UNIVERSITÉ DE STRASBOURG

ÉCOLE DOCTORALE DES SCIENCES CHIMIQUES

Laboratoire de Chimie Inorganique Moléculaire et Catalyse – UMR 7177

THÈSE

présentée par

Rafael GRAMAGE-DORIA

soutenue le **03 janvier 2012**

pour obtenir le grade de

Docteur de l'université de Strasbourg

Discipline/ Spécialité : Sciences Chimiques

Ligands macrocycliques à grande cavité dérivés de cyclodextrines : synthèse, propriétés complexants et catalytiques.

THÈSE dirigée par :

M. MATT Dominique	Directeur de Recherches CNRS, Université de Strasbourg
M. ARMSPACH Dominique	Professeur, Université de Strasbourg

RAPPORTEURS :

Mme CLAVER Carmen	Professeur, Universitat Rovira i Virgili de Tarragona
M. MONFLIER Eric	Professeur, Université d'Artois

MEMBRES DU JURY :

M. BRAUNSTEIN Pierre	Directeur de Recherches CNRS, Université de Strasbourg
M. ROESKY Peter W.	Professeur, Unviersität Karlsruhe
Mme CLAVER Carmen	Professeur, Universitat Rovira i Virgili de Tarragona
M. MONFLIER Eric	Professeur, Université d'Artois
M. MATT Dominique	Directeur de Recherches CNRS, Université de Strasbourg
M. ARMSPACH Dominique	Professeur, Université de Strasbourg

A mes parents, Maria et Rafael

et à mon frère, Vicent

"Genius is one percent inspiration,
ninety-nine percent perspiration"

Thomas Alva Edison (1847-1931)

Cette thèse a été réalisée au sein du Laboratoire de Chimie Inorganique Moléculaire et Catalyse de l'Université de Strasbourg sous la direction du Dr Dominique Matt, directeur de recherche au CNRS et de Monsieur Dominique Armspach, Professeur à l'Université de Strasbourg.

Tout d'abord, je voudrais exprimer ma profonde gratitude aux « deux Dominique » pour m'avoir donné la possibilité de rejoindre ce groupe ainsi que la confiance qu'ils m'ont accordée. Ce travail n'aurait jamais été possible sans leur soutien et les nombreux conseils et discussions à trois. C'est un vrai plaisir et un honneur d'avoir partagé ces trois ans de recherche avec vous !

Je tiens également à exprimer ma gratitude au CNRS et à la Région Alsace pour leur appui financier dans la réalisation de cette thèse.

Mes remerciements vont également au Dr Pierre Braunstein et aux Professeurs Carmen Claver, Eric Monflier et Peter W. Roesky qui ont bien voulu me faire l'honneur d'être membres de mon jury de thèse. Qu'ils trouvent ici l'expression de ma profonde reconnaissance.

Les travaux présentés dans ce manuscrit n'auraient pu être menés à bien sans le concours des différents services communs de l'Institut de Chimie. Je voudrais remercier toute l'équipe de la RMN et en particulier Messieurs Lionel Allouche, Jean-Daniel Sauer et Maurice Coppe. Ma gratitude va également à M. Loïc Toupet (Université de Rennes 1) pour son investissement dans la résolution (jamais évidente) des structures moléculaires et au Dr David Sémeril pour son aide dans la mise en œuvre des tests catalytiques, sans oublier le Dr Rubén D. Costa et le Professeur Enrique Ortí (Université de Valencia) pour la réalisation des calculs préliminaires DFT.

Merci à tous les membres permanents du laboratoire, en particulier les Drs Eric Brenner et Catherine Jeunesse d'avoir non seulement su m'épauler dans les périodes difficiles, mais aussi d'avoir partagé de très bons moments avec moi souvent autour d'un café. Je ne saurais oublier les différents thésards et stagiaires que j'ai eu le plaisir de côtoyer au laboratoire : Hani El Moll, Mouhamad Awada, Julien Mutschler, Soheila Sameni, Coraline Egloff,

Mickaël Henrion, Laure Monnereau, Belkacem Benmerad, Sakina Ouis, Matthieu Jouffroy, Matthieu Teci et Christelle Jenffer.

Durant les deux premières années de thèse, j'ai eu l'opportunité d'enseigner à l'IUT d'Illkirch. Je tiens à remercier tout particulièrement les Drs Nicolas Girard, Anne Bodlenner et Eric Brenner avec lesquels j'ai partagé des moments de convivialité.

Un grand merci aux Docteurs Laurence Bonnafoux, Rafael Ballesteros-Garrido et Frédéric R. Leroux du Laboratoire de Stéréochimie de l'Université de Strasbourg, trois personnes qui ont été déterminantes dans ma décision de me lancer dans un tel projet et sans lesquelles je ne serais pas en train d'écrire ce manuscrit. Ils ont su me transmettre leur motivation pour la science.

Enfin, je tiens à remercier l'ensemble des personnes qui m'ont accompagné dans ce long voyage qui a débuté à mon arrivée à Strasbourg en septembre 2006 en tant qu'étudiant Erasmus. Je n'aurais jamais pu imaginer que je croiserais un jour des gens aussi exceptionnels et dont le souvenir restera gravé en moi à jamais. Je ne les nommerai pas car la liste serait trop longue. Merci pour toutes les soirées passées ensemble, les voyages, les discussions enrichissantes et plein d'autres choses que nous avons eu l'occasion de partager.

Partie rédigée exceptionnellement en valencià :

Finalment, voldria agrair i dedicar aquest treball als meus pares, Rafa i Maria, i al meu germà Vicent. Ells han sigut el meu suport incondicional de l'altre costat del telèfon. Des del primer dia m'han recolzat i han tingut que aguantar també molt. No hi ha res fàcil i com bé diuen ells : "qui algo vol, algo li costa" i a mi m'ha costat estar físicament lluny dels meus. Ara bé, puc dir que ha valgut la pena, i que ha sigut una experiència inoblidable. Ha sigut gràcies a vosaltres que he arribat fins ací i és un orgull poder dir que sóc com vosaltres m'heu ensenyat a ser en aquesta vida. Ja per acabar voldria recordar-me de la resta de la meua familia (sobre tot de Mario i Anna, els meus cosins) i especialment de dos persones que no podràn estar el dia de la presentació d'aquest treball : el meu avi Vicent i la meua avia Fina, açò també va per ells. Gràcies també a tots els meus amics, en especial als del meu poble, Ontinyent.

A vous tous, merci.

CD	cyclodextrin
COD	cycloocta-1,5-diene
COSY	correlation spectroscopy
δ	chemical shift (ppm)
DMAP	4-dimethylaminopyridine
dmba	*N,N*-dimethylbenzylamine
DMF	*N,N*-dimethylformamide
ESI	electro-spray ionisation
GC	gas chromatography
HMQC	heteronuclear multiple quantum correlation
IR	Infra Red absorption spectroscopy
$^{n}J_{A,B}$	coupling constant (Hz) between nuclei A and B through n bonds
Ms	mesyl / $–SO_2Me$
MS	mass spectrometry
NMR	nuclear magnetic resonance
ppm	parts per million
ROESY	Rotation frame Overhauser Effect SpectroscopY
thf	tetrahydrofuran
tht	tetrahydrothiophene
TOCSY	TOtal Correlation SpectroscopY
VT NMR	Variable Temperature Nuclear Magnetic Resonance

Les cyclodextrines (CDs) sont des oligosaccharides cycliques constituées de monomères D-(+)-glucopyranose liés entre eux par des liaisons glycosidiques α-(1→4). Les plus utilisées sont celles qui comportent six, sept ou huit unités glucose, et sont appelées α-CD, β-CD et γ-CD, respectivement. Grâce à leur structure "cage", les cyclodextrines sont capables de former des complexes d'inclusion avec diverses molécules, ouvrant ainsi la voie à des applications dans de nombreux domaines de la chimie. Un des développements les plus récents, à l'origine des travaux présentés dans cette thèse, concerne l'élaboration de molécules associant de manière covalente une cyclodextrine et un métal de transition, composés particulièrement adaptés à l'étude de réactions catalytiques confinées et/ou fonctionnant en mode supramoléculaire.

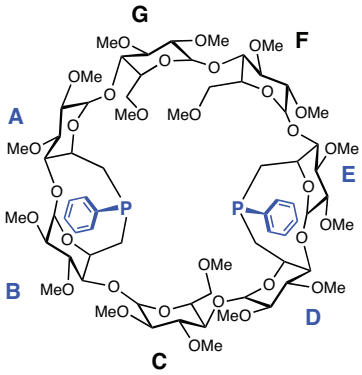

WIDEPHOS

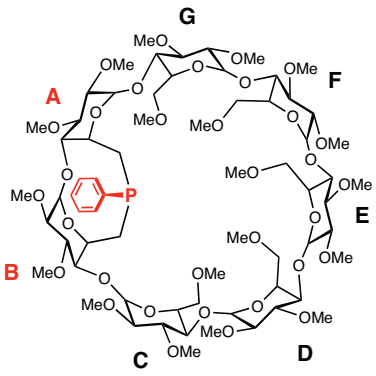

L

La première partie de ce mémoire est une mise au point donnant un aperçu du rôle croissant joué en chimie des métaux de transition par des ligands hybrides associant des centres donneurs et une entité cavitale.

Les chapitres suivants sont consacrés à la synthèse de deux ligands phosphorés originaux construits sur une plateforme β-CD, ainsi qu'à l'étude de leurs propriétés complexantes et catalytiques. Le premier, **WIDEPHOS**, est une β-CD méthylée qui intègre deux unités phenylphosphinidène "PPh" pontant chacune deux unités glucose adjacentes. Dans cette diphosphine qui est conçue comme un chélateur à très grand angle de chélation, les doublets libres des atomes de phosphore pointent vers l'intérieur de la plateforme CD. En présence d'entités MX_2 "carré-plan" (M = Pd, Pt, Rh), **WIDEPHOS** forme des complexes chélate caractérisés par un angle P-M-P proche de 160º, autrement dit conduit à des complexes de stéréochimie *trans* "imparfaite". Cette dernière est à l'origine d'un mouvement de balancier du ligand autour du métal, l'*oschélation*, un mouvement qui permet à chacun des atomes de phosphore d'optimiser, à tour de rôle, la liaison qu'il forme avec le métal complexé. Une autre propriété remarquable de **WIDEPHOS** concerne sa propension à former

des espèces dinucléaires dans lesquelles les deux centres métalliques sont confinés dans l'espace cavital. Les contraintes induites par la formation de tels complexes sont manifestes au niveau de l'angle d'inclinaison τ de l'un des atomes de phosphore ainsi que par l'apparition d'un mouvement d' "oschélation" d'un fragment P,O constitutif de la CD.

Le deuxième ligand étudié dans cette thèse (**L**) correspond à une version "allégée" du ligand introverti précédent. Equipé d'une seule entité phosphinidène, **L** dispose d'un espace cavital sensiblement plus grand que celui de **WIDEPHOS**. Sa structure creuse favorise la formation de complexes monophosphine, autrement dit **L** empêche stériquement la formation de complexes dans lesquels le centre métallique serait, en présence d'une phosphine tertiaire classique, stabilisé par *deux* ligands PR_3. Cette propriété a permis d'isoler le complexe aqua $[PdCl_2(H_2O)\mathbf{L}]$, dont l'entité $PCl_2(H_2O)$ est entièrement piégée dans la cavité CD et dont la stabilité est en partie assurée par des interactions faibles avec les parois internes de la CD. A signaler qu'aucun complexe de type $[PdX_2(PR_3)(H_2O)]$ n'avait été isolé à ce jour. Par ailleurs, la phosphine **L** catalyse efficacement le couplage Heck-Mizoroki entre le styrène et des bromures d'aryle; ses performances se sont avérées supérieures à celle de son analogue diphosphine **WIDEPHOS**. Les résultats catalytiques sont optimaux lorsqu'on applique un ratio monophosphine/palladium de 1, suggérant ainsi la formation d'espèces monocoordinées dans le cycle catalytique.

La dernière partie du manuscrit démontre la possibilité inattendue de former une liaison C–C dans la sphère de coordination d'un atome de palladium lié à la diphosphine **TRANSDIP**, dont les propriétés *trans*-chélatantes exclusives ont été établies récemment. L'étude a permis d'isoler plusieurs intermédiaires clé du mécanisme de formation de cette liaison, notamment celle du complexe κ^1-*P*-$[PdMe_3(\mathbf{TRANSDIP})]Li$.

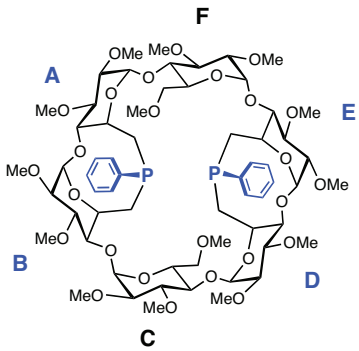

TRANSDIP

Mots-clés : cavitands • cyclodextrines • complexes chélate • complexes dinucléaires • couplage de Heck-Mizoroki • diphosphines *trans*-chélatantes • dynamique moléculaire

Cyclodextrins (CDs) are cyclic oligosaccharides of various sizes containing several α-(1→4)-linked D-(+)-glucopyranose units. The commercially available ones comprise six, seven or eight glucose units, named respectively α-CD, β-CD and γ-CD. Their truncated cone-like and well-defined cavity are particularly attractive for the encapsulation of a variety of substrates. As such, they found numerous applications in many areas of chemistry. A recent development, from which the present work is inspired, consisted in covalently linking transition metals to CD cavities in order to perform and study catalytic reactions in a confined environment featuring steric repulsive or attractive non-covalent interactions with the substrate or/and the metal coordination sphere.

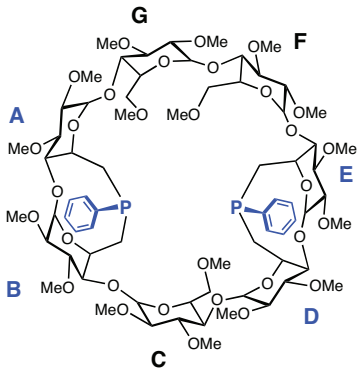

WIDEPHOS

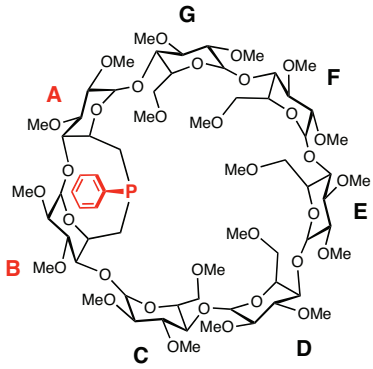

L

The first part of this thesis focuses on reviewing transition metal-based cavitands, for which the first and second metal coordination spheres are controlled by their cavity-shaped ligand. The following chapters are concerned with the synthesis, coordination and catalytic properties of two new phosphane ligands built on a large β-CD scaffold. The first one, named **WIDEPHOS**, is a diphosphine having two phenylphosphinidene "PPh" units capping adjacent glucose units on a methylated β-CD. This ligand features two phosphorus lone pairs pointing to the cavity interior but not aligned. These geometrical features, combined with the large distance separating the two phosphorus atoms, promote the formation of "imperfect" *trans*-chelate complexes in which the metal centre swings about the ligand. This unprecedented molecular movement, christened "oschelation", allows each phosphorus atom to form an optimal bond in turn with the coordinated d^8 and d^{10} transition metal ions. Further studies on **WIDEPHOS** proved that it is better suited for coordinating dinuclear fragments within the confinement of the large β-CD cavity. Severe steric constrains on the metal first sphere of coordination result in the formation of single μ-chlorido bridged dinuclear species.

In this new type of square planar complexes, non-optimal orbital overlapping measured by the so-called tilt angle was also found to take place for one of the phosphorus atom together with an "oschelation" movement involving non identical donor atoms, namely a phosphorus and an oxygen atom. Static gold(I) dinuclear complexes displaying similar imperfect orbital overlapping for one of the phosphorus atom were also prepared.

The second introverted ligand of interest is monophosphane **L**, which can be considered as a "lighter version" of the previous ligand. Featuring only one phenylphosphinidene unit, **L** has more space available for metal complexation than **WIDEPHOS**. Its hollow structure prevents the formation of complexes having two PR_3 ligands coordinated to the metal centre as it is usually the case for standard tertiary phosphines. This property has allowed the preparation of the aqua complex $[PdCl_2(H_2O)\mathbf{L}]$, in which the $PdCl_2(H_2O)$ fragment is fully trapped in the CD cavity and stabilized to some extent by hydrogen bonding with the CD inner walls. Moreover, when coordinated to palladium, phosphine **L** catalyses efficiently Heck-Mizoroki coupling reactions. Its performances were found to be better than its analogue **WIDEPHOS**. Optimal catalytic rates were obtained when employing stoichiometric amounts of monophosphine and palladium, suggesting the formation of monocoordinated species in the catalytic cycle.

The last part of the manuscript is concerned with unexpected C–C coupling reactions mediated by Pd *trans*-chelate complexes of the recently published diphosphine **TRANSDIP**. Several key intermediates involved in the mechanism of C–C bond formation have been isolated and identified, notably the unprecedented κ^1-*P*-[$PdMe_3$(**TRANSDIP**)]Li complex.

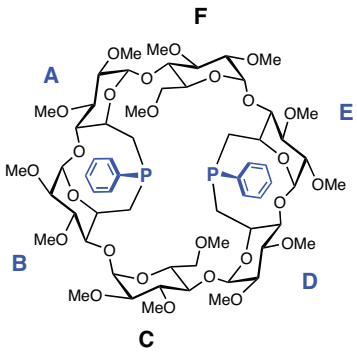

TRANSDIP

Keywords: cavitands • cyclodextrins • chelates complexes • dinuclear complexes Heck reactions • *trans*-chelating diphosphanes • molecular dynamics

General introduction and objectives

During the last three decades molecules that combine the properties of a transition metal with those of an appended cavity have attracted a great deal of attention.[1-3] So far, research in this area has focused on four main objectives: 1) the design and synthesis of systems exploiting the binding properties of a receptor unit linked to a transition-metal centre, with the aim of producing catalysts that mimic an enzyme;[4-8] 2) the study of metal-centred reactions taking place in a confined environment, thereby favouring highly regio-, stereo-, and shape-selective reactions;[9-13] 3) the metal assisted entrapment and recognition of ionic species;[14-16] 4) the construction of sensors capitalizing on an electro- or photoactive metal unit covalently attached to a close, cavity-shaped receptor.[17,18] In this respect, cyclodextrins (CDs) and their chemically modified derivatives occupy a position of choice.[19-27] Their rigid, conical structure as well as the presence of hydroxyl groups that can be substituted in a regioselective manner, offer many possibilities in terms of cavitand design. So far, most studies focused on the smallest member of the family, namely the α-CD, because of the ease with which it can be functionalised, the β-CD derivatives remaining largely unexplored even if their bigger inner space seems more appropriate for taking full advantage of the cavity.

The present thesis is mainly concerned with the preparation of new "introverted" phosphanes derived from multi-functionalised methylated β-CDs and the study of their coordination and catalytic properties. The last part of the manuscript focuses on the use of a smaller α-CD analogue of the aforementioned phosphanes namely the *trans*-chelating diphosphane **TRANSDIP**[28] in palladium-promoted carbon–carbon forming reactions.

The manuscript is divided into six chapters:

Chapitre I. *Contrôle double des première et seconde sphères de coordination d'un métal de transition par des coordinats bâtis sur cavité moléculaire*. This chapter gives an overview on transition metal-based cavitands, for which the first and second metal coordination spheres are controlled by the appended cavity-shaped ligand.

Chapter II. *Regioselective double capping of cyclodextrin scaffolds*. This chapter is devoted to the synthesis of various α- and β-CD derivatives multi-

functionalised at the primary face. The methodology employed relies on the use of difunctional capping reagents.

Chapter III. *Oschelating behaviour of **WIDEPHOS***. This chapter is concerned with the chelating behaviour of **WIDEPHOS**, a β-CD-based diphosphane ligand. **WIDEPHOS** was shown to chelate d^8 and d^{10} transition metal ions exclusively in a *trans* manner. The resulting complexes display fluxional behaviour due to non-optimal orbital overlapping between the metal centre and both "introverted" phosphorus lone pairs.

Chapter IV. *Intra-cavity confinement of two metal centres in a cyclodextrin.* This part of the manuscript describes the way **WIDEPHOS** is able to accommodate two metal centres within its CD cavity. In these heavily strained dinuclear complexes, non-optimal orbital overlapping was shown to be responsible for (1) unusual ^{31}P NMR upfield shifts and (2) fluxional, oschelating behaviour between a P(III) atom and a OMe oxygen atom of the CD scaffold.

Chapter V. *Coordinative and catalytic properties of a β-cyclodextrin bearing an introverted P(III) atom. Comparison with a diphosphine analogue*. This chapter deals with the ability of the monodentate analogue (**L**) of **WIDEPHOS** to form monophosphine complexes with palladium(II) ions. **L** was assessed in the Heck-Mizoroki coupling reaction of arylbromides with styreneand its catalytic properties compared with those of **WIDEPHOS**.

Chapter VI. *Can a cavity-shaped, trans-chelating diphosphine be used in carbon–carbon forming reactions?* The final part of the manuscript focuses on a C–C bond formation reaction promoted by a palladium complex containing the *trans*-spanning chelator **TRANSDIP**.

References

[1] B. Kersting, U. Kehmann, *"Chemistry of Metalated Container Molecules" in Advances in Inorganic Chemistry,* Vol. 61 (Eds.: R. van Eldik, C. D. Hubbard), The Netherlands, Elsevier, pp. 407-470, **2009**.

[2] C. Jeunesse, D. Armspach, D. Matt, *Chem.Commun.* **2005**, 5603-5614.

[3] P. Ballester, A. Vidal-Ferran, *Supramolecular Catalysis* (Ed.: P. W. N. M. van Leeuwen), Willey, Weinheim, pp.1-27, **2008**.

[4] R. Breslow, S. D. Dong, *Chem. Rev.* **1998**, *98*, 1997-2011.

[5] M. T. Reetz, S. R. Waldvogel, *Angew. Chem. Int. Ed.* **1997**, *36*, 865-867.

[6] F. Hapiot, S. Tilloy, E. Monflier, *Chem. Rev.* **2006**, *106*, 767-781.

[7] N. Le Poul, B. Douziech, J. Zeitouny, G. Thiabaud, H. Colas, F. Conan, N. Cosquer, Y. Jabin, C. Lagrost, P. Hapiot, O. Reinaud, Y. Le Mest, *J. Am. Chem. Soc.* **2009**, *131*, 17800-17807.

[8] L. Monnereau, D. Sémeril, D. Matt, L. Toupet, *Chem. Eur. J.* **2010**, *16*, 9237-9247.

[9] J. A. A. W. Elemans, E. J. A. Bijsterveld, A. E. Rowan, R. J. M. Nolte, *Chem. Commun.* **2000**, 2443-2444.

[10] G. Steinfeld, V. Lozan, B. Kersting, *Angew. Chem. Int. Ed.* **2003**, *42*, 2261-2263.

[11] D. Sémeril, C. Jeunesse, D. Matt, L. Toupet, *Angew. Chem. Int. Ed.* **2006**, *45*, 5810-5814.

[12] A. B. C. Deutman, C. Monnereau, J. A. A. W. Elemans, G. Ercolani, R. J. M. Nolte, A. E. Rowan, *Science* **2008**, *322*, 1668-1671.

[13] T. S. Koblenz, J. Wassenaar, J. N. H. Reek, *Chem. Soc. Rev.* **2008**, *37*, 247-262.

[14] M. Staffilani, K. S. B. Hancock, J. W. Steed, K. T. Holman, J. L. Atwood, R. K. Juneja, R. S. Burkhalter, *J. Am. Chem. Soc.* **1997**, *119*, 6324-6335.

[15] F. Fochi, P. Jacopozzi, E. Wegelius, K. Rissanen, P. Cozzini, E. Marastoni, E. Fisicaro, P. Manini, R. Fokkens, E. Dalcanale, *J. Am. Chem. Soc.* **2001**, *123*, 7539-7552.

[16] L. Poorters, D. Armspach, D. Matt, L. Toupet, *Angew. Chem. Int. Ed.* **2007**, *46*, 2663-2665.

[17] P. D. Beer, V. Timoshenko, M. Maestri, P. Passaniti, V. Balzani, *Chem. Commun.* **1999**, 1755-1756.

[18] A. J. Evans, S. E. Matthews, A. R. Cowley, P. D. Beer, *Dalton Trans.* **2003**, 4644-4650.

[19] M. L. Bender, M. Komiyama, *Cyclodextrin Chemistry,* Springer, Berlin, **1978**.

[20] Special Issue "Cyclodextrins" *Chem. Rev.* **1998**, *98*, 1741-2076.

[21] J. L. Atwood, J. E. D. Davies, D. D. Macinol, F. Vögtle, J.-M. Lehn, *'Cyclodextrins', Comprehensive Supramolecular Chemistry,* Pergamon, Oxford, **1996**.

[22] C. J. Easton, S. F. Lincoln, *Modified Cyclodextrins,* Imperial College Press, London **1999**.

[23] M. Sollogoub, *Eur. J. Org. Chem.* **2009**, *9*, 1295-1303.

[24] D. Armspach, D. Matt, *C. R. Chimie* **2011**, *14*, 135-148.

[25] E. Engeldinger, D. Armspach, D. Matt, P. G. Jones, *Chem. Eur. J.* **2003**, *9*, 3091-3105.

[26] S. Guieu, E. Zaborova, Y. Blériot, G. Poli, A. Jutand, D. Madec, G. Prestat, M. Sollogoub, *Angew. Chem. Int. Ed.* **2010**, *49*, 2314-2318.

[27] F. Hapiot, A. Ponchel, S. Tilloy, E. Monflier, *C. R. Chimie*, **2011**, *14*, 149-166.

[28] L. Poorters, D. Armspach, D. Matt, L. Toupet, S. Choua, P. Turek, *Chem. Eur. J.* **2007**, *13*, 9448-9461.

Chapitre I

Contrôle double des première et seconde sphères de coordination d'un métal de transition par des coordinats bâtis sur cavité moléculaire

Chapitre I

Contrôle double des première et seconde sphères de coordination d'un métal de transition par des coordinats bâtis sur cavité moléculaire

I.1. Introduction

L'objet de cette mise au point est de donner un aperçu du rôle croissant joué en chimie des métaux de transition par des ligands hybrides associant un centre donneur et une entité cavitale. Nous nous attacherons principalement à montrer comment, dans un tel ligand, la fonctionnalité "cavité" peut modifier les propriétés d'un centre métallique lié à l'atome coordinateur primaire, soit en créant elle-même une liaison avec l'ion complexé, soit en fonctionnant comme réceptacle vis-à-vis d'entités formant la première sphère de coordination.

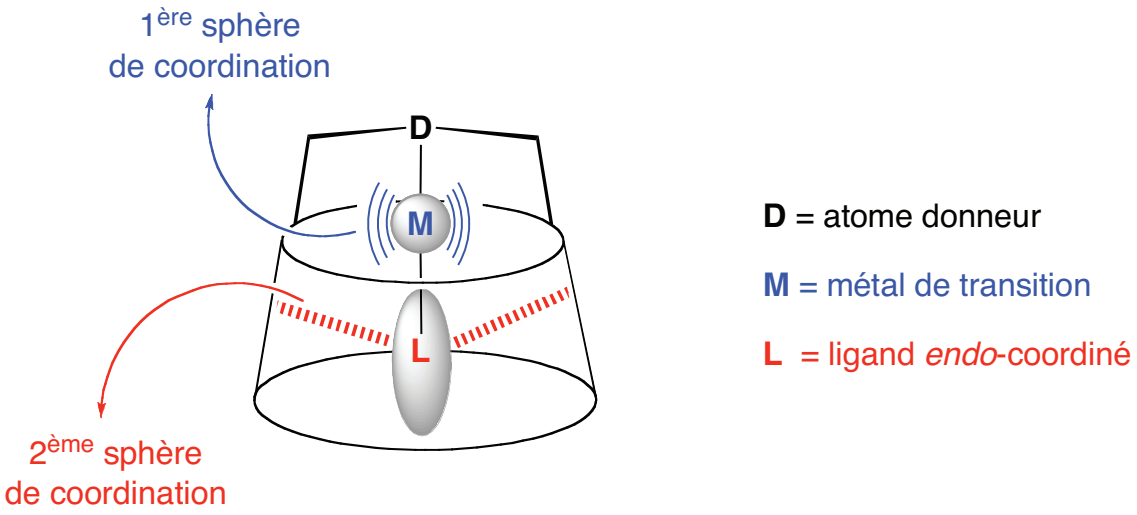

NB: Dans ce chapitre, la numérotation des molécules est indépendante de celle des composés décrits dans les autres chapitres du manuscrit. Les flèches blanches à contour noir renvoient à des structures cristallographiques. Pour celles-ci, les contre-ions, solvants, et atomes d'hydrogène ont été omis par souci de clarté. Les atomes de carbone sont gris, d'oxygène rouges, d'azote bleus, de phosphore oranges et les halogénures verts.

L'apparition de coordinats intégrant des cavités moléculaires remonte à la fin des années 1970, au moment où furent réalisés des progrès très significatifs en synthèse macrocyclique.[1] C'est aussi au cours de cette période que Breslow découvrit les propriétés spectaculaires de métallo-enzymes artificielles dérivées de cyclodextrines dans des réactions d'hydrolyse d'esters.[2,3] Le chapitre est articulé autour de quatre sections, dont les trois premières correspondent aux cavités les plus utilisées de la littérature: calix[*n*]arènes, résorcinarènes, cyclodextrines. La quatrième traite de récepteurs de forme atypique très peu utilisés. Dans la suite de l'article, le mot cavitand désignera toute molécule creuse capable d'héberger une entité chimique, qu'elle soit neutre ou chargée. Ce terme a été introduit en 1983 par Cram, mais ne servait initialement qu'à la description de cavités résorcinaréniques particulières (*vide infra*), dépourvues de toute mobilité conformationnelle.[1]

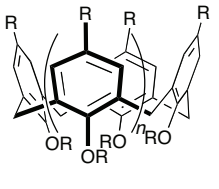

Calix[*n*]arènes
n = 4, 5, 6, 8

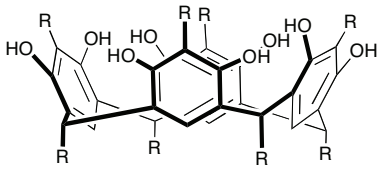

Resorcin[4]arènes

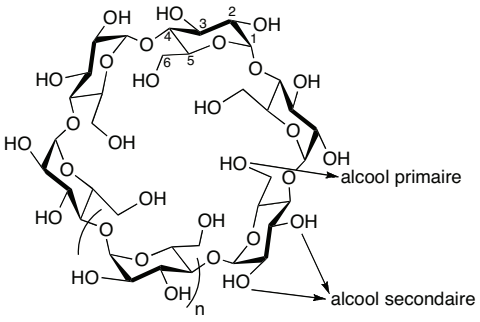

α-CD, n = 1
β-CD, n = 2
γ-CD, n = 3

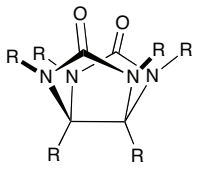

Glycouryle

I.2. Ligands dérivés de calix[*n*]arènes

Ces macrocycles constituent actuellement la classe de cavités la plus utilisée en synthèse moléculaire. Les plus courants sont les calix[*n*]arènes comportant respectivement (*n* =) 4, 6 et 8 entités phénoliques reliées entre elles par des ponts méthyléniques. L'engouement au cours des deux dernières décennies pour ces composés fait suite aux travaux du chimiste américain David Gutsche qui en proposa des synthèses rationnelles à la fin des années 1970.[4-6] De par leur constitution, les calix[*n*]arènes génériques intègrent donc des atomes d'oxygène sur la partie dite inférieure, ces derniers étant des atomes coordinateurs potentiels.

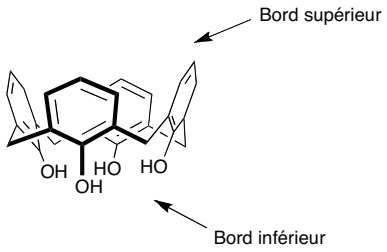

I.2.1. Calix[*n*]arènes porteurs de ligands oxygénés

Le premier exemple de complexe calixarénique comportant un centre métallique ayant un ligand localisé à l'intérieur de la cavité, le complexe **1**, a été décrit par Pedersen à la fin des années 1980. Dans ce complexe de di-titane, obtenu par réaction de *p-tert*-butylcalix[8]arène avec $Ti(O^iPr)_4$, chacune des unités $\{Ti(O^iPr)\}$ est nichée dans une poche conique tri-arylée "$ArCH_2ArCH_2Ar$". En raison du champ magnétique créé par les noyaux phénoliques, les protons des fragments O^iPr *endo*-orientés ont subi un déplacement significatif vers les champs forts ($\Delta\delta$ = *ca.* 2 ppm), comparés à ceux du complexe de départ $Ti(O^iPr)_4$. L'enroulement des noyaux phénoliques autour des deux fragments $\{Ti(O^iPr)\}$ provoque une torsion de l'édifice rendant la molécule chirale.[7] Cette propriété a permis d'envisager une utilisation en reconnaissance chirale. Ainsi, si la base utilisée pour la synthèse du complexe **1** est une amine chirale, on constate la formation de diastéréomères distinguables par RMN ^1H.[7] Les auteurs ont étendu leurs études à des complexes analogues comportant d'autres métaux et d'autres ligands *endo*-orientés (Tableau 1).[8]

Tableau 1. Complexes introvertis derivés de *p-tert*-butylcalix[8]arène.

M	ligand *endo*-coordiné	*exo*-cation
Ti	O^iPr	Li^+, Na^+, K^+, K^+(18-couronne-6), $BnNH_3^+$, RNH_3^+
Ti	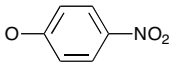	Li^+, Na^+
Ti	OEt	Li^+, Na^+
Ti	O^tBu	K^+, $BnNH_3^+$
Ti	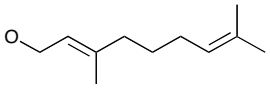	Na^+, $H_2NMe_2^+$
Ti	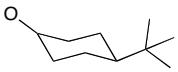	Na
Ti	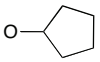	$BnNH_3^+$
Ti	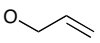	Na^+, K^+
Ti	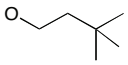	Na^+
Ti	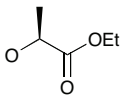	$BnNH_3^+$
Ti	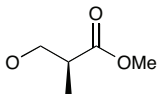	$BnNH_3^+$
Ti	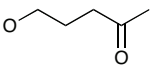	K^+
Zr	O^iPr	K^+
Sn	O^iPr	K^+
Sn	^nBu	K^+
V	O	(*R*)-1-(1-naphtyl)éthylamonium

Pour compléter ce paragraphe, il convient de préciser qu'un seul complexe de titane construit sur une cavité calix[4]arène et ayant un ligand *endo*-orienté est connu, à savoir le complexe benzonitrile **2**.[9]

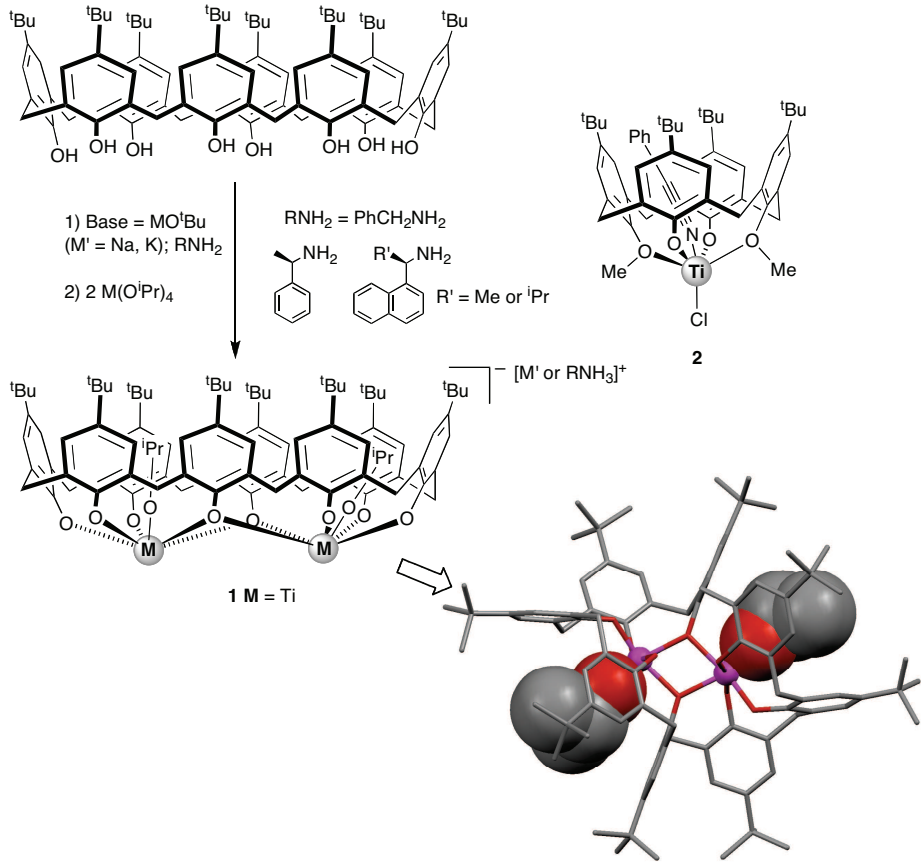

Cependant, des complexes répondant à cette propriété structurale sont connus depuis 1996, notamment les complexes oxo de molybdène **3**[10] et de tungstène **4**[11] qui contiennent respectivement les coordinats eau (O_w) et acétate (travaux de Floriani).

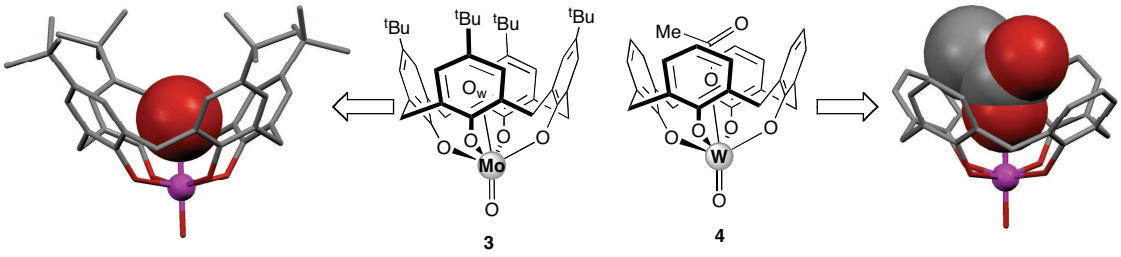

Un autre exemple de métallocalixarène à ligand *endo*-orienté, est le complexe imido **5** décrit par Gibson, comportant un ligand acetonitrile localisé dans la cavité conique.[12] La version calix[8]arène de ce dernier, **6**, reproduit ce type de piégeage deux fois.[12]

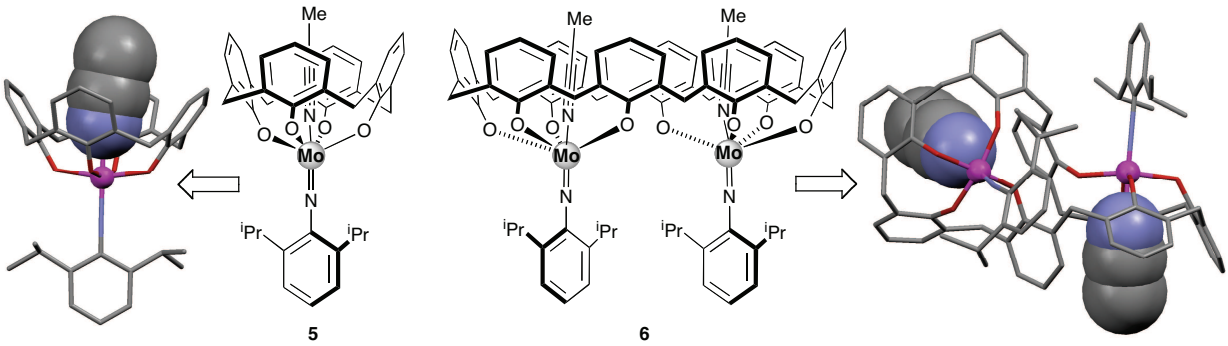

Le complexe **7** est un analogue de **5** dans lequel le groupe aryle du ligand imido est substitué par une fonction alkylaniline. Ce complexe, qui forme des dimères à l'état solide en raison de l'existence de liaisons hydrogène entre fonctions amino, intègre là encore un coordinat nitrile.[13] Cette dernière caractéristique est également observée dans le complexe dinucléaire à pont bis-imido **8**.[13]

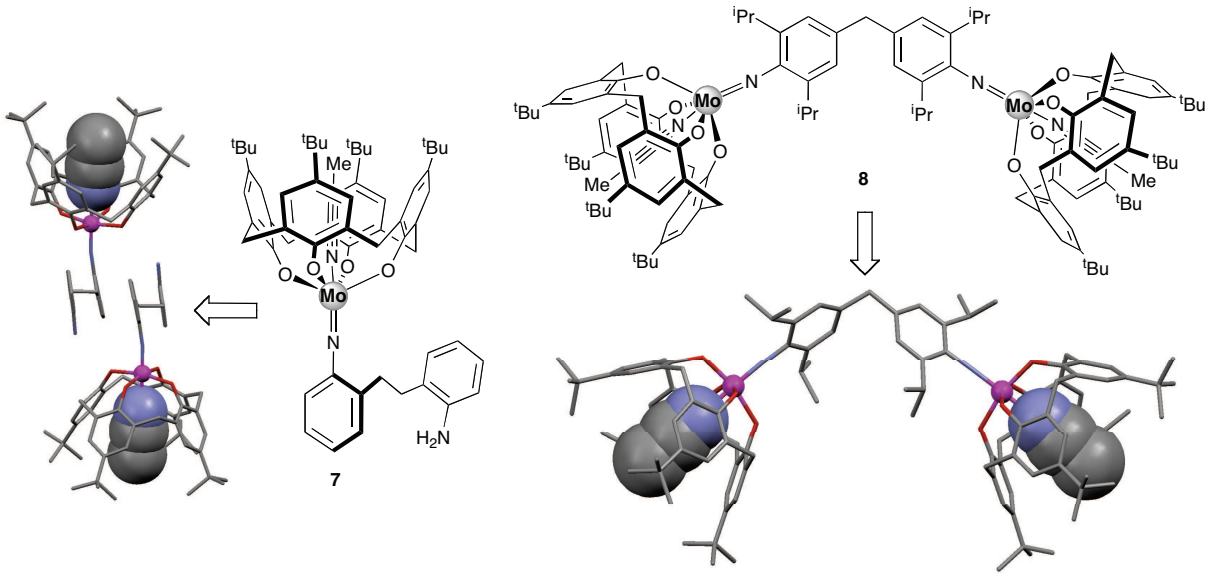

Le complexe chlorido **9**, décrit par Radius, a une structure très voisine de celle de **5**. Ce complexe a servi de composé de départ à la préparation d'un ensemble de complexes (**10**-**14**) ayant chacun une molécule d'acétonitrile incluse dans la cavité.[14]

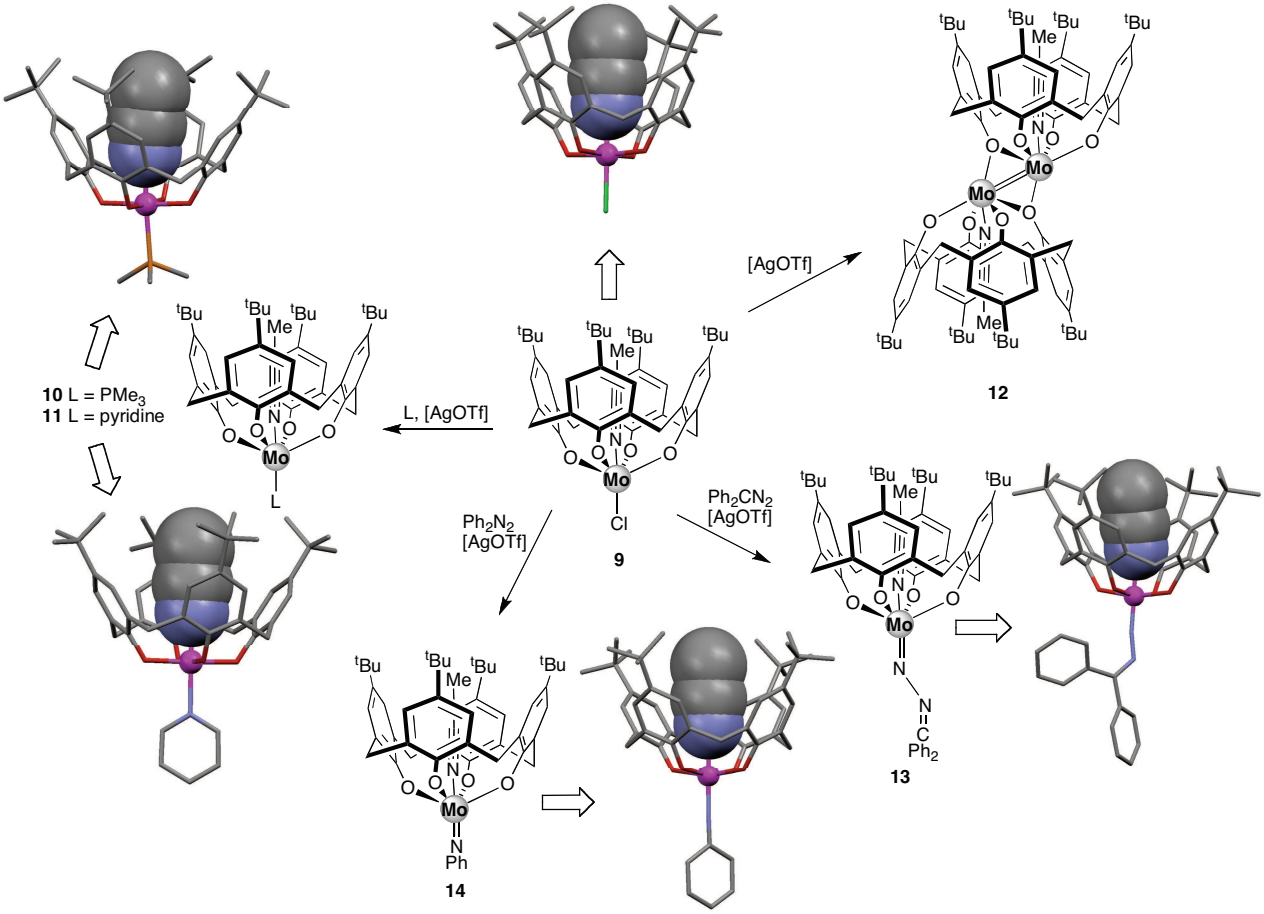

On pourra constater que les complexes imido formés par réaction de *p-tert*-butylcalix[4]arne avec $M(N^tBu)_2(NH^tBu)_2$ ou $M(NMes)_2Cl_2(dme)$ (Mes = 2,4,6-Me_3-C_6H_2, M = Mo, W), ont systématiquement un solvant *endo*-coordiné au métal (H_2O, MeCN, CN^tBu). Il n'a pas été possible de caractériser des variantes de ces métallo-calixarènes dépourvues de solvant. Dans ces complexes (**15-20**), les protons des coordinats piégés ont subi un blindage significatif par rapport à leur forme libre.[15]

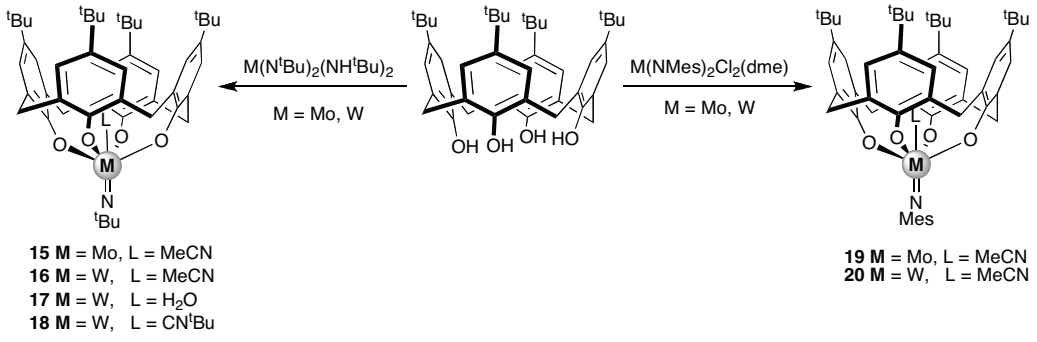

15 M = Mo, L = MeCN
16 M = W, L = MeCN
17 M = W, L = H_2O
18 M = W, L = CN^tBu

19 M = Mo, L = MeCN
20 M = W, L = MeCN

Alors que les complexes **15**-**21** ont tous un ligand imido situé à l'extérieur de la cavité, la situation est différente pour le calix[8]arène **22** décrit par Redshaw, seul exemple connu où des coordinats imido N=NPh$_2$ sont piégés dans une cavité moléculaire.[16]

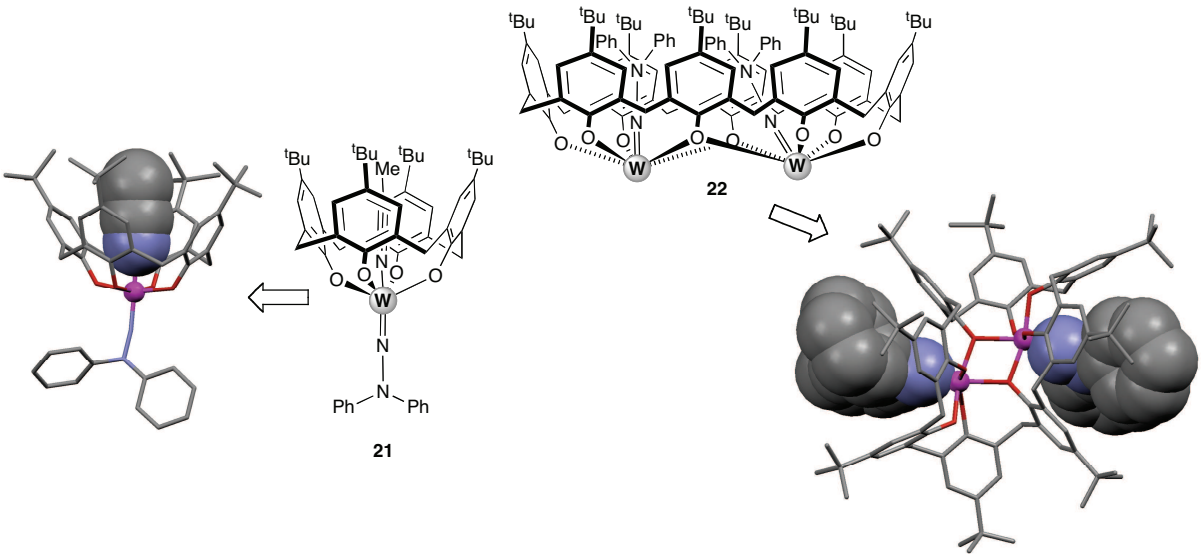

De nombreux travaux ont été consacrés par Floriani et coll. à la synthèse et l'étude de la réactivité de complexes calixaréniques du tungstène. Ces complexes ont notamment servi à l'étude de réactions de formation de liaison carbone–carbone. Il a parfois été possible de suivre ces réactions étape par étape, et ce en raison de la présence de la cavité qui favorise la formation de complexes d'inclusion, et incidemment empêche la poursuite de la réaction (par ex. la formation de **24** à partir de **23**).[17]

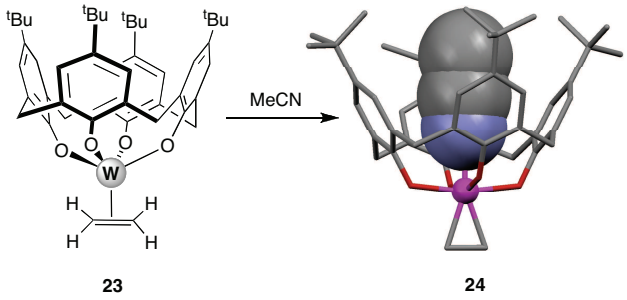

Contrairement aux prévisions, les complexes alkylidène de tungstène **25** et **26** se sont avérés remarquablement stables en présence d'oléfines linéaires.[18] Les auteurs ont postulé qu'au contact du complexe, l'oléfine entrante se positionne en *trans* du carbène, en se nichant à l'intérieur de la cavité. Ce positionnement empêche alors le réarrangement habituel du complexe en complexe *cis* précédant normalement la réaction d'insertion, ce qui explique

donc l'absence de réactivité. L'hypothèse de la formation de complexes *endo* est corroborée par la formation aisée à partir de **25** et **26** de complexes à ligand confiné lors de la réaction avec du benzaldéhyde. Le complexe **25** réagit avec un excès de CN^tBu pour donner le complexe *endo* **27**. Le positionnement *intra*-cavité du ligand isonitrile a été déduit des spectres infrarouges et RMN ^1H. Ainsi, le proton carbénique de l'entité W=C(*H*)Ph a subi un déplacement de 1.2 ppm par rapport à son équivalent dans **25**. En présence d'un large excès de CN^tBu, le complexe **27** conduit au dimère **28** avec deux molécules d'isonitrile incluses et à du distilbène.[19]

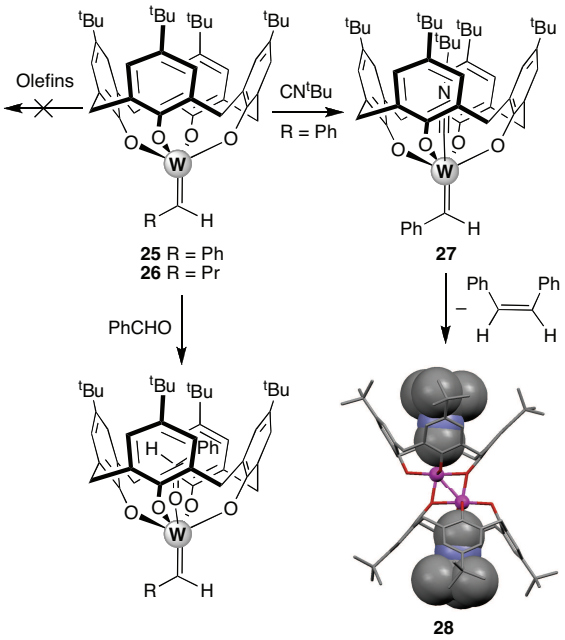

Les propriétés structurales des complexes [W(*exo*-alcène)(calix-O_4)] sont fortement dépendantes de la présence ou non d'un ligand piégé dans la cavité (ce dernier étant localisé en *trans* de l'oléfine). Ainsi, alors que dans le complexe oléfinique **29**, dépourvu de ligand *endo*, la distance C=C est de 1.48 Å, elle est de 1.37 Å dans l'analogue nitrilo **30**.[20] On constate, par ailleurs, que dans ce dernier les quatre atomes d'oxygène sont pratiquement situés dans un même plan (distances O–W: 1.92 Å), alors que dans **29** l'entité O_4 adopte une structure en selle de cheval (O–W: 1.84 Å et 2.02 Å).[20] Une situation similaire est observée dans un analogue molybdique.[21]

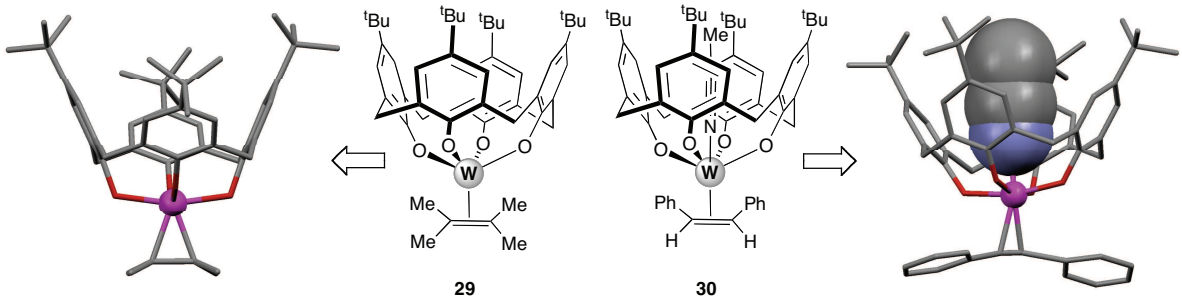

Des complexes calixaréniques de tungstène ont également été employés pour la synthèse de complexes nitrène, intermédiaires clés dans la réduction de N_2 et le clivage de liaisons N–N.[22] Les propriétés réceptrices des complexes imido obtenus par réaction de **31** avec un azoture sont dépendantes de la nature du réactif utilisé. Ainsi, avec l'azoture de triméthylsilyle ou de trityle (R = $SiMe_3$, CPh_3), on forme, après élimination de N_2, respectivement les complexes *exo*-imido **32** et **33**. La réaction de ces derniers avec CN^tBu conduit aux complexes **34** et **35**, ayant chacun un ligand isonitrile logé dans la cavité. La situation est totalement différente si on utilise l'azoture de phényle (PhN_3). Dans ce cas, on forme un imido-complexe *endo* (**36**), pour lequel tout réarrangement squelétal de l'entité W≡NNNR devient impossible, empêchant ainsi l'élimination de N_2.

Le même type de complexe (**37**) est probablement formé avec HN_3 ou $Ph(Me)_2CN_3$ (autre source de HN_3, engendré après départ de α-méthylstyrène), avant sa transformation quasi instantanée en biscalixarène **38**, un complexe où chaque unité calixarène héberge un ligand imido.

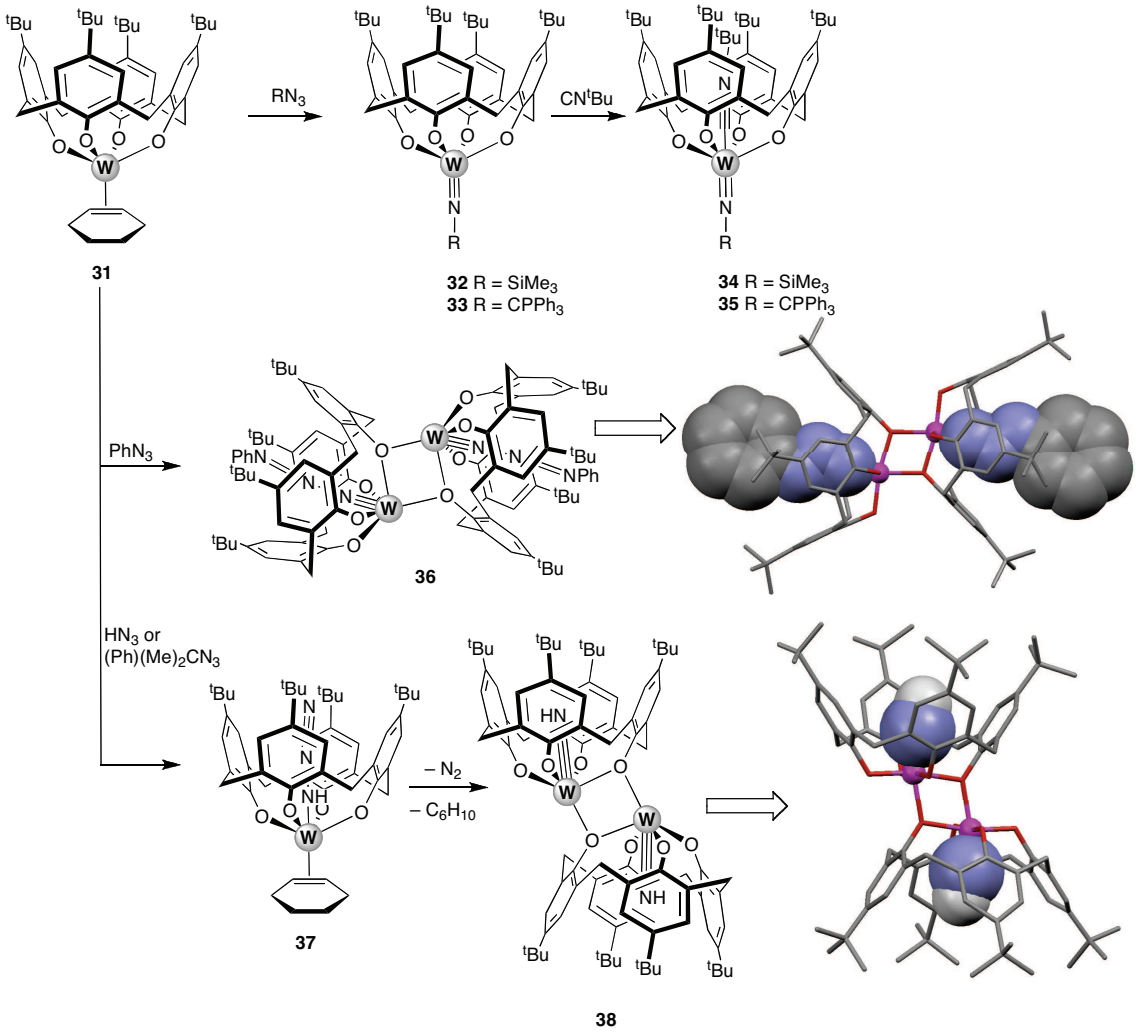

Une autre charactéristique des complexes imido des calixarènes est leur existence sous forme d'équilibre en solution entre monomère et dimère.[22] L'addition de NC^{t}Bu provoque, après coordination-piégeage, la formation d'une seule espèce, mononucléaire (exemple : complexe **39**).

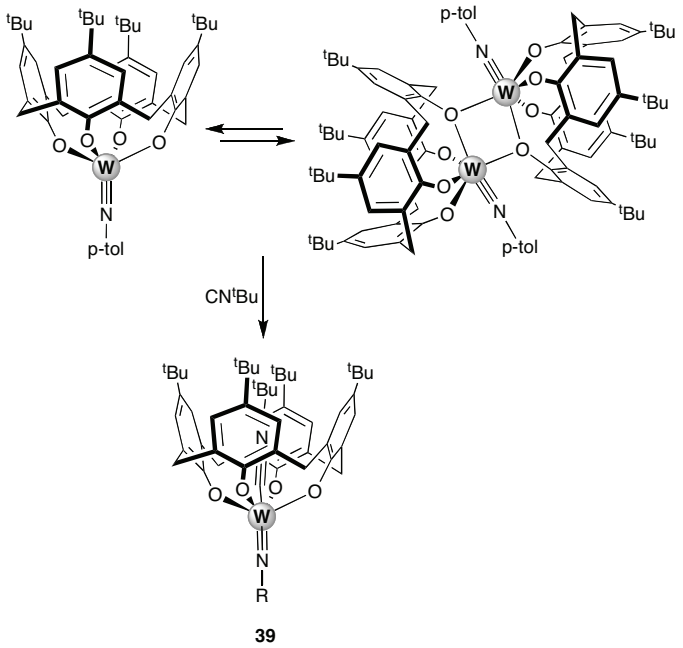

39

La capacité de métallo-calixarènes à base de tungstène de fixer un coordinat positionné à l'intérieur de l'espace conique a été exploité par Swager pour moduler les propriétés de polymères conducteurs, notamment des polymères obtenus par électropolymérisation des bis-thiophènes **40**-**46**.[23]

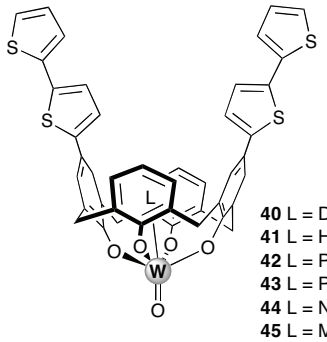

40 L = DMSO
41 L = H_2O
42 L = PhNHCHO
43 L = $PhCH_2NHCHO$
44 L = NH_2CHO
45 L = Me_2NCHO
46 L = $^nBu_2NCHO$

Certains complexes de tungstène dérivés de calix[8]arène peuvent également héberger des ligands venant se nicher dans la partie creuse. Ainsi, le complexe di(oxo-tungstène) **47** se subdivise en deux compartiments cavitaux contenant, chacun, un ligand acétonitrile, comme l'a montré une étude par diffraction des rayons X.[24] A signaler que les tentatives de préparation d'un analogue de **47** à partir d'un calix[6]arène n'ont conduit qu'à des complexes dépourvus de ligands *intra*-cavité .

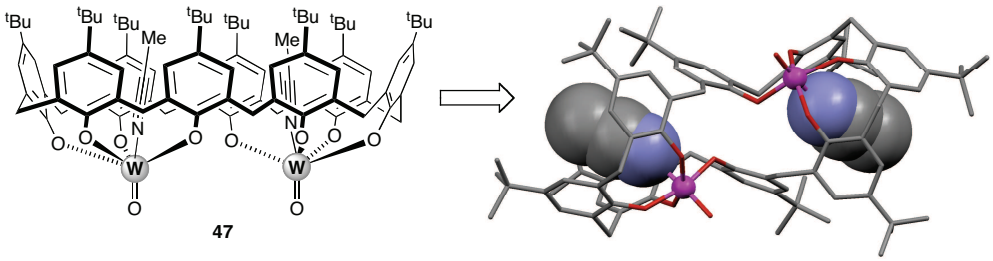

47

Le piégeage d'un ligand, tel qu'il a été observé pour des complexes de tungstène, a également lieu avec d'autres métaux. Ainsi, Lippard et coll. ont décrit les complexes pentaméthyle-cyclopentadiényle-tantale **48** et **49**, ayant respectivement un ligand H_2O (O_w) et MeCN localisé à l'intérieur de la partie conique.[25] Par ailleurs, l'équipe de Floriani a synthétisé le complexe de di-niobium **50**, exemple rare de complexe comportant une entité N=N placée entre deux centres métalliques.[26] Dans ce complexe, un ligand acétonitrile, positionné en *trans* d'un atome d'azote, occupe l'intérieur de chacune des cavités. La même équipe a décrit les complexes dimères de vanadium **51** et **52**, dont les atomes métalliques sont respectivement liés à cinq atomes d'oxygène et un ligand *intra*-cavital (CN^tBu et PhCN, respectivement).[27]

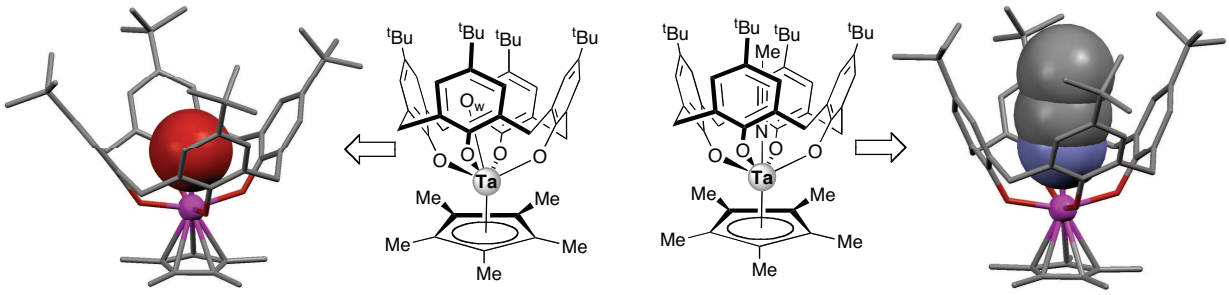

48 49

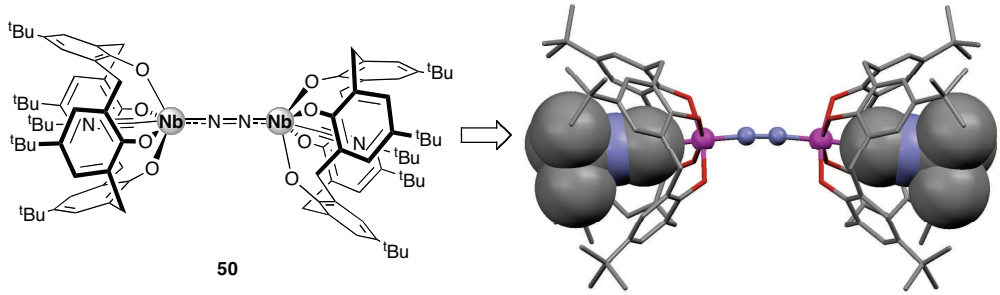

50

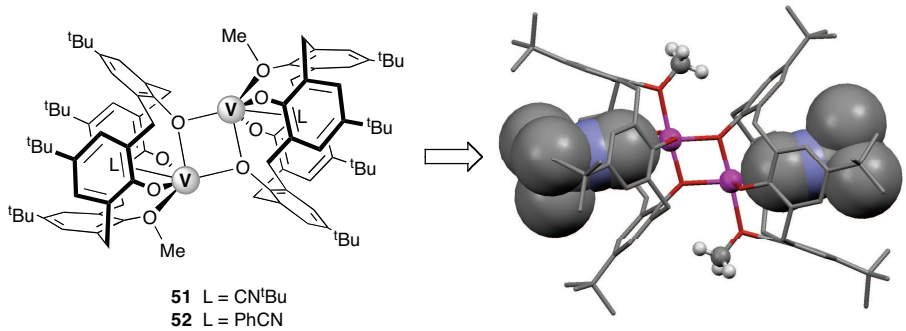

51 L = CN^{t}Bu
52 L = PhCN

Les complexes de chrome **53**-**55** ont été préparés par Redshaw et coll. par réaction de *p-tert*-butylcalix[4]arène avec [$CrCl_3$(thf)], respectivement en présence des bases LiO^tBu, KO^tBu et ^{n}BuLi.[28] Là encore, une molécule d'acétonitrile liée au métal est incluse dans chaque cavité. Dans le complexe **55**, qui peut également être obtenu par réaction d'un calixarène diméthylé avec [$CrCl_3$(thf)] en présence de la base NaH, les entités calixarène sont situées en face l'une de l'autre, par suite de la présence de liaisons hydrogène entre fonctions hydroxyle et phénoxyle de cavités distinctes. De telles liaisons n'existent pas dans le complexe **56**, ce qui explique qu'on se trouve en présence d'une structure où les calixarènes sont disposés de manière décalée, tout en conservant des ligands nitriles piégés.

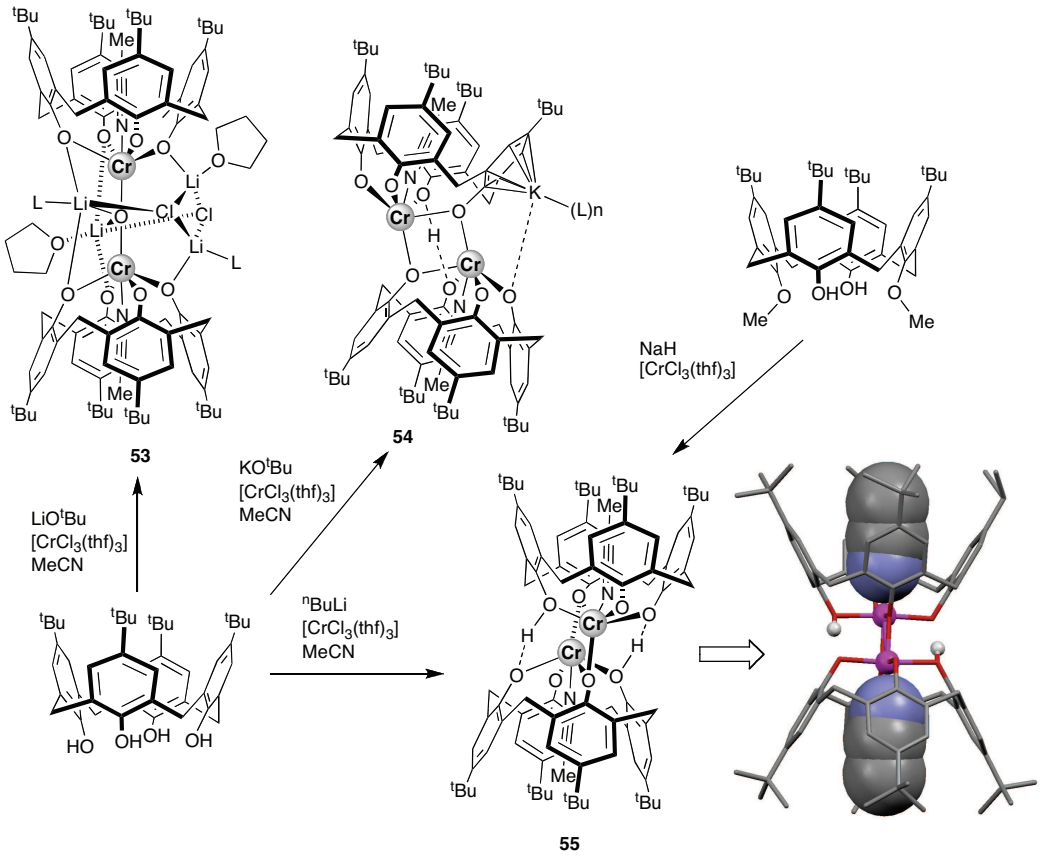

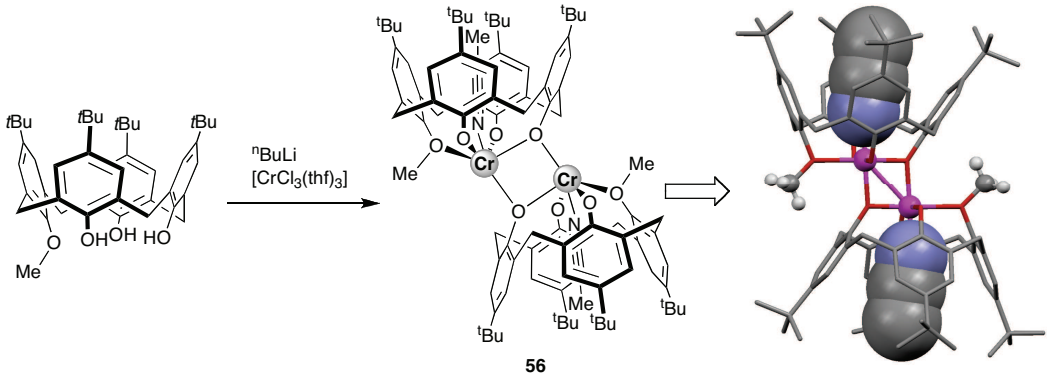

56

Il n'existe que peu de complexes calixaréniques où les atomes d'oxygène phénoliques du calix[4]arène sont liés à des métaux de la droite du tableau périodique. Raston et al. ont synthétisé le complexe **57** comportant cinq atomes de zinc, dont deux sont liés à des fragments alkyle piégés dans des cavités distinctes.[29]

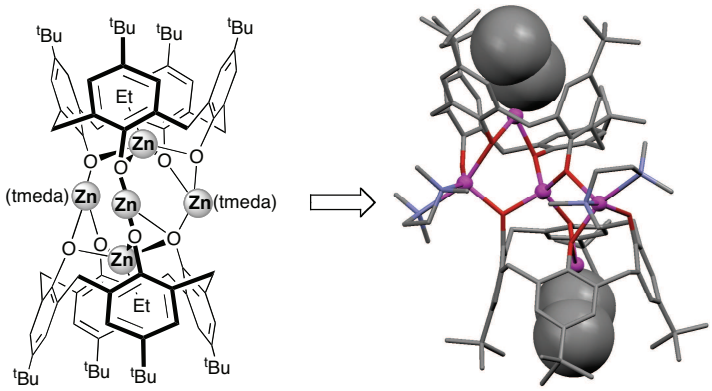

57

D'autres complexes dans lesquels quatre atomes d'oxygène phénoliques prennent en griffe un ion zinc(II) ont été décrits par Vigalok. Dans les complexes **58**-**62**, on observe la présence d'un atome de zinc supplémentaire, qui est d'une part lié à deux oxygènes de l'unité macrocyclique, et d'autre part positionné à l'intérieur du cône calixarénique.[30] La structure moléculaire du complexe éthylzinc **58** a été déterminée par RMN et diffraction des rayons X. Le positionnement du groupement éthyle dans la partie hydrophobe est manifeste au vu du spectre RMN ^{1}H qui montre des signaux blindés. La réaction de 2 équiv. de Ph_2Zn avec **63** conduit au complexe **64**, analogue des complexes d'inclusion précédents, mais où cette fois, c'est une entité ZnPh qui se retrouve piégée à l'intérieur du calixarène. Si on fait réagir **63** avec un mélange équimolaire de Et_2Zn et de Ph_2Zn, seul le complexe ayant un fragment

Ph-Zn dans la cavité, à savoir **65**, est formé, ce qui traduit l'affinité relative de la cavité hydrophobe pour les fragments arène. On peut signaler que si on remplace les groupes C(O)Ph de **63** par des groupes Me, la réaction avec Me_2Zn ou Et_2Zn conduit à un métallocalixarène ayant perdu la conformation cône.[29] Un tel comportement a également été observé avec les calixarènes **66** et **67**, qui sont relativement flexibles, et qui conduisent avec ces mêmes réactifs à un mélange de conformères, l'un cône (**A**) et l'autre 1,2-alterné (**B**). Les proportions relatives de ces derniers dépendent des conditions de réaction.[31] Dans l'isomère **B**, le ligand alkyle lié au zinc n'est que partiellement protégé par les parois calixaréniques. Vigalok a également étudié la réactivité du complexe di-Zn **68** vis-à-vis de certains acides de Lewis. Ainsi, les réactions de **68** avec $B(C_6F_5)_3$ et $BF_3{\cdot}Et_2O$ conduisent, après abstraction du groupe méthyle, à des exemples rares de complexes hexacoordinés du Zn(II), **69** et **70**, respectivement.[32]

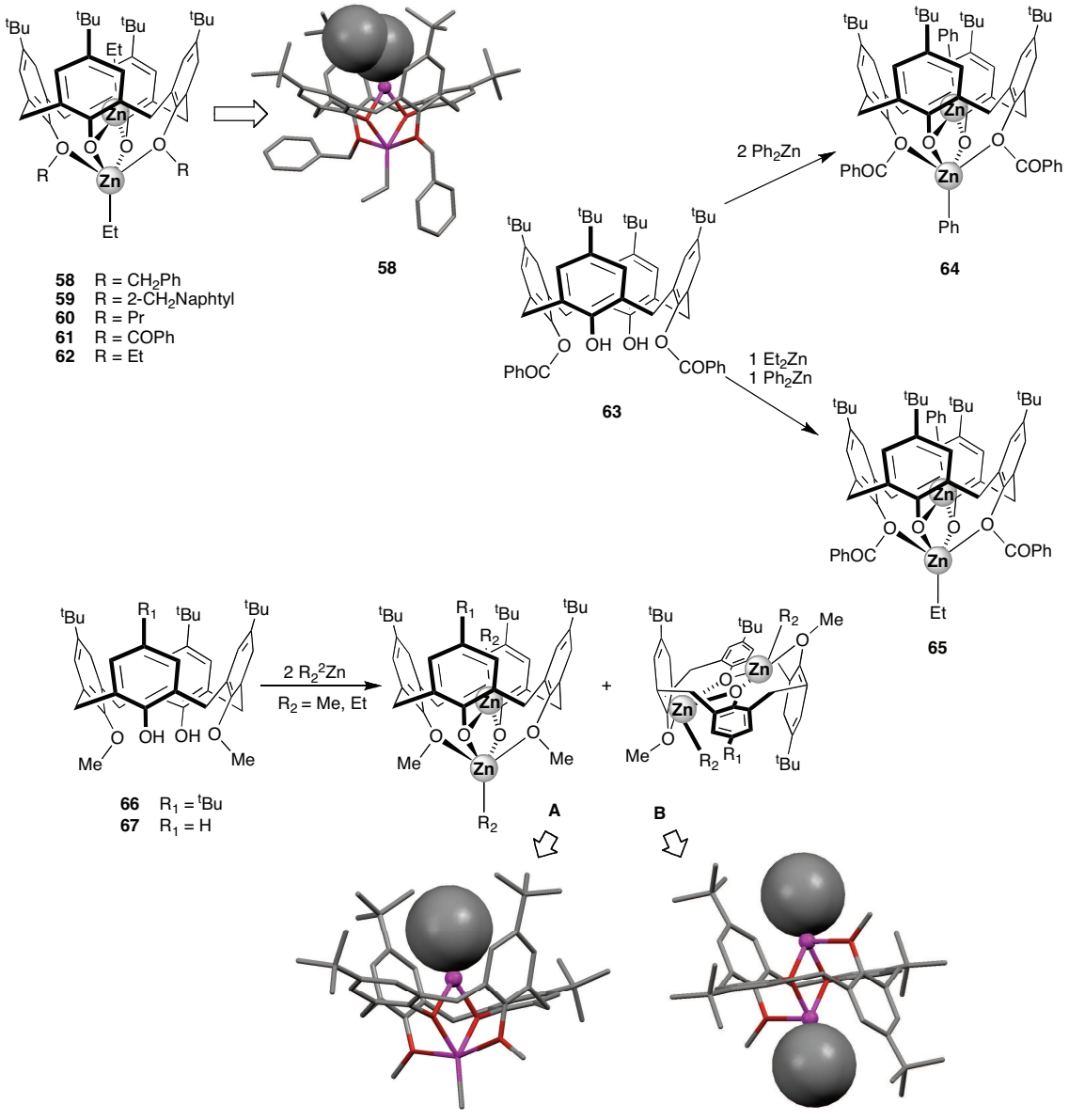

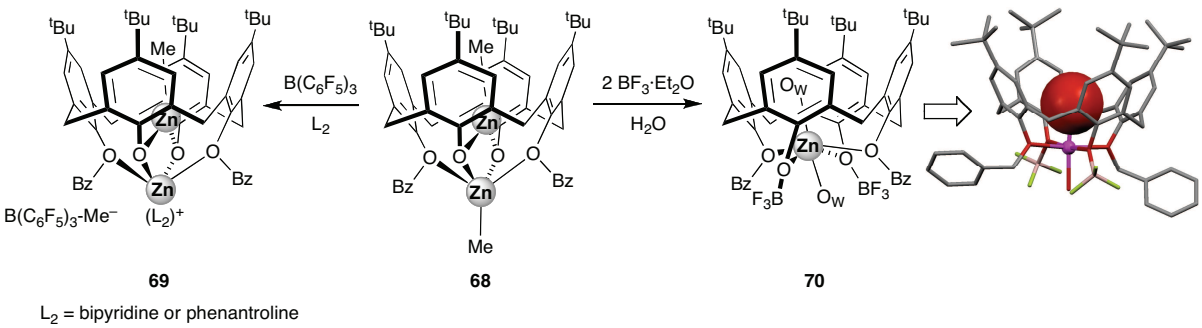

Un seul exemple de calix[4]arène piégeant un centre Pd(II) est connu à ce jour. Il s'agit du complexe **71** formé par réaction d'un précurseur rhénium di-oxo avec [Pd-(η^3-C_3H_5)(acétone)$_2$]$^+$.[33] L'analyse crystallographique révèle une entité "Pd(allyle)" occupant un cône très évasé.

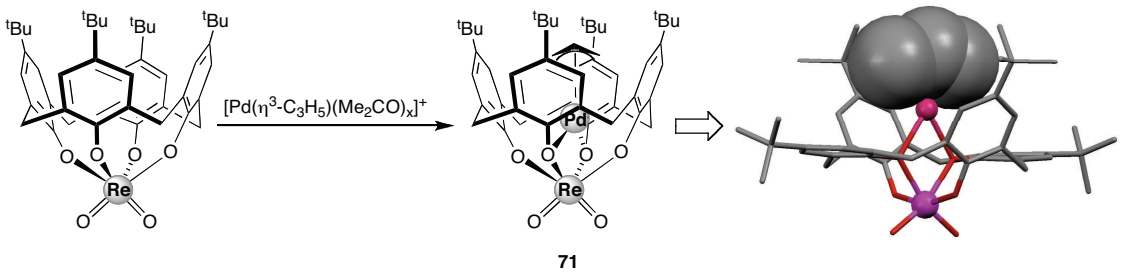

I.2.2. Calix[*n*]arènes porteurs de ligands soufrés

Loeb et coll. ont décrit les premiers complexes comportant un centre métallique positionné en aplomb de la partie évasée d'un calix[4]arène et fixant un ligand qui pointe vers l'intérieur de la cavité. Deux types de calixarènes distalement cappés par des ponts soufrés de longueur différente ont été utilisés à cet effet, **72** et **73**. Ces derniers ont servi à la préparation des complexes palladiés tridentés **74**-**78**, dans lesquels le quatrième coordinat, X, occupe l'embouchure de la cavité.[34] Le positionnement *intra*-cavité de X a été déduit des spectres RMN en solution. Le ligand **73**, qui a une anse plus longue que celle de **72**, est adapté à la reconnaissance de la 4-phénylpyridine en présence de 2-phénylpyridine et 3-phénylpyridine. Les auteurs de ce travail ont proposé que la coordination de 4-phénylpyridine entraînait des interactions de type π–π stacking entre ce ligand et les espaceurs aromatiques du ligand.

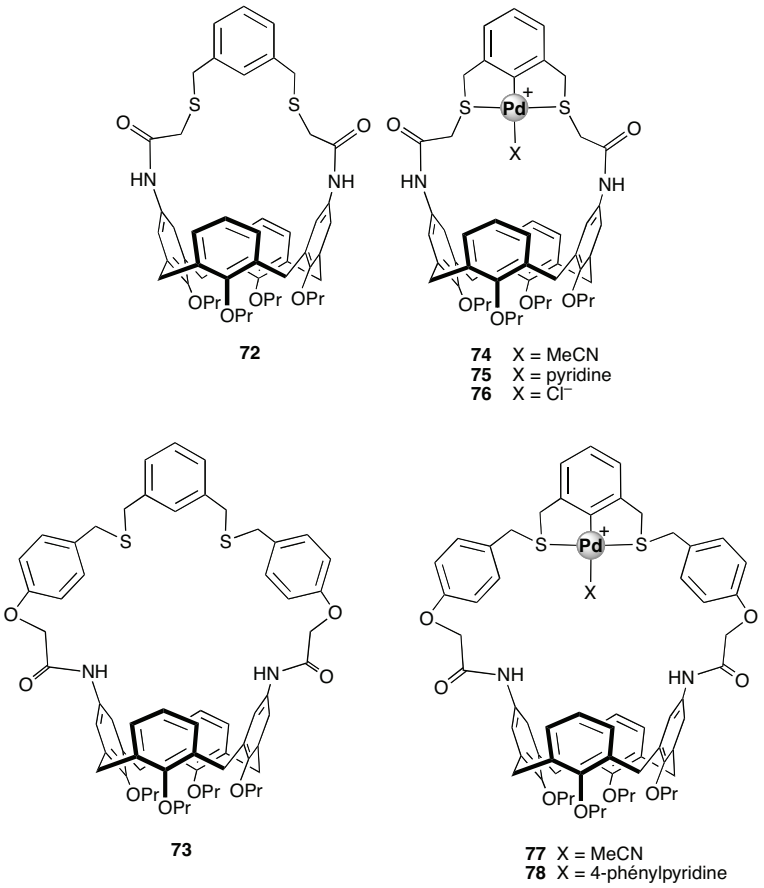

I.2.3. Calix[*n*]arènes porteurs de ligands azotés

La majorité des études concernant des calixarènes substitués par des ligands azotés ont été employés pour simuler l'activité biologique d'enzymes. Ces études ont, logiquement, été menées avec des métaux d'intérêt biologique associés à des calixarènes porteurs de bras azotés susceptibles d'orienter le centre métallique vers l'intérieur de la partie cavitale. Elles ont permis d'appréhender le mode d'action d'un centre métallique dans un environnement de type enzyme, et notamment d'examiner si la cavité peut, par exemple en modifiant la stéréochimie du métal, favoriser des processus d'échange de ligand.

La présence d'ions cuivre confinés dans des récepteurs constitue un élément clé dans de nombreux processus biologiques. De tels systèmes interviennent, par exemple, dans des enzymes biologiques telles que la dopamine β-hydroxylase, la peptidylglycine, l'amidante monooxygénase, les amine oxydases à cuivre, la nitrate réductase, ou encore dans les cytochromes P-450_{cam} et P-450_{BM3}. Le groupe de Reinaud a synthétisé un grand nombre de

calix[6]arènes sur lesquels ont été greffés des ligands azotés capables de chélater, voire prendre en griffe, des ions métalliques (**79**-**91**).[35]

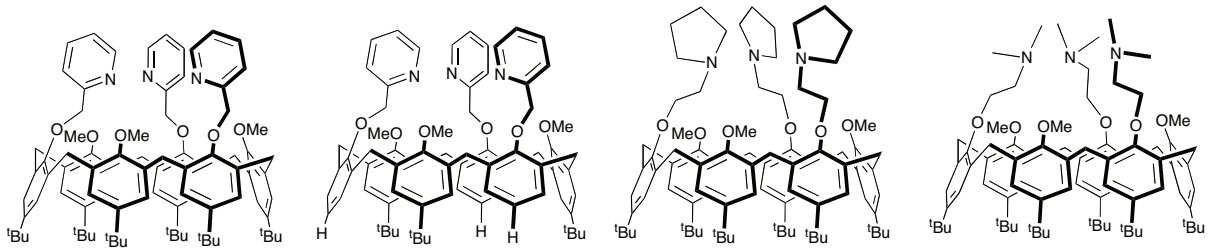

79 **80** **81** **82**

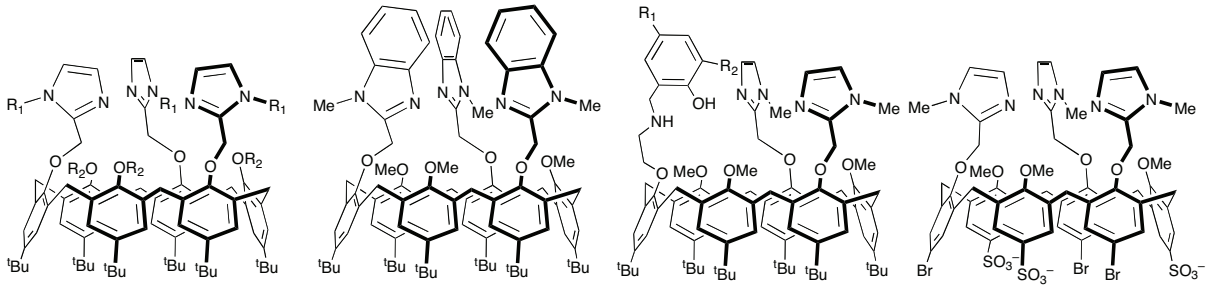

89 **90** **91**

83 R_1 = Me, R_2 = Me
84 R_1 = Et, R_2 = Me
85 R_1 = Me, R_2 = Et
86 R_1 = Et, R_2 = Et
87 R_1 = Me, R_2 = $CH_2{}^iPr$
88 R_1 = Bz, R_2 = Me

Le premier coordinat de ce type, **79**, a été décrit en 1998; il forme un complexe griffe N_3 (**92**) avec un ion Cu(I) dont le quatrième coordinat, du propionitrile, vient se loger entièrement à l'intérieur de la cavité.[36] La substitution de l'acétonitrile par du chlorure est aisée et conduit alors au même type de structure (**93**). Une étude cristallographique révèle qu'à l'état solide la molécule **93** présente une hélicité, qui peut également être mise en évidence par RMN en solution à basse température.[37] La déterbutylation partielle de **79** donne **80**. Cette dernière cavité est plus grande et, dans les complexes de cuivre correspondants, la substitution de l'acétonitrile par d'autres nitriles se fait plus rapidement.[38] La caractéristique principale de ces complexes est d'assurer un contrôle simultané de la première et seconde sphère de coordination. Le ligand **83** est non seulement capable de complexer du cuivre en orientant un ligand à l'intérieur de la cavité calixarénique, mais également de coordiner une molécule additionelle *exo*-positionnée (comme de l'eau dans le complexe **94**).[39] Autrement dit, il est possible, en fonction des solvants présents, de modifier la géométrie de coordination du cuivre (passage de tétraédrique à bipyramide trigonale).[40] Lorsque le quatrième ligand est un anion hydroxyle, les complexes formés existent en équilibre entre une forme monomère (OH à l'extérieur) et une forme dimère.[41,42] Un

complexe entonnoir de cuivre ayant le métal lié à une groupement carbonyle *endo*-orienté a également été obtenu.[43]

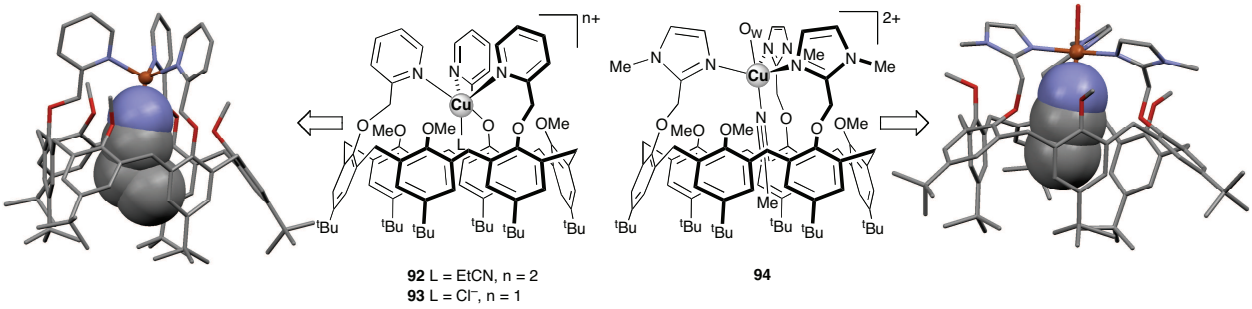

92 L = EtCN, n = 2
93 L = Cl⁻, n = 1

94

Le coordinat N_3O **90** a permis d'élaborer un modèle de galactose oxydase. Dans celui-ci (non dessiné), les trois atomes d'azote occupent le plan équatorial, l'atome d'oxygène venant en position apicale. Le seul site de coordination libre est alors celui situé dans la cavité, ce qui a été confirmé par une analyse de diffraction des rayons X.[44] Quant au ligand tris-imidazole sulfoné **91**, celui-ci s'est avéré capable de chélater du cuivre en formant un complexe soluble dans l'eau, propriété très recherchée lorsqu'on veut mimer des enzymes.[45]

Afin d'assurer le meilleur contrôle possible de la première sphère de coordination, des cavités à chapeau tétraazoté ont été développées, tels que par exemple **95** et **96**. Ces derniers permettent de crypter des ions métalliques de stéréochimie bipyramide trigonale, en tournant le 5ème site de coordination vers la cavité. Le coordinat rigide **95** conduit à des complexes de cuivre(II) capables de piéger des ligands neutres (**97-103**) ainsi que des petits anions (**104-108**).[46] Les complexes de cuivre(II) neutres dérivés de **95** ont des potentiels redox Cu(II)/Cu(I) fortement modifiés par rapport à des complexes calixaréniques dont le centre métallique n'est pas crypté.[47] Par ailleurs, avec ces complexes "cryptés", des phénomènes d'oxydation *intra*-cavité, métallo-assistée, peuvent se produire au niveau du squelette calixarénique.[48] Signalons, enfin, que le coordinat **96**, bien que relativement flexible, donne lieu à des comportements *intra*-cavité similaires à ceux observés avec **95** (exemple, formation du complexe *endo* **109**).[49-51]

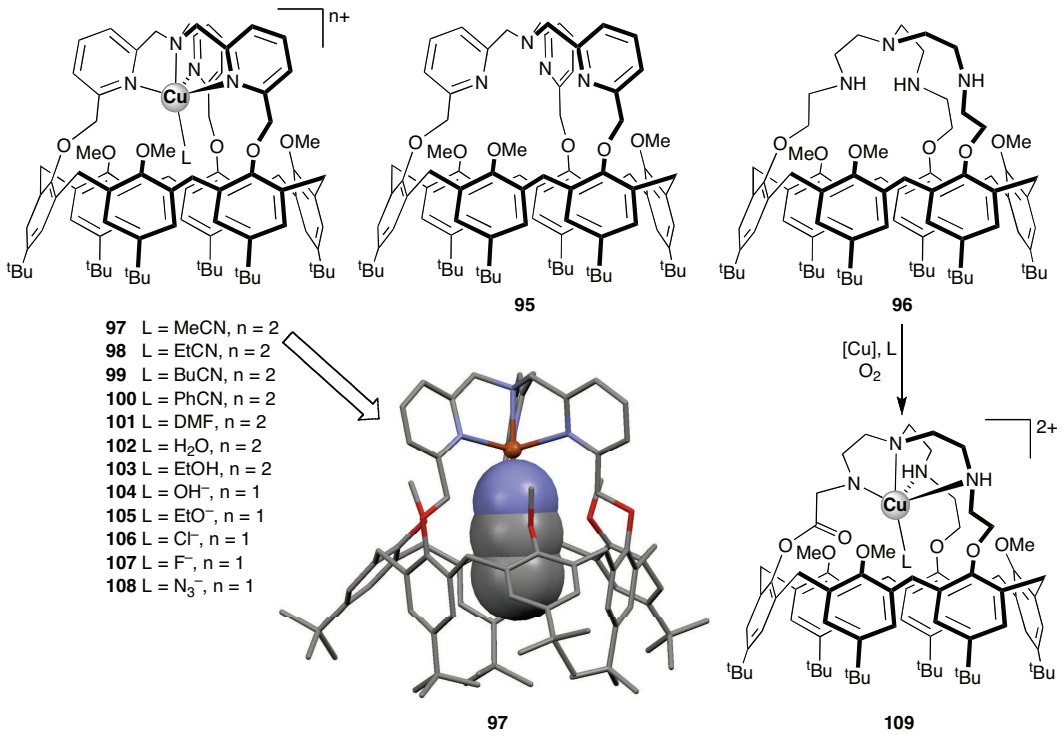

Les calix[6]arènes substitués par des ligands azotés ont fait l'objet de très nombreuses études consacrées à la modélisation de protéines de zinc. Parmi ceux-ci figurent notamment les ligands **83**[52,53] et **86**.[54,55] Ces ligands se sont avérés de très bons agents N_3-chélatants vis-à-vis des ions Zn(II), la complexation laissant à chaque fois un site vacant *intra*-cavital disponible pour la coordination de divers ligands neutres, tels que des amines (comme par ex. dans **110**), qui sont, par ailleurs, facilement échangeables. Des liaisons hydrogène entre ces derniers et des atomes d'oxygène du réceptacle calixarénique, mais également des intéractions CH-π entre l'invité et les parois aromatiques contribuent à la stabilisation des complexes formés.[56] Comme mentionné plus haut pour des complexes du cuivre, les complexes de zinc formés avec ces ligands existent en solution sous forme de paires d'énantiomères en raison de leur structure hélicoïdale. Un aspect remarquable concerne leur capacité à encapsuler de l'eau (liée au zinc), à l'instar de ce qui est connu pour plusieurs enzymes de type zinc-tris(histidine), notamment l'anhydrase carbonique, des métalloprotéases de la matrice ainsi que des métalloprotéinases de venin de serpent.[57,58] Dans le complexe **111**, deux molécules d'eau sont présentes dans la cavité, l'une étant coordinée au métal, l'autre à la première par liaison hydrogène. Lorsque trois des six groupes ^{t}Bu sont remplacés par des groupes amino de petite taille, ce qui conduit à **112**, une seule molécule d'eau reste piégée. Cette dernière peut alors être substituée, dans l'eau, par des coordinats relativement encombrés, tels que la diméthyldopamine ou la benzylamine.[59] Le ligand **113** qui a trois substituants amino au

niveau du bord large est un récepteur particulièrement intéressant. En effet, ses groupes amino, pH-dépendants, sont susceptibles de former des liaisons hydrogène avec des molécules piégées,[60] influencer des transformations se déroulant dans la cavité,[61] ou encore servir de centres coordinateurs pour un deuxième ion Zn(II). Un exemple illustrant ce dernier cas est le complexe **114**, qui comporte un coordinat $(H_3O_2)^-$ fixé aux deux atomes de zinc.[62]

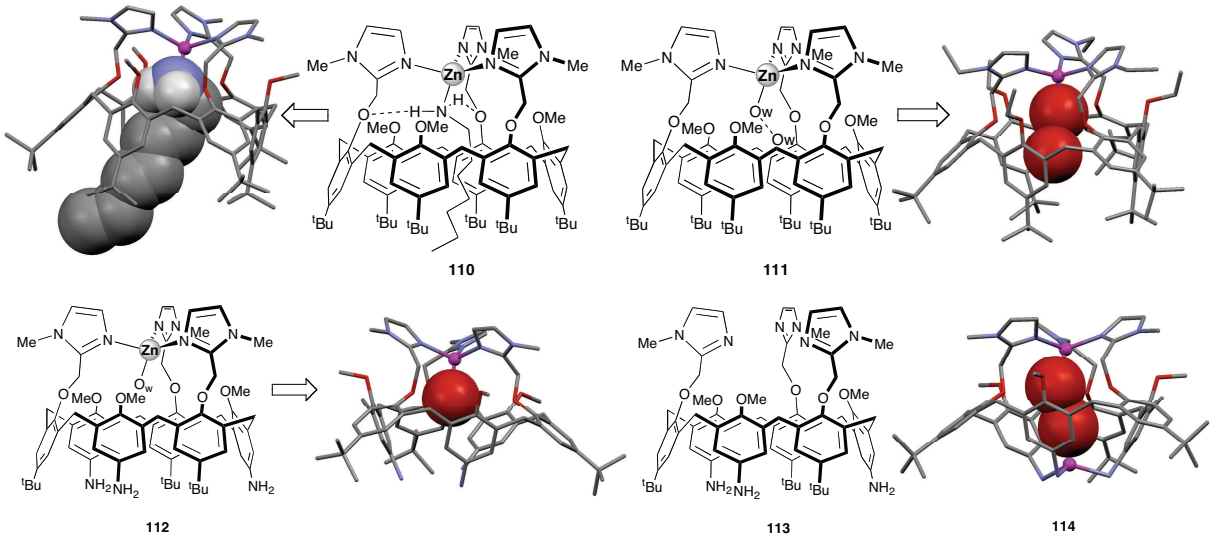

A signaler qu'un analogue de **113** ayant des substituants azotures N_3 à la place des groupes NH_2 a été utilisé comme précurseur pour la préparation de calix[6]arènes tris-fonctionalisés par des triazole-amines au niveau du bord large.[63] La méthodologie mise en œuvre repose sur le piégeage dans la cavité du réactif de couplage, le 5-amino-pentyne (**115-117**).

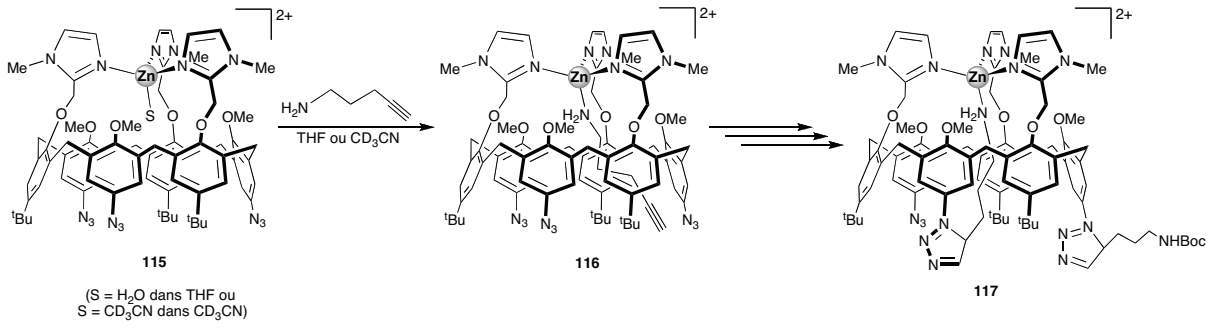

Le calix[6]arène **118**, qui comporte trois imidazoles greffés sur son petit bord et trois groupes triazole sur le bord large est, lui aussi, parfaitement adapté à la complexation de deux centres métalliques. Il a été employé pour la synthèse d'une série de complexes mixtes Zn/Cu (**119-125**) ayant fait l'objet d'études électrochimiques poussées.[64,65]

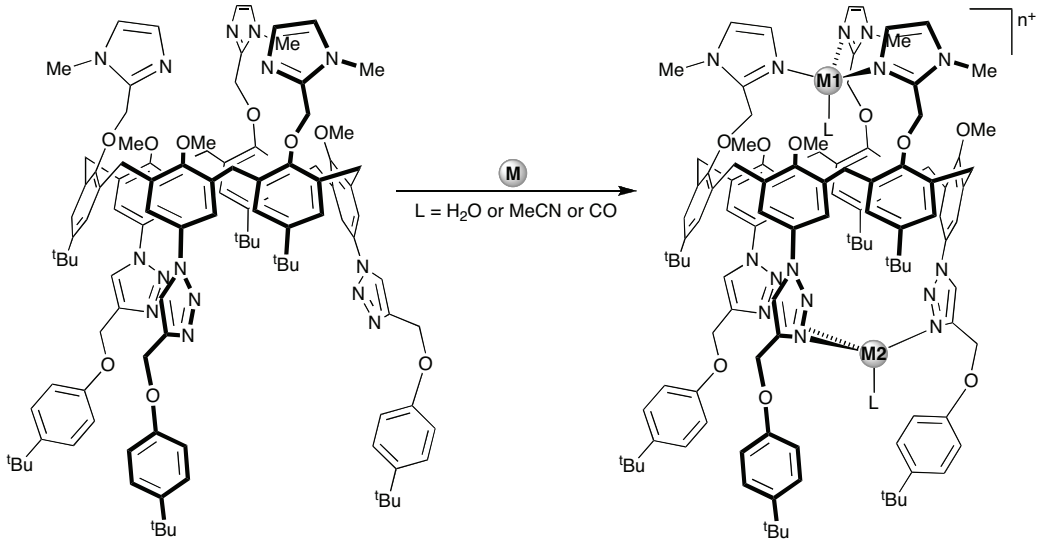

118

119 M1 = Zn(II), n = 2
120 M1 = Cu(I), n = 1
121 M1 = Cu(II), n = 2
122 M1 = M2 = Zn(II), n = 4
123 M1 = M2 = Cu(I), n = 2
124 M1 = Cu(II), M2 = Zn(II), n = 4
125 M1 = Zn(II), M2 = Cu(I), n = 3

Le calix[6]arène N_3O **90** a également été employé pour la synthèse de complexes de zinc ayant un site de coordination *intra*-cavital. Lorsque le 5ème ligand est neutre, ce dernier vient se loger dans la cavité, et la structure conique de l'édifice est conservée. Avec des ligands anioniques tels que OH^-, Cl^-, $PhCOO^-$ ou N_3^-, un ligand imidazole se décoordine, et l'anion se retrouve à l'extérieur de la cavité.[66] Contrairement au ligand **90** dont les bras azotés sont indépendants, le composé **96** peut uniquement former avec des ions Zn(II) des complexes à métal encapsulé. Aussi, avec celui-ci, il a été possible de former un grand nombre de complexes de zinc neutres ou cationiques de stéréochimie bipyramide trigonale.[67,68] Le tris-imidazole-calix[6]arène **126**, substitué au niveau du bord large par une fonction Zn-porphyrine, devient après complexation de zinc un récepteur supramoléculaire ditopique utilisable pour la reconnaissance de molécules bifonctionnellles, telles que par exemple la dodécyldiamine. Avec cette dernière, le complexe **127**, qui comprend une diamine piégée dans la cavité, est formé.[69] Le tris-imidazole **83** a également été utilisé pour la préparation de complexes de cobalt et de nickel. Dans ceux-ci, qu'ils soient de stéréochimie tétraédrique (cobalt) ou de stéréochimie bipyramide trigonale (cobalt, nickel), un solvant organique (typiquement de l'eau, un nitrile, un alcool ou du diméthylformamide) se trouve systématiquement piégé dans la cavité.[70]

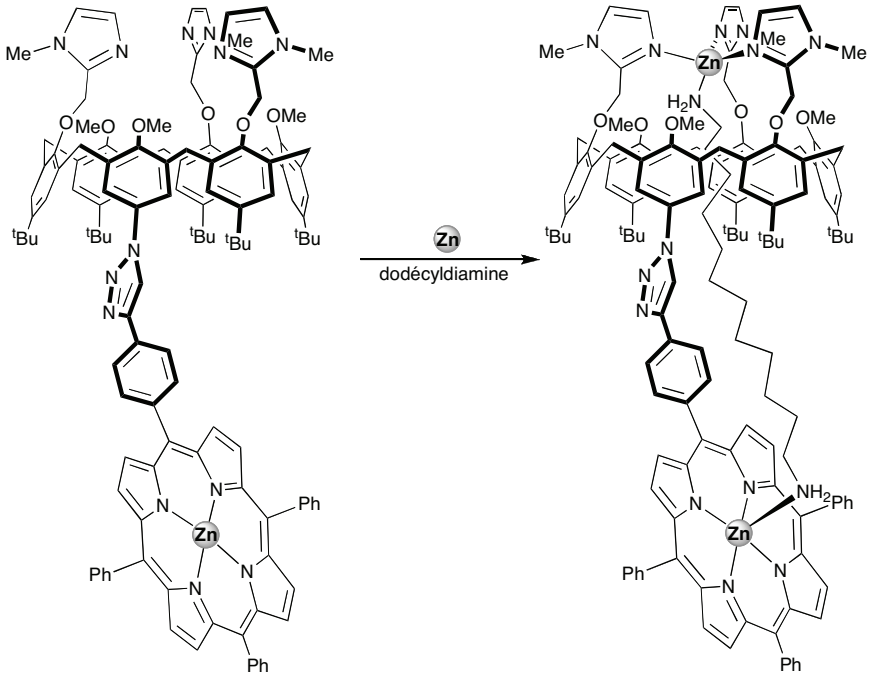

126 127

I.2.4. Calix[*n*]arènes porteurs de ligands phosphorés

Notre laboratoire a récemment décrit plusieurs familles de composés phosphorés construits sur la plateforme calix[4]arène. Parmi les dérivés obtenus qui possèdent des propriétés chélatantes figure le ligand **128**, un calixarène substitué au niveau du bord supérieur (c'est-à-dire sur la partie évasée) par des groupes diphénylphosphino greffés sur deux positions distales. Ce coordinat peut parfois jouer le rôle de seconde sphère de coordination. Ainsi, dans le complexe hydruro de platine **129**, le ligand hydrure est plongé dans la cavité et se trouve ainsi protégé par deux noyaux aromatiques du calixarène. La proximité des cycles phénoliques provoque une apparition du signal hydrure à un déplacement chimique à champ plus fort ($\Delta\delta$ = 1.3 ppm) que celui observé pour [$PtHCl(PPh_3)_2$]. Une situation similaire est rencontrée dans le composé méthyl-palladium **130**, dans lequel la liaison Pd–Me est tournée vers la cavité, comme l'a révélé une expérience de RMN 2D NOESY.[71]

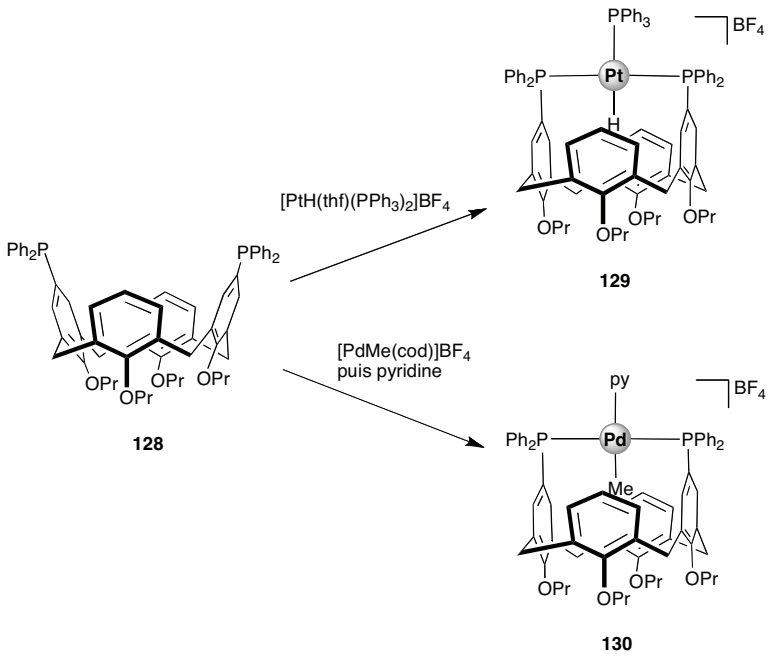

Un autre complexe calixarénique dans lequel la cavité macrocyclique se comporte en réceptacle vis-à-vis d'une entité métal-ligand est le complexe carbonyle *trans*,*trans*,*trans*-**132**, obtenu par isomérisation à la lumière de **131**. Une analyse par diffraction des rayons X révèle qu'à l'état solide un des deux ligands CO est pris en sandwich entre les deux noyaux aromatiques porteurs des atomes de phosphore. La faible distance entre la tige CO et chacun de ces noyaux (2.75 Å) suggère une interaction liante avec ces cycles.[71]

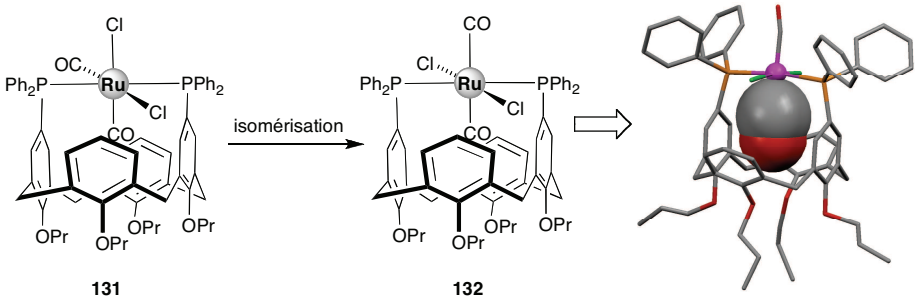

Dans le complexe hydruro **134**, obtenu à partir de la diphosphine **133**, l'hydrure est orienté vers le cœur de la cavité par suite d'interactions avec deux atomes d'oxygène du bord inférieur.[72] En substituant l'atome de chlorure de **134** par des ligands azotés, ce qui conduit à des espèces cationiques, l'orientation de la liaison Pt–H reste inchangée.[73]

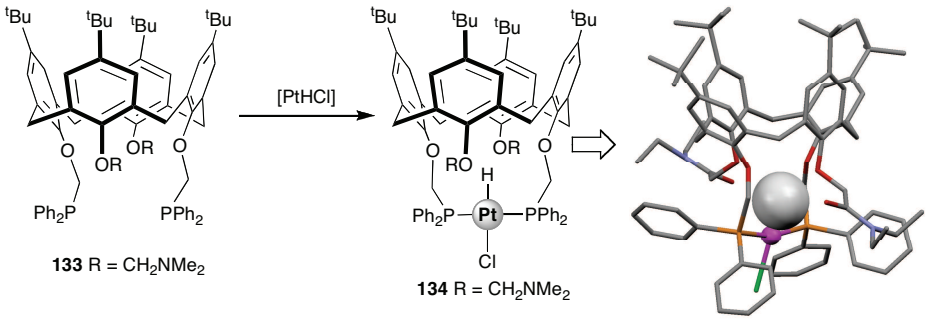

133 R = CH_2NMe_2 **134** R = CH_2NMe_2

Un autre cas intéressant est celui de calix[4]arènes substitués au niveau du bord supérieur par un unique groupe phosphino (appelé dans la suite "calix-monophosphine"). Comme on peut l'anticiper, ces monophosphines forment avec l'entité "$RuCl_2(\eta^6$-*p*-cymène)" des complexes monoligandés par création d'une liaison M–P classique (**135**-**139**).[74,75] Des investigations poussées (RMN, RX) ont montré que, dans ces complexes, le fragment *p*-cymène se plaçait spontanément dans la cavité en raison d'intéractions π–π entre le cycle arène lié au ruthénium et deux cycles phénoliques du macrocycle. La cavité joue donc, là encore, le rôle de seconde sphère de coordination. Ces coordinats ont été qualifiés de chélateurs supramoléculaires.

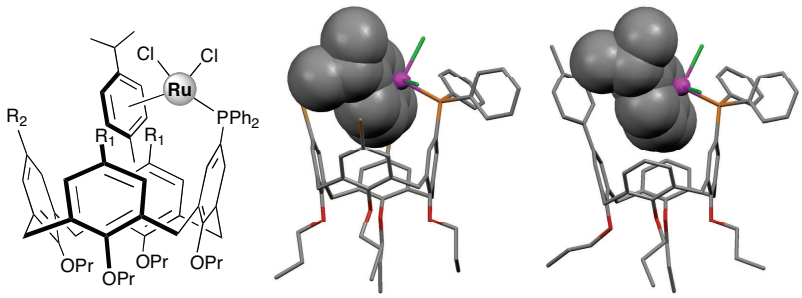

135 $R_1 = R_2$ = Br
136 $R_1 = R_2$ = *p*-tolyl
137 $R_1 = R_2$ = H
138 R_1 = H, R_2 = Br
139 R_1 = H, R_2 = *p*-tolyl

135 **139**

Cette propriété de piégeage d'entités métal-arène a pu être mise à profit dans des réactions pallado-catalysées de couplage croisé impliquant des halogénures d'aryle (type Suzuki-Miyaura[76] et Kumada-Tamao-Corriu[77]). Pour certaines réactions étudiées, la réaction de couplage se produit 40 fois (!) plus rapidement qu'en présence de triphénylphosphine. Les fréquences de rotation remarquables observées avec ces cavitand-phosphines peuvent s'expliquer par leur aptitude à stabiliser des intermédiaires *monoligandés* de palladium zéro [$Pd^0L(ArX)$], dans lesquels l'entité Pd-ArX est piégée dans la cavité. Le

piégeage provoque une augmentation artificielle de l'encombrement du ligand, ce qui en soi favorise la formation d'une espèce monophosphine plutôt que diphosphine.[76,77] Nous rappelons ici au lecteur que des travaux récents de Hartwig ont clairement établi qu'en catalyse de Suzuki, l'étape d'addition oxydante du cycle est réalisée plus facilement à partir d'intermédiaires [$Pd^0L(ArX)$] que de complexes [$Pd^0L_2(ArX)$].[78] Incontestablement, les calix-monophosphines sont donc des ligands donnant lieu à une catalyse supramoléculaire.

Le phénomène de piégeage d'entités "$RuCl_2(\eta^6$-*p*-cymène)" observé avec les calix-monophosphines est transférable à des calixarènes doubles, tels que **140** et **141**. Le fait que dans les complexes **142** et **143**, obtenus à partir de ces ligands, aucun fragment Ru(η^6-*p*-cymène) ne soit orienté vers l'extérieur de la cavité adjacente signifie, qu'une fois que le processus de complexation est amorcé – c'est-à-dire que les deux liaisons Ru–P sont formées –, la molécule se compacte de manière à occuper un volume minimal. Pour l'instant, il n'a pas été possible d'établir la réversibilité de ce curieux phénomène de contraction. Par ailleurs, la diphosphine **141**, malgré sa grande longueur, possède des propriétés de chélateur. En effet, en présence de [$Pd(\eta^3$-$C_3H_5)(thf)_2]BF_4$, espèce cationique ayant deux sites de coordination *cis*-positionnnés, elle conduit au complexe **144**. Dans cette réaction, la complexation non seulement engendre la formation d'une capsule constituée de deux hémisphéres calixarène, elle provoque aussi l'encapsulation du centre métallique en raison du caractère *cis*-orientant du fragment Pd-allyle.[79]

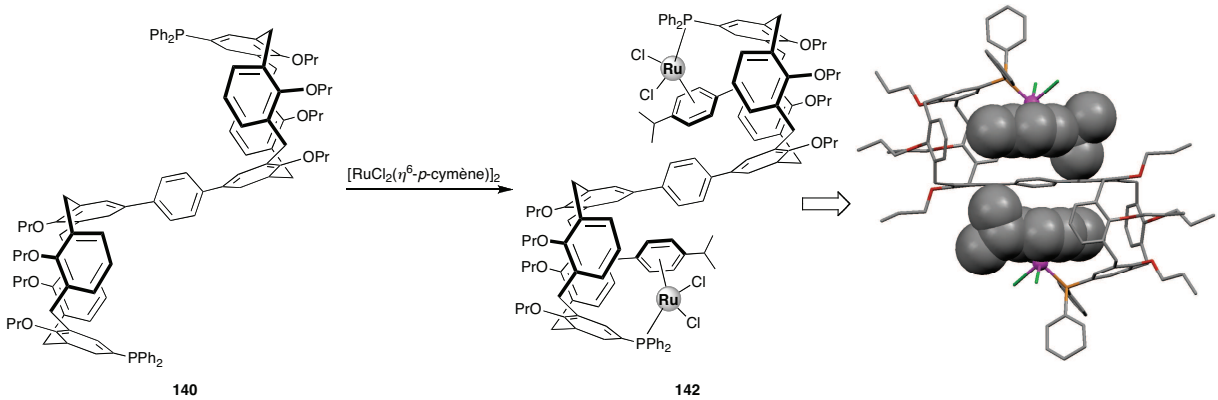

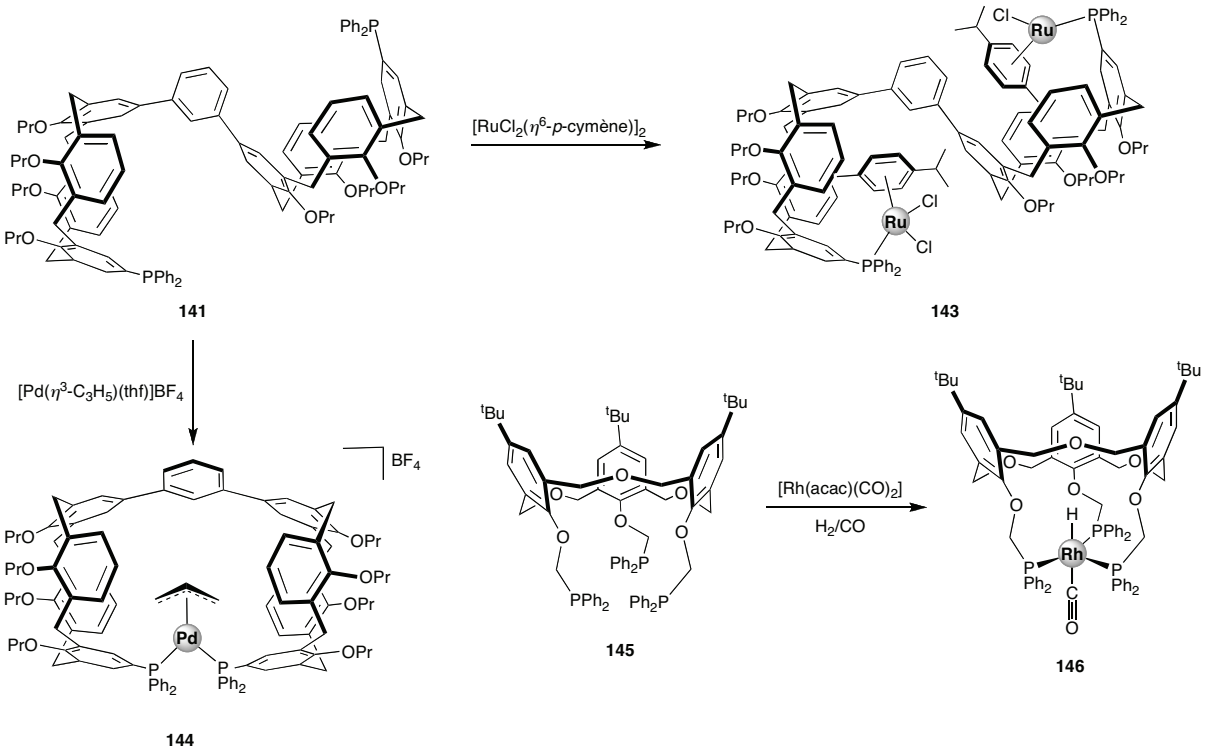

La matrice homooxacalix[3]arène a été utilisée par quelques auteurs pour la confection de podands de symétrie C_{3v}.[80] Rares sont les ligands de cette famille ayant été employés pour la complexation de métaux de transition. L'un d'entre eux, la triphosphine **145**, a permis de préparer le complexe hydruro carbonyle de rhodium **146** dont la liaison Rh–H est orientée vers le cœur calixarénique.[81] Les propriétés hydroformylantes de ce complexes se sont avérées décevantes en raison de la difficulté à dissocier l'un des atomes de phosphore, condition nécessaire pour amorcer la réaction.[82]

Le groupe de Lattman a conçu le phosphoramidite **147** construit sur un calix[5]arène. Dans ce composé où l'atome de phosphore ponte des oxygènes phénoliques adjacents, le doublet du phosphore pointe vers l'axe du calixarène. Ce ligand a permis de synthétiser le complexe imido **148** ayant un atome de tungstène fixé à trois oxygène du calixarène. L'interaction entre l'atome de phosphore et le centre métallique est manifeste au niveau de la faible constante de couplage, $^1J_{PW}$ = 43 Hz. Cependant, à l'état solide, on mesure une distance phosphore-métal (3.15 Å) plus longue que celle habituellement observée pour une liaison P–W, traduisant donc une liaison faible. En traitant **148** avec de l'acide triflique, on forme **149** dans lequel le ligand N^{t}Bu est logé dans la cavité, et où la distance P···W est typiquement celle d'une vraie liaison phosphore–métal. Le passage de **148** à **149** s'accompagne de

modifications structurales importantes, tant au niveau de la sphère de coordination du métal que celui de la forme du calixarène.[83]

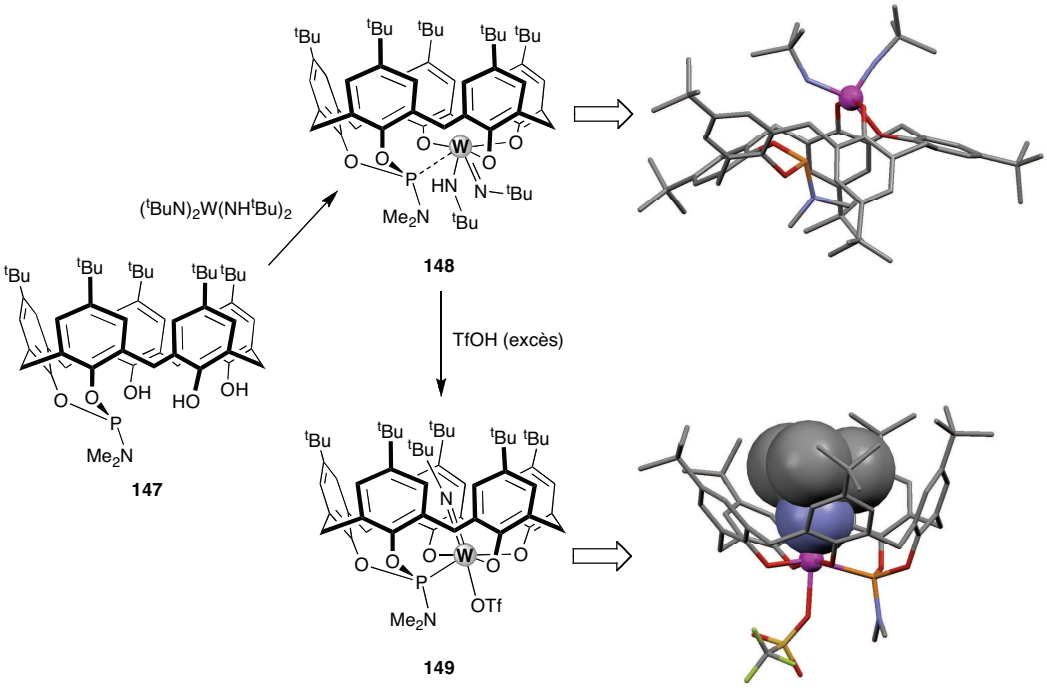

Le phospha-cryptand **150**, ayant un atome de phosphore "introverti", est un excellent complexant des ions cuivre(I) et cuivre(II). Les complexes correspondants possèdent chacun un site vacant *intra*-cavital. L'ion Cu(II) coordine mieux des donneurs σ faibles, tels que MeCN, alors que l'ion Cu(I) préfère des ligands à atome d'oxygène (atome dur), notamment EtOH ou DMF (complexe **151**). Il faut préciser qu'en l'absence de cavité, de tels complexes pentacoordinés ne seraient pas stables. Contrairement à **109**, les complexes de cuivre formés avec **150** ne réagissent pas avec du dioxygène, ce qui reflète la protection stérique efficace de la cavité.[84,85]

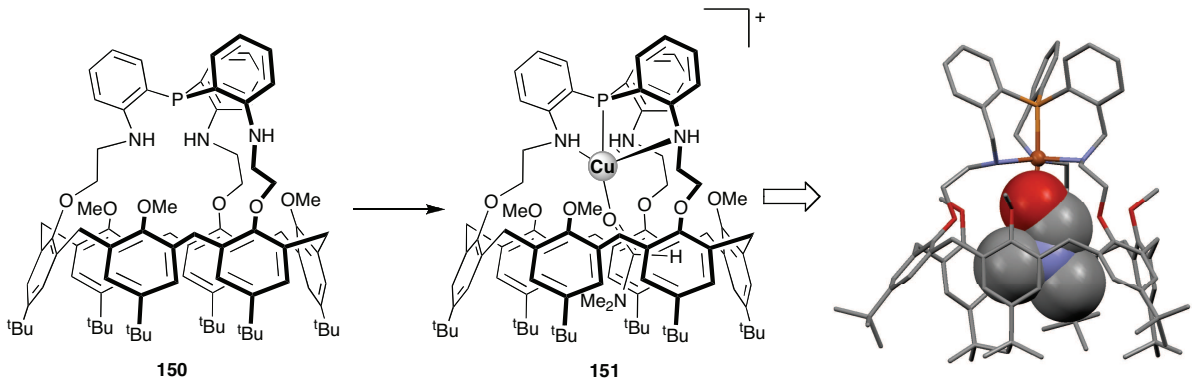

I.3. Ligands dérivés de résorcin[4]arènes

Les résorcinarènes sont des macrocycles qui du point de vue de leur structure sont très proches des calix[4]arènes. Ils sont obtenus par condensation acido-catalysée de résorcinol avec un aldéhyde.[86-89] Contrairement aux calix[4]arènes, leur structure peut être rigidifiée en réalisant un pontage entre unités résorcinoliques adjacents (en général par des ponts méthylènes,[90,91] ou des atomes de phosphore[92-96] ou encore par des entités hétérophénylène[90,97-98]),

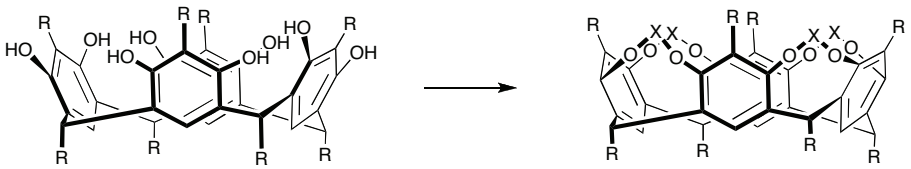

Resorcin[4]arènes Resorcin[4]arènes rigidifiés

I.3.1. Résorcin[4]arènes porteurs de ligands soufrés

Arnott et coll. ont décrit le résorcinarène **152** caractérisé par la présence de deux ligands –SR ancrés sur des positions distales du bord large. La réaction de **152** avec $PdCl_2$ produit le complexe dinucléaire **153** (rdt: 70%), dans lequel le dithioéther fonctionne comme un ligand pontant vis-à-vis de l'entité "ClPd(μ-Cl)$_2$PdCl". En solution, à –50°C, deux conformères sont présents dans un rapport 4:1, l'un d'entre eux étant de symétrie C_2.[99]

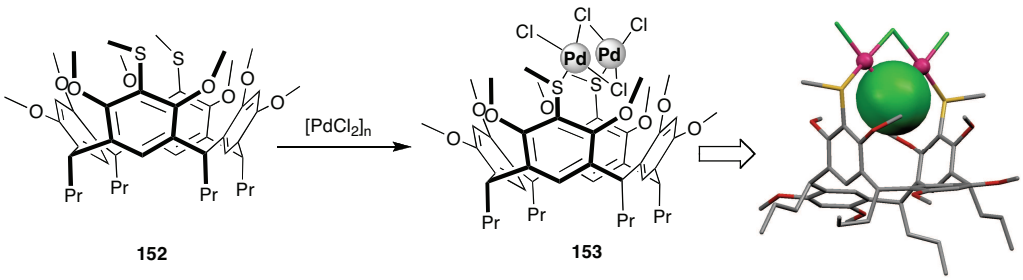

152 153

I.3.2. Résorcin[4]arènes porteurs de ligands azotés

Le résorcinarène **154** est basé sur une cavité rigide substituée par un ligand phénanthroline. Sa réaction avec $ZnCl_2$ en présence de quinuclidine (1-azabicyclo[2.2.2]octane) ou de dabco (dabco = 1,4-diazabicyclo[2.2.2]octane) fournit quantitativement le complexe chélate cationique **155** contenant l'amine fixée au zinc de manière *intra*-cavitale.[100]

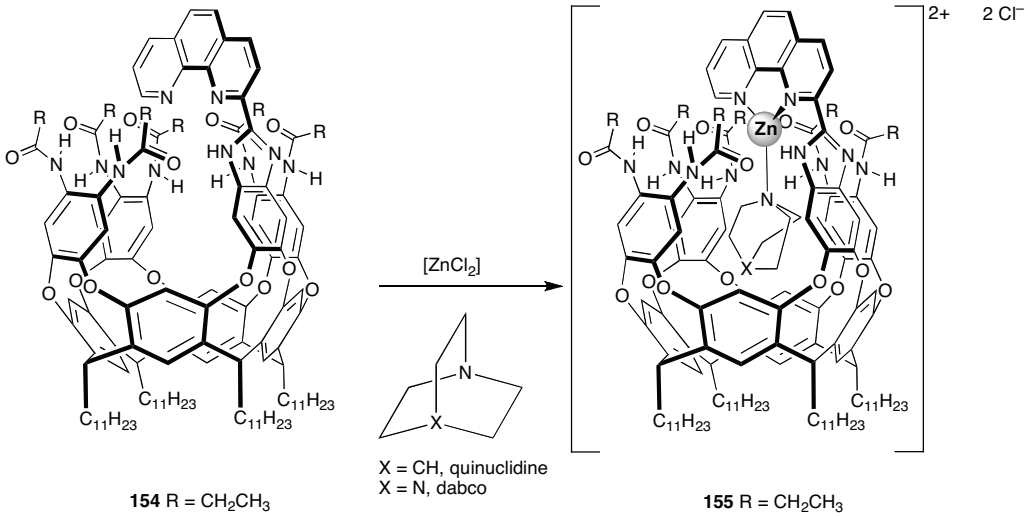

154 R = CH_2CH_3 **155** R = CH_2CH_3

Le cavitand résorcinarénique **156**, substitué par trois fonctions imidazole, a été décrit par Reinaud. Ce ligand tridentate forme avec les ions Zn(II) des complexes de stéréochimie bipytrigonale (**157**) où les trois imidazoles occupent le plan équatorial, l'un des deux sites apicaux pointant vers le centre de la cavité, l'autre vers l'extérieur. Le site *endo* est parfaitement adapté à la fixation d'un groupe acétato, mais pas à celle d'un fragment propionato, de taille légèrement plus grande.[101]

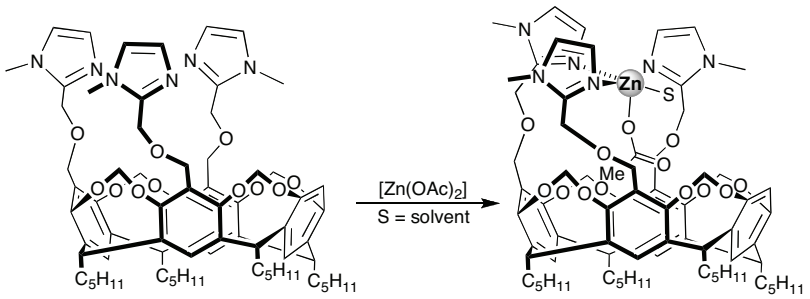

156 **157**

I.3.2. Résorcin[4]arènes porteurs de ligands phosphorés

Rebek et coll. ont préparé le chélateur phosphoramidite-oxazoline **158**, basé sur une cavité résorcinarénique, en vue d'une utilisation en alkylation allylique.[102] Au contact de palladium et d'un acétate allylique, ce ligand conduit à un complexe palladium-allyle, dont l'entité allyle est tourné vers la cavité. La coordination d'une entité allylique $(H_2C^1C^2HC^3HR')^-$ peut se faire de deux manières, selon que le carbone en *trans* du phosphore est le carbone nº 1 ou le carbone nº 3 de l'allyle (complexes **159a** et **159b**). Pour des raisons d'encombrement stérique, l'attaque d'un nucléophile se fait *sélectivement* sur le carbone nº 1, ce qui conduit à un produit linéaire. Par ailleurs, les auteurs ont montré que l'addition oxydante (stœchiométrique), conduisant au complexe allyle, se fait à une vitesse qui décroit dans l'ordre R' = ^{t}Bu (**S3**) > ^{i}Pr (**S2**) >> ^{i}Bu (**S1**). En comparant l'alkylation par du diméthyle malonate de l'acétate allylique **S2** avec celle de **S4** et **S5**, on s'aperçoit que les vitesses de réactions rélatives sont **S4** >> **S2**, **S2** > **S5** et **S4** >> **S5**. Ces sélectivités, qui reflètent les capacités de reconnaissance moléculaire de la cavité, illustrent le potentiel de ligands cavitaux en synthèse organique.

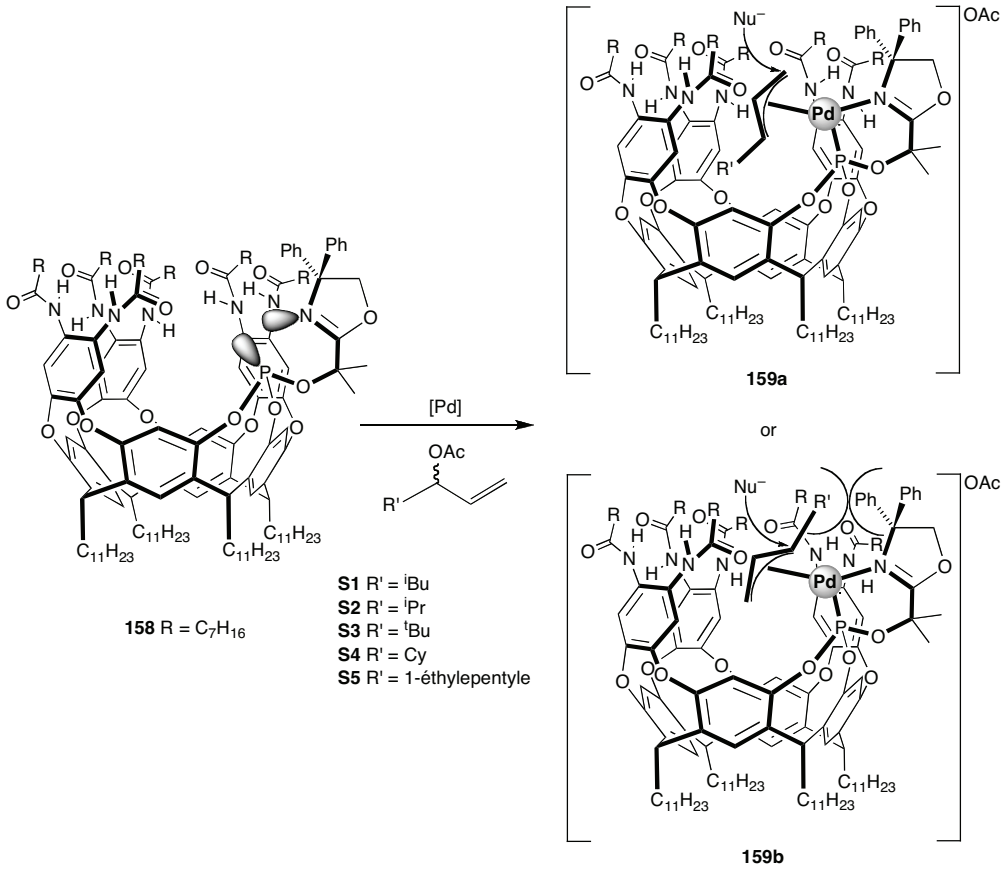

Puddephatt et coll. ont examiné les propriétés complexantes du tétraphosphinito cavitand **160** dans lequel les doublets des quatre atomes de phosphore sont orientés vers l'axe de la cavité (complexes **161**-**163**). Ce ligand fixe quatre entités AuX (X = Cl, Br, I). Le spectre RMN de **161** en solution révèle quatre atomes de phosphore équivalents. A l'état solide, on constate un repli de l'un des fragments P-Au-X vers le cœur du résorcinarène, les trois autres étant légèrement tournés vers l'extérieur du cavitand.[103] Un complexe analogue avec quatre unités "$PtCl_2(SMe)$" coordinées a également été décrit, mais sa structure à l'état solide n'a pas été déterminée.[104]

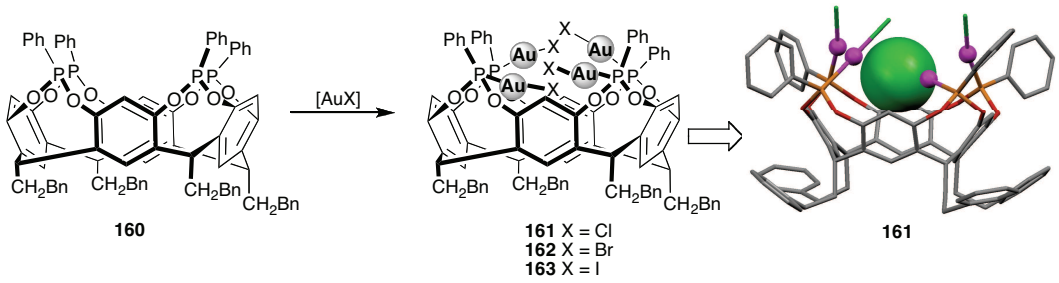

160 **161** X = Cl, **162** X = Br, **163** X = I **161**

Avec les halogénures de Cu(I) et Ag(I) on forme des complexes tétranucléaires dans lesquels les atomes métalliques sont pontés par les halogénures. L'analyse cristallographique du complexe de cuivre **164** révèle la présence, à l'état solide, d'une couronne $Cu_4(\mu^2\text{-}Cl)_4$ couvrant l'embouchure de la cavité, ainsi que d'un ion chlorure isolé formant un pont cappant trois des atomes de cuivre. Au vu des spectres de RMN montrant des atomes de phosphore équivalents, on peut imaginer qu'en solution, cet ion soit lié, probablement de manière dynamique, aux quatre atomes de cuivre. La substitution de tous les ions chlorure de **164** avec un excès de Bu_4NI s'est avérée difficile. Cette réaction conduit au complexe **165** contenant un fragment $Cu_4I_{3.3}Cl_{1.7}$ et où un ligand iodure *endo* ponte les quatre atomes de cuivre. Par contre, lorsqu'on traite **164** avec un équivalent de Bu_4NX (X = Br, I), on forme quantitativement les complexes **166** (X = Br) et **167** (X = Cl) dans lesquels seul l'halogénure piégé a été remplacé. Contrairement à ce qui est observé pour **164**, l'halogénure *endo* du complexe argenté **168** ponte les quatre atomes métalliques. De plus, la totalité des halogénures du complexe ont pu être substitués par du bromure (donnant **169**) ou de l'iodure (**170**). Lorsqu'on traite **168** avec un seul équivalent de bromure ou d'iodure, la substitution se fait sélectivement et quantitativement au niveau de l'halogénure *endo*, conduisant alors respectivement aux complexes **171** et **172**. Des conditions ont également été trouvées pour extraire l'halogénure *endo* de **168** (formation de **173**). Il a aussi pu être remplacé par l'ion S^{2-}

(avec formation de **174**) ainsi que CN^- (formation de **175**).[105,106] A signaler que les complexes **176-178**, porteurs de chaînes ^{i}Bu au niveau du bord inférieur, ont été synthétisés en vue d'une évaluation de leurs propriétés en optique non linéaire.[107,108]

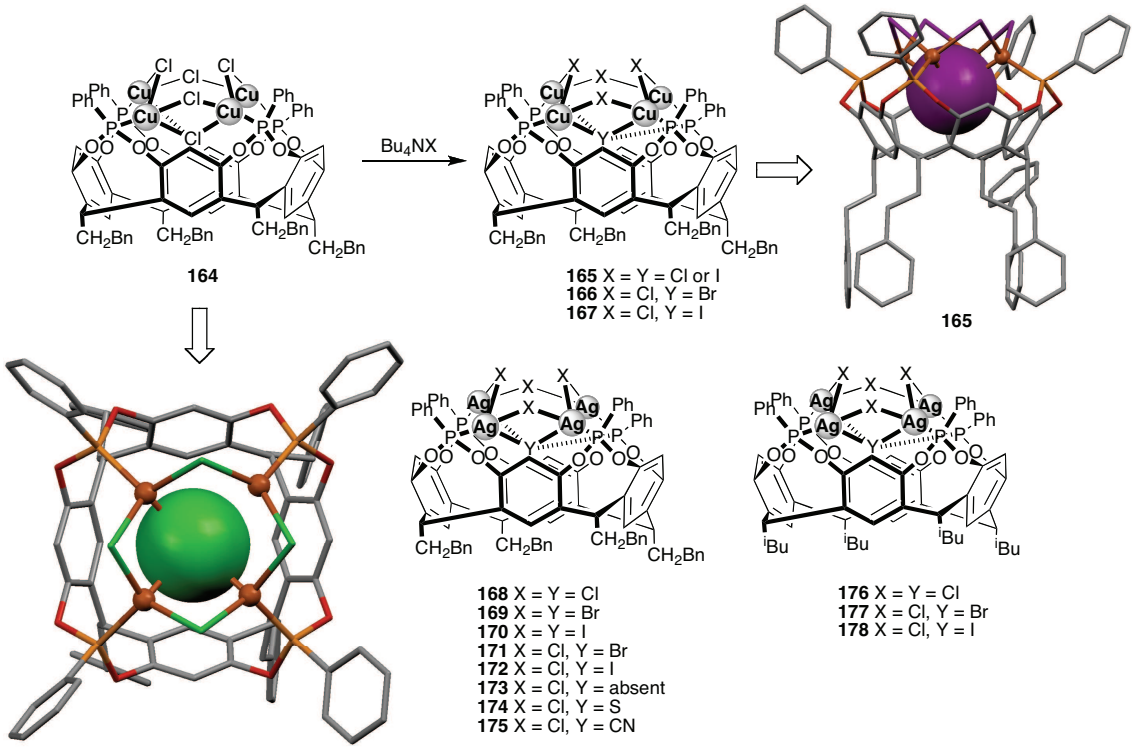

Une série de tétraamidophosphito- et tétraphosphito-résorcinarènes ayant une structure comparable aux phophonites précédents ont été étudiés par Nifantyev.[109,110] Ces ligands introvertis permettent de complexer soit quatre (**179-184**) ou deux (**185-193**) centres métalliques, soit un unique (**194-196**). En raison des contraintes stériques pouvant résulter de la complexation, la structure vue à l'état solide ne correspond pas toujours à celle déduite de l'examen des spectres RMN. Ainsi, alors que les spectres RMN du complexe de rhodium **182** reflètent une symétrie C_{4v} du complexe en solution, on constate qu'à l'état solide une des unités {Rh(acac)CO} présente une orientation opposée à celle des autres fragments de ce type. Les complexes mononucléaires mentionnés ci-dessus ont été employés pour la préparation des complexes hétérobimétalliques **197-200**.[111] Les tétraamidophosphito-résorcinarènes permettent d'héberger une couronne Ag_4Br_4, tout en encapsulant un anion bromure (**201-203**).[112]

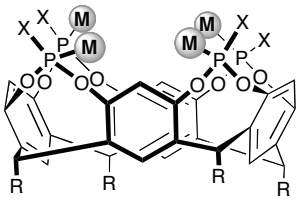

179 X = NEt_2, R = Me, M = [Rh(acac)CO]
180 X = NMe_2, R = Me, M = [Rh(acac)CO]
181 X = NEt_2, R = Pr, M = [Rh(acac)CO]
182 X = O^iPr, R = Me, M = [Rh(acac)CO]
183 X = O^iPr, R = Me, M = $[Cr(CO)_5]$
184 X = O^iPr, R = Me, M = $[Mo(CO)_5]$

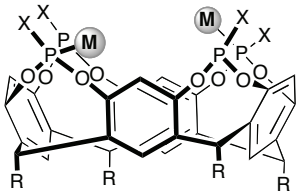

185 X = NMe_2, R = Me, M = $[Cr(CO)_5]$
186 X = NEt_2, R = Me, M = $[Cr(CO)_5]$
187 X = NEt_2, R = Pr, M = $[Cr(CO)_5]$
188 X = NMe_2, R = Me, M = $[Mo(CO)_5]$
189 X = NEt_2, R = Me, M = $[Mo(CO)_5]$
190 X = NEt_2, R = Pr, M = $[Mo(CO)_5]$
191 X = NEt_2, R = Me, M = $[W(CO)_5]$
192 X = NEt_2, R = Me, M = $[MnC_5H_5(CO)_2]$
193 X = NMe_2, R = Pr, M = $[MnC_5H_5(CO)_2]$

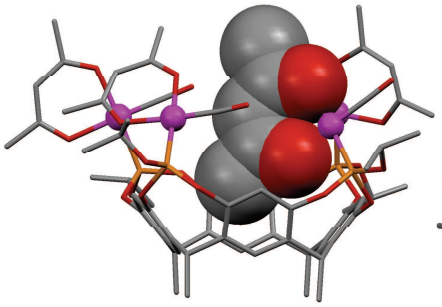

182

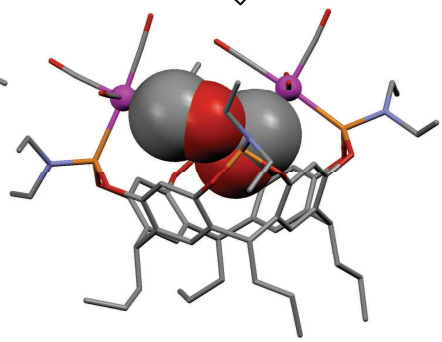

190

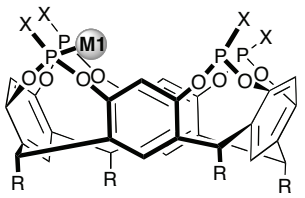

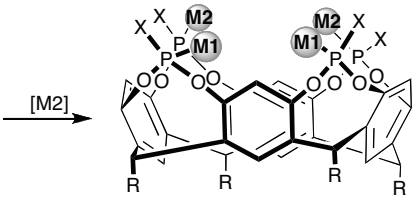

194 X = NEt_2, R = Me, M1 = $[Mo(CO)_5]$
195 X = NMe_2, R = Me, M1 = $[Mo(CO)_5]$
196 X = NEt_2, R = Pr, M1 = $[Mo(CO)_5]$

197 X = NEt_2, R = Me, M1 = $[Mo(CO)_5]$, M2 = [AgBr]
198 X = NEt_2, R = Pr, M1 = $[Mo(CO)_5]$, M2 = [AgBr]
199 X = NEt_2, R = Me, M1 = $[Mo(CO)_5]$, M2 = [Rh(acac)CO]
200 X = NEt_2, R = Pr, M1 = $[Mo(CO)_5]$, M2 = [Rh(acac)CO]

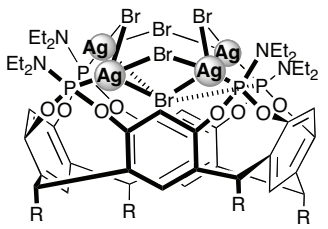

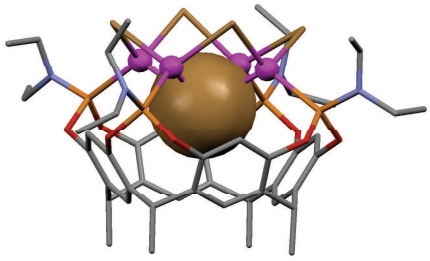

201 R = Me
202 R = Pr
203 R = Nonyl

201

L'effet de substituants ortho (H, Me, Br) dans les cycles résorcinoliques des tétraphosphoramidite-cavitands **204**-**209** a également été étudié. A nouveau, les centres métalliques complexés sont orientés vers l'axe de la cavité conique. [113,114]

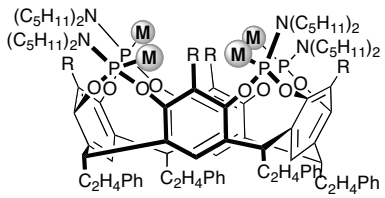

204 R = H, M = [AgBr]
205 R = Me, M = [AgBr]
206 R = Me, M = $[Mo(CO)_5]$

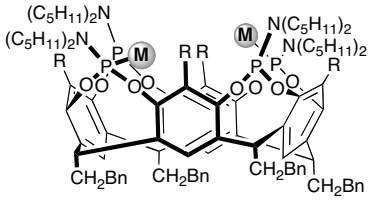

207 R = H, M = $[Mo(CO)_5]$

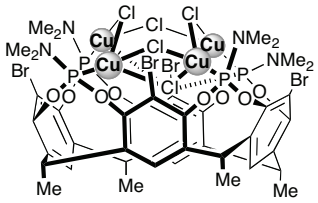

208

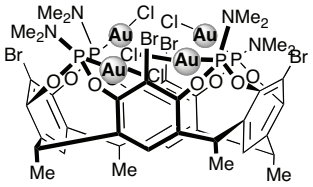

209

I.4. Cyclodextrines

Les cyclodextrines (CDs) sont des oligosaccharides cycliques constitués de monomères α-D-glucopyranose liés entre eux par des ponts 1,4-glycosidiques résultant en une structure conique.[115] Les CDs les plus couramment utilisées comportent six, sept et huit unités glucose nommées respectivement α-, β- et γ-CD.[116,117] De nombreux travaux ont porté sur la fonctionnalisation des différents groupements hyroxyles[118,119] ainsi que le greffage de groupement coordinants. Ces travaux ont largement contribué au dévelopement d'une chimie *intra*-cavité réalisée avec des cyclodextrines.[120]

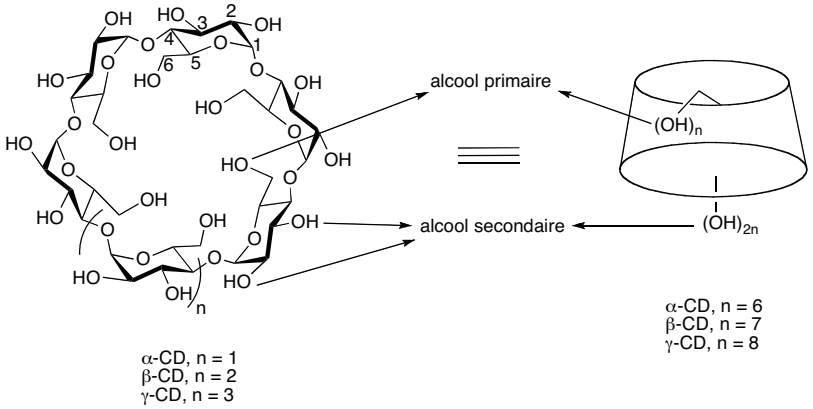

I.4.1. Cyclodextrines porteuses de ligands oxygénés

En faisant réagir de la β-cyclodextrine native avec de l'acétate de Mn(II), Dismukes a obtenu le complexe **210** avec 55% de rendement.[121] La complexation d'une unité $Mn_2(\mu^2\text{-}OH)_2$ a été déduite d'expériences spectrophotométriques et de titrations, et de mesures IR, RPE et voltammétrie cyclique. Le complexe de cuivre **211** a été obtenu par une synthèse similaire en partant d'α-CD (**211**). La coordination intracavitale du fragment $Cu_2(\mu^2\text{-}OH)_2$ a été étudiée par spectroscopie vibrationnelle et dichroïsme circulaire.[122]

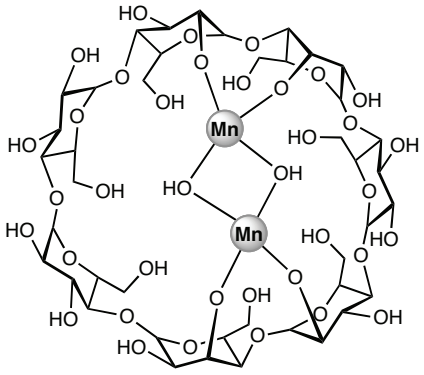

210

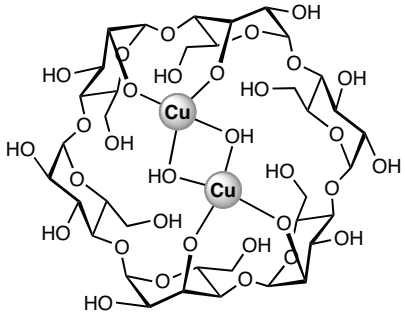

211

I.4.1. Cyclodextrines porteuses de ligands soufrés

La dithioéther-cyclodextrine **212** possède deux atomes de soufre dont l'un des doublets est orienté vers le cœur de la cavité cyclodextrine. En présence de Ag^+, **212** se comporte en agent chélatant en piégeant l'ion argent dans la cavité. Avec $PdCl_2$ et $PtCl_2$, la complexation implique, cette fois, les doublets *exo*-orientés, et des complexes dimère sont alors formés.[123,124] Le complexe d'argent **214** présente la faculté de piéger un ligand butanone dans la cavité, en solution comme à l'état solide.[123,124] Une étude par RMN a permis de mettre en évidence l'encapsulation-coordination de BF_4 dans **213** en solution. Lors de la cristallisation de ce complexe, l'anion est expulsé et remplacé par une molécule d'eau (**215**).[125]

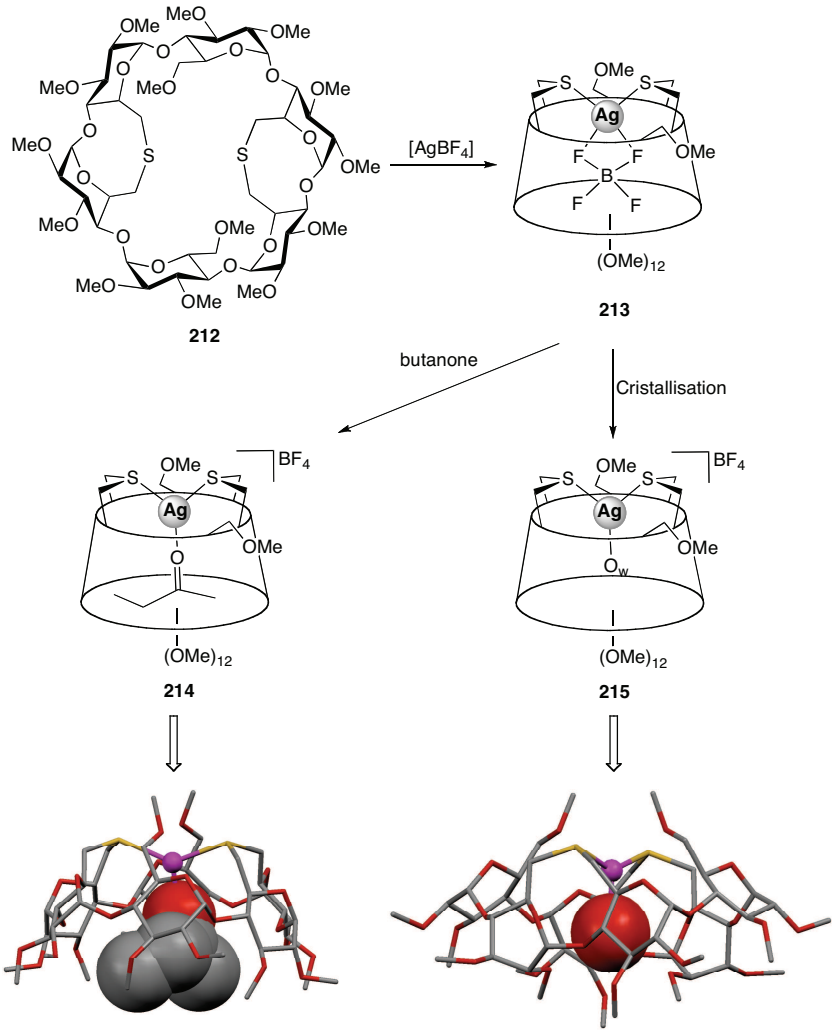

I.4.1. Cyclodextrines porteuses de ligands azotés

Breslow et coll. ont synthétisé la 2,2'-bipyridine **216** symétriquement substituée par deux unités β-CD. En présence d'ions La(III), **216** catalyse efficacement l'hydrolyse d'ester-phosphates.[126] Le même coordinat catalyse l'hydrolyse d'esters simples en présence de Zn(II) et de (*E*)-2-pyridinecarbaldehyde oxime (PAO) dans le rapport 1:1. En l'absence de PAO, **216** est plus actif, mais seulement si on est en présence de Cu(II).[127] Pour expliquer l'efficacité du système, les auteurs ont proposé un modèle dans lequel les deux cavités cyclodextrine piègent le substrat, ce qui a pour effet de positionner favorablement la fonction ester à proximité du centre métallique.

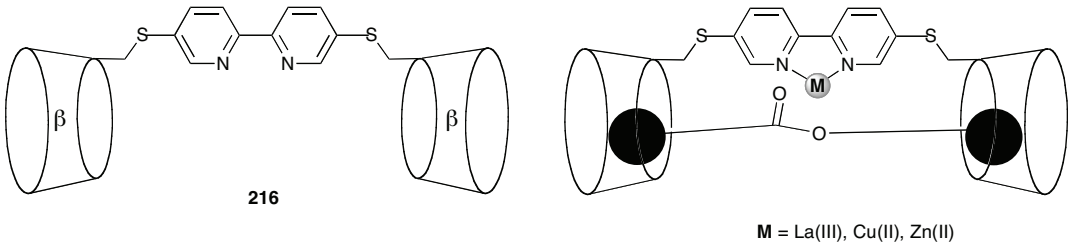

216

M = La(III), Cu(II), Zn(II)

Des cyclodextrines substituées par des ligands azotés ont largement été utilisées en reconnaissance moléculaire. Ainsi, en associant la β-CD **217** à du cuivre(II), on parvient à réaliser la résolution énantiomérique du D,L-tryptophane. Des mesures potentiométriques et de dichroïsme circulaire indiquent que le D-tryptophane (**218**) forme avec la β-CD un complexe d'inclusion, ce qui n'est pas le cas de son énantiomère (**218**). Avec d'autres amino-acides, notamment la D,L-alanine, aucune séparation n'est observée.[128] Le senseur fluorescent **220**, qui présente une affinité plus importante pour le Cu(II) que pour le Fe(II), Ni(II), Co(II) et Zn(II), a également été synthétisé. En présence de Cu(II), il présente une réponse linéaire pour des rapports molaires allant jusqu'à 1:1. Le coordinat **220** et le complexe de Cu(II) **221** donnent chacun lieu à un phénomène d'auto-inclusion en milieu aqueux.[129] En remplaçant la chaîne amino de **220** par un équivalent chiral, on dispose d'un senseur fluorescent optiquement actif pouvant servir à la détermination d'excès énantiomériques.[130]

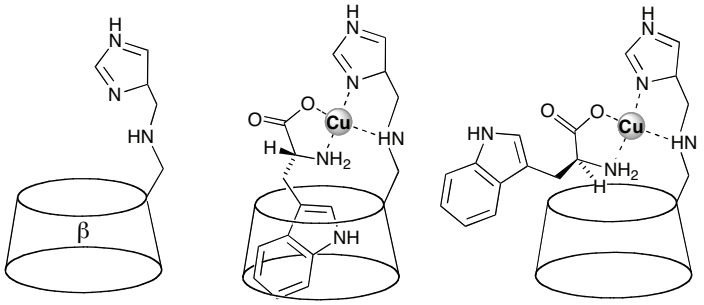

217 218 219

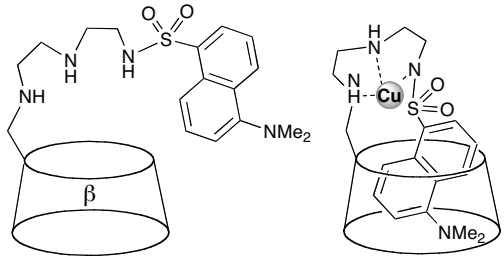

220 221

Un dérivé de β-CD ayant deux groupes amino greffés en positions A et B, forme avec l'entité $PtCl_2$ le complexe *cis*-**222**. Une analyse par diffraction des rayons X montre que le platine est disposé en aplomb de la face primaire.[131]

Harding et Deschenaux ont accroché une unité 2,2'-bipyridyle sur la face primaire d'une β-CD et étudié les propriétés luminescentes d'un dérivé du rhénium. Le complexe **223** existe sous la forme de quatre diastéréoisomères, l'atome de brome pouvant être ou non dans la cavité.[132]

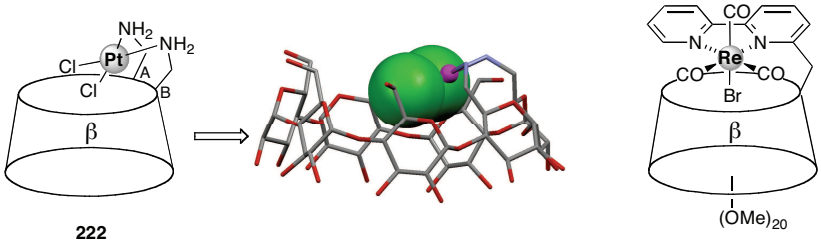

222 223

La cyclodextrine **224**, dont la face primaire est équipée d'une anse 2,2'-bipyridyle ayant ses atomes d'azote orientés vers le cœur de la CD, complexe les ions Ag(I) et Pd(II) en formant des complexes à métal *endo*-orienté. La coordination de l'argent et du palladium a été déduite des spectres de RMN, de masse et infrarouge. Dans le complexe **225**, l'atome d'argent est stabilisé par deux groupes méthoxyle de la face primaire. En traitant **224** avec du palladium acétate, on observe une déprotonation facile de l'un des groupes amide de l'anse et

formation d'un complexe de type pincer, **226**. Dans ce cas encore, le métal se trouve positionné à l'embouchure de la cavité.[133]

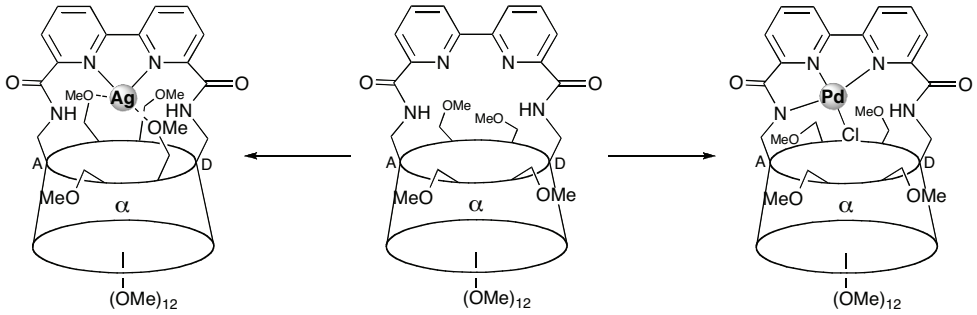

225 **224** **226**

Une expérience de catalyse *intra*-cavitale a été réalisée avec le complexe β-CD **227** contenant une entité $FeCl_2$ rigidement fixée à l'entrée de la CD. Activé avec du méthylaluminoxane (MAO), ce complexe catalyse la polymérisation de l'éthylène en PE. Compte tenu du positionnement particulier de l'atome de fer, la croissance de chaîne se déroule probablement à travers le cône défini par la CD. A signaler que l'équivalent α-CD de **225**, dont la cavité est plus petite, n'est pas actif.[134]

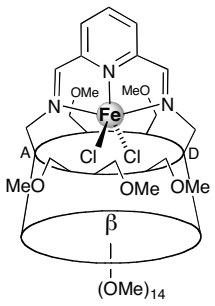

227

I.4.1. Cyclodextrines porteuses de ligands phosphorés

Un groupe strasbourgeois a décrit une variété de cyclodextrines fonctionnalisées par des atomes de P(III). Ces ligands ont été conçus pour assurer le contrôle de la première et de la seconde sphère de coordination des ions complexés. Les ligands **228** et **229** ont chacun deux bras CH_2PPh_2 attachés à la face primaire d'une α-CD, les points d'attache étant situés sur les unités glucose A et D pour la première, A et C pour la seconde. Avec des halogénures de Pd(II), Pt(II) et Rh(I), ces diphosphines forment des complexes de stéréochimie *trans* (**230**-**239**). Le plan de cordination des complexes carré-plan résultants est vertical. En RMN ^1H,

l'inclusion de l'atome X dans la cavité se traduit par un déplacement chimique important des protons *endo*-orientés H-3 et H-5 vers les champs faibles.[135-137]

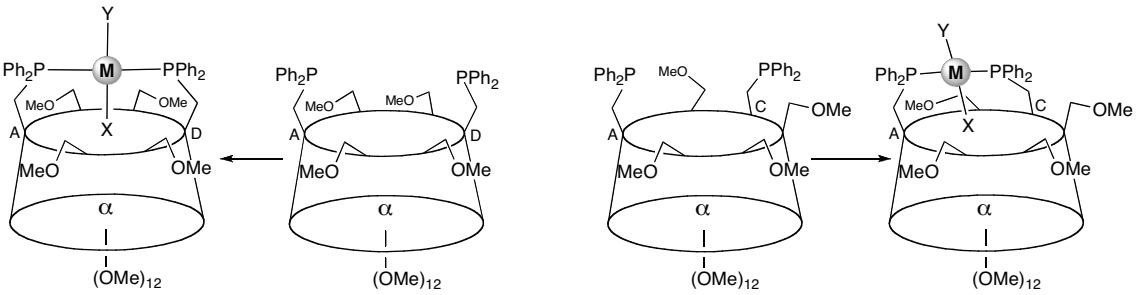

230 M = Pd, X = Y = Cl
231 M = Pt, X = Y = Cl
232 M = Pd, X = Cl, Y = Me
233 M = Rh, X = Cl, Y = CO
234 M = Rh, X = CO, Y = H

228

229

235 M = Pd, X = Y = Cl
236 M = Pt, X = Y = Cl
237 M = Pd, X = Cl, Y = Me
238 M = Rh, X = Cl, Y = CO
239 M = Rh, X = CO, Y = H

Ces diphosphines sont capables de s'adapter à d'autres stéréochimies du métal. Ainsi, le complexe chloro-carbonyle **240** contient un atome de ruthénium octaédrique dont les deux coordinats chlorido sont piégés dans la cavité, les ligands carbonyle ayant une orientation *exo*. Les complexes d'argent **241-244** se sont avérés intéressants pour l'étude de réactions d'échange de nitriles au sein d'une cavité moléculaire.[135-137]

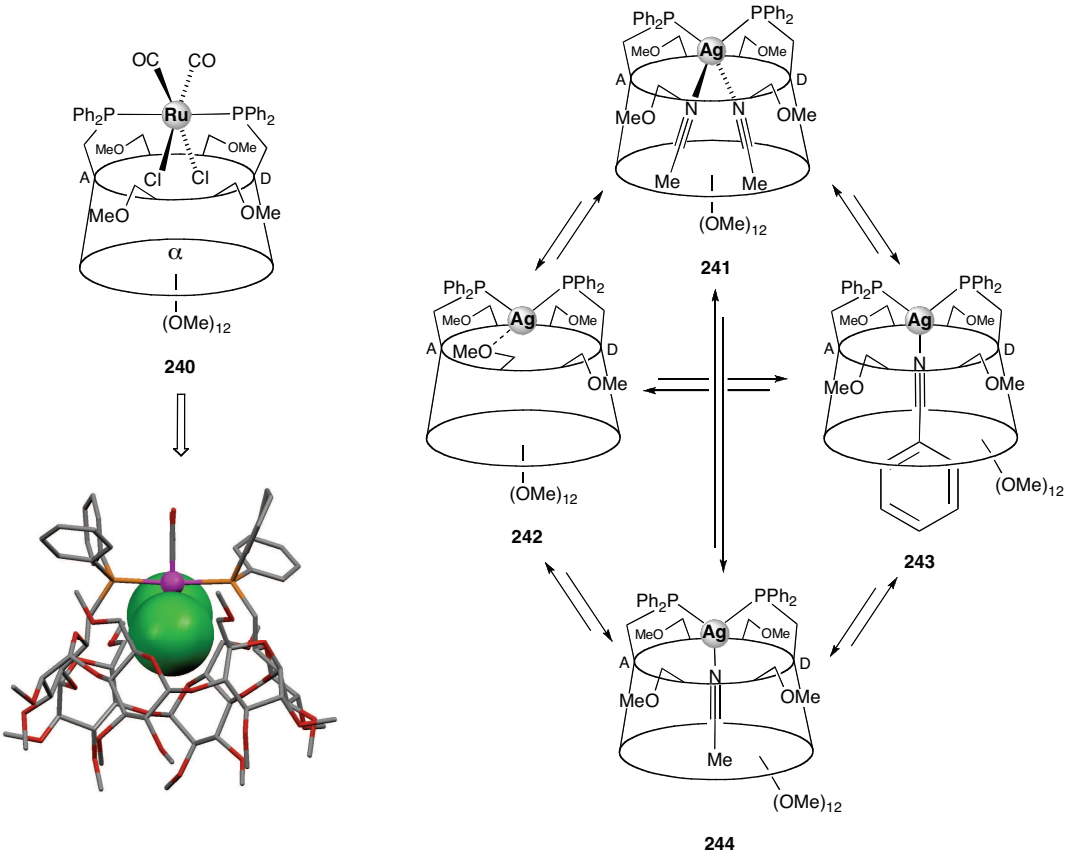

240

241

242

243

244

Le coordinat **245** est un exemple rare de tétraphosphine construite sur une plateforme macrocyclique. La coordination de quatre fragments AuCl conduit au composé **246** présentant la symétrie C_2 attendue pour le complexe. A l'état solide, la stéréochimie vue en solution n'est pas conservée, visiblement pour des raisons stériques. En effet, alors qu'une des tiges P-Au-Cl occupe le cœur de la CD, les trois autres pointent vers l'extérieur de celle-ci.[138,139]

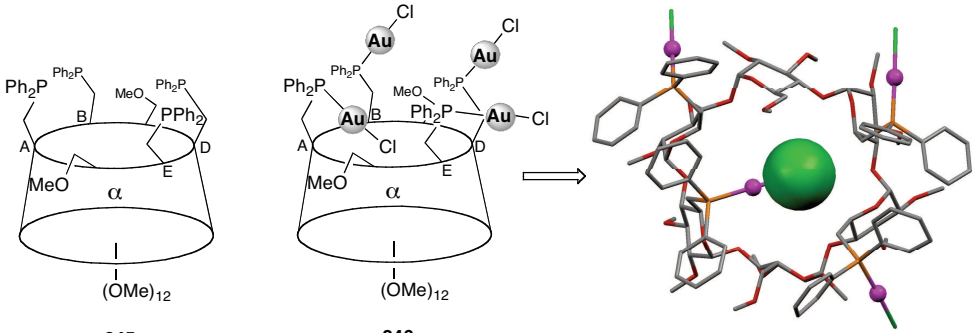

245 **246**

Les phosphines **247** et **248** ont été conçues pour un positionnement *intra*-cavital des ions à complexer. La préorganisation du ligand résulte ici de la présence d'unités phénylphosphinidène ancrées de manière rigide sur la face primaire d'une α-CD, et ayant les doublets du phosphore pointant vers l'intérieur de l'espace cavital. Comme anticipé, les réactions de ces ligands avec $[PdCl(dmba)]_2$ (dmba = *o*-$C_6H_4NMe_2$) conduisent à des complexes ayant le métal positionné à l'embouchure de la CD et le ligand chlorido inclus dans la cavité (**249** et **250**).[140]

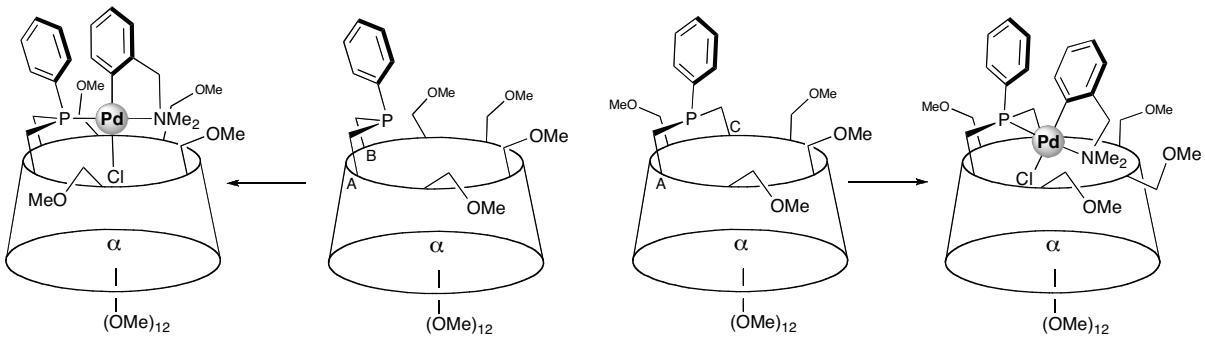

249 **247** **248** **250**

La diphosphine **251** est construite selon le même principe.[140] Elle contient deux atomes de phosphore introvertis et peu mobiles, dont la séparation est parfaitement adaptée à la formation de complexes chélate. La réaction avec des entités MX_2 carré-plan

(X = halogénure) non seulement conduit quantitativement à de tels complexes, mais conduit uniquement des complexes de stéréochimie *trans* (**252**-**260**). Les complexes de nickel **257**-**259** catalysent efficacement, une fois activés avec du MAO, la dimérisation de l'éthylène et du propène.[141] Associée à l'ion Ag^+, la diphosphine **251** devient un récepteur d'anions de taille moyenne.[142] Dans les complexes obtenus (**261**-**267**), l'anion, totalement piégé dans la CD, est lié d'une part au centre métallique, mais également aux parois de la cavité via des interactions faibles impliquant des liaisons CH *endo*-orientées.

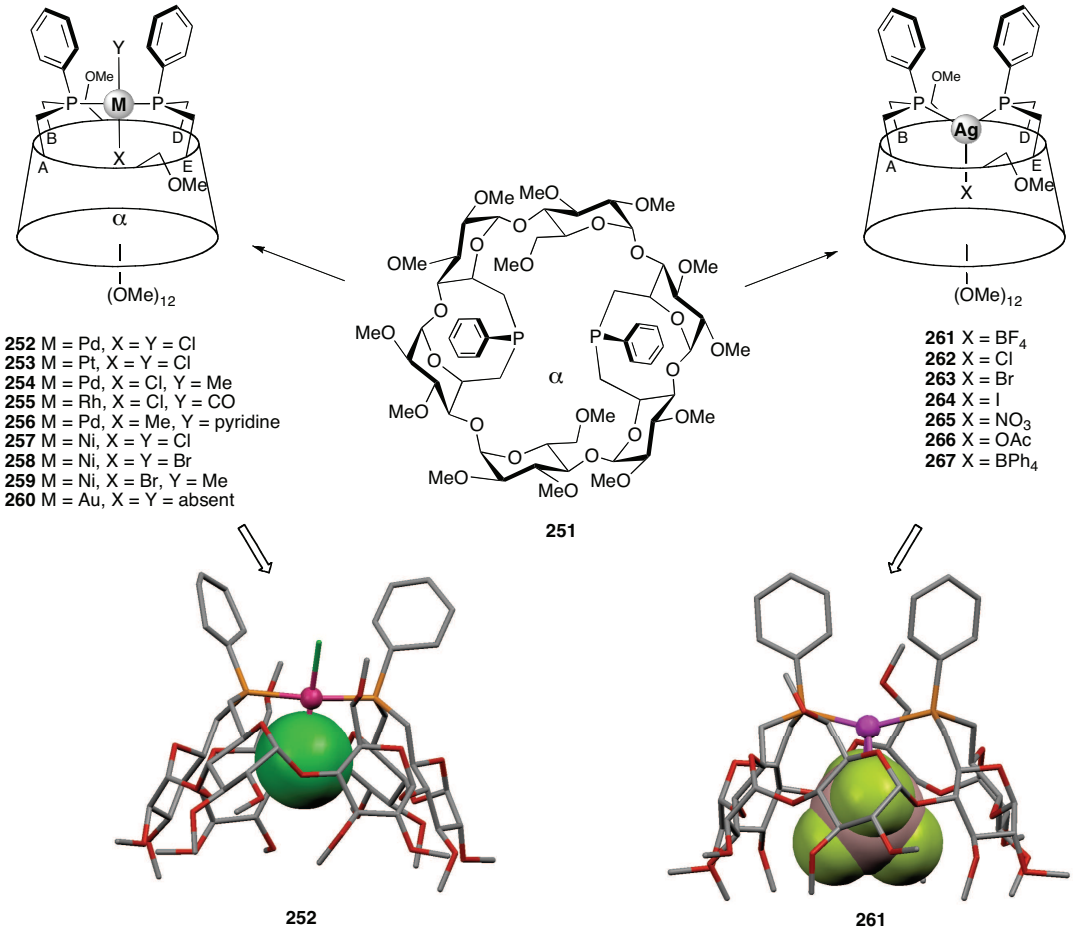

Une "version β-CD" de **251**, la diphosphine **268**, a pu être synthétisée après obtention de précurseurs régiofonctionnalisés A,B,D,E appropriés (voir **Chapitre II** de cette thèse).[143] Ce coordinat est lui aussi adapté à la formation de complexes chélate (**269**-**273**), mais compte tenu de l'orientation relative des doublets du phosphore, ainsi que de la taille de la cavité, il n'est pas possible de former des complexes où l'angle P-M-P serait de 180°. Les modèles moléculaires prévoient, en effet, un angle de chélation proche de 150-160°. C'est précisément cette dernière caractéristique qui déclenche dans les complexes formés le phénomène unique

d'oscillation du ligand diphosphine autour du métal, l'*oschélation* (voir **Chapitre III** de cette thèse). Dans ce mouvement, les doublets des atomes de phosphore cherchent, en alternance, à avoir un recouvrement optimal avec l'orbitale d_{x2-y2} du métal.

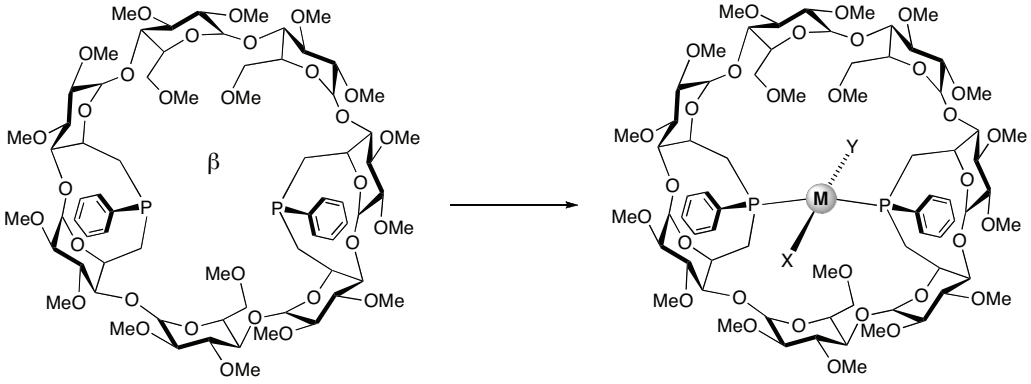

268

269 M = Pd, X = Y = Cl
270 M = Pt, X = Y = Cl
271 M = Pd, X = Cl, Y = Me
272 M = Rh, X = Cl, Y = CO
273 M = Au, X = Y = absent

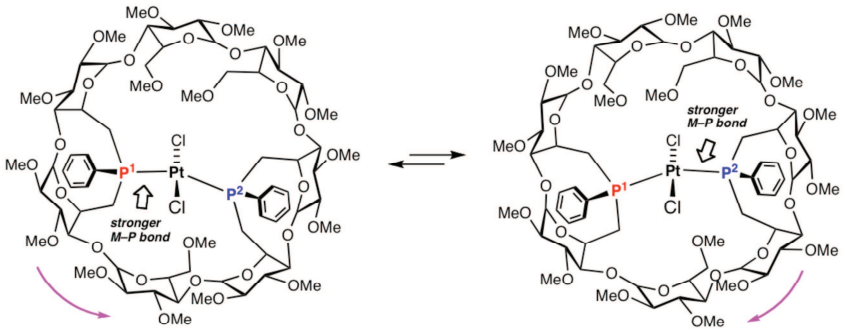

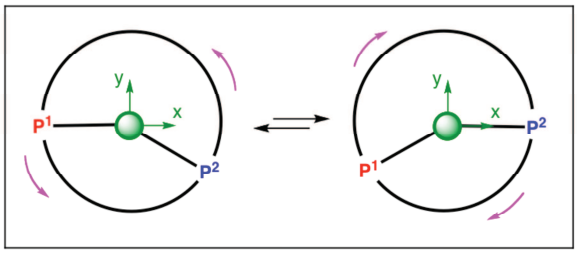

Des réactions de clivage de liaisons M–P ont été réalisées à partir du complexe chélate **269**, soit en mettant celui-ci au contact d'un autre métal (formation de **274**), soit en le faisant réagir avec l'oxygène de l'air (formation des complexes **275** et **276**).[144]

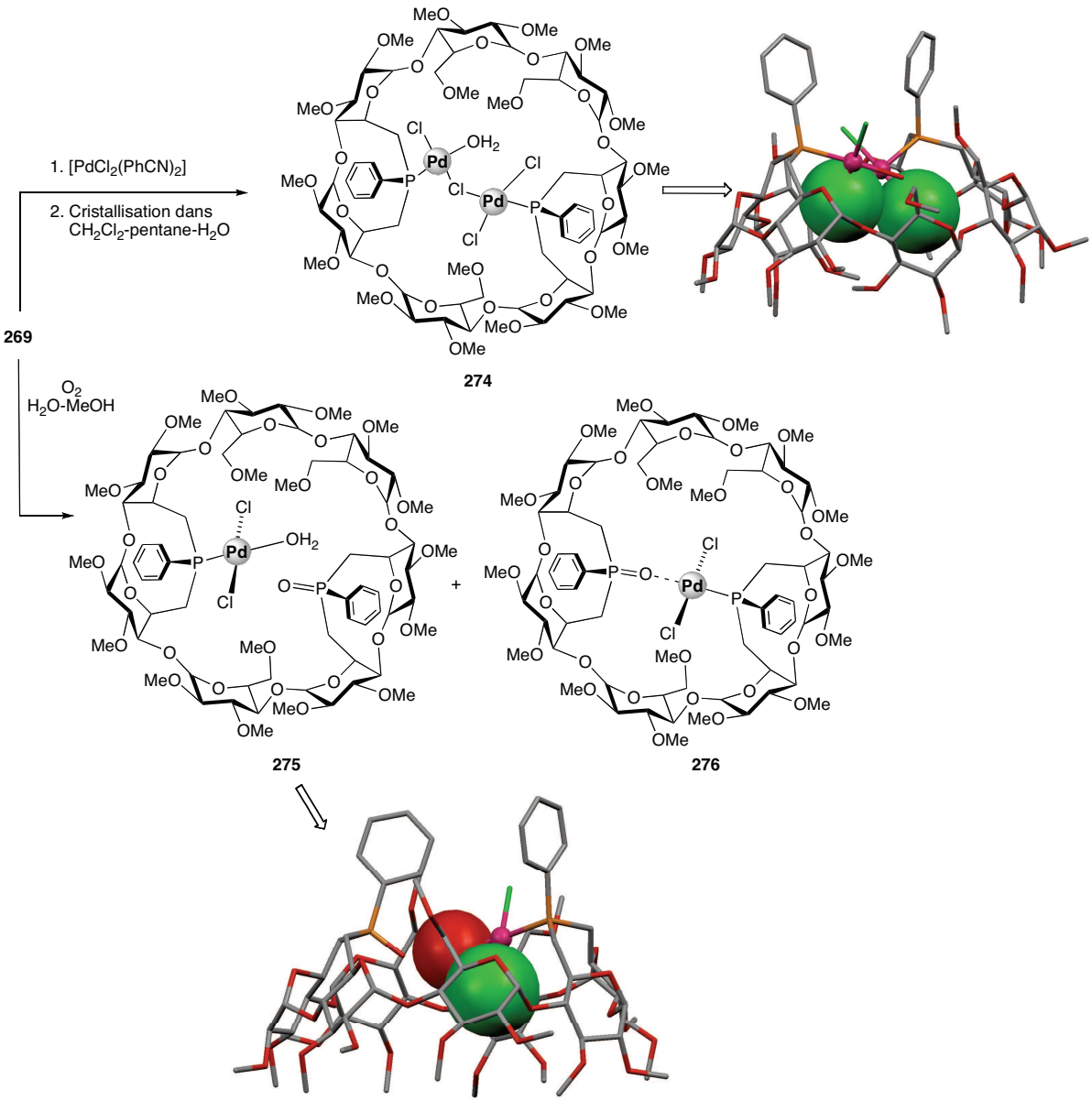

I.5. Ligands intégrant d'autres cavités

Le groupe de Nolte a réalisé un travail très innovant sur des cavités moléculaires dérivées de glycourile. Le composé clé est le métallocavitand **277**, obtenu en greffant un chapeau Zn-porphyrinique sur une entité glycourile, cet ancrage étant réalisé au niveau de quatre fonctions hydroxyle catécholiques. La cage formée s'est avérée être un excellent récepteur des viologènes **G1**-**G7** (formation des complexes **278**-**284**).[145] Le piégeage est réalisé via des liaisons hydrogène impliquant les fonctions carbonyle, des interactions π–π

avec les parois aromatiques de la cavité, des liaisons hydrogène ainsi que des interactions dipolaires avec les espaceurs oxygénés, sans oublier la coordination à l'atome de zinc. La molécule **277** a également été employée pour la translocation de biopolymères à travers son cœur.[146] Le dérivé manganeux **285** est un catalyseur d'époxydation dont le mode de fonctionnement devient entièrement *intra*-cavital à condition d'opérer en présence d'additifs bloquant sélectivement le site de coordination externe du manganèse.[147-149] Le glycouryle-cavitand **286**, comportant deux atomes de cuivre, a été utilisé comme catalyseur d'oxydation d'alcools benzyliques en aldéhydes. L'espèce active est un catalyseur à sélectivité fonctionnelle, car la réaction, qui implique l'encapsulation du substrat, se fait préférentiellement avec des composés benzyliques dérivés de résorcinols.[150] Lors de la complexation de rhodium(I) avec la diamine **287**, une cage est engendrée qui forme des complexes host-guest avec les 5-allyl-dihydroxybenzènes (**288**-**290**). Ces derniers sont convertis catalytiquement en styrènes (par isomérisation) ou en dérivés propylés (par hydrogénation). Les transformations les plus rapides se font avec le substrat 1,3-dihydroxylé (**288**).[151]

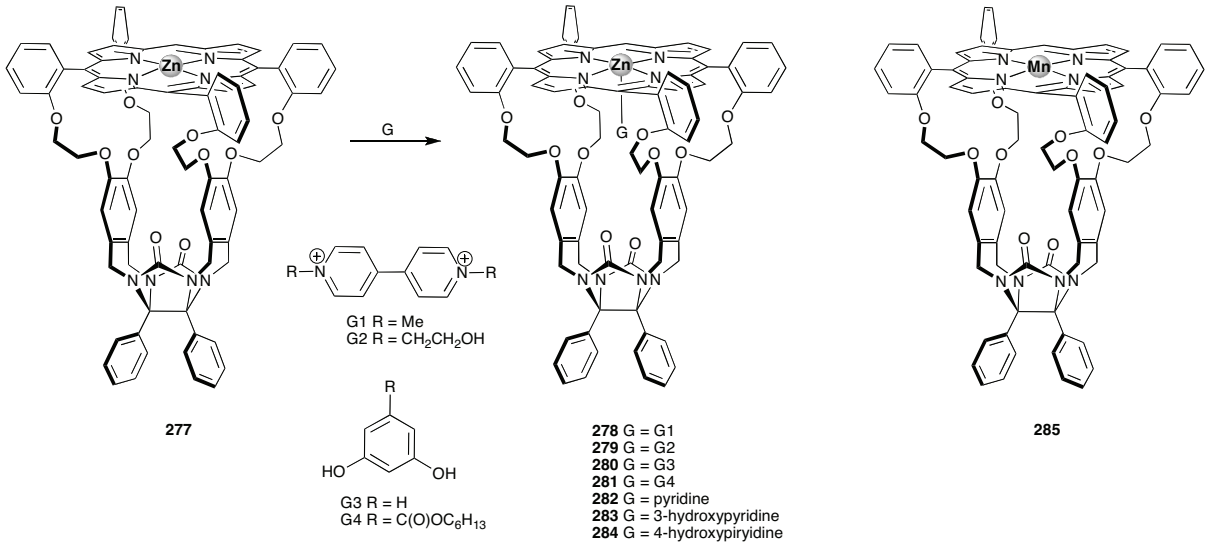

277

278 G = G1
279 G = G2
280 G = G3
281 G = G4
282 G = pyridine
283 G = 3-hydroxypyridine
284 G = 4-hydroxypiryidine

285

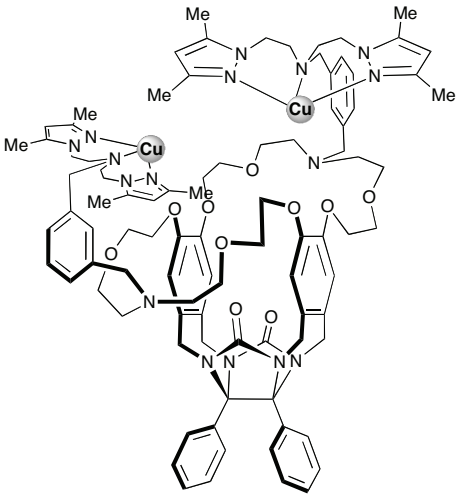

286

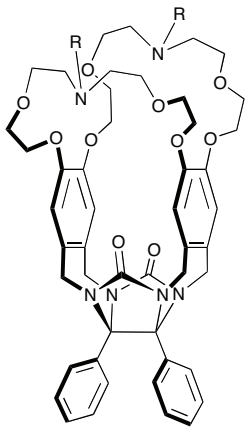

287 R= H_2C—C$_6$H$_4$—$OP(OPh)_2$

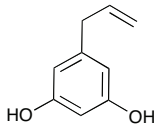

288

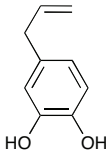

289

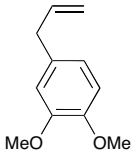

290

Le glycourile **291** et les cyclotrivératrylènes **292** et **293**, équipés de fonctionnalités thioéther, ont été employés pour la stabilisation de clusters [4Fe-4S] qui, une fois complexés, se retrouvent partiellement encapsulés.[152-155]

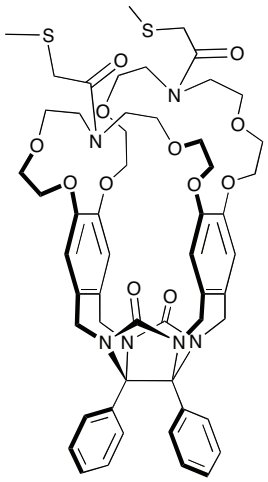

291

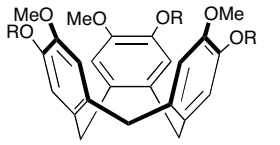

292 R = CH_2CH_2SH
293 R = *m*-$CH_2C_6H_4CH_2SH$

A ce jour, un seul exemple de cavité de type cucurbit[*n*]uryl (CB) fonctionnant comme complexant de métal de transition a été décrit. Il s'agit du coordinat CB7 dont les fragments oxo peuvent coordiner des ions Ag^+. Les complexes correspondants ont été utilisés pour des réactions en milieu biphasique, notamment la photodéazétation [Eq. (1)] du DBO (DBO = 2,3-diazabicyclo[2.2.2]oct-2-ène) et du DBH (DBH = 2,3-diazabicyclo[2.2.1]hept-2-

ène). Dans chacune de ces réactions, le substrat est piégé dans la cavité (formation de **294**).[156]

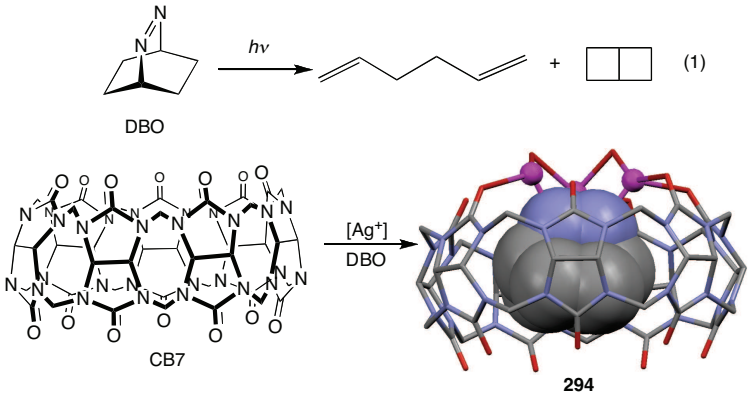

I.6. Conclusion

La présente mise au point a montré comment des ligands associant des atomes coordinateurs classiques à des cavités moléculaires peuvent assurer le double contrôle de la première et de la seconde sphère de coordination d'un métal de transition. Comme l'ont montré les exemples choisis, le rôle de la cavité est multiple: confinement et protection des sites de complexation et, incidemment, stabilisation d'espèces labiles, contrôle de la stéréochimie du métal complexé, assistance supramoléculaire de réactions stoechiométriques ou catalytiques, reconnaissance stérique et fonctionnelle des substrats à transformer, contrôle de la régiosélectivité d'une réaction. Visiblement, cette classe récente de coordinats hybrides a trouvé toute sa place dans la chimie de coordination contemporaine.

I.7. Références

[1] D. J. Cram, *Science* **1983**, *219*, 1177-1183.

[2] J. Emert, R. Breslow, *J. Am. Chem. Soc.* **1974**, *97*, 670-672.

[3] R. Breslow, S. D. Dong, *Chem. Rev.* **1998**, *98*, 1997-2011.

[4] C. D. Gutsche, Muthukrishnan, *J. Org. Chem.* **1978**, *43*, 4905-4906.

[5] C. D. Gutsche, *Calixarenes Revisited, in Monographs in Supramolecular Chemistry,* ed. J. F. Stoddart, Royal Society of Chemistry, Cambridge*,* **1998**.

[6] *Calixarenes in Action,* ed. L. Mandolini, R. Ungaro, Imperial College Press, London **2000**.

[7] G. E. Hofmeister, F. E. Hahn, S. F. Pedersen, *J. Am. Chem. Soc.* **1989**, *111*, 2318-2319.

[8] G. E. Hofmeister, E. Alvarado, J. A. Leary, D. I. Yoon, S. F. Pedersen, *J. Am. Chem. Soc.* **1990**, *112*, 8843-8851.

[9] A. Zanotti-Gerosa, E. Solari, L. Giannini, C. Floriani, N. Re, A. Chiesi-Villa, C. Rizzoli, *Inorg. Chim. Acta* **1998**, *270*, 298-311.

[10] F. Corazza, C. Floriani, A. Chiesi-Villa, C. Guastini, *J. Chem. Soc. Chem. Commun.* **1990**, 640-641.

[11] F. Corazza, C. Floriani, A. Chiesi-Villa, C. Rizzoli, *Inorg. Chem.* **1991**, *30*, 4465-4468.

[12] V. C. Gibson, C. Redshaw, W. Clegg, M. R. J. Elsegood, *J. Chem. Soc. Chem. Commun.* **1995**, 2371-2372.

[13] V. C. Gibson, C. Redshaw, W. Clegg, M. R. J. Elsegood, *Chem. Commun.* **1998**, 1969-1970.

[14] U. Radius, J. Attner, *Inorg. Chem.* **2004**, *43*, 8587-8599.

[15] U. Radius, J. Attner, *Eur. J. Inorg. Chem.* **1999**, 2221-2231.

[16] C. Redshaw, M. R. J. Elsegood, *Inorg. Chem.* **2000**, *39*, 5164-5168.

[17] L. Giannini, E. Solari, C. Floriani, A. Chiesi-Villa, C. Rizzoli, *J. Am. Chem. Soc.* **1998**, *120*, 823-824.

[18] L. Giannini, E. Solari, S. Dovesi, C. Floriani, N. Re, A. Chiesi-Villa, C. Rizzoli, *J. Am. Chem. Soc.* **1999**, *121*, 2784-2796.

[19] L. Giannini, E. Solari, C. Floriani, *Inorg. Chem.* **1999**, *38*, 1438-1445.

[20] G. Guillemot, E. Solari, C. Floriani, *Organometallics* **2000**, *19*, 5218-5230.

[21] G. Guillemot, E. Solari, R. Scopelliti, C. Floriani, *Organometallics* **2001**, *20*, 2446-2448.

[22] G. Guillemot, E. Solari, C. Floriani, *Organometallics* **2001**, *20*, 607-615.

[23] A. Vigalok, T. M. Swager, *Adv. Mater.* **2002**, *14*, 368-371.

[24] C. Redshaw, M. R. J. Elsegood, *Eur. J. Inorg. Chem.* **2003**, 2071-2074.

[25] J. A. Acho, L. H. Doerrer, S. J. Lippard, *Inorg. Chem.* **1995**, *34*, 2542-2556.

[26] A. Caselli, E. Solari, R. Scopelliti, C. Floriani, N. Re, C. Rizzoli, A. Chiesi-Villa, *J. Am. Chem. Soc.* **2000**, *122*, 3652-3670.

[27] B. Castellano, E. Solari, C. Floriani, R. Scopelliti, *Inorg. Chem.* **1999**, *38*, 3406-3413.

[28] C. Redshaw, D. Homden, D. L. Hughes, J. A. Wright, M. R. J. Elsegood, *Dalton Trans.* **2009**, 1231-1242.

[29] M. G. Gardiner, S. M. Lawrence, C. L. Raston, *Chem. Commun.* **1996**, 2491-2492.

[30] E. Bukhaltsev, I. Goldberg, A. Vigalok, *Organometallics* **2004**, *23*, 4540-4543.

[31] E. Bukhaltsev, I. Goldberg, A. Vigalok, *Organometallics* **2005**, *24*, 5732-5736.

[32] N. Kotzen, I. Goldberg, A. Vigalok, *Inorg. Chem. Commun.* **2005**, *8*, 1028-1030.

[33] K. Iwasa, T. Kochi, Y. Ishii, *Angew. Chem. Int. Ed.* **2003**, *42*, 3658-3660.

[34] B. R. Cameron, S. J. Loeb, G. P. A. Yap, *Inorg. Chem.* **1997**, *36*, 5498-5504.

[35] N. Le Poul, M. Campion, B. Douziech, Y. Rondelez, L. Le Clainche, O. Reinaud, Y. Le Mest, *J. Am. Chem. Soc.* **2007**, *129*, 8801-8810.

[36] S. Blanchard, L. Le Clainche, M.-N. Rager, B. Chansou, J.-P. Tuchagues, A. F. Duprat, Y. Le Mest, O. Reinaud, *Angew. Chem. Int. Ed.* **1998**, *37*, 2732-2735.

[37] S. Blanchard, M.-N. Rager, A. F. Duprat, O. Reinaud, *New. J. Chem.* **1998**, 1143-1146.

[38] Y. Rondelez, M.-N. Rager, A. F. Duprat, O. Reinaud, *J. Am. Chem. Soc.* **2002**, *124*, 1334-1340.

[39] L. Le Clainche, M. Giorgi, O. Reinaud, *Inorg. Chem.* **2000**, *39*, 3436-3437.

[40] N. Le Poul, M. Campion, G. Izzet, B. Douziech, O. Reinaud, Y. Le Mest, *J. Am. Chem. Soc.* **2005**, *127*, 5280-5281.

[41] G. Izzet, Y. M. Frapart, T. Prangé, K. Provost, A. Michalowicz, O. Reinaud, *Inorg. Chem.* **2005**, *44*, 9743-9751.

[42] G. Izzet, H. Akdas, N. Hucher, M. Giorgi, T. Prangé, O. Reinaud, *Inorg. Chem.* **2006**, *45*, 1069-1077.

[43] Y. Rondelez, O. Sénèque, M.-N. Rager, A. F. Duprat, O. Reinaud, *Chem. Eur. J.* **2000**, *6*, 4218-4226.

[44] O. Sénèque, M. Campion, B. Douziech, M. Giorgi, Y. Le Mest, O. Reinaud, *Dalton Trans.* **2003**, 4216-4218.

[45] Y. Rondelez, G. Bertho, O. Reinaud, *Angew. Chem. Int. Ed.* **2002**, *41*, 1044-1046.

[46] G. Izzet, X. Zeng, H. Akdas, J. Marrot, O. Reinaud, *Chem. Commun.* **2007**, 810-812.

[47] N. Le Poul, B. Douziech, J. Zeitouny, G. Thiabaud, H. Colas, F. Conan, N. Cosquer, I. Jabin, C. Lagrost, P. Hapiot, O. Reinaud, Y. Le Mest, *J. Am. Chem. Soc.* **2009**, *131*, 17800-17807.

[48] G. Thiabaud, G. Guillemot, I. Schmitz-Alfonso, B. Colasson, O. Reinaud, *Angew. Chem. Int. Ed.* **2009**, *48*, 7383-7386.

[49] G. Izzet, B. Douziech, T. Prangé, A. Tomas, I. Jabin, Y. Le Mest, O. Reinaud, *PNAS* **2005**, *102*, 6831-6836.

[50] G. Izzet, M.-N. Rager, O. Reinaud, *Dalton Trans.* **2007**, 771-780.

[51] G. Izzet, J. Zeitouny, H.-K. Akdas, Y. M. Frapart, S. Ménage, B. Douziech, I. Jabin, Y. Le Mest, O. Reinaud, *J. Am. Chem. Soc.* **2008**, *130*, 9514-9523.

[52] O. Sénèque, M.-N. Rager, M. Giorgi, O. Reinaud, *J. Am. Chem. Soc.* **2000**, *122*, 6183-6189.

[53] O. Sénèque, M. Giorgi, O. Reinaud, *Supramolecular Chemistry* **2003**, *15*, 573-580.

[54] O. Sénèque, Y. Rondelez, L. Le Clainche, C. Inisan, M.-N. Rager, M. Giorgi, O. Reinaud, *Eur. J. Inorg. Chem.* **2001**, 2597-2604.

[55] S. Redon, Y. Li, O. Reinaud, *J. Org. Chem.* **2003**, *68*, 7004-7008.

[56] O. Sénèque, M. Giorgi, O. Reinaud, *Chem. Commun.* **2001**, 984-985.

[57] O. Sénèque, M.-N. Rager, M. Giorgi, O. Reinaud, *J. Am. Chem. Soc.* **2001**, *123*, 8442-8443.

[58] D. Coquière, J. Marrot, O. Reinaud, *Org. Lett.* **2007**, *9*, 3271-3274.

[59] D. Coquière, J. Marrot, O. Reinaud, *Org. Biomol. Chem.* **2008**, *6*, 3930-3934.

[60] D. Coquière, A. de la Lande, S. Martí, O. Parisel, T. Prangé, O. Reinaud, *PNAS* **2009**, *106*, 10449-10454.

[61] D. Coquière, A. de la Lande, O. Parisel, T. Prangé, O. Reinaud, *Chem. Eur. J.* **2009**, *15*, 11912-11917.

[62] D. Coquière, J. Marrot, O. Reinaud, *Chem. Commun.* **2006**, 3924-3926.

[63] B. Colasson, O. Reinaud, *J. Am. Chem. Soc.* **2008**, *130*, 15226-15227.

[64] B. Colasson, M. Save, P. Milko, J. Roithová, D. Schröder, O. Reinaud, *Org. Lett.* **2007**, *9*, 4987-4990.

[65] B. Colasson, N. Le Poul, Y. Le Mest, O. Reinaud, *J. Am. Chem. Soc.* **2010**, *132*, 4393-4398.

[66] O. Sénèque, M.-N. Rager, M. Giorgi, T. Prangé, A. Tomas, O. Reinaud, *J. Am. Chem. Soc.* **2005**, *127*, 14833-14840.

[67] U. Darbost, X. Zeng, M.-N. Rager, M. Giorgi, I. Jabin, O. Reinaud, *Eur. J. Inorg. Chem.* **2004**, 4371-4374.

[68] U. Darbost, M.-N. Rager, S. Petit, I. Jabin, O. Reinaud, *J. Am. Chem. Soc.* **2005**, *127*, 8517-8525.

[69] C. Monnereau, J.-N. Rebilly, O. Reinaud, *Eur. J. Org. Chem.* **2011**, 166-175.

[70] O. Sénèque, M. Campion, M. Giorgi, Y. Le Mest, O. Reinaud, *Eur. J. Inorg. Chem.* **2004**, 1817-1826.

[71] C. Wieser-Jeunesse, D. Matt, A. De Cian, *Angew. Chem. Int. Ed.* **1998**, *37*, 2861-2864.

[72] C. Wieser, D. Matt, L. Toupet, H. Bourgeois, J.-P. Kintzinger, *J. Chem. Soc. Dalton Trans.* **1996**, 4041-4043.

[73] C. Wieser, D. Matt, J. Fischer, A. Harriman, *J. Chem. Soc. Dalton Trans.* **1997**, 2391-2402.

[74] M. Lejeune, C. Jeunesse, D. Matt, N. Kyritsakas, R. Welter, J.-P. Kintzinger, *J. Chem. Soc. Dalton Trans.* **2002**, 1642-1650.

[75] S. Sameni, M. Lejeune, C. Jeunesse, D. Matt, R. Welter, *Dalton Trans.* **2009**, 7912-7923.

[76] L. Monnereau, D. Sémeril, D. Matt, L. Toupet, *Chem. Eur. J.* **2010**, *16*, 9237-9247.

[77] L. Monnereau, D. Sémeril, D. Matt, *Chem. Commun.* **2011**, *47*, 6626-6628.

[78] F. Barrios-Landeros, J. F. Hartwig, *J. Am. Chem. Soc.* **2005**, *127*, 6944-6945.

[79] S. Sameni, C. Jeunesse, D. Matt, L. Toupet, *Chem. Eur. J.* **2009**, *15*, 10446-10456.

[80] M. Takeshita, F. Inokuchi, S. Shinkai, *Tetrahedron Lett.* **1995**, *36*, 3341-3344.

[81] C. B. Dieleman, D. Matt, I. Neda, R. Schmutzler, A. Harriman, R. Yaftian, *Chem. Commun.* **1999**, 1911-1912.

[82] Résultats non publiés.

[83] M. Fan, H. Zhang, M. Lattman, *Chem. Commun.* **1998**.

[84] G. Izzet, X. Zeng, D. Over, B. Douziech, J. Zeitouny, M. Giorgi, I. Jabin, Y. Le Mest, O. Reinaud, *Inorg. Chem.* **2007**, *46*, 375-377.

[85] D. Over, A. de la Lande, X. Zeng, O. Parisel, O. Reinaud, *Inorg. Chem.* **2009**, *48*, 4317-4330.

[86] A. Bayer, *Ber. Dtsh. Chem. Ges.* **1872**, *5*, 25.

[87] A. Michael, A. Comey, *Am. Chem. J.* **1883**, *5*, 349.

[88] J. B. Niederl, H. J. Vogel, *J. Am. Chem. Soc.* **1940**, *62*, 2512-2514.

[89] H. Erdtman, S. Högberg, S. Abrahamsson, B. Nilsson, *Tetrahedron Lett.* **1968**, *9*, 1679-1682.

[90] J. R. Moran, S. Karbach, D. J. Cram, *J. Am. Chem. Soc.* **1982**, *104*, 5826-5828.

[91] D. J. Cram, S. Karbach, H.-E. Kim, C. B. Knobler, E. F. Maverick, J. L. Ericson, R. C. Helgeson, *J. Am. Chem. Soc.* **1988**, *110*, 2229-2237.

[92] P. Delangle, J.-P. Dutasta, *Tetrahedron Lett.* **1995**, *36*, 9325-9328.

[93] T. Lippmann, H. Wilde, E. Dalcanale, L. Mavilla, G. Mann, U. Heyer, S. Spera, *J. Org. Chem.* **1995**, *60*, 235-242.

[94] P. Jacopozzi, E. Dalcanale, S. Spera, L. A. J. Chrisstoffels, D. N. Reinhoudt, T. Lippmann, G. Mann, *J. Chem. Soc. Perkin. Trans. 2* **1998**, 671-677.

[95] I. L. Nikolaeva, A. R. Burilov, D. I. Kharitonov, M. A. Pudovik, W. D. Habicher, A. I. Konovalov, *Russ. J. Gen. Chem.* **2001**, *71*, 379-382.

[96] B. Bibal, J.-P. Declercq, J.-P. Dutasta, B. Tinant, A.-G. Valade, *Tetrahedron* **2003**, *59*, 5849-5854.

[97] J. R. Moran, J. L. Ericson, E. Dalcanale, J. A. Bryant, C. B. Knobler, D. J. Cram, *J. Am. Chem. Soc.* **1991**, *113*, 5707-5714.

[98] B. A. Azov, A. Beeby, M. Cacciarini, A. G. Cheetham, F. Diederich, M. Frei, J. K. Gimzewski, V. Gramlich, B. Hecht, B. Jaun, T. Latychevskaia, A. Lieb, Y. Lill, F. Marotti, A. Schlegel, R. R. Schlittler, P. J. Skinner, P. Seiler, Y. Yamakoshi, *Adv. Funct. Mater.* **2006**, *16*, 147-156.

[99] D. J. Kleinhans, G. E. Arnott, *Dalton Trans.* **2010**, *39*, 5780-5782.

[100] U. Lücking, J. Chen, D. M. Rudkevich, J. Rebek Jr., *J. Am. Chem. Soc.* **2001**, *123*, 9929-9934.

[101] A. Visnjevac, J. Gout, N. Ingert, O. Bistri, O. Reinaud, *Org. Lett.* **2010**, *12*, 2044-2047.

[102] C. Gibson, J. Rebek Jr., *Org. Lett.* **2002**, *4*, 1887-1890.

[103] W. Xu, J. P. Rourke, J. J. Vittal, R. J. Puddephatt, *J. Chem. Soc. Chem. Commun.* **1993**, 145-147.

[104] W. Xu, J. P. Rourke, J. J. Vittal, R. J. Puddephatt, *Inorg. Chem.* **1995**, *34*, 323-329.

[105] W. Xu, J. J. Vittal, R. J. Puddephatt, *J. Am. Chem. Soc.* **1993**, *115*, 6456-6457.

[106] W. Xu, J. J. Vittal, R. J. Puddephatt, *J. Am. Chem. Soc.* **1995**, *117*, 8361-8371.

[107] S. Miao, W.-R. Yao, D.-S. Guo, Q.-F. Zhang, *Journal of Molecular Structure* **2003**, *660*, 159-165.

[108] Q.-F. Zhang, R. D. Adams, D. Fenske, *Journal of Molecular Structure* **2005**, *741*, 129-134.

[109] E. E. Nifantyev, V. I. Maslennikova, S. E. Goryukhina, L. K. Vasyanina, K. A. Lyssenko, M. Y. Antipin, *Russ. Chem Bull.* **1998**, *47*, 1805-1811.

[110] E. E. Nifantyev, V. I. Maslennikova, S. E. Goryukhina, M. Y. Antipin, K. A. Lyssenko, L. K. Vasyanina, *J. Organomet. Chem.* **2001**, *631*, 1-8.

[111] V. I. Maslennikova, S. E. Goryukhina, O. S. Serkova, L. K. Vasyanina, E. E. Nifantyev, *Russ. J. Gen. Chem.* **2002**, *72*, 816-817.

[112] V. I. Maslennikova, O. S. Serkova, L. K. Vasyanina, K. A. Lyssenko, M. Y. Antipin, E. E. Nifantyev, *J. Organomet. Chem.* **2003**, *677*, 21-27.

[113] P. Sakhaii, I. Neda, M. Freytag, H. Thönessen, P. G. Jones, R. Schmutzler, *Z. Anorg. Allg. Chem.* **2000**, *626*, 1246-1254.

[114] V. I. Maslennikova, T. V. Guzeeva, O. S. Serkova, L. K. Vasyanina, K. A. Lyssenko, E. E. Nifantyev, *Russ. J. Gen. Chem.* **2008**, *78*, 175-184.

[115] M. L. Bender, M. Komiyama, *Cyclodextrin Chemistry*; Springer, Berlin, **1978**.

[116] J. L. Atwood, J. E. Davies, D. D. Macinol, F. Vögtle, J.-M. Lehn, *Cyclodextrins, Comprehensive Supramolecular Chemistry*; Pergamon, Oxford, **1996**.

[117] J. Szejtli, *Chem. Rev.* **1998**, *98*, 1743-1754.

[118] A. R. Khan, P. Forgo, K. J. Stine, V. T. D'Souza, *Chem. Rev.* **1998**, *98*, 1977-1996.

[119] C. J. Easton, S. F. Lincoln, *Modified Cyclodextrins*; Imperial College Press, London, **1999**.

[120] S. A. Nepogodiev, J. F. Stoddart, *Chem. Rev.* **1998**, *98*, 1959-1976.

[121] B. U. Nair, G. C. Dismukes, *J. Am. Chem. Soc.* **1983**, *105*, 124-125.

[122] P. K. Bose, P. L. Polavarapu, *Carohydrate Research* **2000**, *323*, 63-72.

[123] B. Benmerad, P. Clair, D. Armspach, D. Matt, F. Balegroune, L. Toupet, *Chem. Commun.* **2006**, 2678-2680.

[124] D. Armspach, L. Poorters, D. Matt, B. Benmerad, P. G. Jones, I. Dix, L. Toupet, *J. Incl. Phenom. Macrocycl. Chem.* **2007**, *57*, 243-250.

[125] D. Armspach, D. Matt, L. Poorters, R. Gramage-Doria, P. G. Jones, L. Toupet, *Polyhedron* **2011**, *30*, 573-578.

[126] R. Breslow, B. Zhang, *J. Am. Chem. Soc.* **1994**, *116*, 7893-7894.

[127] B. Zhang, R. Breslow, *J. Am. Chem. Soc.* **1997**, *119*, 1676-1681.

[128] G. Impellizzeri, G. Maccarrone, E. Rizzarelli, G. Vecchio, R. Corradini, R. Marchelli, *Angew. Chem. Int. Ed.* **1991**, *30*, 1348-1349.

[129] R. Corradini, A. Dossena, G. Galaverna, R. Marchelli, A. Panagia, G. Sartor, *J. Org. Chem.* **1997**, *62*, 6283-6289.

[130] S. Pagliari, R. Corradini, G. Galaverna, S. Sforza, A. Dossena, M. Montalti, L. Prodi, N. Zaccheroni, R. Marchelli, *Chem. Eur. J.* **2004**, *10*, 2749-2758.

[131] V. Cucinotta, G. Grasso, S. Pedotti, E. Rizzarelli, G. Vecchio, B. Di Blasio, C. Isernia, M. Saviano, C. Pedone, *Inorg. Chem.* **1996**, *35*, 7535-7540.

[132] R. Deschenaux, M. M. Harding, R. Ruch, *J. Chem. Soc. Perkin. Trans. 2* **1993**, 1251-1258.

[133] D. Armspach, D. Matt, N. Kyritsakas, *Polyhedron* **2001**, *20*, 663-668.

[134] D. Armspach, D. Matt, F. Peruch, P. Lutz, *Eur. J. Inorg. Chem.* **2003**, 805-809.

[135] E. Engeldinger, D. Armspach, D. Matt, *Angew. Chem. Int. Ed.* **2001**, *40*, 2526-2529.

[136] E. Engeldinger, D. Armspach, D. Matt, P. G. Jones, R. Welter, *Angew. Chem. Int. Ed.* **2002**, *41*, 2593-2596.

[137] E. Engeldinger, D. Armspach, D. Matt, P. G. Jones, *Chem. Eur. J.* **2003**, *9*, 3091-3105.

[138] L. Poorters, D. Armspach, D. Matt, *Eur. J. Org. Chem.* **2003**, 1377-1381.

[139] L. Poorters, D. Armspach, D. Matt, L. Toupet, *Dalton Trans.* **2007**, 3195-3202.

[140] E. Engeldinger, L. Poorters, D. Armspach, D. Matt, L. Toupet, *Chem. Commun.* **2004**, 634-635.

[141] L. Poorters, D. Armspach, D. Matt, L. Toupet, S. Choua, P. Turek, *Chem. Eur. J.* **2007**, *13*, 9448-9461.

[142] L. Poorters, D. Armspach, D. Matt, L. Toupet, P. G. Jones, *Angew. Chem. Int. Ed.* **2007**, *46*, 2663-2665.

[143] R. Gramage-Doria, D. Rodriguez-Lucena, D. Armspach, C. Egloff, M. Jouffroy, D. Matt, L. Toupet, *Chem. Eur. J.* **2011**, *17*, 3911-3921.

[144] R. Gramage-Doria, D. Armspach, D. Matt, L. Toupet, *Angew. Chem. Int. Ed.* **2011**, *50*, 1554-1559.

[145] J. A. A. W. Elemans, M. B. Claase, P. P. M. Aarts, A. E. Rowan, A. P. H. J. Schenning, R. J. M. Nolte, *J. Org. Chem.* **1999**, *64*, 7009-7016.

[146] A. B. C. Deutman, C. Monnereau, J. A. A. W. Elemans, G. Ercolani, R. J. M. Nolte, A. E. Rowan, *Science* **2008**, *322*, 1668-1671.

[147] J. A. A. W. Elemans, E. J. A. Bijsterveld, A. E. Rowan, R. J. M. Nolte, *Chem. Commun.* **2000**, 2443-2444.

[148] P. Thodarson, E. J. A. Bijsterveld, A. E. Rowan, R. J. M. Nolte, *Nature* **2003**, *424*, 915-918.

[149] J. A. A. W. Elemans, E. J. A. Bijsterveld, A. E. Rowan, R. J. M. Nolte, *Eur. J. Org. Chem.* **2007**, 751-757.

[150] C. F. Martens, R. J. M. Klein Gebbink, M. C. Feiters, R. J. M. Nolte, *J. Am. Chem. Soc.* **1994**, *116*, 5667-5670.

[151] H. K. A. C. Coolen, P. W. N. M. van Leeuwen, R. J. M. Nolte, *Angew. Chem. Int. Ed.* **1992**, *31*, 905-907.

[152] J. G. M. van der Linden, G. Beurskens, P. T. Beurskens, J. M. M. Smits, R. J. M. Nolte, *J. Chem. Soc. Chem. Commun.* **1991**, 1623-1625.

[153] C. F. Martens, M. C. Feiters, H. L. Blonk, J. G. M. van der Linden, R. J. M. Nolte, *J. Inorg. Biochem.* **1991**, *43*, 244.

[154] G. P. F. van Strijdonck, J. A. E. H. van Haare, J. G. M. van der Linden, J. J. Steggerda, R. J. M. Nolte, *Inorg. Chem.* **1994**, *33*, 999-1000.

[155] C. F. Martens, M. M. G. Bongers, P. J. A. Kenis, R. Czajka, M. C. Feiters, J. G. M. van der Linden, R. J. M. Nolte, *Chem. Ber./Recueil* **1997**, *130*, 23.

[156] A. L. Koner, C. Márquez, M. H. Dickman, W. M. Nau, *Angew. Chem. Int. Ed.* **2011**, *50*, 545-548.

Chapter II

Regioselective double capping of cyclodextrin scaffolds

Chapter II

Regioselective double capping of cyclodextrin scaffolds

SUMMARY – CHAPTER II

Four different regioselective double capping reactions were applied either to α- or β-cyclodextrin (CD) scaffolds. The first, which relied on the use of a rigid, bulky dialkylating reagent containing two trityl-like subunits, gave access to an A,B,D,E-tetrafunctionalised β-CD regioisomer in large scale reactions. Two further capping reactions, involving the phenylphosphide (PPh^{2-}) and sulfide (S^{2-}) dianions, led to the synthesis of new C_1-symmetrical β-cyclodextrins in which pairs of neighbouring glucose units are linked by very short spacers. For comparison, introverted monophosphanes were also synthesized from either A,B- or A,C-derived β-CDs by treatment with phenylphosphide dianion. The last double capping reaction described allowed the high-yield preparation of unprecedented α- and β-cyclodextrins containing two sulfate handles. Proximal capping turned out to be favoured for each of the above difunctional reagents. The structural characterisation of the capped species was achieved by thorough NMR investigations as well as by single-crystal X-ray diffraction studies.

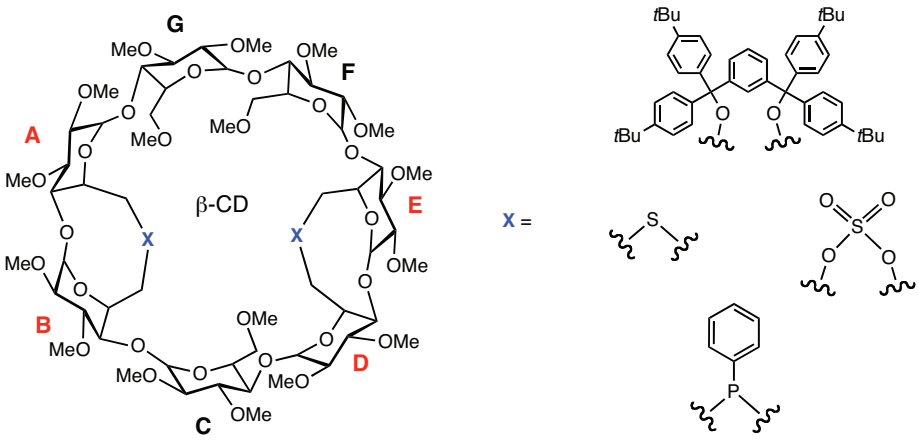

II.1. Introduction

At the end of the XIX century, Villiers reported for the first time the existence of a new type of non-reducing naturally-occuring oligosaccharides.[1] About a decade after his first report, the same compounds were isolated by Schardinger who realised that the substance described by Villiers was actually a mixture of two different compounds he called α-dextrin and β-dextrin.[2-5] Then, in the 30s, Freudenberg managed to establish their α-(1→4) cyclic structure, hence their present name of cyclodextrins (CDs).[6-9] Research on the enzymatic production of pure CDs carried out during the 50s by French[10] and Cramer[11] opened the way to the study of their remarquable properties. Even if some CDs contain more than eight glucose units, the most common, as well as useful ones are those with a well-defined chiral cavity, namely α-, β- and γ-CD (Figure 1).[12-16]

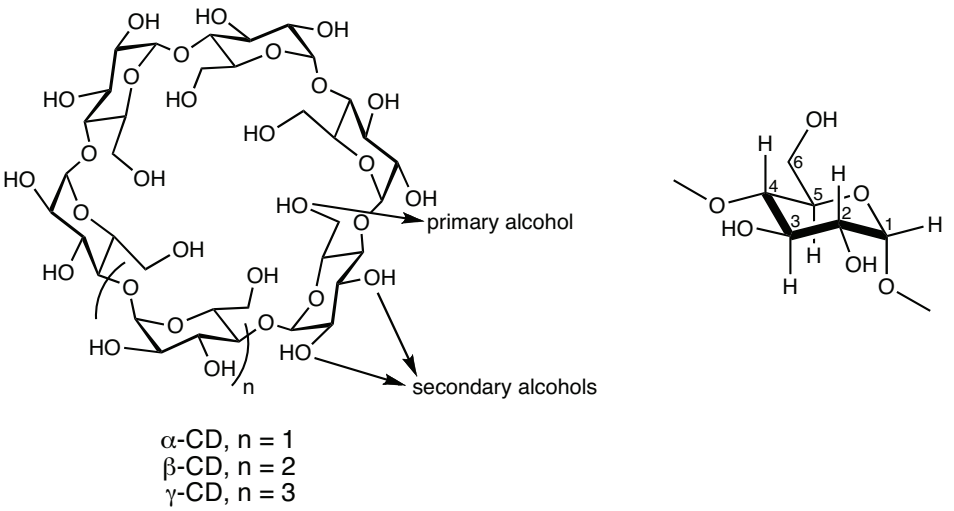

Figure 1. Structure of native CDs and atom labelling for a given glucose unit.

The presence of a large number of hydroxyl groups on their surface makes CDs water-soluble. Moreover, the hydrophobic character of their interior is responsible for the inclusion of a wide range of hydrophobic compounds, mainly organic ones, in aqueous solution, and this supramolecular property, which is retained in many chemically-modified CDs, has been extensively exploited in molecular recognition,[17-19] biphasic catalysis,[20,21] supramolecular chemistry,[22-24] drug delivery[25-29] and many other applications. More recently, the possibility of grafting specific functions at given positions on the CD macrocycle, altering in the process their inclusion properties, has led to promising

developments in fields such as enzyme mimics,[30-40] coordination chemistry and transition metal catalysis, including asymmetric one.[41-83]

Three types of hydroxyl group are present in each CD glucose unit: one primary alcohol at the 6-position and two secondary ones at the 2- and 3-positions (Figure 1). The secondary hydroxyl groups are all located at the wider rim, called secondary face, whilst primary ones dot the narrower rim or primary face. Although substituting all hydroxyl groups of the same type, also called persubstitution, or only one of them is relatively easy,[84] differentiating between identical hydroxyl groups is much more challenging[85] as only a few methods have so far proven their efficacy, mostly for the synthesis of disubstituted[86-107] and trisubstituted species.[108-112]

The more challenging task of obtaining tetrafunctionalised species in a regioselective manner has been recently addressed by several groups.[113,114] For example, one-step diisobutylaluminum hydride (DIBAL-H) induced deprotections of perbenzylated[115] CDs have been employed to produce tetrafunctionalised α-, β- and γ-CDs in low to moderate yields, but with high regioselectivity.[116] Tetrafunctionalised α- and β-CDs are also accessible through multi-step syntheses involving two non-consecutive debenzylation steps.[117,118] In the case of perbenzylated species, deprotection usually takes place at the primary rim, although the O-3 positions of the secondary rim are also affected by C–O bond cleavage for the more sterically demanding perbenzylated α-CD.[119] On the other hand, permethylated β-CD undergoes tetrademethylation solely at the secondary rim.[120,121] Another strategy that has been applied to α-CD, consists of reacting the cyclic oligosaccharide with an excess of bulky monoalkylating agents such as trityl[122,123] or supertrityl chlorides,[124] thereby giving rise to tetrasubstituted species at the primary rim with good regioselectivity. Surprisingly, little attention has been paid to double capping reactions for targeting tetrasubstituted CDs since the early work of Tabushi, who relied on the use of rigid disulfonyl chlorides.[125,126] In the present chapter, we describe a short and convenient synthesis of a $6^A,6^B$:$6^D,6^E$ doubly-capped β-CD, which provides easy access to valuable $6^A,6^B,6^D,6^E$-functionalised β-CDs in gram-scale quantities. Capping methodology was also used for the preparation of new α- and β-CD-derived phosphanes, phosphane oxides, thioethers and sulfates.

II.2. Results and discussion

II.2.1. $6^A,6^B,6^D,6^E$-Tetrafunctionalisation of β-cyclodextrin

Our strategy for the preparation of A,B,D,E-tetrasubstituted β-CDs at the primary face is based on the use of a particular dialkylating reagent, namely "bis-trityl" dichloride **1** (Figure 2).

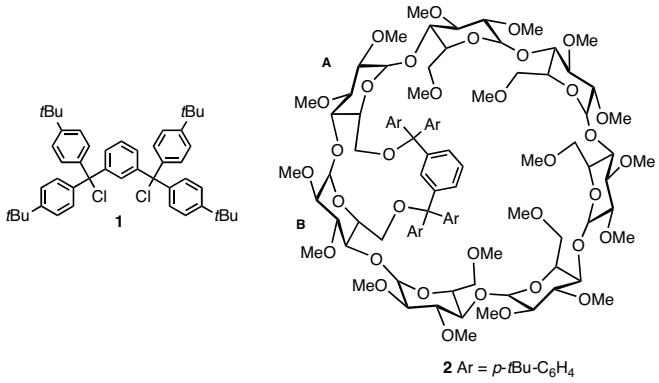

Figure 2. Bis-trityl dichloride **1** and $6^A,6^B$-capped β-CD derivative **2**.

As shown recently, alkylation of β-CD with one equivalent of **1** and subsequent methylation of the non-alkylated hydroxyl groups led to the A,B-capped CD **2**.[106] We anticipated that the use of two equivalents of **1** for the first alkylation step would lead regioselectively to a A,B:D,E doubly-capped β-CD, as a result of both the capacity of the difunctional reagent to strap adjacent glucose units and the steric bulk of the "bis-trityl" cap possibly preventing attachment of two distinct bis-trityl units onto adjacent sugar units. Thus, once A,B cap is formed, the second bis-trityl unit should either form a D,E or a E,F cap, both routes leading to the same regioisomer (Scheme 1).

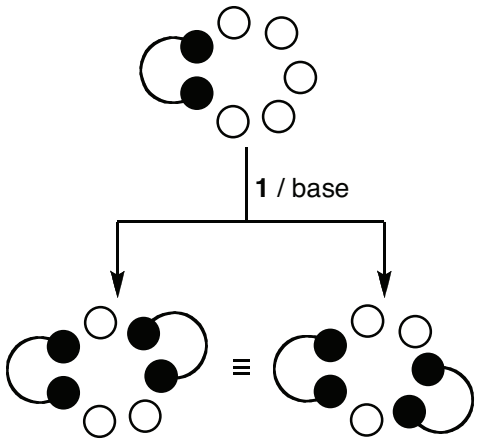

Scheme 1. Double capping strategy based on the use of the bulky reagent **1**.

In fact, doubly-capped **3** could be prepared in 50% isolated yield by reacting **β-CD** with two equivalents of "bis-trityl" dichloride **1**[106] in pyridine in the presence of 4-(*N,N*-dimethylamino)pyridine (DMAP) at 70ºC followed by methylation with NaH and MeI in *N,N*-dimethylformamide (DMF) (Scheme 2). Only one doubly-capped species was detected. The product was conveniently separated from over- and under-tritylated species as well as non-bridged species by standard column chromatography. Note that applying the same reaction conditions to the smaller **α-CD** were rather ineffective as they led to only very small amounts of doubly-capped compound. Clearly, only a wide enough macrocycle like the β-CD torus is able to accommodate *two* of such large handles.

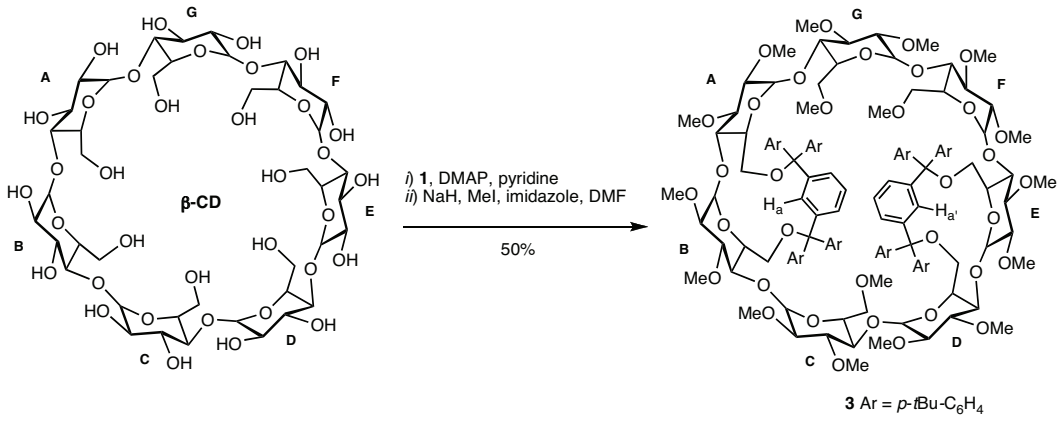

Scheme 2. Synthesis of the doubly-capped β-CD derivative **3**.

The formation of the doubly-capped **3** was inferred from its mass spectrum, which shows intense peaks at *m/z* = 2673.4 and 2657.4 with isotopic profiles exactly as expected for the $[M + K]^+$ and $[M + Na]^+$ ions, respectively. Proof for A,B,D,E-substitution came from a single crystal X-ray diffraction study on the phosphorus-containing CD **4** (*vide infra*), which is derived from **1**. The ^{1}H NMR spectrum of **3** displays 17 singlets for methyoxy groups, in agreement with the expected double cyclisation (Figure 3). It is worth mentioning here that the anomeric region of the ^{1}H NMR spectrum of **3** bears strong resemblance with the singly capped-CD **2**.[106] In particular, two low-field signals for the H_a and $H_{a'}$ protons of the central aromatic rings of the "bis-trityl" fragments at respectively δ = 7.61 and 7.72 ppm, are typical of non-dangling 6^A,6^B capping units.[106]

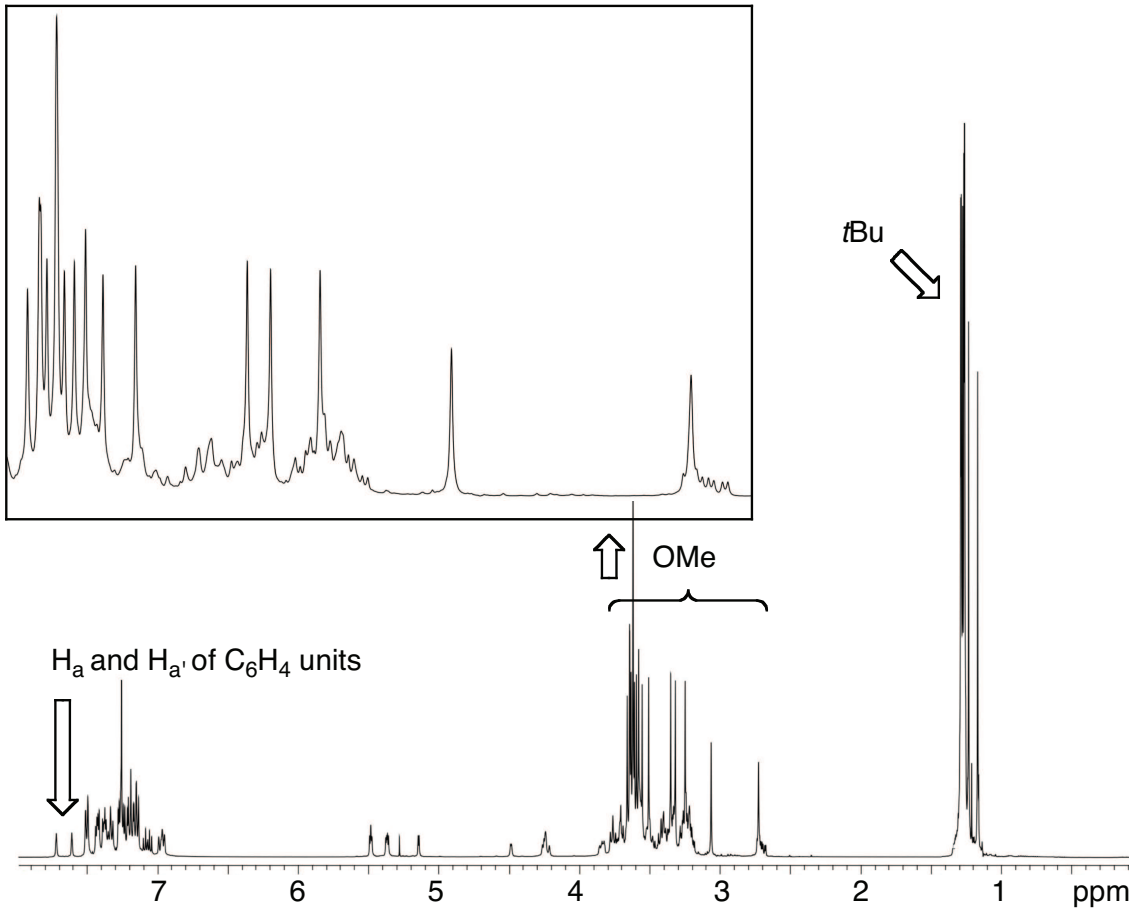

Figure 3. ^{1}H NMR spectrum of **3** recorded in $CDCl_3$ (500.1 MHz) and zoom showing the 17 singlets for the methoxy groups (top left).

The specific formation of A,B and D,E caps was deduced from a combination of ^{1}H-^{1}H COSY, ^{1}H-^{1}H TOCSY, ^{1}H-^{13}C{^{1}H} HMQC and ^{1}H-^{1}H ROESY experiments. Once the connectivity between the individual glucose units was established, 2D ^{1}H-^{1}H ROESY experiments unambiguously showed that some H-6 protons of neighbouring capped sugar units correlates with the central aromatic proton (H_a or $H_{a'}$) of the capping unit, this observation constituting the ultimate proof for A,B:D,E double capping (Figure 4 and Figure 5).

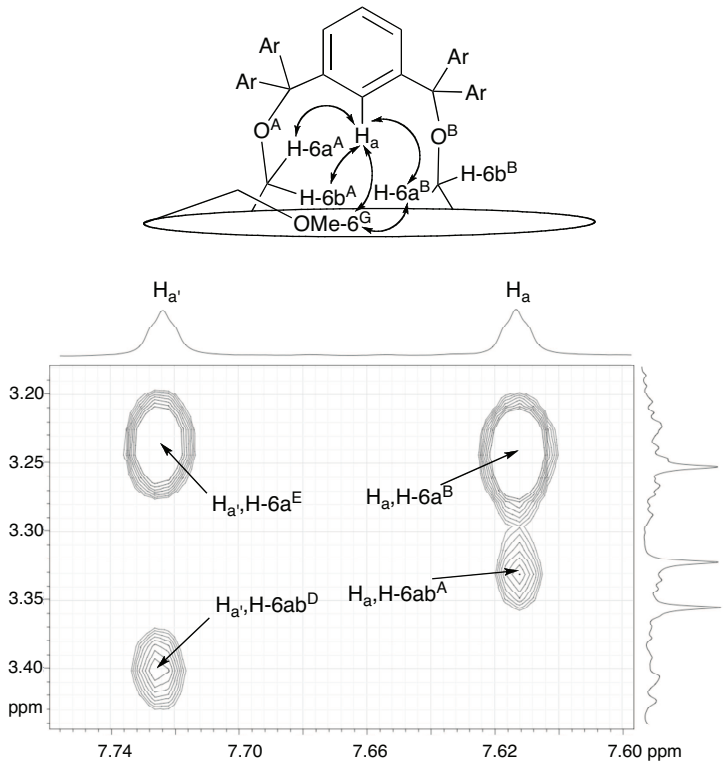

Figure 4. Part of the ^{1}H-^{1}H ROESY NMR spectrum of compound **3** recorded in $CDCl_3$ at 500.1 MHz. The drawing above the spectrum represents one of the two capping units (A,B). The arrows represent important through-space correlations involving the A,B cap. H_a and $H_{a'}$ represent the central, endo-oriented aromatic protons of each capping unit.

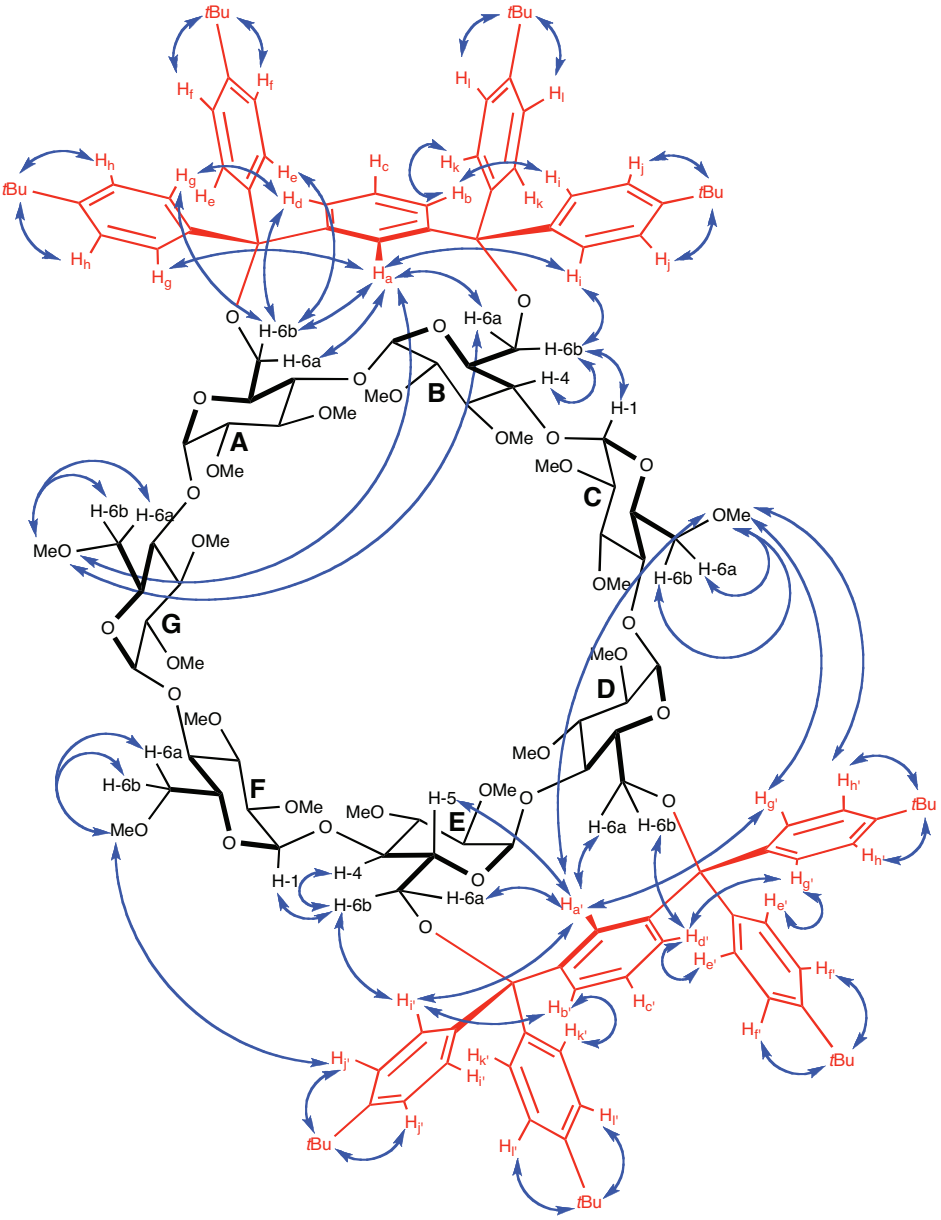

Figure 5. Assignment of selected ROESY cross peaks arising from through-space correlations between aromatic and some CD protons in **3**. View from the primary face.

II.2.2. β-Cyclodextrins capped with PPh^{2-} dianion

Recent studies on double capping of $6^A,6^B,6^D,6^E$-tetramesylated α-CD **5** with small phenylphosphide,[75,79] or very small sulfide dianions[77,78] showed that these cyclisation processes are highly regioselective, even regiospecific (since only adjacent glucose units were being bridged) in the case of the more sterically crowded phenylphosphide, towards $6^A,6^B:6^D,6^E$-double capped ligands **6** (**TRANSDIP**)[79] or **7**[77] (Figure 6).

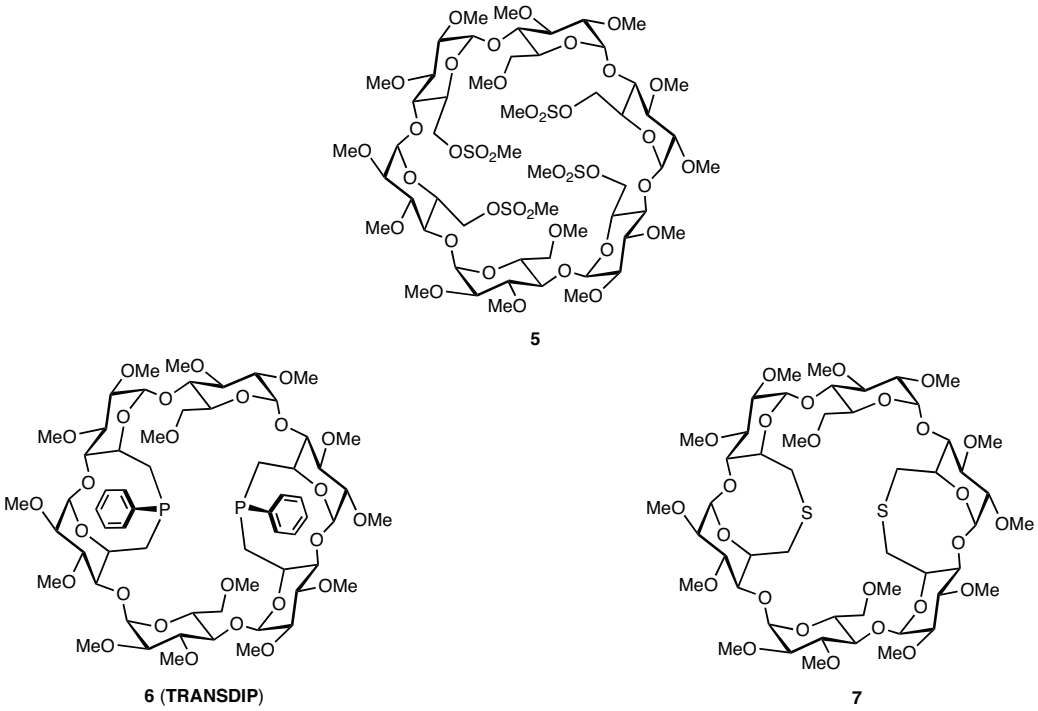

Figure 6. Some tetrafunctionalised permethylated α-CD derivatives.

The synthesis of $6^A,6^B:6^D,6^E$ doubly-capped **3** made it possible to access further double capping reactions on a β-CD scaffold. To that aim, we first prepared $6^A,6^B,6^D,6^E$-tetramesylated β-CD **9**, which was obtained in 96% yield from **3** after hydrolysis of the "bis-trityl" caps with aqueous HBF_4 in MeCN followed by reaction of the intermediate tetrol **8** with mehylsulfonylchloride (MsCl) in DMAP/pyridine (Scheme 3).

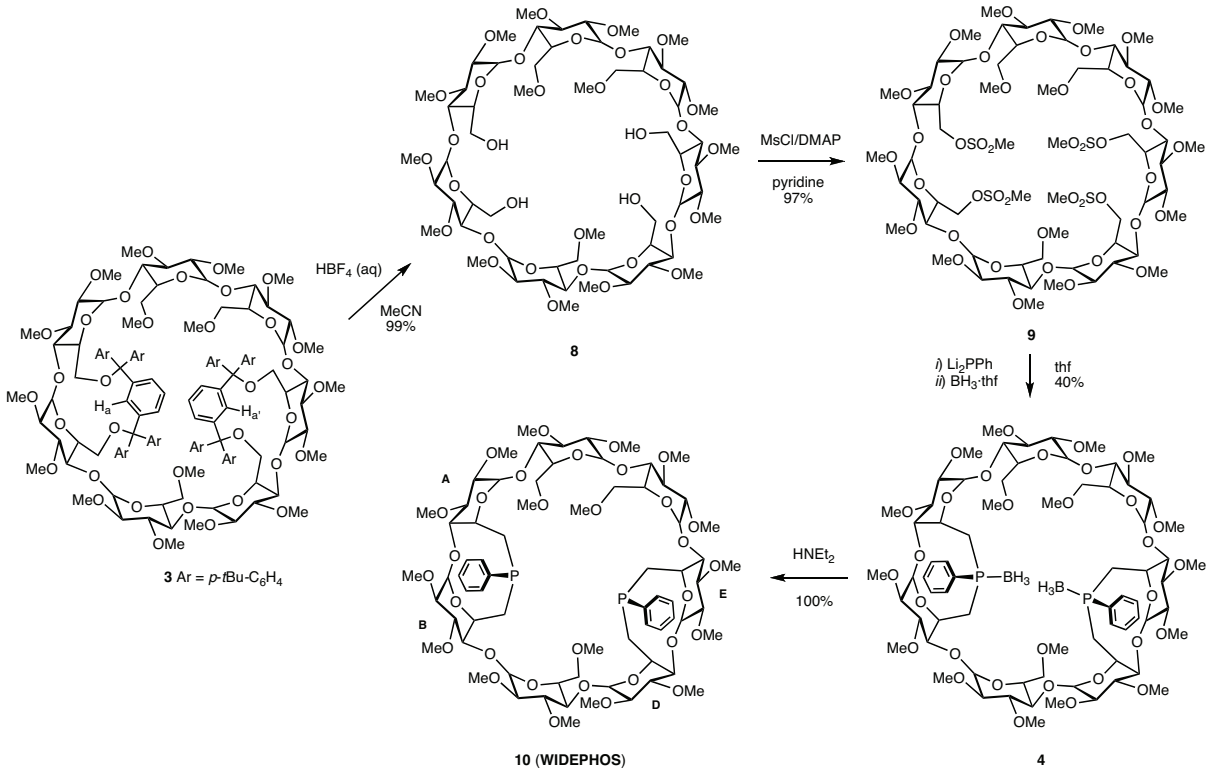

Scheme 3. Stepwise buildup of the $6^A,6^B$:$6^D,6^E$ doubly-capped diphosphane **10**.

Evidence for the cleavage of the capping units came from the presence of four triplets at respectively δ = 2.61, 2.68, 2.78 and 2.96 ppm in the ^{1}H NMR spectrum of **8** corresponding to the four non-equivalent hydroxyl protons. As in the latter compound, the ^{1}H NMR spectrum of tetramesylate **9** is in keeping with a C_1-symmetrical molecule (Figure 7).

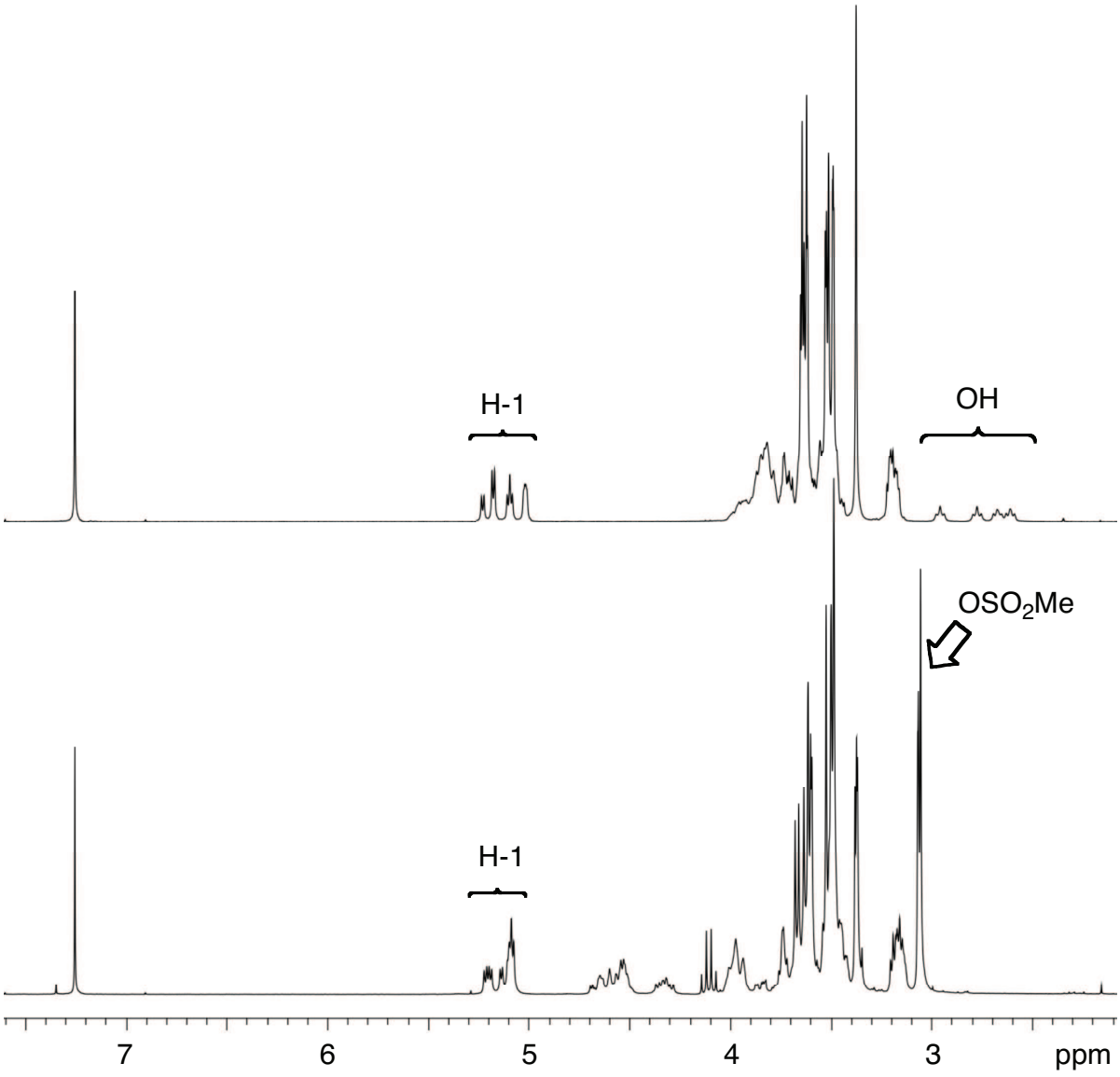

Figure 7. ^{1}H NMR spectra of **8** (top) and **9** (bottom) recorded in $CDCl_3$ at 300.1 MHz.

As expected, reaction of excess Li_2PPh (5 equiv.) in thf (thf = tetrahydrofuran) with **9** afforded the "introverted" diphosphane **10**, named **WIDEPHOS**, as the major product together with unidentified side products. The $^{31}P\{^{1}H\}$ NMR spectrum of the reaction mixture, recorded in C_6D_6, revealed that the side products were a mixture of several regioisomers (Figure 8), each of them possessing a capping PhP unit (–15.4 ppm < δ < –14.7 ppm) as well as a dangling PhPH unit (δ = –39.8 ppm for all regioisomers). The ^{1}H NMR spectrum of the mixture in $CDCl_3$ displays signals between δ = 5.55 ppm and 5.85 ppm that are in agreement with the presence of olefinic protons.

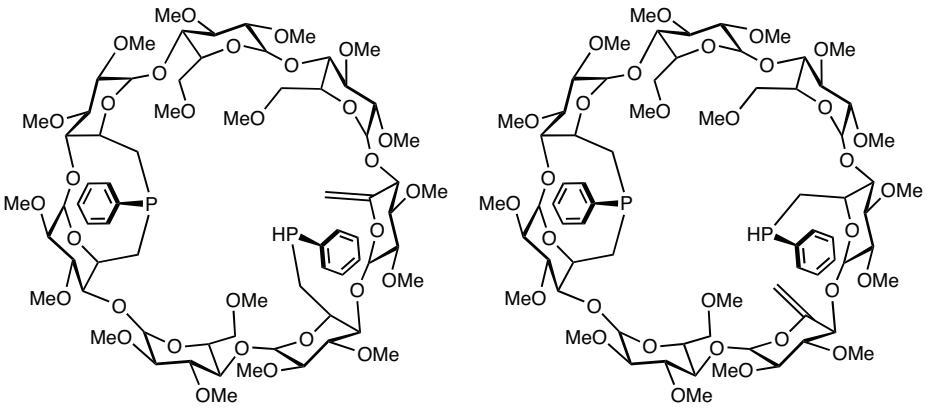

Figure 8. Some possible regioisomers produced when the phosphination of **9**.

In order to purify **WIDEPHOS**, the reaction mixture had to be treated with BH_3·thf to afford the protected diphosphane **4**, which was isolated in 40% overall yield from **9** after standard column chromatography (overnight-dried SiO_2). Removal of the BH_3 protecting groups was carried out quantitatively in boiling $HNEt_2$.[80] The $^{31}P\{^1H\}$ NMR spectrum of pure **WIDEPHOS**, recorded in C_6D_6, displayed two nearly identical singlets at respectively δ = –15.2 and –15.0 ppm, values that are typical of dialkylphenylphosphanes. However, in $CDCl_3$ the spectrum showed a unike peak at δ = –14.6 ppm because of the very similar electronical environment. The "introverted" character of **WIDEPHOS** was revealed by a $^{31}P\{^1H\}$-$^{31}P\{^1H\}$ COSY NMR experiment (Figure 9, left). Although the two non-equivalent phosphorus atoms are too wide apart for large enough $^{31}P\{^1H\}$-$^{31}P\{^1H\}$ through space coupling constants[127] to be observed directly, the $^{31}P\{^1H\}$-$^{31}P\{^1H\}$ COSY NMR spectrum displayed correlations between the two P signals, thus proving that the two phosphorus lone pairs temporarely overlap. Clearly, the only diastereomer in agreement with the previous observation is the one in which two phosphorus lone pairs face each other within the cavity. Interestingly, a rare $^{31}P\{^1H\}$-$^{13}C\{^1H\}$ through space spin coupling ($^{TS}J(PC\text{-}6^C)$ = 2.6 Hz) was observed between the C-6 atom of the non-bridged glucose unit C and one of the introverted P atoms (Figure 9, right).

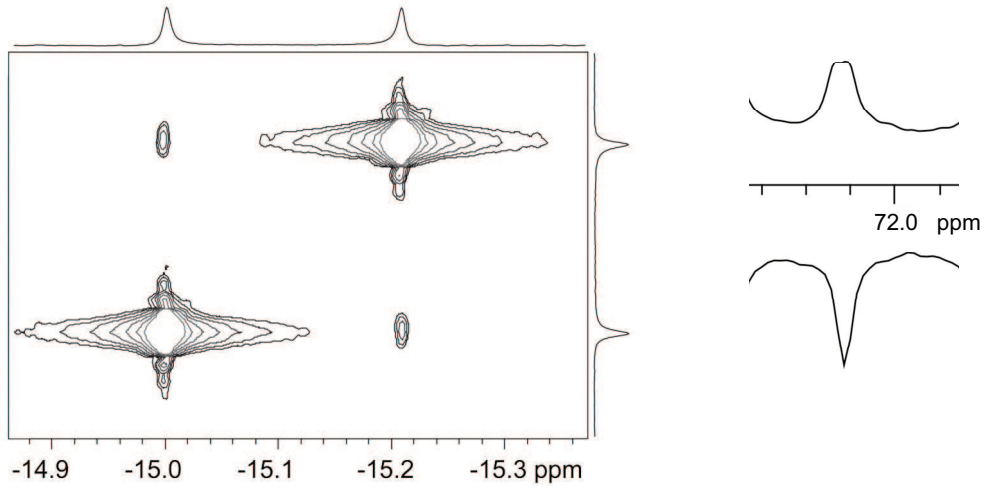

Figure 9. $^{31}P\{^{1}H\}$-$^{31}P\{^{1}H\}$ COSY NMR spectrum of **WIDEPHOS** recorded in C_6D_6 at 202.5 MHz (left). $^{13}C\{^{1}H\}$ NMR (top, right) and $^{13}C\{^{1}H,^{31}P\}$ NMR (bottom, right) spectra of **WIDEPHOS** in C_6D_6 at 125.8 MHz showing the C-6^C signal.

Note that despite its strong basicity, **WIDEPHOS** is difficult to oxidise with air, probably because access of oxygen to the buried phosphorus lone pairs is limited. The solid state structure of the phosphane-borane adduct **4** was determined by a single crystal X-ray diffraction study (Figure 10).

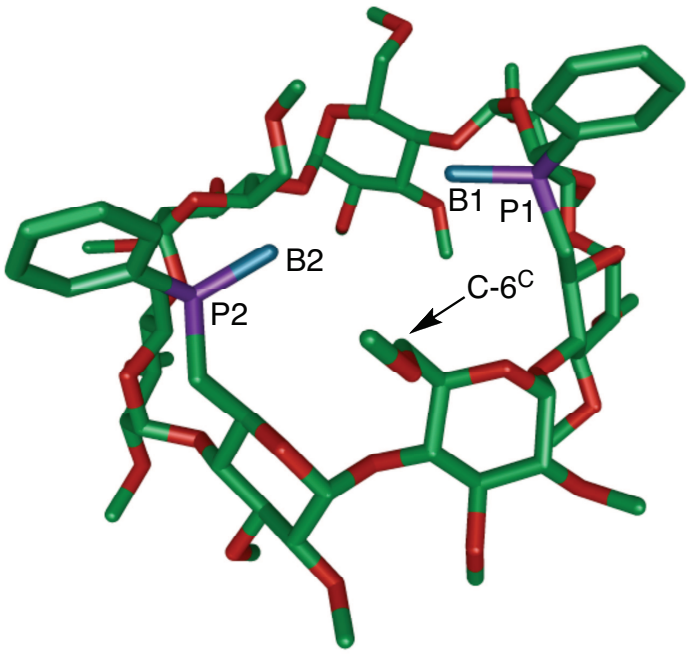

Figure 10. X-ray structure of the borane-diphosphane adduct **4** (top view). For clarity, the solvent molecules have been omitted. Important distances [Å]: P(1)···P(2) 8.23; B(1)···B(2) 4.67; B(2)···C-6^C 3.66; P(2)···C-6^C 4.72.

This study confirmed the capping of adjacent A,B as well as D,E glucose units. The cavity, which hosts a molecule of pentane, has a familiar circular shape, all the glucose units adopting the standard $^4C_1$ conformation. Both P–B vectors are almost perpendicular to the axis that runs through the middle of the cavity and point towards its centre. They are not aligned because of the non-symmetrical nature of the molecule (angle between the P–B vectors = 146.5º). The P(1)···P(2) distance (8.23 Å) is rather large compared to that observed in **TRANSDIP** (4.7 Å as calculated in the X-ray structure of a *trans*-chelate palladium dichloride complex).[79] Moreover, the BH_3 protecting groups, which tend to repel each other, undoubtedly increase the P···P separation. We note also that one of the phosphorus atoms is in relatively short distance with the C-6 atom of the neighbouring glucose unit C (P(2)···C-6^C distance: 4.72 Å). This finding is consistent with the existence of a through space spin coupling between these two nuclei in **WIDEPHOS**. The observed absence of deformation comes to no surprise since all the anomeric CD protons resonate within a narrow range ($\Delta\delta$ = 0.2 ppm) in the ^{1}H NMR spectrum of **4** (Figure 11).[55]

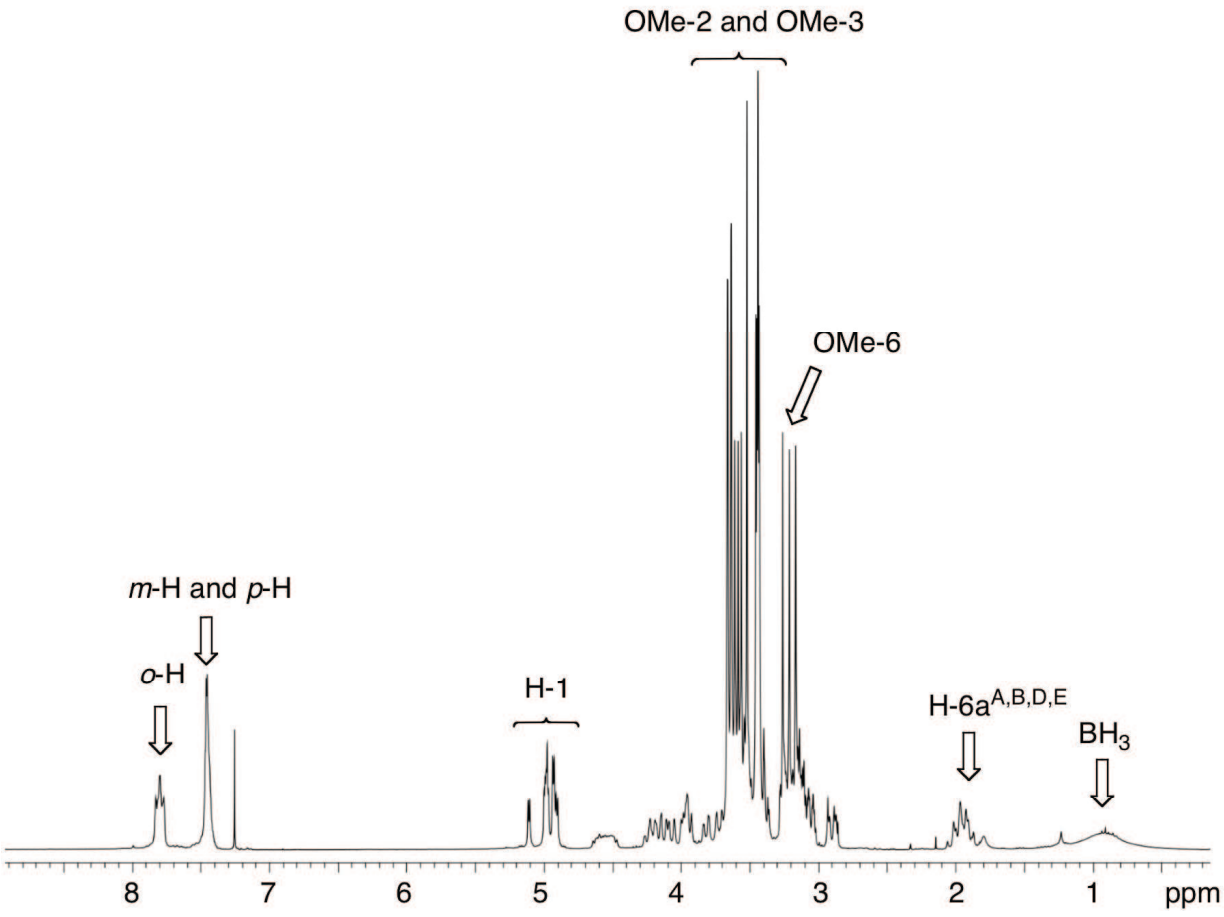

Figure 11. ^{1}H NMR spectrum of diphoshane-borane **4** recorded in $CDCl_3$ at 300.1 MHz.

Attempts were made to improve the synthesis of **WIDEPHOS** by varying the solvents (toluene, heptane) and temperature (–78ºC, –40ºC, 25ºC, 50ºC and 110ºC) of the capping reaction, to no avail as the composition of the reaction mixture varied little. Note that the first cyclisation is probably quantitative as observed for the synthesis of monophosphane **12**, which was obtained from dimesylate **11**[97] according to Scheme 4. Oxidation of **12** in air into the corresponding phosphane oxide **13** occurs readily, in contrast to that of **WIDEPHOS**. For storage purposes, **12** is best converted into the borane adduct **14** (Figure 12).

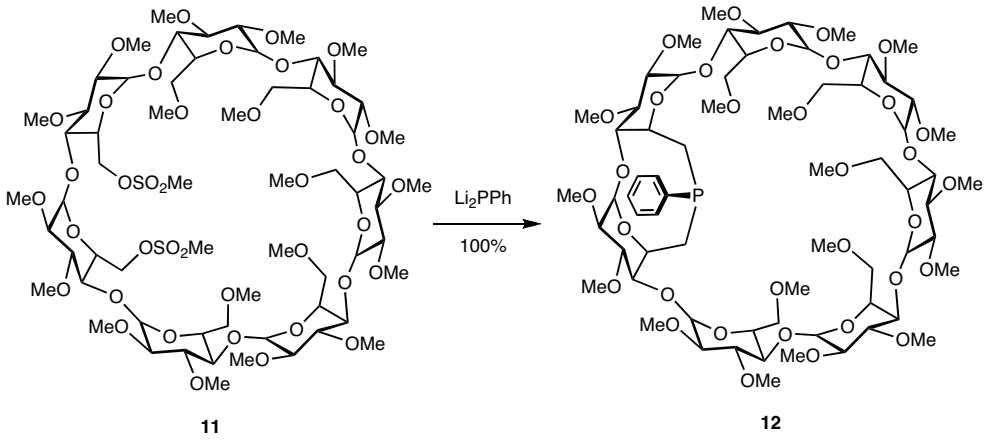

Scheme 4. Synthesis of the $6^A,6^B$-capped monophosphane **12**.

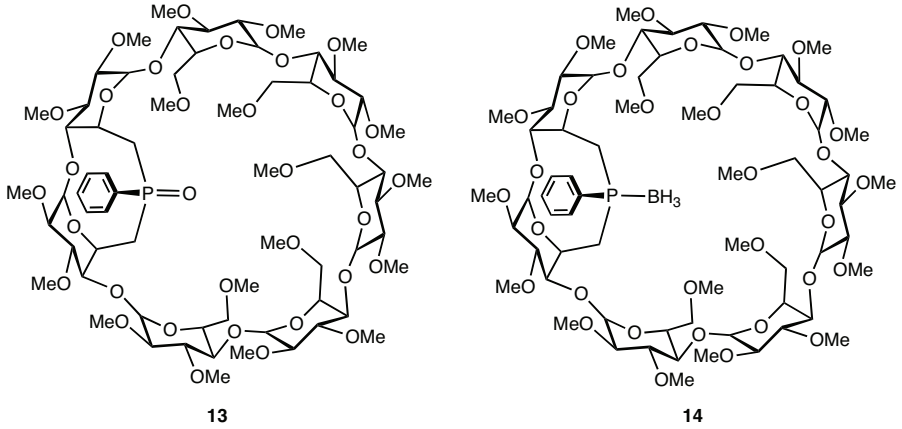

Figure 12. Compounds **13** and **14**.

As for the α-CD series,[75] the same capping reaction did not proceed as smoothly with CDs having mesylated glucose units further apart. Indeed, the A,C-dimesylate **15**[128] reacted with Li_2PPh to afford phosphane-borane adduct **17** in only 35% overall yield after quantitative protection of the cyclisation product **16** with borane. Even if the

A,C-monophosphane **16** is less sensitive to oxidation than **12**, probably because its phosphorus lone pair is more deeply buried in the cavity, phosphine protection was necessary for purification purposes. Analytically pure phosphane **16** was recovered quantitatively upon treating **17** with boiling $HNEt_2$ (Scheme 5).

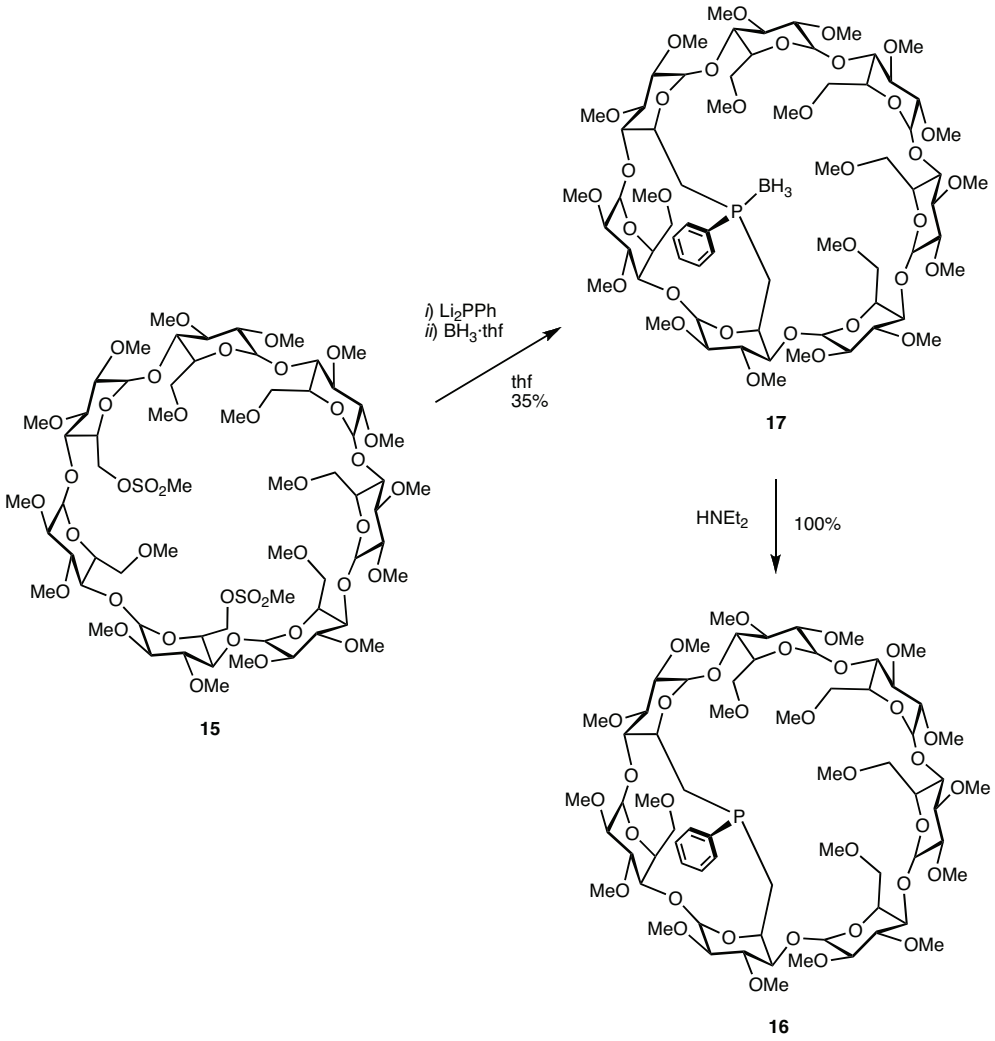

Scheme 5. Synthesis of the $6^A,6^C$-capped monophosphane **16**.

In keeping with a heavily distorted torus, the ^{1}H NMR signals corresponding to the anomeric H-1 protons of **16** are much more widespread ($\Delta\delta$ = 1.12 ppm) that those of its A,B-analogue **12** ($\Delta\delta$ = 0.24 ppm, Figure 13).

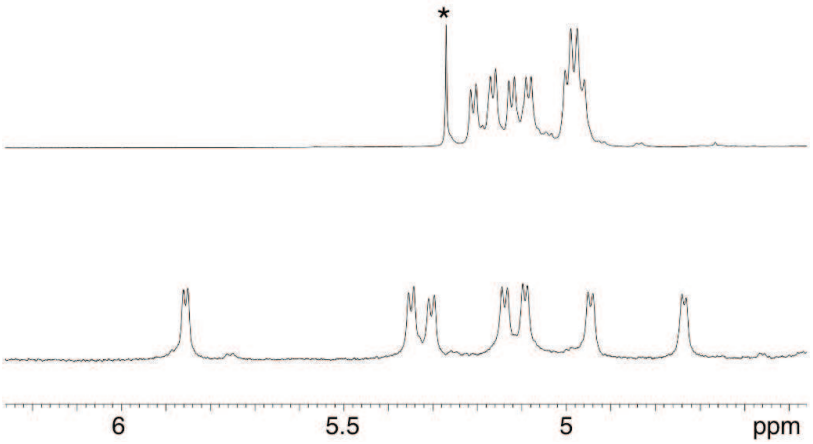

Figure 13. Anomeric regions in the ^{1}H NMR spectra of monophoshanes **12** (top) and **16** (bottom) recorded in $CDCl_3$ at 300.1 MHz. Asterisk denotes residual CH_2Cl_2.

The $^{31}P\{^{1}H\}$ NMR spectrum of A,C-monophosphane **16** consists of a singlet at δ = –17.3 ppm, slightly downfield shifted compared to its A,B-counterpart. Again, a similar trend has been observed for the α-CD series (**18** and **19**, Figure 14).[75]

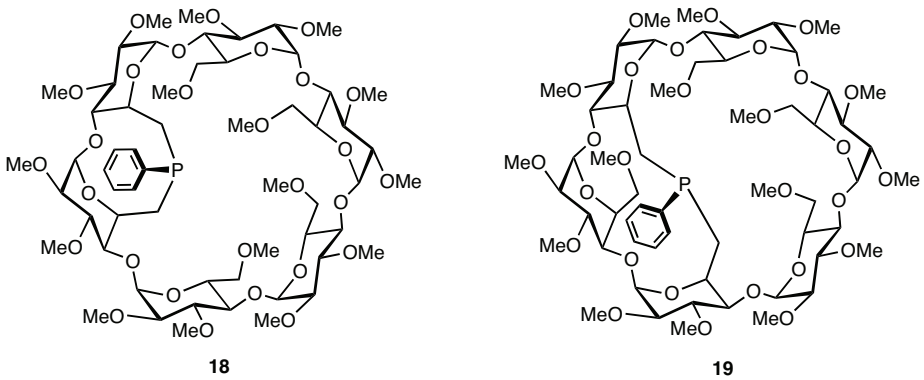

Figure 14. Introverted A,B- and A,C-monophosphanes **18** and **19** based on permethylated α-CDs.

Monophosphanes derived from α-CD such as **18** and **19** were obtained as single stereoisomers. In these introverted ligands, the phenyl ring is located outside the cavity whereas the phosphorus lone pair points towards the cavity interior. Unlike its smaller relative, the β-CD cavity in monophosphanes **12** and **16** is large enough for accommodating a phenyl ring,[129] so that the formation of a stereoisomer with opposite configuration at phosphorus cannot be ruled out. In order to determine the exact configuration of the new phosphorus stereocentre in **12** and **16**, both ligands were reacted with 0.5 equivalents of $[(o\text{-}C_6H_4CH_2NMe_2)PdCl]_2$ (Scheme 6) to afford quantitatively palladium complexes **20** and

21, respectively. Both complexes gave rise to singlets at δ = 25.5 and 15.3 ppm, respectively, in ^{31}P NMR spectroscopy. Their mass spectra revealed the presence of intense peaks at *m/z* = 1774.27 and 1714.67 with the expected isotopic profiles for $[M + Na]^+$ and $[M - Cl]^+$ ions.

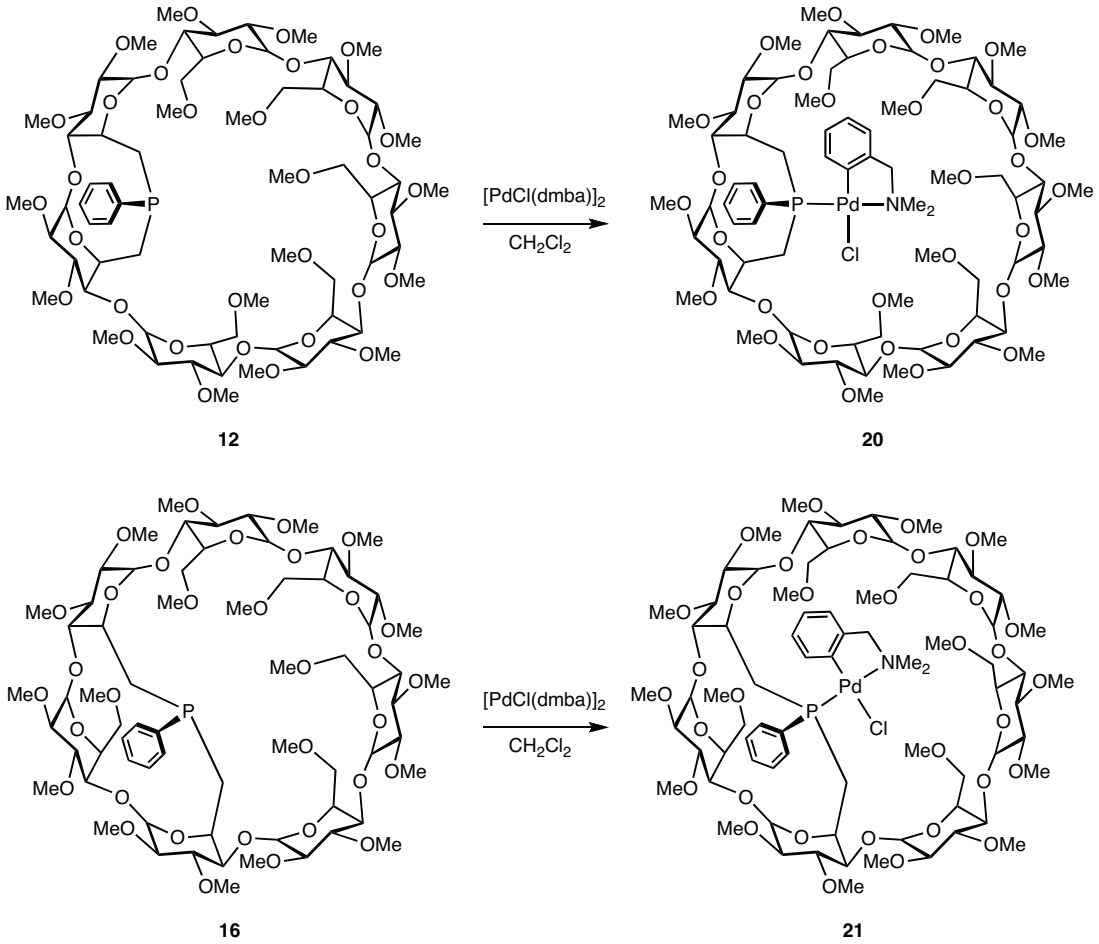

Scheme 6. Synthesis of the introverted complexes **20** and **21**. dmba = *o*-$C_6H_4CH_2NMe_2$.

Interestingly, the H-5 protons of glucose units A and B in **12** undergo an important downfield shift upon complexation ($\Delta\delta$ = 0.7 ppm, Figure 15), revealing the likely presence of a chloridopalladium unit inside the CD cavity in the corresponding complex.[72] On the contrary, no such downfield shifts were detected for ligand **16**. However, 2D ^{1}H-^{1}H ROESY experiments performed on both complexes **20** and **21** unequivocally confirmed metal encapsulation in both cases as strong correlations between the NMe_2 group and several primary face CD protons (H-6 and OMe-6) were revealed. In contrast, no correlations involving phenyl and inner-cavity H-3 or H-5 protons were observed, thus excluding the inclusion of the phenyl group.

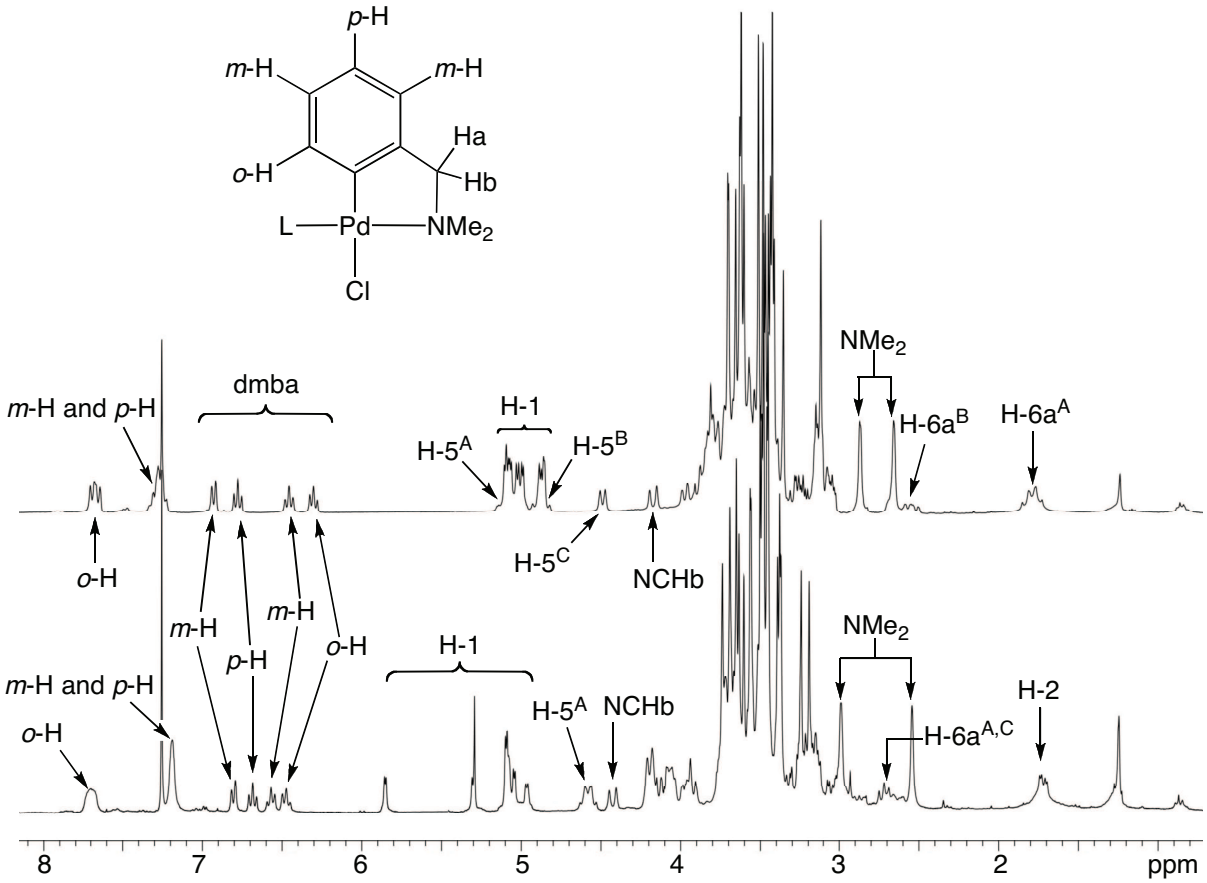

Figure 15. ^{1}H NMR spectrum of complexes **20** (top) and **21** (bottom) recorded in $CDCl_3$ at 300.1 MHz.

All in all, these data are consistent with a stereospecific capping process in which the diatereoisomer being produced is always the one with an introverted phosphine, no matter the size of the cyclodextrin torus. It is likely that privileged conformations within the reacting glucose units are responsible for this outcome (Scheme 7).

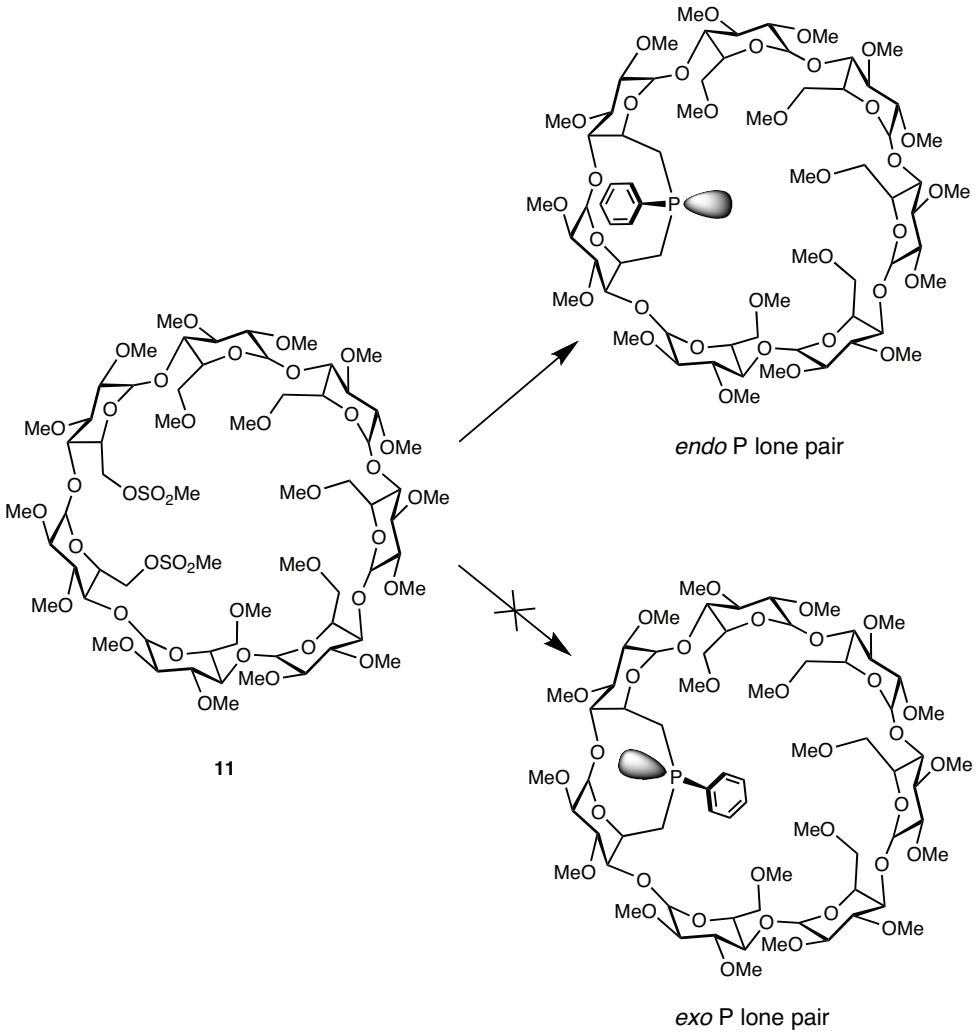

***Scheme** 7*. Possible stereoisomers resulting from capping dimesylate **11** with "PPh^{2-}" phenylphosphide dianion.

II.2.3. β-Cyclodextrins capped with S^{2-} dianion

Aiming at double capping reactions involving a dianion smaller than the crowded phenylphosphide, we also decided to synthesise the β-CD version of **7**. Treatment of tetramesylate **9** with the small sulfide dianion in acetone in the presence of 18-crown-6 gave the expected $6^A,6^B$:$6^D,6^E$-sulfur-capped CD **22** in 50% isolated yield (Scheme 8). The ESI mass spectrum of **22** confirmed the formation of a doubly-capped species, as revealed by the presence of a unique peak at *m/z* = 1391.6 corresponding to the $[M + Na]^+$ ion.

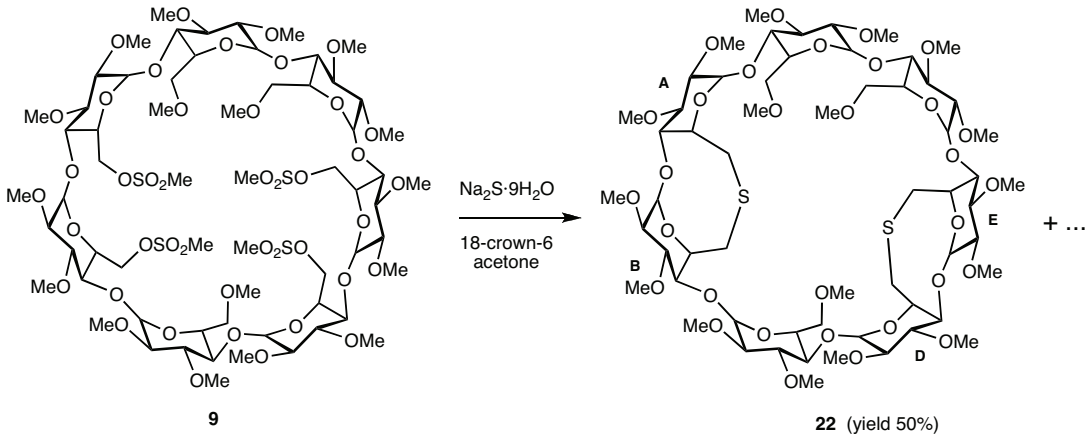

9 **22** (yield 50%)

Scheme 8. Synthesis of the double sulfur-capped species **22**.

As for the phosphinidene-capped derivative **10**, the ^{1}H NMR spectrum of **22** is in agreement with an overall circular CD torus, all anomeric protons lying in a narrow range ($\Delta\delta$ = 0.24 ppm). Again, ^{1}H-^{1}H COSY, ^{1}H-^{1}H TOCSY, ^{1}H-^{13}C{^{1}H} HMQC and ^{1}H-^{1}H ROESY experiments recorded at 500.1 MHz were used to establish the molecular structure of compound **22**.

In particular, these experiments allowed unambiguous identification of the C-6 atoms linked to a sulfur atom and the corresponding H-6 atoms. S-capping of the A and B units was inferred from 2D ^{1}H-^{1}H ROESY experiments (Figure 16) showing the spatial proximity between the H-6a proton of glucose unit A and the H-5 proton of the neighbouring glucose unit B. The same H-6a^{A} proton correlates also with the vicinal H-5^{A} proton. The observation of *both* correlations is only consistent with proximal S-capping. The same type of correlations were observed within the other pair of capped glucose units, namely D and E (Figure 17).

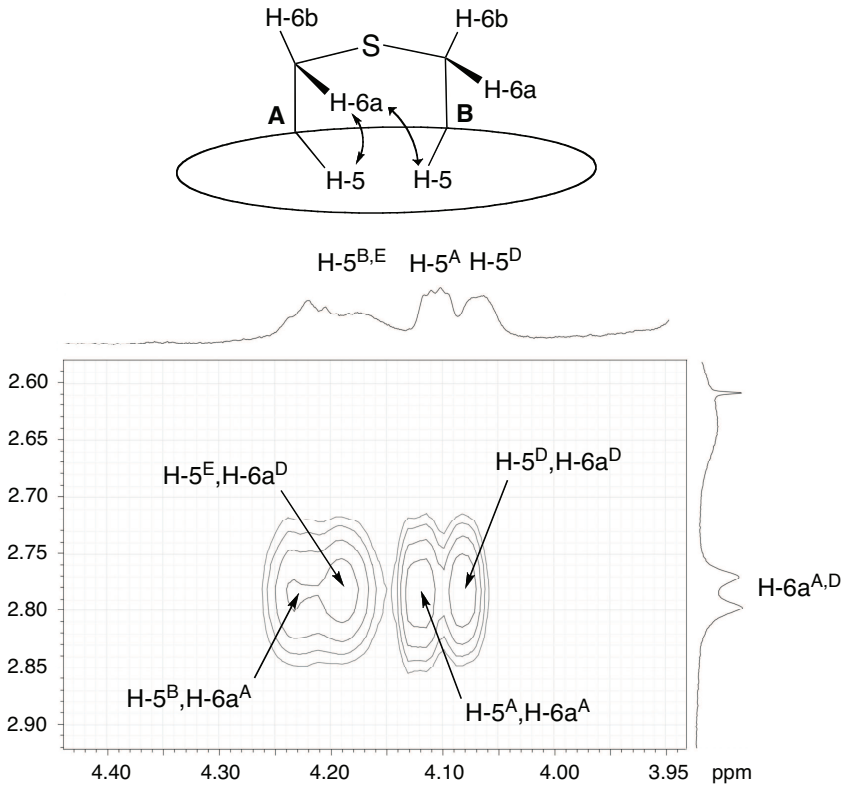

Figure 16. Part of the 2D ^{1}H-^{1}H ROESY NMR spectrum of compound **22** recorded in $CDCl_3$ at 500.1 MHz. The drawing above the spectrum shows one of the two capping units (A,B). The arrows represent through-space correlations involving the A,B cap.

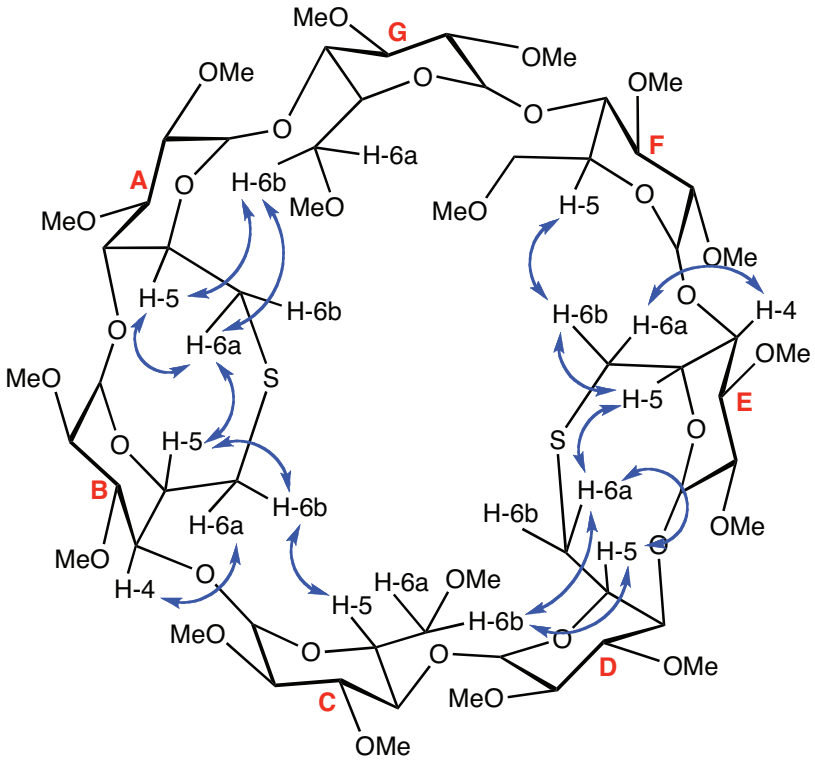

Figure 17. Assignment of selected ROESY cross peaks arising from through-space correlations between CD protons of **22**.

Careful examination of the ^{1}H NMR spectrum of **22** further revealed a broadening of some H-6a, H-6b, H-5, and H-1 signals belonging to capped glucose units, suggesting rapid conformational mobility of the capped glucose residues. Such a feature has previously been detected in another $6^{A},6^{B}$-sulfide-capped methylated β-CD, but not in its $6^{A},6^{C}$-regioisomer,[128] nor in smaller α-CD analogues such as **7**. It should be mentioned here that beside **22** a minor product was formed (**23**) that could not be isolated, to which we tentatively assign a A,C:D,G doubly-capped structure (Figure 18).

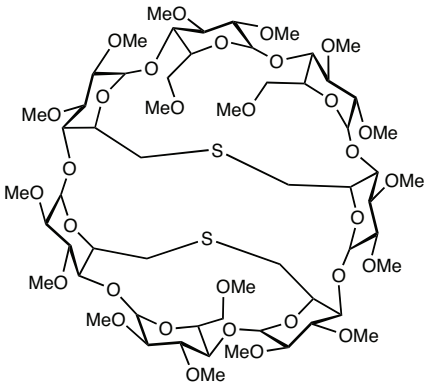

23

Figure 18. Proposed molecular structure for compound **23**.

This structural assignement is based on the mass spectrum of **23** as well as its ^{1}H NMR spectrum, in which the signals of the anomeric protons are much more widespread ($\Delta\delta$ = 0.93 ppm) than those of **22**, reflecting a significant shape distortion of the macrocyclic core brought about by the A,C:D,G double capping (Figure 19).

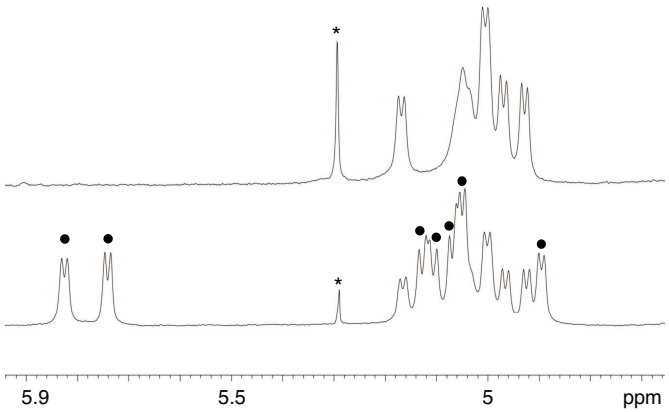

Figure 19. Anomeric regions in the ^{1}H NMR spectra in $CDCl_3$ recorded at 300.1 MHz of compounds **22**(top) and **23** in presence of 40% of **22** (bottom). Peaks marked with dots belong to **23** and asterisks denote residual CH_2Cl_2.

II.2.4. α- and β-Cyclodextrins capped with two sulfate moieties

Bols *et al*. recently managed to cap benzylated α- and β-CDs with a sulfate unit linking the C-6^A and C-6^D carbon atoms in order to study the latter nucleophilic attack on these positions, which turned out to be exclusively in the C-6^A atom.[130] Double capping of methylated α- and β-CD scaffolds with sulfate units can also be achieved, provided Bols's reaction conditions are modified. Indeed, both tetrols **24**[124] and **8** react with thionyl chloride in CH_2Cl_2 and NEt_3 at low temperature (–78ºC) to give a mixture of diastereomeric cyclic disulfites, the corresponding mass spectra displaying in each case a single signal for the corresponding $[M + Na]^+$ cation. Purification of these mixtures was not necessary, as in each case a single product was formed after oxidation with $RuCl_3$ and $NaIO_4$, namely disulfate **25** and **26** (Scheme 9).

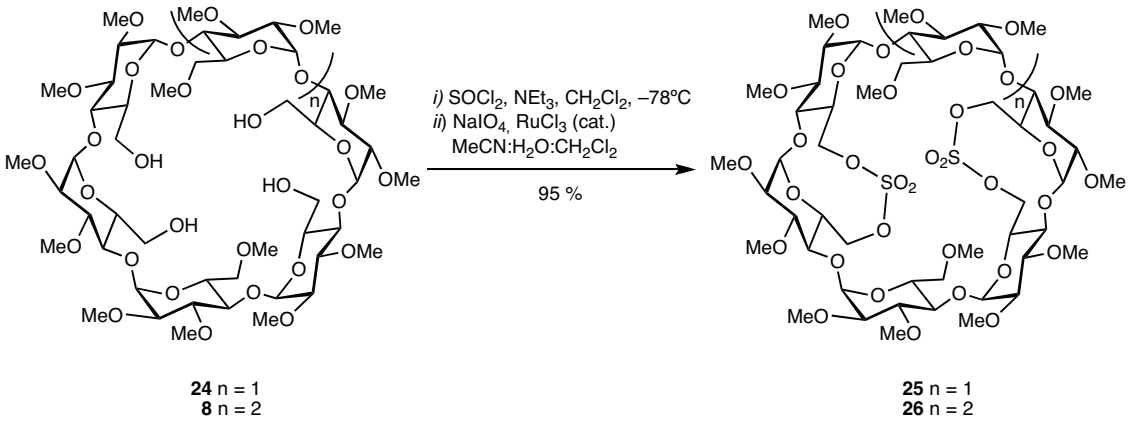

Scheme 9. Synthesis of the disulfate doubly-capped compounds **25** and **26**.

Remarkably, for both α- and β-CD disulfates the overall yield was virtually quantitative (95%). Only the use of a base and a reaction mixture kept at low temperature allowed reaching this level of regioselectivity for these cyclisations.

The regioselectivity of the reaction leading to **25** was unambigously established by a single crystal X-ray diffraction study on this disulfate (Figure 20).

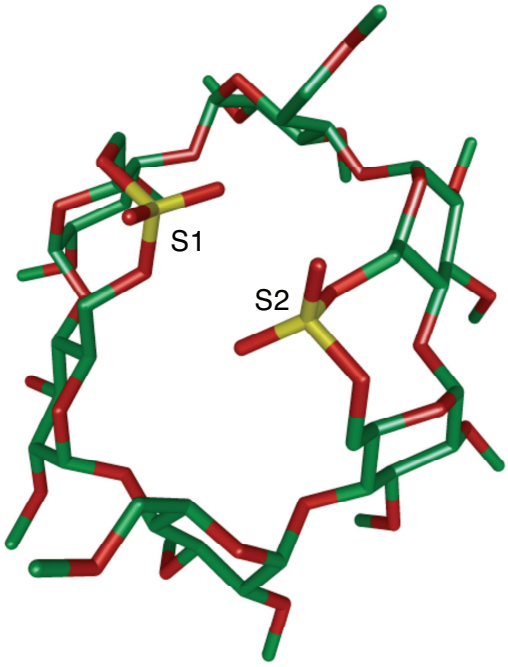

Figure 20. X-ray structure of disulfate doubly-capped derivative **25**. For clarity, the solvent molecules which are each hydrogen-bonded to a sulfate oxygen atom have been omitted. Important distance [Å]: S(1)···S(2) 4.01.

Interestingly, the two sulfate caps of **25**, which link the A,B and D,E glucose units respectively, are intertwined so as to block the cavity entrance. As for doubly-capped CD **4**, the CD macrocycle hosts a molecule of pentane and comprises glucose units having all undistorted standard $^4C_1$ conformations. However, the ones that are being capped (A,B:D,E) are tilted towards the cavity interior. The cavity adopts a slightly elongated shape, the longest O(4)–O'(4) distance being 8.95 Å, and the shortest one 8.00 Å. Careful analysis on the X-ray structure of **25** shows that the C-6^B carbon atom appears more sterically hindered because of the proximity of several hydrogens, specially H-4^B and H-1^C protons, remaining the C-6^A carbon atom more accessible for nucleophilic attacks (the same feature was observed in the D,E cap). Thus, opening a new way for tridifferentiating CDs.

The capping mode in **26** was established by NMR analysis. In keeping with caps involving neighbouring glucose units, the H-1 protons of **26** resonate within a narrow range of chemical shifts ($\Delta\delta$ = 0.3 ppm vs. 0.15 ppm for **25**, Figure 21), in agreement with the presence of undistorted glucose units.

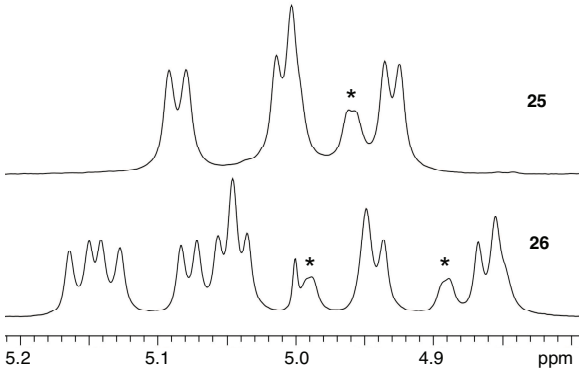

Figure 21. Partial view of the ^{1}H NMR spectra in $CDCl_3$ recorded at 300.1 MHz of compounds **25** (top) and **26** (bottom), showing the anomeric protons (H-1). Asteriks denote H-$6^{A,D}$ protons.

Again, full structural characterisation was achieved through combined ^{1}H-^{1}H COSY, ^{1}H-^{1}H TOCSY, ^{1}H-$^{13}C\{^{1}H\}$ HMQC and ^{1}H-^{1}H ROESY studies (Figure 22). As for disulfide capped **22**, ROESY cross peaks arising from through-space correlations between the H-6a proton of capped glucose unit A and two H-5 protons, namely H-5^{A} and H-5^{B}, unequivocally establish proximal capping. Similar correlations could be seen between a H-6a atom of capped glucose D and H-5^{D} and H-5^{E}. Interestingly, the 2D ^{1}H-^{1}H ROESY NMR spectrum also showed a spatial proximity between the H-6b proton of glucose unit A and H-6a of glucose unit B, suggesting a high degree of flexibility of the AB cap.

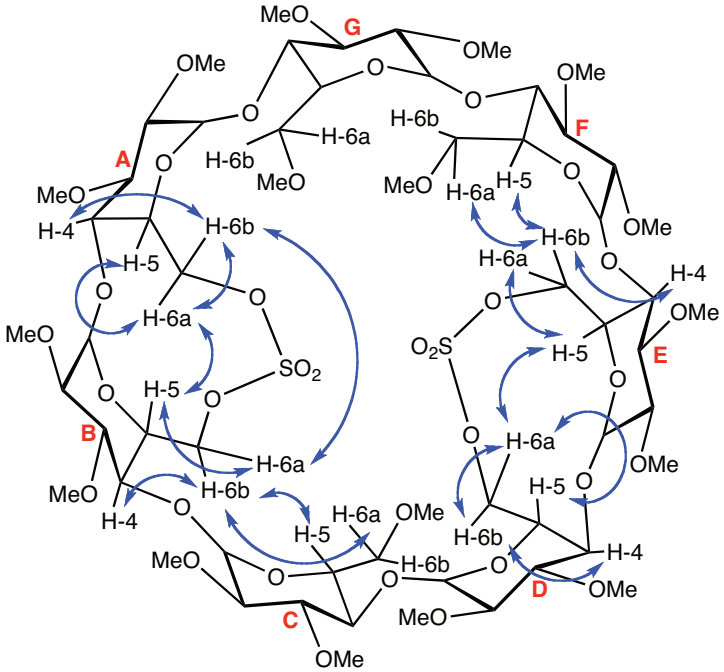

Figure 22. Assignment of selected ROESY cross peaks arising from through-space correlations between CD protons in **26**.

II.3. Conclusion

We have shown that double capping is a powerful mean of tetrasubstituting native β-CD, as well as for introducing useful functionalities on methylated CDs. The diphosphane **10** (**WIDEPHOS**) as well as monophosphanes **12** and **16** are the first examples of introverted phosphanes built on a β-CD scaffold. Alongside disulfide **22**, they constitute a new class of ligands designed for metal encapsulation and intra-cavity catalysis. The coordination of metal fragments of various sizes within their large chiral cavity will be explored in the following chapters together with some of their catalytic properties. In addition, cyclic sulfates **25** and **26** constitute promising starting materials for the tridifferentiation of permethylated α- and β-CDs, in particular as regards the synthesis of CD-based heterotetradentate ligands.

II.4. Experimental section

II.4.1. General procedures

All manipulations were performed in Schlenk-type flasks under dry nitrogen. Solvents were dried by conventional methods and distilled immediately prior to use. $CDCl_3$ was passed down a 5 cm-thick alumina column and stored under nitrogen over molecular sieves (4 Å). Routine ^1H and $^{13}C\{^1H\}$ spectra were recorded with Bruker FT instruments (AVANCE 300, 500, and 600 spectrometers). ^1H NMR spectral data were referenced to residual protiated solvents (δ = 7.26 ppm for $CDCl_3$ and δ = 7.16 ppm for C_6D_6), $^{13}C\{^1H\}$ chemical shifts are reported relative to deuterated solvents (δ = 77.00 ppm for $CDCl_3$ and δ = 128.06 ppm for C_6D_6) and the $^{31}P\{^1H\}$ NMR data are given relative to external H_3PO_4. Mass spectra were recorded either on a ZAB HF VG analytical spectrometer using *m*-nitrobenzyl alcohol as matrix or on a Bruker MicroTOF spectrometer (ESI) using CH_2Cl_2, MeCN or MeOH as solvent. Elemental analyses were performed by the Service de Microanalyse, Institut de Chimie, Strasbourg. Melting points were determined with a Büchi 535 capillary melting-point apparatus. All commercial reagents were used as supplied. 1,3-bis[bis(4-*tert*-Butylphenyl)chloromethyl]benzene (**1**),[106] A,B-dimesylate **11**,[97] A,C-dimesylate **15**,[128] α-tetrol **24**[124] and $[PdCl(o\text{-}C_6H_4CH_2NMe_2)]_2$[131] were synthesised according to literature procedures. The numbering of the atoms within a glucose unit is as follows:

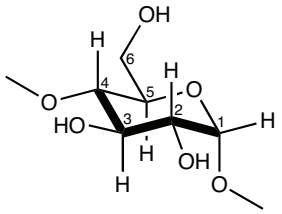

II.4.2. General procedure for full assignment in cyclodextrins

Our strategy for full structural assignment began with the differentiation between capped and non-capped C-6 carbon atoms by DEPT 135. These appear as two distinct sets of signals. The H-6 protons could then be identified using ^{1}H-$^{13}C\{^{1}H\}$ HMQC (Heteronuclear Multiple Qantum Coherence spectroscopy). By using ^{1}H-^{1}H TOCSY (TOtal Correlation SpectroscopY) and COSY (COrrelated SpectroscopY), each H-6 proton was correlated to the set of protons belonging to the same glucose residue. The connectivity between individual glucose units was then established via a ^{1}H-^{1}H ROESY (Rotating frame Overhause Effect SpectroscopY) experiment showing the proximity between H-4^{N} and H-1^{N+1} protons (N and N+1 standing for neighbouring glucose moieties labeled in the alphabetical order).[132]

In the case of **3** a ^{1}H-^{1}H ROESY experiment unambiguously showed that some H-6 protons of neighbouring capped sugar units correlate with the central aromatic proton (H_a or $H_{a'}$) of the capping unit, this observation constituting the ultimate proof for A,B:D,E double capping.

For **22** and **26**, which lack hydrogen atoms in their capping units, the corresponding ^{1}H-^{1}H ROESY spectra revealed the spatial proximity between H-$6a^{A}$ and vicinal H-5^{A} as well as H-5^{B}. Similar correlations were observed for glucose units D and E. Molecular models show that the simultaneous observation of both types of correlations are only compatible with A,B:D,E capped species and not regioisomeric A,C:D,G ones. In particular, if A,C:D,G regioisomers were formed, no H-$6a^{A}$,H-5^{A} correlations should show up. Note also that in compounds **22** and **26** the H-1 protons lie in a very narrow range, in keeping with a non-distorted CD. Molecular models further revealed that A,C:D,G doubly-capped CDs containing "SO_4" or "S" linkers (such a structure has been proposed for **23**) are strongly distorted, this deformation being expected to produce widespread H-1 signals.

II.4.3. Synthesis of compounds

$6^A,6^B,6^D,6^E$-Tetra-*O*-bis{benzene-1,3-bis[bis(4-*tert*-butylphenyl)methyl]}-$2^A,2^B,2^C,2^D,2^E,2^F,2^G,3^A,3^B,3^C,3^D,3^E,3^F,3^G,6^C,6^F,6^G$-heptadeca-*O*-methyl-β-cyclodextrin (3)

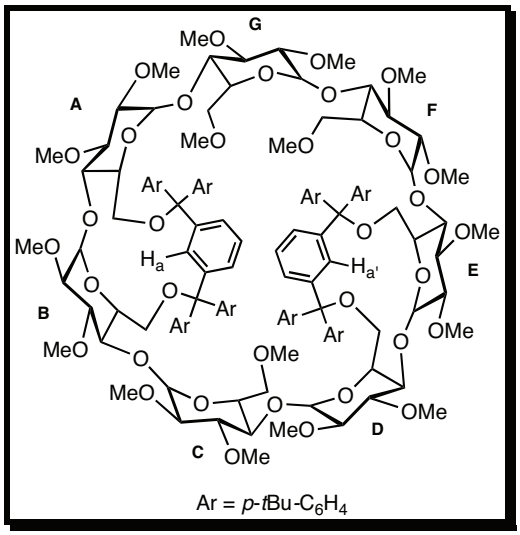

1,3-bis[bis(4-*tert*-butylphenyl)chloromethyl]benzene **1** (5.42 g, 7.7 mmol) was added to a solution of **β-CD** (3.97 g, 3.5 mmol) and DMAP (0.51 g, 4.2 mmol) in pyridine (90 mL). The reaction mixture was stirred at 70ºC for 12 h before being cooled down to room temperature. Pyridine was then removed *in vacuo*. Addition of water (500 mL) to the residue produced a suspension that was filtrated. The cake was dried *in vacuo* at 50ºC for 12 h. The colourless solid was dissolved in DMF (150 mL) and NaH (5.88 g, 147 mmol) was added carefully followed by the addition of catalytic amounts of imidazole (0.010 g, 0.15 mmol). The reaction mixture was stirred at room temperature for 1 h before being cooled at 0ºC whereupon MeI (17.88 g, 7.8 mL, 126 mmol) was added dropwise at 0ºC. The yellow suspension was stirred for 12 h at room temperature. MeOH (50 mL) was then added slowly to quench excess NaH. The reaction mixture was poured into water (500 mL) under stirring before being extracted with Et_2O (3 × 300 mL). The organic extract was dried ($MgSO_4$) and evaporated to dryness to afford a brown residue. The crude material was purified by column chromatography (SiO_2, petroleum ether/AcOEt, 80:20 to 65:35, *v*/*v*) to give the desired product **3** (yield: 4.63 g, 50%) as a colourless solid.

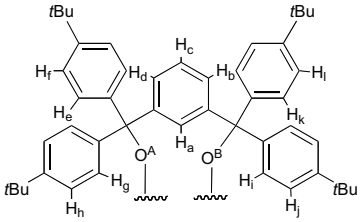

Labeling of aromatic protons in the A,B cap (noted with a dash in the corresponding D,E cap) R_f (SiO_2, petroleum ether/AcOEt, 60:40, *v*/*v*) = 0.60; m.p. dec. >250ºC; ^{1}H NMR (500.1 MHz, $CDCl_3$, 25ºC): δ (assignment by COSY, TOCSY and ROESY) = 1.17 (s, 6 H, *t*Bu), 1.18 (s, 6 H, *t*Bu), 1.20 (s, 6 H, *t*Bu), 1.24 (s, 6 H, *t*Bu), 1.27–1.29 (48 H, *t*Bu), 2.69 (d, 1 H, $^3J_{H\text{-}2,H\text{-}1}$ = 4.0 Hz, H-2^E), 2.73 (s, 3 H, OMe-6^G), 2.73 (d, 1 H, $^3J_{H\text{-}2,H\text{-}1}$ = 3.7 Hz, H-2^B), 3.07 (s, 3 H, OMe-6^C), 3.25 (s, 3 H, OMe-6^F), 3.32 (s, 3 H, OMe-2^B), 3.36 (s, 3 H, OMe-2^E), 3.51 (s, 3 H, OMe-2^G), 3.56 (s, 3 H, OMe-2^A), 3.58 (s, 3 H, OMe-2^F), 3.60 (s, 3 H, OMe-2^C), 3.62 (s, 3 H, OMe-2^D), 3.63 (s, 9 H, OMe-3), 3.64 (s, 3 H, OMe-3), 3.65 (s, 3 H, OMe-3), 3.66 (s, 3 H, OMe-3), 3.67 (s, 3 H, OMe-3), 3.20–4.05 (38 H, H-2, H-3, H-4, H-5, H-6a^{B,E}, H-6^{A,C,D,F,G}), 4.22–4.28 (3 H, H-1^B, H-6b^{B,E}), 4.49 (d, 1 H, $^3J_{H\text{-}1,H\text{-}2}$ = 3.5 Hz, H-1^E), 5.15 (d, 1 H, $^3J_{H\text{-}1,H\text{-}2}$ = 3.4 Hz, H-1^G), 5.36 (d, 1 H, $^3J_{H\text{-}1,H\text{-}2}$ = 3.8 Hz, H-1^A), 5.38 (d, 1 H, $^3J_{H\text{-}1,H\text{-}2}$ = 3.3 Hz, H-1^F), 5.48 (d, 1 H, $^3J_{H\text{-}1,H\text{-}2}$ = 3.9 Hz, H-1^C), 5.49 (d, 1 H, $^3J_{H\text{-}1,H\text{-}2}$ = 3.9 Hz, H-1^D), 6.96 (d, 1 H, $^3J_{Hd\text{-}Hc}$ = 7.5 Hz, H$_{d'}$), 6.97 (d, 1 H, $^3J_{Hb\text{-}Hc}$ = 7.9 Hz, H$_b$), 6.99 (d, 1 H, $^3J_{Hb'\text{-}Hc'}$ = 8.0 Hz, H$_{b'}$), 7.06 (t, 1 H, $^3J_{Hc'\text{-}Hb'}$ = $^3J_{Hc\text{-}Hd}$ = 7.8 Hz, H$_{c'}$), 7.08 (t, 1 H, $^3J_{Hc\text{-}Hb}$ = $^3J_{Hc\text{-}Hd}$ = 7.8 Hz, H$_c$), 7.14–7.29 (17 H, H$_d$, H$_f$, H$_{f'}$, H$_h$, H$_{h'}$, H$_j$, H$_{j'}$, H$_l$ and H$_{l'}$), 7.32–7.45 (12 H, H$_e$, H$_{e'}$, H$_i$, H$_{i'}$, H$_k$ and H$_{k'}$), 7.51 (d, 4 H, $^3J_{Hg\text{-}Hh}$ = 7.8 Hz, H$_g$), 7.61 (br s, H$_a$), 7.72 (br s, H$_{a'}$) ppm; ^{13}C{^{1}H} NMR (75.5 MHz $CDCl_3$, 25ºC): δ (assignment by HMQC) = 31.43 [×24] (Me of *t*Bu), 34.3 [×8] (C of *t*Bu), 57.80, 57.88, 58.06, 58.14, 58.25, 58.42, 58.80, 59.03, 59.51, 59.70, 60.60, 61.03, 61.52, 61.70, 61.75, 61.84, 61.98 (OMe), 61.68, 61.70, 62.73, 63.18 (C-6^{A,B,D,E}), 71.09, 71.75, 72.54 (C-6^{C,F,G}), 70.46, 70.49, 70.61, 70.76, 71.20, 71.57, 71.65 (C-5), 77.21, 78.74, 80.19, 80.54, 80.98, 81.04, 81.19, 81.27, 81.64, 81.77 [×4], 82.13, 82.23, 82.26, 82.59 [×2], 82.74 [×2], 82.86 (C-2, C-3, C-4), 85.74, 86.11, 87.51, 87.85 [$OC(Ar)_3$], 97.74, 98.24, 98.51, 98.63, 98.77 [×3] (C-1), 124.11 [×5], 124.33, 124.43, 124.48 [×2], 124.59, 126.29, 126.44, 126.50, 126.83, 127.28, 127.46, 128.11, 128.14, 130.52, 131.00, 131.53, 131.88, 134.37, 134.95 (*o*-C and *m*-C), 140.09, 140.20, 140.41, 140.59, 140.94, 141.59, 141.92, 142.37, 142.83, 144.58, 144.96, 145.24, 148.46, 148.52, 148.54, 148.56, 148.60, 148.66 [×2], 148.92 (*ipso*-C) ppm; elemental analysis (%) calcd for $C_{155}H_{212}O_{35}{\cdot}CH_2Cl_2$ (2635.32 + 83.95): C 68.88, H 7.93, found: C 68.77, H 8.09; MS (ESI-TOF): *m/z* (%): 2673.36 (15) $[M + K]^+$, 2657.38 (78) $[M + Na]^+$, 2641.41 (9) $[M + Li]^+$.

2^A,2^B,2^C,2^D,2^E,2^F,2^G,3^A,3^B,3^C,3^D,3^E,3^F,3^G,6^C,6^F,6^G-Heptadeca-*O*-methyl-β-cyclodextrin (8)

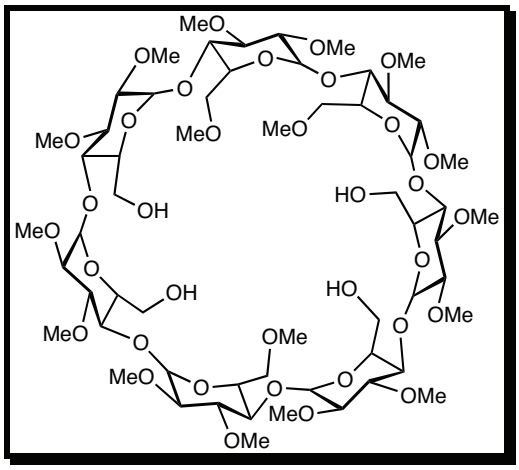

HBF_4 (34 wt % aq, 7.5 g, 7.5 mL, 29 mmol) was added dropwise to a stirred solution of capped cyclodextrin **3** (2.55 g, 0.97 mmol) in MeCN (30 mL) at room temperature. After 30 min, NEt_3 (1.47 g, 2.0 mL) was added dropwise under stirring. Addition of water (100 mL) to the reaction mixture caused the carbinol to precipitate. The resulting suspension was filtrated and the filtrate extracted with $CHCl_3$ (3 × 50 mL). The combined organic extracts were washed with a saturated aqueous $NaHCO_3$ solution (100 mL) before being dried ($MgSO_4$). Removal of the solvent *in vacuo* gave tetrol **8** (yield: 1.32 g, 99%) as a colourless solid. R_f (SiO_2, CH_2Cl_2/MeOH, 92:8, *v*/*v*) = 0.18; m.p. 153ºC; ^{1}H NMR (300.1 MHz, $CDCl_3$, 25ºC): δ (assignment by COSY) = 2.61 (t, 1 H, $^3J_{OH\text{-}H\text{-}6}$ = 6.2 Hz, OH), 2.68 (t, 1 H, $^3J_{OH\text{-}H\text{-}6}$ = 5.9 Hz, OH), 2.78 (t, 1 H, $^3J_{OH\text{-}H\text{-}6}$ = 6.1 Hz, OH), 2.96 (t, 1 H, $^3J_{OH\text{-}H\text{-}6}$ = 5.8 Hz, OH), 3.17–3.22 (7 H, H-2), 3.30–4.00 (35 H, H-3, H-4, H-5, H-6) 3.37 (s, 9 H, OMe), 3.49 (s, 9 H, OMe), 3.51 (s, 6 H, OMe), 3.52 (s, 3 H, OMe), 3.53 (s, 3 H, OMe), 3.62 (s, 9 H, OMe), 3.63 (s, 3 H, OMe), 3.64 (s, 6 H, OMe), 3.65 (s, 3 H, OMe), 5.01–5.03 (2 H, H-1), 5.09 (d, 1 H, $^2J_{H\text{-}1,H\text{-}2}$ = 3.8 Hz, H-1), 5.10 (d, 1 H, $^2J_{H\text{-}1,H\text{-}2}$ = 3.8 Hz, H-1), 5.17 (d, 2 H, $^2J_{H\text{-}1,H\text{-}2}$ = 3.5 Hz, H-1), 5.23 (d, 1 H, $^2J_{H\text{-}1,H\text{-}2}$ = 3.8 Hz, H-1) ppm; ^{13}C{^{1}H} NMR (75.5 MHz $CDCl_3$, 25ºC): δ (assignment by HMQC) = 58.25 [×3], 58.68, 58.77, 58.95, 59.00, 59.06, 59.19 [×2], 61.05, 61.09, 61.25, 61.28, 61.53, 61.63, 61.78 (OMe), 61.78, 61.97 [×2], 62.05 (C-$6^{A,B,D,E}$), 71.18, 71.32, 71.47 (C-$5^{C,F,G}$), 71.39, 71.54, 71.69 (C-$6^{C,F,G}$), 71.83, 72.03, 72.33, 72.53 (C-$5^{A,B,D,E}$), 78.29, 79.11 [×2] 79.96, 80.44, 80.69, 81.09, 81.24, 81.41, 81.45, 81.60 [×2], 81.73, 81.77 [×2], 81.98 [×4], 82.07, 82.14 (C-2, C-3, C-4), 98.37, 98.60, 98.70 [×2], 98.85 [×2], 98.92 (C-1) ppm; elemental analysis (%) calcd for $C_{59}H_{104}O_{35}$ (1373.44): C 51.60, H 7.63, found: C 51.68, H 7.57; MS (ESI-TOF): *m/z* (%): 1395.63 (100) $[M + Na]^+$.

6^A,6^B,6^D,6^E-Tetra-*O*-methylsulfonyl-2^A,2^B,2^C,2^D,2^E,2^F,2^G,3^A,3^B,3^C,3^D,3^E,3^F,3^G,6^C,6^F,6^G-heptadeca-*O*-methyl-β-cyclodextrin (9)

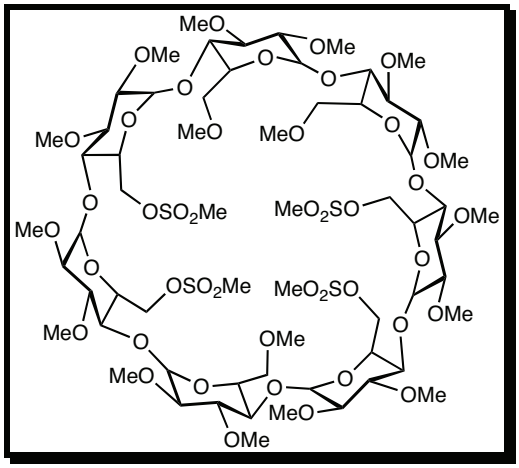

Methanesulfonyl chloride (0.34 g, 0.23 mL, 2.94 mmol) was added to a solution of tetrol **8** (0.96 g, 0.70 mmol) and DMAP (0.35 g, 2.87 mmol) in dry pyridine (30 mL) at 0ºC. The reaction mixture was stirred at room temperature for 12 h before adding water (100 mL). The solution was extracted with AcOEt (3 × 50 mL). The combined organic extracts were washed sequentially with HCl 2 M (2 × 50 mL), NaOH 2 M (2 × 50 mL) and water (50 mL) before being dried ($MgSO_4$). Removal of the solvent *in vacuo* gave pure tetramesylate **9** (yield: 1.14 g, 97%) as a colourless solid. R_f (SiO_2, CH_2Cl_2/MeOH, 92:8, *v*/*v*) = 0.40; m.p. 201ºC; ^{1}H NMR (300.1 MHz, $CDCl_3$, 25ºC): δ (assignment by COSY) = 3.06 (s, 6 H, OSO_2Me), 3.07 (s, 3 H, OSO_2Me), 3.08 (s, 3 H, OSO_2Me), 3.14–3.21 (7 H, H-2), 3.37 (s, 3 H, OMe), 3.38 (s, 3 H, OMe), 3.39 (s, 3 H, OMe), 3.49 (s, 9 H, OMe), 3.50 (s, 6 H, OMe), 3.53 (s, 6 H, OMe), 3.60 (s, 3 H, OMe), 3.61 (s, 3 H, OMe), 3.62 (s, 6 H, OMe), 3.64 (s, 3 H, OMe), 3.66 (s, 3 H, OMe), 3.68 (s, 3 H, OMe), 3.40–4.05 (27 H, H-3, H-4, H-5, H-$6^{C,F,G}$), 4.32–4.34 (2 H, H-$6a^{A,D\text{ or }B,E}$), 4.53–4.70 (6 H, H-$6a^{B,E\text{ or }A,D}$, H-$6b^{A,B,D,E}$), 5.08–5.11 (4 H, H-1), 5.14 (d, 1 H, $^3J_{H\text{-}1,H\text{-}2}$ = 3.6 Hz, H-1), 5.20 (d, 1 H, $^3J_{H\text{-}1,H\text{-}2}$ = 3.9 Hz, H-1), 5.22 (d, 1 H, $^3J_{H\text{-}1,H\text{-}2}$ = 3.9 Hz, H-1) ppm; $^{13}C\{^1H\}$ NMR (75.5 MHz $CDCl_3$, 25ºC): δ (assignment by HMQC) = 37.17, 37.30 [×2], 37.50 (OSO_2Me), 58.26, 58.39 [×2], 58.46, 58.74, 59.10, 59.15 [×2], 59.36, 59.44, 61.11, 61.21, 61.62 [×3], 61.76, 61.80 (OMe), 69.32 [×2], 69.88 [×2] (C-$6^{A,B,D,E}$), 69.56 [×2], 69.67 [×2] (C-$5^{A,B,D,E}$), 70.87, 70.96 [×2] (C-$6^{C,F,G}$), 71.16 [×2], 71.32 (C-$5^{C,F,G}$), 78.10, 78.35, 80.13, 80.20, 80.63, 80.67 [×2], 81.01, 81.47, 81.61 [×5], 81.69, 81.75, 81.85 [×3], 81.95, 82.04 (C-2, C-3, C-4), 97.66, 98.41, 98.94 [×2], 99.12 [×2], 99.17

(C-1) ppm; elemental analysis (%) calcd for $C_{63}H_{112}O_{43}S_4$ (1685.80): C 44.89, H 6.70, found: C 44.88 , H 6.65; MS (ESI-TOF): *m/z* (%): 1707.54 (100) $[M + Na]^+$.

_P,P'_-{6^A,6^B,6^D,6^E-Tetradeoxy-6^A,6^B:6^D,6^E-bis[(*R*)-phenylphosphinidene]-2^A,2^B,2^C,2^D, 2^E,2^F,2^G,3^A,3^B,3^C,3^D,3^E,3^F,3^G,6^C,6^F,6^G-heptadeca-*O*-methyl-β-cyclodextrin} diborane (4)

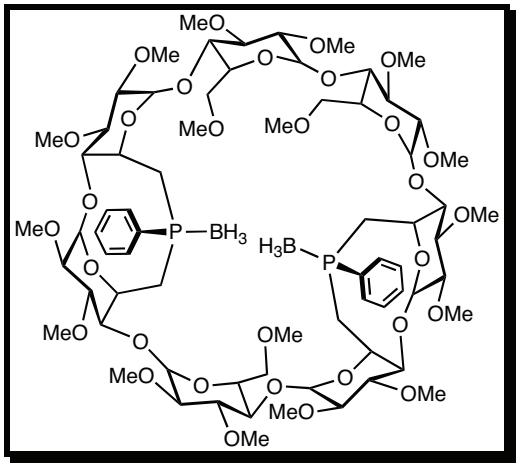

A solution of *n*BuLi in hexane (1.60 M, 1.22 mL, 1.96 mmol) was added dropwise to a stirred solution of H_2PPh (0.098 g, 0.098 mL, 0.89 mmol) in thf (16.5 mL) at –78ºC. The yellow solution was allowed to rise to room temperature over 1 h whereupon the phosphide dianion precipitated. The resulting yellow suspension was cannulated slowly, within 1 h, into a stirred solution of tetramesylate **9** (0.300 g, 0.18 mmol) in thf (25 mL). The reaction mixture was stirred for 12 h at room temperature. The solvent was then removed *in vacuo* and excess Li_2PPh was protonated with MeOH (15 mL). After removal of the solvent *in vacuo*, toluene (100 mL) was added and the resulting suspension filtered over celite. Evaporation of the solvent gave a colourless residue, which was dissolved in thf (10 mL) before adding a solution of BH_3·thf in thf (1.00 M, 0.9 mL, 0.9 mmol) dropwise at 0ºC. After stirring for 12 h at room temperature, the solvent was removed *in vacuo* and the resulting colourless residue subjected to column chromatography (dried SiO_2, CH_2Cl_2/MeOH, 97:3, *v*/*v*) to afford pure **4** (yield: 0.120 g, 40%) as a colourless solid. R_f (SiO_2, CH_2Cl_2/MeOH, 92:8, *v*/*v*) = 0.35; m.p. 185ºC; ^{1}H NMR (300.1 MHz, $CDCl_3$, 25ºC): δ (assignment by COSY) = 0.89 (br s, 6 H, P-BH_3), 1.62–1.64 (4 H, H-6a^{A,B,D,E}), 2.89–2.91 (2 H, H-6b$^{A,D\ or\ B,E}$), 3.17 (s, 3 H, OMe), 3.22 (s, 3 H, OMe), 3.27 (s, 3 H, OMe), 3.44 (s, 3 H, OMe), 3.45 (s, 6 H, OMe), 3.45 (s, 3 H, OMe), 3.46 (s, 3 H, OMe), 3.53, (s, 6 H, OMe), 3.57 (s, 3 H, OMe), 3.59 (s, 3 H, OMe), 3.62 (s, 3 H, OMe), 3.64 (s, 6 H, OMe), 3.67 (s, 3 H, OMe), 3.67 (s, 3 H, OMe), 3.10–4.27 (34 H,

H-2, H-3, H-4, H-5$^{B,E \text{ or } A,D}$, H-5^{C,F,G}, H-6b$^{B,E \text{ or } A,D}$, H-6^{C,F,G}), 4.60–4.62 (2 H, H-5$^{A,D \text{ or } B,E}$), 4.91 (d, 1 H, $^{3}J_{H\text{-}1,H\text{-}2}$ = 3.8 Hz, H-1), 4.94 (d, 2 H, $^{3}J_{H\text{-}1,H\text{-}2}$ = 3.3 Hz, H-1), 4.97–5.00 (3 H, H-1), 5.11 (d, 1 H, $^{3}J_{H\text{-}1,H\text{-}2}$ = 3.6 Hz, H-1), 7.46–7.47 (6 H, *m*-H, *p*-H), 7.77–7.83 (4 H, *o*-H) ppm; $^{13}C\{^{1}H\}$ NMR (75.5 MHz $CDCl_3$, 25ºC): δ (assignment by HMQC) = 27.21 (d, $^{1}J_{C,P}$ = 35.3 Hz), 27.91 (d, $^{1}J_{C,P}$ = 34.4 Hz) (C-6$^{A,D \text{ or } B,E}$), 34.25 (d, $^{1}J_{C,P}$ = 30.0 Hz), 35.15 (d, $^{1}J_{C,P}$ = 30.0 Hz) (C-6$^{B,E \text{ or } A,D}$), 57.91 [×3], 58.00, 58.21, 58.45, 58.49, 58.66, 58.82, 58.90, 61.45, 61.57 [×2], 61.82, 61.91, 62.20, 62.22 (OMe), 64.52, 64.74 (C-5$^{A,D \text{ or } B,E}$), 68.67 (d, $^{2}J_{C,P}$ = 6.4 Hz), 68.99 (d, $^{2}J_{C,P}$ = 5.5 Hz) (C-5$^{B,E \text{ or } A,D}$), 70.86, 71.05, 71.44 (C-5^{C,F,G}), 70.57, 71.15, 71.42 (C-6^{C,F,G}), 80.06, 80.44, 80.48, 81.16, 81.28, 81.54, 81.80, 82.03, 82.26 [×5], 82.38, 82.46, 83.14, 83.30 (C-2, C-3, C-4^{C,F,G}), 86.73 (d, $^{3}J_{C,P}$ = 10.1 Hz), 86.98 (d, $^{3}J_{C,P}$ = 10.1 Hz) (C-4$^{A,D \text{ or } B,E}$), 89.09, 89.46 (C-4$^{B,E \text{ or } A,D}$), 98.46, 98.54, 99.55, 100.28, 100.45, 100.78, 101.18 (C-1), 128.73, 128.85 (*m*-C), 131.12, 131.19 (*p*-C), 131.55 (d, $^{2}J_{C\text{-}P}$ = 3.7 Hz), 131.67 (d, $^{2}J_{C\text{-}P}$ = 3.7 Hz) (*o*-C), 131.34 (d, $^{1}J_{C\text{-}P}$ = 11.4 Hz), 132.17 (d, $^{1}J_{C\text{-}P}$ = 11.4 Hz) (*ipso*-C) ppm; $^{31}P\{^{1}H\}$ NMR (121.5 MHz $CDCl_3$, 25ºC): δ = 17.8 (s), 18.4 (s) ppm; elemental analysis (%) calcd for $C_{71}H_{116}B_2O_{31}P_2 \cdot MeOH$ (1549.23 + 32.04): C 54.69, H 7.65, found: C 54.56, H 7.69; MS (ESI-TOF): *m/z* (%): 1571.71 (100) $[M + Na]^+$.

6^A,6^B,6^D,6^E-Tetradeoxy-6^A,6^B:6^D,6^E-bis[(*R*)-phenylphosphinidene]-2^A,2^B,2^C,2^D,2^E,2^F,2^G, 3^A,3^B,3^C,3^D,3^E,3^F,3^G,6^C,6^F,6^G-heptadeca-*O*-methyl-β-cyclodextrin (10, WIDEPHOS)

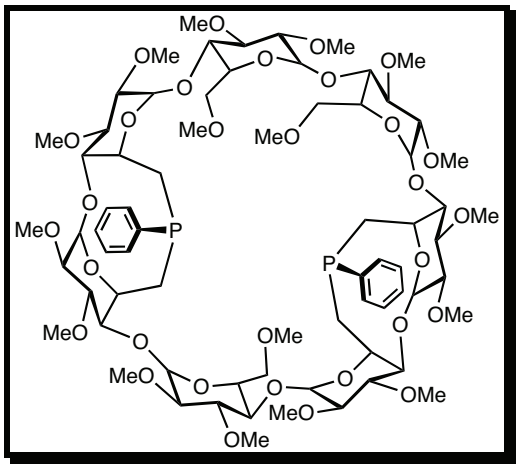

A solution of **4** (0.080 g, 0.52 mmol) in $HNEt_2$ (8 mL) was refluxed for 12 h. After cooling down to room temperature, the suspension was filtered over celite and the filtrate evaporated to dryness *in vacuo* to afford analytically pure **10** (yield: 0.080 g, 99%). R_f (SiO_2, CH_2Cl_2/MeOH, 92:8, *v*/*v*) = 0.40; m.p. 195ºC; ^{1}H NMR (300.1 MHz, $CDCl_3$, 25ºC): δ

(assignment by COSY) = 1.72–1.74 (2 H, H-6a$^{A,D\text{ or }B,E}$), 1.86–1.88 (2 H, H-6a$^{B,E\text{ or }A,D}$), 2.81 (td, 2 H, $^{2}J_{H\text{-}6b,P}$ = $^{2}J_{H\text{-}6b,H\text{-}6a}$ = 13.5 Hz, $^{3}J_{H\text{-}6b,H\text{-}5}$ = 3.9 Hz, H-6b$^{A,D\text{ or }B,E}$), 3.05–3.29 (12 H, H-2, H-6a^{C,F,G}, H-6b$^{B,E\text{ or }A,D}$), 3.11 (s, 3 H, OMe), 3.20 (s, 3 H, OMe), 3.27 (s, 3 H, OMe), 3.30–3.72 (14 H, H-3, H-4), 3.47 (s, 3 H, OMe), 3.48 (s, 3 H, OMe), 3.49 (s, 3 H, OMe), 3.50 (s, 6 H, OMe), 3.55 (s, 6 H, OMe), 3.60 (s, 3 H, OMe), 3.62 (s, 3 H, OMe), 3.65 (s, 9 H, OMe), 3.66 (s, 6 H, OMe), 3.81–3.42 (8 H, H-5$^{A,D\text{ or }B,E}$, H-5^{C,F,G}, H-6b^{C,F,G}), 4.29–4.31 (2 H, H-5$^{B,E\text{ or }A,D}$), 4.95–5.05 (6 H, H-1), 5.22 (d, 1 H, $^{3}J_{H\text{-}1,H\text{-}2}$ = 3.7 Hz, H-1), 7.20–7.28 (6 H, *m*-H, *p*-H), 7.41–7.51 (4 H, *o*-H) ppm; $^{13}C\{^{1}H\}$ NMR (125.8 MHz C_6D_6, 25ºC): δ (assignment by HMQC) = 28.66 (d, $^{1}J_{C,P}$ = 15.4 Hz, C-6$^{A\text{ or }D}$), 28.69 (d, $^{1}J_{C,P}$ = 16.2 Hz, C-6$^{D\text{ or }A}$), 34.99 (d, $^{1}J_{C,P}$ = 19.1 Hz, C-6$^{B\text{ or }E}$), 35.06 (d, $^{1}J_{C,P}$ = 19.7 Hz, C-6$^{E\text{ or }B}$), 58.14 [×2], 58.20, 58.32, 58.71, 59.10, 59.14, 59.44, 59.68, 59.74, 61.77, 61.79, 61.90, 62.00, 62.05, 62.25 [×2] (OMe), 67.54 (d, $^{2}J_{C,P}$ = 11.7 Hz, C-5$^{A\text{ or }D}$), 67.57 (d, $^{2}J_{C,P}$ = 11.7 Hz, C-5$^{D\text{ or }A}$), 71.53 [×2], 71.80 (C-5^{C,F,G}), 72.13 (d, $^{TS}J_{C,P}$ = 2.6 Hz, C-6^{C}), 72.39 [×2] (C-6^{F,G}), 73.95 (d, $^{2}J_{C,P}$ = 14.3 Hz, C-5$^{B\text{ or }E}$), 74.26 (d, $^{2}J_{C,P}$ = 13.6 Hz, C-5$^{E\text{ or }B}$), 79.75, 82.22, 82.31, 82.37, 82.42, 82.97, 83.15, 83.23, 83.36 [×3], 83.42, 83.46, 83.58, 84.07, 84.55, 84.70 (C-2, C-3, C-4^{C,F,G}), 87.15 (d, $^{3}J_{C,P}$ = 8.0 Hz, C-4$^{B\text{ or }E}$), 87.32 (d, $^{3}J_{C,P}$ = 8.0 Hz, C-4$^{E\text{ or }B}$), 90.23 (d, $^{3}J_{C,P}$ = 2.7 Hz, C-4$^{A\text{ or }D}$), 90.38 (d, $^{3}J_{C,P}$ = 2.6 Hz, C-4$^{D\text{ or }A}$), 99.27, 99.32, 99.69, 99.90, 99.96 [×2], 101.19 (C-1), 128.96, 129.03 (*p*-C), 129.15 [×2] (overlapping d, $^{3}J_{C,P}$ = 4.8 Hz, *m*-C), 132.47 (d, $^{2}J_{C,P}$ = 18.7 Hz), 132.51 (d, $^{2}J_{C,P}$ = 18.7 Hz) (*o*-C), 142.33 [×2] (d, $^{1}J_{C,P}$ = 11.7 Hz, *ipso*-C_{quat}) ppm; $^{31}P\{^{1}H\}$ NMR (202.5 MHz, C_6D_6, 25ºC): δ = –15.0 (s), –15.2 (s) ppm; $^{31}P\{^{1}H\}$ NMR (121.5 MHz, $CDCl_3$, 25ºC): δ = –14.6 (s) ppm; elemental analysis (%) calcd for $C_{71}H_{110}O_{31}P_2 \cdot 0.5CH_2Cl_2$ (1521.56 + 42.47): C 54.91, H 7.15, found: C 54.82, H 7.35; MS (ESI-TOF): *m/z* (%): 1521.57 (100) $[M + H]^{+}$.

6^A,6^B-Dideoxy-6^A,6^B-[(*R*)-phenylphosphinidene]-2^A,2^B,2^C,2^D,2^E,2^F,2^G,3^A,3^B,3^C,3^D,3^E,3^F,3^G, 6^C,6^D,6^E,6^F,6^G-nonadeca-*O*-methyl-β-cyclodextrin (12)

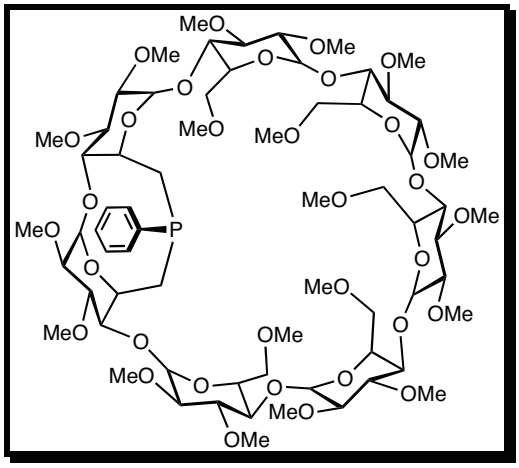

A solution of *n*BuLi in hexane (1.60 M, 4.06 mL, 6.50 mmol) was added dropwise to a stirred solution of H_2PPh (0.35 g, 0.35 mL, 3.24 mmol) in thf (40 mL) at –78ºC. The yellow solution was allowed to rise to room temperature over 1 h whereupon the phosphide dianion precipitated. The resulting yellow suspension was cannulated slowly, within 1 h, into a stirred solution of dimesylate **11** (1.26 g, 0.81 mmol) in thf (110 mL). The reaction mixture was stirred for 12 h at room temperature. The solvent was then removed *in vacuo* and excess Li_2PPh was protonated with MeOH (75 mL). After removal of the solvent *in vacuo*, toluene (200 mL) was added and the resulting suspension filtered over celite. Evaporation of the solvent to dryness *in vacuo* afforded analytically pure **12** (yield: 1.16 g, 97%) as a colourless solid. R_f (SiO_2, CH_2Cl_2/MeOH, 92:8, *v*/*v*) = 0.35; ^{1}H NMR (300.1 MHz, $CDCl_3$, 25ºC): δ (assignment by COSY) = 1.77 (m, 1 H, H-6a$^{A\text{ or }B}$), 1.85 (m, 1 H, H-6a$^{B\text{ or }A}$), 2.86 (t, 1 H, $^2J_{H\text{-}6b,H\text{-}6a} = {}^2J_{H\text{-}6b,P}$ = 13.5 Hz, H-6b$^{A\text{ or }B}$), 3.16–3.46 (17 H, H-2, H-3, H-6b$^{B\text{ or }A}$, H-4^{A,B}), 3.23 (s, 3 H, OMe), 3.28 (s, 3 H, OMe), 3.35 (s, 3 H, OMe), 3.37 (s, 6 H, OMe), 3.47 (s, 3 H, OMe), 3.50 (s, 9 H, OMe), 3.51 (2s, 6 H, OMe), 3.54 (s, 3 H, OMe), 3.61 (s, 3 H, OMe), 3.65 (s, 9 H, OMe), 3.66 (s, 6 H, OMe), 3.67 (s, 3 H, OMe), 3.95-3.32 (20 H, H-4^{C,D,E,F,G}, H-5^{C,D,E,F,G}, H-6^{C,D,E,F,G}), 4.00 (m, 1 H, H-5$^{A\text{ or }B}$), 4.27 (m, 1 H, H-5$^{B\text{ or }A}$), 5.00 (d, 1 H, $^3J_{H\text{-}1,H\text{-}2}$ = 4.8 Hz, H-1), 5.01 (d, 1 H, $^3J_{H\text{-}1,H\text{-}2}$ = 4.2 Hz, H-1), 5.02 (d, 1 H, $^3J_{H\text{-}1,H\text{-}2}$ = 4.2 Hz, H-1), 5.11 (d, 1 H, $^3J_{H\text{-}1,H\text{-}2}$ = 3.6 Hz, H-1), 5.15 (d, 1 H, $^3J_{H\text{-}1,H\text{-}2}$ = 3.9 Hz, H-1), 5.19 (d, 1 H, $^3J_{H\text{-}1,H\text{-}2}$ = 3.3 Hz, H-1), 5.24 (d, 1 H, $^3J_{H\text{-}1,H\text{-}2}$ = 3.9 Hz, H-1), 7.30–7.32 (3 H, *m*-H, *p*-H), 7.44-7.49 (m, 2 H, *o*-H) ppm; ^{13}C{^{1}H} NMR (75.5 MHz, $CDCl_3$, 25ºC): δ (assignment by HMQC) = 27.46 (d, $^1J_{C,P}$ = 14.3 Hz, C-6$^{A\text{ or }B}$), 34.58 (d, $^1J_{C,P}$ = 18.6 Hz, C-6$^{B\text{ or }A}$), 58.03,

58.25, 58.33, 58.40, 58.67 [×3], 58.93, 59.00 [×3], 59.09, 61.05, 61.31, 61.44 [×2], 61.53 [×2], 61.63 (OMe), 66.79 (d, $^{2}J_{C,P}$ = 11.4 Hz, C-5$^{A\text{ or }B}$), 70.66 [×2], 70.99, 71.03 [×2], 71.27, 71.32 [×2], 71.64, 71.68 (C-5^{C,D,E,F,G}, C-6^{C,D,E,F,G}), 73.26 (d, $^{2}J_{C,P}$ = 38.9 Hz, C-5$^{B\text{ or }A}$), 78.13, 79.29, 79.89, 80.49, 81.08, (C-4^{C,D,E,F,G}), 81.10 [×2], 81.82 [×2], 81.97 [×3], 82.06 [×3], 82.25 [×2], 83.68 [×2] (C-2, C-3), 86.05 (C-4$^{A\text{ or }B}$), 88.86 (C-4$^{B\text{ or }A}$), 98.42, 98.50 [×2], 98.73, 98.91, 99.14, 99.69 (C-1), 128.37 (d, $^{3}J_{C,P}$ = 6.6 Hz, *m*-C), 128.55 (*p*-C), 131.58 (d, $^{2}J_{C,P}$ = 18.7 Hz, *o*-C), 140.55 (d, $^{1}J_{C,P}$ = 9.6, Hz, *ipso*-C) ppm; $^{31}P\{^{1}H\}$ NMR (121.5 MHz, $CDCl_3$, 25ºC): δ = –15.1 (s) ppm; elemental analysis (%) calcd for $C_{67}H_{111}O_{33}P{\cdot}2CH_2Cl_2$: (1475.55 + 169.86): C 50.37, H 7.07, found: C 50.28, H 7.21; MS (ESI-TOF): *m/z* (%): 1497.7 $[M + Na]^+$.

6^{A},6^{B}-Dideoxy-6^{A},6^{B}-[(*S*)-phenyloxophosphinidene]-2^{A},2^{B},2^{C},2^{D},2^{E},2^{F},2^{G},3^{A},3^{B},3^{C},3^{D},3^{E},3^{F},3^{G},6^{C},6^{D},6^{E},6^{F},6^{G}-nonadeca-*O*-methyl-β-cyclodextrin (13)

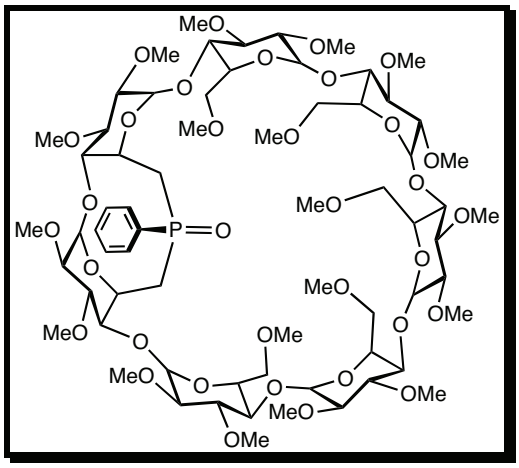

The phosphane oxide **13** was obtained by bubbling air through a solution of **12** in MeOH for 1 h at room temperature. Removal of the solvent *in vacuo* gave analytically pure **13** as a colourless solid. R_f (SiO_2, CH_2Cl_2/MeOH, 98:2, *v*/*v*) = 0.30; m.p. 201ºC; ^{1}H NMR (300.1 MHz, $CDCl_3$, 25ºC): δ (assignment by COSY) = 1.93 (t, 1 H, $^{2}J_{H\text{-}6a,H\text{-}6b}$ = $^{2}J_{H\text{-}6a,P}$ = 13.2 Hz, H-6a$^{A\text{ or }B}$), 2.15 (t, 1 H, $^{2}J_{H\text{-}6a,H\text{-}6b}$ = $^{2}J_{H\text{-}6a,P}$ = 16.4 Hz, H-6a$^{B\text{ or }A}$), 2.90–3.03 (2 H, H-6b^{A,B}), 3.11 (s, 3 H, OMe), 3.13 (s, 3 H, OMe), 3.19–3.94 (36 H, H-2, H-3, H-4, H-5^{C,D,E,F,G}, H-6^{C,D,E,F,G}), 3.35 (s, 6 H, OMe), 3.37 (s, 3 H, OMe), 3.41 (s, 3 H, OMe), 3.44 (s, 9 H, OMe), 3.46 (s, 3 H, OMe), 3.47 (s, 3 H, OMe), 3.50 (s, 3 H, OMe), 3.55 (s, 3 H, OMe), 3.58 (s, 3 H, OMe), 3.61 (s, 9 H, OMe), 3.62 (s, 3 H, OMe), 3.63 (s, 3 H, OMe), 4.38 (m, 1 H, H-5$^{A\text{ or }B}$), 4.62 (m, 1 H, H-5$^{B\text{ or }A}$), 4.90 (d, 1 H, $^{3}J_{H\text{-}1,H\text{-}2}$ = 3.6 Hz, H-1), 4.94 (d, 1 H, $^{3}J_{H\text{-}1,H\text{-}2}$

= 3.3 Hz, H-1), 4.98 (d, 1 H, $^{3}J_{H\text{-}1,H\text{-}2}$ = 4.5 Hz, H-1), 5.05 (d, 1 H, $^{3}J_{H\text{-}1,H\text{-}2}$ = 3.3 Hz, H-1), 5.06 (d, 1 H, $^{3}J_{H\text{-}1,H\text{-}2}$ = 3.0 Hz, H-1), 5.10 (d, 1 H, $^{3}J_{H\text{-}1,H\text{-}2}$ = 3.6 Hz, H-1), 5.12 (d, 1 H, $^{3}J_{H\text{-}1,H\text{-}2}$ = 3.6 Hz, H-1), 7.41–7.49 (3 H, *m*-H, *p*-H), 7.64 (m, 2 H, *o*-H) ppm; $^{13}C\{^{1}H\}$ NMR (75.5 MHz, $CDCl_3$, 25ºC): δ (assignment by HMQC) = 33.35 (d, $^{1}J_{C,P}$ = 68.0 Hz, C-$6^{A\text{ or }B}$), 38.15 (d, $^{1}J_{C,P}$ = 66.4 Hz, C-$6^{B\text{ or }A}$), 58.13, 58.25 [×2], 58.37, 58.50, 58.58, 58,66, 58.77 [×2], 59.00 [×3], 61.20, 61.36, 61.54, 61.61 [×2], 61.70, 61.89 (OMe), 63.20 (d, $^{2}J_{C,P}$ = 5.7 Hz, C-$5^{A\text{ or }B}$), 66.33 (C-$5^{B\text{ or }A}$), 70.62 [×4], 70.94 [×3], 71.25 [×3] (C-$5^{C,D,E,F,G}$, C-$6^{C,D,E,F,G}$), 77.33, 78.70, 79.77, 80.53, 80.62, 81.01, 81.41, 81.53, 81.65 [×2], 81.80, 82.01, 82.09 [×3], 82.19, 82.38, 83.60, 86.12 (C-2, C-3, C-$4^{C,D,E,F,G}$), 86.20 (d, $^{3}J_{C,P}$ = 11.3 Hz, C-$4^{A\text{ or }B}$), 88.92 (C-$4^{B\text{ or }A}$), 98.76, 98.86, 99.00, 99.22 [×2], 99.58, 100.25 (C-1), 128.80 (d, $^{3}J_{C,P}$ = 11.3 Hz, *m*-C), 129.21 (d, $^{2}J_{C,P}$ = 9.1 Hz, *o*-C), 132.02 (*p*-C), 135.00 (d, $^{1}J_{C,P}$ = 97.4, Hz, *ipso*-C) ppm; $^{31}P\{^{1}H\}$ NMR (121.5 MHz, $CDCl_3$, 25ºC): δ = 35.9 (s) ppm; elemental analysis (%) calcd for $C_{67}H_{111}O_{34}P{\cdot}2CH_2Cl_2$ (1491.55 + 169.86): C 49.88, H 6.98, found: C 50.20, H 7.15; MS (ESI-TOF): *m/z* (%): 1513.7 $[M + Na]^{+}$.

_P_-{6^{A},6^{B}-Dideoxy-6^{A},6^{B}-[(_R_)-phenylphosphinidene]-2^{A},2^{B},2^{C},2^{D},2^{E},2^{F},2^{G},3^{A},3^{B},3^{C},3^{D},3^{E},3^{F},3^{G},6^{C},6^{D},6^{E},6^{F},6^{G}-nonadeca-_O_-methyl-β-cyclodextrin} borane (14)

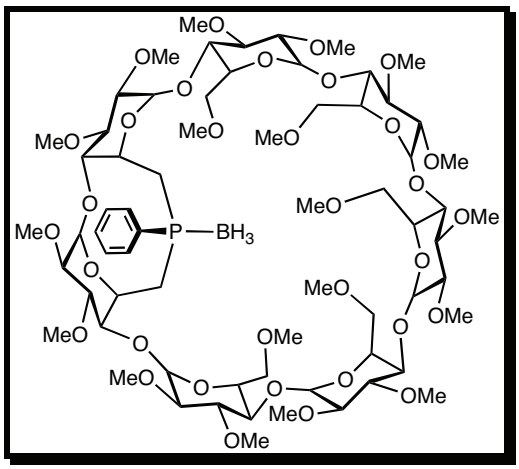

A solution of BH_3·thf in thf (1.00 M, 0.31 mL, 0.31 mmol) was added dropwise to a solution of monophosphane **12** (0.150 g, 0.10 mmol) together with traces of **13** in thf (10 mL) at 0ºC. After stirring for 12 h at room temperature, the solvent was removed *in vacuo* and the resulting colourless residue subjected to column chromatography (dried SiO_2, CH_2Cl_2/MeOH, 97:3, *v*/*v*) to afford pure **14** (yield: 0.140 g, 95%) as a colourless solid. R_f (SiO_2, CH_2Cl_2/MeOH, 92:8, *v*/*v*) = 0.35; m.p. 183ºC; ^{1}H NMR (300.1 MHz, $CDCl_3$, 25ºC):

δ (assignment by COSY) = 0.70 (br s, 3 H, P-BH_3), 1.78 (m, 1 H, H-6a$^{A\ or\ B}$), 1.98 (m, 1 H, H-6a$^{B\ or\ A}$), 2.85 (dd, 1 H, $^{2}J_{H\text{-}6b,H\text{-}6a}$ = 13.9 Hz, $^{3}J_{H\text{-}6b,H\text{-}5}$ = 4.1 Hz, 6b$^{B\ or\ A}$), 3.21 (s, 3 H, OMe), 3.26 (s, 3 H, OMe), 3.34 (s, 3 H, OMe), 3.37 (s, 3 H, OMe), 3.42 (s, 3 H, OMe), 3.45 (s, 3 H, OMe), 3.48 (s, 9 H, OMe), 3.50 (s, 3 H, OMe), 3.52 (s, 3 H, OMe), 3.54 (s, 3 H, OMe), 3.61 (s, 3 H, OMe), 3.64 (s, 6 H, OMe), 3.65 (s, 3 H, OMe), 3.68 (s, 9 H, OMe), 3.09–4.18 (38 H, H-2, H-3, H-4, H-5$^{B\ or\ A\ and\ C,D,E,F,G}$, H-6b$^{A\ or\ B}$, H-6^{C,D,E,F,G}), 4.50 (m, 1 H, H-5$^{A\ or\ B}$), 4.94 (d, 1 H, $^{3}J_{H\text{-}1,H\text{-}2}$ = 3.4 Hz, H-1), 5.00 (m, 2 H, H-1), 5.13 (d, 1 H, $^{3}J_{H\text{-}1,H\text{-}2}$ = 2.6 Hz, H-1), 5.18 (d, 1 H, $^{3}J_{H\text{-}1,H\text{-}2}$ = 2.9 Hz, H-1), 5.26 (d, 1 H, $^{3}J_{H\text{-}1,H\text{-}2}$ = 3.7 Hz, H-1), 5.32 (d, 1 H, $^{3}J_{H\text{-}1,H\text{-}2}$ = 3.3 Hz, H-1), 7.44–7.48 (3 H, *m*-H, *p*-H), 7.71 (t, 2 H, $^{3}J_{o\text{-}H,m\text{-}H}$ = 8.3 Hz, *o*-H) ppm; $^{13}C\{^{1}H\}$ NMR (75.5 MHz $CDCl_3$, 25ºC): δ (assignment by HMQC) = 27.89 (d, $^{1}J_{C,P}$ = 34.9 Hz, C-6$^{B\ or\ A}$), 34.19 (d, $^{1}J_{C,P}$ = 31.4 Hz, C-6$^{A\ or\ B}$), 57.76, 58.08, 58.15, 58.18, 58.53, 58.61, 58.84, 58.85 [×2], 58.98, 59.18, 59.29, 60.87, 61.09, 61.29, 61.53, 61.60, 61.76, 61.91 (OMe), 64.34 (C-5$^{B\ or\ A}$), 68.05 (d, $^{2}J_{C,P}$ = 6.8 Hz, C-5$^{A\ or\ B}$), 70.24, 70.66 [×4] (C-5^{C,D,E,F,G}), 70.43, 70.90, 71.12 [×2], 71.24 (C-6^{C,D,E,F,G}), 75.93, 78.26, 78.80, 79.89, 80.65, 80.89, 81.55, 81.65, 81.71, 81.85 [×2], 81.96[×4], 82.13, 82.19, 82.55, 83.23, (C-2, C-3, C-4^{C,D,E,F,G}), 85.32 (d, $^{3}J_{C,P}$ = 9.9 Hz, C-4$^{A\ or\ B}$), 89.11 (C-4$^{B\ or\ A}$), 97.60, 98.08, 98.20, 98.24, 98.34, 98.70, 99.74 (C-1), 128.81 (d, $^{3}J_{C,P}$ = 9.7 Hz, *m*-C), 131.20 (d, $^{2}J_{C,P}$ = 8.5 Hz, *o*-C), 131.25 (*p*-C), 131.66 (d, $^{3}J_{C,P}$ = 52.9 Hz, *ipso*-C) ppm; $^{31}P\{^{1}H\}$ NMR (121.5 MHz, $CDCl_3$, 25ºC): δ = 17.9 (s) ppm; elemental analysis (%) calcd for $C_{67}H_{114}BO_{33}P{\cdot}EtOH$ (1489.39 + 46.06): C 53.97, H 7.88, found: C 53.83, H 8.00; MS (ESI-TOF): *m/z* (%): 1527.67 (25) $[M + K]^+$, 1511.70 (70) $[M + Na]^+$.

_P_-{6^{A},6^{C}-Dideoxy-6^{A},6^{C}-[(_R_)-phenylphosphinidene]-2^{A},2^{B},2^{C},2^{D},2^{E},2^{F},2^{G}, 3^{A},3^{B},3^{C},3^{D},3^{E},3^{F},3^{G},6^{B},6^{D},6^{E},6^{F},6^{G}-nonadeca-_O_-methyl-β-cyclodextrin} borane (17)

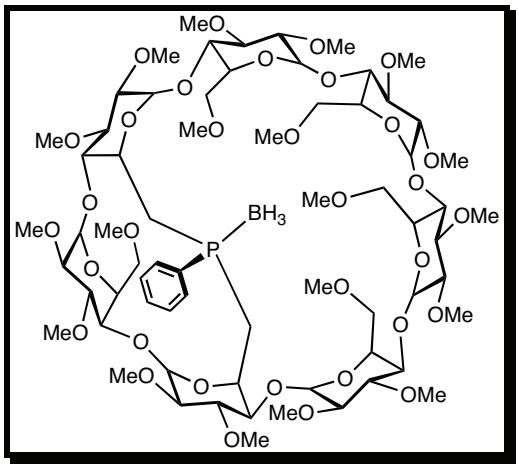

A solution of *n*BuLi in hexane (1.60 M, 0.51 mL, 0.81 mmol) was added dropwise to a stirred solution of H_2PPh (0.042 g, 0.042 mL, 0.39 mmol) in thf (5 mL) at –78ºC. The yellow solution was allowed to rise to room temperature over 1 h whereupon the phosphide dianion precipitated. The resulting yellow suspension was cannulated slowly, within 30 min, into a stirred solution of dimesylate **15** (0.200 g, 0.13 mmol) in thf (12 mL). The reaction mixture was stirred for 12 h at room temperature. The solvent was then removed *in vacuo* and excess Li_2PPh was protonated with MeOH (10 mL). After removal of the solvent *in vacuo*, toluene (70 mL) was added and the resulting suspension filtered over celite. Evaporation of the solvent gave a colourless residue, which was dissolved in thf (10 mL) before adding a solution of BH_3·thf in thf (1.00 M, 0.39 mL, 0.39 mmol) dropwise at 0ºC. After stirring for 12 h at room temperature, the solvent was removed *in vacuo* and the resulting colourless residue subjected to column chromatography (dried SiO_2, CH_2Cl_2/MeOH, 97:3, *v*/*v*) to afford pure **17** (yield: 0.068 g, 35%) as a colourless solid. R_f (SiO_2, CH_2Cl_2/MeOH, 92:8, *v*/*v*) = 0.37; m.p. 179ºC; ^{1}H NMR (300.1 MHz, $CDCl_3$, 25ºC): δ (assignment by COSY) = 1.63 (br s, 3 H, P-BH_3), 1.70 (m, 1 H, H-6a$^{A\text{ or }C}$), 2.24 (m, 1 H, H-6a$^{C\text{ or }A}$), 2.33 (td, 1 H, $^2J_{H\text{-}6b,H\text{-}6a} = {}^2J_{H\text{-}6b,P}$ = 14.8 Hz, $^3J_{H\text{-}6b,H\text{-}5}$ = 5.0 Hz, H-6b$^{A\text{ or }C}$), 2.73 (td, 1 H, $^2J_{H\text{-}6b,H\text{-}6a} = {}^2J_{H\text{-}6b,P} = {}^3J_{H\text{-}6b,H\text{-}5}$ = 9.4 Hz, H-6b$^{C\text{ or }A}$), 2.82 (s, 3 H, OMe), 3.17 (s, 3 H, OMe), 3.39 (s, 3 H, OMe), 3.41 (s, 3 H, OMe), 3.42 (s, 3 H, OMe), 3.44 (s, 3 H, OMe), 3.45 (s, 3 H, OMe), 3.49 (s, 3 H, OMe), 3.51 (s, 6 H, OMe), 3.53 (s, 3 H, OMe), 3.54 (s, 3 H, OMe), 3.57 (s, 6 H, OMe), 3.62 (s, 3 H, OMe), 3.64 (s, 3 H, OMe), 3.70 (s, 3 H, OMe), 3.73 (s, 3 H, OMe), 3.76 (s, 3 H, OMe), 3.09–3.83 (31 H, H-2, H-3, H-4, H-5$^{B,D,E\text{ or }B,D,F\text{ or }B,D,G\text{ or }D,E,F\text{ or }D,E,G\text{ or }E,F,G}$, H-6a^{B,D,E,F,G}, H-6b$^{B,D\text{ or }B,E\text{ or }B,F\text{ or }B,G\text{ or }D,E\text{ or }D,F\text{ or }D,G\text{ or }E,F\text{ or }E,G\text{ or }F,G}$), 3.97–4.27 (6 H, H-5$^{(A\text{ or }C)\text{ and }(F,G\text{ or }E,G\text{ or }E,F\text{ or }D,G\text{ or }D,F\text{ or }D,E\text{ or }B,G\text{ or }B,F\text{ or }B,E\text{ or }B,D)}$, H-6b$^{E,F,G\text{ or }D,E,G\text{ or }D,E,F\text{ or }B,D,G\text{ or }B,D,F\text{ or }B,D,E}$), 4.43 (td, 1 H, $^3J_{H\text{-}5,H\text{-}6a} = {}^3J_{H\text{-}5,H\text{-}4}$ = 9.9 Hz, $^3J_{H\text{-}5,H\text{-}4}$ = 9.7 Hz, H-5$^{C\text{ or }A}$), 4.60 (d, 1 H, $^3J_{H\text{-}1,H\text{-}2}$ = 2.9 Hz, H-1), 4.96 (d, 1 H, $^3J_{H\text{-}1,H\text{-}2}$ = 3.3 Hz, H-1), 5.10 (d, 1 H, $^3J_{H\text{-}1,H\text{-}2}$ = 3.8 Hz, H-1), 5.12 (d, 1 H, $^3J_{H\text{-}1,H\text{-}2}$ = 4.6 Hz, H-1), 5.13 (d, 1 H, $^3J_{H\text{-}1,H\text{-}2}$ = 3.5 Hz, H-1), 5.34 (d, 1 H, $^3J_{H\text{-}1,H\text{-}2}$ = 3.7 Hz, H-1), 5.86 (d, 1 H, $^3J_{H\text{-}1,H\text{-}2}$ = 2.7 Hz, H-1), 7.47 (s, 3 H, *m*-H, *p*-H), 7.75 (m, 2 H, *o*-H) ppm; ^{13}C{^{1}H} NMR (75.5 MHz, $CDCl_3$, 25ºC): δ (assignment by HMQC) = 25.27 (d, $^1J_{C,P}$ = 33.2 Hz, C-6$^{C\text{ or }A}$), 32.57 (d, $^1J_{C,P}$ = 39.6 Hz, C-6$^{A\text{ or }C}$), 57.76, 58.45 [×3], 58.61 [×2], 58.66, 58.80, 58.91, 59.07, 59.38, 59.56, 59.85, 59.94, 60.88, 61.23, 61.59 [×2], 62.11 (OMe), 66.96 (C-5$^{A\text{ or }C}$), 68.50 (C-5$^{C\text{ or }A}$), 70.20 [×2], 70.91, 71.26, 71.55 (C-5^{B,D,E,F,G}), 70.41 [×2], 71.32, 71.55, 71.68 (C-6^{B,D,E,F,G}), 74.19 (d, $^3J_{C,P}$ = 10.9 Hz, C-4$^{A\text{ or }C}$), 77.21, 77.79, 79.46, 80.33, 80.91, 81.10, 81.29 [×2], 81.49, 81.82 [×2], 81.90, 82.06 [×2], 82.29, 82.45, 82.86, 83.37, 85.53 (C-2, C-3, C-4^{B,D,E,F,G}), 83.19 (d, $^3J_{C,P}$ = 9.5 Hz, C-4$^{C\text{ or }A}$), 91.94, 93.91, 95.79, 98.95, 99.47, 99.84, 99.99 (C-1),

128.51 (d, $^{3}J_{C,P}$ = 9.6 Hz, *m*-C), 130.86 (*p*-C), 131.61 (d, $^{1}J_{C,P}$ = 51.5 Hz, *ipso*-C), 131.76 (d, $^{2}J_{C,P}$ = 8.9 Hz, *o*-C) ppm; $^{31}P\{^{1}H\}$ NMR (121.5 MHz $CDCl_3$, 25ºC): δ = 18.1 (s) ppm; elemental analysis (%) calcd for $C_{67}H_{114}BO_{33}P{\cdot}CHCl_3$ (1489.39 + 46.06): C 50.77, H 7.21, found: C 50.82, H 7.16; MS (ESI-TOF): *m/z* (%): 1487.90 (100) $[M - H]^{+}$.

6^{A},6^{C}-Dideoxy-6^{A},6^{C}-[(*R*)-phenylphosphinidene]-2^{A},2^{B},2^{C},2^{D},2^{E},2^{F},2^{G},3^{A},3^{B},3^{C},3^{D},3^{E},3^{F},3^{G}, 6^{B},6^{D},6^{E},6^{F},6^{G}-nonadeca-*O*-methyl-β-cyclodextrin (16)

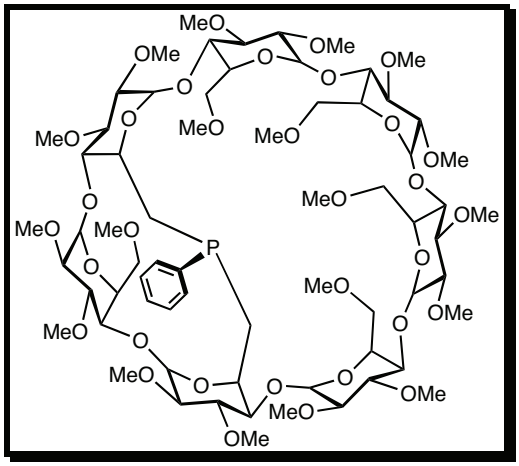

A solution of **17** (0.067 g, 0.045 mmol) in $HNEt_2$ (5 mL) was refluxed for 12 h. After cooling down to room temperature, the suspension was filtered over celite and the filtrate evaporated to dryness *in vacuo* to afford analytically pure **16** (yield: 0.066 g, 99%) as a colourless solid. R_f (SiO_2, CH_2Cl_2/MeOH, 92:8, *v*/*v*) = 0.40; m.p. 175ºC; ^{1}H NMR (300.1 MHz, $CDCl_3$, 25ºC): δ (assignment by COSY) = 1.68 (m, 1 H, H-6a$^{A\ or\ C}$), 2.15 (m, 1 H, H-6a$^{C\ or\ A}$), 2.26 (m, 1 H, H-6b$^{A\ or\ C}$), 2.52 (d, 1 H, $^{2}J_{H\text{-}6b,H\text{-}6a}$ = 14.5 Hz, H-6b$^{C\ or\ A}$), 2.60 (d, 1 H, $^{2}J_{H\text{-}6a,H\text{-}6b}$ = 11.2 Hz, H-6a), 3.04–3.24 (9 H, H-2, H-4$^{A\ or\ C}$, H-6b), 2.79 (s, 3 H, OMe), 3.20 (s, 3 H, OMe), 3.37 (s, 3 H, OMe), 3.41 (s, 3 H, OMe), 3.42 (s, 3 H, OMe), 3.44 (s, 6 H, OMe), 3.47 (s, 3 H, OMe), 3.48 (s, 3 H, OMe), 3.52 (s, 3 H, OMe), 3.54 (s, 3 H, OMe), 3.55 (s, 3 H, OMe), 3.56 (s, 3 H, OMe), 3.57 (s, 3 H, OMe), 3.58 (s, 3 H, OMe), 3.59 (s, 3 H, OMe), 3.70 (s, 3 H, OMe), 3.76 (s, 3 H, OMe), 3.77 (s, 3 H, OMe), 3.33–3.85 (22 H, H-3, H-4$^{(C\ or\ A)\ and\ B,D,E,F,G}$, H-5, H-6a, H-6b) 3.39 (m, 1 H, H-5$^{A\ or\ C}$), 4.02–4.08 (3 H, H-6b), 4.24 (m, 1 H, H-5$^{C\ or\ A}$), 4.41 (m, 1 H, H-5), 4.74 (d, 1 H, $^{3}J_{H\text{-}1,H\text{-}2}$ = 2.6 Hz, H-1), 4.95 (d, 1 H, $^{3}J_{H\text{-}1,H\text{-}2}$ = 3.3 Hz, H-1), 5.09 (d, 1 H, $^{3}J_{H\text{-}1,H\text{-}2}$ = 3.1 Hz, H-1), 5.14 (d, 1 H, $^{3}J_{H\text{-}1,H\text{-}2}$ = 3.6 Hz, H-1), 5.30 (d, 1 H, $^{3}J_{H\text{-}1,H\text{-}2}$ = 3.8 Hz, H-1), 5.35 (d, 1 H, $^{3}J_{H\text{-}1,H\text{-}2}$ = 3.5 Hz, H-1), 5.86 (d, 1 H, $^{3}J_{H\text{-}1,H\text{-}2}$ = 2.7 Hz, H-1), 7.32–7.34 (3 H, *m*-H, *p*-H), 7.54–7.58 (m, 2 H, *o*-H) ppm; $^{13}C\{^{1}H\}$

NMR (75.5 MHz, $CDCl_3$, 25ºC): δ (assignment by HMQC) = 30.55 (d, $^1J_{C,P}$ = 16.8 Hz, C-$6^{A \text{ or } C}$), 33.05 (d, $^1J_{C,P}$ = 11.4 Hz, C-$6^{C \text{ or } A}$), 57.77, 57.95, 58.18, 58.35 [×2], 58.45, 58.76, 58.98, 59.04 [×2], 59.29, 59.38, 59.53, 60.20, 60.57, 61.33, 61.68, 62.00, 62.18 (OMe), 69.74, 70.34, 70.99, 71.42, 75.94 (C-$6^{C,D,E,F,G}$), 69.99 (d, $^2J_{C,P}$ = 13.8 Hz, C-$5^{A \text{ or } C}$), 70.28, 70.70, 71.21, 71.61 [×2] (C-$5^{C,D,E,F,G}$), 74.87 (d, $^2J_{C,P}$ = 9.1 Hz, C-$5^{C \text{ or } A}$), 78.79, 79.28, 79.77, 80.98 [×2], 81.24, 81.30, 81.69 [×4], 81.94, 82.12, 82.33 [×2], 82.46, 82.52, 82.80, 83.00 (C-2, C-3, C-$4^{B,D,E,F,G}$), 85.27 (C-$4^{A \text{ or } C}$), 90.43 (C-$4^{C \text{ or } A}$), 92.21, 93.63, 97.19, 99.10, 99.23, 99.56, 99.68 (C-1), 128.36 (d, $^3J_{C,P}$ = 6.5 Hz, *m*-C), 128.66 (*p*-C), 132.06 (d, $^2J_{C,P}$ = 18.5 Hz, *o*-C) 134.68 (d, $^1J_{C,P}$ = 45.3 Hz, *ipso*-C) ppm; $^{31}P\{^1H\}$ NMR (121.5 MHz $CDCl_3$, 25ºC): δ = –17.3 (s) ppm; elemental analysis (%) calcd for $C_{67}H_{111}O_{33}P{\cdot}CH_2Cl_2$ (1475.55 + 84.93): C 52.34, H 7.30, found: C 52.41, H 7.00; MS (ESI-TOF): *m/z* (%): 1497.72 (25) $[M + Na]^+$, 1475.74 (100) $[M + H]^+$.

***P*-{6^A,6^B-Dideoxy-6^A,6^B-[(*R*)-phenylphosphinidene]-2^A,2^B,2^C,2^D,2^E,2^F,2^G,3^A,3^B,3^C,3^D,3^E,3^F,3^G,6^C,6^D,6^E,6^F,6^G-nonadeca-*O*-methyl-β-cyclodextrin}-[chloro(*o*-dimethylbenzyl-aminomethylphenyl-*C*,*N*)]palladium(II) (20)**

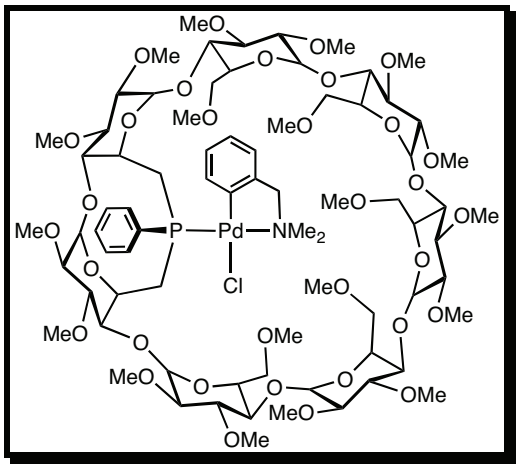

A solution of $[(o\text{-}C_6H_4CH_2NMe_2)PdCl]_2$ (0.017 g, 0.03 mmol) in CH_2Cl_2 (2 mL) was added to a solution of monophosphane **12** (0.090 g, 0.06 mmol) in CH_2Cl_2 (5 mL). After 15 min, the solvent was removed *in vacuo* and the residue was subjected to column chromatography (CH_2Cl_2/MeOH, 97:3, *v*/*v*) to afford pure **20** (yield: 0.090 g, 86%) as a pale yellow solid. R_f (SiO_2, CH_2Cl_2/MeOH, 94:6, *v*/*v*) = 0.35; m.p. dec. >250ºC; ^1H NMR (300.1 MHz, $CDCl_3$, 25 ºC): δ (assignment by COSY) = 1.73–1.86 (m, H-6a^A), 2.51–2.59 (m, 1 H, H-6a^B), 2.66 (s, NMe), 2.88 (s, NMe), 3.03–3.31 (10 H, H-2, H-4^{A,B}, H-6a^C), 3.12 (s, 3 H,

OMe-6), 3.36 (s, 3 H, OMe-6), 3.41 (s, 3 H, OMe-6), 3.43 (s, 6 H, OMe-6), 3.44 (s, 3 H, OMe), 3.45 (s, 3 H, OMe), 3.47 (s, 3 H, OMe), 3.48 (s, 6 H, OMe), 3.51 (s, 6 H, OMe), 3.60 (s, 3 H, OMe), 3.62 (s, 6 H, OMe), 3.63 (s, 3 H, OMe), 3.66 (s, 3 H, OMe), 3.70, (s, 3 H, OMe), 3.71 (s, 3 H, OMe), 3.40–3.91 (27 H, H-3, H-4^{C,D,E,F,G}, H-5^{D,E,F,G}, H-6^{D,E,F,G}, H-6b^{A,B}, NCH_2), 3.98 (d, $^2J_{H\text{-}6b,H\text{-}6a}$ = 10.1 Hz, H-6b^{C}), 4.17 (d, 1 H, ^2J = 12.9 Hz, NCH_2), 4.49 (d, $^3J_{H\text{-}5,H\text{-}6}$ = 9.3 Hz, H-5^{C}), 4.86 (d, $^3J_{H\text{-}1,H\text{-}2}$ = 1.7 Hz, H-1), 4.87 (m, H-5^{B}), 4.88 (d, $^3J_{H\text{-}1,H\text{-}2}$ = 3.9 Hz, H-1), 5.00 (d, $^3J_{H\text{-}1,H\text{-}2}$ = 3.3 Hz, H-1), 5.03 (d, $^3J_{H\text{-}1,H\text{-}2}$ = 4.6 Hz, H-1), 5.04 (m, H-5^{A}), 5.07 (d, $^3J_{H\text{-}1,H\text{-}2}$ = 3.1 Hz, H-1), 5.09 (d, $^3J_{H\text{-}1,H\text{-}2}$ = 4.0 Hz, H-1), 5.10 (d, $^3J_{H\text{-}1,H\text{-}2}$ = 3.8 Hz, H-1), 6.31 (t, J = 6.9 Hz, *o*-H of dmba), 6.46 (t, J = 7.5 Hz, *m*-H of dmba), 6.78 (t, J = 7.3 Hz, *p*-H of dmba), 6.93 (d, J = 7.5 Hz, *m*-H of dmba), 7.23–7.31 (m, 3 H, *m*-H, *p*-H), 7.65–7.71 (m, 2 H, *o*-H) ppm; $^{13}C\{^1H\}$ NMR (75.5 MHz, $CDCl_3$, 25 ºC): δ (assignment by HMQC) = 32.94 (d, $^1J_{C,P}$ = 23.5 Hz, C-6$^{A\text{ or }B}$), 33.6 (d, $^1J_{C,P}$ = 29.4 Hz, C-6$^{B\text{ or }A}$), 49.63 (br s, NCH_3), 50.44 (br s, NCH_3), 57.81, 57.96, 58.04, 58.19 [×2] (OMe-6), 58.65, 58.75, 58.85 [×2], 58.90 [×2], 59.09, 61.21, 61.30, 61.56, 61.62, 61.70 [×2], 62.05 (OMe), 66.25 (d, $^2J_{C,P}$ = 5.8 Hz, C-5$^{A\text{ or }B}$), 70.17 (d, $^2J_{C,P}$ = 7.8 Hz, C-5$^{B\text{ or }A}$), 70.90 [×2], 71.09 [×2], 71.75 (C-5^{C,D,E,F,G}), 71.09, 71.32, 71.52, 71.64, 72.36 (C-6^{C,D,E,F,G}), 73.01 (NCH_2), 79.91, 79.98, 80.58, 80.89 [×2], 80.98, 81.19, 81.74 [×3], 82.17, 82.36, 82.53,82.68 [×2], 82.82, 82.94, 83.08, 83.45 (C-2, C-3, C-4^{C,D,E,F,G}), 88.02 (d, $^3J_{C,P}$ = 9.5 Hz, C-4$^{A\text{ or }B}$), 88.65 (d, d, $^3J_{C,P}$ = 4.4 Hz, C-4$^{B\text{ or }A}$), 96.57, 97.94, 98.79, 100.20 [×2], 100.29, 101.58 (C-1), 122.01 (d, $^4J_{C,P}$ = 2.3 Hz, *m*-C of dmba), 123.52 (*p*-C of dmba), 125.36 (d, $^4J_{C,P}$ = 6.0 Hz, *m*-C of dmba), 128.15 (d, $^3J_{C,P}$ = 10.4 Hz, *m*-C of dmba), 130.15 (*p*-C), 132.38 (d, $^2J_{C,P}$ = 10.8 Hz, *o*-C), 134.91 (d, $^1J_{C,P}$ = 49.0 Hz, *ipso*-C), 136.47 (d, $^3J_{C,P}$ = 10.0 Hz, *ipso*-C), 147.67 (*quart*-C of dmba), 152.44 (*quart*-C of dmba) ppm; $^{31}P\{^1H\}$ NMR (121.5 MHz $CDCl_3$, 25ºC): δ = 25.5 (s) ppm; elemental analysis (%) calcd for $C_{76}H_{123}ClNO_{33}PPd$ (1751.62): C 52.11, H 7.08, N 0.80, found: C 50.34, H 7.07, N 0.80; MS (ESI-TOF): *m/z* (%):1790.60 (8) $[M + K]^+$, 1774.64 (4) $[M + Na]^+$, 1714.67 (100) $[M - Cl]^+$.

***P*-{6^{A},6^{C}-Dideoxy-6^{A},6^{C}-[(*R*)-phenylphosphinidene]-2^{A},2^{B},2^{C},2^{D},2^{E},2^{F},2^{G}, 3^{A},3^{B},3^{C},3^{D},3^{E},3^{F},3^{G},6^{B},6^{D},6^{E},6^{F},6^{G}-nonadeca-*O*-methyl-β-cyclodextrin}-[chloro(*o*-dimethylbenzyl-aminomethylphenyl-C,N)]palladium(II) (21)**

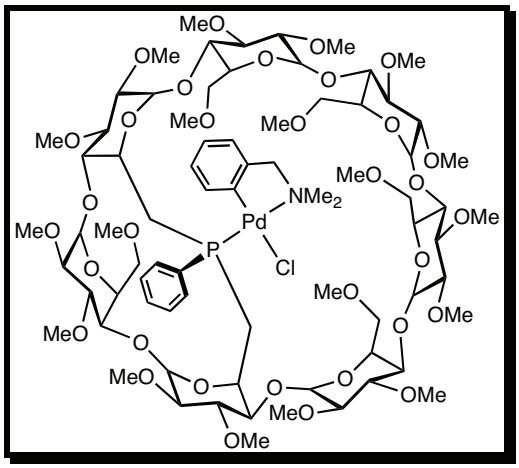

A solution of [(*o*-$C_6H_4CH_2NMe_2$)PdCl]$_2$ (0.022 g, 0.04 mmol) in CH_2Cl_2 (4 mL) was added to a solution of monophosphane **16** (0.100 g, 0.067 mmol) in CH_2Cl_2 (10 mL). After 15 min, the solvent was removed *in vacuo* and the residue was subjected to column chromatography (CH_2Cl_2/MeOH, 97:3, *v*/*v*) to afford pure **21** (yield: 0.098 g, 84%) as a pale yellow solid. R_f (SiO_2, CH_2Cl_2/MeOH, 92:8, *v*/*v*) = 0.40; m.p. dec. >250ºC; ^{1}H NMR (300.1 MHz, $CDCl_3$, 25ºC): δ (assignment by COSY) = 1.72 (dd, 1 H, $^{3}J_{H\text{-}2,H\text{-}3}$ = 10.1 Hz, $^{3}J_{H\text{-}2,H\text{-}1}$ = 3.7 Hz, H-2), 2.55 (br s, 3 H, NMe), 2.59–2.78 (2 H, H-6a^{A,C}), 2.85–3.79 (27 H, H-2, H-3, H-4, H-6a^{B,D,E,F,G}, H-6b^{A,C}, NCHa), 3.19 (s, 3 H, OMe), 3.24 (s, 3 H, OMe), 3.37 (s, 3 H, OMe), 3.38 (s, 3 H, OMe), 3.39 (s, 3 H, OMe), 3.45 (s, 6 H, OMe), 3.46 (s, 3 H, OMe), 3.48 (s, 6 H, OMe), 3.49 (s, 3 H, OMe), 3.59 (s, 3 H, OMe), 3.55 (s, 3 H, OMe), 3.56 (s, 3 H, OMe), 3.60 (s, 3 H, OMe), 3.64 (s, 3 H, OMe), 3.65 (s, 3 H, OMe), 3.69 (s, 3 H, OMe), 3.74 (s, 3 H, OMe), 3.94–4.21 (12 H, H-4, H-5$^{C\text{ or }A\text{ and }B,D,E,F,G}$, H-6b^{B,D,E,F,G}), 4.43 (d, 1 H, $^{2}J_{Hb,Ha}$ = 13.1 Hz, NCHb), 4.57 (m, 1 H, H-5$^{A\text{ or }C}$), 4.97 (d, 1 H, $^{3}J_{H\text{-}1,H\text{-}2}$ = 3.8 Hz, H-1), 5.05 (d, 1 H, $^{3}J_{H\text{-}1,H\text{-}2}$ = 3.2 Hz, H-1), 5.08 (m, 1 H, H-1), 5.10 (d, 2 H $^{3}J_{H\text{-}1,H\text{-}2}$ = 3.1 Hz, H-1), 5.31 (d, 1 H, $^{3}J_{H\text{-}1,H\text{-}2}$ = 3.0 Hz, H-1), 5.86 (d, 1 H, $^{3}J_{H\text{-}1,H\text{-}2}$ = 2.9 Hz, H-1), 6.48 (t, 1 H, $^{3}J_{o\text{-}H,m\text{-}H}$ = $^{3}J_{o\text{-}H,P}$ = 7.1 Hz, *o*-H), 6.57 (t, 1 H, $^{3}J_{m\text{-}H,o\text{-}H}$ = $^{3}J_{m\text{-}H,p\text{-}H}$ = 7.1 Hz, *m*-H), 6.69 (t, 1 H, $^{3}J_{p\text{-}H,m\text{-}H}$ = 7.1 Hz, *p*-H), 6.81 (d, 1 H, $^{3}J_{m\text{-}H,p\text{-}H}$ = 7.1 Hz, *m*-H), 7.19 (3 H, *m*-H, *p*-H), 7.68–7.72 (2 H, *o*-H) ppm; ^{13}C{^{1}H} NMR (75.5 MHz, $CDCl_3$, 25ºC): δ (assignment by HMQC) = 26.84 (d, $^{1}J_{C,P}$ = 22.5 Hz, C-6$^{A\text{ or }C}$), 29.52 (d, $^{1}J_{C,P}$ = 25.2 Hz, C-6$^{C\text{ or }A}$), 49.07, 51.66 (NMe_2), 57.42, 57.56, 58.16,

58.29, 58.51, 58.64, 58.84, 58.90, 58.98, 59.30 [×2], 59.51, 60.23, 60.52, 60.73, 61.03, 61.23, 61.34, 61.82 (OMe), 67.53 (C-5$^{A\text{ or }C}$), 68.30 (C-5$^{C\text{ or }A}$), 70.54, 70.63, 70.76, 71.09 [×2] (C-5^{B,D,E,F,G}), 71.09 (NCH_2), 71.87, 71.98, 72.34, 73.07, 75.24 (C-6^{B,D,E,F,G}), 74.44 (C-4$^{A\text{ or }C}$), 76.76 (d, $^3J_{C,P}$ = 9.9 Hz, C-4$^{C\text{ or }A}$), 77.48, 78.73, 79.95, 80.59, 80.75, 80.85, 80.95, 81.06, 81.30 [×2], 81.60, 82.16 [×2], 82.47 [×2], 82.62, 82.66, 83.06, 85.10 (C-2, C-3, C-4^{B,D,E,F,G}), 90.68, 93.16, 93.60, 98.48, 100.21 [×2], 101.35 (C-1), 122.06 (*m*-C of dmba), 123.29 (*p*-C of dmba), 125.38 (d, $^3J_{C,P}$ = 6.4 Hz, *m*-C of dmba), 127.12 (d, $^3J_{C,P}$ = 10.2 Hz, *m*-C), 129.49 (*p*-C), 133.10 (br, *o*-C), 134.91 (d, $^1J_{C,P}$ = 51.4 Hz, *ipso*-C), 135.46 (d, $^2J_{C,P}$ = 10.8 Hz, *o*-C of dmba), 145.92 (*ipso*-C of dmba), 152.78 (*ipso*-C of dmba) ppm; $^{31}P\{^1H\}$ NMR (121.5 MHz $CDCl_3$, 25ºC): δ = 15.3 (s) ppm; elemental analysis (%) calcd for $C_{76}H_{123}ClNO_{33}PPd$ (1751.62): C 52.11, H 7.08, N 0.80, found: C 51.90, H 7.15, N 0.77; MS (ESI-TOF): *m/z* (%): 1774.72 (86) $[M + Na]^+$, 1714.76 (100) $[M - Cl]^+$.

6^A,6^B,6^D,6^E-Tetradeoxy-6^A,6^B:6^D,6^E-bis(epithio)-2^A,2^B,2^C,2^D,2^E,2^F,2^G,3^A,3^B,3^C,3^D,3^E,3^F,3^G, 6^C,6^F,6^G-heptadeca-*O*-methyl-β-cyclodextrin (22)

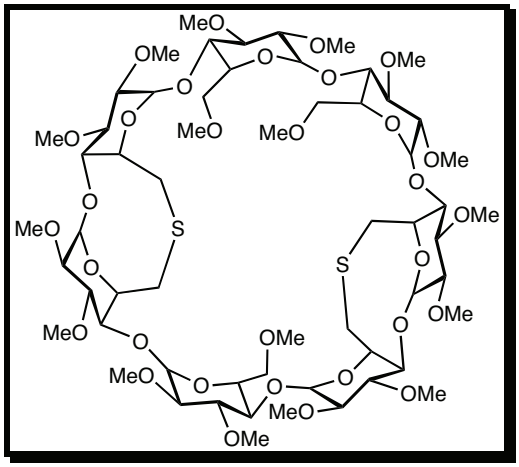

A solution of tetramesylate **9** (0.150 g, 0.089 mmol) in degassed acetone (5 mL) was treated with 18-crown-6 (0.141 g, 0.534 mmol) followed by powdered hydrated sodium sulfide ($Na_2S·9H_2O$, 0.064 g, 0.267 mmol). After 12 h stirring at room temperature, the reaction mixture was evaporated to dryness. The residue was disolved in saturated aqueous KCl solution (30 mL) and extracted with CH_2Cl_2 (3 × 30 mL). The combined organic layers were dried ($MgSO_4$) before removing the solvent. The crude product was purified by column chromatography (SiO_2, CH_2Cl_2/MeOH, 97:3, *v*/*v*) to give the desired product **22** (yield: 0.061 g, 50%) as a colourless solid. R_f (SiO_2, CH_2Cl_2/MeOH, 92:8, *v*/*v*) = 0.42; m.p. 203ºC;

^{1}H NMR (500.1 MHz, $CDCl_3$, 25ºC): δ (assignment by COSY, TOCSY and ROESY) = 2.66 (2 H, H-6a^{B,E}), 2.79 (d, 2 H, $^{2}J_{H\text{-}6a,H\text{-}6b}$ = 16.6 Hz, H-6a^{A,D}), 3.13 (2 H, H-2^{A,D}), 3.17 (dd, 1 H, $^{3}J_{H\text{-}2,H\text{-}3}$ = 9.8 Hz, $^{3}J_{H\text{-}1,H\text{-}2}$ = 3.6 Hz, H-2^{G}), 3.19 (dd, 1 H, $^{3}J_{H\text{-}2,H\text{-}3}$ = 9.8 Hz, $^{3}J_{H\text{-}1,H\text{-}2}$ = 3.6 Hz, H-2^{C}), 3.22 (dd, 1 H, $^{3}J_{H\text{-}2,H\text{-}3}$ = 9.5 Hz, $^{3}J_{H\text{-}1,H\text{-}2}$ = 3.6 Hz, H-2^{F}), 3.28 (d, 2 H, $^{2}J_{H\text{-}6b,H\text{-}6a}$ = 16.6 Hz, H-6b^{B,E}), 3.36–3.64 (21 H, H-2^{A,D}, H-3, H-4, H-6a^{C,F,G}, H-6b^{A,D}), 3.38 (s, 3 H, OMe-6^{G}), 3.39 (s, 6 H, OMe-6^{C,F}), 3.47 (s, 3 H, OMe-2^{G}), 3.48 (s, 3 H, OMe-2^{C}), 3.49 (s, 3 H, OMe-2^{F}), 3.50 (s, 3 H, OMe-2^{A}), 3.51 (s, 3 H, OMe-2^{D}), 3.54 (s, 6 H, OMe-2^{B,E}), 3.58 (s, 3 H, OMe-3), 3.59 (s, 3 H, OMe-3), 3.61 (s, 6 H, OMe-3), 3.62 (s, 3 H, OMe-3), 3.64 (s, 6 H, OMe-3), 3.69 (dd, 1 H, $^{2}J_{H\text{-}6b,H\text{-}6a}$ = 10.3 Hz, $^{3}J_{H\text{-}6b,H\text{-}5}$ = 3.8 Hz, H-6b^{C}), 3.77–3.82 (3 H, H-6b^{F,G}, H-5^{G}), 3.87–3.89 (2 H, H-5^{C,F}), 4.06–4.12 (2 H, H-5^{A,D}), 4.16–4.24 (2 H, H-5^{B,E}), 4.93 (d, 1 H, $^{3}J_{H\text{-}1,H\text{-}2}$ = 3.4 Hz, H-1^{C}), 4.97 (d, 1 H, $^{3}J_{H\text{-}1,H\text{-}2}$ = 3.6 Hz, H-1^{F}), 5.01 (d, 2 H, $^{3}J_{H\text{-}1,H\text{-}2}$ = 3.2 Hz, H-1^{A,D}), 5.05 (br s, 2 H, H-1^{B,E}), 5.17 (d, 1 H, $^{3}J_{H\text{-}1,H\text{-}2}$ = 2.7 Hz, H-1^{G}) ppm; ^{13}C{^{1}H} NMR (150.9 MHz $CDCl_3$, 25ºC): δ (assignment by HMQC) = 30.91 [×2] (br s, C-6^{B,E}), 35.41 [×2] (br s, C-6^{A,D}), 58.13, 58.28, 58.38 [×2], 58.51, 58.60, 59.00 [×2], 59.09, 59.15, 61.60 [×2], 61.29 [×2], 61.47 [×3] (OMe), 70.74 [×3] (C-5^{C,F,G}), 71.05 [×3] (C-6^{C,F,G}), 73.47 [×2] (C-5^{B,E}), 79.01 [×2] (C-5^{A,D}), 80.68, 80.96 [×2], 81.22, 81.33, 81.76 [×2], 81.81 [×3], 81.83 [×3], 81.99 [×2], 82.06, 82.17, 83.48, 84.01, 84.58, 84.69 (C-2, C-3, C-4), 97.83, 97.99, 98.84 [×2], 99.02, 99.28, 99.46 (C-1) ppm; elemental analysis (%) calcd for $C_{59}H_{100}O_{31}S_2$ (1369.54): C 51.74, H 7.36, found: C 51.56, H 7.59; MS (ESI-TOF): *m/z* (%): 1391.56 (100) $[M + Na]^{+}$.

6^{A},6^{B},6^{D},6^{E}-Tetradeoxy-6^{A},6^{B}:6^{D},6^{E}-bis(sulfate)-2^{A},2^{B},2^{C},2^{D},2^{E},2^{F},3^{A},3^{B},3^{C},3^{D},3^{E},3^{F},6^{C},6^{F}-tetradeca-*O*-methyl-α-cyclodextrin (25)

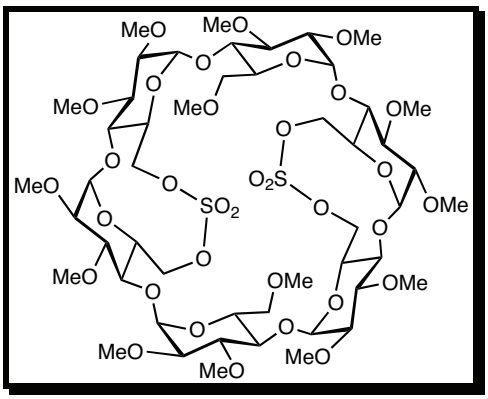

A solution of freshly distilled thionyl chloride (0.72 g, 0.44 mL, 6.08 mmol) in CH_2Cl_2 (25 mL) was added dropwise to a solution of tetrol **24** (1.57 g, 1.35 mmol) and NEt_3 (0.68 g, 0.93 mL, 6.75 mmol) in CH_2Cl_2 (300 mL) at –78ºC. The reaction mixture was stirred for 1 h at –78ºC whereupon it was allowed to reach 0ºC, quenched with a saturated aqueous $NaHCO_3$ solution (200 mL), and extracted with $CHCl_3$ (3 × 150 mL). The combined organic extracts were dried ($MgSO_4$) before being evaporated to dryness to afford a colourless residue, which was dissolved in a mixture of CH_2Cl_2 (18 mL), MeCN (18 mL) and water (36 mL). Ruthenium trichloride (6 mg, 28×10^{-3} mmol) and sodium periodate (0.64 g, 2.97 mmol) were then added and the reaction mixture was stirred for 12 h at room temperature before adding a saturated aqueous $NaHCO_3$ solution (200 mL). Subsequent extraction with $CHCl_3$ (3 × 100 mL) was followed by drying of the organic extracts ($MgSO_4$). Removal of the solvent *in vacuo* gave a colourless residue which was subjected to column chromatography (SiO_2, CH_2Cl_2/MeOH, 97:3, *v*/*v*) to afford **25** (yield: 1.66 g, 95%) as a colourless solid. R_f (SiO_2, CH_2Cl_2/MeOH, 90:10, *v*/*v*) = 0.51; m.p. 189ºC; ^{1}H NMR (300.1 MHz, $CDCl_3$, 25ºC): δ (assignment by COSY) = 3.07 (t, 2 H, $^3J_{H\text{-}4,H\text{-}3} = {}^3J_{H\text{-}4,H\text{-}5}$ = 9.4 Hz, H-4$^{A,D\text{ or }B,E}$), 3.13–3.21 (6 H, H-2), 3.28 (t, 2 H, $^3J_{H\text{-}4,H\text{-}3} = {}^3J_{H\text{-}4,\,H\text{-}5}$ = 9.4 Hz, H-4$^{B,E\text{ or }A,D}$), 3.38 (s, 6 H, OMe), 3.48 (s, 12 H, OMe), 3.54 (s, 6 H, OMe), 3.61 (s, 6 H, OMe), 3.65 (s, 6 H, OMe), 3.66 (s, 6 H, OMe), 3.42–3.60 (8 H, H-3$^{B,E\text{ or }A,D\text{ and }C,F}$, H-4^{C,F}, H-6b^{C,F}), 3.89–3.91 (4 H, H-3$^{A,D\text{ or }B,E}$, H-5^{C,F}), 4.01–4.09 (4 H, H-6b$^{A,D\text{ or }B,E}$, H-6a^{C,F}), 4.17 (dd, 2 H, $^3J_{H\text{-}5,H\text{-}4}$ = 9.9, $^3J_{H\text{-}5,H\text{-}6}$ = 4.6 Hz, H-5$^{B,E\text{ or }A,D}$), 4.37 (d, 2 H, $^2J_{H\text{-}6b,H\text{-}6a}$ = 9.8 Hz, H-6b$^{B,E\text{ or }A,D}$), 4.52 (t, 2 H, $^3J_{H\text{-}5,H\text{-}6a} = {}^3J_{H\text{-}5,H\text{-}6b}$ = 10.2 Hz, H-5$^{A,D\text{ or }B,E}$), 4.69 (dd, 2 H, $^2J_{H\text{-}6a,H\text{-}6b}$ = 9.8, $^3J_{H\text{-}6a,H\text{-}5}$ = 5.1 Hz, H-6a$^{B,E\text{ or }A,D}$), 4.93 (d, 2 H, $^3J_{H\text{-}1,H\text{-}2}$ = 3.2 Hz, H-1), 4.98 (overlapping d, 2 H, H-6a$^{A,D\text{ or }B,E}$), 5.01 (d, 2 H, $^3J_{H\text{-}1,H\text{-}2}$ = 3.2 Hz, H-1), 5.08 (d, 2 H, $^3J_{H\text{-}1,H\text{-}2}$ = 3.6 Hz, H-1) ppm; ^{13}C{^{1}H} NMR (75.5 MHz, $CDCl_3$, 25ºC): δ (assignment by HMQC) = 57.67, 57.98, 58.68, 59.17, 61.59, 61.95, 62.00 (OMe), 67.39 (C-5$^{A,D\text{ or }B,E}$), 69.09 (C-5$^{B,E\text{ or }A,D}$), 70.93 (C-6^{C,F}), 71.39 (C-5^{C,F}), 73.03 (C-6$^{A,D\text{ or }B,E}$), 75.03 (C-6$^{B,E\text{ or }A,D}$), 80.92, 81.24 [×2], 81.44, 81.51, 82.26 [×2], 83.60, 86.83 (C-2, C-3, C-4), 98.34, 100.27, 100.64 (C-1) ppm; elemental analysis (%) calcd for $C_{50}H_{84}O_{34}S_2\cdot0.5CHCl_3$: (1293.31 + 59.69): C 44.83, H 6.29, found: C 44.91, H 6.37; MS (ESI-TOF): *m/z* (%): 1315.42 (100) $[M + Na]^+$.

6^A,6^B,6^D,6^E-Tetradeoxy-6^A,6^B:6^D,6^E-bis(sulfate)2^A,2^B,2^C,2^D,2^E,2^F,2^G,3^A,3^B,3^C,3^D,3^E,3^F, 3^G, 6^C,6^F,6^G-heptadeca-*O*-methyl-β-cyclodextrin (26)

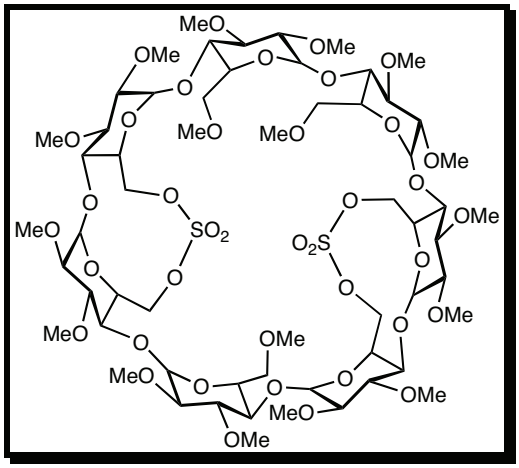

This compound was prepared from **8** (1.28 g, 0.93 mmol) according to the above procedure (yield: 1.34 g, 95%). R_f (SiO_2, CH_2Cl_2/MeOH, 90:10, *v*/*v*) = 0.51; m.p. 191ºC; ^{1}H NMR (600.1 MHz, $CDCl_3$, 25ºC): δ (assignment by COSY, TOCSY and ROESY) = 3.11–3.21 (7 H, H-$2^{A,C,D,F,G}$, H-$4^{B,E}$), 3.26 (dd, 1 H, $^3J_{H\text{-}2,H\text{-}3}$ = 9.1 Hz, $^3J_{H\text{-}1,H\text{-}2}$ = 4.2 Hz, H-2^B), 3.28 (dd, 1 H, $^3J_{H\text{-}2,H\text{-}3}$ = 8.6 Hz, $^3J_{H\text{-}1,H\text{-}2}$ = 4.2 Hz, H-2^E), 3.37–3.72 (14 H, H-3, H-$4^{A,D,F,G}$, H-$6a^{C,F,G}$), 3.39 (s, 3 H, OMe-6^C), 3.39 (s, 3 H, OMe-6^G), 3.40 (s, 3 H, OMe-6^F), 3.49 (s, 12 H, OMe-$2^{B,C,E,G}$), 3.50 (s, 3 H, OMe-2^F), 3.56 (s, 3 H, OMe-2^A), 3.57 (s, 3 H, OMe-2^D), 3.60 (s, 6 H, OMe-3), 3.62 (s, 6 H, OMe-3), 3.64 (s, 3 H, OMe-3),3.65 (s, 6 H, OMe-3), 3.78–3.82 (4 H, H-4^C, H-$5^{C,F,G}$), 3.86 (dd, 1 H, $^2J_{H\text{-}6b,H\text{-}6a}$ = 10.9 Hz, $^3J_{H\text{-}6b,H\text{-}5}$ = 3.2 Hz, H-$6b^F$), 3.94 (dd, 1 H, $^2J_{H\text{-}6b,H\text{-}6a}$ = 11.1 Hz, $^3J_{H\text{-}6b,H\text{-}5}$ = 2.8 Hz, H-$6b^G$), 3.98 (d, 1 H, $^2J_{H\text{-}6b,H\text{-}6a}$ = 11.1 Hz, H-$6b^C$), 4.13–4.18 (3 H, H-$5^{A,D}$, H-$6a^B$), 4.24 (m, 1 H, H-$6a^E$), 4.33 (td, 1 H, $^3J_{H\text{-}5,H\text{-}4}$ = $^3J_{H\text{-}5,H\text{-}6a}$ = 10.0 Hz, $^3J_{H\text{-}5,H\text{-}6b}$ = 1.1 Hz, H-5^B), 4.41 (td, 1 H, $^3J_{H\text{-}5,H\text{-}4}$ = $^3J_{H\text{-}5,H\text{-}6a}$ = 9.9 Hz, $^3J_{H\text{-}5,H\text{-}6b}$ = 1.4 Hz, H-5^E), 4.45 (dd, 1 H, $^2J_{H\text{-}6a,H\text{-}6b}$ = 10.1 Hz, $^3J_{H\text{-}6a,H\text{-}5}$ = 1.0 Hz, H-$6a^A$), 4.50 (dd, 1 H, $^2J_{H\text{-}6a,H\text{-}6b}$ = 10.1 Hz, $^3J_{H\text{-}6a,H\text{-}5}$ = 1.0 Hz, H-$6a^D$), 4.58 (dd, 1 H, $^2J_{H\text{-}6b,H\text{-}6a}$ = 10.1 Hz, $^3J_{H\text{-}6b,H\text{-}5}$ = 4.2 Hz, H-$6b^D$), 4.61 (dd, 1 H, $^2J_{H\text{-}6b,H\text{-}6a}$ = 10.1 Hz, $^3J_{H\text{-}6b,H\text{-}5}$ = 4.4 Hz, H-$6b^A$), 4.86 (d, 1 H, $^3J_{H\text{-}1,H\text{-}2}$ = 3.7 Hz, H-1^C), 4.87 (dd, 1 H, $^2J_{H\text{-}6b,H\text{-}6a}$ = 12.3 Hz, $^3J_{H\text{-}6b,H\text{-}5}$ = 1.7 Hz, H-$6b^E$), 4.95 (d, 1 H, $^3J_{H\text{-}1,H\text{-}2}$ = 3.7 Hz, H-1^F), 4.97 (dd, 1 H, $^2J_{H\text{-}6b,H\text{-}6a}$ = 12.3 Hz, $^3J_{H\text{-}6b,H\text{-}5}$ = 1.2 Hz, H-$6b^B$), 5.05 (d, 1 H, $^3J_{H\text{-}1,H\text{-}2}$ = 3.1 Hz, H-1^D), 5.06 (d, 1 H, $^3J_{H\text{-}1,H\text{-}2}$ = 3.1 Hz, H-1^A), 5.08 (d, 1 H, $^3J_{H\text{-}1,H\text{-}2}$ = 3.3 Hz, H-1^G), 5.14 (d, 1 H, $^3J_{H\text{-}1,H\text{-}2}$ = 4.1 Hz, H-1^E), 5.16 (d, 1 H, $^3J_{H\text{-}1,H\text{-}2}$ = 4.1 Hz, H-1^B) ppm; ^{13}C{^{1}H} NMR (75.5 MHz $CDCl_3$, 25ºC): δ (assignment by HMQC) = 58.20 [×3], 58.52, 58.98, 59.03, 59.12 [×3], 59.44, 61.11, 61.18, 61.25, 61.52,

61.78 [×3] (OMe), 68.42 [×3], 68.55 (C-$5^{A,D,B,E}$), 70.55 [×2], 70.89 (C-$6^{C,F,G}$), 70.89, 71.19, 71.31 (C-$5^{C,F,G}$), 73.79 [×3], 73.88 (C-$6^{A,D,B,E}$), 80.01, 80.70, 81.19, 81.28 [×3], 81.47 [×6], 81.57, 81.65, 81.70, 81.78 [×3], 82.59, 82.75, 82.94 (C-2, C-3, C-4), 97.92, 98.93, 99.09, 99.71 [×2], 100.42, 100.52 (C-1) ppm; elemental analysis (%) calcd for $C_{59}H_{100}O_{39}S_2$: (1497.53): C 47.32, H 6.73, found: C 47.55, H 6.67; MS (ESI-TOF): *m/z* (%): 1519.52 (100) $[M + Na]^+$.

II.4.4. X-ray crystallographic data for 4

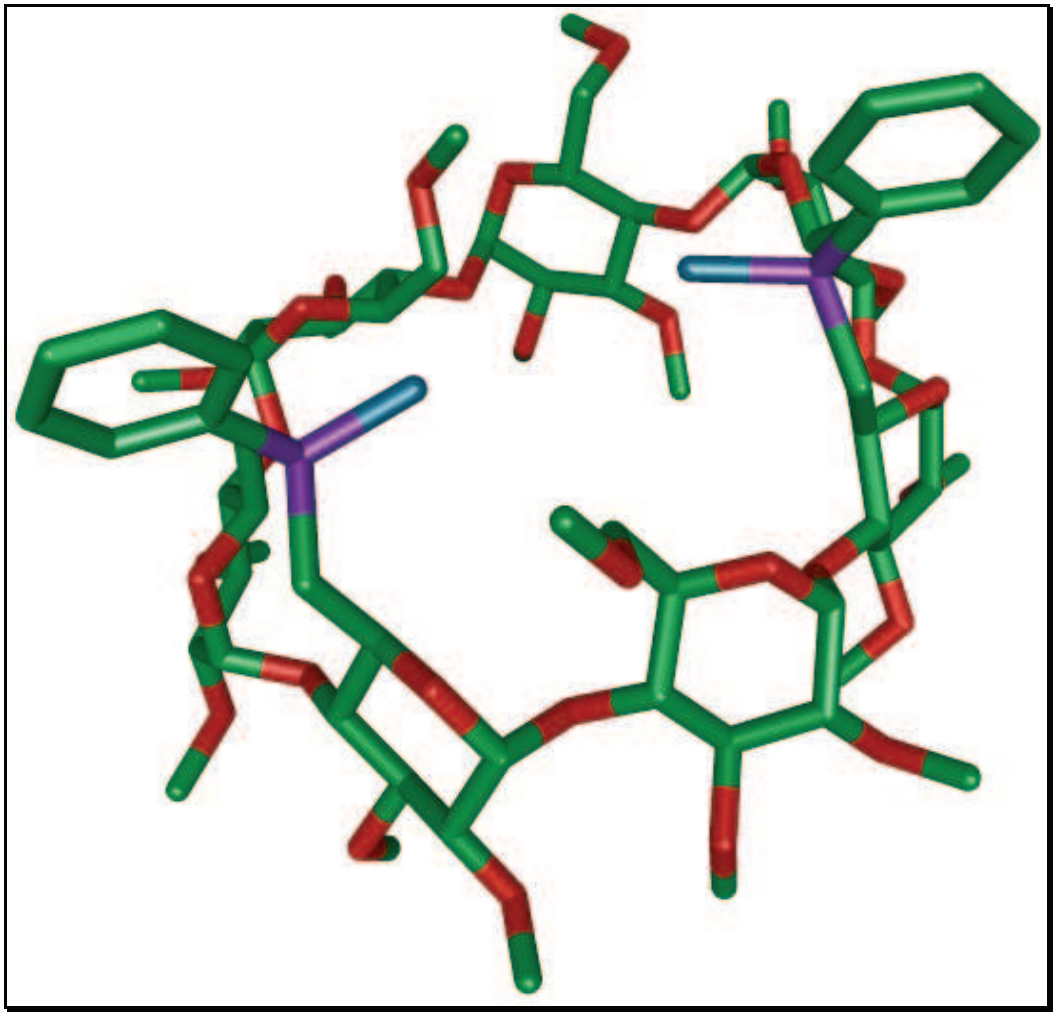

The X-ray structure determination was performed by Dr L. Toupet (University of Rennes, France). Single crystals were obtained by slow diffusion of pentane into a commercial ethyl acetate solution of **4**. The sample was studied on a Oxford Diffraction Xcalibur Saphir 3 CCD with graphite monochromatised MoKα radiation (λ = 0.71073 Å). The structure was solved with SIR-97,[133] which revealed the non-hydrogen atoms of the molecule. After anisotropic refinement, many hydrogen atoms were found with a Fourier difference analysis. The whole structure was refined with SHELX-97[134] and full-matrix least-square techniques (use of F^2 magnitude; x, y, z, β_{ij} for C, B, O, P atoms, x, y, z, in riding mode for H atoms; 1033 variables and 15406 observations with $I > 2.0\sigma(I)$; calcd $w = 1/[\sigma^2(F_o^2) + (0.0840\ P)^2]$ where $P = (F_o^2 + 2\ F_o^2)/3$ with the resulting $R = 0.0475$, $R_w = 0.1241$ and $S_w = 0.954$; $\Delta\rho < 0.592$ eÅ^{-3}. The absolute configuration (and thus the enantiomeric space group assignment) was determined by a *Flack* x parameter of 0.02(6). A summary of the crystallographic data is given in Table 1. CCDC reference number 744760.

Table 1. Crystal data and structure refinement for **4**·0.5($C_4H_8O_2$)·0.5(C_5H_{12})·0.5(H_2O).

Crystal Data	
Crystal size	0.35 × 0.35 × 0.32 mm^3
Empirical formula	$C_{75.5}H_{127}B_2O_{32.5}P_2$
M_r	1638.33
Crystal system	Monoclinic
Space group	$P2_1$
Temperature	150(2) K
Unit cell parameters	
a	13.1531(2) Å
b	21.8818(3) Å
c	16.5539(2) Å
α	90º
β	104.3030 (10)º
γ	90º
V	4616.75(11) $Å^3$
Z	2
D (calculated)	1.179 g/cm^3
F (000)	1760
□	0.474 mm^{-1}
Data Processing and Reduction	
θ range for data collection	2.70 to 27.00º
Index ranges	$-16 \leq h \leq 16$, $-27 \leq k \leq 27$, $-21 \leq l \leq 21$
Reflections collected	62293
Independent reflections	20027 [R(int) = 0.0287]
Refinement method	Full-matrix least-squares on F^2
Data / restraints / parameters	20027 / 1 / 1033
Goodness-on-fir on F^2	1.096
Final R indices [$I > 2\sigma(I)$]	R1 = 0.0475, *w*R2 = 0.1201
R indices (all data)	R1 = 0.0607, *w*R2 = 0.1241
Largest diff. peak and hole	0.592 and -0.493 $eÅ^{-3}$

II.4.5. X-ray crystallographic data for 25

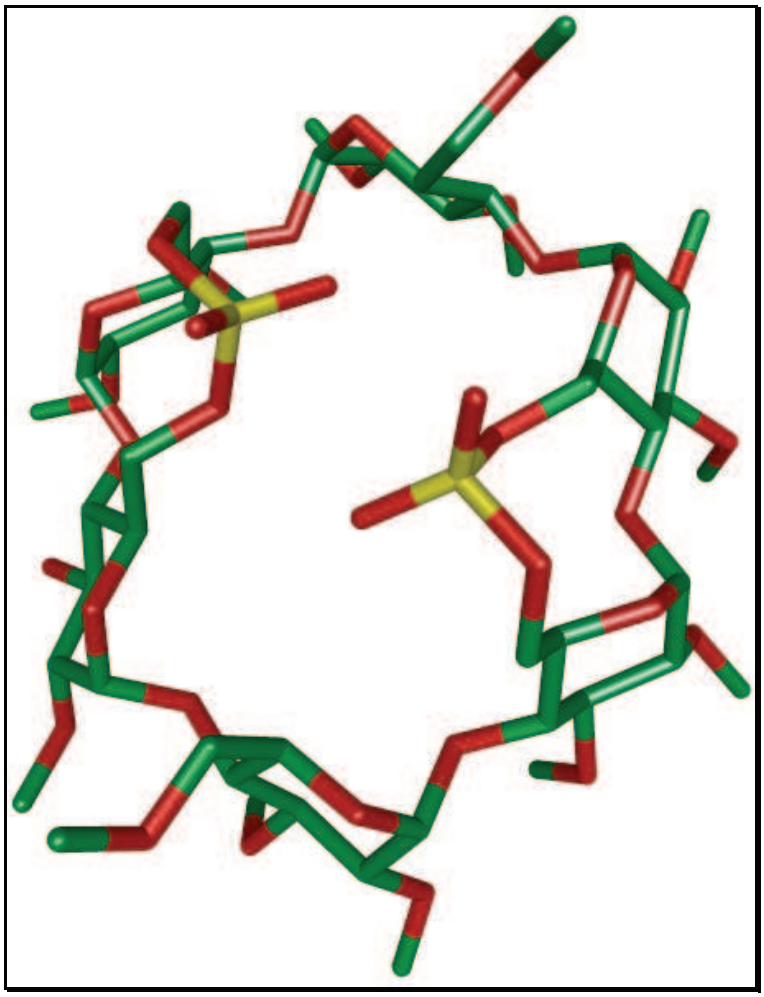

The X-ray structure determination was performed by Dr L. Toupet (University of Rennes, France). Single crystals were obtained by slow diffusion of pentane into a dichloromethane solution of **25**. The sample was studied on a Oxford Diffraction Xcalibur Saphir 3 CCD with graphite monochromatised MoKα radiation (λ = 0.71073 Å). The structure was solved with SIR-97,[133] which revealed the non-hydrogen atoms of the molecule. After anisotropic refinement, many hydrogen atoms were found with a Fourier difference analysis. The whole structure was refined with SHELX-97[134] and full-matrix least-square techniques (use of F^2 magnitude; x, y, z, β_{ij} for C, O, S atoms, x, y, z, in riding mode for H atoms; 874 variables and 15792 observations with $I > 2.0\sigma(I)$; calcd $w = 1/[\sigma^2(F_o^2) + (0.1186\,P)^2]$ where $P = (F_o^2 + 2\,F_o^2)/3$ with the resulting $R = 0.0506$, $R_w = 0.1476$ and $S_w = 0.842$; $\Delta\rho < 1.306$ eÅ^{-3}. The absolute configuration (and thus the enantiomeric space group assignment) was determined by a *Flack* x parameter of 0.00(5). A summary of the crystallographic data is given in Table 2. CCDC reference number 738543.

Table 2. Crystal data and structure refinement for **25**·2(CH_2Cl_2)·0.5(C_5H_{12}).

Crystal Data	
Crystal size	0.26 × 0.22 × 0.22 mm^3
Empirical formula	$C_{54.5}H_{94}Cl_4O_{34}S_2$
M_r	1499.22
Crystal system	Monoclinic
Space group	$P2_1$
Temperature	120(2) K
Unit cell parameters	
a	14.6490(2) Å
b	16.4157(2) Å
c	16.0156(2) Å
α	90º
β	109.1850 (10)º
γ	90º
V	4616.75(11) $Å^3$
Z	2
D (calculated)	1.369 g/cm^3
F (000)	1586
□	0.306 mm^{-1}
Data Processing and Reduction	
θ range for data collection	2.61 to 27.00º
Index ranges	-18 ≤ h ≤ 18, -20≤ k ≤ 20, -20≤ l ≤ 20
Reflections collected	32951
Independent reflections	15792 [R(int) = 0.0256]
Refinement method	Full-matrix least-squares on F^2
Data / restraints / parameters	15792 / 1 / 874
Goodness-on-fir on F^2	0.842
Final R indices [I > 2σ(I)]	R1 = 0.0506, *w*R2 = 0.1409
R indices (all data)	R1 = 0.0665, *w*R2 = 0.1476
Largest diff. peak and hole	1.306 and -0.616 $eÅ^{-3}$

II.5. References

[1] A. Villiers, *Compt. Rend.* **1891**, *112*, 536.

[2] F. Schardinger, *Z. Unters. Nahr. u. Genussm* **1903**, *6*, 865-880.

[3] F. Schardinger, *Wien. Klin. Wochenschr* **1904**, *17*, 207-209.

[4] F. Schardinger, *Zentralbl. Bakteriol. Parasitenk. Abt. 2* **1905**, *14*, 772-781.

[5] F. Schardinger, *Zentralbl. Bakteriol. Parasitenk. Abt. 2* **1911**, *29*, 188-197.

[6] K. Freudenberg, *Ber. Dtsch. Chem. Ges.* **1936**, *69*, 1258-1266.

[7] K. Freudenberg, *Ber. Dtsch. Chem. Ges.* **1936**, *69*, 2041-2045.

[8] K. Freudenberg, *Naturwissenschaften* **1938**, *26*, 123-124.

[9] K. Freudenberg, *Ber. Dtsch. Chem. Ges.* **1938**, *71*, 1596-1600.

[10] D. French, *Carbohydr. Chem.* **1957**, *12*, 189-260.

[11] F. Cramer, *Einschlussverbindungen,* Springer-Verlag, Berlin, **1954**.

[12] A. Hybl, R. E. Rundle, D. E. William, *J. Am. Chem. Soc.* **1965**, *87*, 2779-2788.

[13] W. Saenger, M. Noltemeyer, P. C. Manor, B. Himgerty, B. Klar, *Bioorg. Chem.* **1976**, *5*, 187-195.

[14] M. L. Bender, M. Komiyama, *Cyclodextrin Chemistry,* Springer, Berlin, **1978**.

[15] J. L. Atwood, J. E. D. Davies, D. D. Macinol, F. Vögtle, J.-M. Lehn, *'Cyclodextrins', Comprehensive Supramolecular Chemistry,* Pergamon, Oxford, **1996**.

[16] C. J. Easton, S. F. Lincoln, *Modified Cyclodextrins,* Imperial College Press, London **1999**.

[17] M. V. Rekharsky, Y. Inoue, *Chem. Rev.* **1998**, *98*, 1875-1917.

[18] S. A. Nepogodiev, J. F. Stoddart, *Chem. Rev.* **1998**, *98*, 1959-1976.

[19] D. Wilson, L. Perlson, R. Breslow, *Bioorg. Med. Chem.* **2003**, *11*, 2649-2653.

[20] S. Tilloy, H. Bricout, E. Monflier, *Green Chemistry* **2002**, *4*, 188-193.

[21] H. Bricout, F. Hapiot, A. Ponchel, S. Tilloy, E. Monflier, *Sustainability* **2009**, *1*, 294-945.

[22] I. Tabushi, *Acc. Chem. Res.* **1982**, *15*, 66-72.

[23] R. Breslow, J. W. Canary, M. Varney, S. T. Waddell, D. Yang, *J. Am. Chem. Soc.* 1990, *112*, 5212-5219.

[24] G. Wenz, *Angew. Chem., Int. Ed. Engl.* **1994**, *33*, 803-822.

[25] A. W. Coleman, C.-C. Ling, M. Miocque, *Angew. Chem.* **1992**, *104*, 1402-1404.

[26] S. Li, W. C. Purdy, *Chem. Rev.* **1992**, *92*, 1457-1470.

[27] V. J. Stella, V. M. Rao, E. A. Zannou, V. Zia, *Adv. Drug. Deliv. Rev.* **1999**, *36*, 3-16.

[28] F. Hirayama, K. Uekama, *Adv. Drug. Deliv. Rev.* **1999**, *36*, 125-141.

[29] L. Marinescu, M. Bols, *Curr. Org. Chem.* **2010**, *14*, 1380-1398.

[30] R. Breslow, S. Dong, *Chem. Rev.* **1998**, *98*, 1997-2011.

[31] K. Takahashi, *Chem. Rev.* **1998**, *98*, 2013-2033.

[32] C. Rousseau, B. Christensen, T. E. Petersen, M. Bols, *Org. Biomol. Chem.* **2004**, *2*, 3476-3482.

[33] F. Ortega-Caballero, J. Bjerre, L. S. Laustsen, M. Bols, *J. Org. Chem.* **2005**, *70*, 7217-7226.

[34] F. Ortega-Caballero, C. Rousseau, B. Christensen, T. E. Petersen, M. Bols, *J. Am. Chem. Soc.* **2005**, *127*, 3238-3239.

[35] R. Villalonga, R. Cao, A. Fragoso, *Chem. Rev.* **2007**, *107*, 3088-3116.

[36] J. Bjerre, C. Rousseau, L. Marinescu, M. Bols, *Appl. Microbiol. Biotechnol.* **2008**, *81*, 1-11.

[37] T. H. Fenger, J. Bjerre, M. Bols, *Chem. Bio. Chem.* **2009**, *10*, 2494-2503.

[38] T. H. Fenger, L. G. Marinescu, M. Bols, *Org. Biomol. Chem.* **2009**, *7*, 933-943.

[39] T. H. Fenger, M. Bols, *Chem. Commun.* **2010**, *46*, 7769-7771.

[40] T. H. Fenger, M. Bols, *J. Incl. Phenom. Macrocyclic Chem.* **2011**, *69*, 397-402.

[41] I. Tabushi, Y. J. Kuroda, *J. Am. Chem. Soc.* **1984**, *106*, 4580-4584.

[42] I. Tabushi, Y. J. Kuroda, T. Mizutani, *Tetrahedron* **1984**, *40*, 545-552.

[43] E. U. Akkaya, A. W. Czarnik, *J. Am. Chem. Soc.* **1988**, *110*, 8553-8554.

[44] E. U. Akkaya, A. W. Czarnik, *J. Phys. Org. Chem.* **1992**, *5*, 540-548.

[45] A. W. Coleman, C.-C. Ling, M. Miocque, *J. Coord. Chem.* **1992**, *26*, 137-141.

[46] C.-C. Ling, M. Miocque, A. W. Coleman, *J. Coord. Chem.* **1993**, *28*, 313-317.

[47] M. T. Reetz, J. Rudolph, *Tetrahedron: Assymetry* **1993**, *4*, 2405-2406.

[48] M. Sawamura, K. Kitayama, Y. Ito, *Tetrahedron: Assymetry* **1993**, *4*, 1829-1832.

[49] I. Nicolis, A. W. Coleman, P. Charpin, C. de Rango, *Angew. Chem. Int. Ed.* **1995**, *34*, 2381-2383.

[50] R. P. Bonomo, S. Pedotti, G. Vecchio, E. Rizzarelli, *Inorg. Chem.* **1996**, *35*, 6873-6877.

[51] R. P. Bonomo, E. Conte, G. De Guidi, G. Maccarrone, E. Rizzarelli, G. Vecchio, *J. Chem. Soc., Dalton Trans.* **1996**, 4351-4355.

[52] V. Cucinotta, G. Grasso, S. Pedotti, E. Rizzarelli, G. Vecchio, B. Di Blasio, C. Isernia, M. Saviano, C. Pedone, *Inorg. Chem.* **1996**, *35*, 7535-7540.

[53] M. T. Reetz, S. R. Waldvogel, *Angew. Chem. Int. Ed.* **1997**, *36*, 865-867.

[54] M. T. Reetz, *Catal. Today* **1998**, *42*, 399-411.

[55] D. Armspach, D. Matt, *Chem. Commun.* **1999**, 1073-1074.

[56] F. Charbonnier, T. Humbert, A. Marsura, *Tetrahedron Lett.* **1999**, *40*, 4047-4050.

[57] R. M. Deshpande, A. Fukuoka, M. Ichikawa, *Chem. Lett.* **1999**, 13-14.

[58] M. T. Reetz, C. Frömbgen, *Synthesis* **1999**, 1555-1557.

[59] M. Selktim, I. Nicolis, A. Navaza, *J. Coord. Chem.* **1999**, *47*, 541-549.

[60] D. Armspach, D. Matt, *Inorg. Chem.* **2001**, *40*, 3505-3509.

[61] D. Armspach, D. Matt, N. Kyritsakas, *Polyhedron* **2001**, *20*, 663-668.

[62] E. Engeldinger, D. Armspach, D. Matt, *Angew. Chem. Int. Ed.* **2001**, *40*, 2526-2529.

[63] M. T. Reetz, J. Rudolph, R. Goddard, *Can. J. Chem.* **2001**, *79*, 1806-1811.

[64] M. Wagner, P. Engrand, J.-B. Regnouf-de-Vains, A. Marsura, *Tetrahedron Lett.* **2001**, *42*, 5207-5209.

[65] C. Yang, Y. K. Cheung, J. Yao, Y. T. Wong, J. G., *Organometallics* **2001**, *20*, 424-429.

[66] C. Yang, Y. T. Wong, Z. Li, J. J. Krepinsky, G. Jia, *Organometallics* **2001**, *20*, 5220-5224.

[67] E. Engeldinger, D. Armspach, D. Matt, P. G. Jones, R. Welter, *Angew. Chem. Int. Ed.* **2002**, *41*, 2593-2596.

[68] E. Engeldinger, D. Armspach, D. Matt, L. Toupet, M. Wesolek, *C. R. Chimie* **2002**, *5*, 359-372.

[69] R. Heck, F. Dumarcay, A. Marsura, *Chem. Eur. J.* **2002**, *8*, 2438-2445.

[70] M. T. Reetz, I. D. Kostas, S. R. Waldvogel, *Inorg. Chem. Commun.* **2002**, *5*, 252-254.

[71] Y. T. Wong, C. Yang, K.-C. Ying, G. Jia, *Organometallics* **2002**, *21*, 1782-1787.

[72] E. Engeldinger, D. Armspach, D. Matt, P. G. Jones, *Chem. Eur. J.* **2003**, *9*, 3091-3105.

[73] R. Heck, A. Marsura, *Tetrahedron Lett.* **2003**, *44*, 1533-1536.

[74] M. Badis, A. Van der Heyden, R. Heck, A. Marsura, B. Gauthier-Manuel, A. Zywocinski, E. Rogalska, *Langmuir* **2004**, *20*, 5338-5346.

[75] E. Engeldinger, L. Poorters, D. Armspach, D. Matt, L. Toupet, *Chem. Commun.* **2004**, *6*, 634-635.

[76] R. Heck, A. Marsura, *Tetrahedron Lett.* **2004**, *45*, 281-284.

[77] B. Benmerad, P. Clair, D. Armspach, D. Matt, F. Balegroune, L. Toupet, *Chem. Commun.* **2006**, 2678-2680.

[78] D. Armspach, L. Poorters, D. Matt, B. Benmerad, P. G. Jones, I. Dix, L. Toupet, *J. Incl. Phenom. Macrocyclic Chem.* **2007**, *57*, 243-250.

[79] L. Poorters, D. Armspach, D. Matt, L. Toupet, S. Choua, P. Turek, *Chem. Eur. J.* **2007**, *13*, 9448-9461.

[80] L. Poorters, D. Armspach, D. Matt, L. Toupet, *Dalton Trans.* **2007**, *29*, 3195-3202.

[81] L. Poorters, D. Armspach, D. Matt, L. Toupet, P. G. Jones, *Angew. Chem. Int. Ed.* **2007**, *46*, 2663-2665.

[82] L. Poorters, M. Lejeune, D. Armspach, D. Matt, *Actualite Chimique* **2009**, *326*, 15-18.

[83] D. Armspach, D. Matt, *C. R. Chimie* **2010**, *14*, 135-148.

[84] P. Fügedi, P. Nánási, J. Szejtli, *Carbohydr. Res.* **1988**, *175*, 173-181.

[85] A. R. Khan, P. Forgo, K. J. Stine, T. D'Souza, *Chem. Rev.* **1998**, *98*, 1977-1996.

[86] B. Brady, N. Lynam, T. O'Sullivan, C. Ahern, R. Darcy, *Org. Synth.* **2000**, *77*, 220-224.

[87] I. Tabushi, Y. Kuroda, K. Yokota, L. C. Yuan, *J. Am. Chem. Soc.* **1981**, *103*, 711-712.

[88] K. Fujita, A. Matsunaga, T. Imoto, *J. Am. Chem. Soc.* **1984**, *106*, 5740-5741.

[89] I. Tabushi, K. Yamamura, T. Nabeshima, *J. Am. Chem. Soc.* **1984**, *106*, 5267-5270.

[90] I. Tabushi, Y. Kuroda, M. Yamada, M. Higashimura, R. Breslow, *J. Am. Chem. Soc.* **1985**, *107*, 5545-5546.

[91] I. Tabushi, T. Nabeshima, K. Fujita, A. Matsunaga, T. Imoto, *J. Org. Chem.* **1985**, *50*, 2638-2643.

[92] K. Fujita, T. Ishizu, K. Oshiro, K. Obe, *Bull. Chem. Soc. Jpn.* **1989**, *62*, 2960-2962.

[93] A. Ueno, F. Moriwaki, A. Azuma, T. Osa, *J. Org. Chem.* **1989**, *54*, 295-299.

[94] K. Fujita, H. Yamamura, T. Imoto, *Tetrahedron Lett.* **1991**, 6737-6740.

[95] T. Tanimoto, T. Sakaki, K. Koizumi, *Chem. Pharm. Bull.* **1993**, *41*, 866-869.

[96] T. Tanimoto, T. Sakaki, T. Iwanaga, K. Koizumi, *Chem. Pharm. Bull.* **1994**, *42*, 385-387.

[97] Z. Chen, J. S. Bradshaw, Y.-F. Shen, Y. Habata, M. L. Lee, *J. Org. Chem.* **1997**, *62*, 8529-8534.

[98] D. Armspach, D. Matt, *Carbohydr. Res.* **1998**, *310*, 129-133.

[99] V. Cucinotta, G. Grasso, G. Vecchio, *J. Incl. Phenom. Mol. Recog. Chem.* **1998**, *31*, 43-55.

[100] A. J. Pearce, P. Sinaÿ, *Angew. Chem. Int. Ed.* **2000**, *39*, 3610-3612.

[101] K. Teranishi, *Tetrahedron Lett.* **2000**, *41*, 7085-7088.

[102] K. Matsuoka, Y. Shiraishi, D. Terunuma, H. Kuzuhara, *Tetrahedron Lett.* **2001**, *42*, 1531-1533.

[103] K. Teranishi, *Tetrahedron Lett.* **2001**, *42*, 5477-5480.

[104] W. Wang, A. J. Pearce, Y. Zhang, P. Sinaÿ, *Tetrahedron: Assymetry* **2001**, *12*, 517-523.

[105] K. Teranishi, *Tetrahedron* **2003**, *59*, 2519-2538.

[106] D. Armspach, L. Poorters, D. Matt, B. Benmerad, F. Balegroune, L. Toupet, *Org. Biomol. Chem.* **2005**, *3*, 2588-2592.

[107] E. Zaborova, Y. Blériot, M. Sollogoub, *Tetrahedron Lett.* **2010**, *51*, 1254-1256.

[108] J. Boger, D. G. Brenner, J. R. Knowles, *J. Am. Chem. Soc.* **1979**, *101*, 7630-7631.

[109] K. Fujita, A. Matsunaga, H. Yamamura, T. Imoto, *Chem. Lett.* **1988**, 1947-1950.

[110] K. Fujita, T. Tahara, H. Yamamura, T. Imoto, T. Koga, T. Fujioka, K. Mihashi, *J. Org. Chem.* **1990**, *55*, 877-880.

[111] S. Hanessian, A. Benalil, C. Laferrière, *J. Org. Chem.* **1995**, *60*, 4786-4797.

[112] M. Atsumi, M. Izumida, D.-Q. Yuan, K. Fujita, *Tetrahedron Lett.* **2000**, *41*, 8117-8120.

[113] S. Guieu, M. Sollogoub, *J. Org. Chem.* **2008**, *73*, 2819-2828.

[114] M. Sollogoub, *Eur. J. Org. Chem.* **2009**, *9*, 1295-1303.

[115] T. Lecourt, A. Herault, A. J. Pearce, M. Sollogoub, P. Sinaÿ, *Chem. Eur. J.* **2004**, *10*, 2960-2971.

[116] G. K. Rawal, S. Rani, S. Ward, C.-C. Ling, *Org. Biomol. Chem.* **2010**, *8*, 171-180.

[117] O. Bistri, P. Sinaÿ, M. Sollogoub, *Tetrahedron Lett.* **2005**, *46*, 7757-7760.

[118] O. Bistri, P. Sinaÿ, J. J. Barbero, M. Sollogoub, *Chem. Eur. J.* **2007**, *13*, 9757-9774.

[119] G. K. Rawal, S. Rani, C.-C. Ling, *Tetrahedron Lett.* **2009**, *50*, 4633-4636.

[120] X. Luo, Y. Chen, G. Huber, Y. Zhang, P. Sinaÿ, *C. R. Chimie* **2004**, *7*, 25-28.

[121] S. Xiao, M. Yang, P. Sinaÿ, Y. Blériot, M. Sollogoub, Y. Zhang, *Eur. J. Org. Chem.* **2010**, 1510-1516.

[122] C.-C. Ling, A. W. Coleman, M. Miocque, *Carbohydr. Res.* **1992**, *223*, 287-291.

[123] S. Ward, P. Zhang and C.-C. Ling, *Carbohydr. Res.* **2009**, *344*, 808-814.

[124] L. Poorters, D. Armspach, D. Matt, *Eur. J. Org. Chem.* **2003**, *8*, 1377-1381.

[125] I. Tabushi, K. Shimokawa, N. Shimizu, H. Shirakata, K. Fujita, *J. Am. Chem. Soc.* **1976**, *98*, 7855-7856.

[126] I. Tabushi, L. C. Yuan, K. Shimokawa, K. Yokota, T. Mizutani, Y. Kuroda, *Tetrahedron Lett.* **1981**, *22*, 2273-2276.

[127] J.-C. Hierso, D. Armspach, D. Matt, *C. R. Chimie* **2009**, *12*, 1002-1013.

[128] D. Armspach, D. Matt, L. Toupet, *Angew. Chem. Int. Ed.* **2009**, *48*, 4555-4558.

[129] C. Machut-Binkowski, F.-X. Legrand, N. Azaroual, S. Tilloy, E. Monflier, *Chem. Eur. J.* **2010**, *16*, 10195-10201.

[130] M. Petrillo, L. Marinescu, C. Rousseau, M. Bols, *Org. Lett.* **2009**, *11*, 1983-1985.

[131] A. C. Cope, E. C. Friedrich, *J. Am. Chem. Soc.* **1968**, *90*, 909-913.

[132] H.-J. Schneider, F. Hacket, V. Rüdiger, *Chem. Rev.* **1998**, *98*, 1755-1785.

[133] A. Altomare, M. C. Burla, M. Camalli, G. Cascarano, C. Giacovazzo, A. Guagliardi, G. Moliterni, G. Polidori, R. Spagna, *J. Appl. Crystallogr.* **1998**, *31*, 74-77.

[134] G. M. Sheldrick, SHELXL-97, *Program for Crystal Structure Refinement,* University of Göttingen, Göttingen (Germany) **1997**.

Chapter III

Oschelating behaviour of WIDEPHOS

Chapter III

Oschelating behaviour of WIDEPHOS

Summary – Chapter III 143

SUMMARY – CHAPTER III

The first large-bite-angle diphosphane built upon a methylated β-cyclodextrin, **WIDEPHOS**, was shown to display unusual *trans*-chelating properties towards various d^8 and d^{10} transition metal ions. Being unsymmetrically disposed on the CD macrocycle, the two rigid and introverted donor atoms force the chelate complexes into a metastable state, in which the P-M-P angles are smaller than the standard value of 180º. Variable temperature ^{1}H NMR and ^{31}P NMR studies revealed the presence of a fast oscillatory motion about the metal ion, christened *oschelation*, which is associated with a weakening of one of the phosphorus–metal bond.

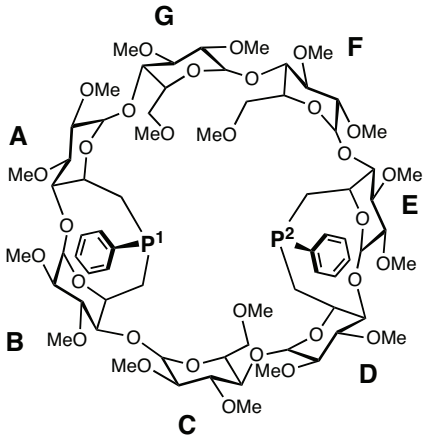

WIDEPHOS

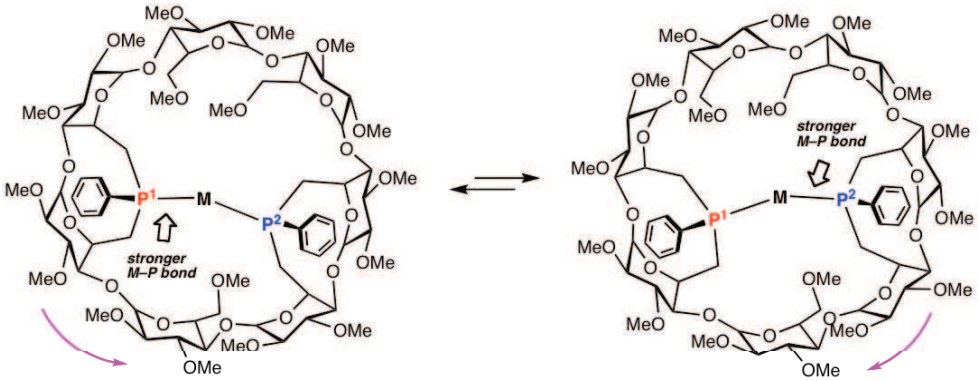

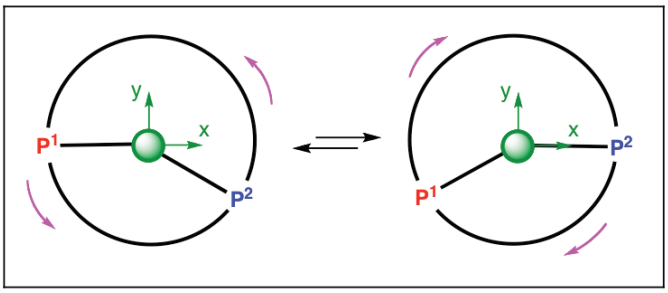

III.1. Introduction

Because of their ubiquitous use in transition metal catalysis, polyphosphane ligands have been extensively sought after over the last four decades.[1-4] Grafting phosphane units onto preorganisation platforms was shown to produce chelating ligands exhibiting enhanced catalytic properties when coordinated to a relevant transition metal centre.[5-8] In this respect, *rigid* molecular cavities such as calix[4]arenes,[9-11] resorcin[4]arenes[9,12] or cyclodextrins (CDs)[13-15] occupy a place of choice. These are also attractive scaffolds because they are easily functionalised in a regioselective manner so that coordinating units can be introduced at different locations onto the macrocyclic scaffold.[16,17] Examples of chelating diphosphanes built upon a molecular cavity that display high performances in homogeneous catalysis include the calixarenes displayed in Figure 1, which have their donor atoms positioned at different rims of the macrocyclic backbone.[18-20]

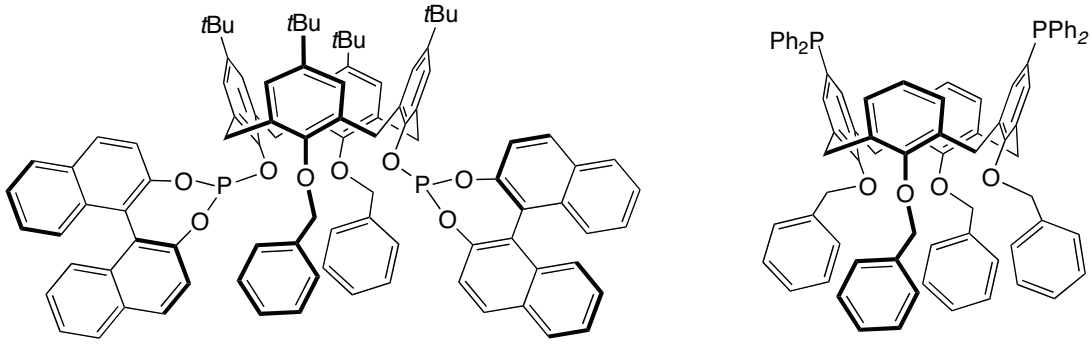

Figure 1. Lower- and upper-rim distal diphosphanes derived from calix[4]arene.

Phosphanes built on CD scaffolds were first reported in 1993 when the groups of Ito[21] and Reetz[22] synthesised phosphanes covalently linked to the secondary and primary face of a native β-CD, respectively (Figure 2), but it is not until 1999 that Armspach and Matt began to use CDs as preorganization platforms for the design of chelating diphosphanes.

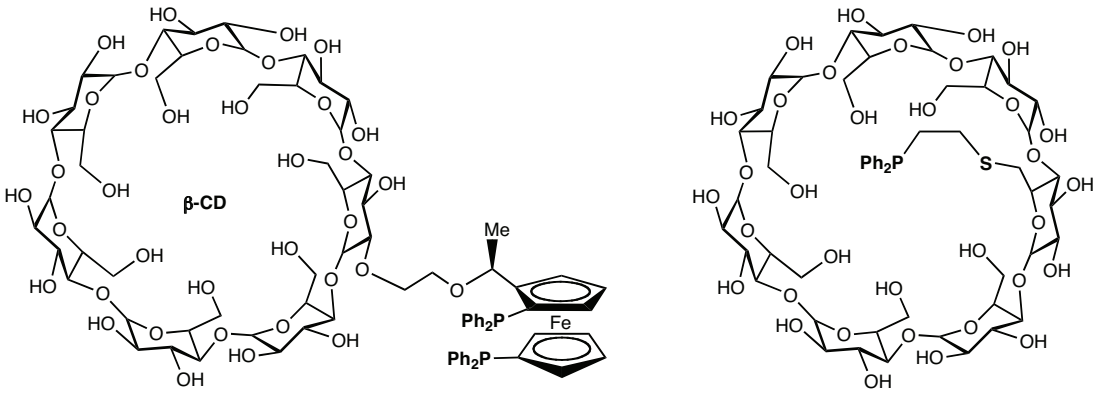

Figure 2. Ito's diphosphane (left)[21] and Reetz's heterotopic P,S ligand (right).[22]

Unlike the first generation of phosphanes which are all derived from monosubstituted CDs,[23-32] the polyphosphanes designed by Armspach and Matt[33-37], and others[38-40] rely on grafting at least two coordinating units directly onto the macrocyclic structure (Figure 3). In this way, metals can be brought much closer to the CD torus by means of chelation in order to force them to interact with the cavity interior. A marked affinity for metal-chloride fragments was notably observed in the case of α-CD derivatives.[41-43]

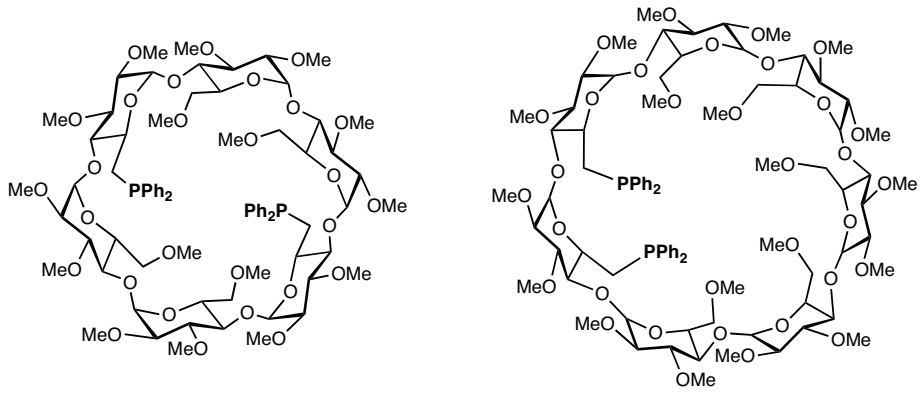

Figure 3. A,D-diphosphane-α-CD (left)[42] and A,B-diphosphane-β-CD (right).[38]

Because of its increased rigidity, this property is reinforced for the so-called **TRANSDIP** ligand (Figure 4, left), which comprises a permethylated α-CD moiety doubly-capped by two phenylphosphinidene units at the primary face.[44] Both phosphorus lone pairs of **TRANSDIP** point towards the cavity centre and are ideally placed for coordinating d^8 and

d^{10} transition metal ions in a *trans*-fashion.[43] The *trans*-chelating properties of **TRANSDIP** are unique as, unlike other *trans*-spanning diphosphanes such as **TRANSPHOS**,[45-48] **XANTPHOS**,[49-52] and **SPANPHOS,**[53,54] *cis*-chelate complexes, dimeric species or higher oligomers are not formed upon complexation.[43] In **Chapter II**, we described a new method for getting hold of gram-scale quantities of a β-CD macrocycle specifically tetrasubstituted at the A, B, D, E positions of the primary face. Such a regioisomer proved to be a key starting material for the synthesis of an extended version of **TRANSDIP**, christened **WIDEPHOS** (Figure 4, right). In this chapter, we show how this *trans*-chelator, which is characterised by a long P···P separation and non equivalent, introverted donor atoms, behaves as a balance wheel swinging about its central metal unit when chelating d^8 and d^{10} metal ions.

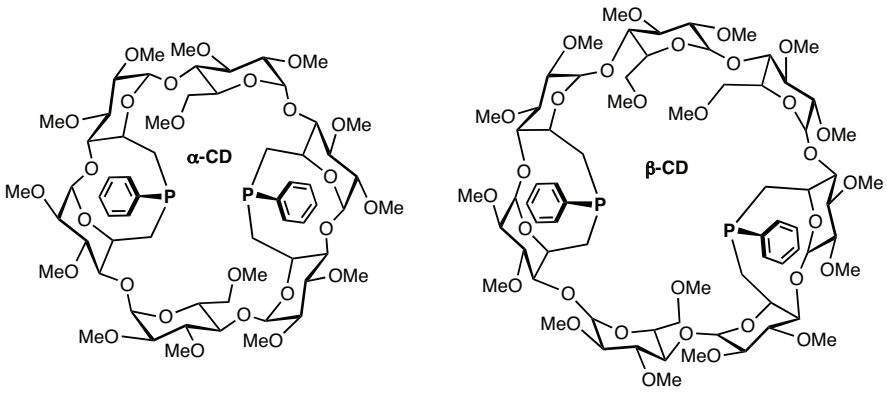

Figure 4. α-CD-based **TRANSDIP** (left) and β-CD-based **WIDEPHOS** (right).

III.2. Results and discussion

III.2.1. General features of WIDEPHOS

The synthesis and full characterisation of **WIDEPHOS** are described in **Chapter II**. When dissolved in MeOH, this diphosphane could be oxidised on prolonged standing to air to afford the corresponding di(phosphane oxide) **27** (Scheme 1), the structure of which was determined by a single-crystal X-ray diffraction study (Figure 5).

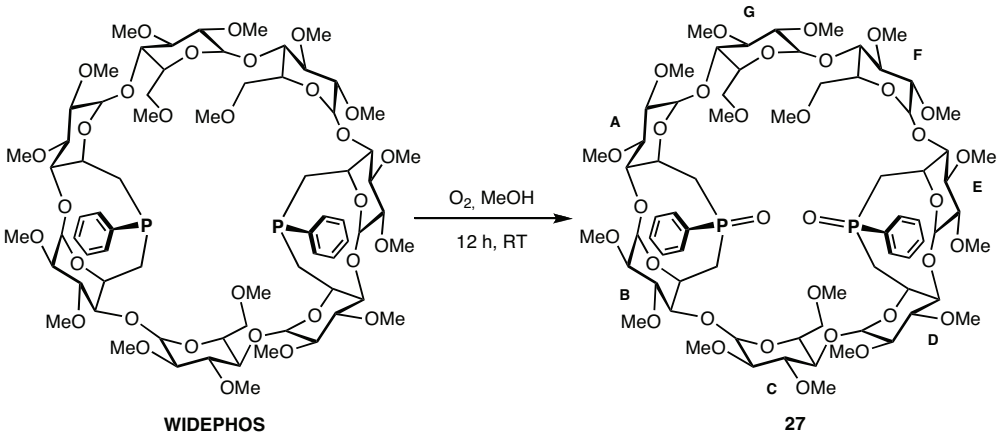

Scheme 1. Synthesis of di(phosphane oxide) **27**.

In the solid state, the two P=O vectors of **27** point towards the cavity interior, the P···P separation being rather large as predicted (6.91 Å). Being unsymmetrically disposed on the CD macrocycle, the two P=O vectors are not aligned, the angle between them (151.8º) departing significantly from 180º. The cavity is filled with two solvent molecules, namely a pentane and a dichloromethane one. Two non-bridged glucose units (C and F) are slightly tipped towards the CD axis, but no major conformational changes within the individual 6-membered glucose rings were detected, all of them adopting the standard $^4C_1$ conformation.

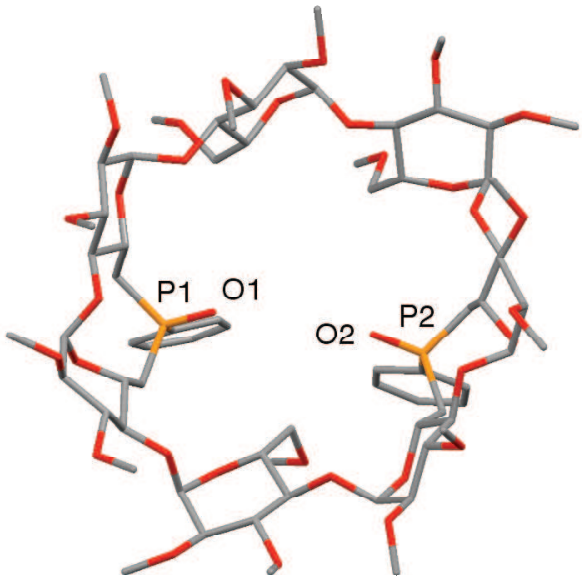

Figure 5. X-ray structure of di(phosphane oxide) **27** (view from the secondary face). Solvent molecules have been omitted for clarity. Important distances [Å]: P(1)···P(2) 6.91; O(1)···O(2) 4.32.

The narrow range within which the anomeric protons H-1 resonate ($\Delta\delta$ = 0.22 ppm) reflects the lack of deformation of the β-CD torus. Moreover, identical chemical shifts dispersion for **WIDEPHOS** ($\Delta\delta$ = 0.22 ppm) and dioxide **27** suggest that both compounds have very similar structures (Figure 6). It is therefore not unreasonable to think that the location of the P=O bonds in **27** is close to that of the phosphorus lone pairs in **WIDEPHOS**.

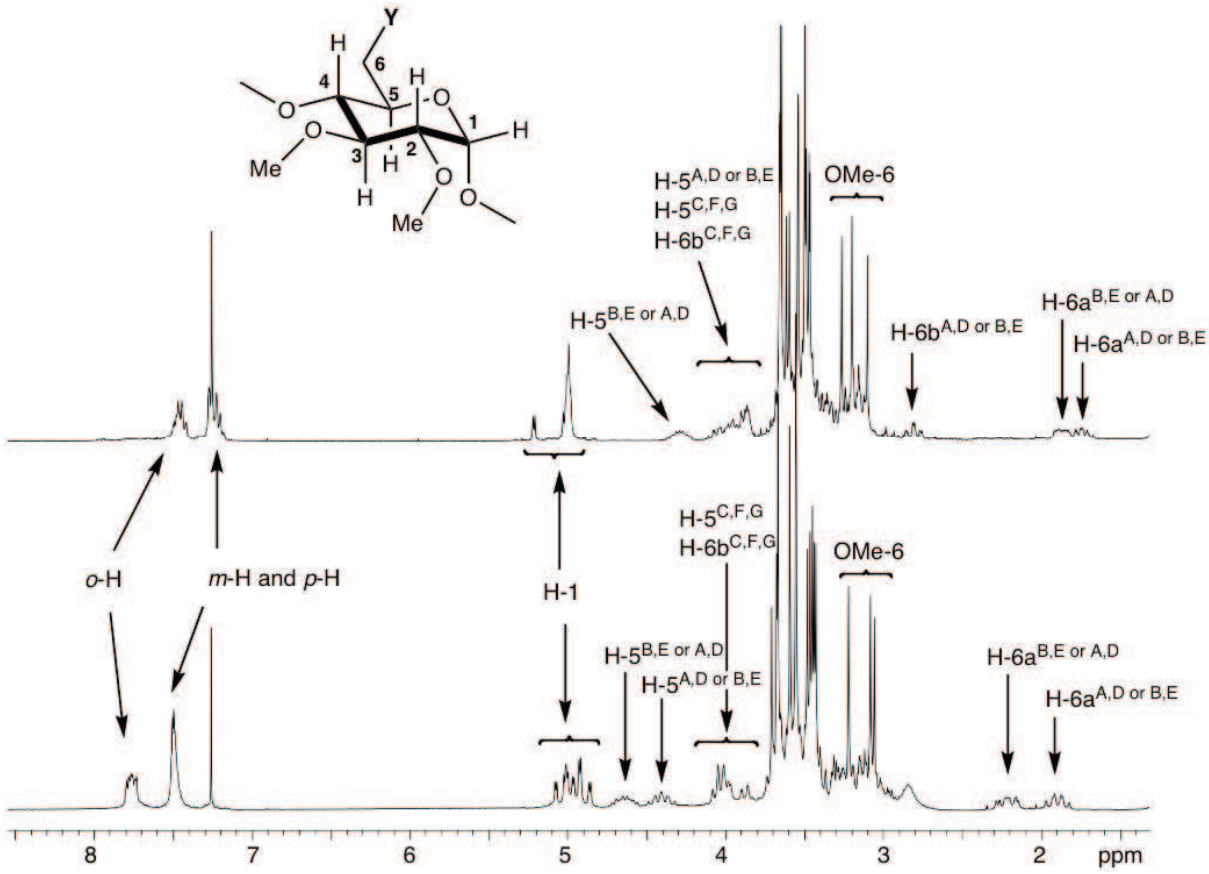

Figure 6. ^{1}H NMR spectra of **WIDEPHOS** (top) and **27** (bottom) recorded in $CDCl_3$ at 300.1 MHz.

III.2.2. Oschelating behaviour of WIDEPHOS

Despite the long separation between both phosphorus atoms, **WIDEPHOS** turned out to be suitable for chelation. Thus, for example, reaction with 1 equivalent of [Au(tht)(thf)] (tht = tetrahydrothiophene; thf = tetrahydrofuran) led quantitatively to complex **28** (Scheme 2). The mass spectrum of **28** showed an intense peak at *m/z* = 1717.62 having exactly the isotopic profile expected for $[M - PF_6]^+$ ion. Furthermore, the $^{31}P\{^1H\}$ NMR (CD_2Cl_2, 25ºC) spectrum displayed an AB pattern with a ^2J(PP) coupling constant of 326 Hz, which is in accord with a very large bite angle or a *trans*-chelate complex. However, CPK[55] models indicate that the bite angle is close to 160º; in other terms the ligand cannot behave as a perfect *trans*-chelator because of the non-symmetrical nature of **WIDEPHOS**. The good chelating properties of **WIDEPHOS** were further confirmed by the *quantitative* formation of the *trans*-chelate complex **29** (Scheme 2), even in the presence of excess $[PtCl_2(PhCN)_2]$.

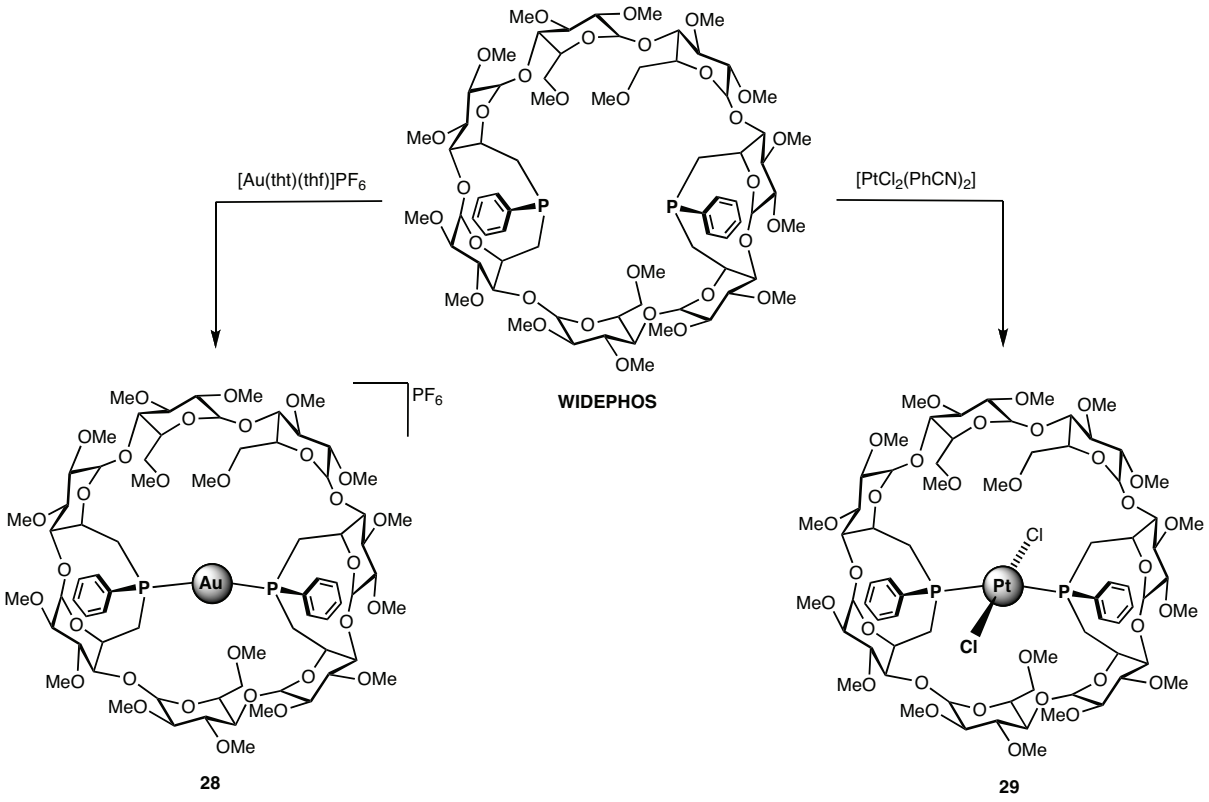

Scheme 2. Synthesis of gold chelate complex **28** and platinum chelate complex **29**.

The chelate structure of **29** was revealed by its mass spectrum, which comprises a strong peak at *m/z* = 1792.45 for $[M + Li]^+$ ion. The ^{1}H NMR signals corresponding to anomeric protons are much more widespread than in **WIDEPHOS** ($\Delta\delta$ = 0.74 ppm), which is consistent with a more distorted CD torus. Intriguingly, some protons appear larger than usual, especially those close to the phosphorus atoms such as H-6, H-5 and aromatic *o*-H protons (Figure 7; see Figure 6 for numbering of a given glucose unit). Also, the aromatic *o*-H protons in complex **29** are downfield shifted compared to complex **28**, probably because of their spatial proximity to chloride atoms. The ^{13}C{^{1}H} NMR signals for C-6 atoms belonging to glucose units capped by phenylphosphinidene moieties (A, B, D and E) are broad at room temperature in both **28** and **29** and cannot be sharpened by raising the temperature. However, their unambiguous assignment was achieved thanks to 2D ^{1}H-^{13}C{^{1}H} HMQC NMR techniques.

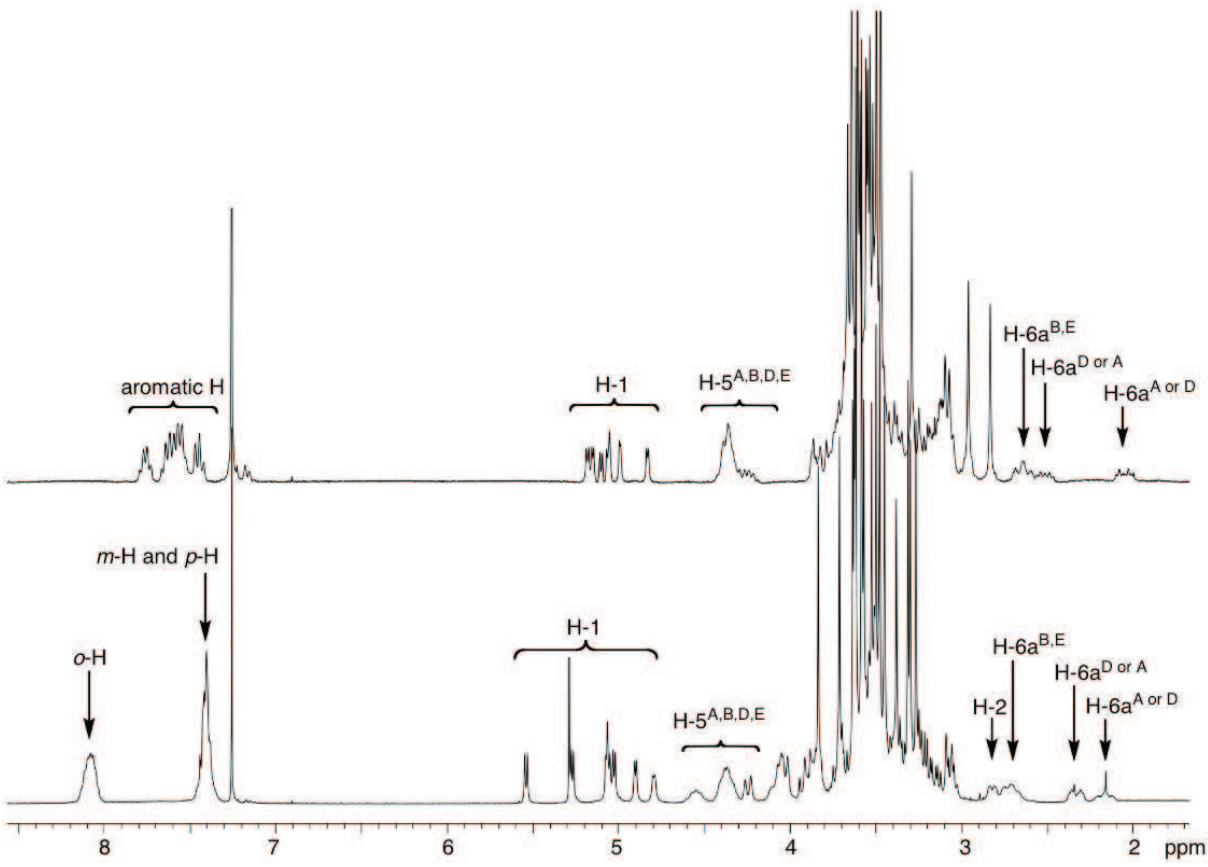

Figure 7. ^{1}H NMR spectra of gold chelate complex **28** (top) and platinum chelate complex **29** (bottom) recorded in $CDCl_3$ at 300.1 MHz.

Surprisingly, the $^{31}P\{^{1}H\}$ NMR spectrum of complex **29** consists of a broad signal at room temperature. As shown by a variable-temperature NMR study, complex **29** displays fluxional behaviour in solution (Figure 8). The $^{31}P\{^{1}H\}$ NMR (CD_2Cl_2) spectrum of **29**, measured at –80ºC, revealed the presence of two species (**29a** and **29b,** Scheme 3) present in a 1:1 ratio, each characterised by an ABX pattern (^{2}J(AB) = 492 Hz and 476 Hz respectively, ^{1}J(PPt) coupling poorly resolved). Upon raising the temperature, the signals first broadened, then coalesced near –15ºC, and finally merged into a single ABX spectrum at 80ºC (^{2}J(AB) = 496 Hz, ^{1}J(PPt) = 2510 Hz).

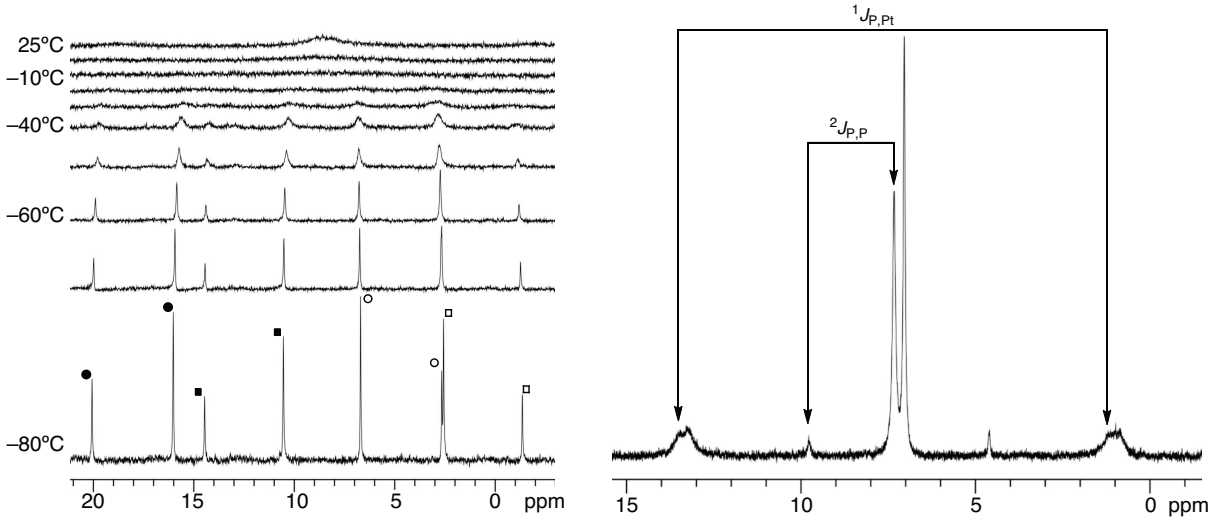

Figure 8. Variable temperature $^{31}P\{^{1}H\}$ NMR study recorded in CD_2Cl_2 at 121.5 MHz (left) and $^{31}P\{^{1}H\}$ NMR at +80ºC recorded in $C_2D_2Cl_4$ at 202.5 MHz (right) of the platinum chelate complex **29**. The AB patterns of the two equilibrating species are represented by dots and squares. Filled symbols are for the A parts, open symbols for the B parts.

The observed data are consistent with exchange between two complexes both of which contain a close to linear P-Pt-P unit. A variable temperature ^{1}H NMR study was also carried out which confirmed the 1:1 stoichiometry of the equilibrating species (Figure 9). Both series of experiments led to a free energy of activation $\Delta G^{\neq} = (11.3 \pm 0.2)$ kcal mol^{-1}.

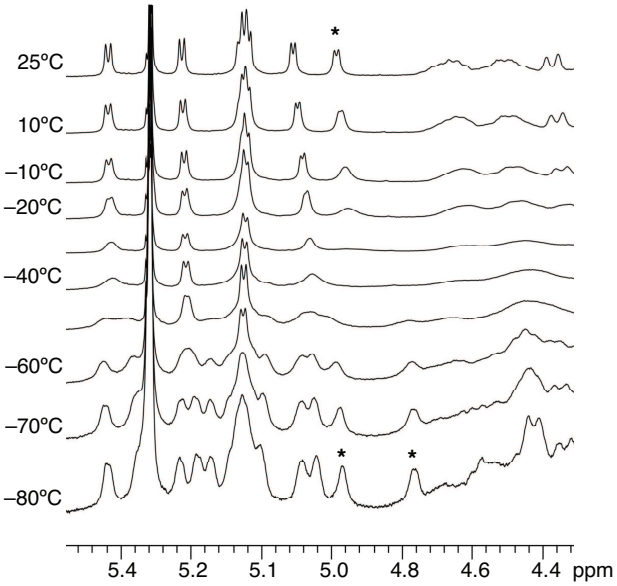

Figure 9. ^{1}H NMR spectra showing the anomeric protons zone in the range –80ºC/25ºC recorded in CD_2Cl_2 at 500.1 MHz of platinum chelate complex **29**. Asterisks show a given proton signal at room temperature splitting up in two proton signals at –80ºC.

Interestingly, the low-temperature $^{31}P\{^{1}H\}$ NMR spectra revealed two AB patterns with a large separation between the A and B parts (ca. 12 ppm). Note that for each equilibrating species, one of the phosphorus signals (e.g. δ = 1.0 ppm) appears near the midpoint between the signal of the free ligand (δ = –14.6 ppm) and that of the other signal (e.g. δ = 12.2 ppm), indicating that the two P atoms of each complex are coordinated to the platinum atom with unequal strength. As shown by an off-resonance 2D $^{31}P\{^{1}H\}$-$^{31}P\{^{1}H\}$ ROESY NMR experiment, the *strongly* coordinated phosphorus atom of each species is in exchange with the *weakly* coordinated phosphorus atom of the other isomer (Figure 10).

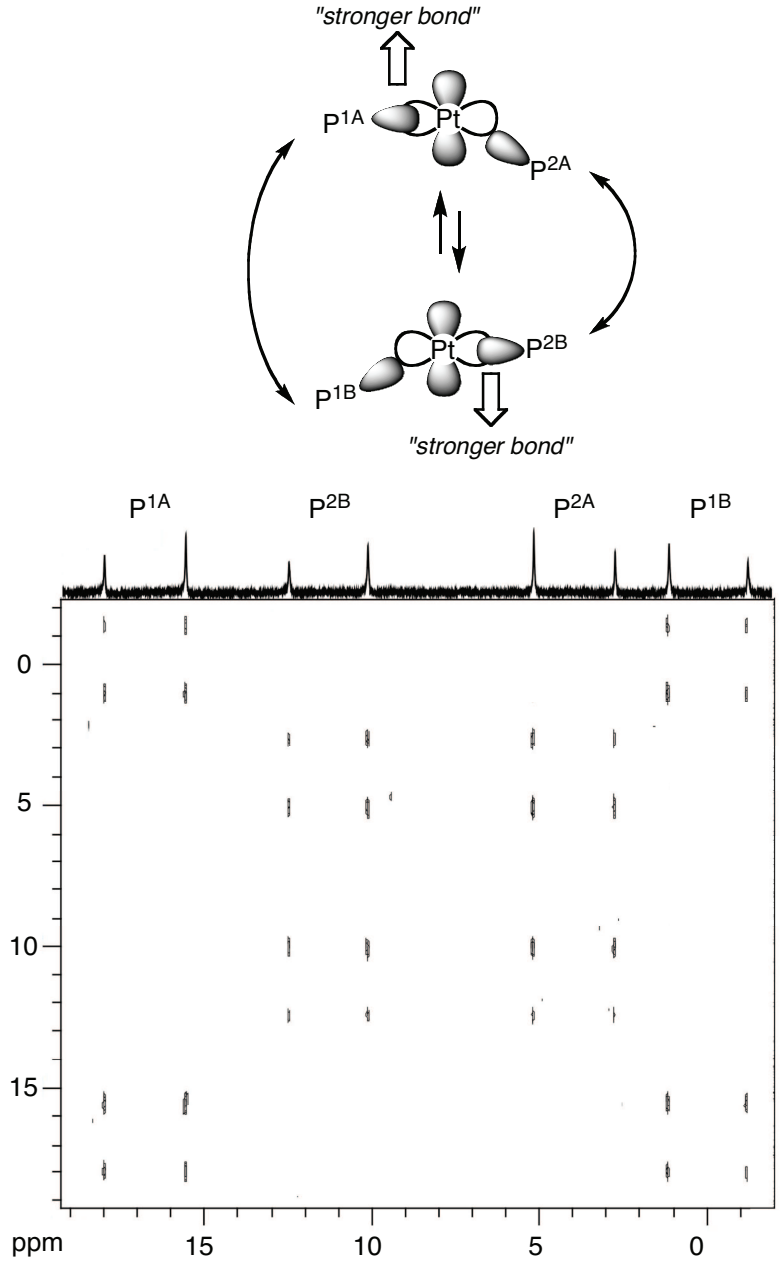

Figure 10. $^{31}P\{^{1}H\}$ NMR spectrum and off resonance $^{31}P\{^{1}H\}$-$^{31}P\{^{1}H\}$ ROESY NMR spectrum of platinum chelate complex **29** at –60ºC recorded in CD_2Cl_2 at 202.5 MHz.

Overall, the best way to describe these findings is to consider that the d_{x2-y2} orbital involved in formation of the M–P bonds changes its orientation in a pendular fashion so as to adopt in alternation different overlaps with each of the two convergent, but non-aligned phosphorus lone pairs. Consequently, metal binding to the two phosphorus donor atoms is non-equivalent in a given species. The observed isomerization is probably also accompanied by a slight displacement of the metal centre. Thus, being unable to form an authentic *trans*-complex (i.e. with a P-M-P angle of 180ºC), **WIDEPHOS** may be regarded as a frustrated chelator, which compensates the metal electron deficiency generated at one

coordination site by oscillating about the complexed metal ion (Scheme 3). We propose to term this type of bidentate ligand an oschelating (contraction of oscillating and chelating) species.

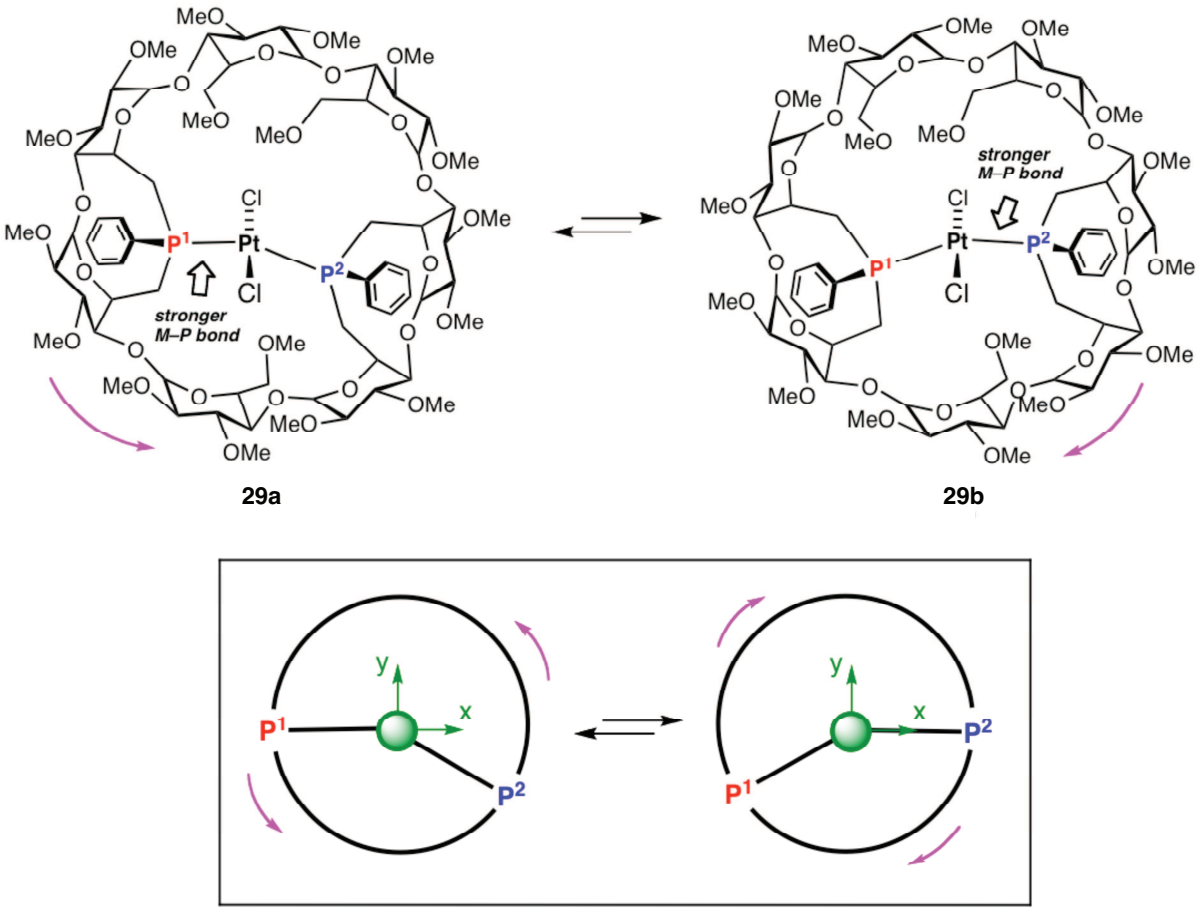

Scheme 3. Balance wheel movement of **WIDEPHOS** in complex **29** (view along the CD axis). The x and y arrows in the lower part indicate the orientations of the d_{x2-y2} orbital involved in formation of the two M–P bonds.

It is worth mentioning here that the observed fluxionality is different from that found in complexes containing hemilabile ligands, the latter leading to intermediates in which one end is totally dissociated.[56-59] Furthermore, the coupling constants persisted over the temperature range –80ºC to +80ºC. In other words, the observed dynamic behaviour occurs without dissociation of the M–P bonds. This phenomenon may be regarded as a variant of bond-stretch isomerism.[60,61]

Variable temperature studies were also performed with cationic gold complex **28**. Again, they revealed the same oschelating behaviour in solution with identical free energy of activation, $\Delta G^{\neq}$ = (11.3 ± 0.2) kcal mol^{-1}, thus discarding dynamics involving the chlorido ligands in complex **29**.

Another illustration of the good chelating properties of **WIDEPHOS** was provided by its reaction with 1 equivalent of $[PdCl_2(PhCN)_2]$, [PdClMe(cod)] (cod = cycloocta-1,5-diene) and 0.5 equivalents of $[\{RhCl(CO)_2\}_2]$, which afforded complexes **30**-**32** (Scheme 4) in high yields (90-99%). Note that in this case small amounts of dimetallic species were detected upon complexation (these findings will be discussed in **Chapter IV**.).

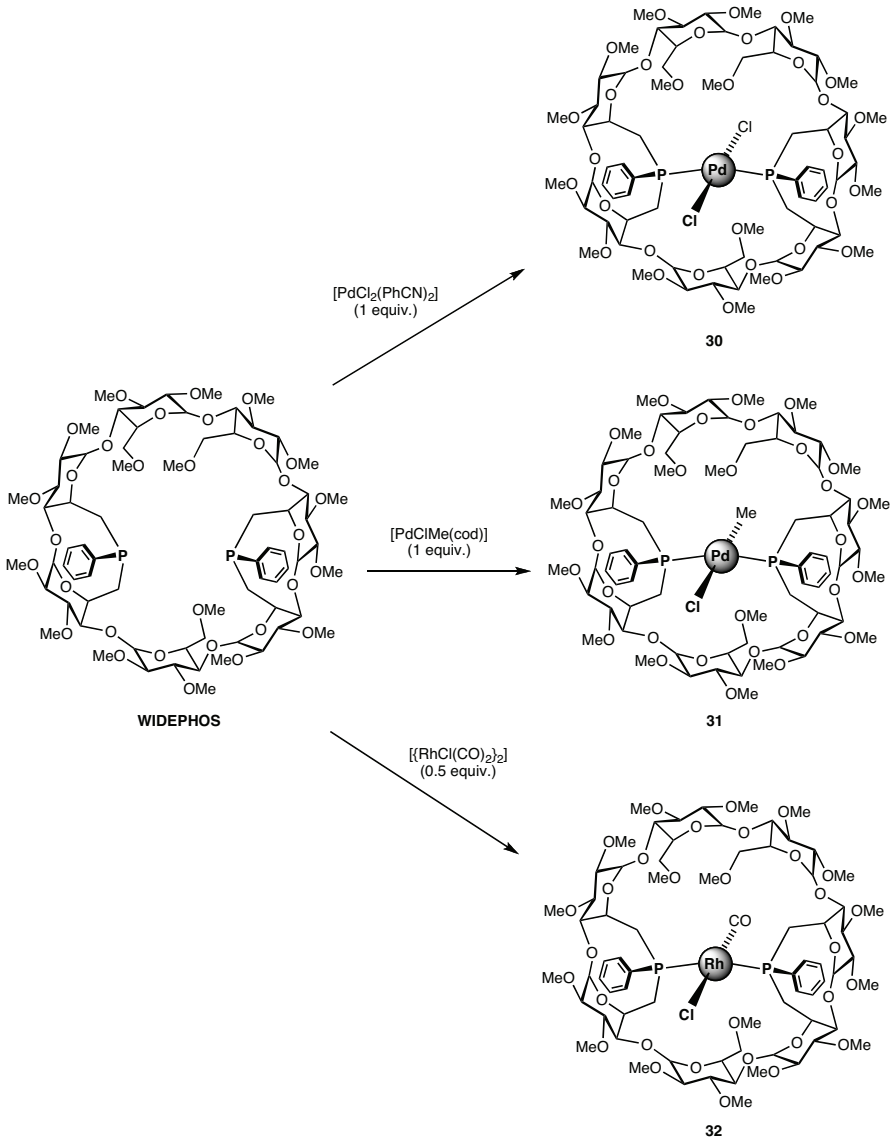

Scheme 4. Synthesis of palladium and rhodium chelate complexes **30**-**32**.

The coordination of a palladium dichloride moiety in complex **30** was deduced by its mass spectrum which revealed a strong peak at *m/z* = 1737.46 and 1721.47 having the expected isotopic profile for $[M + K]^+$ and $[M + Na]^+$ ions, respectively. The ^{1}H NMR and $^{13}C\{^1H\}$ NMR spectra show the same features as those observed for oschelate platinum complex **29**. As its analogues **28** and **29**, the palladium complex **30** also displays oschelating behaviour in solution. The $^{31}P\{^1H\}$ NMR spectrum at room temperature comprises a broad signal, which splits up in two AB patterns having the A and B parts separated by ca. 11 ppm. The ^2J(PP) = 564 Hz and ^2J(PP) = 549 Hz at –80ºC (Figure 11), and ^2J(PP) = 569 Hz at 100ºC (the ^2J(PP) coupling constants were only resolved after 27724 scans, which represents 12 h (!) recording; Figure 12) are in agreement with two phosphorus atoms in a *trans*-arrangement over the entire temperature range.

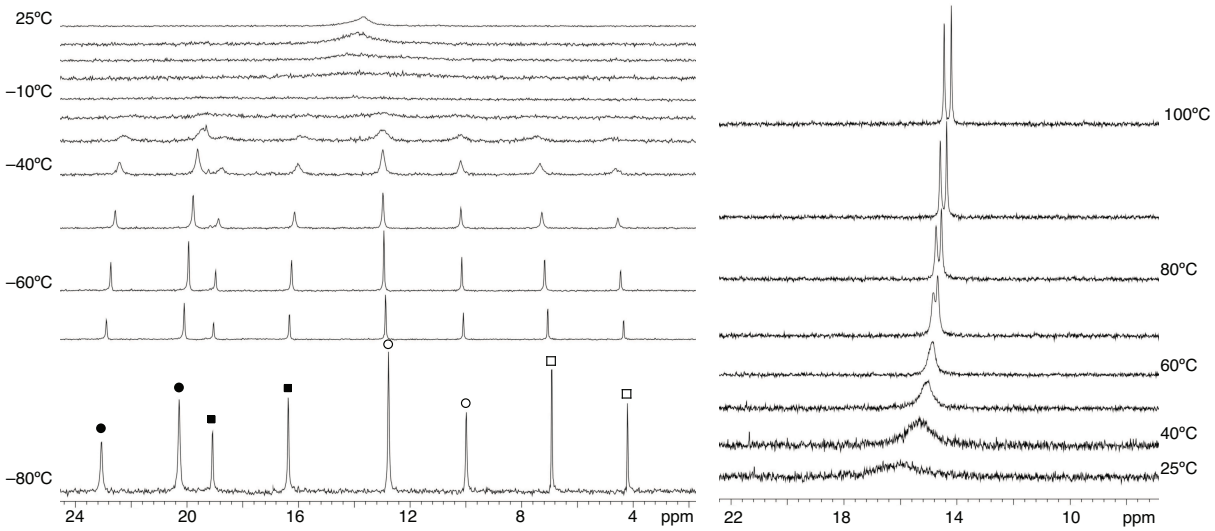

Figure 11. Variable temperature $^{31}P\{^1H\}$ NMR study at low temperatures recorded in CD_2Cl_2 at 202.5 MHz (left) and variable temperature $^{31}P\{^1H\}$ NMR study at high temperatures recorded in $C_2D_2Cl_4$ at 121.5 MHz (right) of the palladium complex **30**. The AB patterns of the two equilibrating species are represented by dots and squares. Filled symbols are for the A parts, open symbols for the B parts.

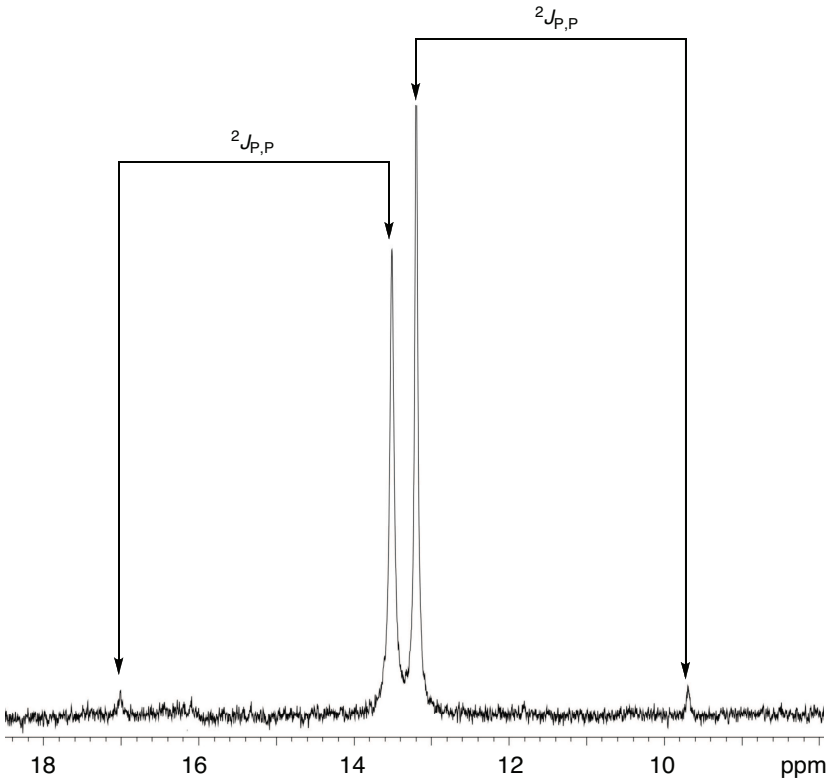

Figure 12. $^{31}P\{^1H\}$ NMR spectrum recorded in $C_2D_2Cl_4$ at 162.0 MHz of palladium complex **30** after 27724 scans (equivalent to 12 h (!) recording) at 100ºC.

As expected, an equimolar ratio of each equilibrating species was revealed by a VT ^1H NMR study (Figure 13) and the same free energy of activation as in oschelate complexes **28** and **29** was found, $\Delta G^{\neq} = (11.3 \pm 0.2)$ kcal mol^{-1}.

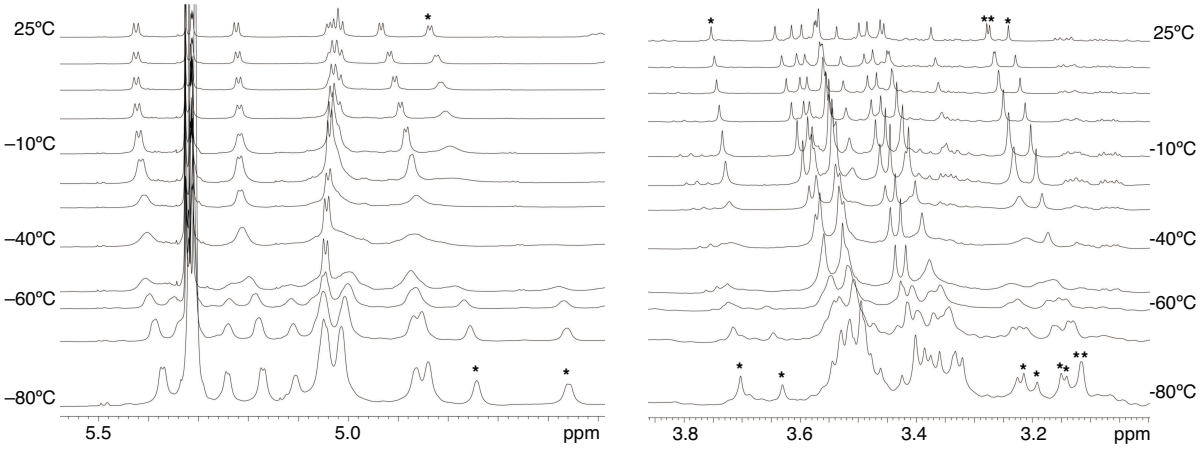

Figure 13. ^1H NMR spectra showing the anomeric protons zone (left) and in the methoxy zone (right) in the range –80ºC/25ºC recorded in CD_2Cl_2 at 500.1 MHz of the palladium complex **30**. Asterisks show a signal at room temperature splitting up into two signals at –80ºC.

The chelate structure of chlorido-methyl palladium complex **31** was also deduced from the mass spectrum, which displayed strong peaks at *m/z* = 1699.54 and 1641.58 for $[M + Na]^+$ and $[M - Cl]^+$ ions, respectively. The coordinated methyl group appeared as a triplet at δ = 0.09 ppm in the ^{1}H NMR spectrum with a coupling constant of ^3J(PH) = 6.4 Hz, a value typical of a *trans*-arrangement of the two phosphorus atoms about the palladium centre. The presence of a methyl group coordinated to a palladium centre allowed a more in-depth exploration of the metal coordination sphere by means of a 2D ^{1}H-^{1}H ROESY NMR experience. In particular, spatial proximity between this methyl group and H-6 protons as well as aromatic *o*-H protons belonging to one of the phenyl rings was established. Correlations with some *intra*-cavity H-5 protons were also observed (Figure 14), suggesting that the [PdClMe] rod is not located perpendicular to the CD axis, but rather tilted away from it.

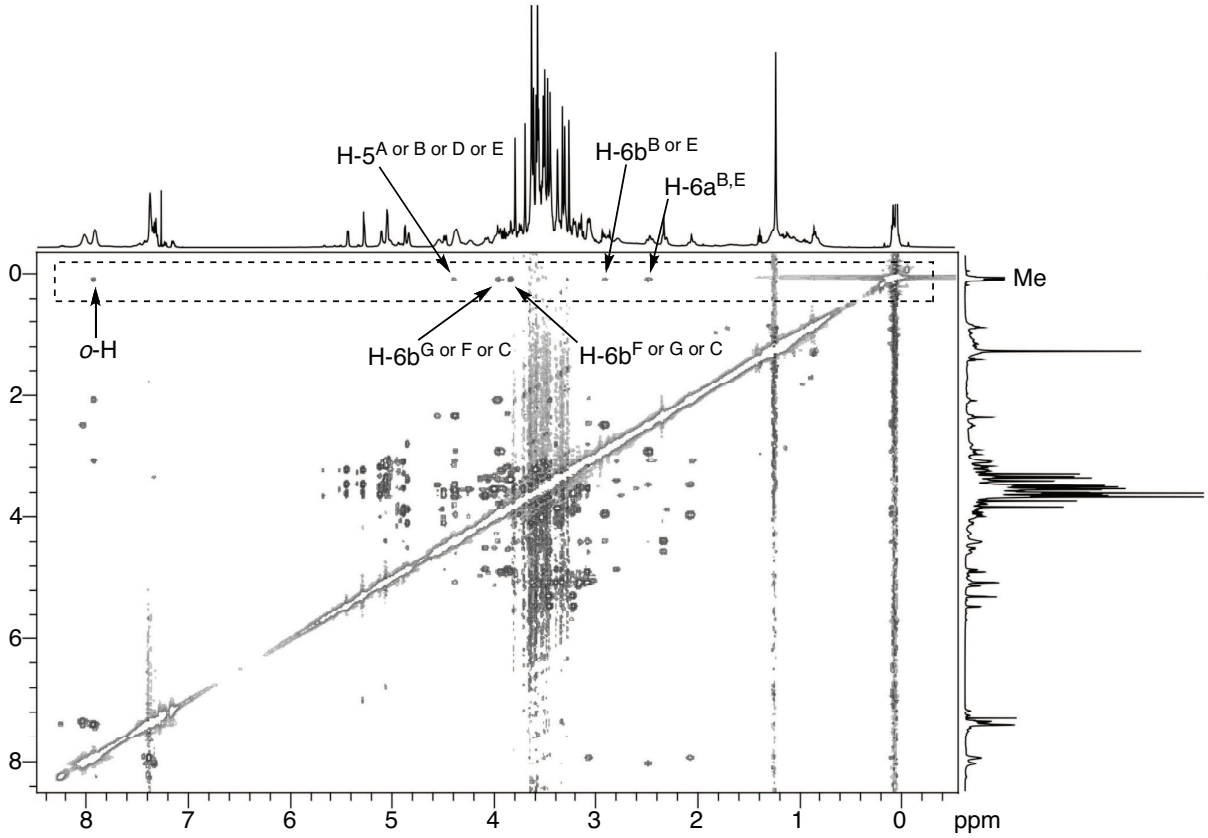

Figure 14. 2D ^{1}H-^{1}H ROESY NMR spectrum of palladium chelate complex **31** recorded in $CDCl_3$ at 500.1 MHz.

Complex **31** displays also oschelating behaviour in solution as revealed by variable temperature ^{1}H NMR and ^{31}P{^{1}H} NMR studies. In the ^{31}P{^{1}H} NMR spectrum recorded at –80ºC, two AB patterns were clearly identified with the A and B parts separated by about $\Delta\delta$ = 10 ppm for both equilibrating species, which are present in equimolar amounts. Coupling constants of ^{2}J(PP) = 442 Hz and 455 Hz for each species in exchange confirmed the *trans*-stereochemistry about the metal centre. Upon prolonged standing in $CDCl_3$ solution, which is well known for releasing Cl^- anions, complex **31** is slowly converted into the dichlorido complex **30**.

Similarly, the rhodium(I) chelate complex **32** was obtained in quantitative yield by reacting **WIDEPHOS** with 0.5 equivalents of dimeric $[RhCl(CO)_2]_2$. Again, the monomeric nature of this complex was deduced from its mass spectrum, which showed strong peaks at *m/z* = 1725.48, 1709.51 and 1652.55 having the expected isotopic profiles for $[M + K]^+$, $[M + Na]^+$ and $[M - Cl]^+$ ions, respectively. As in oschelate complexes containing $[MX_2]$ rods **29-31**, the ^{1}H NMR spectrum of **32** comprises relatively widespread H-1 signals ($\Delta\delta$ = 0.65 ppm) compared to those belonging to the free ligand ($\Delta\delta$ = 0.22 ppm), thus reflecting the marked torus deformation caused by oschelation. In contrast with gold complex **28**, but as observed for other chlorido-containing complexes such as **29-31**, aromatic *o*-H protons underwent a marked downfield shift upon coordination probably because of their spatial proximity to the chlorido ligand (Figure 15). Even if the carbonyl ligand of **32** was not detected by ^{13}C{^{1}H} NMR spectroscopy, the presence of an intense peak at ν = 1970 cm^{-1} in the IR spectrum lifted any doubt about the presence of a carbonyl ligand bonded to a Rh(I) centre. Thanks to variable temperature ^{1}H and ^{31}P{^{1}H} NMR studies, a free energy of activation comparable to the one found for previous oschelate complexes could be determined. Even if the ^{31}P chemical shift differences associated with each equilibrating species are large as in other oschelate complexes ($\Delta\delta$ = 18.6 and 7 ppm respectively), their ^{2}J(PP) = 354 Hz and ^{1}J(PRh) = 118 Hz coupling constants turned out to be identical, in stark contrast with all so far described oschelate complexes. Whether this is pure coincidence or an unusual feature of this particular complex remains to be seen. Nevertheless, both ^{2}J(PP) and ^{1}J(PRh) values reflect the *trans*-arrangement of the phosphorus atoms about the rhodium centre.[43]

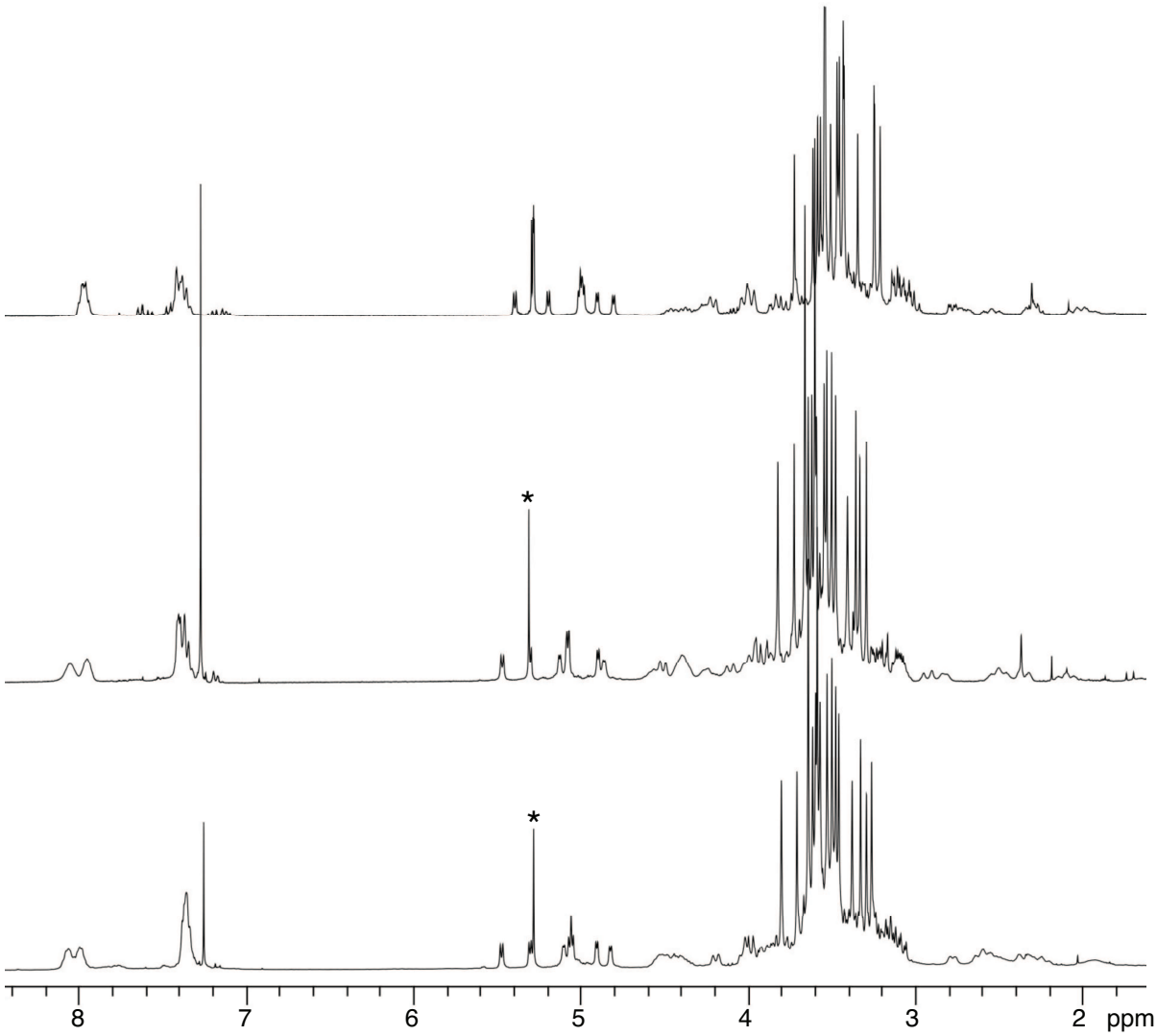

Figure 15. ^{1}H NMR spectra of oschelate complexes **30** (CD_2Cl_2, top), **31** ($CDCl_3$, middle) and **32** ($CDCl_3$, bottom) recorded at 300.1 MHz. Asterisks denote residual CH_2Cl_2.

It must be emphasized that, except for the chelate complexes **28** and **29**, excess metal precursor leads to dinuclear species. Only slow addition of stoichiometric amounts of the metal precursor to a solution of the ligand produced mononuclear complexes exclusively. Even if chelate complexes can be obtained in high yields, **WIDEPHOS** seems to be better adapted for the coordination of dinuclear species (**Chapter IV**).

III.2.3. Breaking M–P bonds in oschelate complexes

Proof of the relative fragility of oschelate complexes came from the decomposition of gold(I) and rhodium(I) complexes **28** and **32**, and to a lesser extent palladium(II) complexes **30** and **31** in solution upon prolonged exposure to air at room temperature, giving rise to the corresponding di(phosphane oxide) **27** after about 1 week. In contrast, complex **29** turned out to be very robust and does not decompose even when dissolved in air-saturated hot methanol.

The platinum(II) oschelate complex **29** only reacted in the presence of a soft metal cation with high affinity for phosphine ligands such as gold(I). The resulting reaction mixture consisted of equimolar amounts of two inseparable regioisomers, respectively **33a** and **33b** (Scheme 5), the $^{31}P\{^{1}H\}$ NMR spectrum of which displayed two peaks (δ = 0.0 and –4.2 ppm) flanked by Pt satellites (^{1}J(PPt) = 3239 Hz and ^{1}J(PPt) = 3454 Hz, respectively) and two overlapping singlets at 34.0 ppm (Figure 16). Each donor atom is alternatively coordinated to platinum or gold depending on the regioisomer envisaged.

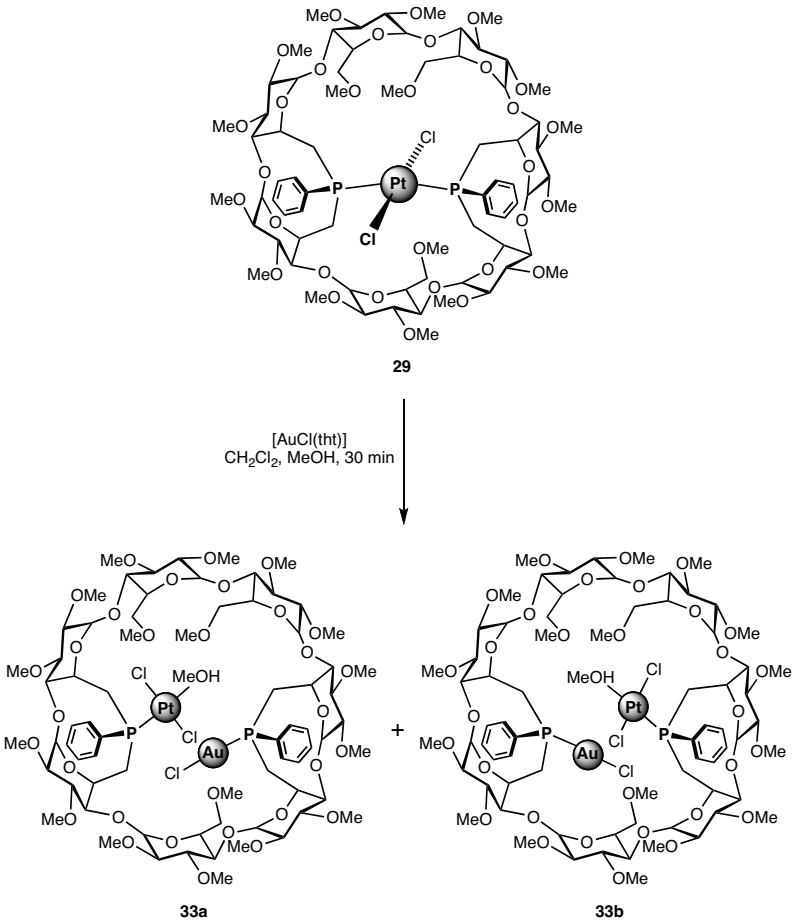

Scheme 5. Breaking the Pt–P bond in complex **29**.

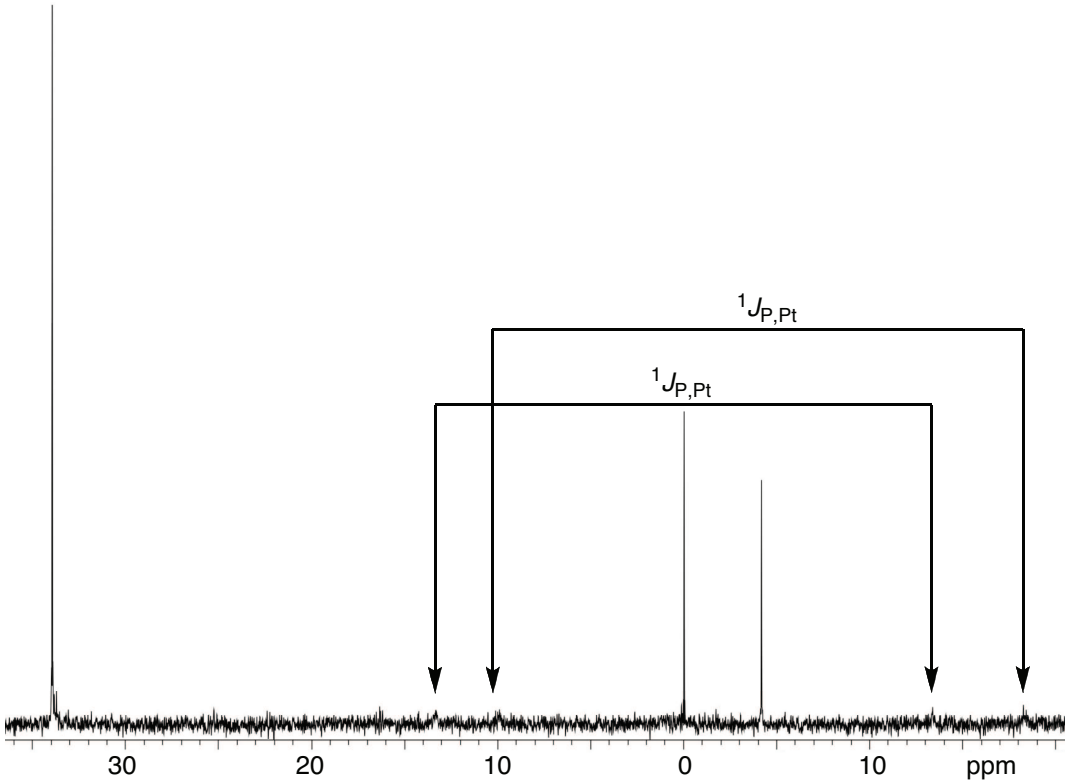

Figure 16. $^{31}P\{^1H\}$ NMR spectrum of **33a** and **33b** recorded in $CDCl_3$ at 121.5 MHz.

The structural assignment of the two regioisomers was based on the mass spectrum of the mixture, which showed a strong peak at *m/z* = 2071.56 corresponding to the $[M + Na]^+$ ion. A coordinated MeOH solvent molecule is here necessary for the platinum(II) cation to fulfil its coordination sphere.

Before being fully oxidised to di(phosphane oxide) **27**, palladium oschelate complex **30** gave rise to equimolar amounts of regioisomeric complexes **34** and **35** (Scheme 6) when dissolved in air saturated aqueous MeOH. The partially oxidised complexes could be separated by standard chromatography on silica.

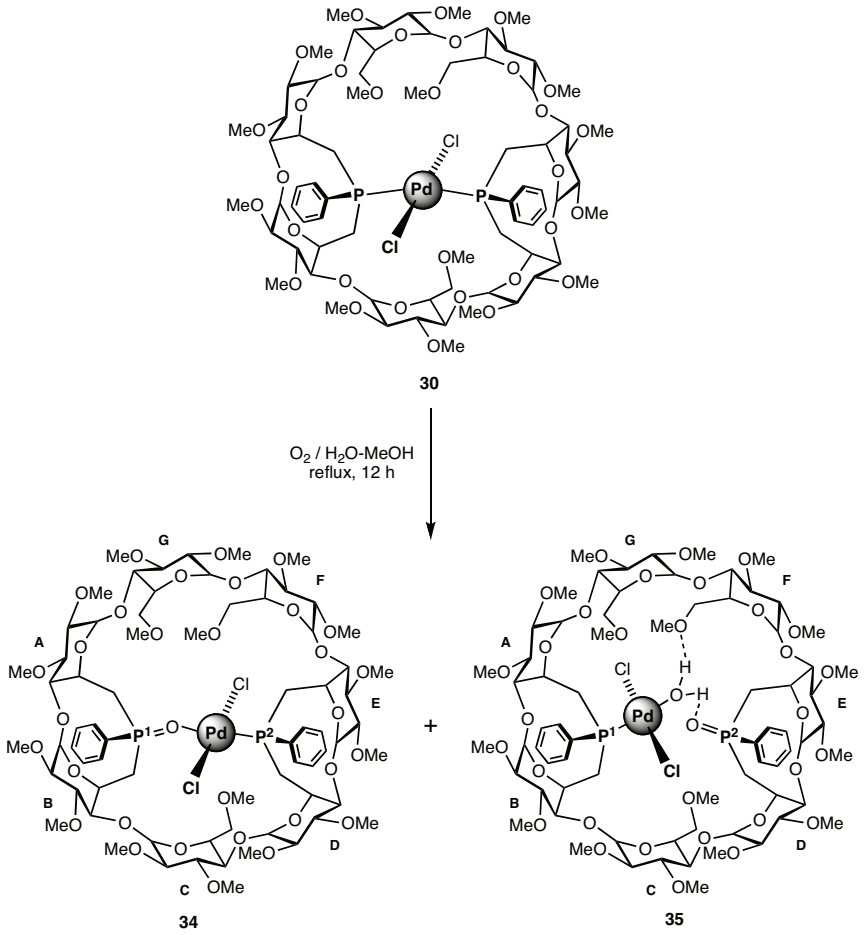

Scheme 6. Breaking the P–Pd bonds in palladium oschelate complex **30**. Dotted lines represent hydrogen bonding of the metal coordinated water molecule.

Complex **34**, which is less polar than **35**, was recovered first and its molecular structure established unambiguously by multidimensional NMR analysis (^{1}H-^{1}H COSY, ^{1}H-^{1}H TOCSY, ^{1}H-^{1}H ROESY, ^{1}H-^{13}C{^{1}H} HMQC and ^{1}H-^{31}P{^{1}H} HMQC) and mass spectrometry. The presence of a coordinated [$PdCl_2$] moiety and one oxidised donor atom in complex **34** were inferred from its mass spectrum, which displayed strong peaks at *m/z* = 1753.49 and 1737.49, corresponding to $[M + K]^+$ and $[M + Na]^+$ ions, respectively. The existence of a small ^{3}J(PP) = 4.4 Hz is consistent with the *P,O* chelate complex **34**. Further proof for such a structure came from the marked downfield shift of the ^{31}P signal (δ = 54.5 ppm) of the phosphane oxide fragment compared to non-coordinating phosphane oxide units such as those present in **27** (δ = 35.7 and 35.9 ppm). As revealed by a single-crystal X-ray diffraction study, complex **35** bears some similarities with regioisomer **34**, but in this case the partially oxidised ligand is no longer chelating the [$PdCl_2$] unit, which is now coordinated by a water molecule together with a P atom *trans*-disposed to oxygen. Careful examination of the

structure (Figure 17) showed that the coordinated water molecule (O_w) is hydrogen bonded to the phosphoryl group (O) on one hand and to the primary methoxy group of glucose unit F (O^F) on the other hand. Another interesting feature of complex **35** concerns the close proximity of the inward-pointing H-5 atom of glucose unit B to the chlorine atom lying inside the cavity. The high-field shift of about $\Delta\delta$ = 0.5 ppm experienced by this H-5 atom upon complexation is hardly surprising given the short distance (Cl(1)···H-5^B 2.65 Å) between the two atoms. It is indicative of a weak C–H···Cl–M interaction as reported on several occasions in other introverted chlorido CD complexes.[42,43]

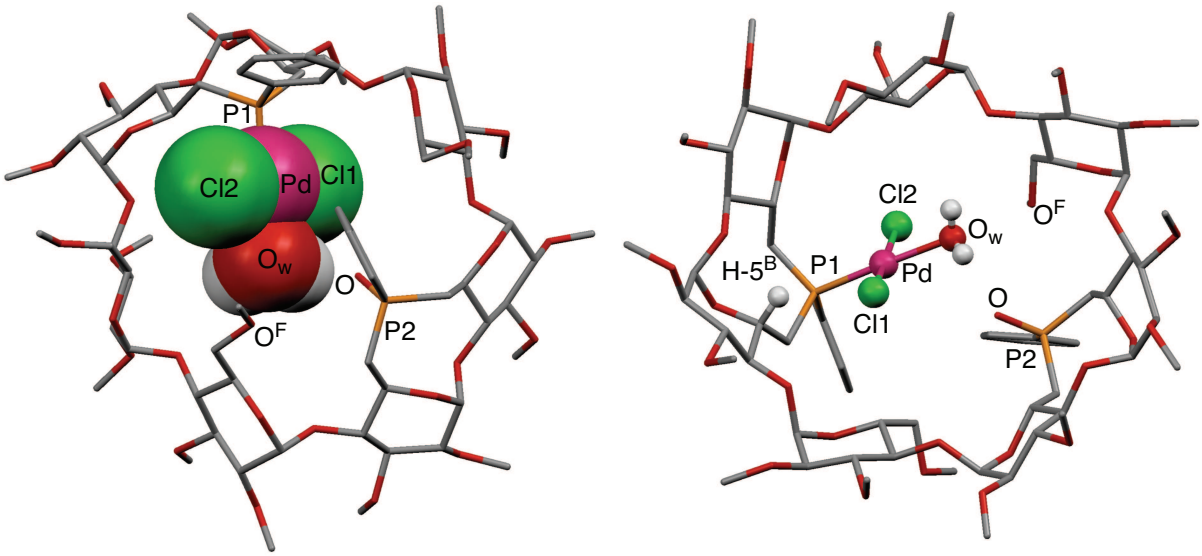

Figure 17. X-ray structure of the palladium complex **35**. Top view (left) and bottom view from the secondary face (right). Solvent molecules have been omitted for clarity. Selected bond lengths [Å], angles [º] and distances[Å]: P(1)–Pd 2.20, Pd–O_w 2.13, Cl(1)–Pd 2.28, Cl(2)–Pd 2.30, P(1)-Pd-O_w 176.27, Cl(1)-Pt-Cl(2) 172.67, Cl(1)-Pd-P(1) 95.94, P(1)-Pd-Cl(2) 89.15, Cl(2)-Pd-O_w 88.24, O_w-Pd-Cl(1) 86.91, H-5^B···Cl(1) 2.65, O_w···O 2.61, O_w···O^F 2.80, P1···P2 6.60.

Unexpectedly, the $^{31}P\{^1H\}$ NMR spectrum of complex **35** displayed two broad signals at room temperature, which sharpened at –80ºC in CD_2Cl_2 (Figure 18). The first signal at δ = 31.4 ppm corresponds to the metal-bound phosphorus atom whereas the second one at δ = 39.9 ppm, is typical of a phosphine oxide unit such as those present in di(phosphane oxide) **27**. Broad ^1H NMR signals corresponding to phenyl and two H-1 protons as well as a OMe-6 group (likely belonging to glucose unit F), which is hydrogen bonded to the coordinated water molecule, also reflect the fluxional behaviour of complex **35**. At –80ºC, all

the signals sharpened (Figure 18) so that even the coordinated water molecule could be observed at 6.1 ppm, a value that is in agreement with previously reported water molecules coordinated to palladium centres.[62-65] All these data are consistent with a rather dynamic hydrogen bonding network in solution involving the coordinated water molecule (O_w) as well as the OMe-6 of glucose unit F (O^F) and P=O units.

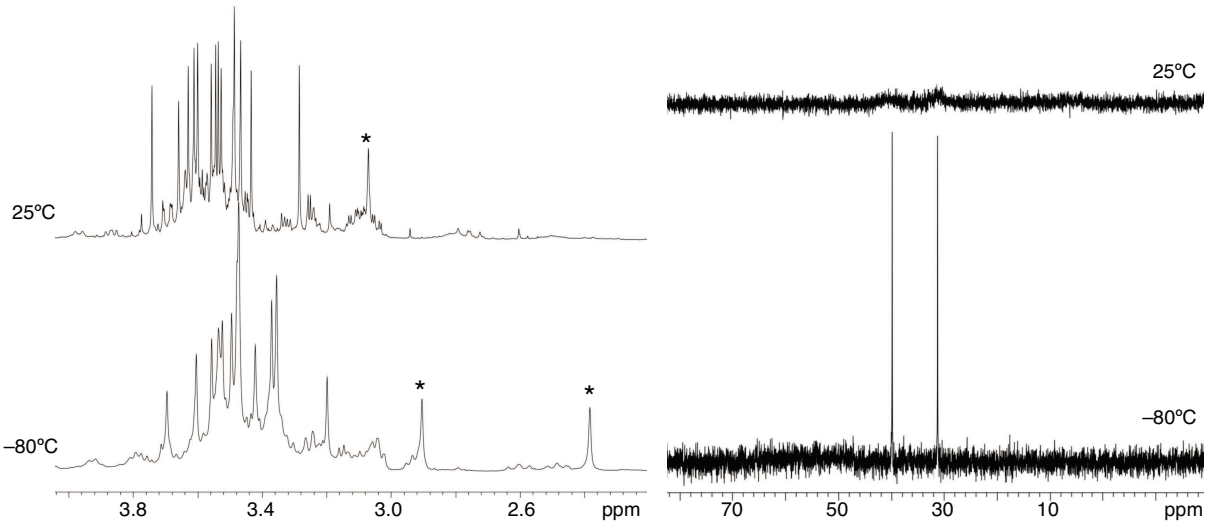

Figure 20. Part of ^{1}H NMR spectra recorded at 500.1 MHz (left) and ^{31}P{^{1}H} NMR spectra recorded at 202.5 MHz (right) in CD_2Cl_2 of the aqua-palladium complex **35** at 25ºC (top) and –80ºC (bottom). The asterisk in the spectrum at 25ºC corresponds to two overlapping OMe-6 signals. These appear as two sharp peaks at –80°C (one of them corresponding to the OMe-6 group of glucose unit F).

All in all, the partially oxidised complexes **34** and **35** are likely to be formed by cleavage of one of the Pd–P bond, whether Pd–P1 or Pd–P2, and subsequent formation of an aqua complex. In the case of **34**, the formation of a *P,O* chelate complex implies the displacement of the coordinated water molecule by the phosphine oxide ligand, whereas in **35** the aqua complex is stabilised by multiple hydrogen bonding with the cavity inner wall (Scheme 7).

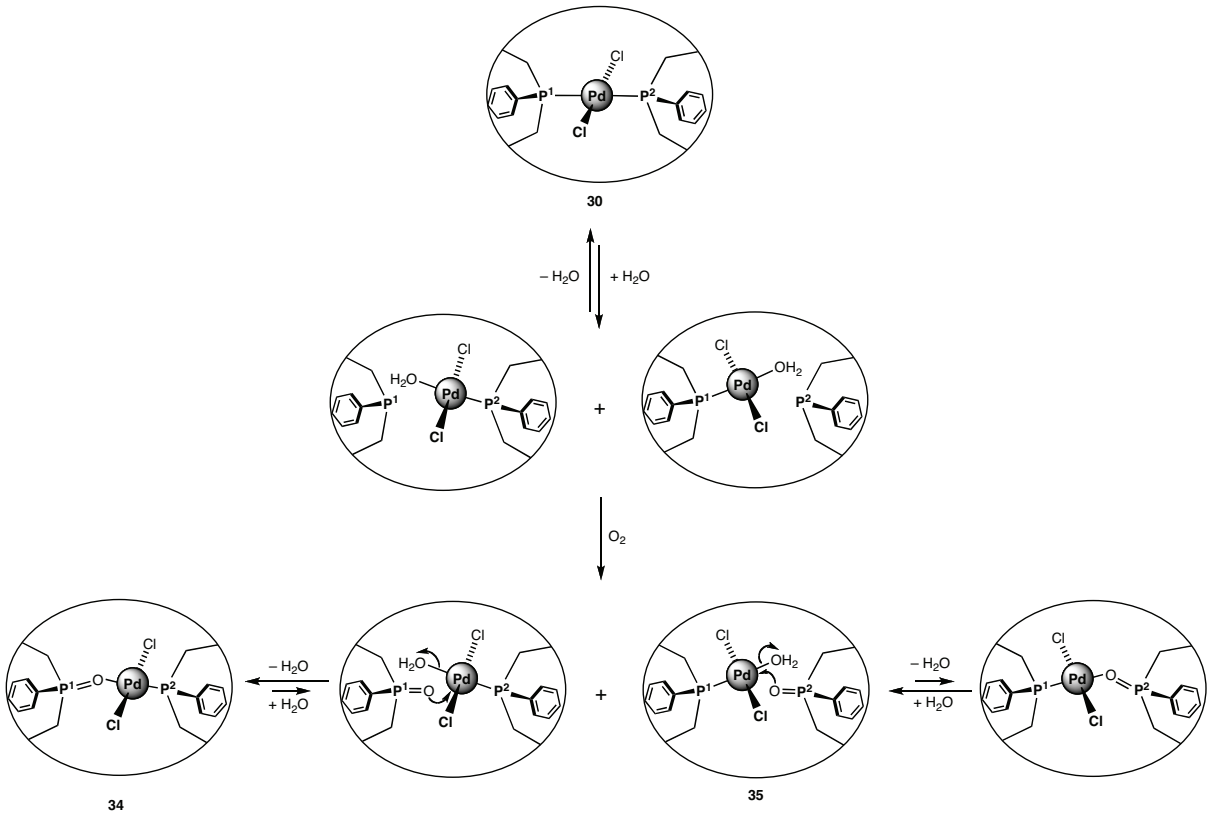

Scheme 7. Proposed mechanism for the formation of complexes **34** and **35**.

III.3. Conclusion

In the present chapter, we have presented the chelating properties of **WIDEPHOS**, the first introverted diphosphane built on a large β-CD cavity. Owing to its rigidity as well as the large separation between the two phosphorus donor atoms, **WIDEPHOS** behaves towards square planar and linear transition-metal ions as an unsymmetrical *trans*-chelator, inducing rapid oscillation of the chelate about the metal centre. This phenomenon occurs without dissociation of the phosphorus atoms. The unprecedented chelating behaviour of **WIDEPHOS** enabled the formation of monophosphane complexes displaying rich *intra*-cavity reactivity, thereby paving the way to the further study of organometallic catalysts operating in a confined environment.

III.4. Experimental section

III.4.1. General procedures

All manipulations were performed in Schlenk-type flasks under dry nitrogen. Solvents were dried by conventional methods and distilled immediately prior to use. Deuterated solvents were passed down a 5 cm-thick alumina column and stored under nitrogen over molecular sieves (4 Å). Routine ^{1}H and $^{13}C\{^{1}H\}$ spectra were recorded on FT Bruker AVANCE 300, AVANCE 400, AVANCE 500 and AVANCE 600 instruments. ^{1}H NMR spectral data were referenced to residual protiated solvents (δ = 7.26 ppm for $CDCl_3$, 7.16 ppm for C_6D_6 and 5.32 ppm for CD_2Cl_2), $^{13}C\{^{1}H\}$ chemical shifts are reported relative to deuterated solvents (δ = 77.00 ppm for $CDCl_3$, 128.06 ppm for C_6D_6 and 54.00 for CD_2Cl_2) and the $^{31}P\{^{1}H\}$ NMR data are given relative to external H_3PO_4. Mass spectra were recorded either on a ZAB HF VG analytical spectrometer using *m*-nitrobenzyl alcohol as matrix or on a Bruker MicroTOF spectrometer (ESI) using CH_2Cl_2, MeCN or MeOH as solvent. Elemental analyses were performed by the Service de Microanalyse, Institut de Chimie, Strasbourg. Melting points were determined with a Büchi 535 capillary melting-point apparatus. All commercial reagents were used as supplied. **WIDEPHOS** was prepared according to the synthesis of compound **10** from **Chapter II**. [AuCl(tht)],[66] $[PtCl_2(PhCN)_2]$,[67] $[PdCl_2(PhCN)_2]$[67] and [PdClMe(cod)][68] were prepared according to literature procedures. The numbering of the atoms within a glucose unit is as follows:

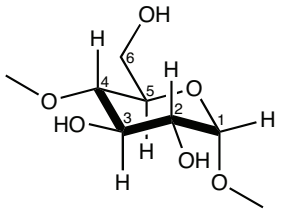

III.4.2. Synthesis of compounds

6^{A},6^{B},6^{D},6^{E}-Tetradeoxy-6^{A},6^{B}:6^{D},6^{E}-bis[(*S*)-phenyloxophosphinidene]-2^{A},2^{B},2^{C},2^{D},2^{E},2^{F}, 2^{G},3^{A},3^{B},3^{C},3^{D},3^{E},3^{F},3^{G},6^{C},6^{F},6^{G}-heptadeca-*O*-methyl-β-cyclodextrin (27)

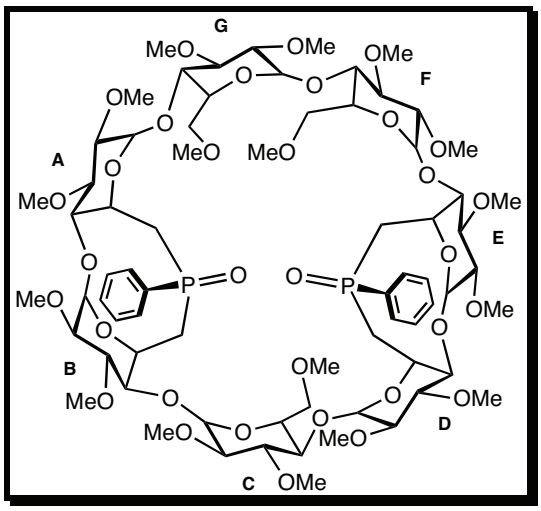

The bis(phosphane oxide) **27** was quantitavely obtained by bubbling air through a solution of **WIDEPHOS** in MeOH for 3 h at room temperature. Removal of the solvent *in vacuo* gave **27** as a colourless analytically pure product. R_f (SiO_2, CH_2Cl_2/MeOH, 92:8, *v*/*v*) = 0.30; m.p. 213ºC; ^{1}H NMR (300.1 MHz, $CDCl_3$, 25ºC): δ (assignment by COSY) = 1.91–1.93 (2 H, H-6a$^{A,D\text{ or }B,E}$), 2.21–2.23 (2 H, 6a$^{B,E\text{ or }A,D}$), 2.91–3.74 (28 H, H-2, H-3, H-4, H-6b^{A,B,D,E}, H-6a^{C,F,G}), 3.06 (s, 3 H, OMe), 3.08 (s, 3 H, OMe), 3.22 (s, 3 H, OMe), 3.43 (s, 3 H, OMe), 3.44 (s, 3 H, OMe), 3.45 (s, 3 H, OMe), 3.47 (s, 3 H, OMe), 3.48 (s, 3 H, OMe), 3.56 (s, 9 H, OMe), 3.60 (s, 6 H, OMe), 3.67 (s, 6 H, OMe), 3.68 (s, 3 H, OMe), 3.71 (s, 3 H, OMe), 3.86–4.08 (6 H, H-5^{C,F,G}, H-6b^{C,F,G}), 4.40–4.42 (2 H, H-5$^{A,D\text{ or }B,E}$), 4.62–4.64 (2 H, H-5$^{B,E\text{ or }A,D}$), 4.86 (d, 1 H, $^3J_{H\text{-}1,H\text{-}2}$ = 3.3 Hz, H-1), 4.93 (d, 2 H, $^3J_{H\text{-}1,H\text{-}2}$ = 3.3 Hz, H-1), 4.97 (d, 1 H, $^3J_{H\text{-}1,H\text{-}2}$ = 3.3 Hz, H-1), 5.02 (d, 2 H, $^3J_{H\text{-}1,H\text{-}2}$ = 3.3 Hz, H-1), 5.08 (d, 1 H, $^3J_{H\text{-}1,H\text{-}2}$ = 3.3 Hz, H-1), 7.45–7.54 (6 H, *m*-H, *p*-H), 7.72–7.80 (4 H, *o*-H) ppm; ^{13}C{^{1}H} NMR (75.5 MHz $CDCl_3$, 25ºC): δ (assignment by HMQC) = 33.41 (d, $^2J_{C,P}$ = 68.1 Hz), 33.50 (d, $^2J_{C,P}$ = 68.1 Hz) (C-6$^{A,D\text{ or }B,E}$), 37.82 (d, $^2J_{C,P}$ = 65.5 Hz), 37.87 (d, $^2J_{C,P}$ = 65.5 Hz) (C-6$^{B,E\text{ or }A,D}$), 57.89, 58.14, 58.17 [×2], 58.21, 58.25 [×2], 58.66, 58.73, 58.81, 61.48, 61.50, 61.62 [×2], 61.93, 62.10, 62.22 (OMe), 63.33 [×2] (C-5$^{A,D\text{ or }B,E}$), 66.22, 66.83 (C-5$^{B,E\text{ or }A,D}$), 70.30, 70.74, 70.83 (C-5^{C,F,G}), 70.89, 70.96, 71.04 (C-6^{C,F,G}), 80.31, 80.57, 81.25, 81.50 [×2], 81.67, 81.85 [×2],

82.04, 82.41 [×4], 82.65[×2], 83.37, 83.57 (C-2,C-3, C-4^{C,F,G}), 86.25 (d, $^{3}J_{C,P}$ = 11.8 Hz), 87.21 (d, $^{3}J_{C,P}$ = 11.8 Hz) (C-4$^{A,D\text{ or }B,E}$), 89.29 [×2] (C-4$^{B,E\text{ or }A,D}$), 98.81, 98.94, 99.73, 100.35 [×2], 100.65, 101.15 (C-1), 128.71 [×2] (d, $^{2}J_{C,P}$ = 11.8 Hz, *o*-C), 129.44 [×2] (d, $^{3}J_{C,P}$ = 9.3 Hz, *m*-C), 131.69 [×2] (*p*-C), 135.16 (d, $^{1}J_{C,P}$ = 98.1 Hz, *ipso*-C), 135.36 (d, $^{1}J_{C,P}$ = 98.1 Hz, *ipso*-C) ppm; $^{31}P\{^{1}H\}$ NMR (121.5 MHz $CDCl_3$, 25ºC): δ = 35.7 (s), 35.9 (s) ppm; elemental analysis (%) calcd for $C_{71}H_{110}O_{33}P_2$ (1553.56): C 54.89, H 7.14, found: C 54.82, H 7.43; MS (ESI-TOF): *m/z* (%): 1575.56 (100) $[M + Na]^+$.

_P,P'_-{6^{A},6^{B},6^{D},6^{E}-Tetradeoxy-6^{A},6^{B}:6^{D},6^{E}-bis[(*R*)-phenylphosphinidene]-2^{A},2^{B},2^{C},2^{D},2^{E}, 2^{F},2^{G},3^{A},3^{B},3^{C},3^{D},3^{E},3^{F},3^{G},6^{C},6^{F},6^{G}-heptadeca-*O*-methyl-β-cyclodextrin}gold(I) hexafluorophosphate (28)

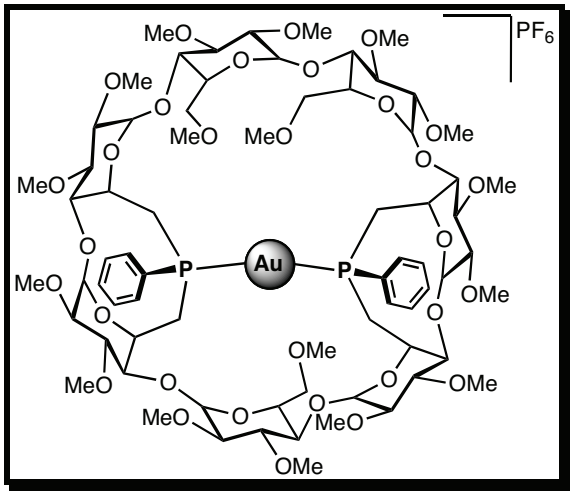

A solution of thallium hexafluorophosphate (0.020 g, 0.058 mmol) in thf (2 mL) was added to a solution of [AuCl(tht)] (0.016 g, 0.053 mmol) in CH_2Cl_2 (10 mL). After stirring for 30 min, the solution was filtered through celite to eliminate thallium chloride, then added to a solution of **WIDEPHOS** (0.080 g, 0.053 mmol) in CH_2Cl_2 (5 mL). After 30 min, the solution was filtered through celite and the filtered solution was concentrated to *ca.* 2 mL. Addition of pentane afforded complex **28** (yield: 0.099 g, 99%) as a pale brown precipitate. R_f (SiO_2, CH_2Cl_2/MeOH, 92:8, *v*/*v*) = 0.33; m.p. dec. >250ºC; ^{1}H NMR (300.1 MHz, $CDCl_3$, 25ºC): δ (assignment by COSY) = 2.06 (dt, 1 H, $^{2}J_{H\text{-}6a,H\text{-}6b}$ = 15.4 Hz, $^{2}J_{H\text{-}6a,P}$ = $^{3}J_{H\text{-}6a,H\text{-}65}$ = 5.7 Hz, H-6a$^{A\text{ or }D}$), 2.52 (m, 1 H, H-6a$^{D\text{ or }A}$), 2.65 (2 H, H-6a^{B,E}), 2.84 (s, 3 H, OMe), 2.95–3.70 (30 H, H-2, H-3, H-4$^{A,B,D,E\text{ and }C,F\text{ or }F,G\text{ or }C,G}$, H-5$^{C\text{ or }F\text{ or }G}$, H-6$^{C,F\text{ or }F,G\text{ or }C,G}$, H-6a$^{G\text{ or }C\text{ or }F}$, H-6b^{A,B,D,E}), 2.96 (s, 3 H, OMe), 3.30 (s, 3 H, OMe), 3.47 (s, 6 H, OMe), 3.50 (s, 6 H, OMe),

3.52 (s, 3 H, OMe), 3.54 (s, 3 H, OMe), 3.55 (s, 3 H, OMe), 3.56 (s, 3 H, OMe), 3.60 (s, 3 H, OMe), 3.61 (s, 6 H, OMe), 3.64 (s, 6 H, OMe), 3.67 (s, 3 H, OMe), 3.80–3.90 (2 H, H-4$^{G\text{ or }C\text{ or }F}$, H-6b$^{G\text{ or }C\text{ or }F}$), 4.21–4.43 (6 H, H-5$^{A,B,D,E\text{ and }F,G\text{ or }C,F\text{ or }C,G}$), 4.83 (d, 1 H, $^{3}J_{H\text{-}1,H\text{-}2}$ = 3.1 Hz, H-1), 4.99 (d, 1 H, $^{3}J_{H\text{-}1,H\text{-}2}$ = 2.0 Hz, H-1), 5.06 (d, 1 H, $^{3}J_{H\text{-}1,H\text{-}2}$ = 3.1 Hz, H-1), 5.07 (d, 1 H, $^{3}J_{H\text{-}1,H\text{-}2}$ = 3.3 Hz, H-1), 5.10 (d, 1 H, $^{3}J_{H\text{-}1,H\text{-}2}$ = 4.5 Hz, H-1), 5.15 (d, 1 H, $^{3}J_{H\text{-}1,H\text{-}2}$ = 3.3 Hz, H-1), 5.18 (d, 1 H, $^{3}J_{H\text{-}1,H\text{-}2}$ = 3.9 Hz, H-1), 7.42–7.47 (2 H, *m*-H), 7.55–7.67 (6 H, *m*-H, *p*-H, *o*-H), 7.73–7.79 (2 H, *o*-H) ppm; $^{13}C\{^{1}H\}$ NMR (75.5 MHz, $CDCl_3$, 25ºC): δ (assignment by HMQC) = 28.27, 28.96 (C-6$^{B,E\text{ or }A,D}$), 36.23, 38.66 (C-6$^{A,D\text{ or }B,E}$), 57.77 [×2], 58.14 [×2], 58.22, 58.27, 58.50, 58.80, 59.09, 59.29, 59.51, 59.59, 60.04, 60.96, 60.97 [×2], 61.40 (OMe), 64.40, 65.05 (C-5$^{A,D\text{ or }B,E}$), 69.52, 70.43 [×2] (C-5$^{B,E\text{ or }A,D\text{ and }C\text{ or }F\text{ or }G}$), 72.64, 74.03 (C-5$^{F,G\text{ or }C,F\text{ or }C,G}$), 71.26, 71.95, 72.77 (C-6^{C,F,G}), 76.90, 77.07, 78.07 (C-4^{C,F,G}), 80.29, 80.67, 81.23, 81.28 [×2], 81.70, 81.79 [×3], 81.84, 82.36 [×2], 82.78, 83.91 (C-2, C-3), 88.61 [×2] (C-4$^{A,B\text{ or }D,E}$), 86.21 [×2] (C-4$^{D,E\text{ or }A,B}$), 95.20, 97.01, 97.44, 97.61, 98.73, 99.42, 99.54 (C-1), 129.59, 129.76 (*m*-C), 132.48 [×2] (*p*-C), 132.30, 132.69 (*o*-C), 137.75 [×2] (*ipso*-C) ppm; $^{31}P\{^{1}H\}$ NMR (121.5 MHz, $CDCl_3$, 25ºC): δ = 34.2 (br s), –144.3 (hept, $^{1}J_{P,F}$ = 716 Hz) ppm; $^{31}P\{^{1}H\}$ NMR (121.5 MHz, CD_2Cl_2, 25ºC): δ = 37.6 and 34.6 (2 d, AB system, $^{2}J_{P1,P2}$ = 326 Hz), –144.3 (hept, $^{1}J_{P,F}$ = 716 Hz) ppm; $^{31}P\{^{1}H\}$ NMR (121.5 MHz, CD_2Cl_2, –80ºC): δ = 40.6 and 31.6 (2d, AB system, $^{2}J_{P1,P2}$ = 326 Hz), 38.0 and 33.8 (2d, AB system, $^{2}J_{P1,P2}$ = 326 Hz), –144.3 (hept, $^{1}J_{P,F}$ = 716 Hz) ppm; elemental analysis (%) calcd for $C_{71}H_{110}AuF_6O_{31}P_3$ (1863.49): C 45.76, H 5.95, found: C 45.76, H 5.95; MS (ESI-TOF): *m/z* (%): 1717.62 (100) $[M - PF_6]^+$.

***trans-P,P'*-Dichlorido-{6^{A},6^{B},6^{D},6^{E}-tetradeoxy-6^{A},6^{B}:6^{D},6^{E}-bis[(*R*)-phenylphosphinidene]-2^{A},2^{B},2^{C},2^{D},2^{E},2^{F},2^{G},3^{A},3^{B},3^{C},3^{D},3^{E},3^{F},3^{G},6^{C},6^{F},6^{G}-heptadeca-*O*-methyl-β-cyclodextrin} platinum(II) (29)**

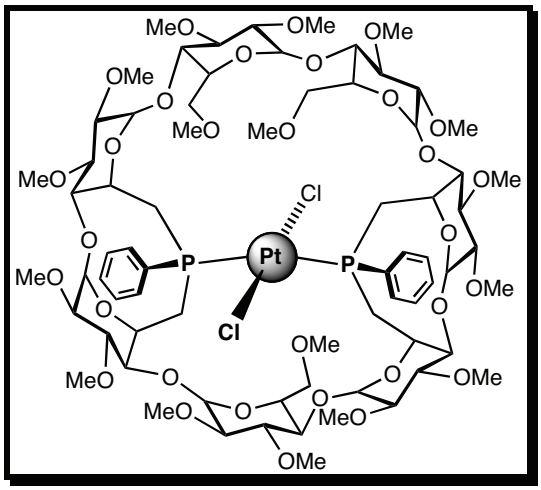

A solution of $[PtCl_2(PhCN)_2]$ (0.025 g, 0.053 mmol) in CH_2Cl_2 (5 mL) was added dropwise to a solution of **WIDEPHOS** (0.080 g, 0.053 mmol) in CH_2Cl_2 (10 mL) within 30 min at room temperature. After 30 min, the reaction mixture was evaporated to dryness affording analytically pure **29** (yield: 0.089 g, 99%) as a pale yellow solid. R_f (SiO_2, CH_2Cl_2/MeOH, 92:8, *v*/*v*) = 0.40; m.p. dec. >250ºC; ^{1}H NMR (300.1 MHz, $CDCl_3$, 25ºC): δ (assignment by COSY) = 2.12–2.21 (m, 1 H, H-6a$^{A\text{ or }D}$), 2.34 (dt, 1 H, $^{3}J_{H\text{-}6a,P}$ = 15.5 Hz, $^{2}J_{H\text{-}6a,H\text{-}6b}$ = 7.7 Hz, $^{3}J_{H\text{-}6a,H\text{-}5}$ = 7.7 Hz, H-6a$^{D\text{ or }A}$), 2.68–2.76 (2 H, H-6a^{B,E}), 2.82 (dd, 1 H, $^{3}J_{H\text{-}2,H\text{-}3}$ = 9.2 Hz, $^{3}J_{H\text{-}2,H\text{-}1}$ = 3.1 Hz, H-2), 3.05–3.75 (22 H, H-2, H-3, H-4^{A,B,D,E}, H-6a^{C,F,G}, H-6b^{B,E}), 3.27 (s, 3 H, OMe), 3.30 (s, 3 H, OMe), 3.32 (s, 3 H, OMe), 3.38 (s, 3 H, OMe), 3.45 (s, 3 H, OMe) 3.48 (s, 3 H, OMe), 3.50 (s, 3 H, OMe), 3.53 (s, 3 H, OMe), 3.57 (s, 3 H, OMe), 3.59 (s, 6 H, OMe), 3.62 (s, 6 H, OMe), 3.63 (s, 3 H, OMe), 3.64 (s, 3 H, OMe), 3.72 (s, 3 H, OMe), 3.84 (s, 3 H, OMe), 3.86–3.95 (6 H, H-4^{C,F,G}, H-6b$^{A,D\text{ and }C\text{ or }F\text{ or }G}$), 4.02–4.11 (4 H, H-5$^{F,G\text{ or }C,F\text{ or }C,G}$, H-6b$^{F,G\text{ or }C,F\text{ or }C,G}$), 4.25 (d, 1 H, $^{3}J_{H\text{-}5,H\text{-}6a}$ = 9.7 Hz, H-5$^{C\text{ or }F\text{ or }G}$), 4.33–4.39 (3 H, H-5$^{A\text{ or }D\text{ and }B,E}$), 4.55 (m, 1 H, H-5$^{D\text{ or }A}$), 4.80 (d, 1 H, $^{3}J_{H\text{-}1,H\text{-}2}$ = 3.3 Hz, H-1), 4.91 (d, 1 H, $^{3}J_{H\text{-}1,H\text{-}2}$ = 3.4 Hz, H-1), 5.03 (d, 1 H, $^{3}J_{H\text{-}1,H\text{-}2}$ = 4.0 Hz, H-1), 5.06 (d, 2 H, $^{3}J_{H\text{-}1,H\text{-}2}$ = 4.3 Hz, H-1), 5.27 (d, 1 H, $^{3}J_{H\text{-}1,H\text{-}2}$ = 4.1 Hz, H-1), 5.54 (d, 1 H, $^{3}J_{H\text{-}1,H\text{-}2}$ = 4.7 Hz, H-1), 7.39–7.42 (6 H, *m*-H, *p*-H), 8.06–8.10 (4 H, *o*-H) ppm; ^{13}C{^{1}H} NMR (75.5 MHz, $CDCl_3$, 25ºC): δ (assignment by HMQC) = 22.80, 26.50 (C-6$^{A,D\text{ or }B,E}$), 32.00, 33.00 (C-6$^{B,E\text{ or }A,D}$), 56.73,

57.74, 57.91, 58.15, 58.79, 58.84, 58.93, 59.02, 59.78, 60.42, 60.62, 60.96, 61.27, 61.40, 61.54, 61.72, 61.89 (OMe), 63.54, 64.29 (C-$5^{B,E\text{ or }A,D}$), 67.97, 69.10 (C-$5^{A,D\text{ or }B,E}$), 70.37, 70.45, 70.69 (C-$5^{C,F,G}$), 71.02, 71.89, 72.05 (C-$6^{C,F,G}$), 77.90 [×2], 78.07 (C-$4^{C,F,G}$), 79.02 [×2], 79.70 [×2], 80.54, 81.13 [×2], 81.37, 81.61, 82.11, 82.43, 82.95, 83.05, 83.44 (C-2, C-3), 84.50 [×2] (C-$4^{A,D\text{ or }B,E}$), 89.39 [×2] (C-$4^{B,E\text{ or }A,D}$), 94.64, 94.75, 96.97, 98.14, 98.26, 98.75, 99.25 (C-1), 127.95 (virtual t, $|^3J_{C,P} + {}^5J_{C,P'}| = 10.0$ Hz, *m*-C), 128.52 (virtual t, $|^3J_{C,P} + {}^5J_{C,P'}| = 10.0$ Hz, *m*-C), 130.28 [×2] (*p*-C), 133.25 (virtual t, $|^2J_{C,P} + {}^4J_{C,P'}| = 12.3$ Hz, *o*-C), 133.69 (virtual t, $|^2J_{C,P} + {}^4J_{C,P'}| = 12.3$ Hz, *o*-C), 135.57 [×2] (virtual t, $|^1J_{C,P} + {}^3J_{C,P'}| = 52.0$ Hz, *ipso*-C) ppm; $^{31}P\{^1H\}$ NMR (121.5 MHz, $CDCl_3$, 25ºC): $\delta = 8.9$ (br s with br Pt satellites, $^1J_{P,Pt} \approx 2500$ Hz) ppm; ^{31}P $\{^1H\}$ NMR (121.5 MHz, CD_2Cl_2, –80ºC) = 12.2 and 1.0 (2 d, AB system, $^2J_{P1,P2} = 476$ Hz), 17.8 and 5.0 (2 d, AB system, $^2J_{P1,P2} = 492$ Hz) ppm ($^1J_{Pt,P}$ poorly resolved); ^{31}P $\{^1H\}$ NMR (202.5 MHz, $C_2D_2Cl_4$, 80ºC) = 7.35 and 7.0 (2 d with Pt satellites, ABX system, $^1J_{Pt,P1} = 2507$ Hz, $^1J_{Pt,P2} = 2481$ Hz, $^2J_{P1,P2} = 496$ Hz) ppm; elemental analysis (%) calcd for $C_{71}H_{110}Cl_2O_{31}P_2Pt$ (1785.55): C 47.71, H 6.20, found: C 47.91, H 6.31; MS (ESI-TOF): *m/z* (%): 1792.45 (100) $[M + Li]^+$.

***trans-P,P'*-Dichlorido-{6^A,6^B,6^D,6^E-tetradeoxy-6^A,6^B:6^D,6^E-bis[(*R*)-phenylphosphinidene]-2^A,2^B,2^C,2^D,2^E,2^F,2^G,3^A,3^B,3^C,3^D,3^E,3^F,3^G,6^C,6^F,6^G-heptadeca-*O*-methyl-β-cyclodextrin} palladium(II) (30)**

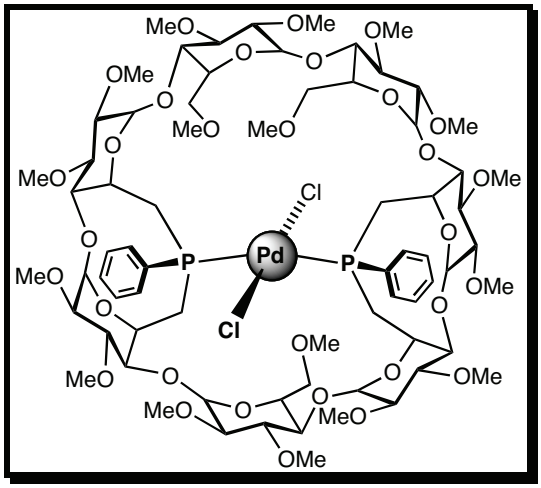

A solution of $[PdCl_2(PhCN)_2]$ (0.020 g, 0.053 mmol) in CH_2Cl_2 (5 mL) was added dropwise to a solution of **WIDEPHOS** (0.080 g, 0.053 mmol) in CH_2Cl_2 (10 mL) within 30 min at room temperature. After 30 min, the reaction mixture was evaporated to dryness and

the residue subjected to column chromatography (SiO_2, CH_2Cl_2/MeOH, 96:4, *v*/*v*) to give pure **30** (yield: 0.081 g, 90%) as a pale yellow powder. R_f (SiO_2, CH_2Cl_2/MeOH, 92:8, *v*/*v*) = 0.40; m.p. dec. >250ºC; ^{1}H NMR (300.1 MHz, CD_2Cl_2, 25ºC): δ (assignment by COSY) = 2.0 (m, 1 H, H-6a$^{A\text{ or }D}$), 2.29 (m, 1 H, H-6a$^{D\text{ or }A}$), 2.55 (m, 1 H, H-6a$^{B\text{ or }E}$), 2.70 (m, 1 H, H-6a$^{E\text{ or }B}$), 2.78 (dd, 1 H, $^3J_{H\text{-}2,H\text{-}3}$ = 9.6 Hz, $^3J_{H\text{-}2,H\text{-}1}$ = 3.5 Hz, H-2), 2.98–3.14 (8 H, H-2, H-4^{D,E}), 3.25–3.88 (20 H, H-3, H-4^{A,B,C,F,G}, H-6a^{C,F,G}, H-6b$^{A,B,D,E\text{ and }C\text{ or }F\text{ or }G}$), 3.22 (s, 3 H, OMe), 3.24 (s, 3 H, OMe), 3.25 (s, 3 H, OMe), 3.35 (s, 3 H, OMe), 3.43 (s, 3 H, OMe), 3.44 (s, 3 H, OMe), 3.46 (s, 3 H, OMe), 3.47 (s, 3 H, OMe), 3.51 (s, 3 H, OMe), 3.54 (s, 6 H, OMe), 3.55 (s, 6 H, OMe), 3.57 (s, 3 H, OMe), 3.59 (s, 3 H, OMe), 3.62 (s, 3 H, OMe), 3.73 (s, 3 H, OMe), 3.97–4.11 (3H, H-5$^{C\text{ or }F\text{ or }G}$, H-6b$^{C,F\text{ or }C,G\text{ or }F,G}$), 4.20–4.33 (4 H, H-5$^{A,B\text{ and }F,G\text{ or }C,F\text{ or }C,G}$), 4.36–4.41 (m, 1 H, H-5$^{E\text{ or }D}$), 4.44–4.90 (m, 1 H, H-5$^{D\text{ or }E}$), 4.81 (d, 1 H, $^3J_{H\text{-}1,H\text{-}2}$ = 3.6 Hz, H-1), 4.91 (d, 1 H, $^3J_{H\text{-}1,H\text{-}2}$ = 3.4 Hz, H-1), 4.99 (d, 1 H, $^3J_{H\text{-}1,H\text{-}2}$ = 3.1 Hz, H-1), 5.00 (d, 1 H, $^3J_{H\text{-}1,H\text{-}2}$ = 3.3 Hz, H-1), 5.01 (d, 1 H, $^3J_{H\text{-}1,H\text{-}2}$ = 3.1 Hz, H-1), 5.20 (d, 1 H, $^3J_{H\text{-}1,H\text{-}2}$ = 4.0 Hz, H-1), 5.40 (d, 1 H, $^3J_{H\text{-}1,H\text{-}2}$ = 4.4 Hz, H-1), 7.36–7.42 (6 H, *m*-H, *p*-H), 7.95–8,01 (4 H, *o*-H) ppm; ^{13}C{^{1}H} NMR (75.5 MHz, CD_2Cl_2, 25ºC): δ (assignment by HMQC) = 22.86, 25.06 (C-6$^{A,D\text{ or }B,E}$), 31.51, 32.00 (C-6$^{B,E\text{ or }A,D}$), 54.74, 55.93, 55.88 [×2], 56.50, 56.56 [×2], 56.74, 57.64, 58.09, 58.37, 58.45, 58.86 [×2], 59.27 [×2], 59.45 (OMe), 61.71, 62.31 (C-5$^{A,D\text{ or }B,E}$), 66.18, 67.25 (C-5$^{B,E\text{ or }A,D}$), 68.58, 68.73, 68.87 (C-5^{C,F,G}), 69.07, 69.84, 70.03 (C-6^{C,F,G}), 75.71, 75.83 [×2] (C-4 ^{C,F,G}), 77.25, 77.45, 78.64, 79.08, 79.16, 79.33, 79.39, 79.47 [×2], 79.74, 80.12, 80.45, 80.96 [×2] (C-2, C-3), 82.50 [×2], 87.28 [×2] (C-4^{A,B,D,E}), 92.46, 92.84, 94.98, 95.99, 96.35, 96.79, 96.89 (C-1), 125.92 (virtual t, $|^3J_{C,P} + {}^5J_{C,P'}|$ = 9.8 Hz, *m*-C), 126.57 (virtual t, $|^3J_{C,P} + {}^5J_{C,P'}|$ = 9.5 Hz, *m*-C), 128.11, 128.33 (*p*-C), 130.97 (virtual t, $|^2J_{C,P} + {}^4J_{C,P'}|$ = 12.7 Hz, *o*-C), 131.37 (virtual t, $|^2J_{C,P} + {}^4J_{C,P'}|$ = 12.7 Hz, *o*-C), 132.87 [×2] (virtual t, $|^2J_{C,P} + {}^4J_{C,P'}|$ = 51.0 Hz, *ipso*-C) ppm; ^{31}P{^{1}H} NMR (121.5 MHz, $CDCl_3$, 25ºC): δ = 15.5 (br s) ppm; ^{31}P {^{1}H} NMR (121.5 MHz, CD_2Cl_2, –80ºC) = 21.7 and 11.4 (2 d, AB system, $^2J_{P1,P2}$ = 564 Hz), 17.7 and 5.6 (2 d, AB system, $^2J_{P1,P2}$ = 549 Hz) ppm; elemental analysis (%) calcd for $C_{71}H_{110}Cl_2O_{31}P_2Pd$ (1698.89): C 50.20, H 6.53, found: C 50.12, H 6.74; MS (ESI-TOF): *m/z* (%): 1737.46 (19) $[M + K]^+$, 1721.47 (76) $[M + Na]^+$, 1661.51 (5) $[M - Cl]^+$.

***trans-P,P'*-Chlorido-methyl-{6^{A},6^{B},6^{D},6^{E}-tetradeoxy-6^{A},6^{B}:6^{D},6^{E}-bis[(*R*)phenylphosphinidene]-2^{A},2^{B},2^{C},2^{D},2^{E},2^{F},2^{G},3^{A},3^{B},3^{C},3^{D},3^{E},3^{F},3^{G},6^{C},6^{F},6^{G}-heptadeca-*O*-methyl-β-cyclodextrin}palladium(II) (31)**

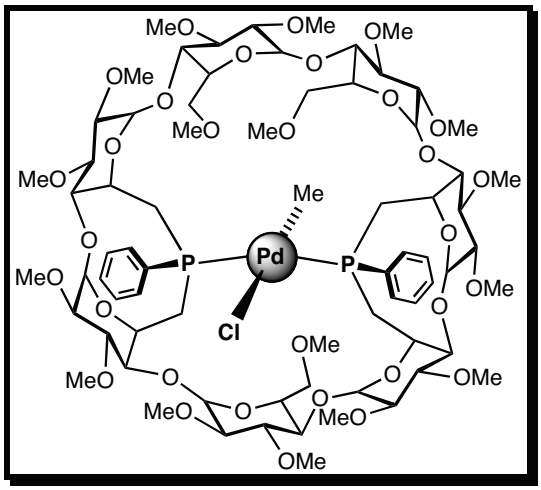

A solution of [PdClMe(cod)] (0.012 g, 0.046 mmol) in CH_2Cl_2 (5 mL) was added dropwise to a solution of **WIDEPHOS** (0.070 g, 0.046 mmol) in CH_2Cl_2 (10 mL) within 30 min at room temperature. After 30 min, the reaction mixture was evaporated to dryness and the residue subjected to column chromatography (SiO_2, CH_2Cl_2/MeOH, 96:4, *v*/*v*) to give pure **31** (yield: 0.069 g, 90%) as a pale yellow powder. R_f (SiO_2, CH_2Cl_2/MeOH, 92:8, *v*/*v*) = 0.40; m.p. dec. >250ºC; ^{1}H NMR (300.1 MHz, $CDCl_3$, 25ºC): δ (assignment by COSY) = 0.09 (t, 3 H, $^{2}J_{H,P}$ = 6.4 Hz, Me), 2.01–2.11 (2 H, H-6a$^{A,D\text{ or }B,E}$), 2.42–2.51 (2 H, H-6a$^{B,E\text{ or }A,D}$), 2.78–2.80 (m, 1 H, H-2), 2.87–2.93 (m, 1 H, H-6b$^{B\text{ or }E}$), 3.15 (m, 1 H, H-6b$^{E\text{ or }B}$), 3.26 (s, 3 H, OMe), 3.28 (s, 3 H, OMe), 3.32 (s, 3 H, OMe), 3.37 (s, 3 H, OMe), 3.44 (s, 3 H, OMe), 3.47 (s, 3 H, OMe), 3.49 (s, 3 H, OMe), 3.51 (s, 3 H, OMe), 3.56 (s, 3 H, OMe), 3.57 (s, 6 H, OMe), 3.58 (s, 3 H, OMe), 3.61 (s, 3 H, OMe), 3.63 (s, 6 H, OMe), 3.69 (s, 3 H, OMe), 3.79 (s, 3 H, OMe), 3.10–3.90 (25 H, H-2, H-3, H-4, H-6a$^{C\text{ or }F\text{ or }G}$, H-6$^{F,G\text{ or }C,G\text{ or }C,F}$), 3.89–3.96 (2 H, H-6b$^{A,D\text{ or }B,E}$), 4.08 (d, 1 H, $^{2}J_{H\text{-}6b,H\text{-}6a}$ = 11.3 Hz, H-6b$^{C\text{ or }F\text{ or }G}$), 4.22 (m, 1 H, H-5$^{C\text{ or }F\text{ or }G}$), 4.36 (4 H, H-5^{A,B,D,E}), 4.48 (m, 1 H, H-5$^{F\text{ or }G\text{ or }C}$), 4.53 (m, 1 H, H-5$^{G\text{ or }F\text{ or }C}$), 4.83 (d, 1 H, $^{3}J_{H\text{-}1,H\text{-}2}$ = 2.9 Hz, H-1), 4.87 (d, 1 H, $^{3}J_{H\text{-}1,H\text{-}2}$ = 3.4 Hz, H-1), 5.04 (d, 2 H, $^{3}J_{H\text{-}1,H\text{-}2}$ = 3.8 Hz, H-1), 5.09 (d, 1 H, $^{3}J_{H\text{-}1,H\text{-}2}$ = 3.1 Hz, H-1), 5.27 (d, 1 H, $^{3}J_{H\text{-}1,H\text{-}2}$ = 2.3 Hz, H-1), 5.44 (d, 1 H, $^{3}J_{H\text{-}1,H\text{-}2}$ = 4.5 Hz, H-1), 7.31–7.37 (6 H, *m*-H, *p*-H), 7.92 (2 H, *o*-H), 8.02 (2 H, *o*-H) ppm; ^{13}C{^{1}H} NMR (75.5 MHz, $CDCl_3$, 25 ºC): δ = –2.37 (br s, Me), 27.01 (br s,

C-6$^{A,D\text{ or }B,E}$), 32.27 (br s, C-6$^{B,E\text{ or }A,D}$), 56.63, 57.70, 57.79, 57.95, 58.85 [×5], 59.56, 60.38, 60.41, 60.95, 61.16, 61.21, 61.65, 61.74 (OMe), 64.15, 64.34, 68.71, 69.35 (C-5^{A,B,D,E}), 70.14, 70.23, 70.70 (C-5^{C,F,G}), 71.01, 71.29, 72.35 (C-6^{C,F,G}), 77.20, 77.94, 79.72 [×2], 80.66, 80.93, 81.13 [×2], 81.44 [×3], 82.15. 82.42, 83.01 [×2], 83.62, 84.32 (C-2, C-3, C-4^{C,F,G}), 84.90 [×2], 89.32 [×2] (C-4^{A,B,D,E}), 94.65 [×2], 96.91, 97.95, 98.56 [×2], 99.14 (C-1), 127.77 [×2] (s with triplet shape, *m*-C), 128.51 [×2] (virtual t, $|^3J_{C,P} + {}^5J_{C,P'}| = 8.6$ Hz, *m*-C), 129.72, 129.84 (*p*-C), 133.03 (virtual t, $|^2J_{C,P} + {}^4J_{C,P'}| = 13.2$ Hz, *o*-C), 133.71 (s with triplet shape, *o*-C), 136.58 [×2] (virtual t, $|^1J_{C,P} + {}^3J_{C,P'}| = 40.0$ Hz, *ipso*-C) ppm; $^{31}P\{^1H\}$ NMR (121.5 MHz, $CDCl_3$, 25ºC): $\delta = 15$ (br s) ppm; $^{31}P\ \{^1H\}$ NMR (202.5 MHz, CD_2Cl_2, –80ºC): $\delta = 22.6$ and 13.9 (2 d, AB system, $^2J_{P1,P2} = 454$ Hz), 19.4 and 5.1 (2 d, AB system, $^2J_{P1,P2} = 442$ Hz) ppm; elemental analysis (%) calcd for $C_{72}H_{113}ClO_{31}P_2Pd{\cdot}0.5CH_2Cl_2$ (1678.47 + 42.47): C 49.72, H 6.57, found: C 49.82, H 6.51; MS (ESI-TOF): *m/z* (%): 1699.54 (3) $[M + Na]^+$, 1673.47 (100) $[M + MeOH - Cl]^+$, 1641.58 (38) $[M - Cl]^+$.

***trans-P,P'*-Chlorido-carbonyl-{6^A,6^B,6^D,6^E-tetradeoxy-6^A,6^B:6^D,6^E-bis[(*R*)-phenylphosphinidene]-2^A,2^B,2^C,2^D,2^E,2^F,2^G,3^A,3^B,3^C,3^D,3^E,3^F,3^G,6^C,6^F,6^G-heptadeca-*O*-methyl-β-cyclodextrin}rhodium(I) (32)**

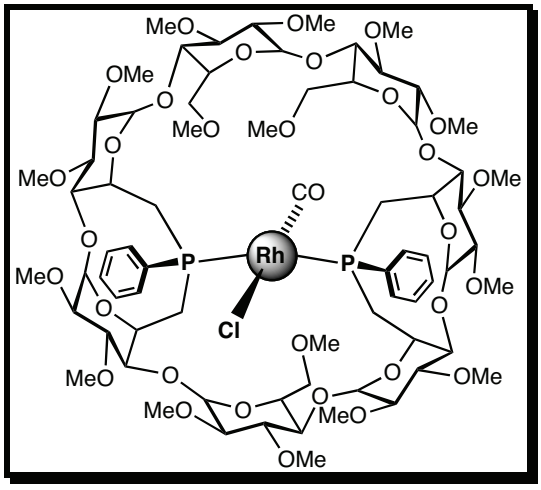

A solution of $[RhCl(CO)_2]_2$ (0.010 g, 0.026 mmol) in CH_2Cl_2 (5 mL) was added dropwise to a solution of **WIDEPHOS** (0.080 g, 0.053 mmol) in CH_2Cl_2 (10 mL) within 30 min at room temperature. After stirring for 30 min, the reaction mixture was evaporated to dryness affording analytically pure **32** (yield: 0.089 g, 99%) as an orange-yellow solid. R_f (SiO_2, CH_2Cl_2/MeOH, 92:8, *v*/*v*) = 0.40; m.p. dec. >250ºC; IR (KBr) *v*/cm^{-1}: 1970; ^1H NMR

(300.1 MHz, $CDCl_3$, 25ºC): δ (assignment by COSY) = 2.25–2.38 (2 H, H-6a$^{A,D\text{ or }B,E}$), 2.55–2.65 (2 H, H-6a$^{B,E\text{ or }A,D}$), 2.78 (d, 1 H, $^3J_{H\text{-}2,H\text{-}3}$ = 9.0 Hz, H-2), 3.05–4.05 (32 H, H-2, H-3, H-4, H-5$^{C,F\text{ or }C,G\text{ or }F,G}$, H-6^{C,F,G}, H-6b^{A,B,D,E}), 3.27 (s, 3 H, OMe), 3.30 (s, 3 H, OMe), 3.33 (s, 3 H, OMe), 3.38 (s, 3 H, OMe), 3.46 (s, 3 H, OMe) 3.48 (s, 3 H, OMe), 3.50 (s, 3 H, OMe), 3.53 (s, 3 H, OMe), 3.57 (s, 3 H, OMe), 3.59 (s, 6 H, OMe), 3.60 (s, 3 H, OMe), 3.62 (s, 3 H, OMe), 3.64 (s, 6 H, OMe), 3.71 (s, 3 H, OMe), 3.81 (s, 3 H, OMe), 4.20 (d, 1 H, $^3J_{H\text{-}5,H\text{-}6a}$ = 9.4 Hz, H-5$^{G\text{ or }F\text{ or }C}$), 4.38–4.53 (4 H, H-5^{A,B,D,E}), 4.83 (d, 1 H, $^3J_{H\text{-}1,H\text{-}2}$ = 3.4 Hz, H-1), 4.91 (d, 1 H, $^3J_{H\text{-}1,H\text{-}2}$ = 3.1 Hz, H-1), 5.06 (d, 1 H, $^3J_{H\text{-}1,H\text{-}2}$ = 4.1 Hz, H-1), 5.07 (d,1 H, $^3J_{H\text{-}1,H\text{-}2}$ = 4.5 Hz, H-1), 5.11 (d, 1 H, $^3J_{H\text{-}1,H\text{-}2}$ = 2.9 Hz, H-1), 5.31 (d, 1 H, $^3J_{H\text{-}1,H\text{-}2}$ = 4.1 Hz, H-1), 5.48 (d, 1 H, $^3J_{H\text{-}1,H\text{-}2}$ = 4.5 Hz, H-1), 7.35–7.39 (6 H, *m*-H, *p*-H), 7.99–8.07 (4 H, *o*-H) ppm; $^{13}C\{^1H\}$ NMR (75.5 MHz, $CDCl_3$, 25ºC): δ (assignment by HMQC) = 28.40 [×2] (virtual t, $|^1J_{C,P} + {}^3J_{C,P'}|$ = 9.9 Hz, C-6$^{A,D\text{ or }B,E}$), 30.19 [×2] (virtual t, $|^1J_{C,P} + {}^3J_{C,P'}|$ = 11.4 Hz, C-6$^{B,E\text{ or }A,D}$), 56.75, 57.89 [×2], 58.10, 58.72, 58.82, 58.92, 50.00, 59.44, 60.31, 60.57, 60.93 [×2], 61.06, 61.18, 61.69, 61.72 (OMe), 64.10, 64.79 (C-5$^{A,D\text{ or }B,E}$), 68.60, 69.63 (C-5$^{B,E\text{ or }A,D}$), 69.92, 70.41, 70.90 (C-5^{C,F,G}), 71.08, 71.69, 72.30 (C-6^{C,F,G}), 77.21 [×2], 77.64 (C-4^{C,F,G}), 79.57, 79.82, 80.34, 80.97, 81.24, 81.36 [×3], 82.38, 82.53, 83.08 [×2], 83.50, 84.42, (C-2, C-3), 84.95 [×2] (C-4$^{A,D\text{ or }B,E}$), 89.51 [×2] (C-4$^{B,E\text{ or }A,D}$), 94.36, 94.57, 97.01, 98.02, 98.34, 98.47, 99.08 (C-1), 127.68 (virtual t, $|^3J_{C,P} + {}^5J_{C,P'}|$ = 4.5 Hz, *m*-C), 128.39 (virtual t, $|^3J_{C,P} + {}^5J_{C,P'}|$ = 4.5 Hz, *m*-C), 129.72, 129.82 (*p*-C), 133.21 (virtual t, $|^2J_{C,P} + {}^4J_{C,P'}|$ = 6.3 Hz, *o*-C), 133.58 (virtual t, $|^2J_{C,P} + {}^4J_{C,P'}|$ = 5.8 Hz, *o*-C), 137.97 [×2] (virtual t, $|^1J_{C,P} + {}^3J_{C,P'}|$ = 22.5 Hz, *ipso*-C) ppm; $^{31}P\{^1H\}$ NMR (121.5 MHz, $CDCl_3$, 25ºC): δ = 18.7 (br d, $^1J_{P,Rh} \approx$ 120 Hz) ppm; $^{31}P\ \{^1H\}$ NMR (162.0 MHz, CD_2Cl_2, –80ºC) = 28.0 and 9.4 (2 dd, ABX system, $^2J_{P1,P2}$ = 354 Hz, $^1J_{P,Rh}$ = 118 and 118), 16.4 and 9.4 (2 dd, ABX system, $^2J_{P1,P2}$ = 354 Hz, $^1J_{P,Rh}$ = 118 and 118) ppm; elemental analysis (%) calcd for $C_{72}H_{110}ClO_{32}P_2Rh$ (1687.93): C 51.23, H 6.57, found: C 51.15, H 6.44; MS (ESI-TOF): *m/z* (%): 1725.48 (23) $[M + K]^+$, 1709.51 (58) $[M + Na]^+$, 1652.51 (16) $[M - Cl]^+$.

Platinum(II)-gold(I) complexes 33a and 33b

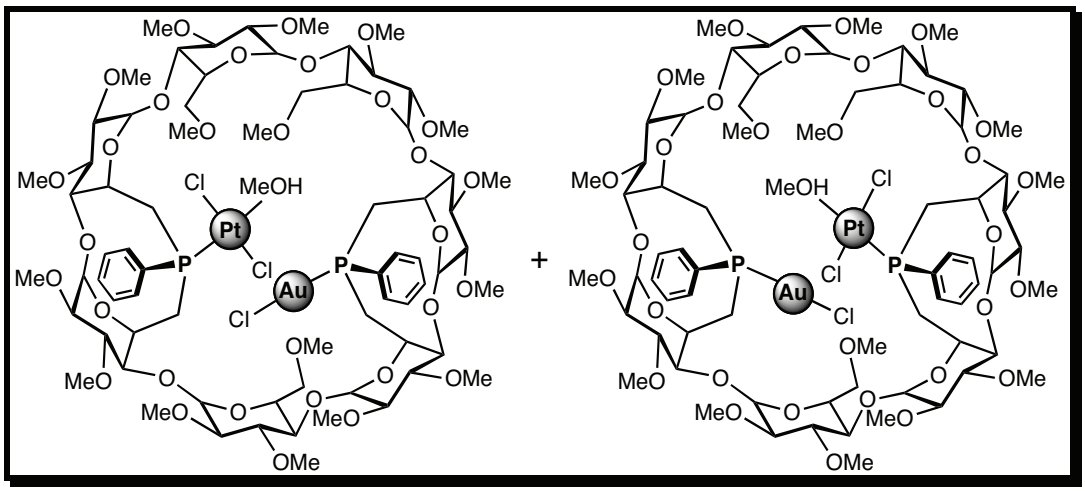

A solution of [AuCl(tht)] (0.011 g, 0.035 mmol) in CH_2Cl_2 (5 mL) was added to a solution of complex **29** (0.054 g, 0.030 mmol) in MeOH (10 mL). After 12 h at room temperature, the solution was filtered through a bed of celite. The solvent was then removed *in vacuo* affording a brown powder (yield: 0.061 g, 99%) containing both regioisomers **33a** and **33b**. m.p. dec. >250ºC; $^{31}P\{^{1}H\}$ NMR (121.5 MHz, $CDCl_3$, 25ºC): δ = 0.0 (s with Pt satellites, $^{1}J_{Pt,P}$ = 3239 Hz), –4.2 (s with Pt satellites, $^{1}J_{Pt,P}$ = 3454 Hz), 34.0 (s, 2 P); MS (ESI-TOF): *m/z* (%): 2071.56 (100) $[M + Na]^{+}$.

Synthesis of complexes 34 and 35:

Air was bubbled through a solution of complex **30** (0.080 g, 0.047 mmol) in undistilled MeOH for 30 min. After refluxing the solution for 12 h, the solvent was removed *in vacuo*

and the crude product was purified by column chromatography (SiO_2, CH_2Cl_2/MeOH, 97:3, *v*/*v*).

Palladium(II) complex 34

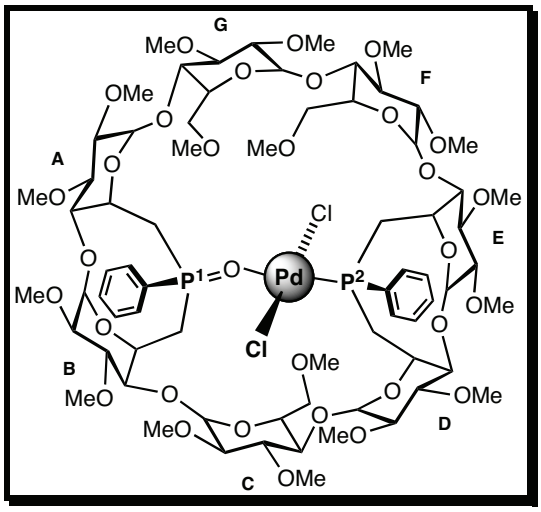

Complex **34** (yield: 0.034 g, 43%) eluted first. R_f (SiO_2, CH_2Cl_2/MeOH, 92:8, *v*/*v*) = 0.40; m.p. dec. >250ºC; ^{1}H NMR (600.1 MHz, $CDCl_3$, 25ºC): δ (assignment by COSY, ROESY, ^{1}H-^{13}C{^{1}H} HMQC and ^{1}H-^{31}P{^{1}H} HMQC) = 2.09 (m, 1 H, H-6a^E), 2.17 (m, 1 H, H-6a^A), 2.38 (m, 1 H, H-6a^B), 2.52 (ddd, 1 H, $^2J_{H\text{-}6a,H\text{-}6b}$ = 15.2 Hz, $^2J_{H\text{-}6a,P}$ = 14.0 Hz, $^2J_{H\text{-}6a,H\text{-}5}$ = 6.0 Hz, H-6a^D), 2.75 (t, 1 H, $^2J_{H\text{-}6b,H\text{-}6a}$ = $^2J_{H\text{-}6b,P}$ = 15.2 Hz, H-6b^D), 2.80 (dd, 1 H, $^2J_{H\text{-}6b,H\text{-}6ba}$ = 16.4 Hz, $^3J_{H\text{-}6b,H\text{-}5}$ = 7.3 Hz, H-6b^A), 3.01–3.82 (25 H, H-2, H-3, H-4, H-6a^{C,F,G}, H-6b^B), 3.24 (s, 3 H, OMe), 3.31 (s, 3 H, OMe), 3,32 (s, 3 H, OMe), 3.46 (s, 3 H, OMe), 3.47 (s, 3 H, OMe), 3.48 (s, 3 H, OMe), 3.49 (s, 6 H, OMe), 3.59 (s, 6 H, OMe), 3.60 (s, 3 H, OMe), 3.62 (s, 6 H, OMe), 3.64 (s, 3 H, OMe), 3.65 (s, 3 H, OMe), 3.74 (s, 3 H, OMe), 3.85 (s, 3 H, OMe), 3.95 (dd, 1 H, $^2J_{H\text{-}6b,H\text{-}6a}$ = 11.5 Hz, $^3J_{H\text{-}6b,H\text{-}5}$ = 1.5 Hz, H-6b^C), 4.05 (d, 1 H, $^2J_{H\text{-}6b,H\text{-}6a}$ = 11.7 Hz, $^3J_{H\text{-}6b,H\text{-}5}$ = 1.9 Hz, H-6b^G), 4.11 (m, 1 H, H-5), 4.12 (d, 1 H, $^2J_{H\text{-}6b,H\text{-}6a}$ = 9.8 Hz, H-6b^E), 4.15 (dd, 1 H, $^2J_{H\text{-}6b,H\text{-}6a}$ = 10.9 Hz, $^3J_{H\text{-}6b,H\text{-}5}$ = 2.4 Hz, H-6b^F), 4.29 (m, 1 H, H-5^E), 4.34 (m, 1 H, H-5^F), 4.41–4.42 (2 H, H-5$^{G\text{ and }D}$), 4.58–4.60 (2 H, H-5$^{A\text{ and }B}$), 4.84 (d, 1 H, $^3J_{H\text{-}1,H\text{-}2}$ = 3.3 Hz, H-1^D), 4.97 (d, 1 H, $^3J_{H\text{-}1,H\text{-}2}$ = 4.3 Hz, H-1^E), 4.99 (d, 1 H, $^3J_{H\text{-}1,H\text{-}2}$ = 4.3 Hz, H-1^B), 5.06 (d, 1 H, $^3J_{H\text{-}1,H\text{-}2}$ = 3.8 Hz, H-1^G), 5.07 (d, 1 H, $^3J_{H\text{-}1,H\text{-}2}$ = 4.5 Hz, H-1^A), 5.22 (d, 1 H, $^3J_{H\text{-}1,H\text{-}2}$ = 4.2 Hz, H-1^F), 5.26 (d, 1 H, $^3J_{H\text{-}1,H\text{-}2}$ = 4.3 Hz, H-1^C), 7.42–7.45 (td, 2 H, $^3J_{m\text{-}H,o\text{-}H}$ = $^3J_{m\text{-}H,p\text{-}H}$ = 7.9 Hz, $^4J_{m\text{-}H,P}$ = 2.0 Hz, *m*-H of PhPPd), 7.47 (m, 1 H, *p*-H of PhPPd), 7.58 (td, 2 H, $^3J_{m\text{-}H,o\text{-}H}$ = $^3J_{m\text{-}H,p\text{-}H}$ = 7.6 Hz, $^4J_{m\text{-}H,P}$ = 2.6 Hz, *m*-H of PhP(O)), 7.62 (m, 1 H, *p*-H of PhP(O)), 8.05–8.10 (4 H, *o*-H) ppm; ^{13}C{^{1}H} NMR (150.9 MHz, $CDCl_3$, 25ºC):

δ (assignment by HMQC) = 31.77 (d, $^{1}J_{C,P}$ = 26.8 Hz, C-6^{E}), 32.12 (d, $^{1}J_{C,P}$ = 59.4 Hz, C-6^{B}), 37.61 (d, $^{1}J_{C,P}$ = 31.9 Hz, C-6^{D}), 42.14 (d, $^{1}J_{C,P}$ = 72.4 Hz, C-6^{A}), 59.84, 56.96, 57.84, 58.10, 58.79, 58.85 [×2], 58.92, 60.29, 60.39, 60.61, 60.93, 61.70, 61.73 [×2], 61.94 [×2] (OMe), 61.98 (C-5^{B}), 63.21 (d, $^{2}J_{C,P}$ = 4.0 Hz, C-5^{E}), 66.06 (C-5^{A}), 68.27 (d, $^{2}J_{C,P}$ = 3.5 Hz, C-5^{D}), 70.42 [×2], 70.09 (C-5^{C,F,G}), 71.20, 71.57, 72.22 (C-6^{C,F,G}), 77.29, 80.27, 80.36, 80.47, 80.54, 81.00, 81.14, 81.17, 81.68, 81.75, 81.84, 81.90, 82.06, 82.08, 82.43, 82.82, 82.93, 83.45, 83.81, 84.26 (C-2, C-3, C-4$^{A \text{ or } D \text{ and } B,C,E,F,G}$), 89.31 (d, $^{3}J_{C,P}$ = 12.8 Hz, C-4$^{D \text{ or } A}$), 94.20 (C-1^{D}), 97.42 (C-1^{E}), 98.11 (C-1^{B}), 98.90 (C-1$^{A \text{ or } G}$), 99.49 (C-1$^{G \text{ or } A}$), 99.64 (C-1^{C}), 99.78 (C-1^{F}), 128.66 (d, $^{3}J_{C,P}$ = 5.9 Hz, *m*-C of PhPPd), 128.73 (d, $^{3}J_{C,P}$ = 6.2 Hz, *m*-C of PhP(O)), 130.11 (d, $^{2}J_{C,P}$ = 9.1 Hz, *o*-C of PhP), 131.03 (*p*-C of PhPPd), 132.13 (*p*-C of PhP(O)), 132.74 (d, $^{2}J_{C,P}$ = 9.1 Hz, *o*-C of PhP), 133.72 (d, $^{1}J_{C,P}$ = 6.7 Hz, *ipso*-C of PhP), 134.24 (d, $^{1}J_{C,P}$ = 6.7 Hz, *ipso*-C of PhP) ppm; $^{31}P\{^{1}H\}$ NMR (121.5 MHz $CDCl_3$, 25ºC): 33.8 (d, $^{2}J_{P1,P2}$ = 4.4 Hz, PPd), 54.5 (d, $^{2}J_{P1,P2}$ = 4.4 Hz, P(O)) ppm; elemental analysis (%) calcd for $C_{71}H_{110}Cl_2O_{32}P_2Pd$ (1714.89): C 49.73, H 6.47, found: C 49.60, H 6.55; MS (ESI-TOF): *m/z* (%): 1753.47 (30) $[M + K]^+$, 1737.49 (70) $[M + Na]^+$.

Palladium(II) complex 35

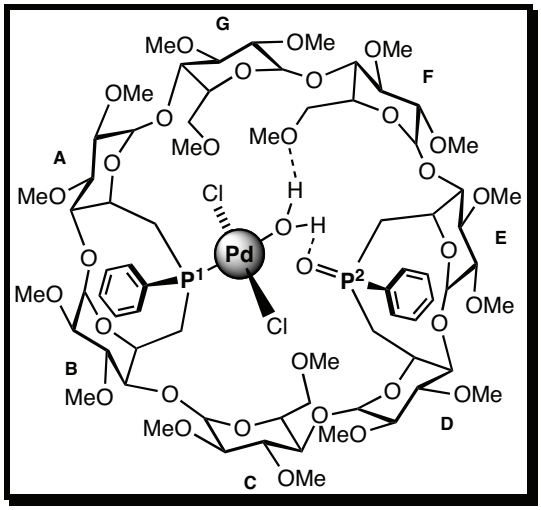

Complex **35** (yield: 0.036 g, 45%) was isolated as a pale yellow solid. R_f (SiO_2, CH_2Cl_2/MeOH, 92:8, *v*/*v*) = 0.35; m.p. dec. >250ºC; ^{1}H NMR (600.1 MHz, $CDCl_3$, 25ºC): δ (assignment by COSY; the symbols ¶, $, #, §, denotes a given bridged glucose unit A or B or D or E) = 1.85 (m, 1 H, H-6a¶), 1.91–1.96 (2 H, H-6a$^{\$}$, H-6a$^{\#}$), 2.80 (dd, 1 H, $^{1}J_{H\text{-}6a,P}$ = 18.6 Hz, $^{2}J_{H\text{-}6a,H\text{-}6b}$ = 15.8 Hz, H-6b$^{\#}$), 2.99–3.04 (2 H, H-6a§, H-6b§), 3.07–3.80 (31 H, H-2, H-3,

H-4, H-5¶, H-5$^{\$}$, H-6^{C,F,G}, H-6b¶, H-6b$^{\$}$), 3.15 (s, 6 H, OMe), 3.35 (s, 3 H, OMe), 3,46 (s, 3 H, OMe), 3.50 (s, 3 H, OMe), 3.51 (s, 3 H, OMe), 3.52 (s, 3 H, OMe), 3.53 (s, 3 H, OMe), 3.54 (s, 6 H, OMe), 3.59 (s, 3 H, OMe), 3.64 (s, 6 H, OMe), 3.67 (s, 3 H, OMe), 3.69 (s, 3 H, OMe), 3.74 (s, 3 H, OMe), 3.76 (s, 3 H, OMe), 3.96–4.02 (2 H, H-5$^{C,F\text{ or }C,G\text{ or }F,G}$), 4.25 (d, 1 H, $^{3}J_{H\text{-}5,H\text{-}6}$ = 10.4 Hz, H-5$^{G\text{ or }F\text{ or }C}$), 4.54 (m, 1 H, H-5$^{\#}$), 4.82 (m, 1 H, H-5§), 4.94 (d, 2 H, $^{3}J_{H\text{-}1,H\text{-}2}$ = 2.7 Hz, H-1), 4.99 (d, 1 H, $^{3}J_{H\text{-}1,H\text{-}2}$ = 3.9 Hz, H-1), 5.00 (d, 1 H, $^{3}J_{H\text{-}1,H\text{-}2}$ = 3.9 Hz, H-1), 5.03 (d, 1 H, $^{3}J_{H\text{-}1,H\text{-}2}$ = 3.9 Hz, H-1), 5.06 (m, 1 H, H-1), 5.09 (m, 1 H, H-1), 7.35 (td, 2 H, $^{3}J_{m\text{-}H,o\text{-}H} = {}^{3}J_{m\text{-}H,p\text{-}H}$ = 7.9 Hz, $^{4}J_{m\text{-}H,P}$ = 0.5 Hz, *m*-H of PhP(O)), 7.41 (t, 1 H, $^{3}J_{p\text{-}H,m\text{-}H}$ = 7.9 Hz, *p*-H of PhP(O)), 7.57–7.59 (3 H, *m*-H and *p*-H of PhPPd), 7.86 (dd, 2 H, $^{3}J_{o\text{-}H,P}$ = 11.8 Hz, $^{3}J_{o\text{-}H,m\text{-}H}$ = 7.9 Hz, *o*-H of PhP(O)), 8.22 (m, 2 H, *o*-H of PhPPd) ppm (the protons of the coordinated water molecule appear as a broad singlet at 6.1 ppm in the ^{1}H NMR spectrum recorded in CD_2Cl_2 at –80°C); $^{13}C\{^{1}H\}$ NMR (75.5 MHz, $CDCl_3$, 25ºC): δ (assignment by HMQC) = 57.31, 57.87, 58.07, 58.54, 58.78, 58.83, 58.91, 59.12, 59.32, 59.55, 61.26, 61.38, 61.72 [×2], 61.83 [×2], 62.09 (OMe), 62.98 (C-5$^{\#}$), 66.38 (C-5§), 70.46 [×2] (C-6$^{C,F\text{ or }C,G\text{ or }F,G}$), 70.66 [×2] (C-5$^{C,F\text{ or }C,G\text{ or }F,G}$), 71.50 (C-6$^{G\text{ or }F\text{ or }C}$), 71.68 (C-5$^{G\text{ or }F\text{ or }C}$), 73.45 [×2] (C-5¶, C-5$^{\$}$), 78.39 [×2], 80.79, 81.03 [×2], 81.13, 81.24, 81.71, 81.87, 81.96, 82.94 [×2], 83.04 [×2], 83.24, 83.58, 83.68 (C-2, C-3, C-4^{C,F,G}), 86.40, 86.93 (C-4¶, C-4$^{\$}$), 89.36 [×2] (C-4$^{\#}$, C-4§), 95.33, 97.94, 98.86, 100.61, 100.65, 100.90, 101.23 (C-1), 128.16 (d, $^{3}J_{C,P}$ = 11.7 Hz, *m*-C of PhP(O)), 128.87 (d, $^{3}J_{C,P}$ = 11.4 Hz, *m*-C of PhPPd), 130.25 (d, $^{2}J_{C,P}$ = 10.2 Hz, *o*-C of PhPPd), 130.74 (*p*-C of PhP(O)), 132.11 (d, $^{2}J_{C,P}$ = 9.7 Hz, *o*-C of PhP(O)), 132.48 (*p*-C of PhPPd) ppm (C-6^{A,B,D,E} and both *ipso*-C's could not be detected); $^{31}P\{^{1}H\}$ NMR (202.5 MHz CD_2Cl_2, –80ºC): 31.4 (s, PPd), 39.9 (s, P(O)) ppm; elemental analysis (%) calcd for $C_{71}H_{112}Cl_2O_{33}P_2Pd$ (1732.90): C 49.21, H 6.51, found: C 49.39, H 5.69; MS (ESI-TOF): *m/z* (%): 1737.52 (50) $[M + Li]^+$, 1735.48 (50) $[M - H_2O + Na]^+$.

III.4.3. X-ray crystallographic data for 27

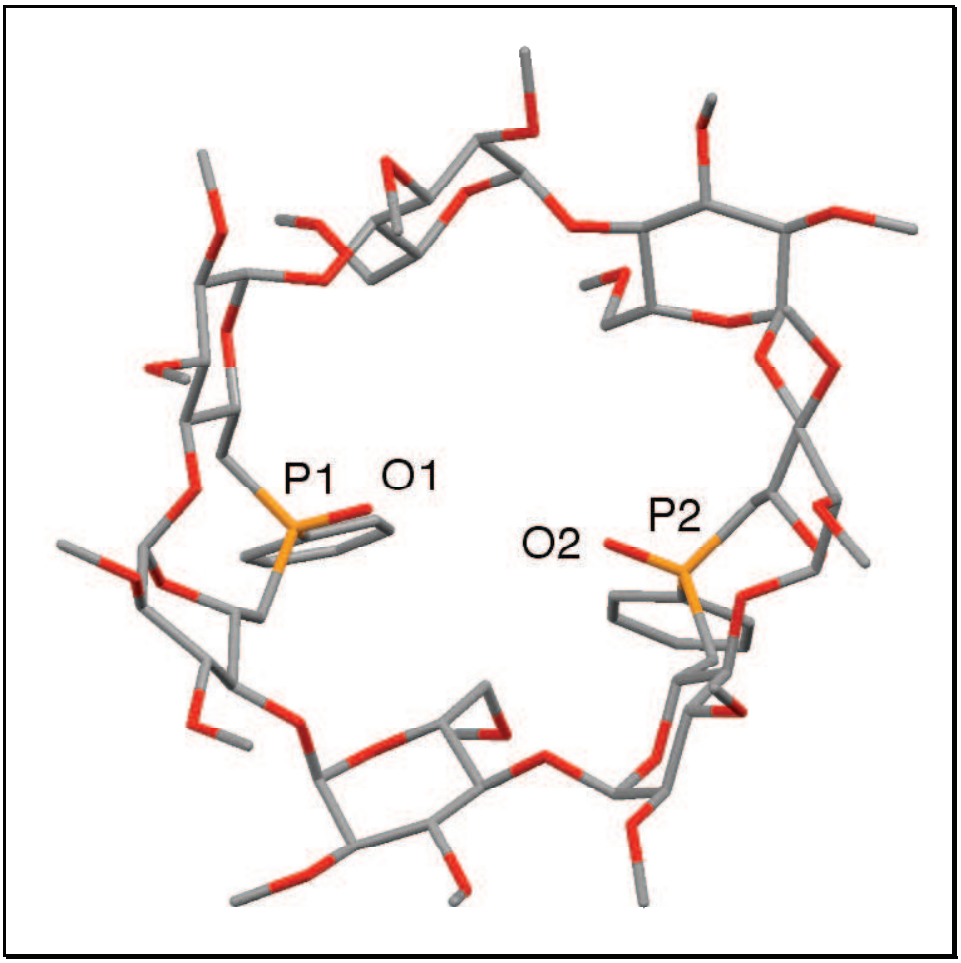

The X-ray structure determination was performed by Dr L. Toupet (University of Rennes, France). Single crystals were obtained by slow diffusion of pentane into a solution of **27** in dichloromethane. The sample was studied on a Oxford Diffraction Xcalibur Saphir 3 CCD with graphite monochromatised MoKα radiation (λ = 0.71073 Å). The structure was solved with SIR-97,[69] which revealed the non-hydrogen atoms of the molecule. After anisotropic refinement, many hydrogen atoms were found with a Fourier difference analysis. The whole structure was refined with SHELX-97[70] and full-matrix least-square techniques (use of F^2 magnitude; x, y, z, β_{ij} for C, O, P atoms, x, y, z, in riding mode for H atoms; 988 variables and 18635 observations with $I > 2.0\sigma(I)$; calcd $w = 1/[\sigma^2(F_o^2) + (0.0985\ P)^2]$ where $P = (F_o^2 + 2\ F_o^2)/3$ with the resulting R = 0.071, R_w = 0.190 and S_w = 0.791; $\Delta\rho < 0.646$ eÅ^{-3}. The absolute configuration (and thus the enantiomeric space group assignment) was determined by a *Flack* x parameter of 0.07 (13). A summary of the crystallographic data is

given in Table 1. CCDC reference number 756653. The alerts level A in the checkcif are mainly due to disordered MeO groups and solvent molecules.

Table 1. Crystal data and structure refinement for **27**·0.5(CH_2Cl_2)·0.5(C_5H_{12}).

Crystal Data	
Crystal size	0.32 × 0.22 × 0.14 mm^3
Empirical formula	$C_{74}H_{117}ClO_{33}P_2$
M_r	1632.07
Crystal system	Orthorombic
Space group	$P2_12_12_1$
Temperature	150(2) K
Unit cell parameters	
a	15.1479(3) Å
b	15.6542(3) Å
c	36.0599(9) Å
α	90º
β	90º
γ	90º
V	8550.8(3) $Å^3$
Z	4
D (calculated)	1.268 g/cm^3
F (000)	3488
□	0.163 mm^{-1}
Data Processing and Reduction	
θ range for data collection	2.52 to 27.00º
Index ranges	-19 ≤ h ≤ 19, -19≤ k ≤ 19, -46≤ l ≤ 46
Reflections collected	110163
Independent reflections	18635 [R(int) = 0.1159]
Refinement method	Full-matrix least-squares on F^2
Data / restraints / parameters	18635 / 4 / 988
Goodness-on-fir on F^2	0.791
Final R indices [I > 2σ(I)]	R1 = 0.0708, *w*R2 = 0.1636
R indices (all data)	R1 = 0.1777, *w*R2 = 0.1904
Largest diff. peak and hole	0.646 and -0.316 $eÅ^{-3}$

III.4.4. X-ray crystallographic data for 35

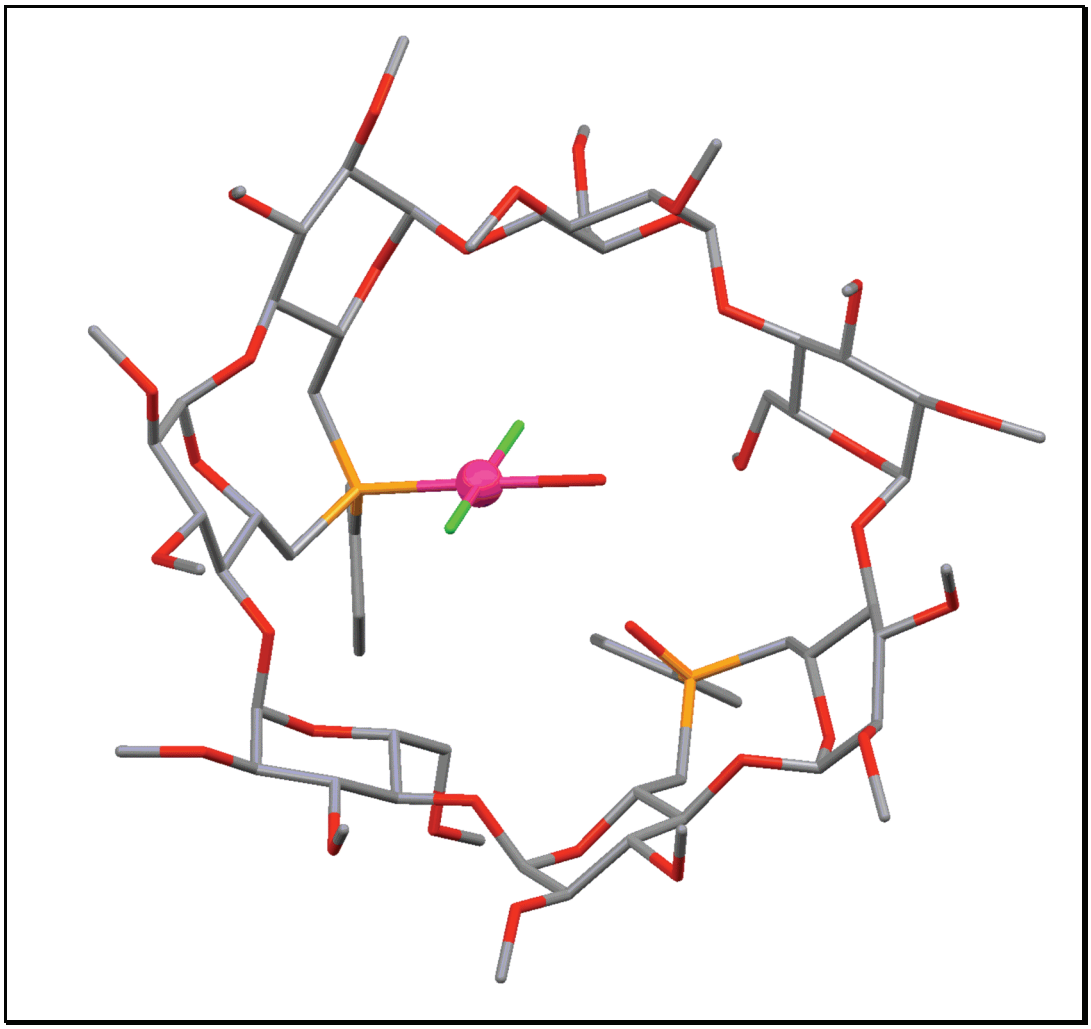

The X-ray structure determination was performed by Dr L. Toupet (University of Rennes, France). Single crystals were obtained by slow diffusion of pentane into a solution of **35** in dichloromethane. The sample was studied on a Oxford Diffraction Xcalibur Saphir 3 CCD with graphite monochromatised MoKα radiation (λ = 0.71073 Å). The structure was solved with SIR-97,[69] which revealed the non-hydrogen atoms of the molecule. After anisotropic refinement, many hydrogen atoms were found with a Fourier difference analysis. The whole structure was refined with SHELX-97[70] and full-matrix least-square techniques (use of F^2 magnitude; x, y, z, β_{ij} for Pd, Cl, C, O, P atoms, x, y, z, in riding mode for H atoms; 1002 variables and 20360 observations with $I > 2.0\sigma(I)$; calcd $w = 1/[\sigma^2(F_o^2) + (0.0600\ P)^2]$ where $P = (F_o^2 + 2\ F_o^2)/3$ with the resulting R = 0.055, R_w = 0.131 and S_w = 0.769; $\Delta\rho < 1.608$ eÅ^{-3}. The absolute configuration (and thus the enantiomeric space group assignment) was

determined by a *Flack* x parameter of 0.04 (2). A summary of the crystallographic data is given in Table 2. CCDC reference number 770728.

Table 2. Crystal data and structure refinement for **35**·(C_5H_{12}).

Crystal Data	
Crystal size	0.25 × 0.12 × 0.12 mm^3
Empirical formula	$C_{76}H_{124}Cl_2O_{33}P_2Pd$
M_r	1804.99
Crystal system	Orthorombic
Space group	$P2_12_12_1$
Temperature	100(2) K
Unit cell parameters	
a	17.6384(7) Å
b	19.4659(5) Å
c	27.2535(8) Å
α	90º
β	90º
γ	90º
V	9357.4(5) $Å^3$
Z	4
D (calculated)	1.281 g/cm^3
F (000)	3816
μ	0.366 mm^{-1}
Data Processing and Reduction	
θ range for data collection	2.50 to 27.00º
Index ranges	$-22 \leq h \leq 22$, $-24 \leq k \leq 24$, $-34 \leq l \leq 34$
Reflections collected	195217
Independent reflections	20360 [R(int) = 0.1656]
Refinement method	Full-matrix least-squares on F^2
Data / restraints / parameters	20360 / 2 / 1002
Goodness-on-fir on F^2	0.769
Final R indices [$I > 2\sigma(I)$]	R1 = 0.0549, *w*R2 = 0.1150
R indices (all data)	R1 = 0.1392, *w*R2 = 0.1312
Largest diff. peak and hole	1.608 and -0.460 $eÅ^{-3}$

III.5. References

[1] A.-M. Caminade, J.-P. Majoral, R. Mathieu, *Chem. Rev.* **1991**, *91*, 575-162.

[2] C. Bianchini, A. Meli, M. Peruzzini, F. Vizza, F. Zanobini, *Coord. Chem. Rev.* **1992**, *120*, 193-208.

[3] F. A. Cotton, B. Hong, *Prog. Inorg. Chem.* **1992**, *40*, 179-289.

[4] J.-C. Hierso, R. Amardeil, E. Bentabet, R. Broussier, B. Gautheron, P. Meunier, P. Kalck, *Coord. Chem. Rev.* **2003**, *236*, 143-206.

[5] M. E. Broussard, B. Juma, S. G. Train, W.-J. Peng, S. A. Laneman, G. G. Stanley, *Science* **1993**, *260*, 1784-1788.

[6] W.-J. Peng, S. G. Train, D. K. Howell, F. R. Fronczek, G. G. Stanley, *Chem. Commun.* **1996**, 2607-2612.

[7] H. Jiang, Y. Xu, S. Liao, D. Yu, H. Chen, X. Li, *J. Mol. Catal. A: Chem.* **1999**, *142*, 147-152.

[8] D. Laurenti, M. Feuerstein, G. Pèpe, H. Doucet, M. Santelli, *J. Org. Chem.* **2001**, *66*, 1633-1637.

[9] C. Wieser, C. B. Dieleman, D. Matt, *Coord. Chem. Rev.* **1997**, *165*, 93-161.

[10] S. D. Alexandratos, S. Natesan, *Ind. Eng. Chem. Res.* **2000**, *39*, 3998-4010.

[11] D. M. Homden, C. Redshaw, *Chem. Rev.* **2008**, *108*, 5086-5130.

[12] R. J. Puddephatt, *Can. J. Chem.* **2006**, *84*, 1505-1514.

[13] E. Engeldinger, D. Armspach, D. Matt, *Chem. Rev.* **2003**, *103*, 4147-4173.

[14] S. S. Braga, *Curr. Org. Chem.* **2010**, *14*, 1356-1361.

[15] D. Armspach, D. Matt, *C. R. Chimie* **2011**, *14*, 135-148.

[16] C. Jeunesse, D. Armspach, D. Matt, *Chem. Commun.* **2005**, *45*, 5603-5614.

[17] H. El Moll, D. Semeril, D. Matt, L. Toupet, *Eur. J. Org. Chem.* **2010**, *6*, 1158-1168.

[18] D. Sémeril, C. Jeunesse, D. Matt, L. Toupet, *Angew. Chem. Int. Ed.* **2006**, *45*, 5810-5814.

[19] D. Semeril, D. Matt, L. Toupet, *Chem. Eur. J.* **2008**, *14*, 7144-7155.

[20] L. Monnereau, D. Semeril, D. Matt, L. Toupet, A. J. Mota, *Adv. Synth. Cat.* **2009**, *351*, 1383-1389.

[21] M. Sawamura, K. Kitayama, Y. Ito, *Tetrahedron: Assymetry* **1993**, *4*, 1829-1832.

[22] M. T. Reetz, J. Rudolph, *Tetrahedron: Assymetry* **1993**, *4*, 2405-2406.

[23] M. T. Reetz, S. R. Waldvogel, *Angew. Chem. Int. Ed.* **1997**, *36*, 865-867.

[24] M. T. Reetz, *Catal. Today* **1998**, *42*, 399.

[25] M. T. Reetz, C. Frömbgen, *Synthesis* **1999**, 1555.

[26] R. M. Deshpande, A. Fukuoka, M. Ichikawa, *Chem. Lett.* **1999**, *28*, 13-14.

[27] M. T. Reetz, J. Rudolph, R. Goddard, *Can. J. Chem.* **2001**, *79*, 1806-1811.

[28] C. Yang, Y. T. Wong, Z. Li, J. J. Krepinsky, G. Jia, *Organometallics* **2001**, *20*, 5220-5224.

[29] C. Yang, Y. K. Cheung, J. Yao, Y. T. Wong, G. Jia, *Organometallics* **2001**, *20*, 424-429.

[30] M. T. Reetz, I. D. Kostas, S. R. Waldvogel, *Inorg. Chem. Commun.* **2002**, *5*, 252-254.

[31] C. Machut-Binkowski, F.-X. Legrand, N. Azaroual, S. Tilloy, E. Monflier, *Chem. Eur. J.* **2010**, *16*, 10195-10201.

[32] F.-X. Legrand, N. Six, C. Slomianny, H. Bricout, S. Tilloy, E. Monflier, *Adv. Synth. Cat.* **2011**, *353*, 1325-1334.

[33] D. Armspach, D. Matt, *Chem. Commun.* **1999**, 1073-1074.

[34] E. Engeldinger, D. Armspach, D. Matt, *Angew. Chem. Int. Ed.* **2001**, *40*, 2526-2529.

[35] E. Engeldinger, D. Armspach, D. Matt, L. Toupet, M. Wesolek, *C. R. Chimie* **2002**, *5*, 359-372.

[36] L. Poorters, D. Armspach, D. Matt, *Eur. J. Org. Chem.* **2003**, 1377-1381.

[37] L. Poorters, D. Armspach, D. Matt, L. Toupet, *Dalton Trans.* **2007**, 3195-3202.

[38] Y. T. Wong, C. Yang, K.-C. Ying, G. Jia, *Organometallics* **2002**, *21*, 1782-1787.

[39] S. Guieu, E. Zaborova, Y. Blériot, G. Poli, A. Jutand, D. Madec, G. Prestat, M. Sollogoub, *Angew. Chem. Int. Ed.* **2010**, *49*, 2314-2318.

[40] E. Zaborova, J. Deschamp, S. Guiei, Y. Blériot, G. Poli, M. Ménand, D. Madec, G. Prestat, M. Sollogoub, *Chem. Commun.* **2011**, *47*, 9206-9208.

[41] E. Engeldinger, D. Armspach, D. Matt, P. G. Jones, R. Welter, *Angew. Chem. Int. Ed.* **2002**, *41*, 2593-2596.

[42] E. Engeldinger, D. Armspach, D. Matt, P. G. Jones, *Chem. Eur. J.* **2003**, *9*, 3091-3105.

[43] L. Poorters, D. Armspach, D. Matt, L. Toupet, S. Choua, P. Turek, *Chem. Eur. J.* **2007**, *13*, 9448-9461.

[44] E. Engeldinger, L. Poorters, D. Armspach, D. Matt, L. Toupet, *Chem. Commun.* **2004**, 634-635.

[45] N. J. DeStefano, D. K. Johnson, L. M. Venanzi, *Angew. Chem. Int. Ed.* **1974**, *13*, 133-134.

[46] N. J. DeStefano, D. K. Johnson, R. M. Lane, L. M. Venanzi, *Helv. Chim. Acta* **1976**, *59*, 2674-2682.

[47] F. Bachechi, L. Zambonelli, L. M. Venanzi, *Helv. Chim. Acta* **1977**, *60*, 2815-2823.

[48] G. Bracher, D. M. Grove, L. M. Venanzi, F. Bachechi, P. Mura, L. Zambonelli, *Helv. Chim. Acta* **1980**, *63*, 2519-2530.

[49] P. C. J. Kamer, M. Kranenburg, P. W. N. M. van Leeuwen, *Book of Abstracts, XVIth International Conference Organometallic Chemistry,* University of Sussex, 10-15 July **1994**, The Royal Society of Chemistry - Dalton Division, abstract no. OC18.

[50] S. Hillebrand, J. Bruckmann, C. Krüger, M. W. Haenel, *Tetrahedron Lett.* **1995**, *36*, 75-78.

[51] J. Yin, S. L. Buchwald, *J. Am. Chem. Soc,* **2002**, *124*, 6043-6048.

[52] L. A. van der Veen, P. H. Keeven, G. C. Schoemaker, J. N. H. Reek, P. C. J. Kamer, P. W. N. M. van Leeuwen, M. Lutz, A. L. Spek, *Organometallics* **2000**, *19*, 872-883.

[53] Z. Freixa, M. S. Beentjes, G. D. Batema, C. B. Dieleman, G. P. F. van Strijdonck, J. N. H. Reek, P. C. J. Kamer, J. Fraanje, K. Goubitz, P. W. N. M. van Leeuwen, *Angew. Chem. Int. Ed.* **2003**, *42*, 1284-1287.

[54] C. Jiménez-Rodríguez, F. X. Roca, C. Bo, J. Benet-Buchholz, E. Escudero-Adán, Z. Freixa, P. W. N. M. van Leeuwen, *Dalton Trans.* **2006**, 268-278.

[55] CPK stands for Corey-Pauling-Koltun.

[56] P. Braunstein, D. Matt, F. Mathey, D. Thavard, *J. Chem. Res. Synop.* **1978**, 232-233.

[57] J. C. Jeffrey, T. B. Rauchfuss, *Inorg. Chem.* **1979**, *18*, 2658-2666.

[58] A. Bader, E. Lindner, *Coord. Chem. Rev.* **1991**, *108*, 27-110.

[59] T. Hara, T. Yamagata, K. Mashima, *Organometallics* **2007**, *26*, 110-118.

[60] G. Parkin, *Acc. Chem. Res.* **1992**, *25*, 455-460.

[61] P. Comba, A. Hauser, M. Kerscher, H. Pritzkow, *Angew. Chem. Int. Ed.* **2003**, *42*, 4536-4540.

[62] P. Espinet, J. M. Martínez-Ilarduya, C. Pérez-Briso, A. L. Casado, M. A. Alonso, *J. Organomet. Chem.* **1998**, *551*, 9-20.

[63] J. Vicente, A. Arcas, M.-A. Blasco, J. Lozano, M. C. Ramírez de Arellano, *Organometallics* **1998**, *17*, 5374-5383.

[64] C. Bartolomé, P. Espinet, L. Vicente, F. Villafañe, *Organometallics* **2002**, *21*, 3536-3543.

[65] J. Vicente, A. Arcas, *Coord. Chem. Rev.* **2005**, *249*, 1135-1154.

[66] R. Uson, A. Laguna, M. Laguna, *Inorganic Synthesis* **1989**, *26*, 85-91.

[67] F. R. Hartley, *The Chemistry of Platinum and Palladium;* Wiley, New York **1973**.

[68] R. E. Rülke, J. M. Ernsting, A. L. Spek, C. J. Elsevier, P. W. N. M. van Leeuwen, K. Vrieze, *Inorg. Chem.* **1993**, *32*, 5769-5778.

[69] A. Altomare, M. C. Burla, M. Camalli, G. Cascarano, C. Giacovazzo, A. Guagliardi, G. Moliterni, G. Polidori, R. Spagna, *J. Appl. Crystallogr.* **1998**, *31*, 74-77.

[70] G. M. Sheldrick, SHELXL-97, *Program for Crystal Structure Refinement,* University of Göttingen, Göttingen (Germany), **1997**.

Chapter IV

Intra-cavity confinement of two metal centres in a cyclodextrin

Chapter IV

Intra-cavity confinement of two metal centres in a cyclodextrin

SUMMARY – CHAPTER IV

In stark contrast with its smaller analogue **TRANSDIP**, the highly preorganized cavitand **WIDEPHOS** was shown to have a cavity large enough for accommodating *two* metal fragments. The two metal centres can either be unconnected as in the gold complexes **36-38** and the palladium complex **42**, or bridged by a single μ-chlorido bridge as in the fluxional complexes **43** and **44**. In the first type of compound, steric hindrance about the two metal centres leads either to a distorted CD macrocycle or to non-optimal orbital overlap within the metal–phosphorus bond. The latter phenomenon, which manifests itself by a marked ^{31}P magnetic shielding, has notably been observed in a series of digold complexes (**36-38**) characterised by different steric crowding about the metal centres of each complex. Uncrowded monogold complexes (**39-41**) have also been prepared. Furthermore, in the case of the chlorido-bridged dinuclear complexes **43** and **44**, non-optimal metal-phosphorus orbital overlap was shown to be responsible for the fluxional behaviour of these complexes. The ligand displays oschelating behaviour, but contrary to the oschelation taking place in complexes **28-32**, the ligand motion in **43** and **44** involves two different types of donor atom, namely a phosphorus and an oxygen atom.

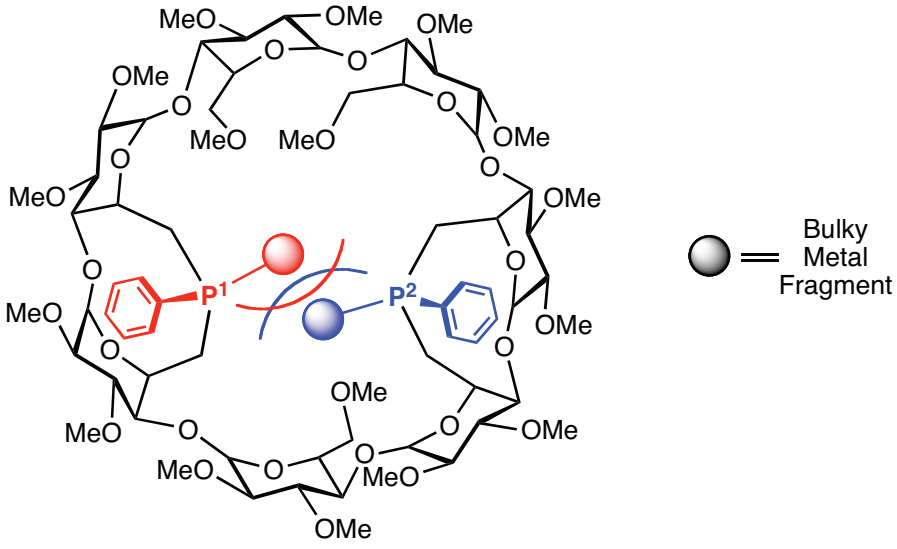

IV.1. Introduction

Inspired by the pioneering work of Issleib and Hohlfeld[1] in the early 60s, many researchers have focused on the design of geometrically constrained diphosphanes.[2-8] Ligands of this type, in particular diphosphanes characterised by a large natural bite angle have been shown to give rise to catalysts with exceptional activities and selectivities.[9-13] So far, most of them were designed to complex a single metal centre in a chelate fashion, so that the geometry around the metal could be tuned at will.[14-16] Conversely, the number of diphosphane ligands meant to complex two metal centres is considerably smaller,[35-39] as the corresponding dinuclear species have often been labelled as undesired side-products of chelation.[16-19] However, because of possible cooperation between the two metal centres, interest for these systems has steadily increased over the years as potential applications have emerged in a variety of fields such as catalysis,[22-28] molecular recognition,[29] material science[30,31] and magnetism.[32-34] Of particular interest are dinuclear complexes featuring a short-bridge between the metal centres.

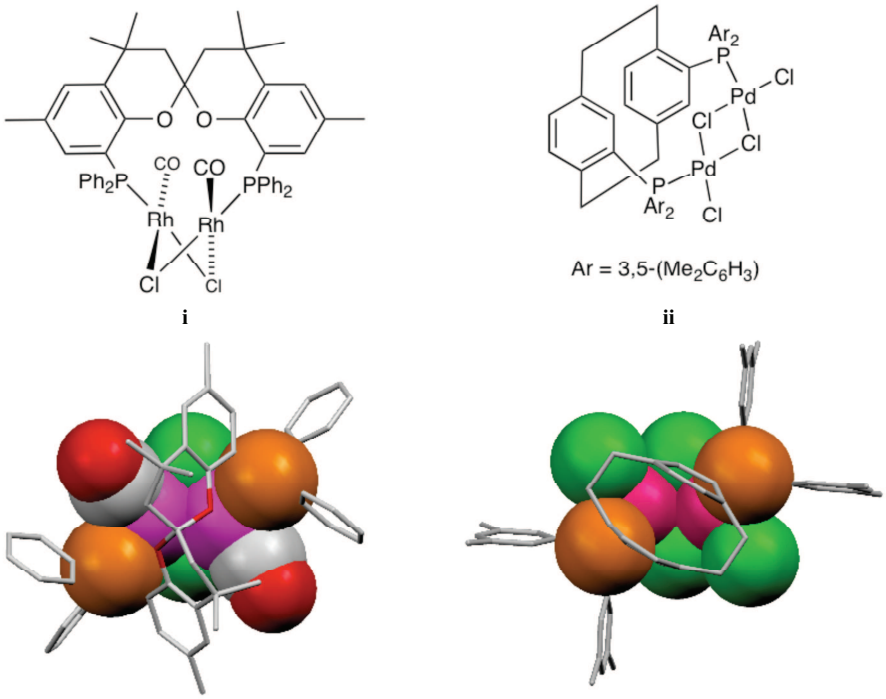

Figure 1. Examples of complexes obtained from dinucleating diphosphanes. Dirhodium complex **i** used in methanol carbonylation (left)[20] and dipalladium complex **ii** used in asymmetric hydroxycarbonylation and alkoxycarbonylation (right).[21]

For example, the diphosphane-capped dinuclear complexes **i** and **ii** (Figure 1), in which a diphosphane spans a $\{M_2(\mu\text{-}X)_2\}$ unit, were shown to be remarkable carbonylation catalysts.[20,21] Interestingly, in both complexes the $\{M_2(\mu\text{-}X)_2\}$ moiety adopts a rare roof-type structure instead of the standard flat geometry.[41-43] Note that distorted $\{M_2(\mu\text{-}Cl)_2\}$ fragments were also found in Gelman's dinuclear complexes of type **iii** obtained by ring-expansion of large bite angle diphosphane complexes (Scheme 1).[40]

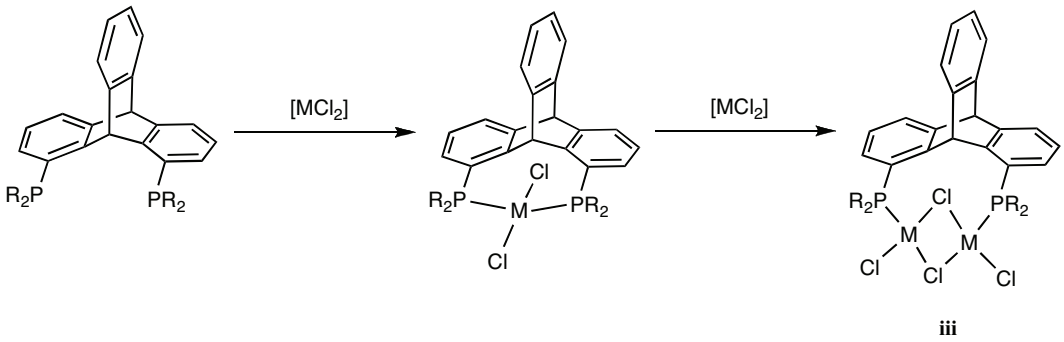

Scheme 1. Schematic representation of the ring expansion process for the synthesis of bridged $[M_2Cl_2(\mu\text{-}Cl)_2(\text{diphosphane})]$ species **iii** based on diphosphanes described by Gelman and co-workers.[40]

Provided the two donor atoms are sufficiently wide apart, diphosphanes built on molecular cavities are also capable of stabilizing dinuclear species, either with independent[44-46] or with bridged metal centres (Figure 2),[47,48] although a high degree of preorganization is required for the simultaneous confinement of the two metal centres.[44,49-53]

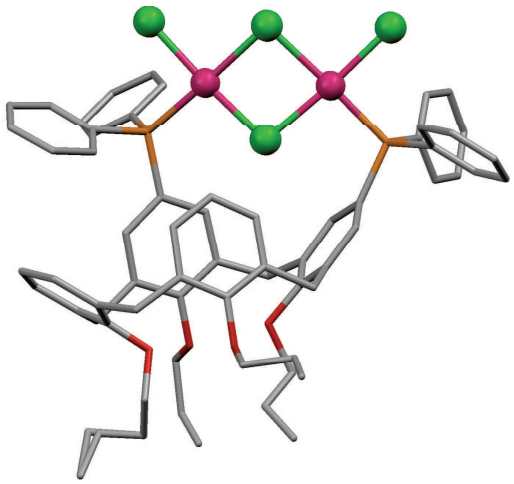

Figure 2. Example of edge-sharing $\{Pd_2Cl_2(\mu\text{-}Cl)_2\}$ complex built on a 1,2-calix[4]arene diphosphane.[48]

Herein, we report on the use of the previously described cavity-shaped diphosphane **WIDEPHOS** (Figure 3) for the entrapment of dinuclear species. Because of the introverted nature of the coordinating atoms, the metal fragments are forced to stay confined in the β-CD cavity, where they give rise to unprecedented, heavily constrained species.

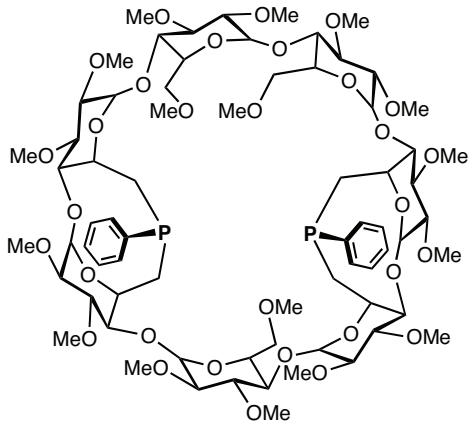

Figure 3. **WIDEPHOS**.

IV.2. Results and discussion

IV.2.1. Non-optimal orbital overlap in dinuclear complexes having two independent metal centres

Reaction of **WIDEPHOS** with 2 equivalents of [AuCl(tht)] (tht = tetrahydrothiophene) gave quantitatively the digold chlorido complex **36** (Scheme 2), the mass spectrum of which showed two intense peaks at *m/z* = 2025.4 and 2007.4 with the isotopic profiles expected for the corresponding $[M + K]^+$ and $[M + Na]^+$ ions, respectively. All NMR spectra are in keeping with the C_1 symmetry of the ligand. The $^{31}P\{^1H\}$ NMR spectrum of **36** displayed two peaks at δ = 31.5 and 22.8 ppm characterised by their large separation ($\Delta\delta$ = 8.7 ppm), which is indicative of phosphorus atoms lying in a different environment. An even larger gap is found in the related gold bromide and iodide complexes **37** and **38** ($\Delta\delta$ = 8.9 and 9.9 ppm, respectively), which were prepared in quantitative yields from **36** by halide metathesis (Scheme 2).

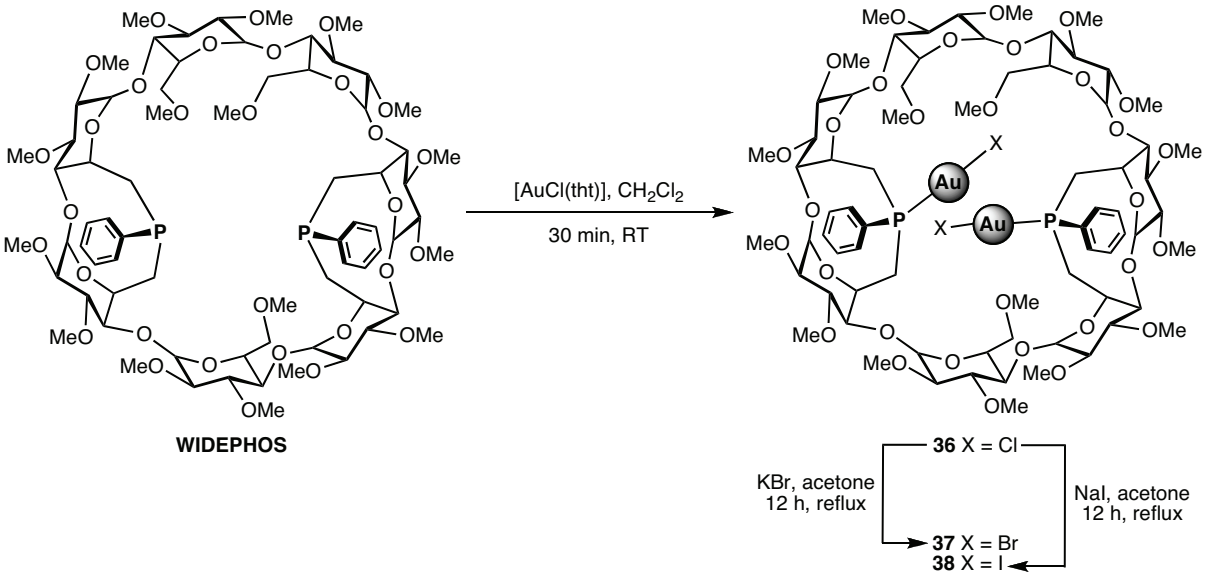

Scheme 2. Synthesis of dinuclear gold(I) halide complexes **36**-**38**

Unlike dipalladium complex **42**, the CD torus of which was found to be distorted (section **IV.2.2.**), complexes **36**-**38** show a preserved circular macrocyclic structure, as can be inferred from the very narrow range ($\Delta\delta$ = ~ 0.2 ppm) in which their anomeric protons H-1 are lying. To get a better understanding of the structure of these complexes, the sterically uncrowded analogues **39**-**41**, based on monophosphane **L,** were also prepared (Scheme 3). For each of the latter, the chemical shift of the corresponding ^{31}P NMR signal approaches that of the signal appearing at lower field in the dinuclear analogue (Table 1). Clearly, one of the gold atoms in **36**-**38** must be coordinated in the same way as in the unconstrained complexes **39**-**41**, whereas the coordination sphere of the second one has probably undergone significant alterations.

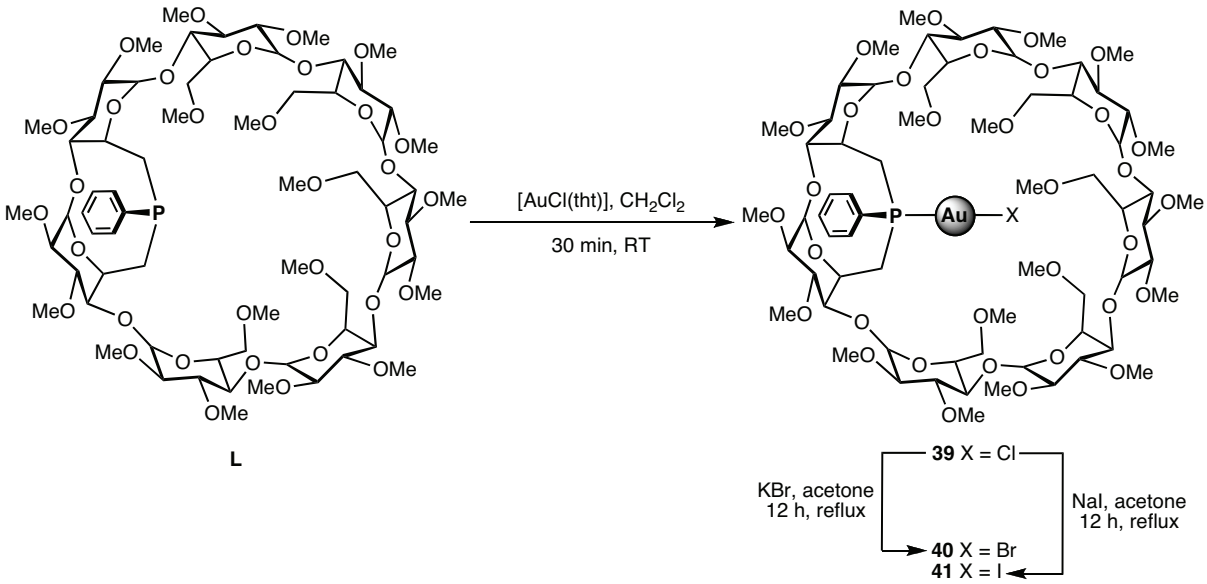

Scheme 3. Synthesis of mono-gold(I) halide complexes **39**-**41**.

Table 1. ^{31}P Chemical shifts of gold(I) complexes **36**-**41** measured in $CDCl_3$ at 121.5 MHz.

	WIDEPHOS·[Au_2X_2]		**L**·[AuX]	
X	Compound	δ (ppm)	Compound	δ (ppm)
Cl	**36**	31.5 and 22.8	**39**	31.0
Br	**37**	32.4 and 23.5	**40**	34.0
I	**38**	33.3 and 23.4	**41**	38.9

As evidenced by an X-ray diffraction study carried out on **36** (Figure 4 and Table 2), the P(1)-Au-Cl fragment, which is linked to the A and B glucose units, lies above that connected to the D and E ones, which points towards the interior of the cavity. Furthermore, the P(1)-Au-Cl unit significantly deviates from linearity (P(1)-Au(1)-Cl(1): 170.52º and 170.25º, for the two molecules present in the unit cell, **36a** and **36b**; Table 2), the angle of the other P-Au-Cl rod being nearly 180º (P(2)-Au(2)-Cl(2): 178.52º and 178.38º; Table 2).[54] As proven by full NMR assignment (^{1}H-^{1}H COSY, ^{1}H-^{1}H TOCSY, ^{1}H-^{1}H ROESY, ^{1}H-^{13}C{^{1}H} HMQC and ^{1}H-^{31}P{^{1}H} HMQC), the ^{31}P NMR signal appearing at higher field belongs to

P(1), that is the phosphorus atom linking glucose units A and B, which is the one being involved in the distorted P-Au-Cl rod.

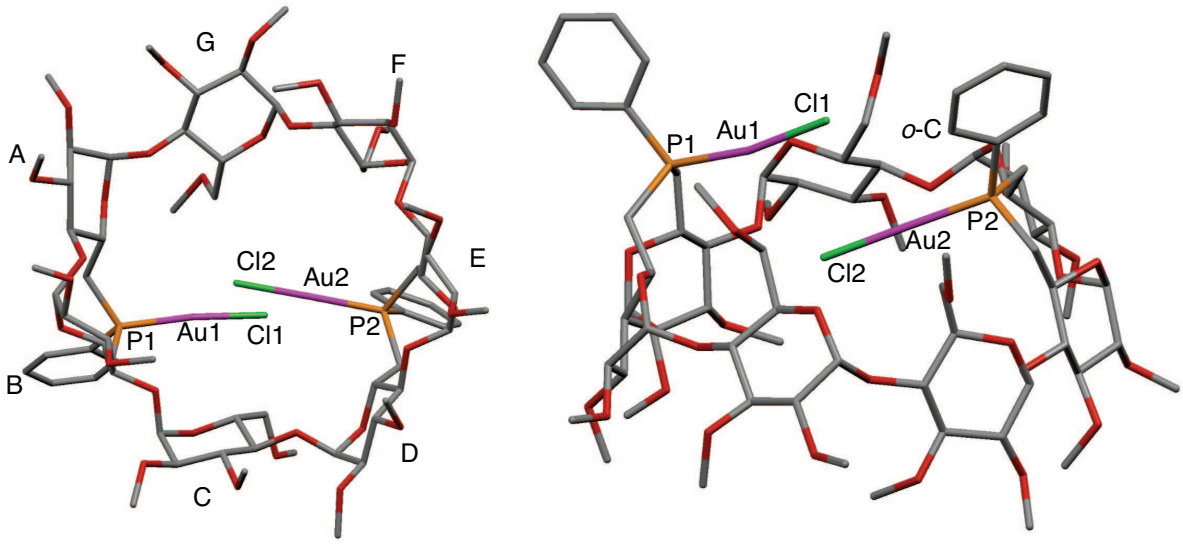

Figure 4. X-ray structure of **36**. View from the secondary face (left) and side view (right). For clarity, only one molecule from the unit cell is shown and solvent molecules have been omitted.

The glucose rings A and B linked to the gold atom that is pushed away from the cavity have their mean ring plane roughly parallel to the CD axis. This shows that the CD wall is flexible enough to depart significantly from its natural, introverted orientation thereby allowing the coordination of a sterically demanding {AuCl} unit. As expected, the P···P separation in **36** is significantly larger than that found in the relaxed, oxidised diphosphane **27** (8.13 and 8.11 Å *vs*. 6.91 Å, respectively). Surprisingly, the chlorine atom included in the cavity, Cl(2), does not interact with any CD proton.[55,56] The one located outside is close to aromatic *o*-H protons of one phenyl ring (Cl(1)···*o*-H distances: 2.60 Å and 2.71 Å for each co-crystallised molecules; Table 2). The small, but significant downfield shift observed for these aromatic *o*-H protons in the ^{1}H NMR spectrum of **36** ($\delta = 8.01$ *vs*. 7.89 ppm for the other aromatic *o*-H protons) points to the existence of weak Au–Cl···H–C interactions in solution. The conformational changes described above do not have any major impact on the CD platform as its overall circular structure is preserved, every glucose units adopting the standard $^{4}C_{1}$ conformation. Note that no gold···gold contacts were detected between the {AuCl} moieties (Au···Au distances: 4.41 and 4.54 Å).[57,58]

Table 2. Selected bond lengths, distances and angles for 2(**36**)·3(C_6H_5Cl)·2(C_5H_{12}). "ct" is the centroid defined as the average point of the three phosphorus-linked carbon atoms.

Molecule **36a**		Molecule **36b**	
Bond lengths and distances [Å]			
P(1)–Au(1)	2.222(2)	P(1)–Au(1)	2.222(3)
Au(1)–Cl(1)	2.291(3)	Au(1)–Cl(1)	2.288(3)
P(2)–Au(2)	2.237(2)	P(2)–Au(2)	2.233(2)
Au(2)–Cl(2)	2.285(3)	Au(2)–Cl(2)	2.289(3)
Cl(1)···*o*-H(P2)	2.711	Cl(1)···*o*-H(P2)	2.598
Angles[º]			
P(1)-Au(1)-Cl(1)	170.52	P(1)-Au(1)-Cl(1)	170.25
ct(1)-P(1)-Au(1)	173.56	ct(1)-P(1)-Au(1)	172.10
P(2)-Au(2)-Cl(2)	178.52	P(2)-Au(2)-Cl(2)	178.38
ct(2)-P(2)-Au(2)	178.29	ct(2)-P(2)-Au(2)	179.73

As mentioned above, one P-Au-Cl fragment of **36** deviates from linearity, while the corresponding phosphorus atom appears at considerably higher field than that of the undistorted P-Au-Cl parent unit. The observation of a P-Au-Cl angle close to 170º suggests that the corresponding phosphorus lone pair imperfectly overlaps with the LUMO orbital of the gold atom. In fact, deviations from optimal overlap of the orbitals involved in phosphorus–metal bonds (also called "bond bending") can be conveniently measured by the so-called "tilt angle" τ,[59] which is expressed as the angle between the M–P vector and the pseudo C_3 axis that runs through the phosphorus atom and the centroid (ct) of the three carbon atoms connected to the former (Figure 5, left).

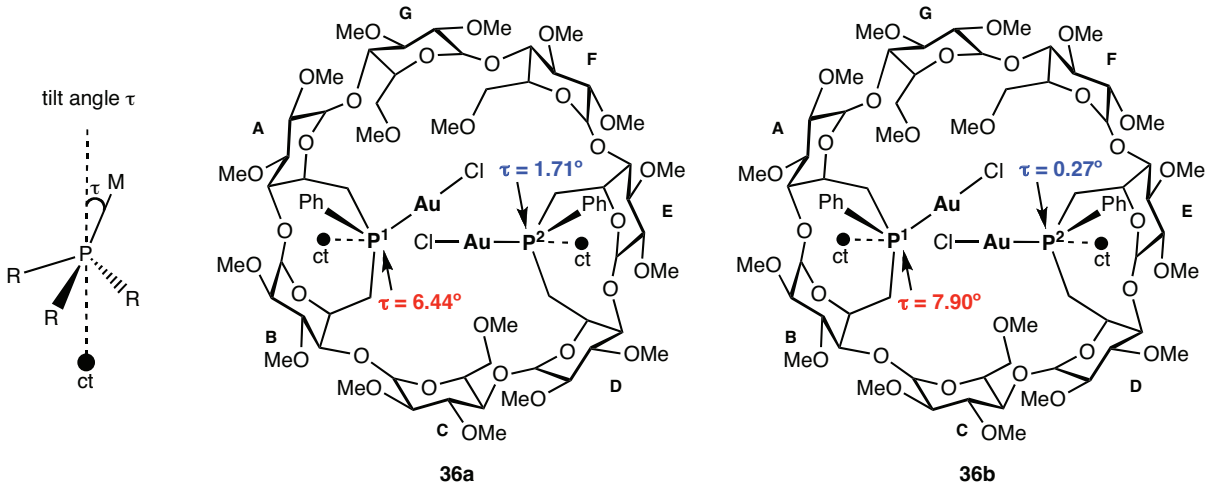

Figure 5. Schematic representation of the tilt angle (left), and tilt angles **τ** calculated from molecular structures determined from an X-ray diffraction study carried out in complex **36** (view from the secondary face, middle and right).

In accord with a linear P-Au-Cl unit, the tilt angle of the P(2) atom is nearly zero (1.71º and 0.27º for **36a** and **36b,** respectively; Figure 5, middle and right). On the other hand, the tilt angles associated with the phosphorus atom of the *bent* P(1)-Au-Cl fragment depart significantly from 0º (6.44º and 7.90º, respectively; Figure 5, middle and right), confirming that the phosphorus lone pair and the interacting metal orbital are non-aligned in this case. It should be noted that, for **36**, a P-Au-Cl bending as small as 6º-8º induces for the corresponding phosphorus atom a remarkably important phosphorus highfield shift with respect to that of the unaffected P-Au-Cl fragment. Similar chemical shift variations were recently observed in **WIDEPHOS**-derived chelate complexes displaying oschelating behaviour, and these were attributed to differences in the way the two phosphorus lone pairs overlap with the metal d_{x2-y2} orbital (**Chapter III**). Finally, we noticed that in the case of iodido species and to a lesser extent bromido ones, a displacement towards higher field was also observed for the low-field signal on going from the mononuclear to the more sterically demanding dinuclear complexes ($\Delta\delta$ = –5.6 ppm for the diodido complex **38**). It is likely that in these complexes both P-Au-X units adopt a slightly bent structure. Undoubtedly, the above findings are a nice illustration that abnormal highfield shifted ^{31}P signals in metal-phosphine complexes may be a result of "imperfect" coordination.

IV.2.2. Two-metal centre complexation within a sterically strained β-CD cavity

In line with its ability to bind two [AuCl] units, **WIDEPHOS** turned out to be also suited for accommodating two bulky [PdCl(dmba)] moieties (dmba = *o*-$C_6H_4CH_2NMe_2$) within its cavity. Thus, treatment of **WIDEPHOS** with 1 equivalent of dimeric $[PdCl(dmba)]_2$ afforded quantitatively the dinuclear palladium complex **42** (Scheme 4).

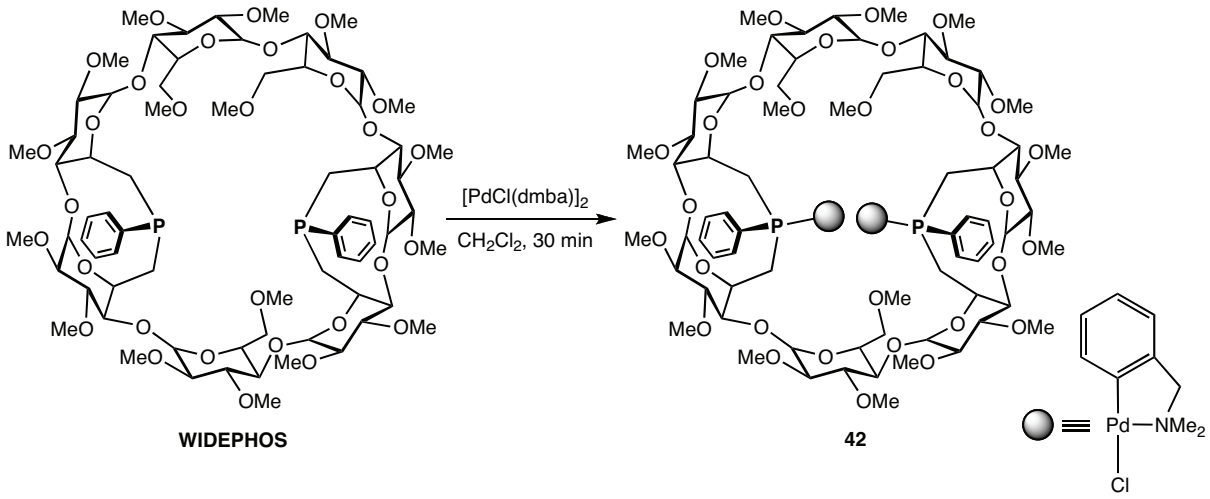

Scheme 4. Synthesis of the dinuclear palladium complex **42**.

The formation of complex **42** was inferred from its mass spectrum, which displayed a strong peak at *m/z* = 2035.62 with the expected isotopic profile corresponding to the $[M - Cl]^+$ ion. Its ^1H NMR as well as $^{13}C\{^1H\}$ NMR spectra are in agreement with an overall C_1-symmetrical molecule.

Since the anomeric protons H-1 lie within a much wider range ($\Delta\delta$ = 0.38 ppm) compared to **WIDEPHOS** ($\Delta\delta$ = 0.22 ppm), it is likely that the presence of two bulky P-coordinated fragments within the cavity causes significant distortions in the CD torus (Figure 5).

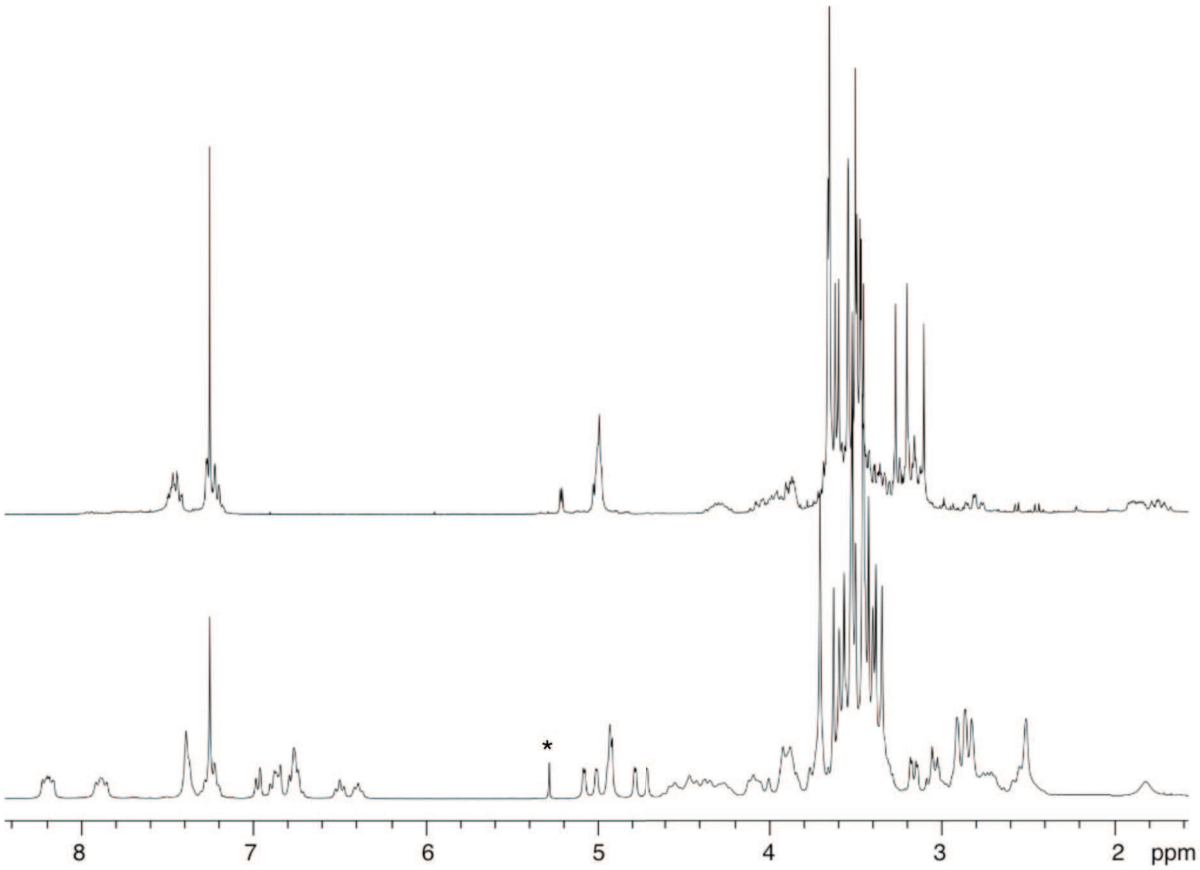

Figure 5. ^{1}H NMR spectra of **WIDEPHOS** (top) and dinuclear palladium complex **42** (bottom) recorded in $CDCl_3$ at 300.1 MHz. Asterisk denotes residual CH_2Cl_2.

The $^{31}P\{^{1}H\}$ NMR spectrum of **42** displays two singlets which are close together (δ = 24.53 and 24.89 ppm), strongly suggesting that the two coordinated phosphorus atoms coordinate the palladium centre in the same way, so that here both phosphorus atoms must be coordinated in an optimal way. Note that these values are very similar to that found in the analogue monophosphane-palladium complex **20** (**Chapter II**). However, one ^{31}P signal was broader than the other at room temperature, suggesting that **42** shows dynamic behaviour. At –80ºC, the ^{1}H NMR spectrum displays exactly the same profile as at room temperature, except for the two aromatic *o*-H protons of the two "PPh" moieties (Figure 6, left), which are no longer equivalent at low temperature. In addition, the initially broad ^{31}P singlet broadened even further on cooling the solution to –20ºC before sharpening again at –80ºC, whereas the second phosphorus signal remained sharp all along the same temperature range (Figure 6, right).

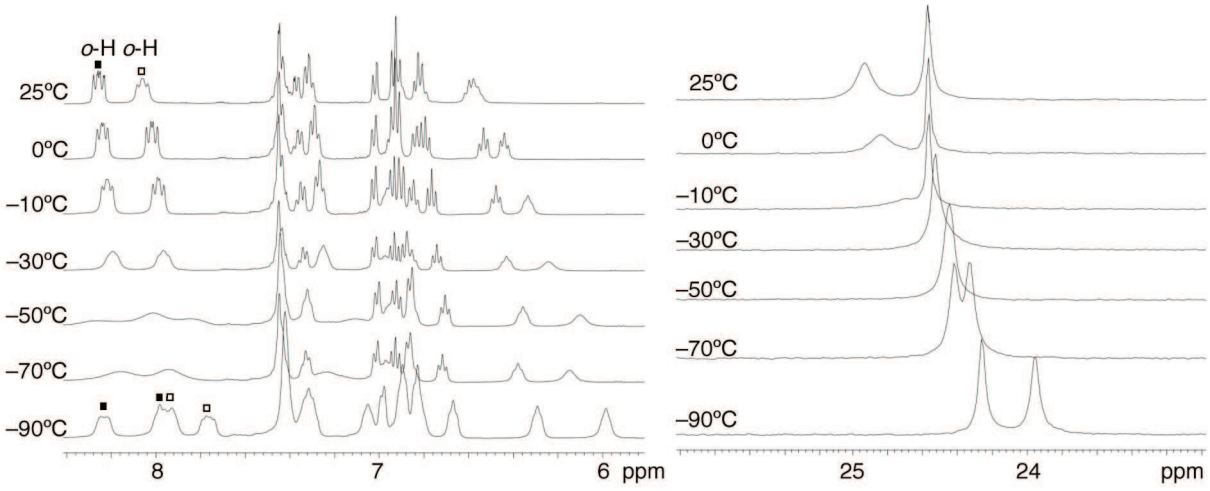

Figure 6. Variable temperature ^{1}H NMR for aromatic protons (left) and $^{31}P\{^{1}H\}$ NMR (right) studies of complex **42** recorded in CD_2Cl_2 at 400.1 MHz and 162.0 MHz, respectively. Open symbols and filled symbols represent a given pair of aromatic *o*-H protons, respectively.

All these data point to phenyl rings rotating slowly about their *ipso*-C–P axis at the ^{1}H NMR time scale. Noticeably, one of them rotates faster than the other, the difference of free energy between the two motions being $\Delta(\Delta G^{\neq}) = 0.14 \pm 0.01$ kcal mol^{-1}. The partial rotational blockage of the phenyl rings is likely to be a result of steric interactions with the large [PdCl(dmba)] units.

IV.2.3. Fluxional, monochlorido-bridged dinuclear complexes

In **Chapter III** we have presented the synthesis of a number of **WIDEPHOS**-derived chelate complexes displaying oschelating behaviour. As mentioned, very small amounts of dinuclear species were detected beside the predominant chelate complexes **30** and **31** formed when **WIDEPHOS** was treated with 1 equivalent of the appropriate metallic precursor, $[PdCl_2(PhCN)_2]$ and [PdClMe(cod)] (cod = cycloocta-1,5-diene), respectively. Raising the metal/ligand ratio to 2 afforded instantly and quantitatively the bridged dinuclear palladium(II) complexes **43** and **44**, respectively. These could also be obtained by treating complexes **30** or **31** with 1 equivalent of the corresponding palladium precursor (Scheme 5). It is noteworthy that mild conditions were applied here for synthesising these dinuclear complexes, in contrast with those reported for other diphosphine-capped dinuclear species, the synthesis of which required higher temperatures and longer reaction times to be complete.[40]

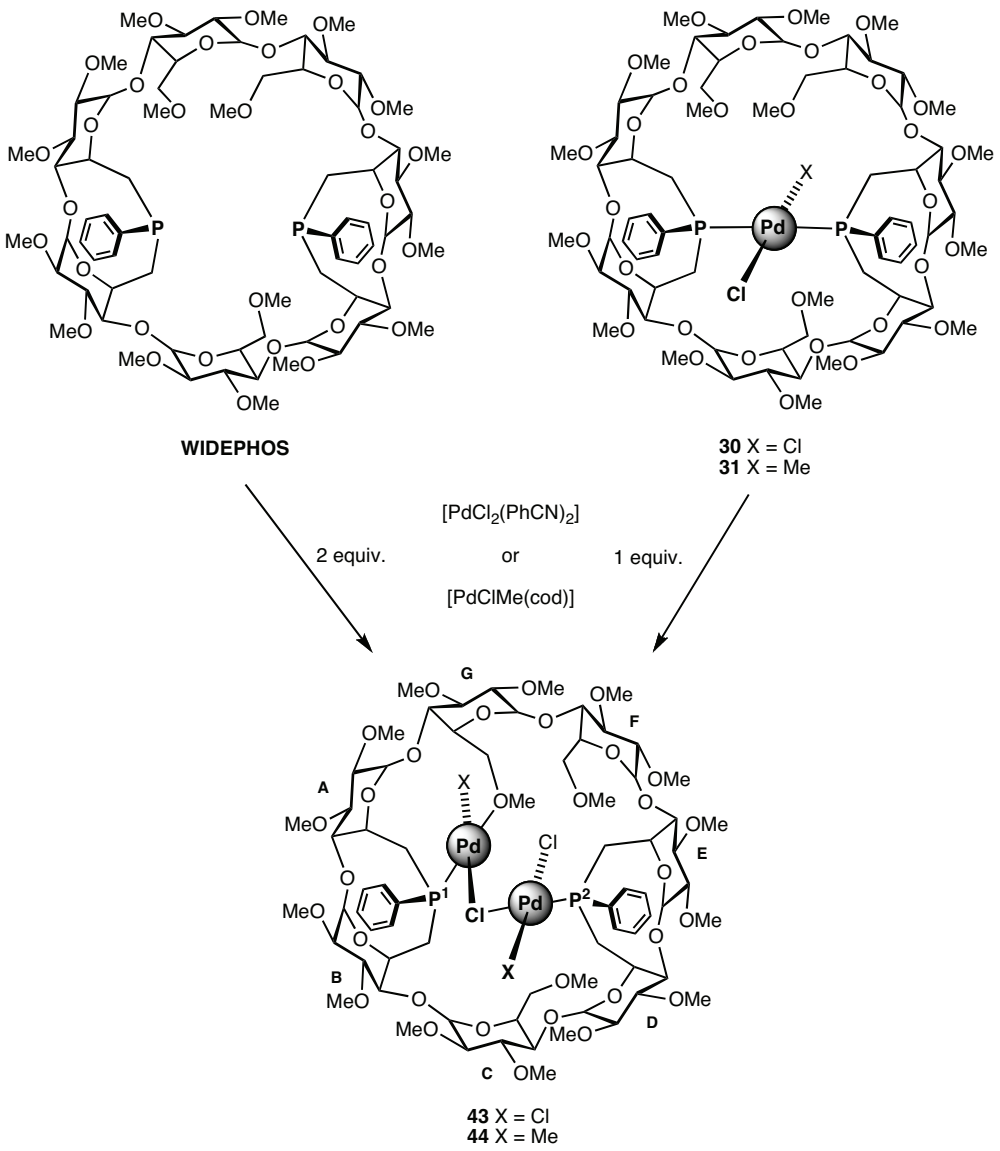

Scheme 5. Synthesis of dinuclear palladium(II) complexes **43** and **44**.

The mass spectra of both complexes **43** and **44** displayed strong peaks for $[M + Na]^+$ and $[M - Cl]^+$ ions with the expected isotopic profiles at respectively *m/z* = 1899.36 and 1841.4 for **43** and *m/z* = 1855.43 and 1797.47 for **44**. Their ^1H and $^{13}C\{^1H\}$ NMR spectra are in agreement with C_1 symmetrical molecules. The ^1H NMR spectra of both complexes comprise anomeric protons lying in a relatively narrow range ($\Delta\delta$ = 0.38 and 0.28 ppm, respectively) compared to the corresponding chelate complexes **30** and **31** ($\Delta\delta$ = 0.59 and 0.61 ppm, respectively), suggesting a less strained cyclodextrin torus in these dinuclear species (Figure 7). **WIDEPHOS** was found to be more inclined to entrap two metal centres than its smaller analogue **TRANSDIP** as the latter, which is perfectly suited for

trans-chelation, only give rise to small amounts of unstable dinuclear species under forcing conditions (12 h reflux in toluene using 3 equivalents of $[PdCl_2(PhCN)_2]$).

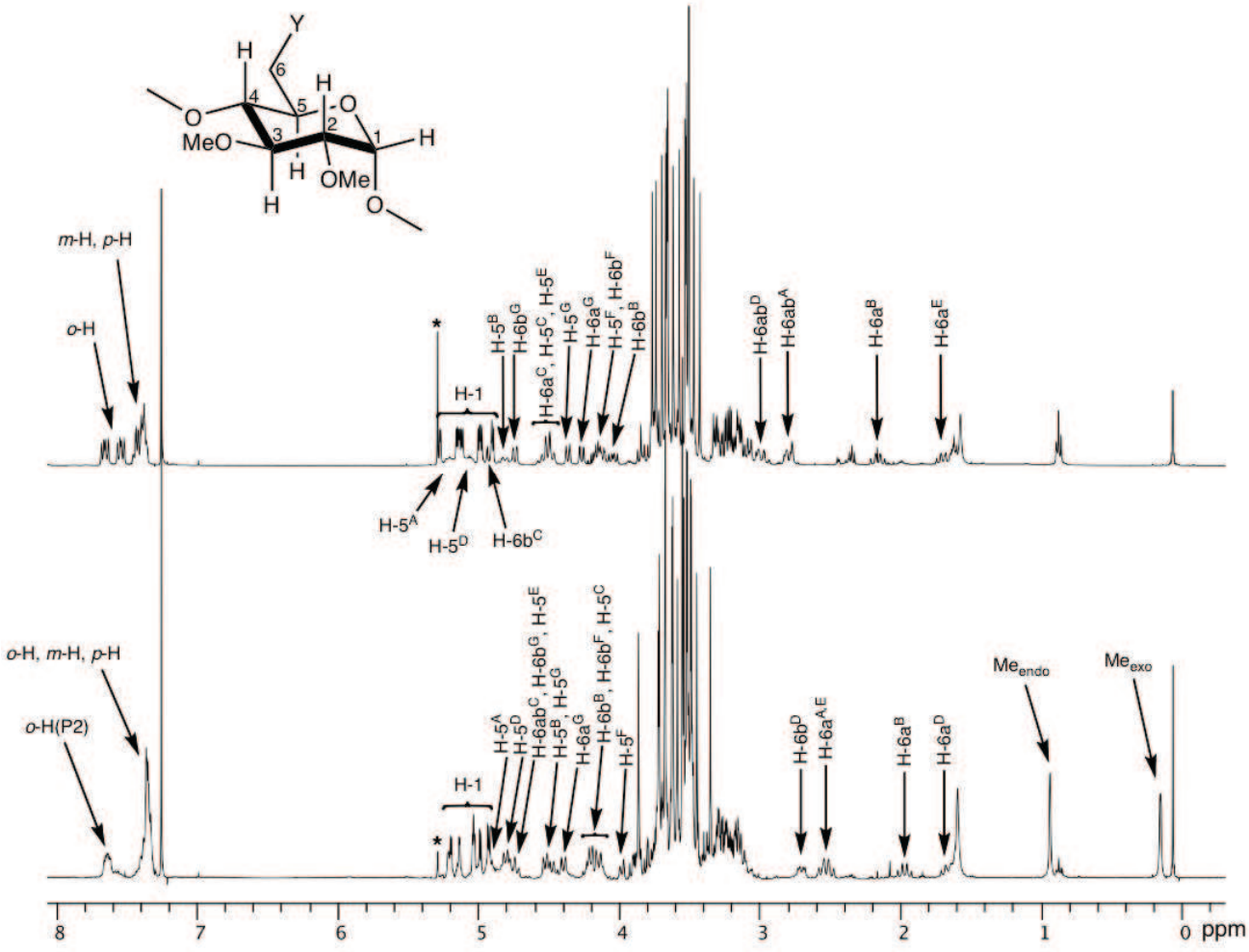

Figure 7. ^{1}H NMR spectra of bridged dinuclear palladium(II) complexes **43** (top) and **44** (bottom) recorded in $CDCl_3$ at 400.1 MHz. Asterisks denote residual CH_2Cl_2.

Full structural assignment based on ^{1}H-^{1}H COSY, ^{1}H-^{1}H TOCSY, ^{1}H-^{1}H ROESY, ^{1}H-^{13}C{^{1}H} HMQC and ^{1}H-^{31}P{^{1}H} HMQC established unambiguously that in complexes **43** and **44**, the OMe-6 group of glucose unit G is significantly downfield shifted compared to the two remaining OMe-6 groups and therefore is likely to be coordinated to one of the metal centres (Figure 8). Similar methoxy coordination was previously observed in other cyclodextrin-derived complexes.[60,61]

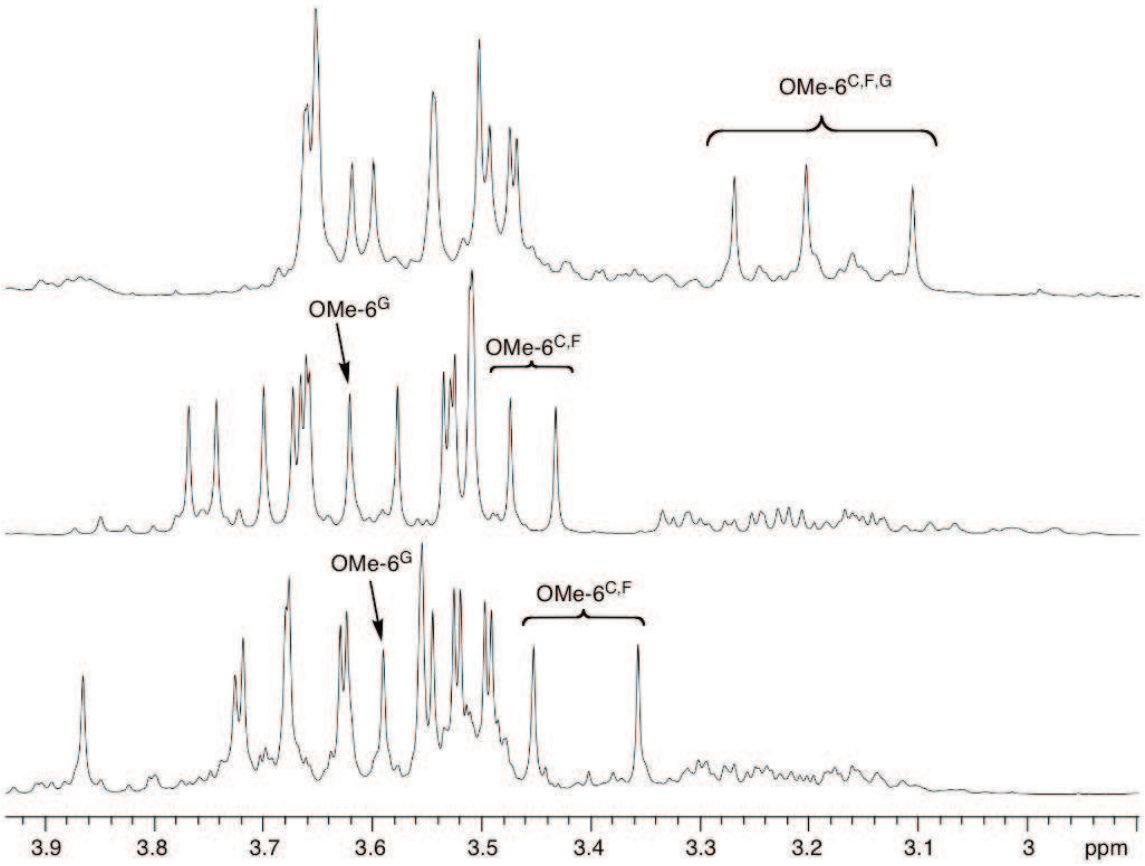

Figure 8. Part of the ^{1}H NMR spectra of **WIDEPHOS** (top), complex **43** (middle) and complex **44** (bottom) recorded in $CDCl_3$ showing the area of the methoxy groups.

Interestingly, a ^{1}H-^{1}H ROESY experiment carried out on complex **44** proved that one coordinated methyl group is located inside the cavity as it gives rise to strong trough-space correlations with H-3 and H-5 *intra*-cavity protons of glucose units D, E and F. On the other hand, the second one is clearly located outside the CD torus, this group strongly correlating with the downfield shifted methoxy group of glucose unit G as well as with aromatic *o*-H protons belonging to the P(1)-substituted phenyl ring (phosphorus atom bridging glucose units A and B; Figure 9). It appears that the inclusion of two chlorido ligands into the CD cavity is not favourable, probably on the ground of electronic repulsions between them. Note that in complex **44**, the proximity of aromatic *o*-H protons to the chlorido ligand, named *o*-H(P2), causes a small displacement to lower field compared to those lying in the vicinity of the methyl group ($\Delta\delta$ = 0.28 ppm; Figure 7, bottom). The ultimate evidence for the bridged nature of **43** and **44** came from the corresponding ^{31}P{^{1}H} NMR spectra (40ºC), which both displayed two doublets with coupling constants of ^{4}J(PP) = 4.4 Hz and ^{4}J(PP) = 3.8 Hz respectively, in agreement with the presence of a link between the metals.

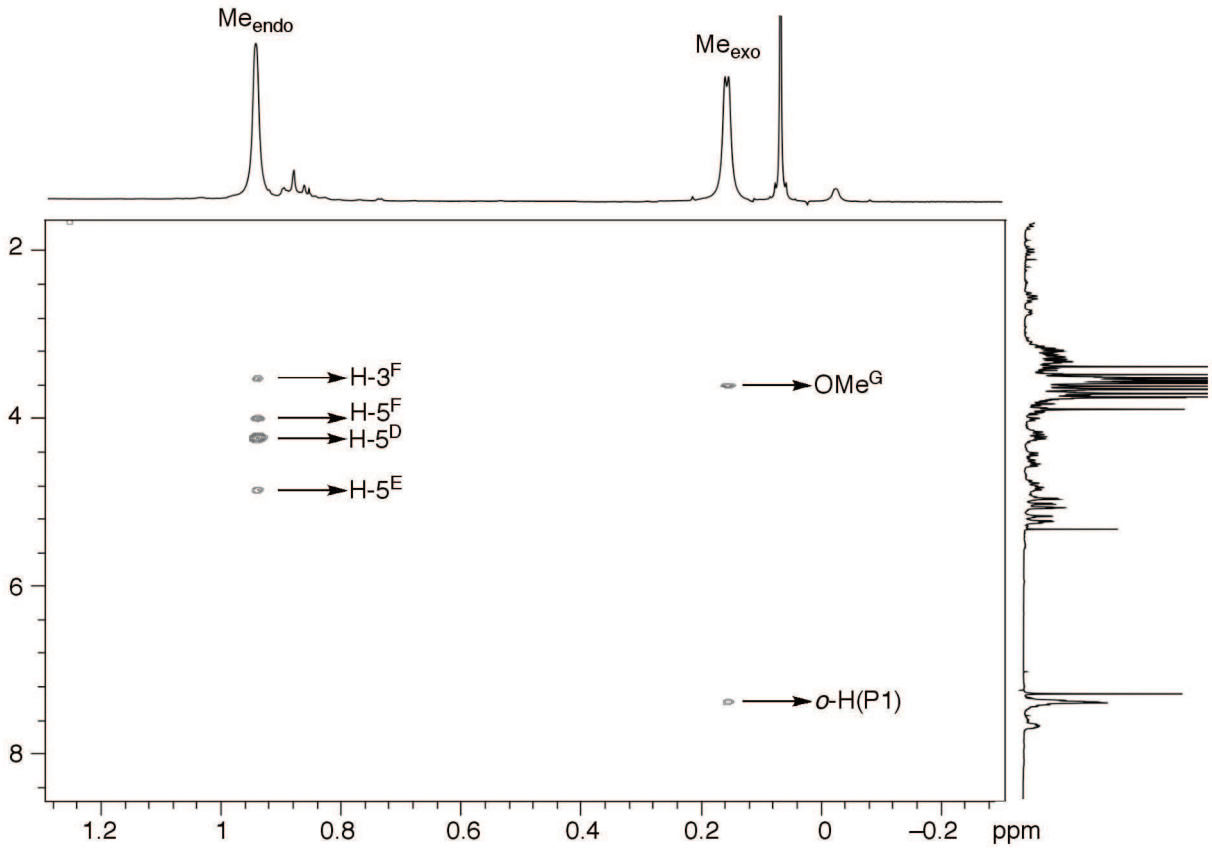

Figure 9. Part of ^{1}H-^{1}H ROESY NMR spectrum of bridged dinuclear palladium(II) complex **44** recorded in $CDCl_3$ at 400.1 MHz.

Unexpectedly, the OMe-6 ligand of glucose unit G was displaced by a water molecule during crystallisation, giving rise to complex **45** (Scheme 6), which was characterized by an X-ray diffraction study. Such a transformation is a good indication of the weakness of the Pd–O bond in complex **43**. It must be emphasized that the coordinated water molecule is only detected in the solid state and does not reflect the structure of complex **43** in solution. Such a feature has already been observed in other CD-based aqua complexes.[62]

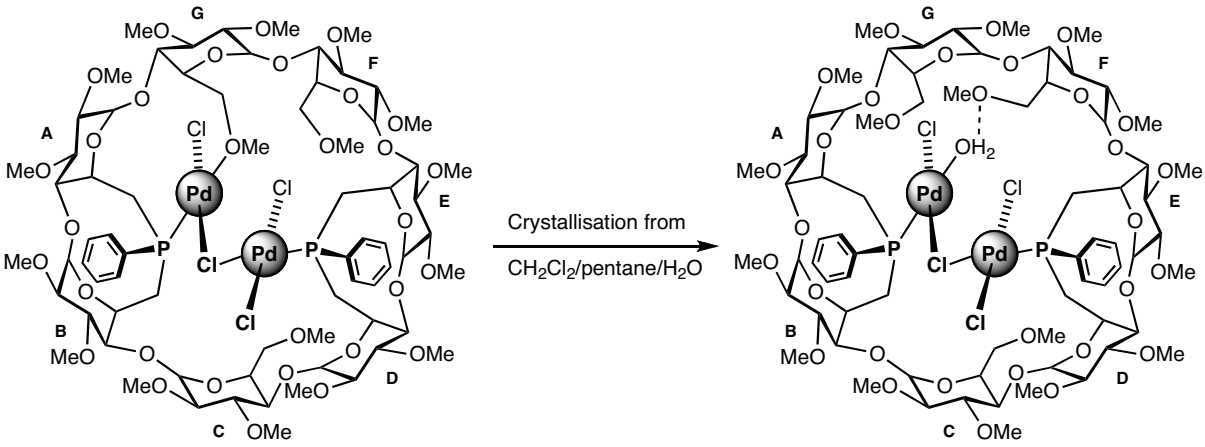

Scheme 6. Formation of aqua complex **45**. Doted lines represent hydrogen bonding between the coordinated water molecule and the primary face methoxy group of glucose unit F.

Complex **45** comprises two chlorido ligands located inside the β-CD cavity and two outside (Figure 10 and Table 3). Only one of the *endo*-chlorido ligands, named Cl(2), bridges two palladium(II) centres. None of the other chlorido ligands is able to behave as μ-bridging unit because of the steric constrains imposed by the macrocyclic ligand onto the metal's first coordination sphere. To the best of our knowledge, the $\{Pd_2Cl_4\}$ moiety of **45** represents the first example reported in the literature in which this unit does not adopt the usual $\{Pd_2Cl_2(\mu\text{-}Cl)_2\}$ flat-like or roof structures, but instead is constituted of two square planar fragments linked by a single μ-chlorido bridge. The Pd(1)-Cl(1)-Cl(2) and Pd(2)-Cl(3)-Cl(4) interplanar angle known as bent angle is here meaningless because the complex is not edge-, but *vertex-sharing*. Interestingly, the distance between the palladium centres (3.17 Å) is slightly longer than that observed for roof-like $\{Pd_2Cl_4\}$ moieties,[40] but much shorter than that observed for flat ones.[63,64] As expected, the P···P separation in **45** (6.19 Å) is only slightly shorter than in the oxidised ligand **27** (6.91 Å, **Chapter III**), hence the absence of major conformational changes in the macrocyclic structure, all glucose units retaining the standard $^4C_1$ conformation. It is important to point out that the coordinated water molecule (O_w) is stabilized by a hydrogen bond involving the OMe-6 group of glucose unit F (O^F). Furthermore, both phosphorus "tilt angles" τ deviate significantly from 0º (τ = 5.19º for P(1) and τ = 3.64º for P(2)), hence reflecting some constraints within the metals' coordination spheres.

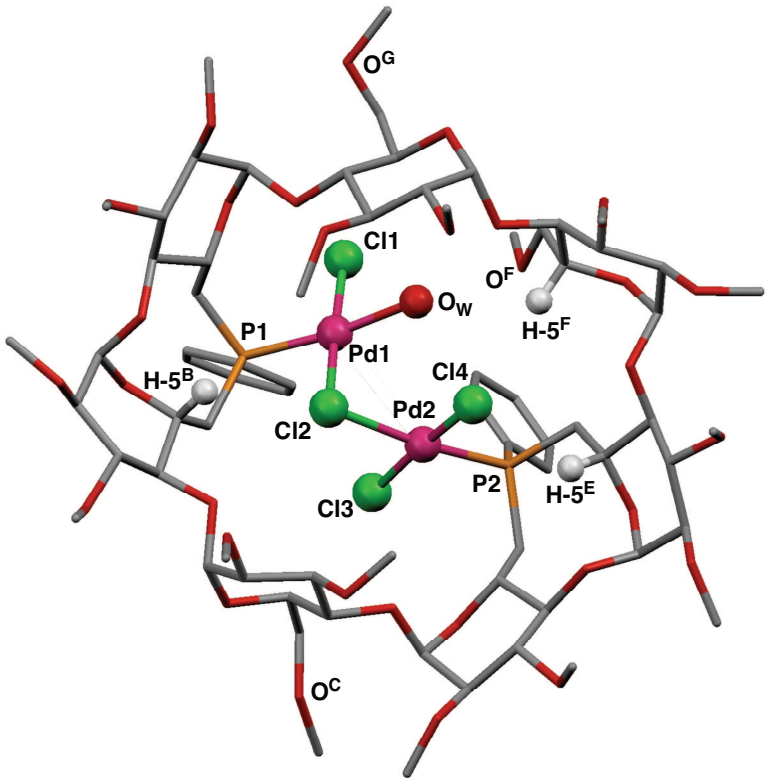

Figure 10. X-ray structure of complex **45** (view from the secondary face). For clarity, solvent molecules have been omitted.

Table 3. Selected bond lengths and angles for **45**·0.5(C_5H_{12}).

Bond lengths and distances [Å]			
P(1)–Pd(1)	2.201(2)	P(2)–Pd(2)	2.204(2)
Pd(1)–Cl(1)	2.287(2)	Pd(2)–Cl(2)	2.433(2)
Pd(1)–Cl(2)	2.325(2)	Pd(2)–Cl(3)	2.306(2)
Pd(1)–O_w	2.077(5)	Pd(2)–Cl(4)	2.305(2)
O_w···O^F	2.828	Cl(4)···H-5^E	2.599
Cl(2)···H-5^B	2.747	Cl(4)···H-5^F	2.801
Angles[º]			
P(1)-Pd(1)-O_w	173.26	P(2)-Pd(2)-Cl(2)	172.26
Cl(1)-Pd(1)-Cl(2)	178.13	Cl(3)-Pd(3)-Cl(4)	174.91
ct(1)-P(1)-Pd(1)	174.81	ct(2)-P(2)-Pd(2)	176.36

Addition of water to a solution of **43** did not produce any changes in its NMR spectra and no indication of aqua complexes such as **45** was found. Complex **45** only formed upon crystallisation and could not be isolated by other means. In fact, complex **43** turned out to be very robust to the extent that it could be purified by standard column chromatography.

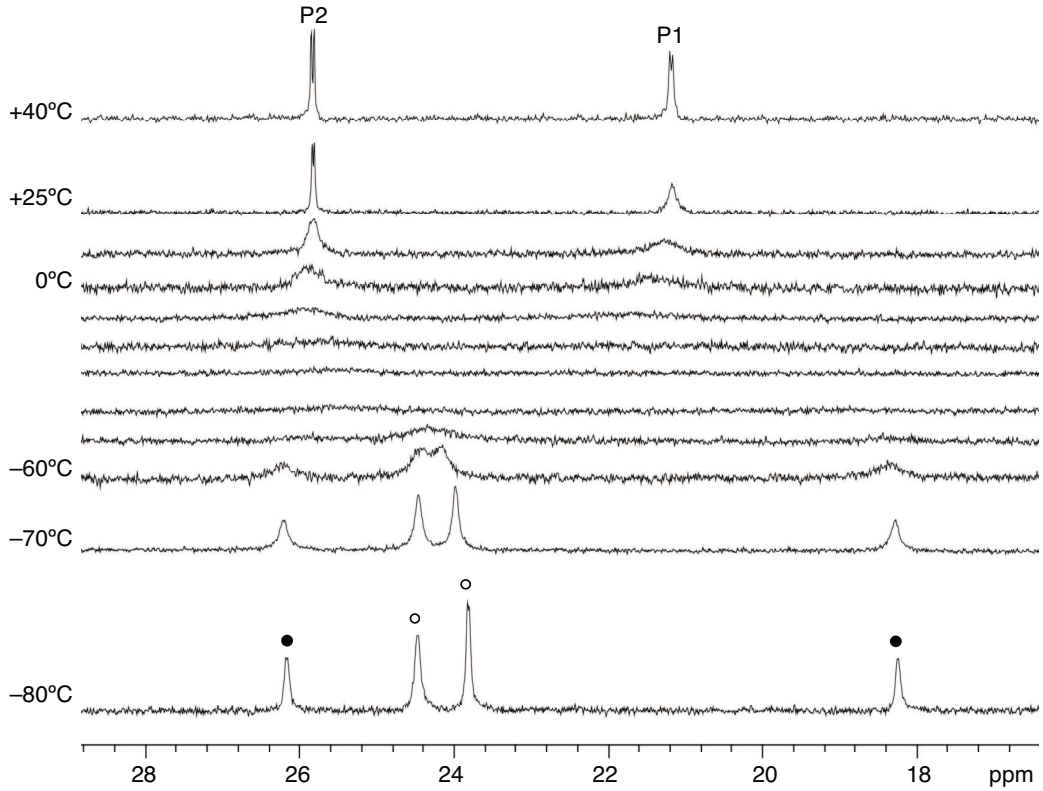

Figure 11. Variable temperature $^{31}P\{^{1}H\}$ NMR study of complex **43** recorded in CD_2Cl_2 at 162.0 MHz. Empty symbols label the phosphorus signals associated with species **A**, whereas filled symbols label those corresponding to species **B**.

Bridged dinuclear palladium(II) complexes **43** and **44** display fluxional behaviour in solution as revealed by their $^{31}P\{^{1}H\}$ NMR spectra (Figure 11). At room temperature, the $^{31}P\{^{1}H\}$ NMR spectra of complexes **43** and **44** recorded in CD_2Cl_2 comprise a broad signal corresponding to the P(1) phosphorus atom (linked to glucose units A and B), which emerges as a doublet at 40ºC. On the other hand, the P(2) phosphorus atom (linked to glucose units D and E) already appears as a doublet at room temperature. Upon cooling the solution of either **43** or **44**, both ^{31}P signals coalesced around –30ºC and emerged as four broad doublets at –80ºC associated with two distinct species present in a 67:33 ratio. The corresponding ^{1}H NMR spectrum measured at –80ºC did not allow a clear distinction between the two species, the structures of which must be very similar. Again the OMe-6 group belonging to

glucose unit G is downfield shifted even at low temperatures, suggesting coordination to palladium.

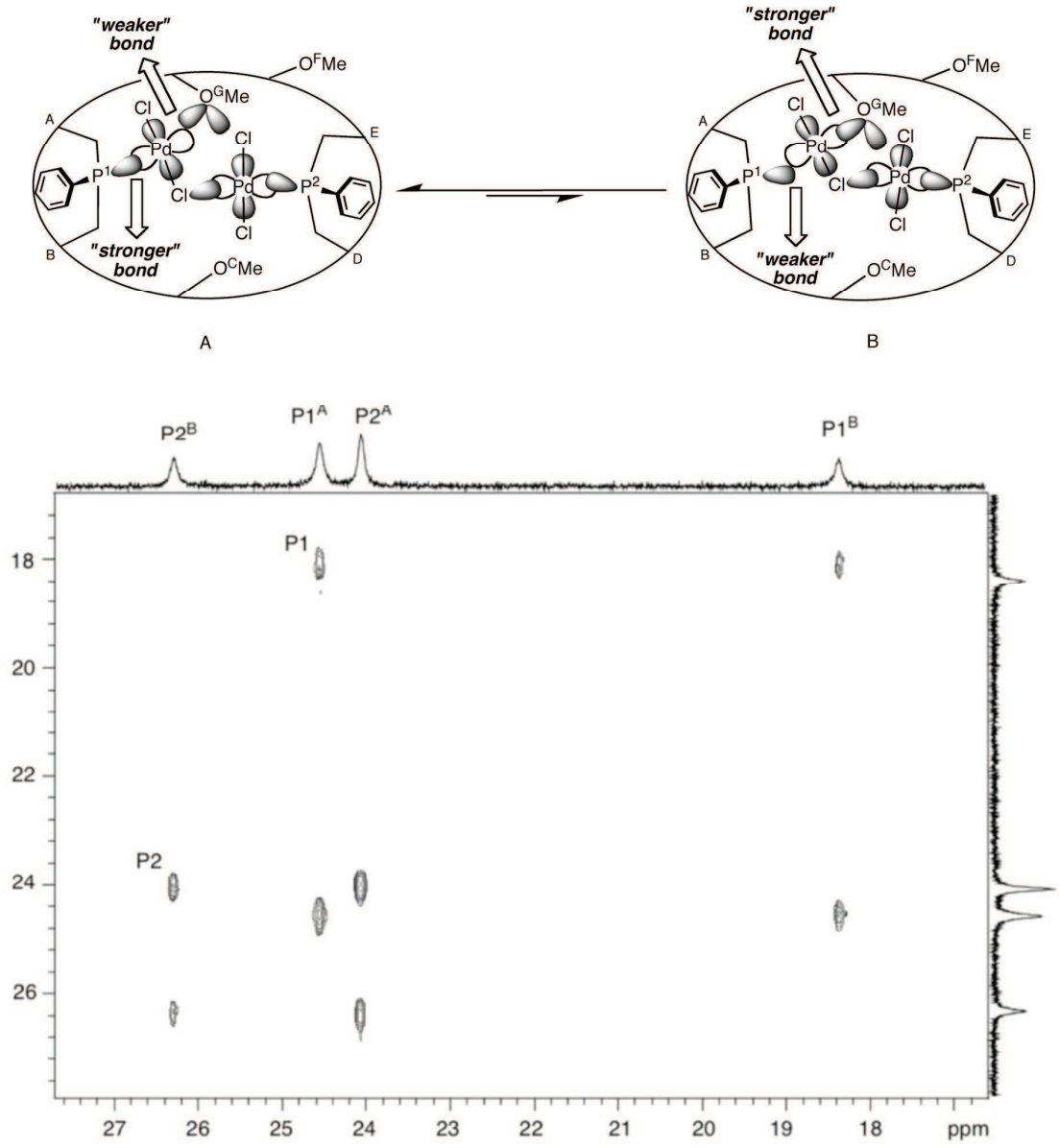

Figure 12. Off resonance 2D $^{31}P\{^{1}H\}$-$^{31}P\{^{1}H\}$ ROESY NMR spectrum of complex **43** at –70ºC recorded in CD_2Cl_2 at 202.5 MHz.

An off-resonance 2D $^{31}P\{^{1}H\}$-$^{31}P\{^{1}H\}$ ROESY NMR experiment carried out on complex **43** (Figure 12) showed that the P(1) atom underwent a dramatic upfield shift ($\Delta\delta$ = 6.2 ppm) on going from one species to the other compared to the P(2) atom, the chemical shift of which remained nearly unchanged ($\Delta\delta$ = 1.7 ppm). As demonstrated above in sections **III.2.2** and **IV.2.1**, a ^{31}P NMR upfield shift of that extent is compatible with a "weakening" of

the metal coordination by the phosphorus atom as a result of non-alignment of the phosphorus lone pair and the metal d_{x2-y2} orbital. This, in turn, should lead to a "strengthening" of the Pd–O^GMe bond.

The coordination of oxygen atom O^G to palladium is obviously weaker than that of P(1), hence the non-equimolar ratio of the species in equilibrium. Overall, all these data point out to the presence of two species in exchange, the major one (**A**) having its P(1) atom better coordinated to palladium than that of the minor species **B**, whereas the O^G atom of **B** is better coordinated to palladium than that of **A**. The free energy of activation $\Delta G^{\neq}$ calculated for this equilibrium is given in Figure 13.[65,66]

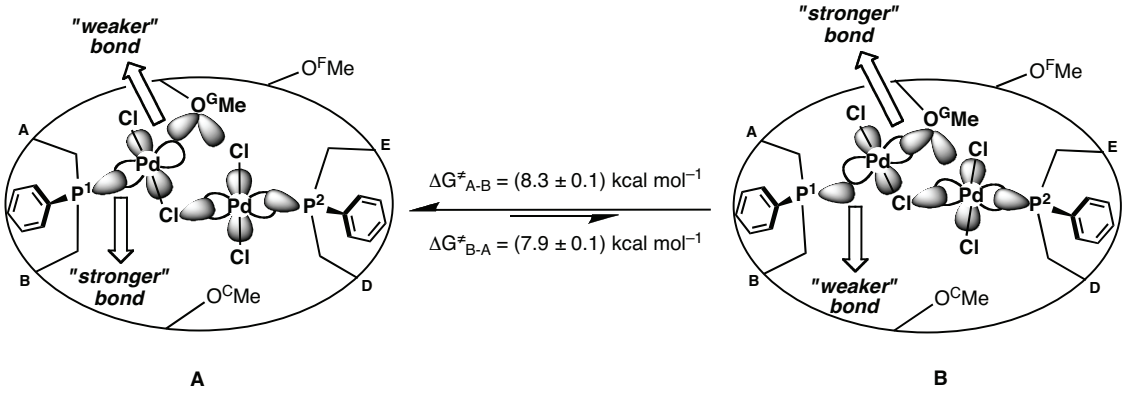

Figure 13. Equilibrium between species **A** and **B**.

As in chelate complexes **28-32**, the dynamics observed for **43** and **44** arise from non-optimal overlap between P and O lone pairs and the d_{x2-y2} metal orbital to which it is bound. In fact non-optimal coordination in **43** and **44** occurs at the same phosphorus atom, P(1), as in dinuclear gold complexes **36-38**. The major difference between the present system and **28-32** is that chelation involves here phosphorus and non-phosphorus atoms. In this respect, this study shows, for the first time, that oschelating behaviour may also occur with hybrid chelators.

The capacity of the β-CD cavity to accommodate two metal centres was further exemplified by the dirhodium(I) complex **46**, obtained quantitatively when **WIDEPHOS** was treated with 1 equivalent of dimeric $[\{RhCl(CO)_2\}_2]$ (Scheme 7). Alternatively, complex **46** can be obtained from the rhodium(I) complex **32** by using only 0.5 equivalent of metal precursor.

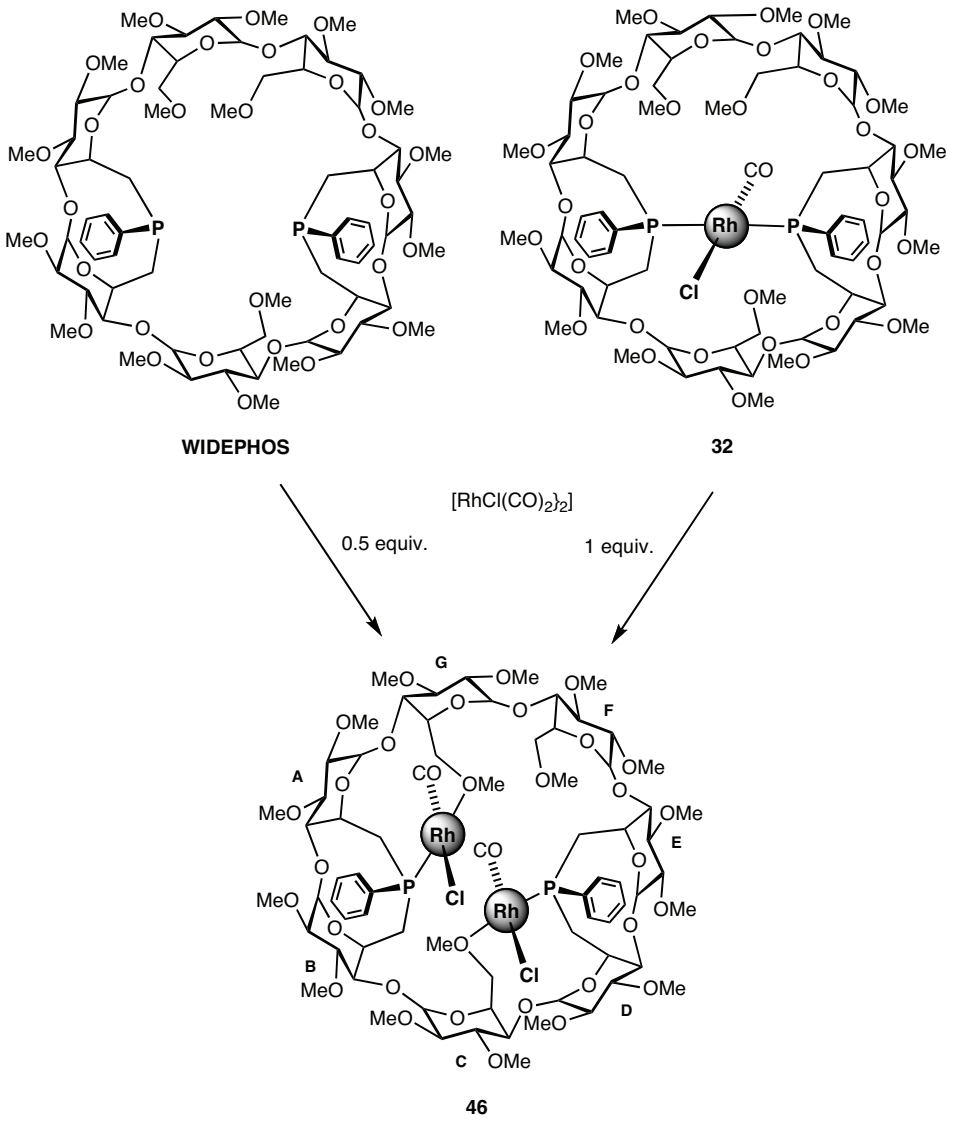

Scheme 7. Synthesis of dinuclear rhodium(I) complex **46**.

Strong peaks at *m/z* = 1891.36, 1875.37 and 1816.39 in the MS spectrum of **46** for the $[M + K]^+$, $[M + Na]^+$ and $[M - Cl]^+$ ions are indicative of the presence of two coordinated rhodium centres. Its $^{13}C\{^1H\}$ NMR spectrum displayed two singlets at δ = 177.49 and 178.75 ppm, belonging to the two non-equivalent carbonyl ligands. In the ^1H NMR spectrum, two OMe-6 groups are unusually downfield shifted (Figure 14), reflecting their coordination to rhodium centres. In the $^{31}P\{^1H\}$ NMR spectrum the phosphorus atoms appear as two broad doublets ($^1J_{P,Rh} \approx 170$Hz). The broadness of the peaks is likely to reflect oschelating behaviour of the individual *P,O*-Rh subunits. The existence of *two* P,O-oschelating units is here likely, but this cannot be stated with certainty.

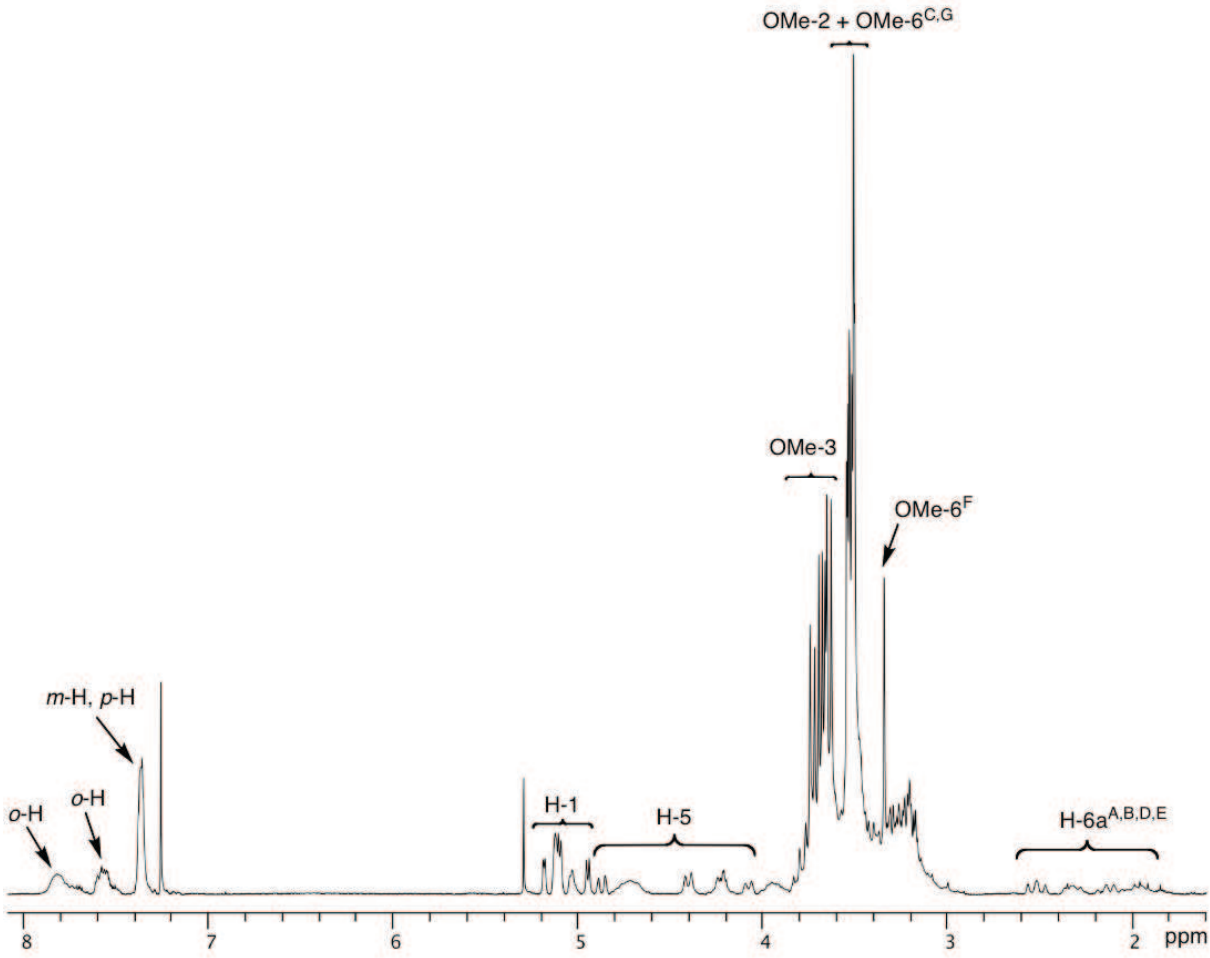

Figure 14. ^{1}H NMR spectrum of dinuclear rhodium(I) complex **46** recorded in $CDCl_3$ at 300.1 MHz.

IV.3. Conclusion

In this work we have shown that **WIDEPHOS** is suitable for hosting two metal centres. The fact that the donor atoms are rigidly held at given positions within the inner-walls imposes considerable strain on dinuclear complexes obtained from this ligand. Non-optimal orbital overlap in phosphorus–metal bonds, which can be detected easily by ^{31}P NMR spectroscopy, leads to significant deviations from standard coordination geometries and this often neglected phenomenon was shown to be central in the release of tension for many complexes derived from **WIDEPHOS**, notably static dinuclear and fluxional bridged ones. In this respect, bridged dinuclear complexes **43** and **44** provide the first examples of complexes containing a heterodentate *P,O* coordinating unit displaying oschelating behaviour. The presence of only one μ-Cl bridge in these systems is a further proof for the high degree of control imposed by the ligand on the dinuclear fragment. It is expected that these non-conventional complexes having two confined metal centres will give rise to unusual selectivities and activities in various catalytic reactions, possibly with cooperativity between the two metals.[22]

IV.4. Experimental section

IV.4.1. General procedures

All manipulations were performed in Schlenk-type flasks under dry nitrogen. Solvents were dried by conventional methods and distilled immediately prior to use. Deuterated solvents were passed down a 5 cm-thick alumina column and stored under nitrogen over molecular sieves (4 Å). Routine ^{1}H and $^{13}C\{^{1}H\}$ spectra were recorded on FT Bruker AVANCE 300, AVANCE 400 and AVANCE 500. ^{1}H NMR spectral data were referenced to residual protiated solvents (δ = 7.26 ppm for $CDCl_3$), $^{13}C\{^{1}H\}$ chemical shifts are reported relative to deuterated solvents (δ = 77.00 ppm for $CDCl_3$) and the $^{31}P\{^{1}H\}$ NMR data are given relative to external H_3PO_4. Mass spectra were recorded either on a ZAB HF VG analytical spectrometer using *m*-nitrobenzyl alcohol as matrix or on a Bruker MicroTOF spectrometer (ESI) using CH_2Cl_2, MeCN or MeOH as solvent. Elemental analyses were performed by the Service de Microanalyse, Institut de Chimie, Strasbourg. Melting points were determined with a Büchi 535 capillary melting-point apparatus. All commercial reagents were used as supplied. **WIDEPHOS** and **L** were prepared according to the synthesis of compound **10** and **12** from **Chapter II**. [AuCl(tht)],[67], $[PdCl(dmba)]_2$[68], $[PdCl_2(PhCN)_2]$[69] and [PdClMe(cod)][70] were prepared according to literature procedures. The numbering of the atoms within a glucose unit is as follows:

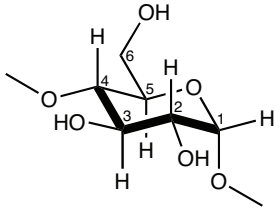

IV.4.2. Synthesis of compounds

***P,P'*-Dichlorido-{6^{A},6^{B},6^{D},6^{E}-tetradeoxy-6^{A},6^{B}:6^{D},6^{E}-bis[(*R*)-phenylphosphinidene]-2^{A},2^{B},2^{C},2^{D},2^{E},2^{F},2^{G},3^{A},3^{B},3^{C},3^{D},3^{E},3^{F},3^{G},6^{C},6^{F},6^{G}-heptadeca-*O*-methyl-β-cyclodextrin} digold(I) (36)**

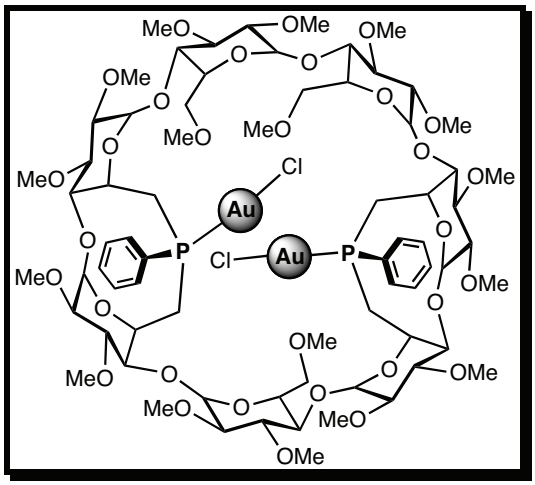

To a stirred solution of **WIDEPHOS** (0.100 g, 0.066 mmol) in CH_2Cl_2 (5 mL) was added a solution of [AuCl(tht)] (0.042 g, 0.132 mmol) in CH_2Cl_2 (2 mL). After 30 min, the reaction mixture was evaporated to dryness and the residue subjected to column chromatography (SiO_2, CH_2Cl_2/MeOH, 96:4, *v*/*v*) to give pure **36** (yield: 0.130 g, 99%) as a colourless powder. R_f (SiO_2, CH_2Cl_2/MeOH, 92:8, *v*/*v*) = 0.40; m.p. dec. >250ºC; ^{1}H NMR (500.1 MHz, $CDCl_3$, 25ºC): δ (assignment by ^{1}H-^{1}H COSY, ^{1}H-^{1}H TOCSY, ^{1}H-^{1}H ROESY, ^{1}H-^{13}C{^{1}H} HMQC, ^{1}H-^{31}P{^{1}H} HMQC) = 2.08 (td, 1 H, $^{2}J_{H\text{-}6a,H\text{-}6b}$ = $^{2}J_{H\text{-}6a,P}$ = 15.1 Hz, $^{3}J_{H\text{-}6a,H\text{-}5}$ = 13.0 Hz, H-6a^{D}), 2.11 (td, 1 H, $^{2}J_{H\text{-}6a,H\text{-}6b}$ = $^{2}J_{H\text{-}6a,P}$ = 15.1 Hz, $^{3}J_{H\text{-}6a,H\text{-}5}$ = 13.0 Hz, H-6a^{A}), 2.30 (m, 1 H, H-6a^{E}), 2.33 (m, 1 H, H-6a^{B}), 3.05 (d, 1 H, $^{3}J_{H\text{-}2,H\text{-}3}$ = 10.2 Hz, $^{3}J_{H\text{-}2,H\text{-}1}$ = 3.0 Hz, H-2^{A}), 3.09 (d, 1 H, $^{3}J_{H\text{-}2,H\text{-}3}$ = 10.1 Hz, $^{3}J_{H\text{-}2,H\text{-}1}$ = 3.2 Hz, H-2^{D}), 3.14 (1 H, H-2^{C}), 3.16 (1 H, H-2^{F}), 3.19 (1 H, H-2^{G}), 3.19 (s, 3 H, OMe-6), 3.22 (1 H, H-4^{A}), 3.23 (s, 3 H, OMe-6), 3.27 (1 H, H-4^{D}), 3.30 (1 H, H-2^{B}), 3.31 (1 H, H-2^{E}), 3.32 (1 H, H-4^{B}), 3.33 (1 H, H-4^{E}), 3.34 (1 H, H-6b^{D}), 3.41 (s, 3 H, OMe-6), 3.44 (1 H, H-6b^{A}), 3.46 (s, 3 H, OMe-2), 3.47 (1 H, H-6b^{E}), 3.47 (s, 3 H, OMe-2), 3.48 (s, 3 H, OMe-2), 3.49 (s, 3 H, OMe-2), 3.50 (s, 3 H, OMe-2), 3.51 (1 H, H-3^{E}), 3.54 (1 H, H-3^{B}), 3.54 (s, 3 H, OMe-2), 3.55 (1 H, H-3^{F}), 3.55 (s, 3 H, OMe-2), 3.56 (1 H, H-6a^{G}), 3.57 (1 H, H-3^{C}), 3.58 (1 H, H-4^{F}), 3.59 (1 H, H-4^{C}), 3.60 (1 H, H-3^{G}), 3.64 (s, 6 H, OMe-3), 3.67 (1 H, H-3^{D}), 3.67 (s, 6 H, OMe-3), 3.68 (s, 3 H, OMe-3), 3.69 (s, 3 H, OMe-3), 3.71 (1 H, H-4^{G}), 3.72 (1 H- H-6b^{B}), 3.75 (s, 3 H, OMe-3),

3.77 (1 H, H-3^{A}), 3.93 (dd, 1 H, $^{2}J_{\text{H-6a,H-6b}}$ = 10.9 Hz, $^{3}J_{\text{H-6a,H-5}}$ =1.6 Hz, H-6a^{C}), 3.94 (d, 1 H, $^{3}J_{\text{H-6b,H-5}}$ = 1.6 Hz, H-6b^{F}), 3.95 (dd, 1 H, $^{2}J_{\text{H-6a,H-6b}}$ = 11.5 Hz, $^{3}J_{\text{H-6a,H-5}}$ =1.8 Hz, H-6a^{G}), 4.01 (dt, 1 H, $^{3}J_{\text{H-5,H-4}}$ = 9.6 Hz, $^{3}J_{\text{H-5,H-6a}}$ = $^{3}J_{\text{H-5,H-6b}}$ = 2.1 Hz, H-5^{F}), 4.11 (1 H, H-6b^{C}), 4.12 (1 H, H-6b^{F}), 4.13 (1 H, H-5^{G}), 4.21 (m, 1 H, H-5^{E}), 4.32 (d, 1 H, $^{3}J_{\text{H-5,H-4}}$ = 9.5 Hz, H-5^{C}), 4.34 (t, 1 H, $^{3}J_{\text{H-5,H-4}}$ = $^{3}J_{\text{H-5,H-6b}}$ = 12.0 Hz, H-5^{B}), 4.46 (m, 1 H, H-5^{A}), 4.64 (m, 1 H, H-5^{D}), 4.91 (d, 1 H, $^{3}J_{\text{H-1,H-2}}$ = 3.6 Hz, H-1^{C}), 4.96 (d, 1 H, $^{3}J_{\text{H-1,H-2}}$ = 3.3 Hz, H-1^{D}), 5.01 (d, 1 H, $^{3}J_{\text{H-1,H-2}}$ = 2.4 Hz, H-1^{A}), 5.02 (d, 1 H, $^{3}J_{\text{H-1,H-2}}$ = 2.5 Hz, H-1^{E}), 5.05 (d, 1 H, $^{3}J_{\text{H-1,H-2}}$ = 4.5 Hz, H-1^{F}), 5.06 (d, 1 H, $^{3}J_{\text{H-1,H-2}}$ = 5.1 Hz, H-1^{B}), 5.08 (d, 1 H, $^{3}J_{\text{H-1,H-2}}$ = 3.6 Hz, H-1^{G}), 7.46–7.50 (6 H, *m*-H, *p*-H), 7.89 (ddd, 2 H, $^{3}J_{o\text{-H,P}}$ = 13.0 Hz, $^{3}J_{o\text{-H},m\text{-H}}$ = 7.6 Hz, $^{3}J_{o\text{-H},p\text{-H}}$ = 1.7 Hz, *o*-H(P1)), 8.01 (ddd, 2 H, $^{3}J_{o\text{-H,P}}$ = 12.9 Hz, $^{3}J_{o\text{-H},m\text{-H}}$ = 7.8 Hz, $^{4}J_{o\text{-H},p\text{-H}}$ = 1.6 Hz, *o*-H(P2)) ppm; ^{13}C{^{1}H} NMR (125.8 MHz, $CDCl_3$, 25ºC): δ (assignment by HMQC) = 29.19 (d, $^{1}J_{\text{C,P}}$ = 37.9 Hz, C-6^{E}), 31.34 (d, $^{1}J_{\text{C,P}}$ = 34.6 Hz, C-6^{B}), 37.75 (d, $^{1}J_{\text{C,P}}$ = 32.5 Hz, C-6^{D}), 40.76 (d, $^{1}J_{\text{C,P}}$ = 32.5 Hz, C-6^{A}), 58.17, 58.28, 58.36, 58.43, 58.49, 58.94, 59.28, 59.34, 59.52, 59.91, 61.80, 61.85, 62.01, 62.13, 62.27, 62.32, 62.59 (OMe), 65.24 (C-5^{E}), 65.33 (d, $^{2}J_{\text{C,P}}$ = 4.7 Hz, C-5^{B}), 70.61 (d, $^{2}J_{\text{C,P}}$ = 6.5 Hz, C-5^{A}), 71.18 (C-5^{G}), 71.22 (C-5^{C}), 71.32 (C-5^{F}), 71.75 (C-6^{G}), 72.90 (C-6^{F}), 73.15 (C-6^{C}), 72.98 (C-5^{D}), 80.00, 80.75, 81.50 [×2], 81.87, 81.93, 81.97, 82.30, 82.55 [×2], 82.67, 82.70, 82.88, 83.04 [×2], 83.18, 84.10 (C-2, C-3, C-4^{C,F,G}), 86.34 (d, $^{3}J_{\text{C,P}}$ = 12.6 Hz), 86.45 (d, $^{3}J_{\text{C,P}}$ = 10.6 Hz) (C-4^{B,E}), 88.88 (d, $^{3}J_{\text{C,P}}$ = 4.2 Hz, C-4^{D}), 90.68 (d, $^{3}J_{\text{C,P}}$ = 4.0 Hz, C-4^{A}), 98.87 (C-1^{E}), 98.94 (C-1^{B}), 99.91 (C-1^{A}), 100.29 (C-1^{D}), 100.54 (C-1^{G}), 100.60 (C-1^{C}), 101.27 (C-1^{F}), 129.51 [×2] (overlapping d, $^{3}J_{\text{C,P}}$ = 11.7 Hz, *m*-C), 130.99 (d, $^{1}J_{\text{C,P}}$ = 61.9 Hz, *ipso*-C), 132.12, 132.32 (*p*-C), 133.19 (d, $^{1}J_{\text{C,P}}$ = 61.9 Hz, *ipso*-C), 133.50 (d, $^{2}J_{\text{C,P}}$ = 14.1 Hz, *o*-CP(P2), 133.69 (d, $^{2}J_{\text{C,P}}$ = 14.1 Hz, *o*-C(P1)) ppm; ^{31}P{^{1}H} NMR (121.5 MHz, $CDCl_3$, 25ºC): δ = 22.8 (s, P1), 31.5 (s, P2) ppm; elemental analysis (%) calcd for $C_{71}H_{110}Cl_2O_{31}P_2Au_2 \cdot C_7H_8$ (1986.40 + 92.14): C 45.07, H 5.72, found: C 45.11, H 6.00; MS (ESI-TOF): *m/z* (%): 2025.41 (67) $[M + K]^+$, 2007.43 (100) $[M + Na]^+$.

***P,P'*-Dibromido-{6^{A},6^{B},6^{D},6^{E}-tetradeoxy-6^{A},6^{B}:6^{D},6^{E}-bis[(*R*)-phenylphosphinidene]-2^{A},2^{B},2^{C},2^{D},2^{E},2^{F},2^{G},3^{A},3^{B},3^{C},3^{D},3^{E},3^{F},3^{G},6^{C},6^{F},6^{G}-heptadeca-*O*-methyl-β-cyclodextrin} digold(I) (37)**

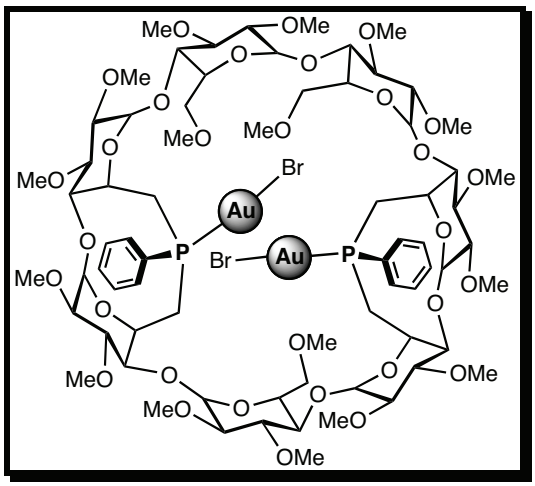

To a stirred solution of **36** (0.100 g, 0.050 mmol) in degassed acetone (5 mL) was added KBr (0.030 g, 0.25 mmol). After 12 h at reflux, the reaction mixture was cooled to room temperature and filtered over celite. The solvent was then removed *in vacuo* affording complex **37** (yield: 0.102 g, 98%) as a pale brown powder. R_f (SiO_2, CH_2Cl_2/MeOH, 92:8, *v*/*v*) = 0.40; m.p. dec. >250ºC; ^{1}H NMR (400.1 MHz, $CDCl_3$, 25ºC): δ (assignment by COSY) = 2.13–2.23 (2 H, H-6a$^{A,D\text{ or }B,E}$), 2.31 (td, 2 H, $^{2}J_{H\text{-}6a,H\text{-}6b} = {}^{2}J_{H\text{-}6a,P}$ = 13.1 Hz, $^{3}J_{H\text{-}6a,H\text{-}5}$ = 12.9 Hz, H-6a$^{B,E\text{ or }A,D}$), 3.04-3.87 (28 H, H-2, H-3, H-4, H-6a^{C,F,G}, H-6b^{A,B,D,E}), 3.19 (s, 3 H, OMe), 3.29 (s, 3 H, OMe), 3.45 (s, 3 H, OMe), 3.47 (s, 6 H, OMe), 3.48 (s, 6 H, OMe), 3.49 (s, 3 H, OMe), 3.55 (s, 3 H, OMe), 3.57 (s, 3 H, OMe), 3.61 (s, 3 H, OMe), 3.64 (s, 3 H, OMe), 3.66 (s, 3 H, OMe), 3.68 (s, 3 H, OMe), 3.69 (s, 3 H, OMe), 3.70 (s, 3 H, OMe), 3.78 (s, 3 H, OMe), 3.94 (dd, 1 H, $^{2}J_{H\text{-}6a,H\text{-}6b}$ = 10.9 Hz, $^{3}J_{H\text{-}6a,H\text{-}5}$ =2.9 Hz, H-6b$^{C\text{ or }F\text{ or }G}$), 4.00–4.37 (7 H, H-5^{B,C,E,F,G}, H-6b$^{F,G\text{ or }C,G\text{ or }C,F}$), 4.50 (m, 1 H, H-5$^{A\text{ or }D}$), 4.66 (m, 1 H, H-5$^{D\text{ or }A}$), 4.88 (d, 1 H, $^{3}J_{H\text{-}1,H\text{-}2}$ = 3.5 Hz, H-1), 4.97 (d, 1 H, $^{3}J_{H\text{-}1,H\text{-}2}$ = 2.9 Hz, H-1), 5.01-5.02 (2 H, H-1), 5.03 (d, 1 H, $^{3}J_{H\text{-}1,H\text{-}2}$ = 5.2 Hz, H-1), 5.06 (d, 1 H, $^{3}J_{H\text{-}1,H\text{-}2}$ = 4.6 Hz, H-1), 5.10 (d, 1 H, $^{3}J_{H\text{-}1,H\text{-}2}$ = 3.4 Hz, H-1), 7.46–7.52 (6 H, *m*-H, *p*-H), 7.90 (ddd, 2 H, $^{3}J_{o\text{-}H,P}$ = 13.0 Hz, $^{3}J_{o\text{-}H,m\text{-}H}$ = 7.3 Hz, $^{4}J_{o\text{-}H,p\text{-}H}$ = 1.7 Hz, *o*-H), 8.03 (ddd, 2 H, $^{3}J_{o\text{-}H,P}$ = 13.0 Hz, $^{3}J_{o\text{-}H,m\text{-}H}$ = 6.5 Hz, $^{4}J_{o\text{-}H,p\text{-}H}$ = 3.2 Hz, *o*-H) ppm; ^{13}C{^{1}H} NMR (75.5 MHz, $CDCl_3$, 25ºC): δ (assignment by HMQC) = 28.79 (d, $^{1}J_{C,P}$ = 36.8 Hz), 30.85 (d, $^{1}J_{C,P}$ = 32.6 Hz), 37.48 (d, $^{1}J_{C,P}$ = 32.2 Hz), 40.55 (d, $^{1}J_{C,P}$ = 30.4 Hz) (C-6^{A,B,D,E}), 57.67, 57.82, 57.88, 57.99, 58.16, 58.31, 58.76, 59.04, 59.19, 59.68, 61.26,

61.31, 61.49, 61.60, 61.83, 62.05, 62.34 (OMe), 65.04 (d, $^{2}J_{C,P}$ = 3.4 Hz), 65.09 (d, $^{2}J_{C,P}$ = 4.6 Hz), 70.16 (d, $^{2}J_{C,P}$ = 6.3 Hz), 70.69 (d, $^{2}J_{C,P}$ = 6.5 Hz) (C-$5^{A,B,D,E}$), 70.77 [×2], 72.39 (C-$5^{C,F,G}$), 71.41, 72.58, 72.94 (C-$6^{C,F,G}$), 79.42, 80.07, 80.98, 81.07, 81.39 [×3], 81.84, 81.90, 82.13, 82.20, 82.40, 82.46, 82.62 [×3], 83.61 (C-2, C-3, C-$4^{C,F,G}$), 86.20 (d, $^{3}J_{C,P}$ = 10.2 Hz), 86.72 (d, $^{3}J_{C,P}$ = 12.4 Hz), 88.62 (d, $^{3}J_{C,P}$ = 3.9 Hz), 90.46 (d, $^{3}J_{C,P}$ = 3.4 Hz) (C-$4^{A,B,D,E}$), 98.63 [×2], 99.55, 99.96, 100.14, 100.27, 100.97 (C-1), 128.98 (d, $^{3}J_{C,P}$ = 11.4 Hz, *m*-C), 129.13 (d, $^{3}J_{C,P}$ = 11.6 Hz, *m*-C), 130.74 (d, $^{1}J_{C,P}$ = 59.9 Hz, *ipso*-C), 131.62, 131.99 (*p*-C), 132.99 (d, $^{2}J_{C,P}$ = 8.3 Hz, *o*-C), 133.17 (d, $^{2}J_{C,P}$ = 9.3 Hz, *o*-C), 133.30 (d, $^{1}J_{C,P}$ = 59.8 Hz, *ipso*-C) ppm; $^{31}P\{^{1}H\}$ NMR (121.5 MHz, $CDCl_3$, 25ºC): δ = 23.5 (s), 32.4 (s) ppm; elemental analysis (%) calcd for $C_{71}H_{110}Br_2O_{31}P_2Au_2 \cdot 2CHCl_3$ (2075.30 + 238.76): C 37.89, H 4.88, found: C 37.66, H 5.16; MS (ESI-TOF): *m/z* (%): 2097.45 (35) $[M + K]^+$, 2053.50 (30) $[M + Na]^+$, 1995.54 (100) $[M - Br]^+$.

_P,P'_-Diiodido-{6^{A},6^{B},6^{D},6^{E}-tetradeoxy-6^{A},6^{B}:6^{D},6^{E}-bis[(*R*)-phenylphosphinidene]-2^{A},2^{B},2^{C},2^{D},2^{E},2^{F},2^{G},3^{A},3^{B},3^{C},3^{D},3^{E},3^{F},3^{G},6^{C},6^{F},6^{G}-heptadeca-*O*-methyl-β-cyclodextrin}digold(I) (38)

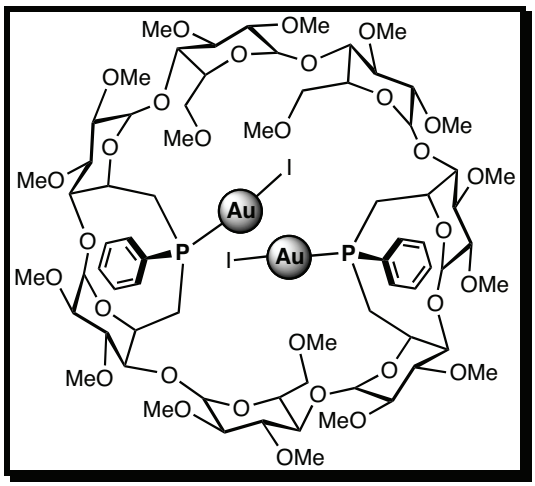

To a stirred solution of **36** (0.100 g, 0.050 mmol) in degassed acetone (5 mL) was added NaI (0.037 g, 0.25 mmol). After 12 h at reflux, the reaction mixture was cooled to room temperature and evaporated to dryness. The residue was taken in CH_2Cl_2 (30 mL) and filtered over celite. The solvent was then removed *in vacuo* affording complex **38** (yield: 0.106 g, 98%) as a pale brown powder. R_f (SiO_2, CH_2Cl_2/MeOH, 92:8, *v*/*v*) = 0.40; m.p. dec. >250ºC; ^{1}H NMR (300.1 MHz, $CDCl_3$, 25ºC): δ (assignment by COSY) = 2.11–2.32 (4 H,

H-6a^{A,B,D,E}), 3.03–3.89 (28 H, H-2, H-3, H-4, H-6a^{C,F,G}, H-6b^{A,B,D,E}), 3.27 (s, 3 H, OMe), 3.38 (s, 3 H, OMe), 3.46 (s, 3 H, OMe), 3.47 (s, 9 H, OMe), 3.48 (s, 6 H, OMe), 3.55 (s, 3 H, OMe), 3.58 (s, 3 H, OMe), 3.59 (s, 3 H, OMe), 3.64 (s, 3 H, OMe), 3.65 (s, 3 H, OMe), 3.68 (s, 3 H, OMe), 3.69 (s, 3 H, OMe), 3.71 (s, 3 H, OMe), 3.81 (s, 3 H, OMe), 3.98 (dd, 1 H, $^{2}J_{\text{H-6b,H-6a}}$ = 11.0 Hz, $^{3}J_{\text{H-6b,H-5}}$ =2.3 Hz, H-6b$^{C\text{ or }F\text{ or }G}$), 4.10–4.19 (3 H, H-5^{C,F,G}), 4.27 (m, 1 H, H-5$^{D\text{ or }E}$), 4.37 (d, 1 H, $^{2}J_{\text{H-6b,H-6a}}$ = 9.3 Hz, H-6b$^{F\text{ or }G\text{ or }C}$), 4.39 (m, 1 H, H-5$^{E\text{ or }D}$), 4.44 (d, 1 H, $^{2}J_{\text{H-6b,H-6a}}$ = 9.3 Hz, H-6b$^{G\text{ or }C\text{ or }F}$), 4.55 (m, 1 H, H-5$^{A\text{ or }D}$), 4.73(m, 1 H, H-5$^{D\text{ or }A}$), 4.88 (d, 1 H, $^{3}J_{\text{H-1,H-2}}$ = 3.2 Hz, H-1), 4.99–5.04 (2 H, H-1), 5.01 (d, 2 H, $^{3}J_{\text{H-1,H-2}}$ = 3.7 Hz, H-1), 5.06 (d, 1 H, $^{3}J_{\text{H-1,H-2}}$ = 4.7 Hz, H-1), 5.11 (d, 1 H, $^{3}J_{\text{H-1,H-2}}$ = 3.3 Hz, H-1), 7.45–7.52 (6 H, *m*-H, *p*-H), 7.84–7.98 (4 H, *o*-H) ppm; $^{13}C\{^{1}H\}$ NMR (75.5 MHz, $CDCl_3$, 25ºC): δ (assignment by HMQC) = 37.08 (d, $^{1}J_{C,P}$ = 28.1 Hz), 37.51 (d, $^{1}J_{C,P}$ = 29.1 Hz), 40.15 (d, $^{1}J_{C,P}$ = 26.3 Hz), 40.85 (d, $^{1}J_{C,P}$ = 27.9 Hz) (C-6^{A,B,D,E}), 57.66, 57.85, 58.09 [×2], 58.19, 58.63, 58.97, 59.46 [×2], 60.02, 61.30, 61.43, 61.67, 61.72, 62.01, 62.34, 62.64 (OMe), 65.27, 65.60, 70.25 (d, $^{2}J_{C,P}$ = 8.0 Hz), 70.60 (C-5^{A,B,D,E}), 70.87, 70.97, 72.40 (C-5^{C,F,G}), 71.58, 72.53, 73.20 (C-6^{C,F,G}), 79.46, 80.04, 81.18, 81.39, 81.52, 81.56, 81.73, 81.88, 82.13, 82.32, 82.41, 82.48, 82.54, 82.79, 82.84, 82.93, 83.81, 87.15, 88.84, 89.92, 90.68 (C-2, C-3, C-4), 98.86, 98.89, 99.89, 100.01, 100.39, 100.80, 101.20 (C-1), 129.12 (d, $^{3}J_{C,P}$ = 12.0 Hz, *m*-C), 129.31 (d, $^{3}J_{C,P}$ = 12.0 Hz, *m*-C), 130.31 (d, $^{1}J_{C,P}$ = 33.7 Hz, *ipso*-C), 131.63, 132.05 (*p*-C), 132.74 (d, $^{2}J_{C,P}$ = 12.6 Hz, *o*-C), 133.11 (d, $^{2}J_{C,P}$ = 31.9 Hz, *o*-C), 135.65 (d, $^{1}J_{C,P}$ = 36.4 Hz, *ipso*-C) ppm; $^{31}P\{^{1}H\}$ NMR (121.5 MHz, $CDCl_3$, 25ºC): δ = 23.4 (s), 33.3 (s) ppm; elemental analysis (%) calcd for $C_{71}H_{110}I_2O_{31}P_2Au_2$ (2169.30): C 39.31, H 5.11, found: C 39.15, H 5.21; MS (ESI-TOF): *m/z* (%): 2207.34 (10) $[M + K]^+$, 2191.36 (100) $[M + Na]^+$, 2041.48 (50) $[M - Br]^+$.

***P*-Chlorido-{6^{A},6^{B}-dideoxy-6^{A},6^{B}-[(*R*)-phenylphosphinidene]-2^{A},2^{B},2^{C},2^{D},2^{E},2^{F},2^{G}, 3^{A},3^{B},3^{C},3^{D},3^{E},3^{F},3^{G},6^{C},6^{D}6^{E},6^{F},6^{G}-nonadeca-*O*-methyl-β-cyclodextrin}gold(I) (39)**

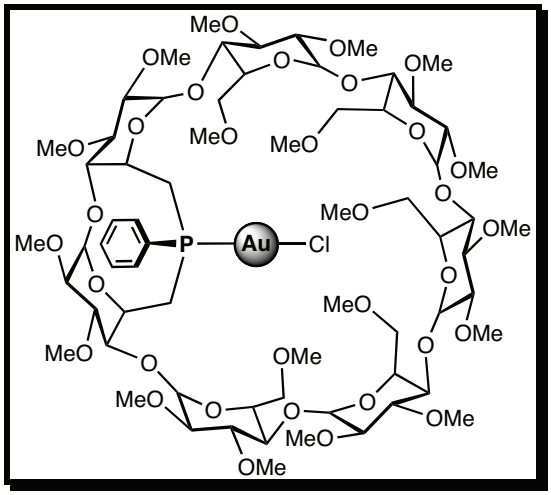

To a stirred solution of monophosphane **L** (0.100 g, 0.067 mmol) in CH_2Cl_2 (10 mL) was added a solution of [AuCl(tht)] (0.021 g, 0.067 mmol) in CH_2Cl_2 (5 mL). After 30 min, the reaction mixture was evaporated to dryness and the residue subjected to column chromatography (SiO_2, CH_2Cl_2/MeOH, 96:4, *v*/*v*) to give pure **39** (yield: 0.114 g, 100%) as a colourless powder. R_f (SiO_2, CH_2Cl_2/MeOH, 92:8, *v*/*v*) = 0.40; m.p. dec. >250ºC; ^{1}H NMR (300.1 MHz, $CDCl_3$, 25ºC): δ (assignment by COSY) = 2.07 (t, 1 H, $^{2}J_{H\text{-}6a,H\text{-}6b} = {}^{2}J_{H\text{-}6a,P} = 14.5$ Hz, H-6a$^{A\text{ or }B}$), 2.27 (td, 1 H, $^{2}J_{H\text{-}6a,H\text{-}6b} = {}^{2}J_{H\text{-}6a,P} = 13.5$ Hz, $^{3}J_{H\text{-}6a,H\text{-}5} = 12.1$ Hz, H-6b$^{B\text{ or }A}$), 3.15–4.11 (39 H, H-2, H-3, H-4, H-5$^{B\text{ or A and C,D,E,F,G}}$, H-6^{C,D,E,F,G}, H-6b^{A,B}), 3.19 (s, 3 H, OMe), 3.21 (s, 3 H, OMe), 3.37 (s, 9 H, OMe), 3.43 (s, 3 H, OMe), 3.45 (s, 12 H, OMe), 3.48 (s, 3 H, OMe), 3.52 (s, 3 H, OMe), 3.57 (s, 6 H, OMe), 3.59 (s, 3 H, OMe), 3.61 (s, 3 H, OMe), 3.62 (s, 6 H, OMe), 3.66 (s, 3 H, OMe), 4.47 (m, 1 H, H-5$^{A\text{ or }B}$), 4.88 (d, 1 H, $^{3}J_{H\text{-}1,H\text{-}2}$ = 3.1 Hz, H-1), 4.98 (2 H. H-1), 5.07 (d, 1 H, $^{3}J_{H\text{-}1,H\text{-}2} = 2.9$ Hz, H-1), 5.11 (d, 1 H, $^{3}J_{H\text{-}1,H\text{-}2}$ = 2.9 Hz, H-1), 5.14 (2 H, H-1), 7.47–7.52 (3 H, *m*-H, *p*-H), 7.76 (dd, 2 H, $^{3}J_{o\text{-}H,P}$= 12.7 Hz, $^{3}J_{o\text{-}H,m\text{-}H} = 6.9$ Hz, *o*-H) ppm; ^{13}C{^{1}H} NMR (75.5 MHz, $CDCl_3$, 25ºC): δ (assignment by HMQC) = 29.78 (d, $^{1}J_{C,P} = 36.1$ Hz, C-6$^{B\text{ or }A}$), 36.91 (d, $^{1}J_{C,P} = 34.2$ Hz, C-6$^{A\text{ or }B}$), 57.93, 58.00, 58.07, 58.21 [×2], 58.44, 58.66, 58.92 [×3], 59.04 [×2], 61.13 [×2], 61.53, 61.57, 61.69, 61.73, 61.95 (OMe), 64.73 (C-5$^{B\text{ or }A}$), 70.59 [×3], 70.85, 70.95 (C-5^{C,D,E,F,G}), 70.76, 71.00, 71.08, 72.10, 72.29 (C-6^{C,D,E,F,G}), 72.55 (d, $^{2}J_{C,P} = 11.4$ Hz, C-5$^{A\text{ or }B}$), 78.66, 78.80, 79.96, 80.89, 81.18, 81.32, 81.51[×2], 81.81 [×3], 81.92 [×3], 82.17 [×2], 82.29, 82.41, 83.09 (C-2, C-3, C-4^{C,D,E,F,G}), 86.16 (d, $^{3}J_{C,P} = 12.0$ Hz, C-4$^{B\text{ or }A}$), 88.81 (d, $^{3}J_{C,P} = 3.4$ Hz, C-4$^{A\text{ or }B}$),

98.76, 98.85, 99.16, 99.66, 100.04, 100.19, 100.26 (C-1), 129.32 (d, $^{3}J_{C,P}$ = 11.5 Hz, *m*-C), 130.98 (d, $^{1}J_{C,P}$ = 62.4 Hz, *ipso*-C), 132.30 (*p*-C), 132.38 (d, $^{2}J_{C,P}$ = 12.4 Hz, *o*-C) ppm; $^{31}P\{^{1}H\}$ NMR (121.5 MHz $CDCl_3$, 25ºC): δ = 31.0 (s) ppm; elemental analysis (%) calcd for $C_{67}H_{111}AuClO_{33}P\cdot 0.5CHCl_3$ (1707.97 + 59.69): C 45.86, H 6.36, found: C 45.52, H 6.53; MS (ESI-TOF): *m/z* (%): 1729.60 (100) $[M + Na]^{+}$.

***P*-Bromido-{6^{A},6^{B}-Dideoxy-6^{A},6^{B}-[(*R*)-phenylphosphinidene]-2^{A},2^{B},2^{C},2^{D},2^{E},2^{F},2^{G}, 3^{A},3^{B},3^{C},3^{D},3^{E},3^{F},3^{G},6^{C},6^{D}6^{E},6^{F},6^{G}-nonadeca-*O*-methyl-β-cyclodextrin}gold(I) (40)**

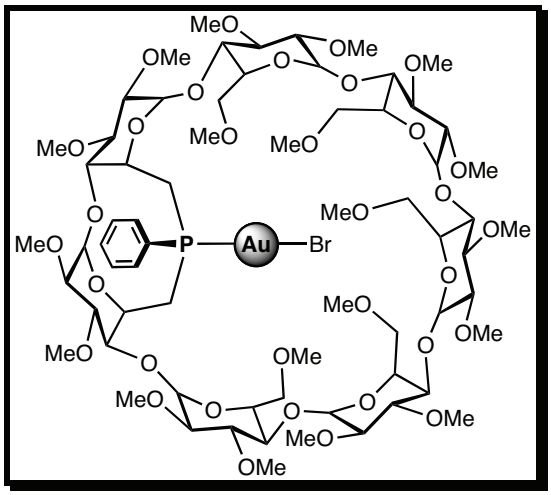

To a stirred solution of **39** (0.100 g, 0.059 mmol) in degassed acetone (5 mL) was added KBr (0.036 g, 0.30 mmol). After 12 h at reflux, the reaction mixture was cooled to room temperature and filtered over celite. The solvent was then removed at vacuum affording complex **40** (yield: 0.102 g, 98%) as a pale brown powder. R_f (SiO_2, CH_2Cl_2/MeOH, 92:8, *v*/*v*) = 0.40; m.p. dec. >250ºC; ^{1}H NMR (400.1 MHz, $CDCl_3$, 25ºC): δ (assignment by COSY) = 2.13 (t, 1 H, $^{2}J_{H\text{-}6a,H\text{-}6b} = {}^{2}J_{H\text{-}6a,P}$ = 14.3 Hz, H-6a$^{A\text{ or }B}$), 2.28 (td, 1 H, $^{2}J_{H\text{-}6a,H\text{-}6b} = {}^{2}J_{H\text{-}6a,P}$ = 13.1 Hz, $^{3}J_{H\text{-}6a,H\text{-}5}$ = 11.6 Hz, H-6b$^{B\text{ or }A}$), 3.08–4.16 (39 H, H-2, H-3, H-4, H-5$^{B\text{ or A and C,D,E,F,G}}$, H-6^{C,D,E,F,G}, H-6b^{A,B}), 3.20 (s, 3 H, OMe), 3.21 (s, 3 H, OMe), 3.40 (s, 3 H, OMe), 3.41 (s, 3 H, OMe), 3.42 (s, 3 H, OMe), 3.47 (s, 3 H, OMe), 3.48 (s, 9 H, OMe), 3.50 (s, 3 H, OMe), 3.52 (s, 3 H, OMe), 3.56 (s, 3 H, OMe), 3.60 (s, 3 H, OMe), 3.61 (s, 3 H, OMe), 3.64 (s, 6 H, OMe), 3.66 (s, 3 H, OMe), 3.67 (s, 3 H, OMe), 3.71 (s, 3 H, OMe), 4.51 (m, 1 H, H-5$^{A\text{ or }B}$), 4.92 (d, 1 H, $^{3}J_{H\text{-}1,H\text{-}2}$ = 3.5 Hz, H-1), 5.00 (d, 1 H, $^{3}J_{H\text{-}1,H\text{-}2}$ = 4.2 Hz, H-1), 5.01 (d, 1 H, $^{3}J_{H\text{-}1,H\text{-}2}$ = 2.8 Hz, H-1), 5.11 (d, 1 H, $^{3}J_{H\text{-}1,H\text{-}2}$ = 2.9 Hz, H-1), 5.11 (d, 1 H, $^{3}J_{H\text{-}1,H\text{-}2}$ = 4.2 Hz, H-1), 5.12 (d, 1 H, $^{3}J_{H\text{-}1,H\text{-}2}$ = 4.0 Hz, H-1), 5.15 (d, 1 H, $^{3}J_{H\text{-}1,H\text{-}2}$ = 3.4 Hz, H-1), 5.16 (d, 1 H,

$^{3}J_{\text{H-1,H-2}}$ = 3.5 Hz, H-1), 7.48–7.56 (3 H, *m*-H, *p*-H), 7.79 (ddd, 2 H, $^{3}J_{o\text{-H,P}}$= 12.9 Hz, $^{3}J_{o\text{-H},m\text{-H}}$ = 7.8 Hz, $^{4}J_{o\text{-H},p\text{-H}}$ = 1.4 Hz, *o*-H) ppm; $^{13}C\{^{1}H\}$ NMR (75.5 MHz, $CDCl_3$, 25ºC): δ (assignment by HMQC) = 29.55 (d, $^{1}J_{C,P}$ = 26.4 Hz, C-$6^{B\text{ or }A}$), 36.95 (d, $^{1}J_{C,P}$ = 25.3 Hz, C-$6^{A\text{ or }B}$), 58.08, 58.13, 58.19, 58.29, 58.35, 58.45, 58.79, 59.06 [×3], 59.13, 59.16, 61.23, 61.43, 61.63, 61.70, 61.80, 61.88, 62.20 (OMe), 64.93 (C-$5^{B\text{ or }A}$), 70.59, 70.72, 70.85 [×2], 71.03 (C-$5^{C,D,E,F,G}$), 70.91, 71.17, 71.26, 72.29, 72.35 (C-$6^{C,D,E,F,G}$), 72.59 (d, $^{2}J_{C,P}$ = 12.0 Hz, C-$5^{A\text{ or }B}$), 79.62, 80.08 [×2], 81.09, 81.38, 81.57 [×2], 81.67 [×3], 81.86, 82.11, 82.20 [×2], 82.30, 82.37 [×2], 82.56, 83.31 (C-2, C-3, C-$4^{C,D,E,F,G}$), 86.63 (d, $^{3}J_{C,P}$ = 12.0 Hz, C-$4^{B\text{ or }A}$), 88.95 (d, $^{3}J_{C,P}$ = 3.4 Hz, C-$4^{A\text{ or }B}$), 99.07, 99.35, 99.79 [×2], 99.95, 100.28, 100.70 (C-1), 129.42 (d, $^{3}J_{C,P}$ = 11.5 Hz, *m*-C), 131.28 (d, $^{1}J_{C,P}$ = 60.9 Hz, *ipso*-C), 132.40 (d, $^{2}J_{C,P}$ = 12.8 Hz, *o*-C), 132.41 (*p*-C) ppm; $^{31}P\{^{1}H\}$ NMR (121.5 MHz $CDCl_3$, 25ºC): δ = 34.0 (s) ppm; elemental analysis (%) calcd for $C_{67}H_{111}AuBrO_{33}P{\cdot}CH_2Cl_2$ (1752.42 + 84.93): C 44.45, H 6.20, found: C 44.40, H 6.17; MS (ESI-TOF): *m/z* (%): 1775.59 (25) $[M + Na]^{+}$.

_P_-Iodido-{6^{A},6^{B}-Dideoxy-6^{A},6^{B}-[(_R_)-phenylphosphinidene]-2^{A},2^{B},2^{C},2^{D},2^{E},2^{F},2^{G},3^{A},3^{B},3^{C},3^{D},3^{E},3^{F},3^{G},6^{C},$6^{D}6^{E}$,6^{F},6^{G}-nonadeca-_O_-methyl-β-cyclodextrin}gold(I) (41)

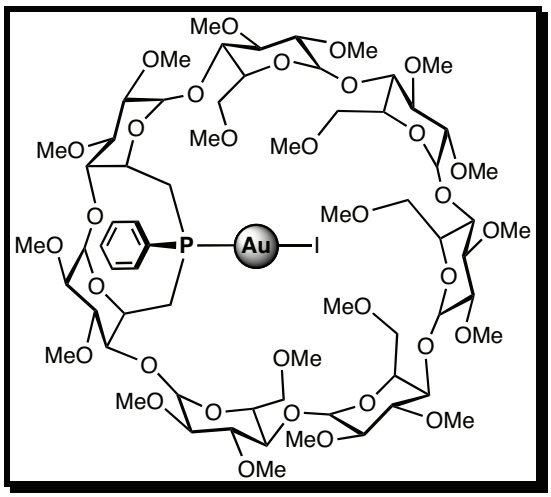

To a stirred solution of **39** (0.100 g, 0.059 mmol) in degassed acetone (5 mL) was added NaI (0.045 g, 0.30 mmol). After 12 h at reflux, the reaction mixture was cooled to room temperature and evaporated to dryness. The residue was taken in CH_2Cl_2 (30 mL) and filtered over celite. The solvent was then removed *in vacuo* affording complex **41** (yield: 0.104 g, 98%) as a pale brown powder. R_f (SiO_2, CH_2Cl_2/MeOH, 92:8, *v*/*v*) = 0.40; m.p. dec. >250ºC; ^{1}H NMR (300.1 MHz, $CDCl_3$, 25ºC): δ (assignment by COSY) = 2.11–2.38 (2 H, H-$6a^{A,B}$),

3.08–3.75 (28 H, H-2, H-3, H-4, H-6a^{C,D,E,F,G}, H-6b^{A,B}), 3.19 (s, 6 H, OMe), 3.40 (s, 3 H, OMe), 3.41 (s, 3 H, OMe), 3.42 (s, 3 H, OMe), 3.47 (s, 3 H, OMe), 3.48 (s, 9 H, OMe), 3.50 (s, 3 H, OMe), 3.52 (s, 3 H, OMe), 3.56 (s, 3 H, OMe), 3.60 (s, 3 H, OMe), 3.62 (s, 3 H, OMe), 3.64 (s, 3 H, OMe), 3.66 (s, 3 H, OMe), 3.67 (s, 6 H, OMe), 3.71 (s, 3 H, OMe), 3.80–4.20 (11 H, H-5$^{A \text{ or } B \text{ and } C,D,E,F,G}$, H-6b^{C,D,E,F,G}), 4.57 (m, 1 H, H-5$^{B \text{ or } A}$), 4.94 (d, 1 H, $^{3}J_{H\text{-}1,H\text{-}2}$ = 3.1 Hz, H-1), 5.00 (d, 2 H, $^{3}J_{H\text{-}1,H\text{-}2}$ = 4.0 Hz, H-1), 5.09 (d, 1 H, $^{3}J_{H\text{-}1,H\text{-}2}$ = 3.2 Hz, H-1), 5.11 (d, 1 H, $^{3}J_{H\text{-}1,H\text{-}2}$ = 3.7 Hz, H-1), 5.14 (d, 2 H, $^{3}J_{H\text{-}1,H\text{-}2}$ = 3.3 Hz, H-1), 7.50–7.53 (3 H, *m*-H, *p*-H), 7.79 (dd, 2 H, $^{3}J_{o\text{-}H,P}$= 12.5 Hz, $^{3}J_{o\text{-}H,m\text{-}H}$ = 7.8 Hz, *o*-H) ppm; $^{13}C\{^{1}H\}$ NMR (75.5 MHz, $CDCl_3$, 25ºC): δ (assignment by HMQC) = 29.06 (d, $^{1}J_{C,P}$ = 32.5 Hz, C-6$^{B \text{ or } A}$), 36.9 (d, $^{1}J_{C,P}$ = 30.2 Hz, C-6$^{A \text{ or } B}$), 58.03 [×2], 58.12 [×2], 58.26 [×2], 58.68, 58.98 [×4], 59.07, 61.08, 61.43, 61.47, 61.63, 61.67, 61.82, 62.22 (OMe), 64.92 (C-5$^{B \text{ or } A}$), 70.35, 70.44, 70.60 [×2], 70.94 (C-5^{C,D,E,F,G}), 70.83, 71.18 [×2], 72.28 [×2] (C-6^{C,D,E,F,G}), 72.41 (d, $^{2}J_{C,P}$ = 6.4 Hz, C-5$^{A \text{ or } B}$), 79.95, 80.23, 81.02, 81.07, 81.20, 81.31 [×2], 81.38, 81.52, 81.66, 81.93, 82.04 [×2], 82.23, 82.28, 82.41 [×2], 82.57, 83.27 (C-2, C-3, C-4^{C,D,E,F,G}), 86.72 (d, $^{3}J_{C,P}$ = 12.2 Hz, C-4$^{B \text{ or } A}$), 88.89 (d, $^{3}J_{C,P}$ = 3.5 Hz, C-4$^{A \text{ or } B}$), 98.99, 99.34, 99.72, 99.85, 100.25, 100.49, 100.74 (C-1), 129.31 (d, $^{3}J_{C,P}$ = 11.4 Hz, *m*-C), 131.40 (d, $^{1}J_{C,P}$ = 58.5 Hz, *ipso*-C), 132.13 (d, $^{2}J_{C,P}$ = 13.6 Hz, *o*-C), 132.22 (*p*-C) ppm; $^{31}P\{^{1}H\}$ NMR (121.5 MHz $CDCl_3$, 25ºC): δ = 38.9 (s) ppm; elemental analysis (%) calcd for $C_{67}H_{111}AuIO_{33}P$ (1799.42): C 44.72, H 6.22, found: C 44.86, H 6.07; MS (ESI-TOF): *m/z* (%): 1816.59 (15) $[M + H_2O + H]^+$, 1821.55 (25) $[M + Na]^+$.

_P,P'_-{6^{A},6^{B},6^{D},6^{E}-tetradeoxy-6^{A},6^{B}:6^{D},6^{E}-bis[(*R*)-phenylphosphinidene]-2^{A},2^{B},2^{C},2^{D},2^{E},2^{F},2^{G},3^{A},3^{B},3^{C},3^{D},3^{E},3^{F},3^{G},6^{C},6^{F},6^{G}-heptadeca-*O*-methyl-β-cyclodextrin}-di[chloro(*o*-dimethylbenzyl-aminomethylphenyl-*C,N*)]dipalladium(II) (42)

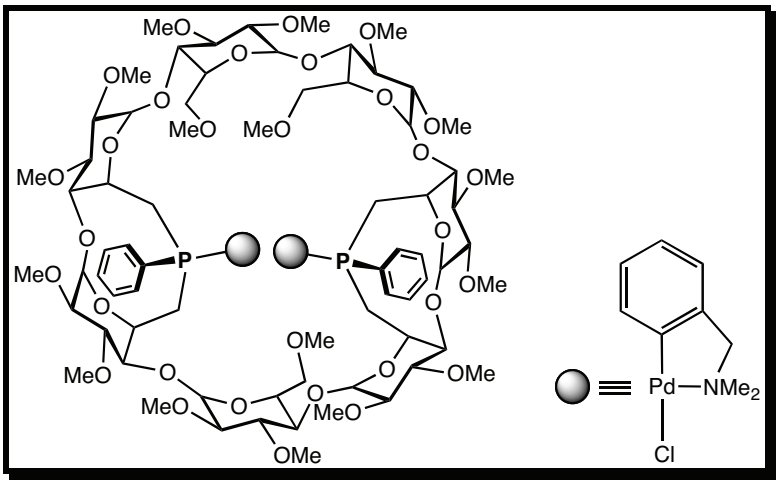

A solution of $[PdCl(dmba)]_2$ (0.033 g, 0.059 mmol) in CH_2Cl_2 (5 mL) was added to a solution of **WIDEPHOS** (0.090 g, 0.059 mmol) in CH_2Cl_2 (10 mL). After 30 min, the reaction mixture was evaporated to dryness and the residue subjected to column chromatography (SiO_2, CH_2Cl_2/MeOH, 96:4, *v*/*v*) to give pure **42** (yield: 0.121 g, 99%) as a yellow solid. R_f (SiO_2, CH_2Cl_2/MeOH, 92:8, *v*/*v*) = 0.45; m.p. dec. >250ºC; ^{1}H NMR (300 MHz, $CDCl_3$, 25ºC): δ (assignment by COSY) = 2.52 (br s, 3 H, NMe), 2.53–2.59 (3 H, H-2, H-6a^{A}), 2.62–2.85 (3 H, H-6a^{B,D,E}), 2.83 (br s, 3 H, NMe), 2.87 (br s, 3 H, NMe), 2.92 (br s, 3 H, NMe), 2.95–3.15 (3 H, H-2, H-4$^{B,D\text{ or }B,E\text{ or }D,E}$), 3.16 (dd, 2 H, $^3J_{H\text{-}2,H\text{-}3}$ = 9.7 Hz, $^3J_{H\text{-}2,H\text{-}1}$ = 3.1 Hz, H-2), 3.33–3.78 (21 H, H-2, H-3, H-4, H-6a$^{F,G\text{ or }C,G\text{ or }C,F}$, H-6b$^{A\text{ and }B,D\text{ or }B,E\text{ or }D,E}$), 3.35 (s, 3 H, OMe), 3.39 (s, 3 H, OMe), 3.40 (s, 3 H, OMe), 3.43 (s, 3 H, OMe), 3.45 (s, 6 H, OMe), 3.46 (s, 3 H, OMe), 3.50 (s, 3 H, OMe), 3.52 (s, 12 H, OMe), 3.57 (s, 3 H, OMe), 3.60 (s, 3 H, OMe), 3.63 (s, 3 H, OMe), 3.71 (s, 6 H, OMe), 3.88–3.92 (7 H, H-5$^{C,F\text{ or }C,G\text{ or }F,G}$, H-6a$^{C\text{ or }F\text{ or }G}$, H-6b$^{B\text{ or }D\text{ or }E\text{ and }F\text{ or }G\text{ or }C}$, NCHa, NCHa), 4.03 (d, 1 H, $^2J_{H\text{-}6b,H\text{-}6a}$ = 14.8 Hz, H-6b$^{G\text{ or }C\text{ or }F}$), 4.09 (m, 1 H, H-5$^{G\text{ or }F\text{ or }C}$), 4.21–4.60 (7 H, H-5^{A,B,D,E}, H-6b$^{C\text{ or }F\text{ or }G}$, NCHb, NCHb), 4.71 (d, 1 H, $^3J_{H\text{-}1,H\text{-}2}$ = 2.0 Hz, H-1), 4.79 (d, 1 H, $^3J_{H\text{-}1,H\text{-}2}$ = 3.0 Hz, H-1), 4.93 (d, 2 H, $^3J_{H\text{-}1,H\text{-}2}$ = 4.0 Hz, H-1), 4.94 (d, 1 H, $^3J_{H\text{-}1,H\text{-}2}$ = 4.2 Hz, H-1), 5.01 (d, 1 H, $^3J_{H\text{-}1,H\text{-}2}$ = 2.4 Hz, H-1), 5.09 (d, 1 H, $^3J_{H\text{-}1,H\text{-}2}$ = 2.9 Hz, H-1), 6.40 (br t, 1 H, $^3J_{o\text{-}H,m\text{-}H}$ = $^3J_{o\text{-}H,P}$ = 6.6 Hz, *o*-H of dmba), 6.50 (br t, 1 H, $^3J_{m\text{-}H,o\text{-}H}$ = $^3J_{m\text{-}H,p\text{-}H}$ = 7.4 Hz, *m*-H of dmba), 6.75–6.80 (3 H, *p*-H of dmba, *o*-H and *m*-H of dmba'), 6.85–6.91 (2 H, *m*-H of dmba and *p*-H of dmba'), 6.98 (d, 1 H, $^3J_{m\text{-}H,p\text{-}H}$ = 7.1 Hz, *m*-H of dmba'), 7.21–7.29 (3 H, *m*-H, *p*-H), 7.40 (3 H, *m*-H, *p*-H), 7.89 (dd, 2 H, $^3J_{o\text{-}H,P}$ = 11.3 Hz, $^3J_{o\text{-}H,m\text{-}H}$ = 6.9 Hz, *o*-H), 8.17–8.23 (2 H, *o*-H) ppm; $^{13}C\{^1H\}$ NMR (75.5 MHz, $CDCl_3$, 25ºC): δ (assignment by HMQC) = 29.70–30.94 (C-6^{A,B,D,E}), 49.02, 50.49 [×2], 51.65 (NMe_2), 57.40, 57.95, 57.79, 58.25, 58.43, 58.74, 58.89, 59.24, 59.77 [×4], 60.46, 60.73, 61.44, 61.51, 61.66, 61.89, 62.08 (OMe), 66.12 (d, $^2J_{C,P}$ = 7.4 Hz), 69.27 (d, $^2J_{C,P}$ = 4.6 Hz), 69.33, 71.25 (C-5^{A,B,D,E}), 71.40 [×2], 71.79 (C-5^{C,F,G}), 71.49, 71.94 [×2] (C-6^{C,F,G}), 73.24, 73.32 (NCH_2), 80.06 [×3], 81.25, 81.41 [×3], 81.50, 81.60 [×2], 81.81 [×2], 82.01 [×3], 82.66, 83.39 [×2], 83.91, 86.52, 86.62 (d, $^3J_{C,P}$ = 2.2 Hz) (C-2, C-3, C-4), 96.32, 97.08, 97.23, 98.44, 98.63, 99.63, 100.35 (C-1), 122.12 (*p*-C of dmba), 123.09 (*m*-C of dmba), 123.52 (*p*-C of dmba'), 123.87 (*m*-C of dmba'), 125.31 [×2] (*m*-C of dmba and dmba'), 127.17 (d, $^3J_{C,P}$ = 10.5 Hz, *m*-C), 127.51 (d, $^3J_{C,P}$ = 10.8 Hz, *m*-C), 129.89, 130.10 (*p*-C), 131.51 (d, $^1J_{C,P}$ = 40.4 Hz, *ipso*-C), 132.33 (d, $^1J_{C,P}$ = 45.0 Hz, *ipso*-C), 133.62 (d, $^2J_{C,P}$ = 11.8 Hz, *o*-C), 133.78 (d, $^2J_{C,P}$ = 11.8 Hz, *o*-C), 135,08 (d, $^3J_{C,P}$ = 9.3 Hz, *o*-CH of dmba), 136.38 (d, $^3J_{C,P}$ = 10.2 Hz, *o*-CH of dmba'), 148.12, 148.29 (*o*-C of dmba and dmba'), 151.09,

152.65 (*ipso*-C of dmba and dmba') ppm; $^{31}P\{^{1}H\}$ NMR (121.5 MHz, $CDCl_3$, 25ºC): δ = 25.4 (s), 26.3 (s) ppm; elemental analysis (%) calcd for $C_{89}H_{134}Cl_2N_2O_{31}P_2Pd_2$ (2073.70): C 51.55, H 6.51, found: C 51.37, H 6.59; MS (ESI-TOF): *m/z* (%): 2037.62 (100) $[M - Cl]^+$, 1760.65 (58) $[M - Cl - PdCl(dmba)]^+$, 1796.63 (29) $[M - PdCl(dmba) + H]^+$.

Dipalladium(II) complex 43

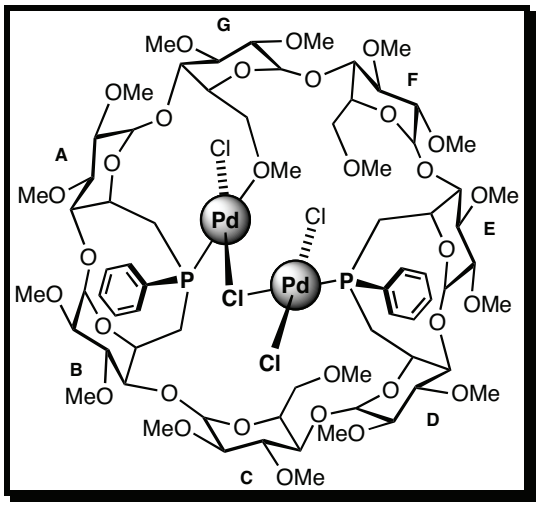

A solution of $[PdCl_2(PhCN)_2]$ (0.040 g, 0.106 mmol) in CH_2Cl_2 (5 mL) was added to a solution of **WIDEPHOS** (0.080 g, 0.053 mmol) in CH_2Cl_2 (10 mL) at room temperature. After 30 min, the reaction mixture was concentrated to *ca.* 2 mL and pentane (50 mL) was added. The suspension was then filtered over celite. Evaporation of pentane afforded **43** as an orange-yellow powder (yield: 0.099 g, 99%). R_f (SiO_2, CH_2Cl_2/MeOH, 92:8, *v*/*v*) = 0.35; m.p. dec. >250ºC; ^{1}H NMR (300.1 MHz, $CDCl_3$, 25ºC): δ (assignment by ^{1}H-^{1}H COSY, ^{1}H-^{1}H TOCSY, ^{1}H-^{1}H ROESY, ^{1}H-$^{13}C\{^{1}H\}$ HMQC and ^{1}H-$^{31}P\{^{1}H\}$ HMQC) = 1.71 (dt, 1 H, $^{2}J_{H\text{-}6a,P}$ = 13.9 Hz, $^{2}J_{H\text{-}6a,H\text{-}6b}$ = $^{3}J_{H\text{-}6a,H5}$ = 12.1 Hz, H-6a^{E}) 2.16 (dt, 1 H, $^{2}J_{H\text{-}6a,P}$ = 13.1 Hz, $^{2}J_{H\text{-}6a,H\text{-}6b}$ = $^{3}J_{H\text{-}6a,H\text{-}5}$ = 12.4 Hz, H-6a^{B}), 2.82 (m, 2 H, H-6^{A}), 3.00 (m, 2H, H-6^{D}), 3.07–3.34 (12 H, H-2, H-4^{A,B,D,E}, H-6b^{E}), 3.48–3.88 (11 H, H-3, H-4^{C,F,G}, H-6a^{F}), 3.43 (s, 3 H, OMe-6^{F}), 3.47 (s, 3 H, OMe-6^{C}), 3.51 (s, 6 H, OMe-2), 3.51 (s, 3 H, OMe-2), 3.52 (s, 3 H, OMe-2), 3.53 (s, 3 H, OMe-2), 3.54 (s, 3 H, OMe-2), 3.58 (s, 3 H, OMe-2), 3.62 (s, 3 H, OMe-6^{G}), 3.65 (s, 3 H, OMe-3), 3.66 (s, 3 H, OMe-3), 3.67 (s, 3 H, OMe-3), 3.68 (s, 3 H, OMe-3), 3.70 (s, 3 H, OMe-3), 3.74 (s, 3 H, OMe-3), 3.77 (s, 3 H, OMe-3), 4.05 (dd, 1 H, $^{2}J_{H\text{-}6b,H\text{-}6a}$ = 14.7 Hz, $^{3}J_{H\text{-}6b,H\text{-}5}$ = 9.2 Hz, H-6b^{B}), 4.12–4.15 (2 H, H-5^{F}, H-6b^{F}), 4.27 (d, 1 H, $^{2}J_{H\text{-}6b,H\text{-}6a}$ = 10.9 Hz, H-6a^{G}), 4.37 (d, 1 H, $^{3}J_{H\text{-}5,H\text{-}6a}$ = 10.0 Hz, H-5^{G}), 4.48–4.54 (3 H, H-5^{E}, H-5^{C}, H-6a^{C}), 4.75

(dd, 1 H, $^{2}J_{\text{H-6b,H-6a}}$ = 10.7 Hz, $^{3}J_{\text{H-6b,H-5}}$ = 1.9 Hz, H-6b^{G}), 4.82 (m, 1 H, H-5^{B}), 4.90 (d, 1 H, $^{3}J_{\text{H-1,H-2}}$ = 4.7 Hz, H-1^{B}), 4.93 (dd, 1 H, $^{2}J_{\text{H-6b,H-6a}}$ = 11.1 Hz, $^{3}J_{\text{H-6b,H-5}}$ = 1.8 Hz, H-6b^{C}), 4.98 (d, 1 H, $^{3}J_{\text{H-1,H-2}}$ = 4.4 Hz, H-1^{E}), 5.00 (d, 1 H, $^{3}J_{\text{H-1,H-2}}$ = 4.1 Hz, H-1^{F}), 5.11 (m, 1 H, H-5^{D}), 5.12 (d, 1 H, $^{3}J_{\text{H-1,H-2}}$ = 4.4 Hz, H-1^{C}), 5.14 (d, 1 H, $^{3}J_{\text{H-1,H-2}}$ = 2.9 Hz, H-1^{A}), 5.16 (d, 1 H, $^{3}J_{\text{H-1,H-2}}$ = 3.6 Hz, H-1^{G}), 5.21 (m, 1 H, H-5^{A}), 5.27 (d, 1 H, $^{3}J_{\text{H-1,H-2}}$ = 2.9 Hz, H-1^{D}), 7.37–7.46 (6 H, *m*-H, *p*-H), 7.52–7.57 (2 H, *o*-H), 7.64–7.67 (2 H, *o*-H) ppm; $^{13}C\{^{1}H\}$ NMR (75.5 MHz, $CDCl_3$, 25ºC): δ (assignment by HMQC) = 31.54 (d, $J_{C,P}$ = 31.8 Hz, C-6^{B}), 31.12 (d, $J_{C,P}$ = 32.5 Hz, C-6^{E}), 35.48(d, $J_{C,P}$ = 29.7 Hz, C-6^{D}), 38.08 (d, $J_{C,P}$ = 23.1 Hz, C-6^{A}), 57.40, 57.83, 58.01, 58.62, 58.66, 58.72, 59.32, 59.36, 59.68 (OMe-2, OMe-6^{C,F}), 59.84 (OMe-6^{G}), 61.31 [×2], 61.55, 61.71, 61.82, 61.86, 61.92 (OMe-3), 64.35 (C-5^{B}), 64.59 (C-5^{E}), 68.67 (C-5^{A}), 69.49 (C-5^{D}), 71.16 (C-5^{G}), 71.45 (C-5^{F}), 71.70 (C-5^{C}), 71.63 (C-6^{F}), 72.78 [×2] (C-6^{C,G}), 79.98, 80.26, 80.49 [×2], 80.92, 81.31, 81.59 [×2], 82.04 [×2], 82.18 [×2], 82.73, 82.83, 82.96, 83.15 [×2] (C-2, C-3, C-4^{C,F,G}), 84.11 (d, $^{3}J_{C,P}$ = 11.4 Hz, C-4^{E}), 87.60 (d, $^{3}J_{C,P}$ = 11.4 Hz, C-4^{B}), 89.64 (C-4^{A}), 89.83 (C-4^{D}), 97.55 (C-1^{E}), 98.14 (C-1^{G}), 98.26(C-1^{B}), 98.85 (C-1^{D}), 99.79 (C-1^{A}), 100.72 (C-1^{F}), 102.07 (C-1^{C}), 128.55 (d, $^{3}J_{C,P}$ = 11.6 Hz, *m*-C), 128.70 (d, $^{3}J_{C,P}$ = 11.6 Hz, *m*-C), 131.02, 131.10 (*p*-C), 131.19, 131.29 (*o*-C), 130.7–131.94 [×2] (*ipso*-C) ppm; $^{31}P\{^{1}H\}$ NMR (121.5 MHz $CDCl_3$, 25ºC): δ = 22.4 (br s), 27.3 (d, $^{4}J_{P1,P2}$ = 4.4 Hz) ppm; elemental analysis (%) calcd for $C_{71}H_{110}Cl_4O_{31}P_2Pd_2$ (1876.21): C 45.45, H 5.91, found: C 45.39, H 6.09; MS (ESI-TOF): *m/z* (%): 1899.32 (75) $[M + Na]^{+}$, 1839.40 (25) $[M - Cl]^{+}$.

Dipalladium(II) complex 44

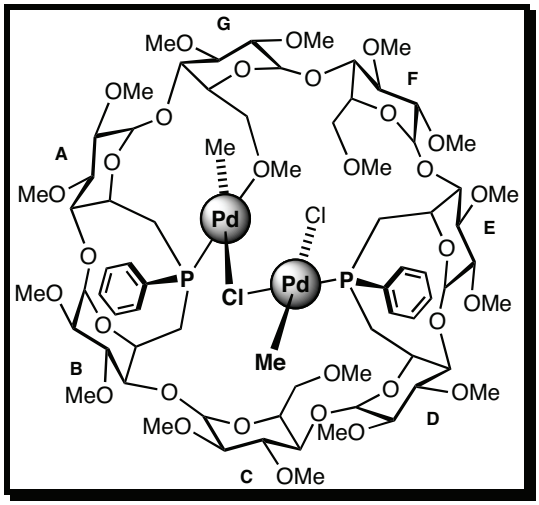

A solution of [PdClMe(cod)] (0.028 g, 0.106 mmol) in CH_2Cl_2 (5 mL) was added to a solution of **WIDEPHOS** (0.080 g, 0.053 mmol) in CH_2Cl_2 (10 mL) at room temperature. After 30 min, the reaction mixture was concentrated to *ca.* 2 mL and pentane (50 mL) was added. The suspension was then filtered over celite. Evaporation of pentane afforded **44** as a pale yellow powder (yield: 0.096 g, 99%). R_f (SiO_2, CH_2Cl_2/MeOH, 92:8, *v*/*v*) = 0.35; m.p. dec. >250ºC; ^{1}H NMR (300.1 MHz, $CDCl_3$, 25ºC): δ (assignment by ^{1}H-^{1}H COSY, ^{1}H-^{1}H TOCSY, ^{1}H-^{1}H ROESY, ^{1}H-^{13}C{^{1}H} HMQC and ^{1}H-^{31}P{^{1}H} HMQC) = 0.16 (d, 3 H, $^3J_{H,P}$ = 2.3 Hz, Me_{exo}), 0.94 (br s , 3 H, Me_{endo}), 1.66 (dt, 1 H, $^2J_{H\text{-}6a,P}$ = 16.2 Hz, $^2J_{H\text{-}6a,H\text{-}6b}$ = $^3J_{H\text{-}6a,H\text{-}5}$ = 13.3 Hz, H-6a^D), 1.96 (dt, 1 H, $^2J_{H\text{-}6a,P}$ = 12.4 Hz, $^2J_{H\text{-}6a,H\text{-}6b}$ = $^3J_{H\text{-}6a,H\text{-}5}$ = 13.2 Hz, H-6a^B), 2.53 (dt, 2 H, $^2J_{H\text{-}6a,P}$ = 12.9 Hz, $^2J_{H\text{-}6a,H\text{-}6b}$ = $^3J_{H\text{-}6a,H\text{-}5}$ = 15.1 Hz, H-6a^{A,E}), 2.71 (dd, 1 H, $^2J_{H\text{-}6b,H\text{-}6a}$ = 13.3 Hz, $^3J_{H\text{-}6b,H\text{-}5}$ = 5.5 Hz, H-6b^D), 3.11–3.41 (14 H, H-2, H-4^{A,B,D,E}, H-6b^{A,E}, H-6a^F), 3.36 (s, 3 H, OMe-6^C), 3.45 (s, 3 H, OMe-6^F), 3.49 (s, 3 H, OMe-2), 3.50 (s, 3 H, OMe-2), 3.52 (s, 3 H, OMe-2), 3.53 (s, 3 H, OMe-2), 3.55 (s, 3 H, OMe-2), 3.56 (s, 6 H, OMe-2), 3.59 (s, 3 H, OMe-6^G), 3.62 (s, 3 H, OMe-3), 3.63 (s, 3 H, OMe-3), 3.67 (s, 3 H, OMe-3), 3.68 (s, 3 H, OMe-3), 3.72 (s, 3 H, OMe-3), 3.73 (s, 3 H, OMe-3), 3.87 (s, 3 H, OMe-3), 3.44–3.92 (10 H, H-3, H-4^{C,F,G}), 3.98 (d, 1 H, $^3J_{H\text{-}5,H\text{-}6b}$ = 9.3 Hz, H-5^F), 4.14–4.21 (4 H, H-6b^{B,F}, H-5^{C,D}), 4.40 (d, 1 H, $^2J_{H\text{-}6a,H\text{-}6b}$ = 11.0 Hz, H-6a^G), 4.48–4.53 (2 H, H-5^B, H-5^G), 4.76 (m, 2 H, H-6^C), 4.81 (m, 1 H, H-6b^G), 4.84 (m, 1 H, H-5^E), 4.92 (m, 1 H, H-5^A), 4.94 (d, 1 H, $^3J_{H\text{-}1,H\text{-}2}$ = 5.1 Hz, H-1^B), 4.99 (d, 1 H, $^3J_{H\text{-}1,H\text{-}2}$ = 4.4 Hz, H-1^F), 5.03 (d, 1 H, $^3J_{H\text{-}1,H\text{-}2}$ = 3.5 Hz, H-1^C), 5.04 (d, 1 H, $^3J_{H\text{-}1,H\text{-}2}$ = 3.5 Hz, H-1^E), 5.14 (d, 1 H, $^3J_{H\text{-}1,H\text{-}2}$ = 2.5 Hz, H-1^D), 5.20 (d, 1 H, $^3J_{H\text{-}1,H\text{-}2}$ = 3.5 Hz, H-1^G), 5.22 (d, 1 H, $^3J_{H\text{-}1,H\text{-}2}$ = 2.3 Hz, H-1^A), 7.34–7.40 (8 H, *o*-H, *m*-H, *p*-H), 7.62–7.67 (2 H, *o*-H) ppm; ^{13}C{^{1}H} NMR (100.6 MHz, $CDCl_3$, 25ºC): δ (assignment by HMQC) = 1.40 (Me_{endo}), 7.97 (Me_{exo}), 31.82 (d, $^1J_{C,P}$ = 26.5 Hz, C-6^D), 32.11 (d, $^1J_{C,P}$ = 26.7 Hz, C-6^B), 33.86 (d, $^1J_{C,P}$ = 21.3 Hz, C-6^E), 37.23 (d, $^1J_{C,P}$ = 20.4 Hz, C-6^A), 57.54, 57.68, 58.24, 58.41, 58.43, 58.90, 59.19, 59.46, 59.65 (OMe-2, OMe-6^{C,F}), 60.02 (OMe-6^G), 61.11, 61.32, 61.64, 61.74, 62.01, 62.27, 62.53 (OMe-3), 64.09 (C-5^D), 65.34 (d, $^2J_{C,P}$ = 3.2 Hz, C-5^B), 70.11 (d, $^2J_{C,P}$ = 5.9 Hz, C-5^A), 70.76 (C-6^F), 71.00 (C-5^G), 71.17 (C-5^C), 71.43 [×2] (C-5^{E,F}), 73.54 (C-6^G), 74.13 (C-6^C), 79.07, 79.78, 80.78, 81.14, 81.53, 81.64, 82.02, 82.17, 82.25, 82.38, 82.60, 83.00, 83.08, 83.30, 83.43, 83.58, 83.96 (C-2, C-3, C-4^{C,F,G}), 87.84 (d, $^3J_{C,P}$ = 6.5 Hz, C-4^B), 87.89 (d, $^3J_{C,P}$ = 4.0 Hz, C-4^D), 89.12 (C-4^E), 90.64 (d, $^3J_{C,P}$ = 4.1 Hz, C-4^A), 96.63 (C-1^G), 97.82 (C-1^F), 98.27 (C-1^B), 98.83 (C-1^A), 100.30 (C-1^E), 100.59 (C-1^D), 101.22 (C-1^C), 128.35 (d, $^3J_{C,P}$ = 11.4 Hz, *m*-C), 128.46 (d, $^3J_{C,P}$ = 10.8 Hz, *m*-C), 129.64, 130.34 (*p*-C), 130.39 (d, $^2J_{C,P}$ = 6.4 Hz, *o*-C), 131.33 (d, $^2J_{C,P}$ =

10.3 Hz, *o*-C), 134.16 (d, $^{1}J_{C,P}$ = 46.7 Hz, *ipso*-C), 134.67 (d, $^{1}J_{C,P}$ = 52.9 Hz, *ipso*-C) ppm; $^{31}P\{^{1}H\}$ NMR (121.5 MHz $CDCl_3$, 25ºC): δ = 14.5 (br s), 23.7 (d, $^{4}J_{P,P'}$ = 3.8 Hz) ppm; elemental analysis (%) calcd for $C_{73}H_{116}Cl_2O_{31}P_2Pd_2 \cdot 0.5CH_2Cl_2$ (1835.38 + 42.47): C 46.88, H 6.22, found: C 46.72, H 6.52; MS (ESI-TOF): *m/z* (%): 1877.39 (5) $[M + K]^+$, 1857.43 (100) $[M + Na]^+$, 1799.47 (45) $[M - Cl]^+$.

Dirhodium(I) complex 46

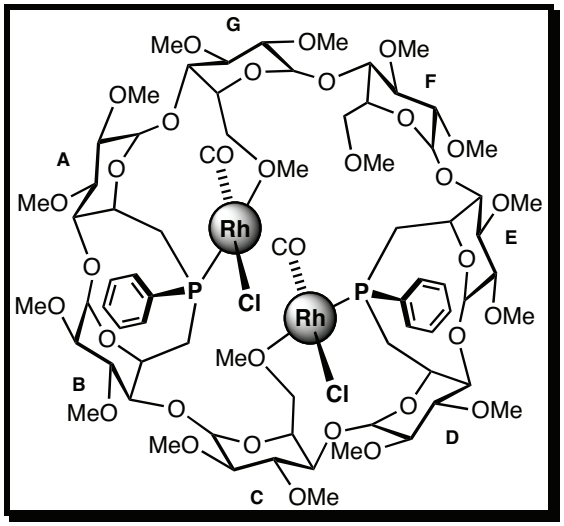

A solution of $[RhCl(CO)_2]_2$ (0.020 g, 0.053 mmol) in CH_2Cl_2 (5 mL) was added dropwise to a solution of **WIDEPHOS** (0.080 g, 0.053 mmol) in CH_2Cl_2 (10 mL) within 30 min at room temperature. After stirring for 30 min, the reaction mixture was evaporated to dryness affording analytically pure **46** (yield: 0.089 g, 99%) as a dark orange powder. R_f (SiO_2, CH_2Cl_2/MeOH, 92:8, *v*/*v*) = 0.35; m.p. dec. >250ºC; ^{1}H NMR (300.1 MHz, $CDCl_3$, 25ºC): δ (assignment by COSY) = 1.96 (m, 1 H- H-6a$^{A \text{ or } D}$), 2.12 (td, 1 H, $^{2}J_{H\text{-}6a,H\text{-}6b} = {}^{2}J_{H\text{-}6a,P}$ = 13.3 Hz, $^{3}J_{H\text{-}6a,H\text{-}5}$ = 12.4 Hz, H-6$^{B \text{ or } E}$), 2.35 (m, 1 H, H-6a$^{E \text{ or } B}$), 2.52 (t, 1 H $^{2}J_{H\text{-}6a,H\text{-}6b}$ = 14.1 Hz, H-6b$^{D \text{ or } A}$), 3.13–3.83 (30 H, H-2, H-3, H-4, H-6^{C,F,G}, H-6b$^{B,E \text{ and } D \text{ or } A}$), 3.34 (s, 3 H, OMe-6^{C}), 3.50 (s, 3 H, OMe), 3.51 (s, 9 H, OMe), 3.52 (s, 3 H, OMe), 3.53 (s, 6 H, OMe), 3.54 (s, 3 H, OMe), 3.55 (s, 3 H, OMe), 3.63 (s, 3 H, OMe-3), 3.65 (s, 3 H, OMe-3), 3.66 (s, 3 H, OMe-3), 3.68 (s, 3 H, OMe-3), 3.70 (s, 3 H, OMe-3), 3.72 (s, 3 H, OMe-3), 3.75 (s, 3 H, OMe-3), 3.96 (m ,1 H, H-6b$^{A \text{ or } D}$), 4.08 (d, 1 H, $^{3}J_{H\text{-}5,H\text{-}6b}$ = 9.6 Hz, H-5$^{C \text{ or } F \text{ or } G}$), 4.20–4.25 (2 H, H-5$^{A \text{ or } D \text{ and } B \text{ or } E}$), 4.40 (d, 1 H, $^{3}J_{H\text{-}5,H\text{-}6b}$ = 10.0 Hz, H-5$^{E \text{ or } B}$), 4.62–4.80 (2 H, H-5$^{F,G \text{ or } G,C \text{ or } C,F}$), 4.87 (d, 1 H, $^{3}J_{H\text{-}5,H\text{-}6b}$ = 10.6 Hz, H-5$^{D \text{ or } A}$), 4.95 (d, 1 H, $^{3}J_{H\text{-}1,H\text{-}2}$ = 4.3 Hz, H-1),

5.04 (d, 1 H, $^{3}J_{\text{H-1,H-2}}$ = 4.0 Hz, H-1), 5.10 (d, 2 H, $^{3}J_{\text{H-1,H-2}}$ = 4.0 Hz, H-1), 5.13 (2 H, H-1), 5.18 (d, 1 H, $^{3}J_{\text{H-1,H-2}}$ = 2.6 Hz, H-1), 7.36–7.37 (6 H, *m*-H, *p*-H), 7.55–7.60 (2 H, *o*-H), 7.80–7.83 (2 H, *o*-H) ppm; $^{13}C\{^{1}H\}$ NMR (75.5 MHz, $CDCl_3$, 25ºC): δ (assignment by HMQC) = 29.27 (d, $^{1}J_{\text{C,P}}$ = 58.0 Hz), 29.98 (d, $^{1}J_{\text{C,P}}$ = 49.8 Hz), 31.55 (d, $^{1}J_{\text{C,P}}$ = 27.4 Hz), 32.33 (d, $^{1}J_{\text{C,P}}$ = 23.4 Hz) (C-$6^{\text{A,B,D,E}}$), 57.53, 58.24 [×3], 58.27 [×2], 59.00, 59.24, 59.27, 59.36, 61.29 [×2], 61.44, 61.90 [×2], 62.15, 62.21 (OMe), 63.85 [×2], 68.11 [×2] (C-$5^{\text{A,B,D,E}}$), 70.71 [×2], 71.07 (C-$5^{\text{C,F,G}}$), 70.97 [×3] (C-$6^{\text{C,F,G}}$), 79.80, 80.27, 80.34, 81.24 [×4], 81.66, 82.03, 82.16, 82.24 [×2], 82.61, 83.02, 83.09, 83.50, 83.57 (C-2,C-3,C-$4^{\text{C,F,G}}$), 87.89 [×2] (d, $^{3}J_{\text{C,P}}$ = 10.7 Hz) 88.89, 89.00 (C-$4^{\text{A,B,D,E}}$), 97.71, 97.86, 98.66, 99.83, 99.98, 10.58, 101.83 (C-1), 128.28 [×2] (d, $^{3}J_{\text{C,P}}$ = 10.0 Hz, *m*-C), 130.01 (*p*-C), 130.32 (*p*-C), 130.37 (d, $^{2}J_{\text{C,P}}$ = 7.7 Hz, *o*-C), 131.14 [×2] (d, $^{1}J_{\text{C,P}}$ = 42.9 Hz, *ipso*-C), 131.82 (d, $^{2}J_{\text{C,P}}$ = 9.7 Hz, *o*-C), 177.49 (CO), 178.50 (CO) ppm; $^{31}P\{^{1}H\}$ NMR (121.5 MHz $CDCl_3$, 25ºC): δ = 31.2 (br d, $^{1}J_{\text{P,Rh}} \approx 170$ Hz), 45.7 (br d, $^{1}J_{\text{P,Rh}} \approx 170$ Hz) ppm; $C_{73}H_{110}Cl_2O_{33}P_2Rh_2$ (1854.30); MS (ESI-TOF): *m/z* (%): 1891.36 (30) $[M + K]^+$, 1857.37 (25) $[M + Na]^+$, 1816.39 (20) $[M - Cl]^+$. We do not provide microanalytical data for this complex due to rapid decomposition.

IV.4.3. X-ray crystallographic data for 36

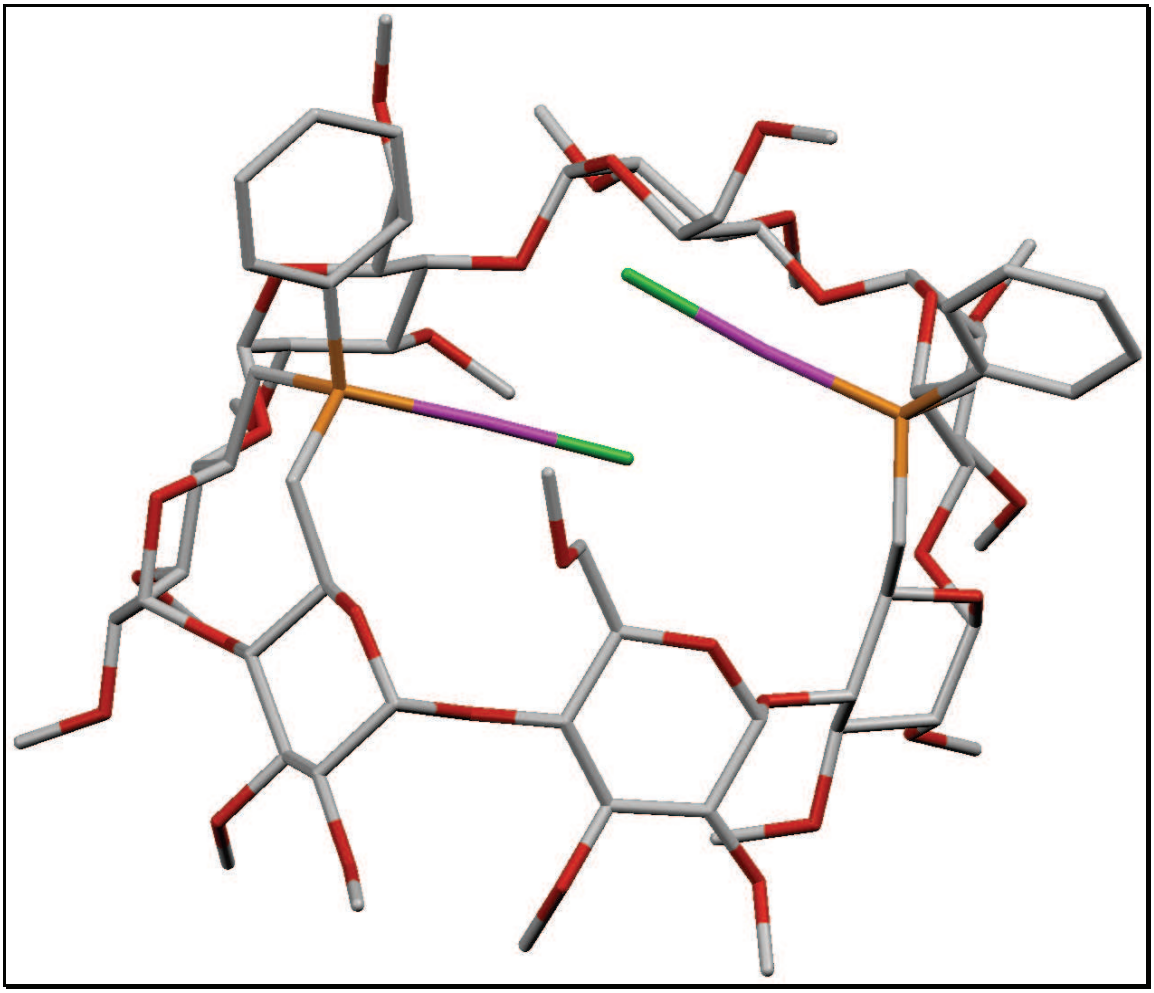

The X-ray structure determination was performed by Dr L. Toupet (University of Rennes, France). Single crystals were obtained by slow diffusion of pentane into a solution of **36** in chlorobenzene. The sample was studied on a Oxford Diffraction Xcalibur Saphir 3 CCD with graphite monochromatised MoKα radiation (λ = 0.71073 Å). The structure was solved with SIR-97,[71] which revealed the non-hydrogen atoms of the molecule. After anisotropic refinement, many hydrogen atoms were found with a Fourier difference analysis. The whole structure was refined with SHELX-97[72] and full-matrix least-square techniques (use of F^2 magnitude; x, y, z, β_{ij} for Au, Cl, C, O, P atoms, x, y, z, in riding mode for H atoms; 1535 variables and 41397 observations with $I > 2.0\sigma(I)$; calcd $w = 1/[\sigma^2(F_o^2) + (0.0673\ P)^2]$ where $P = (F_o^2 + 2\ F_o^2)/3$ with the resulting R = 0.052, R_w = 0.125 and S_w = 0.836; $\Delta\rho < 1.599$ eÅ^{-3}. The absolute configuration (and thus the enantiomeric space group assignment) was determined by a *Flack* x parameter of 0.01 (4). A summary of the crystallographic data is given in Table 4. CCDC reference number 801259.

Table 4. Crystal data and structure refinement for 2(**36**)·3(C_6H_5Cl)·2(C_5H_{12}).

Crystal Data	
Crystal size	0.28 × 0.12 × 0.10 mm^3
Empirical formula	$C_{170}H_{259}Au_4Cl_7O_{62}P_4$
M_r	4454.67
Crystal system	Triclinic
Space group	*P*1
Temperature	120(2) K
Unit cell parameters	
a	13.5343(2) Å
b	14.9731(2) Å
c	24.5351(4) Å
α	85.968(1)º
β	83.148(1)º
γ	87.986(1)º
V	4922.52(13) $Å^3$
Z	1
D (calculated)	1.503 g/cm^3
F (000)	2270
□	3.180 mm^{-1}
Data Processing and Reduction	
θ range for data collection	2.61 to 27.00º
Index ranges	$-17 \leq h \leq 17$, $-19 \leq k \leq 19$, $-31 \leq l \leq 31$
Reflections collected	73437
Independent reflections	41397 [R(int) = 0.0504]
Refinement method	Full-matrix least-squares on F^2
Data / restraints / parameters	41397 / 3 / 1535
Goodness-on-fir on F^2	0.837
Final R indices [$I > 2\sigma(I)$]	R1 = 0.0522, *w*R2 = 0.1119
R indices (all data)	R1 = 0.0967, *w*R2 = 0.1252
Largest diff. peak and hole	1.599 and -0.728 $eÅ^{-3}$

IV.4.4. X-ray crystallographic data for 45

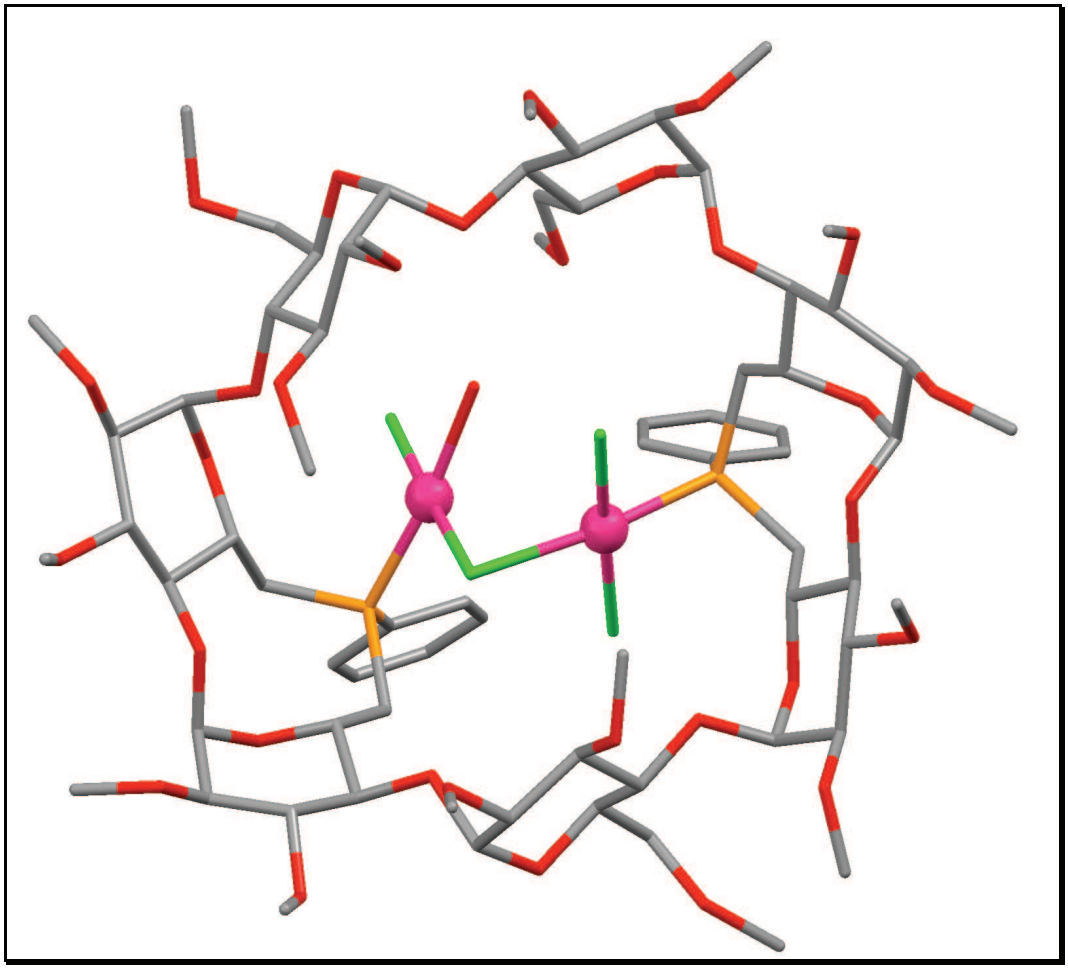

The X-ray structure determination was performed by Dr L. Toupet (University of Rennes, France). Single crystals were obtained by slow diffusion of pentane into a solution of **43** in non-distilled dichloromethane. The sample was studied on a Oxford Diffraction Xcalibur Saphir 3 CCD with graphite monochromatised MoKα radiation (λ = 0.71073 Å). The structure was solved with SIR-97,[71] which revealed the non-hydrogen atoms of the molecule. After anisotropic refinement, many hydrogen atoms were found with a Fourier difference analysis. The whole structure was refined with SHELX-97[72] and full-matrix least-square techniques (use of F^2 magnitude; x, y, z, β_{ij} for Pd, Cl, C, O, P atoms, x, y, z, in riding mode for H atoms; 1010 variables and 19198 observations with $I > 2.0\sigma(I)$; calcd $w = 1/[\sigma^2(F_o^2) + (0.0815\ P)^2]$ where $P = (F_o^2 + 2\ F_o^2)/3$ with the resulting R = 0.057, R_w = 0.143 and S_w = 0.851; $\Delta\rho < 3.114$ eÅ^{-3}. The absolute configuration (and thus the enantiomeric space group assignment) was determined by a *Flack* x parameter of 0.03 (2). A summary of the crystallographic data is given in Table 5. CCDC reference number 758028.

Table 5. Crystal data and structure refinement for **45**·0.5(C_5H_{12}).

Crystal Data	
Crystal size	0.20 × 0.18 × 0.08 mm^3
Empirical formula	$C_{73.5}H_{118}Cl_4O_{32}P_2Pd_2$
M_r	1930.22
Crystal system	Monoclinic
Space group	$P2_1$
Temperature	130(2) K
Unit cell parameters	
a	13.6733(3) Å
b	24.1680(5) Å
c	14.1445(3) Å
α	90º
β	109.022(2)º
γ	90º
V	4418.90(16) $Å^3$
Z	2
D (calculated)	1.451 g/cm^3
F (000)	2010
□	0.643 mm^{-1}
Data Processing and Reduction	
θ range for data collection	2.66 to 27.00º
Index ranges	$-17 \leq h \leq 17$, $-30 \leq k \leq 30$, $-18 \leq l \leq 18$
Reflections collected	5782
Independent reflections	19198 [R(int) = 0.0678]
Refinement method	Full-matrix least-squares on F^2
Data / restraints / parameters	19198 / 5 / 1010
Goodness-on-fir on F^2	0.851
Final R indices [$I > 2\sigma(I)$]	R1 = 0.0570, *w*R2 = 0.1314
R indices (all data)	R1 = 0.1001, *w*R2 = 0.1433
Largest diff. peak and hole	3.114 and -0.731 $eÅ^{-3}$

IV.5. References

[1] K. Issleib, G. Hohlfeld, *Z. Anorg. Allg. Chem.* **1961**, *312*, 169-179.

[2] Z. Freixa, M. S. Beentjes, G. D. Batema, C. B. Dieleman, G. P. F. van Strijdonck, J. N. H. Reek, P. C. J. Kamer, J. Fraanje, K. Goubitz, P. W. N. M. van Leeuwen, *Angew. Chem. Int. Ed.* **2003**, *42*, 1284-1287.

[3] C. Jeunesse, D. Armspach, D. Matt, *Chem. Commun.* **2005**, 5603-5614.

[4] B. Breit, *Angew. Chem. Int. Ed.* **2005**, *44*, 6816-6825.

[5] E. Kossoy, M. A. Iron, B. Rybtchinski, Y. Ben-David, L. J. W. Shimon, L. Konstantinovski, J. M. L. Martin, D. Milstein, *Chem. Eur. J.* **2005**, *11*, 2319-2326.

[6] P. Le Floch, *Coord. Chem. Rev.* **2006**, *250*, 627-680.

[7] C. Jiménez-Rodríguez, F. X. Roca, C. Bo, J. Benet-Buchholz, E. Escudero-Adán, Z. Freixa, P. W. N. M. van Leeuwen, *Dalton Trans.* **2006**, 268-278.

[8] R. C. J. Atkinson, V. C. Gibson, N. L. Long, A. J. P. White, *Dalton Trans.* **2010**, *39*, 7540-7546.

[9] M. Sundermeier, A. Zapf, M. Beller, *Eur. J. Inorg. Chem.* **2003**, 3513-3526.

[10] M. Weis, C. Waloch, W. Seiche, B. Breit, *J. Am. Chem. Soc.* **2006**, *128*, 4188-4189.

[11] D. Semeril, D. Matt, L. Toupet, *Chem. Eur. J.* **2008**, *14*, 7144-7155.

[12] L. Monnereau, D. Semeril, D. Matt, L. Toupet, A. J. Mota, *Adv. Synth. Cat.* **2009**, *351*, 1383-1389.

[13] J. Meeuwissen, A. J. Sandee, Bas de Bruin, M. A. Siegler, A. L. Spek, J. N. H. Reek, *Organometallics* **2010**, *29*, 2413-2421.

[14] C. A. Bessel, P. Aggarwal, A. C. Marschilok, K. J. Takeuchi, *Chem. Rev.* **2001**, *101*, 1031-1066.

[15] L. Poorters, D. Armspach, D. Matt, L. Toupet, P. G. Jones, *Angew. Chem. Int. Ed.* **2007**, *46*, 2663-2665.

[16] Z. Freixa, P. W. N. M. van Leeuwen, *Coord. Chem. Rev.* **2008**, *252*, 1755-1786.

[17] C. Woodcock, R. Eisenberg, *Inorg. Chem.* **1984**, *23*, 4207-4211.

[18] J. García-Antón, J. Pons, X. Solans, M. Font-Bardia, J. Ros, *Eur. J. Inorg. Chem.* **2002**, 3319-3327.

[19] V. K. Jain, L. Jain, *Coord. Chem. Rev.* **2005**, *249*, 3075-3197.

[20] Z. Freixa, P. C. J. Kamer, M. Lutz, A. L. Spek, P. W. N. M. van Leeuwen, *Angew. Chem. Int. Ed.* **2005**, *44*, 4385-4388.

[21] T. M. Konrad, J. A. Fuentes, A. M. Z. Slawin, M. L. Clarke, *Angew. Chem. Int. Ed.* **2010**, *49*, 9197-9200.

[22] M. E. Broussard, J. Booker, S. G. Train, W.-J. Peng, S. A. Laneman, G. G. Stanley, *Science* **1993**, *260*, 1784-1787.

[23] P. Hofmann, C. Meier, W. Hiller, M. Heckel, J. Riede, M. U. Schmidt, *J. Organomet. Chem.* **1995**, *490*, 51-70.

[24] C. M. Thomas, R. Mafua, B. Therrien, E. Rusanov, E. Stoeckli-Evans, G. Süss-Fink, *Chem. Eur. J.* **2002**, *8*, 3343-3352.

[25] I. A. Guzei, K. Li, G. A. Bikzhanova, J. Darkwa, S. F. Mapolie, *Dalton Trans.* **2003**, 715-722.

[26] F. Speiser, P. Braunstein, L. Saussine, R. Welter, *Organometallics* **2004**, *23*, 2613-2624.

[27] I. P. Beletskaya, V. P. Ananikov, *Eur. J. Org. Chem.* **2007**, 3431-3444.

[28] J. M. López-Valbuena, E. C. Escudero-Adan, J. Benet-Buchholz, Z. Freixa, P. W. N. M. van Leeuwen, *Dalton Trans.* **2010**, *39*, 8560-8574.

[29] D. C. Smith Jr., C. H. Lake, G. M. Gray, *Chem. Commun.* **1998**, 2771-2772.

[30] E. Ruckenstein, R. Tsekov, *J. Chem. Phys.* **1994**, *100*, 7696-7699.

[31] P. Nalla, S.-H. Huang, Y. Shang, O. Chyan, M. G. Richmond, M. El Bouanani, *Chem. Mater.* **2005**, *17*, 5951-5956.

[32] C. R. Hess, T. Weyhermüller, E. Bill, K. Wieghardt, *Angew. Chem. Int. Ed.* **2009**, *48*, 3703-3706.

[33] S. Piligkos, L. D. Slep, T. Weyhermüller, P. Chaudhuri, E. Bill, F. Neese, *Coord. Chem. Rev.* **2009**, *253*, 2352-2362.

[34] A. Soncini, T. Mallah, L. F. Chibotaru, *J. Am. Chem. Soc.* **2010**, *132*, 8106-8114.

[35] V. C. Gibson, N. J. Long, A. J. P. White, C. K. Williams, D. J. Williams, *Organometallics* **2000**, *19*, 4425-4428.

[36] S.-M. Kuang, P. E. Fanwick, R. A. Walton, *Inorganica Chimica Acta* **2002**, *338*, 219-227.

[37] S.-M. Kuang, P. E. Fanwick, R. A. Walton, *Inorg. Chem.* **2002**, *41*, 1036-1038.

[38] J.-C. Hierso, F. Lacassin, R. Broussier, R. Amardeil, P. Meunier, *J. Organomet. Chem.* **2004**, *689*, 766-769.

[39] O. Grossman, C. Azerraf, D. Gelman, *Organometallics* **2006**, *25*, 375-381.

[40] C. Azerraf, S. Cohen, D. Gelman, *Inorg. Chem.* **2006**, *45*, 7010-7017.

[41] R. C. Schnabel, D. M. Roddick, *Inorg. Chem.* **1993**, *32*, 1513-1518.

[42] G. Aullón, G. Ujaque, A. Lledós, S. Alvarez, P. Alemany, *Inorg. Chem.* **1998**, *37*, 804-813.

[43] G. Aullón, G. Ujaque, A. Lledós, S. Alvarez, *Chem. Eur. J.* **1999**, *5*, 1391-1410.

[44] X. Fang, B. L. Scott, J. G. Watkin, C. A. G. Carter, G. J. Kubas, *Inorganica Chimica Acta* **2001**, *317*, 276-281.

[45] E. Engeldinger, D. Armspach, D. Matt, L. Toupet, M. Wesolek, *C. R. Chimie* **2002**, *5*, 359-372.

[46] H. El Moll, D. Semeril, D. Matt, L. Toupet, *Eur. J. Org. Chem.* **2010**, *6*, 1158-1168.

[47] D. J. Eisler, R. J. Puddephatt, *Can. J. Chem.* **2004**, *82*, 1423-1427.

[48] M. Awada, C. Jeunesse, D. Matt, L. Toupet, R. Welter, *Dalton Trans.* **2011**, *40*, 10063-10070.

[49] C. Loeber, D. Matt, P. Briard, D. Grandjean, *J. Chem. Soc. Dalton Trans.* **1996**, 513-524.

[50] F. Plourde, K. Gilbert, J. Gagnon, P. D. Harvey, *Organometallics* **2003**, *22*, 2862-2875.

[51] P. Mongrain, P. D. Harvey, *Macromol. Rapid Commun.* 2008, *29*, 1752-1757.

[52] M. Awada, C. Jeunesse, E. Brenner, D. Matt, L. Toupet, *Zeitschrift fuer Kristallographie* **2010**, *225*, 176-178.

[53] H. El Moll, D. Sémeril, D. Matt, L. Toupet, *Adv. Synth. Catal.* **2010**, *352*, 901-908.

[54] N. C. Baenziger, W. E. Bennett, D. M. Soboroff, *Acta Cryst. B* **1976**, *32*, 962-963.

[55] E. Engeldinger, D. Armspach, D. Matt, P. G. Jones, *Chem. Eur. J.* **2003**, *9*, 3091-3105.

[56] L. Poorters, D. Armspach, D. Matt, L. Toupet, S. Choua, P. Turek, *Chem. Eur. J.* **2007**, *13*, 9448-9461.

[57] T. L. Stott, M. O. Wolf, B. O. Patrick, *Inorg. Chem.* **2005**, *44*, 620-627.

[58] T. S. Teets, D. G. Nocera, *J. Am. Chem. Soc.* **2009**, *131*, 7411-7420.

[59] J. Powell, *J. Chem. Soc., Chem. Commun.* **1989**, 200-202.

[60] E. Engeldinger, D. Armspach, D. Matt, *Angew. Chem. Int. Ed.* **2001**, *40*, 2526-2529.

[61] D. Armspach, D. Matt, N. Kyritsakas, *Polyhedron* **2001**, *20*, 663-668.

[62] D. Armspach, D. Matt, L. Poorters, R. Gramage-Doria, P. Jones, L. Toupet, *Polyhedron* **2011**, *30*, 573-578.

[63] J. O. Yu, E. Lam, J. L. Sereda, N. C. Rampersad, A. J. Lough, C. S. Browning, D. H. Farrar, *Organometallics* **2005**, *24*, 37-47.

[64] S. Vuoti, M. Haukka, J. Pursiainen, *J. Organomet. Chem.* **2007**, *692*, 5044-5052.

[65] H. S. Gutowsky, C. H. Holm, *J. Chem. Phys.* **1956**, *25*, 1128-1234.

[66] H. Shanan-Atidi, K. H. Bar-Eli, *J. Phys. Chem.* **1970**, *74*, 961-963.

[67] R. Uson, A. Laguna, M. Laguna, *Inorganic Synthesis* **1989**, *26*, 85-91.

[68] A. C. Cope, E. C. Friedrich, *J. Am. Chem. Soc.* **1968**, *90*, 909-913.

[69] F. R. Hartley, *The Chemistry of Platinum and Palladium;* Wiley, New York **1973**.

[70] R. E. Rülke, J. M. Ernsting, A. L. Spek, C. J. Elsevier, P. W. N. M. van Leeuwen, *Inorg. Chem.* **1993**, *32*, 5769-5778.

[71] A. Altomare, A. C. Burla, M. Camalli, G. Cascarano, C. Giacovazzo, A. Guagliardi, A. G. G. Moliterni, G. Polidori, R. Spagna, *J. Appl. Crystallogr.* **1998**, *31*, 74-77.

[72] G. M. Sheldrick, SHELXL-97, *Program for Crystal Structure Refinement*, University of Göttingen (Germany) **1997**.

IV.6. Annex – Comments about the tilt angle

The *tilt angle* τ is expressed as the angle between the M–P vector and the pseudo C_3 axis that runs through the phosphorus atom and the centroid (ct) of the three carbon atoms connected to the former (Figure A1, right). The presence of non-optimal orbital overlap in P–M bonds is not uncommon amongst complexes displaying constrain about both chelated and non-chelated metal centres. Such deviations from ideal orbital overlap were notably observed in *cis*-[$PdCl_2$(**XANTPHOS**)] (τ = 9.83º and 8.00º),[73] *trans*-[$PdCl_2$(**TRANSPHOS**)] (τ = 5.03º and 3.19º),[74] *trans*-[PtHCl(**TRANSPHOS**)] (τ= 6.26º and 4.51º),[75] and also in a palladium(0)-complex containing a Buchwald monophosphane (τ = 8.30º).[76]

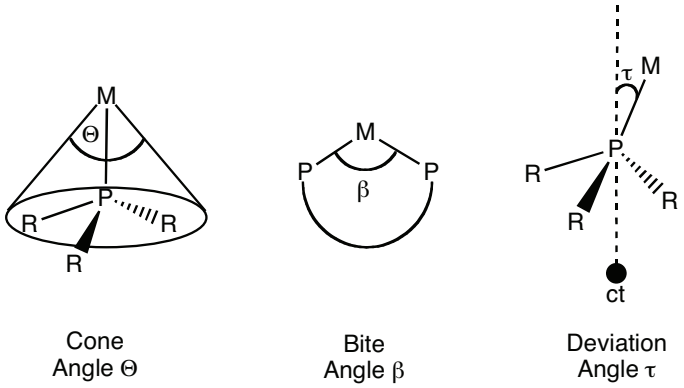

Figure A1. Schematic representation of relevant parameters used in metal coordination phosphorus chemistry.

Although seldom mentioned compared to other geometrical parameters like the Tolman cone angle Θ (Figure A1, left)[77-79] or P-M-P bite angle β (Figure A1, middle) of diphosphanes involved in chelate complexes,[80-88] the "tilt angle" may have a key role in the metal's reactivity, notably in catalytic reactions[89] and was shown to be responsible for important ^{31}P chemical shifts variations.[90] Surprisingly, the influence of the "tilt angle" τ on ^{31}P chemical shifts has rarely been addressed, except for studies in which five-membered chelate complexes were compared with four, five, six, seven and eight-membered ones. However, with these chelating diphosphanes, correlating the ^{31}P chemical shifts with the geometrical deviation of the phosphorus atom from its ideal position is problematic, as in the

corresponding chelate complexes a ring contribution needs to be considered, the extent of which is hard to predict.[91]

The precise location of the phosphorus lone pairs in **WIDEPHOS** can conveniently be inferred from its oxidised form, **27**. Note that, for tilt angle measurements on oxide derivatives, an oxygen atom replaces the metal atom. Not surprisingly, the tilt angles τ in **27** are not far of 0º (1.70º and 1.34º for each P atom; Figure A2)[92-94] We believe that **WIDEPHOS**, when binding two independent metal centres in a non-equivalent manner as in **36**, constitutes an ideal ligand for understanding the relationship between the ^{31}P NMR data and the tilt angle because here non-optimal orbital overlap is not induced by ring strain, but by simple steric effects. Moreover, one of its phosphorus atoms can be taken as an internal reference.

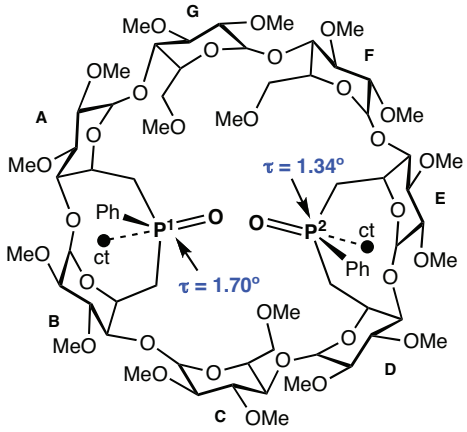

27

Figure A2. **WIDEPHOS** oxide **27** showing the tilt angles **τ** calculated from the molecular structure determined from X-ray diffraction studies (view from the secondary face).

Similar chemical shifts separation between the ^{31}P NMR signals of the two phosphorus nuclei has already been noticed and previously discussed for the so-called oschelate complexes **28**-**32**, also derived from **WIDEPHOS**. DFT calculations were performed on the platinum oschelate complex **29** and the tilt angles each associated with one of the two phosphorus atoms, were measured from one of the optimized structures (Figure A3). As expected, the difference between them turned out to be quite large (7.07º and 13.35º). This means that in the dynamic species **29**, the lone pair of one of the phosphorus atom overlaps better than the other with the d_{x2-y2} metal orbital. ^{31}P NMR chemical shifts calculations were performed on the optimized structure of **29** and revealed a large separation of *ca.* 14 ppm

between the two phosphorus nuclei, a value that is very close to the one determined experimentally (*ca.* 12 ppm). It is worth mentioning here that no abnormal phosphorus–metal bond distances were found in the computer simulated structure, which means that in both cases out of axis coordination of the metal by the ligand is likely to be responsible for this dramatic differentiation.

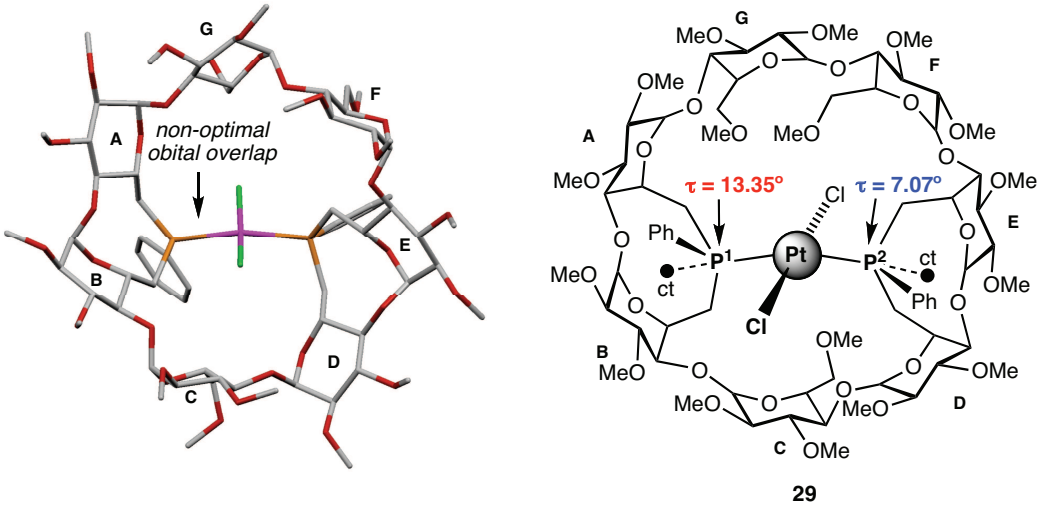

Figure A3. Optimized molecular structure of **29** (left) and schematic representation showing the tilt angles **τ** about each phosphorus atom (right). View from the secondary face. Selected angles [º] and bond lengths [Å]: P(1)-Pt-P(2) 165.36, Cl(1)-Pt-Cl(2) 168.81, ct(1)-P(1)-Pt 166.65, ct(2)-Pt-Cl(2) 172.93, P(1)–Pt 2.377, P(2)–Pt 2.380, Cl(1)–Pt 2.395, Cl(2)–Pt 2.389.

References

[73] A. M. Johns, M. Utsunomiya, C. D. Incarvito, J. F. Hartwig, *J. Am. Chem. Soc.* **2006**, *128*, 1828-1839.

[74] F. Bachechi, L. Zambonelli, L. M. Venanzi, *Helv. Chim. Acta* **1977**, *60*, 2815-2823.

[75] G. Bracher, B. Kellenberger, L. M. Venanzi, F. Bachechi, L. Zambonelli, *Helv. Chim. Acta* **1988**, *71*, 1442-1457.

[76] S. D. Walker, T. E. Barder, J. R. Martinelli, S. L. Buchwald, *Angew. Chem. Int. Ed.* **2004**, *43*, 1871-1876.

[77] C. A. Tolman, *Chem. Rev.* **1977**, *3*, 313-348.

[78] A. Immirzi, A. Musco, *Inorganica Chimica Acta* **1977**, *25*, 41-42.

[79] T. Niksch, H. Görls, W. Weigand, *Eur. J. Inorg. Chem.* **2010**, 95-105.

[80] C. P. Casey, G. T. Whiteker, *Israel J. Chem.* **1990**, *30*, 299-304.

[81] C. P. Casey, G. T. Whiteker, M. G. Melville, L. M. Petrovich, J. A. Gavney Jr., D. R. Powell, *J. Am. Chem. Soc.* **1992**, *114*, 5535-5543.

[82] J. M. Brown, P. J. Guiry, *Inorganica Chimica Acta* **1994**, *220*, 249-259.

[83] M. Kranenburg, Y. E. M. van der Burgt, P. C. J. Kamer, P. W. N. M. van Leeuwen, *Organometallics* **1995**, *14*, 3081-3089.

[84] L. A. van der Veen, M. D. K. Boele, F. R. Bregman, P. C. J. Kamer, P. W. N. M. van Leeuwen, K. Goubitz, J. Fraanje, H. Schenk, C. Bo, *J. Am. Chem. Soc.* **1998**, *120*, 11616-11626.

[85] P. Dierkes, P. W. N. M. van Leeuwen, *J. Chem. Soc. Dalton Trans.* **1999**, 1519-1529.

[86] L. A. van der Veen, P. H. Keeven, G. C. Schoemaker, J. N. H. Reek, P. C. J. Kamer, P. W. N. M. van Leeuwen, M. Lutz, A. L. Spek, *Organometallics* **2000**, *19*, 872-883.

[87] Z. Freixa, P. W. N. M. van Leeuwen, *Dalton Trans.* **2003**, 1890-1901.

[88] W.-J. van Zeist, R. Visser, F. M. Bickelhaupt, *Chem. Eur. J.* **2009**, *15*, 6112-6115.

[89] R. Fornika, H. Görls, B. Seemann, W. Leitner, *J. Chem. Soc. Chem. Commun.* **1995**, 1479-1481.

[90] E. Lindner, R. Fawzi, H. A. Mayer, K. Eichele, W. Hiller, *Organometallics* **1992**, *11*, 1033-1043.

[91] W. Leitner, M. Bühl, R. Fornika, C. Six, W. Baumann, E. Dinjus, M. Kessler, C. Krüger, A. Rufinska, *Organometallics* **1999**, *18*, 1196-1206.

[92] V. V. Tkachev, L. O. Atovmyan, L. V. Goncharova, A. A. Shvets, O. A. Osipov, *Zh. Strukt. Khim.* **1982**, *23*, 168-170.

[93] O. Orama, J. T. Koskinen, *Acta Cryst. C* **1994**, *50*, 608-609.

[94] B. Machura, A. Swietlicka, M. Wolff, R. Kruszynski, *Polyhedron* **2010**, *29*, 2061-2069.

Chapter V

Coordinative and catalytic properties of a β-cyclodextrin bearing an introverted P(III) donor atom. Comparison with a diphosphine analogue

Chapter V

Coordinative and catalytic properties of a β-cyclodextrin bearing an introverted P(III) donor atom. Comparison with a diphosphine analogue

SUMMARY – CHAPTER V

A permethylated β-cyclodextrin containing a phenylphosphinidene ("PPh") unit that caps two adjacent glucose units (**L**), thereby orientating the phosphorus lone pair towards the CD interior, straightforwardly forms monophosphine complexes when reacted with palladium(II) complexes. The complex *trans*-[$PdCl_2(H_2O)$**L**], obtained in high yield from [$PdCl_2(PhCN)_2$], provides a rare example of square planar Pd(II) aqua complex stabilised by a single tertiary phosphine that behaves both as a first and second coordination sphere ligand.

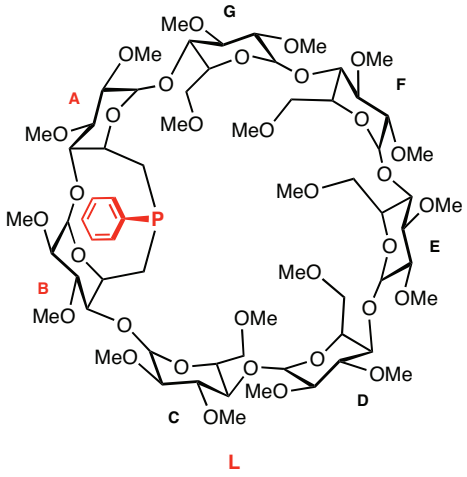

L

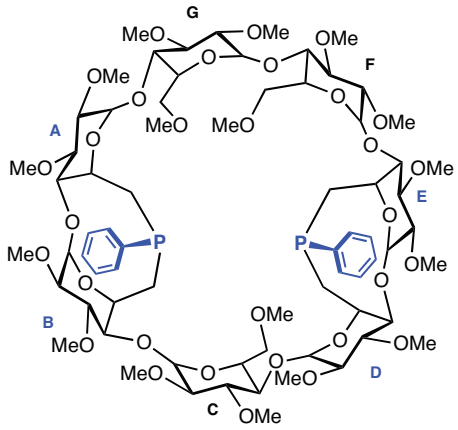

WIDEPHOS

In combination with palladium, **L** turned out to be active in Heck couplings of arylbromides with styrene. Highest activities were obtained when applying a phosphine/palladium ratio of 1:1, suggesting that a monophosphine complex is operative during catalysis. The performance of **L** was higher than that obtained with the diphosphine **WIDEPHOS**, a doubly-phosphinated variant of the ligand.

V.1. Introduction

Since the recent studies of Buchwald[1,2] and Hartwig[3,4] on the role of some particular monodentate ligands in cross-coupling reactions, there is a renewed interest for tertiary phosphines that favour the formation of monophosphine complexes when opposed to transition metal ions. Such a behaviour is classically achieved either with very bulky phosphines,[5-9] including dendrimeric ones,[10,11] or with hybrid ligands that may potentially act as chelating ligands so as to prevent coordination of a second phosphorus atom.[12] An alternative approach that was recently developed by us, consists in using medium-sized molecular cavities integrating an "introverted" P(III) atom able to position a metal-organic fragment inside the cavity.[13] The steric crowding of such a ligand is expected to inhibit the binding of more than one phosphine unit. In the present study, we show, for the first time, that the previously reported β-cyclodextrin-phosphine **L** (**Chapter II**; Figure 1, left) meets the criteria for forming such complexes. The study further establishes that **L** promotes the palladium-catalysed Heck coupling of arylbromides with styrene. Its performance was compared with that of **WIDEPHOS** (Figure 1, right), a doubly-phosphinated variant of **L**.

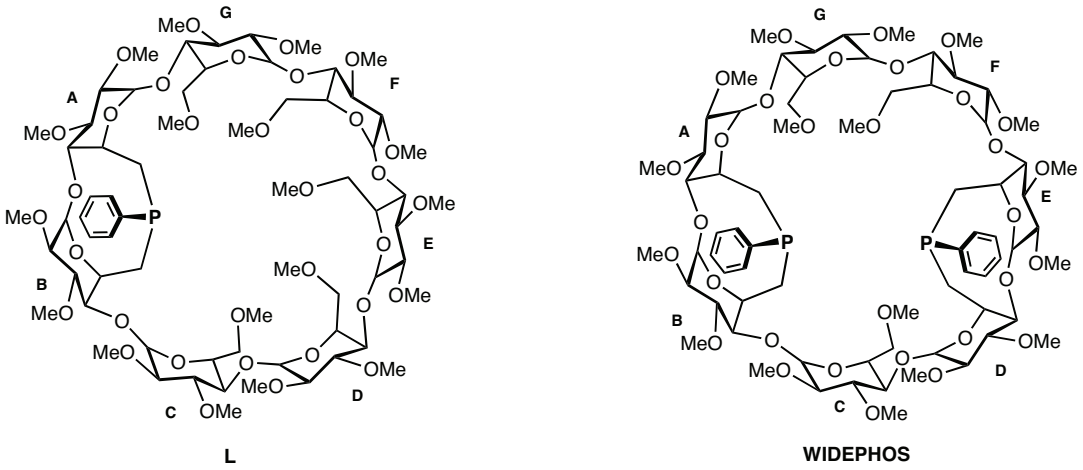

Figure 1. β-CD-based introverted phosphines used in this study.

V.2. Results and discussion

V.2.1. Coordination properties of β-CD-based monophosphine L

Monophoshine **L** contains a phenylphosphinidene ("PPh") unit linking the carbon atoms 6^A and 6^B of a permethylated β-CD. In this CD, the phosphorus lone pair is pointing towards the interior of the cavity. This allowed the preparation of complex **20** (Figure 2), presented in **Chapter II**.

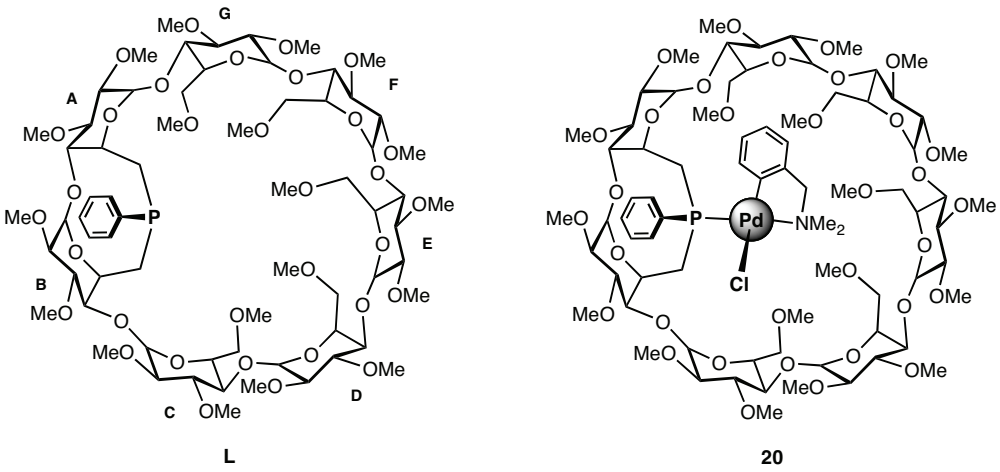

Figure 2. 6^A,6^B-capped ligand **L** and complex **20**.

Dropwise addition of monophosphine **L** to an excess (3 equiv.) of $[PdCl_2(PhCN)_2]$ in CH_2Cl_2 produced a mixture of several equilibrating species (probably involving benzonitrile complexes), which could not be identified. After standard column chromatography of the reaction mixture, complex **47** was recovered in high yield (90%, Scheme 1).

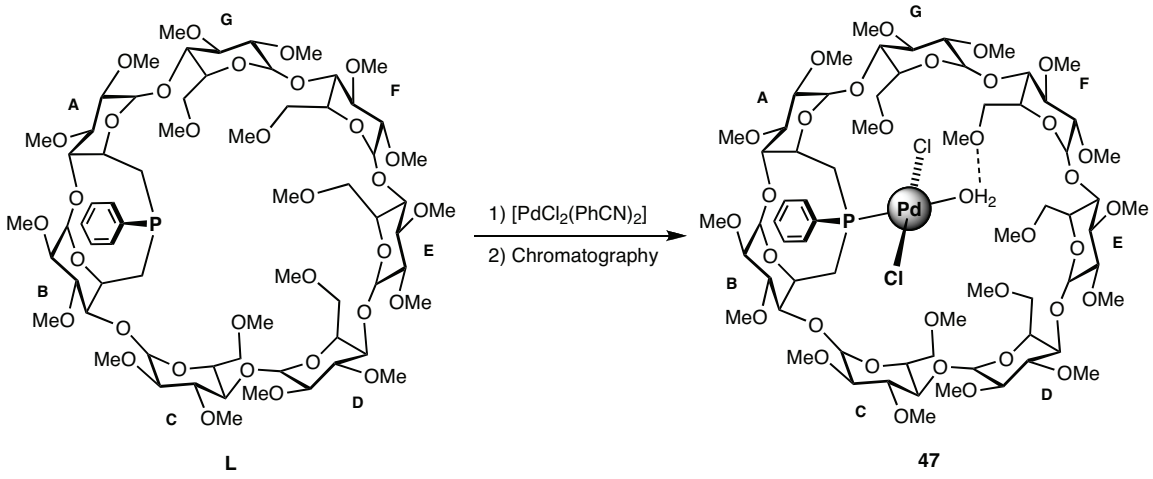

Scheme 1. Synthesis of the aqua-palladium complex **47**.

The P-monoligated nature of the complex was deduced from its mass spectrum, which displays a strong peak at *m/z* = 1675.52 corresponding to the $[M + Li]^+$ ion. Its $^{31}P\{^1H\}$ NMR spectrum shows a single, slightly broad singlet at δ = 34.4 ppm. The ^1H NMR spectrum reflects the presence of a non-distorted cavity, all H-1 anomeric protons lying in a very narrow range ($\Delta\delta$ = 0.18 ppm). The H-5 *intra*-cavity protons of glucose units A and B are significantly less downfield shifted (δ = 4.36 ppm and 4.79 ppm) than those of complexes **20**, in which the chlorine atom lies deep in the β-CD cavity.

Although not visible at room temperature, the coordinated water molecule appeared as a broad singlet at δ = 5.64 ppm when the ^1H NMR spectrum was recorded at –80ºC (Figure 3). This chemical shift is typical of aqua-palladium complexes.[14-16]

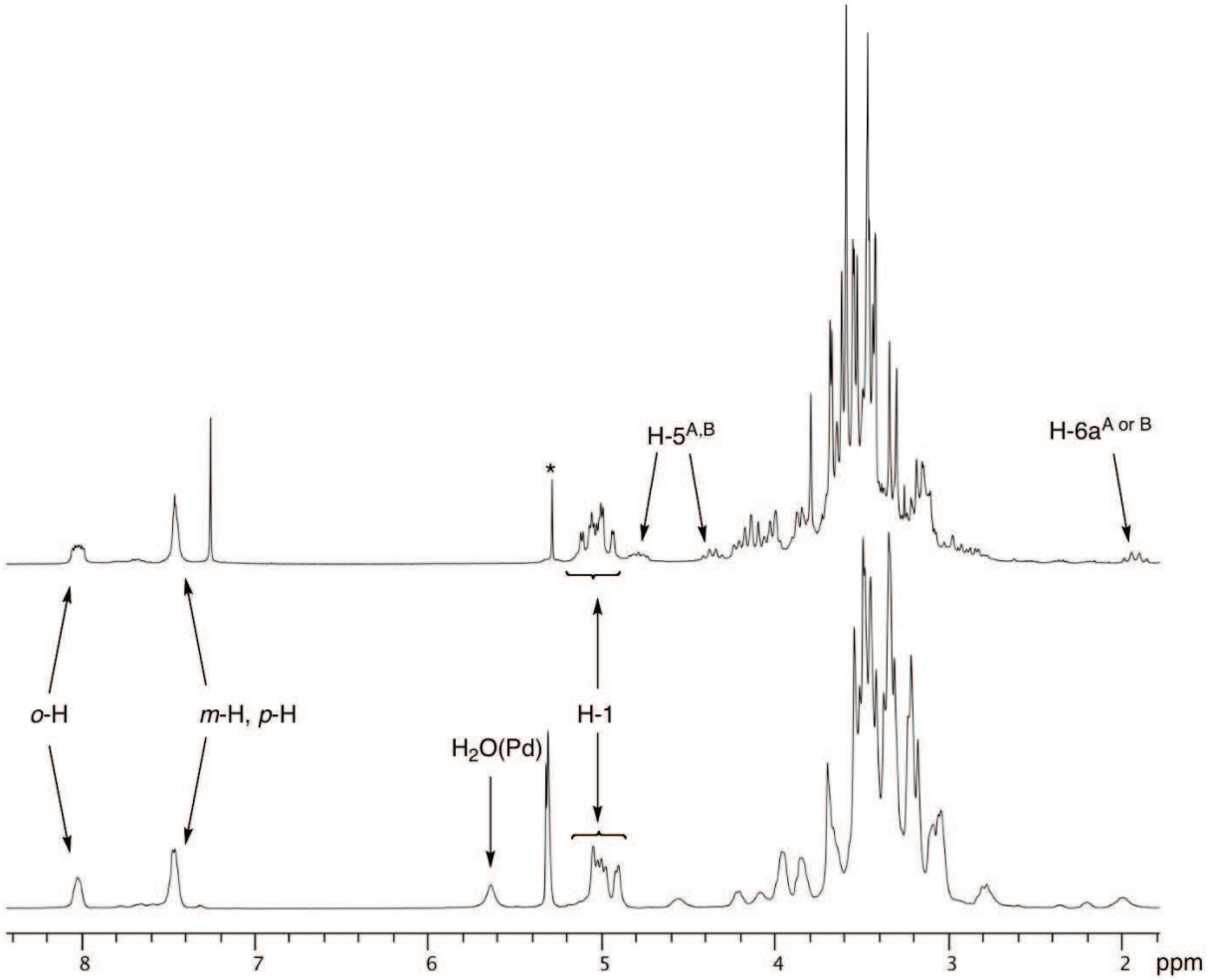

Figure 3. ^{1}H NMR spectra of compound **47** recorded in $CDCl_3$ at 300.1 MHz at 25ºC (top) and recorded in CD_2Cl_2 at 500.1 MHz at –80ºC (bottom). Asterisk denotes residual CH_2Cl_2.

The solid state structure of **47** was determined by an X-ray diffraction study (Figure 4 and Table 1), which confirmed the coordination of a single $\{PdCl_2(H_2O)\}$ fragment inside the β-CD cavity. Its most striking feature is the presence of a unique *intra*-cavity hydrogen-bonding network that literally fills the cavity with water molecules. The coordinated water molecule (O_w) is not only hydrogen-bonded to the OMe-6 group of glucose unit F (O^F), but also to an additional water molecule (O1), itself weakly bonded to the Cl(1) chlorine atom and a third water molecule (O2). The latter is connected to the CD secondary rim via a hydrogen bond with the OMe-2 group of glucose unit G (2-O^G). Interestingly, the P–Pd vector is not perfectly oriented towards the CD core, but slightly tilted towards one side of the cavity, close to glucose residues F and G. Moreover, the OMe-6 group of unit F underwent a major directional change so that *intra*-cavity hydrogen-bonding can take place

between its now inward-looking oxygen atom and the water molecule coordinated to the palladium centre.

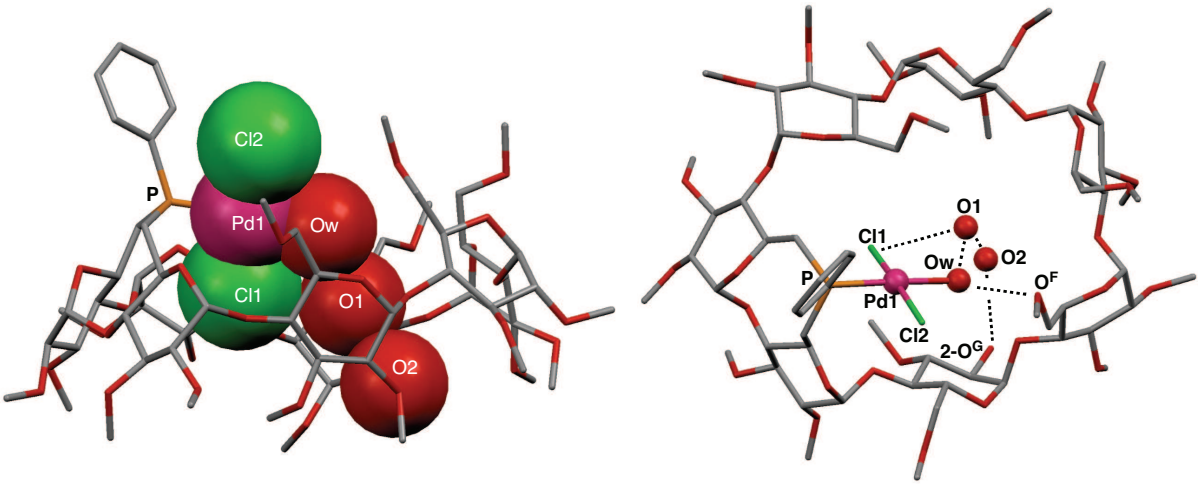

Figure 4. X-ray structure of aqua-palladium complex **47** (side view, left, and top view, right). Doted lines indicate hydrogen-bonding. Solvent molecules have been removed for clarity.

Table 1. Selected bond lengths, distances and angles for **47**·CH_2Cl_2·C_2H_6O·2(H_2O).

Bond lengths and distances [Å]			
P(1)–Pd(1)	2.208(3)	O_w···O^F	2.753
Pd(1)–Cl(1)	2.301(3)	O_w···O1	2.696
Pd(1)–Cl(2)	2.274(3)	O1···O2	2.810
Pd(1)–O_w	2.136(7)	O2···2-O^G	2.800
Cl(1)···H-5^A	2.696	Cl(1)···O1	3.202
Cl(1)···H-5^B	2.732	Cl(1)···H-5^C	2.779
Angles[°]			
P(1)-Pd(1)-O_w	177.42	P(1)-Pd(1)-Cl(1)	91.69
Cl(1)-Pd(1)-Cl(2)	173.14	P(1)-Pd(1)-Cl(2)	90.82
Cl(1)-Pd(1)-O_w	87.16	Cl(2)-Pd(1)-O_w	90.07

In the aqua-palladium complex **47**, the coordinated water molecule (O_w) is strongly stabilized by two hydrogen bonds. This is quite different from the related aqua complex **45** (**Chapter IV**; Figure 5, right), the water molecule of which is only involved in a single hydrogen bond, but more like the situation in complex **35** (**Chapter IV**; Figure 5, left), which

shares common features with **47,** hence the difference of stability between **45** on one hand and both **35** and **47** on the other. Note that complexes with a methanol solvent molecule and a monophosphine coordinating a palladium centre have been reported.[17]

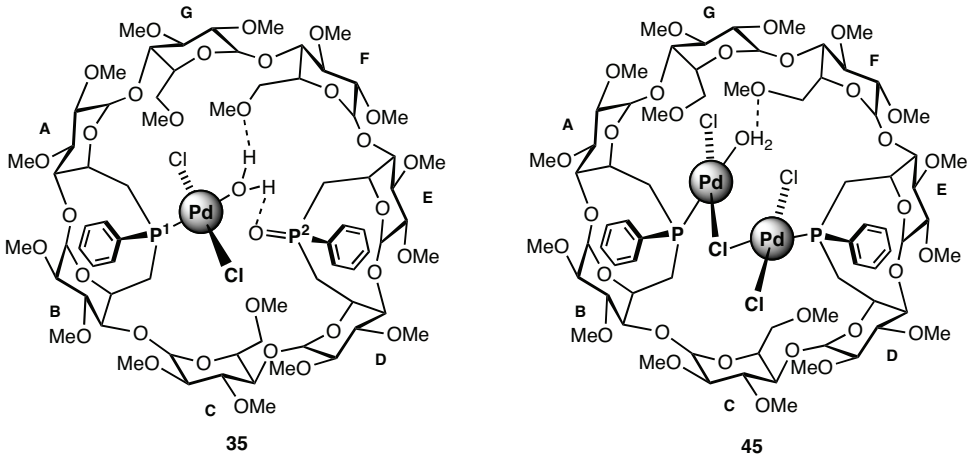

Figure 5. Aqua-palladium(II) complex **35** and **45**.

The aqua-palladium complex **47** could be dehydrated using a Dean-Stark apparatus to give the corresponding methoxy-bonded complex **48** (Scheme 2). The latter is rather unstable and is readily rehydrated upon standard column chromatography. The mass spectrum of **48** shows a strong peak at *m/z* = 1673.52 having the expected isotopic profile to $[M + Na]^+$ ion. The ^1H NMR and $^{13}C\{^1H\}$ NMR of both compounds are very similar, however some differences could be detected, in particular in the chemical shift range where methoxy protons resonate. Although it was not possible to determine which methoxy group was bonded to the metal centre because of overlapping signals, coordination of the one belonging to glucose unit G seemed to be the most favourable according to CPK models.

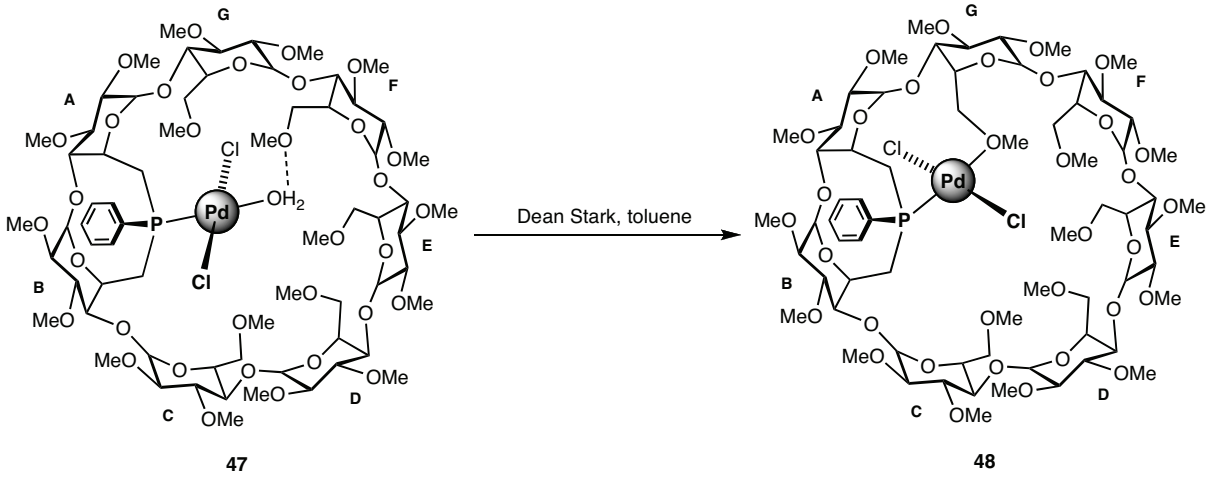

Scheme 2. Synthesis of the dehydrated palladium(II) complex **48**.

Also, the anomeric protons of **48** lie in a wider range ($\Delta\delta$ = 0.36 ppm) than those of less distorted **47** ($\Delta\delta$ = 0.18 ppm). Clearly, coordination of the methoxy group to palladium requires significant conformational changes in the CD torus. The most significant spectroscopic changes concern the $^{31}P\{^{1}H\}$ NMR signals. The $^{31}P\{^{1}H\}$ NMR spectrum of **48** consists of a sharp singlet at δ = 19.8 ppm corresponding to the single phosphorus atom, which resonates at a much higher field than that of its hydrated counterpart **47** (δ = 34.4 ppm). Such an unexpected large upfield shift ($\Delta\delta$ = 14.6 ppm), which is reminiscent of the observations made for **43** and **44** (**Chapter IV**), is consistent with a weakening of the Pd–P bond on going from **47** to **48**, probably as a result of a non optimal overlap between the phosphorus lone pair and the metal orbital in chelate **48**.

V.2.2. Using β-CDs bearing "introverted" phosphine ligands in Heck reactions

Monophosphine **L** was evaluated in combination with $Pd(OAc)_2$ as catalyst for Heck coupling[18] of styrene with arylbromides. In a preliminary study, 4-bromoanisole was reacted for 1 h with styrene at 110ºC in the presence of Cs_2CO_3 in *N,N*-dimethylformamide (DMF) (Table 2). Under these conditions the highest yield (46.5%) was obtained when using one equivalent of **L** per palladium operating under 1 mol % of catalyst (Table 2, entry 4). Higher phosphine/Pd ratios did not improve the catalytic outcome (Table 2, entry 3). These results clearly indicate that a single phosphine ligand is sufficient to stabilize the active palladium species. Finally, we observed that by raising the temperature to 130º, the conversions remained practically unchanged (Table 2, entry 5).

Table 2. Heck cross-coupling of 4-bromoanisole with styrene – the search for optimal conditions.

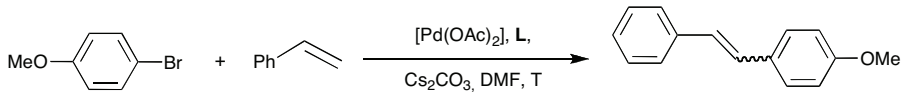

Entry	**L** /[$Pd(OAc)_2$]	T (ºC)	Conversion (%)
1[a]	0/1	110	4.3
2[a]	1/2	110	17.6
3[a]	2/1	110	45.7
4[a]	1/1	110	46.5
5[b]	1/1	130	45.5

[a] Conditions: [$Pd(OAc)_2$] (5 x 10^{-3} mmol, 1 mol %), ligand, 4-bromoanisole (0.5 mmol), styrene (1.0 mmol), Cs_2CO_3 (1.0 mmol), DMF (1.5 mL), decane (0.05 mL), 1 h.
[b] Conditions: [$Pd(OAc)_2$] (2.5 x 10^{-3} mmol, 1 mol %), ligand, 4-bromoanisole (0.25 mmol), styrene (0.5 mmol), Cs_2CO_3 (0.5 mmol), DMF (0.75 mL), decane (0.025 mL), 1 h. Conversions were determined by GC, the calibrations being based on decane.

We then applied the aforementioned optimal conditions in the coupling of styrene with different arylbromides (Table 3). The reaction appeared to depend on the steric hindrance of the bromide used. Thus, a conversion of 61.0% was observed for 4-bromotoluene, while the 3- and 2-substituted isomers led to conversions of 37.9% and 28.6%, respectively (Table 3, entry 1 and 2). As expected, the activated 2-bromo-6-methoxynaphtalene afforded the corresponding coupling product in relatively high yield (71%; Table 3, entry 4). It is noteworthy that the activities obtained in Heck coupling with the above catalytic system lie in

the range obtained with other phosphines,[19,20] these being, however, generally used in excess.[3,21]

Table 3. Palladium-catalysed Heck cross-coupling of arylbromides with styrene using **L**.[a]

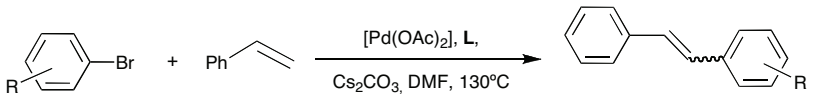

Entry	Substrate	Conversion (%)
1	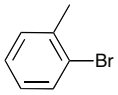	28.6
2	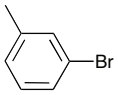	37.9
3	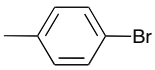	61.0
4	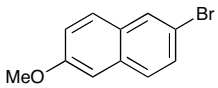	71.1

[a] Conditions: $[Pd(OAc)_2]$ (2.5 x 10^{-3} mmol, 1 mol %), ligand (2.5 x 10^{-3} mmol, 1 mol %), arylbromide (0.25 mmol), styrene (0.5 mmol), Cs_2CO_3 (0.5 mmol), DMF (0.75 mL), decane (0.025 mL), 1 h. Conversions were determined by GC, the calibrations being based on decane.

Until 2000, the mechanism for the Pd-phosphine catalysed Heck reaction was assumed to involve a step in which a bis-phosphine complex undergoes dissociation of a phosphine ligand leading to an olefin intermediate (Scheme 3, left).[22-26] Recent mechanistic studies by Amatore and Jutand[27] have shown that the whole catalytic cycle may take place via intermediates that all contain two coordinated phosphines. As shown above, the catalytic results outlined in the present study are in keeping with the formation of active monocoordinated $[Pd^0\mathbf{L}]$ species. Clearly, the formation of a bis-phosphine $[Pd\mathbf{L}_2]$ intermediate is not favoured owing to the particular structure of the phosphine. On the other hand, the coordination of methoxy groups in the active palladium species cannot be ruled out (Scheme 3, right).

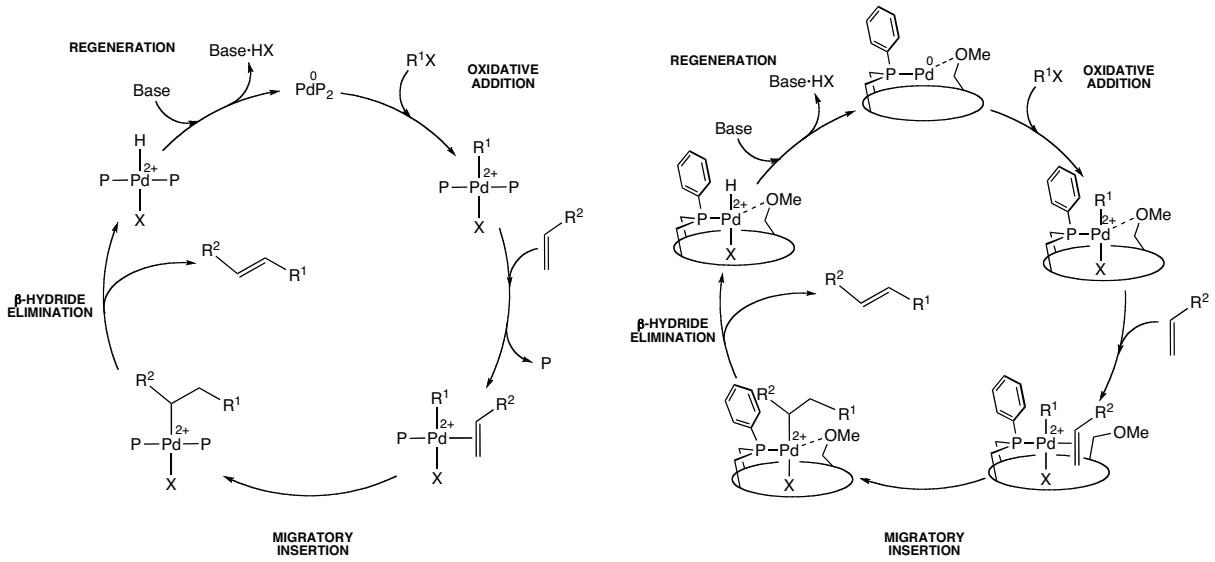

Scheme 3. Traditional mechanism of the Heck reaction (P = monophosphine, left) and possible mechanism when using **L** as ligand (right). R^1 = Ar or vinyl; R^2 = preferentially an electron withdrawing group; X = Br, I.

We also assessed the catalytic behaviour of the *trans*-chelating ligand **WIDEPHOS** in Heck reactions. Again, 4-bromoanisole was reacted with styrene to search for optimal conditions. When using a 1:1 ligand/Pd ratio, no conversion was observed (Table 4, entry 2). This poor result is probably caused by the formation of a stable *trans*-complex, which does not allow easy dissociation of a phosphine end. However, when applying a ligand/Pd ratio of 1:2, the reaction proceeded with 10.4% conversion (Table 4, entry 3). With this ratio and by increasing the temperature from 110ºC to 130ºC, the conversion raised to 20.7% (Table 4, entry 4). These results suggest that under these particular conditions **WIDEPHOS** operates as a ligand with two independent *monophosphine* arms, each of which binds a palladium atom. The lower conversions observed for **WIDEPHOS** *vs*. those obtained with **L**, is likely to arise from the important steric crowding generated about the two metal centres located in the CD.

Table 4. Heck cross-coupling of 4-bromoanisole with styrene – the search for optimal conditions.

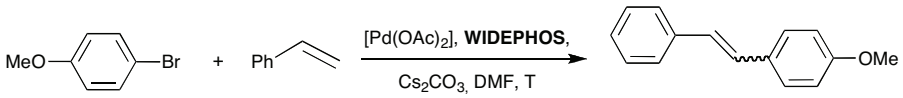

Entry	**WIDEPHOS**/[Pd(OAc)$_2$]	T (ºC)	Conversion (%)
1[a]	0/1	110	5.6
2[a]	1/1	110	/
3[a]	1/2	110	10.4
4[b]	1/2	130	20.7

[a] Conditions: [Pd(OAc)$_2$] (5 x 10^{-3} mmol, 1 mol %), ligand, 4-bromoanisole (0.5 mmol), styrene (1.0 mmol), Cs_2CO_3 (1.0 mmol), DMF (1.5 mL), decane (0.05 mL), 1 h.
[b] Conditions: [Pd(OAc)$_2$] (2.5 x 10^{-3} mmol, 1 mol %), ligand, 4-bromoanisole (0.25 mmol), styrene (0.5 mmol), Cs_2CO_3 (0.5 mmol), DMF (0.75 mL), decane (0.025 mL), 1 h. Conversions were determined by GC, the calibrations being based on decane.

Table 5. Palladium-catalysed Heck cross-coupling of arylbromides with styrene by using **WIDEPHOS**.[a]

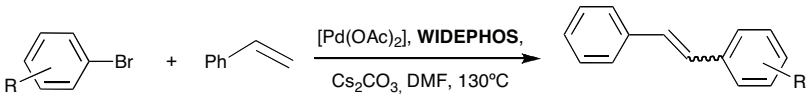

Entry	Substrate	Conversion (%)
1	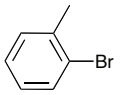	16.0
2	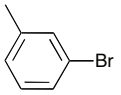	25.5
3	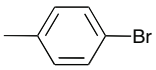	31.1
4	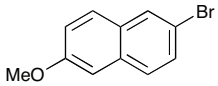	74.2

[a] Conditions: [Pd(OAc)$_2$] (2.5 x 10^{-3} mmol, 1 mol %), ligand (1.25 x 10^{-3} mmol, 0.5 mol %), arylbromide (0.25 mmol), styrene (0.5 mmol), Cs_2CO_3 (0.5 mmol), DMF (0.75 mL), decane (0.025 mL), 1 h. Conversions were determined by GC, the calibrations being based on decane.

Applying the above conditions to reactions carried out with the arylbromides outlined in Table 5, led, in general, to lower yields than those observed with **L** (Table 3). However, as for **L**, the less bulky 4-bromotoluene led to a higher conversion (31.1%) than that obtained with 3- or 2-bromotoluene (25% and 16.0%, respectively; Table 5, entries 1-3). In contrast, the catalytic outcome for 2-bromo-6-methoxynaphtalene (74.2%; Table 5, entry 4) was similar to that observed when using monophosphine **L** (71.1%; Table 3, entry 4). We have no rational explanation for the poor discrimination between the two ligands towards this particular substrate.

Overall, the rather poor performances obtained with the chelating ligand **WIDEPHOS** are in accord with previous observations made for *trans*-binding diphosphines in the cross coupling of aryl halides with olefins.[5,21,28,29] Obviously, the formation of stable *trans*-complexes prevents decoordination of a phosphine end, which seems vital for completion of the whole catalytic cycle. Finally, we found that none of the two ligands assessed in this study were suitable for Suzuki-Miyaura cross coupling of arylhalides with phenylboronic acid. This again could reflect the steric limitations imposed by the ligands.

V.3. Conclusion

In this study, we have shown that when opposed to palladium(II) centres, the cavity-shaped phosphine **L** selectively forms monophosphine complexes. This property allowed isolation of the first Pd(II) aqua complex, *trans*-[$PdCl_2(H_2O)$**L**], in which the {$PdCl_2(H_2O)$} fragment is fully embedded in the CD cavity. Mixing the ligand with an equivalent of palladium resulted in a catalyst active in Heck couplings of styrene with arylbromides. The study revealed that the catalytically active species is likely to contain only one phosphine ligand and that the catalytic system exhibits superior activity compared to that obtained with the sterically more crowded chelating diphosphine **WIDEPHOS**. To the best of our knowledge, **L** is the first tertiary phosphine that has been successfully employed for the efficient cross coupling of 4-bromoanisole with styrene using only one equivalent of phosphine per palladium.[3,30]

V.4. Experimental section

V.4.1. General procedures

All manipulations were performed in Schlenk-type flasks under dry nitrogen. Solvents were dried by conventional methods and distilled immediately prior to use. Deuterated solvents were passed down a 5 cm-thick alumina column and stored under nitrogen over molecular sieves (4 Å). Routine ^{1}H and $^{13}C\{^{1}H\}$ spectra were recorded on FT Bruker AVANCE 300, AVANCE 400 and AVANCE 500. ^{1}H NMR spectral data were referenced to residual protiated solvents (δ = 7.26 ppm for $CDCl_3$), $^{13}C\{^{1}H\}$ chemical shifts are reported relative to deuterated solvents (δ = 77.00 ppm for $CDCl_3$) and the $^{31}P\{^{1}H\}$ NMR data are given relative to external H_3PO_4. Mass spectra were recorded either on a ZAB HF VG analytical spectrometer using *m*-nitrobenzyl alcohol as matrix or on a Bruker MicroTOF spectrometer (ESI) using CH_2Cl_2, MeCN or MeOH as solvent. Elemental analyses were performed by the Service de Microanalyse, Institut de Chimie, Strasbourg. Melting points were determined with a Büchi 535 capillary melting-point apparatus. All commercial reagents were used as supplied. **WIDEPHOS** and **L** were prepared according to the synthesis of compound **10** and **12** from **Chapter II**. $[PdCl_2(PhCN)_2]$[31] was prepared according to literature procedures. The numbering of the atoms within a glucose unit is as follows:

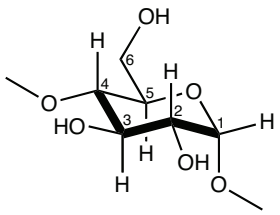

V.4.2. Synthesis of compounds

Aqua-palladium(II) complex 47

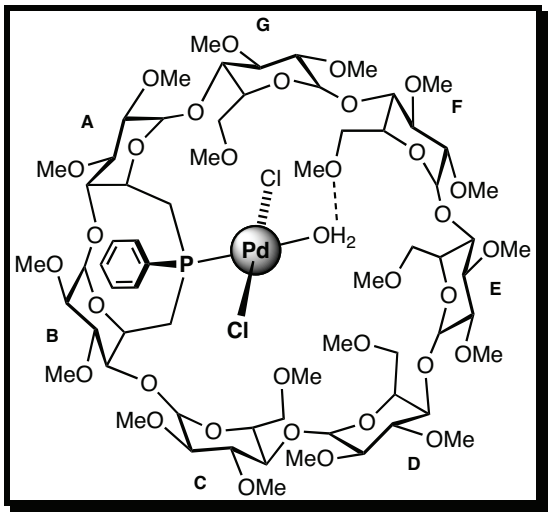

A solution of monophosphine **L** (0.150 g, 0.102 mmol) in CH_2Cl_2 (15 mL) was added dropwise to a solution of $[PdCl_2(PhCN)_2]$ (0.117 g, 0.306 mmol) in CH_2Cl_2 (15 mL) over 30 min. The reaction mixture was stirred for 1 h at room temperature before being evaporated to dryness. The crude product was purified by column chromatography (SiO_2, CH_2Cl_2/MeOH, 94:6, *v*/*v*) affording the aqua-palladium complex **47** (yield: 0.153 g, 90%) as an orange solid. R_f (SiO_2, CH_2Cl_2/MeOH, 92:8, *v*/*v*) = 0.35; m.p. dec. >250ºC; ^{1}H NMR (300.1 MHz, $CDCl_3$, 25ºC): δ (assignment by COSY) = 1.92 (td, 1 H, $^2J_{H\text{-}6a,H\text{-}6b} = {}^2J_{H\text{-}6a,P}$ = 12.9 Hz, $^3J_{H\text{-}6a,H\text{-}5}$ = 12.6 Hz, H-6a$^{A\text{ or }B}$), 2.78–3.02 (2 H, H-6$^{B\text{ or }A}$), 3.07–3.73 (20 H, H-3, H-4, H-6b$^{A\text{ or }B}$, H-6a^{C,D,E,F,G}), 3.81–4.24 (10 H, H-5^{C,D,E,F,G}, H-6a^{C,D,E,F,G}), 3.30 (s, 3 H, OMe), 3.34 (s, 3 H, OMe), 3.43 (s, 6 H, OMe), 3.44 (s, 3 H, OMe), 3.46 (s, 3 H, OMe), 3.47 (s, 9 H, OMe), 3.53 (s, 3 H, OMe), 3.55 (s, 3 H, OMe), 3.56 (s, 3 H, OMe), 3.59 (s, 9 H, OMe), 3.62 (s, 3 H, OMe), 3.68 (s, 3 H, OMe), 3.69 (s, 3 H, OMe), 3.80 (s, 3 H, OMe), 4.36 (td, 1 H, $^3J_{H\text{-}5,H\text{-}6a} = {}^2J_{H\text{-}5,P}$ = 10.4 Hz, $^3J_{H\text{-}5,H\text{-}6b}$ = 11.5 Hz, H-5$^{B\text{ or }A}$), 4.79 (m, 1 H, H-5$^{A\text{ or }B}$), 4.94 (d, 1 H, $^3J_{H\text{-}1,H\text{-}2}$ = 3.1 Hz, H-1), 5.00 (d, 2 H, $^3J_{H\text{-}1,H\text{-}2}$ = 3.7 Hz, H-1), 5.02 (d, 1 H, $^3J_{H\text{-}1,H\text{-}2}$ = 4.4 Hz, H-1), 5.05 (d, 1 H, $^3J_{H\text{-}1,H\text{-}2}$ = 3.8 Hz, H-1), 5.07 (d, 1 H, $^3J_{H\text{-}1,H\text{-}2}$ = 3.8 Hz, H-1), 5.12 (d, 1 H, $^3J_{H\text{-}1,H\text{-}2}$ = 4.2 Hz, H-1), 7.47 (3 H, *m*-H, *p*-H), 7.99–8.06 (m, 2 H, *o*-H) ppm; ^{13}C{^{1}H} NMR (75.5 MHz, $CDCl_3$, 25ºC): δ (assignment by HMQC) = 32.51 (d, $^1J_{C,P}$ = 33.8 Hz, C-6$^{A\text{ or }B}$), 36.66 (d, $^1J_{C,P}$ = 31.5 Hz, C-6$^{B\text{ or }A}$), 56.97, 57.88, 57.94, 58.10, 58.76, 58.83, 58.94 [×2], 59.12, 59.30, 59.44, 60.12, 60.75, 61.26, 61.62, 61.67, 61.71 [×2], 61.85 (OMe), 63.57 (d,

$^{2}J_{C,P}$ = 4.6 Hz, C-5$^{A\text{ or }B}$), 69.07 (d, $^{2}J_{C,P}$ = 4.6 Hz, C-5$^{B\text{ or }A}$), 70.20, 70.58, 70.65, 71.01, 71.44 (C-5^{C,D,E,F,G}), 71.11 [×2], 71.59, 73.14, 73.52 (C-6^{C,D,E,F,G}), 81.02 [×3], 81.10. 81.21, 81.40, 81.44, 81.63, 81.76 [×2], 82.12, 82.22, 82.32 [×2], 82.47, 82.81, 82.96, 83.13, 83.57, 83.76 (C-2, C-3, C-4$^{B\text{ or }A,C,D,E,F,G}$), 89.36 (d, $^{3}J_{C,P}$ = 4.6 Hz, C-4$^{A\text{ or }B}$), 95.02, 97.51, 99.22, 99.70, 100.15, 100.21, 100.80 (C-1), 128.68 (d, $^{3}J_{C,P}$ = 11.5 Hz, *m*-C), 131.10 (*p*-C), 132.09 (d, $^{2}J_{C,P}$ = 9.9 Hz, *o*-C) 133.60 (d, $^{1}J_{C,P}$ = 60.9 Hz, *ipso*-C) ppm; $^{31}P\{^{1}H\}$ NMR (121.5 MHz $CDCl_3$, 25ºC): δ = 34.4 (s) ppm; elemental analysis (%) calcd for $C_{67}H_{113}PdCl_2O_{34}P$ (1670.89): C 48.16, H 6.82, found: C 48.35, H 6.56; MS (ESI-TOF): *m/z* (%): 1741.43 (10) [*M* + MeOH + K]$^{+}$, 1675.52 (20) [*M* + Li]$^{+}$, 1673.51 (20) [*M* – H_2O + Na]$^{+}$.

Palladium(II) complex 48

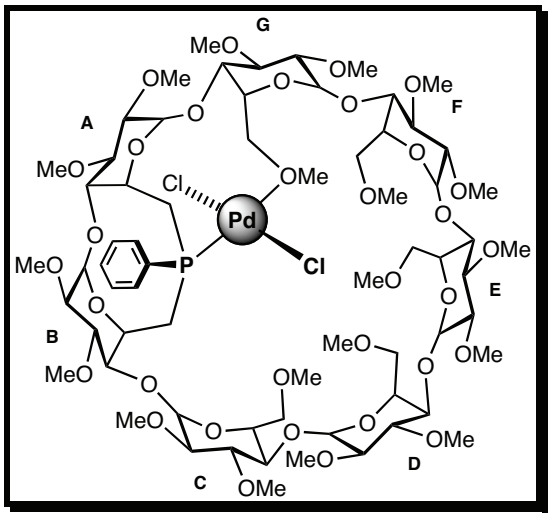

Water was removed over 12 h by azeotropic distillation of a refluxing toluene solution (100 mL) of compound **47** using a Dean Stark apparatus. After allowing the solution to reach room temperature, the solvent was removed *in vacuo* affording quantitatively compound **48**. Compound **48** rehydrates when absorbed to silica giving back compound **47**. m.p. dec. >250ºC; ^{1}H NMR (300.1 MHz, $CDCl_3$, 25ºC): δ (assignment by COSY) = 2.37 (m, 1 H, H-6a$^{A\text{ or }B}$), 2.59 (m, 1 H, H-6a$^{A\text{ or }B}$), 2.69 (dd, 1 H, $^{3}J_{H\text{-}2,H\text{-}3}$ = 9.9 Hz, $^{3}J_{H\text{-}2,H\text{-}1}$ = 2.8 Hz, H-2), 2.93–3.07 (2 H, H-6b^{A,B}), 3.12–3.26 (5 H, H-2), 3.30–3.93 (28 H, H-2, H-3, H-4, H-5, H-6), 3.99 (dd, 1 H, , $^{2}J_{H\text{-}6b,H\text{-}6a}$ = 9.7 Hz, $^{3}J_{H\text{-}6b,H\text{-}5}$ = 2.7 Hz, H-6b), 4.19 (dd, 1 H, , $^{2}J_{H\text{-}6b,H\text{-}6a}$ = 11.0 Hz, $^{3}J_{H\text{-}6b,H\text{-}5}$ = 2.4 Hz, H-6b), 4.25 (m, 1 H, H-5), 4.42 (m, 1 H, H-5$^{A\text{ or }B}$), 4.50 (m, 1 H, H-5$^{B\text{ or }A}$), 4.85 (d, 1 H, $^{3}J_{H\text{-}1,H\text{-}2}$ = 4.7 Hz, H-1), 4.98 (d, 1 H, $^{3}J_{H\text{-}1,H\text{-}2}$ = 2.6 Hz, H-1), 5.06 (d, 1 H, $^{3}J_{H\text{-}1,H\text{-}2}$ = 3.7 Hz, H-1), 5.08 (d, 1 H, $^{3}J_{H\text{-}1,H\text{-}2}$ = 3.6 Hz, H-1), 5.11 (d, 1 H, $^{3}J_{H\text{-}1,H\text{-}2}$ = 3.1 Hz,

H-1), 5.15 (d, 1 H, $^{3}J_{\text{H-1,H-2}}$ = 3.1 Hz, H-1), 5.21 (d, 1 H, $^{3}J_{\text{H-1,H-2}}$ = 3.1 Hz, H-1), 7.33–7.45 (3 H, *m*-H, *p*-H), 7.97 (ddd, 2 H, $^{3}J_{o\text{-H,P}}$ = 12.1 Hz, $^{3}J_{o\text{-H},m\text{-H}}$ = 6.9 Hz, $^{3}J_{o\text{-H},p\text{-H}}$ = 1.0 Hz, *o*-H) ppm; $^{13}C\{^{1}H\}$ NMR (75.5 MHz, $CDCl_3$, 25ºC): δ (assignment by HMQC) = 27.94–28.09 (overlapping d, $^{1}J_{\text{C,P}}$ = 27.5 Hz, C-$6^{\text{A,B}}$), 57.89, 58.29 [×2], 58.59, 58.62 [×3], 59.01, 59.05, 59.11, 59.25 [×2], 60.77, 60.98, 61.04, 61.32 [×2], 61.65, 61.71 (OMe), 65.36 (d, $^{2}J_{\text{C,P}}$ = 8.6 Hz, C-$5^{\text{A or B}}$), 69.30 (d, $^{2}J_{\text{C,P}}$ = 3.9 Hz, C-$5^{\text{B or A}}$), 70.80, 71.09 [×2], 71.26, 71.52 (C-$5^{\text{C,D,E,F,G}}$), 71.10, 71.36 [×2], 71.43, 71.61 (C-$6^{\text{C,D,E,F,G}}$), 79.15, 79.39, 79.91, 80.03, 80.12, 80.82, 80.87, 81.19, 81.32, 81.42, 81.49, 81.84 [×2], 81.89 [×2], 82.10, 82.24, 82.35, 82.41, 83.53, 84.17 (C-2, C-3, C-4), 96.98, 97.26, 98.79, 98.97, 99.36, 99.47, 99.64 (C-1), 128.57 (*p*-C), 128.97 (d, $^{3}J_{\text{C,P}}$ = 5.8 Hz, *m*-C), 131.46 (d, $^{1}J_{\text{C,P}}$ = 50.6 Hz, *ipso*-C), 132.53 (d, $^{2}J_{\text{C,P}}$ = 10.5 Hz, *o*-C) ppm; $^{31}P\{^{1}H\}$ NMR (121.5 MHz $CDCl_3$, 25ºC): δ = 19.8 (s) ppm; MS (ESI-TOF): *m/z* (%): 1673.52 (40) $[M + Na]^{+}$. We do not provide microanalytical data for this compound because of fast rehydration in air.

V.4.3. General procedure for palladium-catalysed Heck cross-coupling reactions

In an oven-dried Schlenk tube in an inert atmosphere a solution of $[Pd(OAc)_2]$ in DMF, a solution of ligand in DMF, aryl bromide (1 equiv.), styrene (2 equiv.), Cs_2CO_3 (2 equiv.), decane (internal reference) and a complementary amount of DMF were introduced. The reaction mixture was then heated for 1 h. After cooling to room temperature, a small amount (0.5 mL) of the resulting solution was passed through a Millipore filter and analyzed by GC.

V.4.4. X-ray crystallographic data for 47

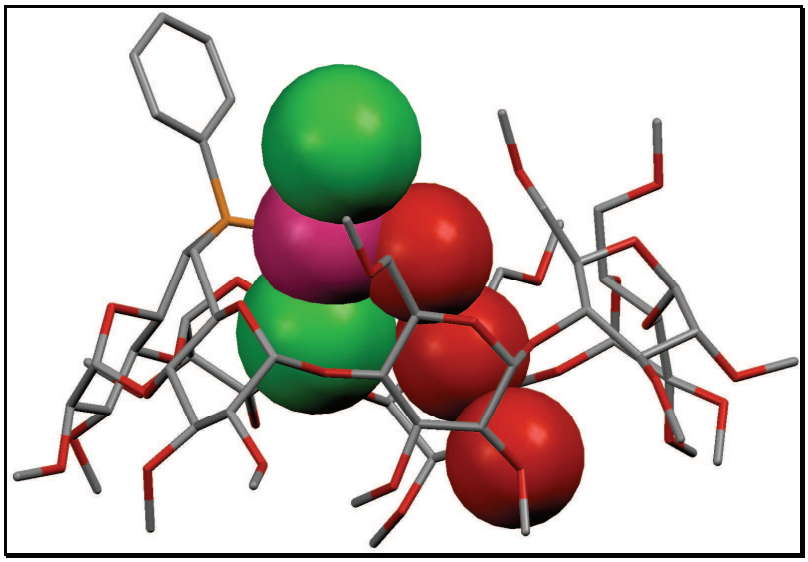

The X-ray structure determination was performed by Dr L. Toupet (University of Rennes, France). Single crystals were obtained by slow diffusion of pentane into a solution of **47** in non-distilled dichloromethane and ethanol. The sample was studied on a Oxford Diffraction Xcalibur Saphir 3 CCD with graphite monochromatised MoKα radiation (λ = 0.71073 Å). The structure was solved with SIR-97,[32] which revealed the non-hydrogen atoms of the molecule. After anisotropic refinement, many hydrogen atoms were found with a Fourier difference analysis. The whole structure was refined with SHELX-97[33] and full-matrix least-square techniques (use of F^2 magnitude; x, y, z, β_{ij} for Pd, Cl, C, O, P atoms, x, y, z, in riding mode for H atoms; 1000 variables and 18926 observations with $I > 2.0\sigma(I)$; calcd $w = 1/[\sigma^2(F_o^2) + (0.0348\ P)^2]$ where $P = (F_o^2 + 2\ F_o^2)/3$ with the resulting R = 0.064, R_w = 0.142 and S_w = 0.641; $\Delta\rho < 0.977$ eÅ^{-3}. The absolute configuration (and thus the enantiomeric space group assignment) was determined by a *Flack* x parameter of 0.08 (3). A summary of the crystallographic data is given in Table 6. CCDC reference number 780374. The samples were grown in CH_2Cl_2 solution. Only one cristal (size 0.11x0.04x0.04) was considered suitable for X-ray analysis. Due to the size and the poor diffracting quality of the sample, it was necessary to use a long time for the CCD images. The compound crystallizes with one molecule of ethanol, two half molecules of CH_2Cl_2 and three water molecules, one of them being chelated on Pd atom. The many Alert level A (maxshift/error, ADP, ...) are due to the size and the quality of the sample. In these conditions, the ratio 4547 Fo > 4sig(Fo) for 1000 parameters may be considered as a good result.

Table 6. Crystal data and structure refinement for **47**·CH_2Cl_2·C_2H_6O·2(H_2O).

Crystal Data	
Crystal size	0.11 × 0.04 × 0.04 mm^3
Empirical formula	$C_{70}H_{125}Cl_4O_{37}PPd$
M_r	1837.87
Crystal system	Orthorombic
Space group	$P2_1P2_1P2_1$
Temperature	120(2) K
Unit cell parameters	
a	10.4085(5) Å
b	24.645(2) Å
c	35.506(3) Å
α	90º
β	90º
γ	90º
V	9107.9(12) $Å^3$
Z	4
D (calculated)	1.340 g/cm^3
F (000)	3880
□	0.420 mm^{-1}
Data Processing and Reduction	
θ range for data collection	2.61 to 27.00º
Index ranges	$-13 \leq h \leq 11$, $-27 \leq k \leq 31$, $-45 \leq l \leq 26$
Reflections collected	32803
Independent reflections	18926 [R(int) = 0.1258]
Refinement method	Full-matrix least-squares on F^2
Data / restraints / parameters	18926 / 12 / 1000
Goodness-on-fir on F^2	0.635
Final R indices [$I > 2\sigma(I)$]	R1 = 0.0644, *w*R2 = 0.1134
R indices (all data)	R1 = 0.2426, *w*R2 = 0.1420
Largest diff. peak and hole	0.977 and -0.445 $eÅ^{-3}$

V.5. References

[1] J. P. Wolfe, R. A. Singer, B. H. Yang, S. L. Buchwald, *J. Am. Chem. Soc.* **1999**, *121*, 9550-9561.

[2] S. D. Walker, T. E. Barder, J. R. Martinelli, S. L. Buchwald, *Angew. Chem. Int. Ed.* **2004**, *43*, 1871-1876.

[3] J. P. Stambuli, S. R. Stauffer, K. H. Shaughnessy, J. F. Hartwig, *J. Am. Chem. Soc.* **2001**, *123*, 2677-2678.

[4] N. Kataoka, Q. Shelby, J. P. Stambuli, J. F. Hartwig, *J. Org. Chem.* **2002**, *67*, 5553-5566.

[5] A. F. Littke, G. C. Fu, *J. Org. Chem.* **1999**, *64*, 10-11.

[6] A. F. Littke, G. C. Fu, *J. Am. Chem. Soc.* **2001**, *123*, 6989-7000.

[7] Y. Ohzu, K. Goto, T. Kawashima, *Angew. Chem. Int. Ed.* **2003**, *42*, 5714-5717.

[8] T. Iwasawa, T. Komano, A. Tajima, M. Tokunaga, Y. Obora, T. Fujihara, Y. Tsuji, *Organometallics* **2006**, *25*, 4665-4669.

[9] H. Ohta, M. Tokunaga, Y. Obora, T. Iwai, T. Iwasawa, T. Fujihara, Y. Tsuji, *Org. Lett.* **2007**, *9*, 89-92.

[10] T. Fujihara, S. Yoshida, H. Ohta, Y. Tsuji, *Angew. Chem. Int. Ed.* **2008**, *47*, 8310-8314.

[11] D. J. M. Snelders, G. van Koten, R. J. M. K. Gebbink, *J. Am. Chem. Soc.* **2009**, *131*, 11407-11416.

[12] F. Y. Kwong, A. S. C. Chan, *Synlett* **2008**, *10*, 1440-1448.

[13] E. Engeldinger, L. Poorters, D. Armspach, D. Matt, L. Toupet, *Chem. Commun.* **2004**, 634-635.

[14] P. Espinet, J. M. Martínez-Ilarduya, C. Pérez-Briso, A. L. Casado, M. A. Alonso, *J. Organomet. Chem.* **1998**, *551*, 9-20.

[15] C. Bartolomé, P. Espinet, L. Vicente, F. Villafañe, *Organometallics* **2002**, *21*, 3536-3543.

[16] J. Vicente and A. Arcas, *Coord. Chem. Rev.* **2005**, *249*, 1135-1154.

[17] G. H. Queck, P.-H. Leung, K. F. Mok, *Inorganica Chimica Acta* **1995**, *239*, 185-188.

[18] R. F. Heck, J. P. Nolley Jr., *J. Org. Chem.* **1972**, *37*, 2320-2322.

[19] D. Sémeril, M. Lejeune, C. Jeunesse, D. Matt, *J. Mol. Catal. A* **2005**, *239*, 257-262.

[20] H. El Moll, D. Sémeril, D. Matt, M.-T. Youinou, L. Toupet, *Org. Biomol. Chem.* **2009**, *7*, 495-501.

[21] K. H. Shaughnessy, P. Kim, J. F. Hartwig, *J. Am. Chem. Soc.* **1999**, *121*, 2123-2132.

[22] Y. Ben-David, M. Portnoy, M. Gozin, D. Milstein, *Organometallics* **1992**, *11*, 1995-1996.

[23] G. T. Crisp, *Chem. Soc. Rev.* **1998**, *27*, 427-436.

[24] I. P. Beletskaya, A. V. Cheprakov, *Chem. Rev.* **2000**, *100*, 3009-3066.

[25] N. J. Whitcombe, K. K. Hii, S. E. Gibson, *Tetrahedron* **2001**, *57*, 7449-7476.

[26] P. Surawatanawong, Y. Fan, M. B. Hall, *J. Organomet. Chem.* **2008**, *693*, 1552-1563.

[27] C. Amatore, A. Jutand, *Acc. Chem. Res.* **2000**, *33*, 314-321.

[28] M. Qadir, T. Möchel and K. K. Hii, *Tetrahedron* **2000**, *56*, 7975-7979.

[29] R. C. Smith, C. R. Bodner, M. J. Earl, N. C. Sears, N. E. Hill, L. M. Bishop, N. Sizemore, D. T. Hehemann, J. J. Bohn, J. D. Protasiewicz, *J. Organomet. Chem.* **2005**, *690*, 477-481.

[30] M. D. Sliger, G. A. Broker, S. T. Griffin, R. D. Rogers, K. H. Shaughnessy, *J. Organomet. Chem.* **2005**, *690*, 1478-1486.

[31] F. R. Hartley, *The Chemistry of Platinum and Palladium;* Wiley, New York **1973**.

[32] A. Altomare, M. C. Burla, M. Camalli, G. Cascarano, C. Giacovazzo, A. Guagliardi, G. Moliterni, G. Polidori, R. Spagna, *J. Appl. Crystallogr.* **1998**, *31*, 74-77.

[33] G. M. Sheldrick, SHELXL-97, *Program for Crystal Structure* Refinement, University of Göttingen, Göttingen (Germany) **1997**.

Chapter VI

Can a cavity-shaped, trans-chelating diphosphine be used in carbon–carbon forming reactions?

Chapter VI

Can a cavity-shaped, *trans*-chelating diphosphine be used in carbon–carbon forming reactions?

SUMMARY – CHAPTER VI

Herein, we show how the *trans*-spanning ligand **TRANSDIP**, an α-cyclodextrin-derived, rigid diphosphane, participates in a palladium promoted carbon–carbon bond forming reaction. The study essentially focuses on the clear identification of relevant reaction intermediates. It reveals in particular that the cavity-shaped ligand is able to accommodate pentacoordinated palladium(II) complexes and that bond dissociation of one of the two M–P bonds occurs before the reductive elimination step.

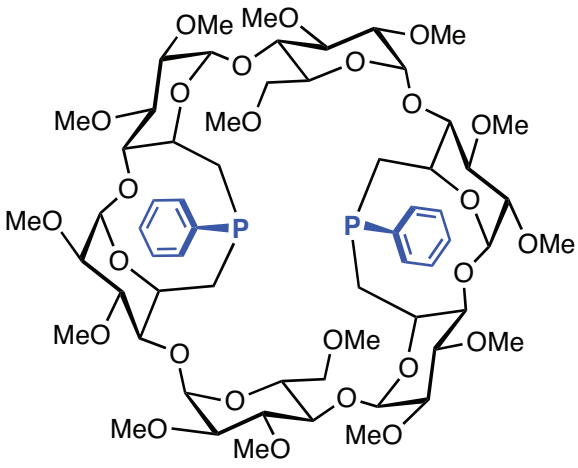

TRANSDIP

We further describe the synthesis of the anionic complex [Pd^0Cl(**TRANSDIP**)]Li, which is readily converted into [PdO_2(**TRANSDIP**)], a complex having a dioxygen ligand embedded in the cavity and which, therefore, opens the way to the study of *intra*-cavity oxidation processes occurring in a confined environment. Finally, the solvent dependent encapsulation of a chloride anion in the cationic complex [Au(**TRANSDIP**)]Cl will be described.

VI.1. Introduction

The quest for *trans*-spanning diphosphanes has been a long and difficult road[1-3] since the pioneering work of Issleib and Hohfeld in the 1960s.[4] Early efforts to synthesise such chelators culminated in the exhaustive studies of Venanzi on the first diphosphane, **TRANSPHOS** (Figure 1, left), claimed to be a *trans*-chelating ligand,[5-7] although its rigid benzo[*c*]phenanthrene backbone turned out to be flexible enough to allow *cis*-coordination.[8] Since then, such elusive ligands have been actively sought after, but most of them suffer from the lack of control of the metal first coordination sphere, in other terms they may also lead to other types of coordination complex, namely *cis*-chelates, dimers, oligomers or dinuclear species.[2] In 2004, we described the synthesis of the first authentic *trans*-spanning ligand, **TRANSDIP** (Figure 1, right).[9]

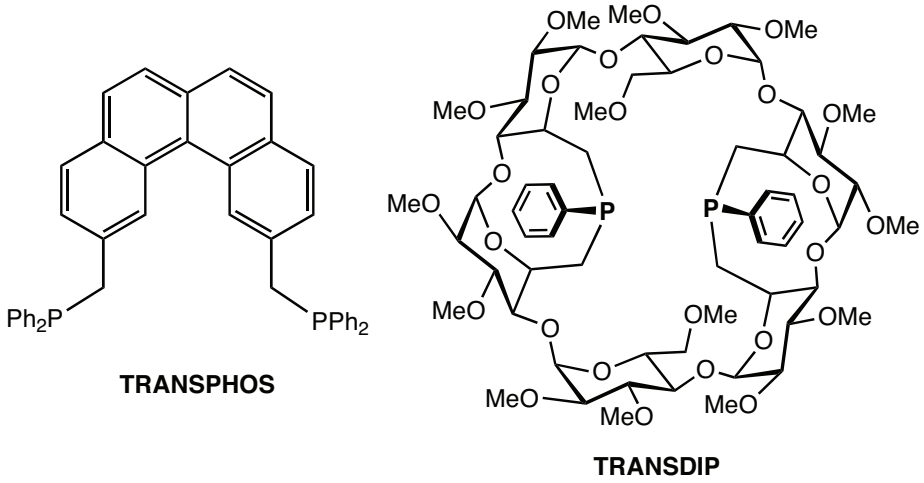

Figure 1. *trans*-Chelators **TRANSPHOS** (left) and **TRANSDIP** (right).

TRANSDIP rigid cyclodextrin (CD) platform does not allow the two inward-looking phosphorus donor atoms to coordinate a metal centre other than in a chelate fashion.[3,10,11] In addition, exclusive *trans*-coordination is believed to be the result of not only an ideal P···P separation, but also of the incapacity of the α-CD cavity to host more than one small metal-bound ligand such as a chlorido at a time.[12]

Palladium-catalysed coupling reactions have been extensively studied over the last 40 years.[13-16] They all require *cis*-coordination of the groups undergoing migratory insertion or reductive elimination.[17,18] Interestingly, some *trans*-chelating diphosphanes have been successfully employed in C–C bond forming reactions despite the fact that *cis*-chelation is strongly disfavoured with these ligands.[2,10,19-21] The lack of evidence for the real active species in these systems prompted us to study the behaviour of the authentic *trans*-chelator **TRANSDIP** in reductive, palladium promoted carbon–carbon coupling reactions. Here, we describe how **TRANSDIP** controls effectively the metal first sphere of coordination, so that previously postulated, but never identified intermediates could be stabilized for the first time in an unprecedented cascade of reactions leading to the formation of a carbon–carbon bond. Also, we report the first example of a metallated CD capable of trapping dioxygen within its cavity.

VI.2. Results and discussion

VI.2.1. Use of TRANSDIP in a C–C bond forming reaction

Previously, we had shown that upon reaction with MeLi the complex [$NiBr_2$(**TRANSDIP**)] (**49**) undergoes selective monomethylation to give **50**, no matter the amount of anion being used.[10] Steric protection provided by the cavity was invoked to explain the lack of reactivity of the second bromido ligand. As expected, when the palladium analogue **51** was treated with one equivalent of MeLi in thf (thf = tetrahydrofuran), the monomethylated complex **52** was recovered quantitatively after work-up. However, repeating the reaction in benzene, also with one equivalent of MeLi, caused the quantitative formation of the anionic five-coordinate complex **53**, that immediately precipitated out of solution and was isolated by simple filtration (Scheme 1).

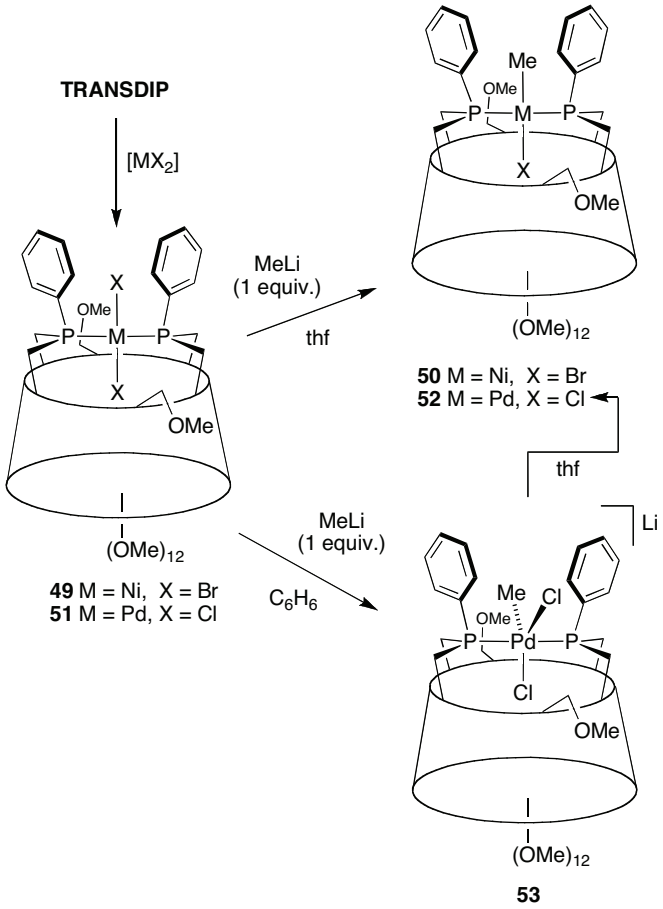

Scheme 1. Monomethylation of *trans*-chelate complexes **49** and **51**.

The ESI-MS-spectrum of **53**, recorded in negative ion mode, displays major peaks at *m/z* = 1509.5 and 1525.5 for $[M]^-$ and $[M + O]^-$ ions, respectively. The $^{31}P\{^1H\}$ NMR spectrum of **53**, recorded in C_6D_6, consists of a single, broad peak at δ = 10.7 ppm, the broadness of this peak possibly arising from partial insolubility of the complex. Conversely, **53** is perfectly soluble in thf, but is then slowly converted into **52** at room temperature (full conversion after 10 h). Complex **53** displays apparent C_2 symmetry, as deduced from its $^{31}P\{^1H\}$ NMR (d_8-thf) spectrum, which revealed a sharp singlet at δ = 11.1 ppm. Cooling the solution down to –80ºC caused this signal to broaden, however without reaching coalescence, unlike the signal of **52**, the singlet of which remained sharp over the considered temperature range. In keeping with *trans*-bonded phosphorus atoms, the ^1H NMR (d_8-thf, 25ºC) spectrum of **53** shows a well-defined methyl triplet at δ = –0.65 ppm, with ^3J(PH) = 6.2 Hz. Moreover, a 2D ^1H-$^{31}P\{^1H\}$ HMQC NMR experiment neatly revealed the presence of downfield shifted *intra*-cavity H-5 protons belonging to glucose units A, B, D and E (δ = 4.51 and 4.86 ppm; Figure 2, top), typical of chlorido encapsulation. In addition, a 2D ^1H-^1H ROESY NMR

experiment showed cross peaks between the palladium-bound methyl ligand and H-5 *intra*-cavity protons as well as aromatic *o*-H protons (Figure 2, bottom).

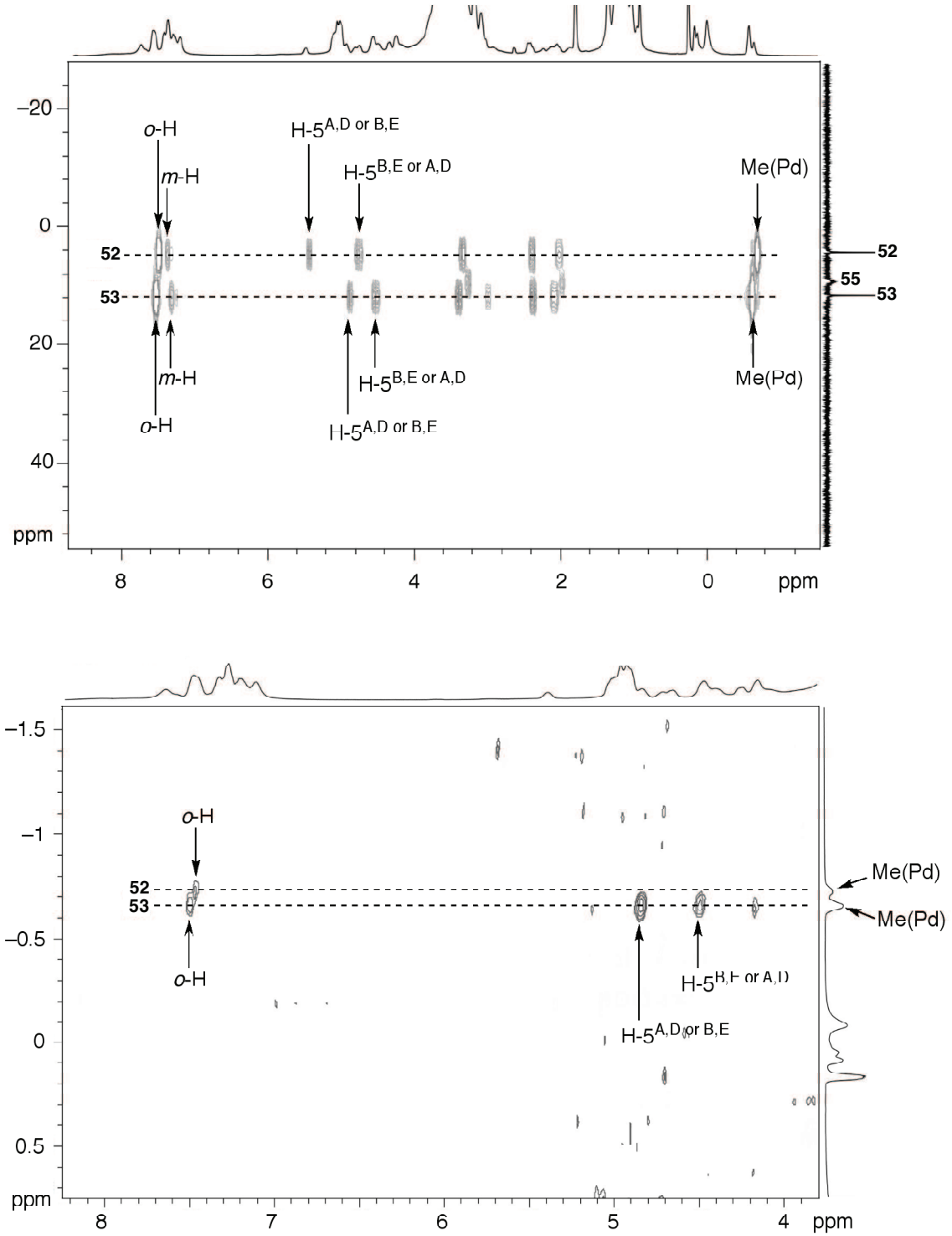

Figure 2. ^{1}H-^{31}P{^{1}H} HMQC (top) and part of the ^{1}H-^{1}H ROESY NMR (bottom) spectra of a mixture of **52**, **53** and **55** in the presence of an excess of MeLi recorded in d_8-thf at 500.1 MHz at 25ºC.

Overall, the above NMR data are consistent with a "$PdMeCl_2$" unit freely spinning around the P-Pd-P axle (Figure 3), the behaviour of complex **53** being reminiscent of Gray's molecular gyroscope obtained by *trans*-complexation of a $Mo(CO)_4$ moiety with a long α,ω-bis(phosphorus-donor)polyether ligand.[22] Clearly, the CD cavity plays here a major role in stabilizing the anionic intermediate **53**, which turned out to be much more stable than pentacoordinated palladium complexes coordinated to two independent phosphines.[23-25] Interestingly, this is not the case for the nickel analogue of **53**, which rapidly transforms into **50**. It is noteworthy that complex **53** constitutes the *first* spectroscopically characterised trigonal bipyramidal palladium complex with *trans*-disposed phosphorus atoms. Pentacoordinated, anionic alkyl-Pd(II) complexes containing phosphine ligands have already been identified, both spectroscopically and electrochemically, but their exact stereochemistry could not be established.[23-25] Note also that these were generated by oxidative addition of an aryl halide to a palladium(0) species and not by nucleophilic substitution on a palladium(II) centre.

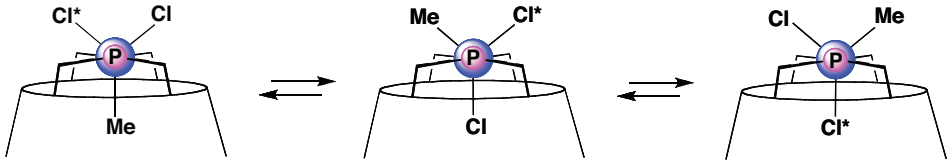

Figure 3. Fast rotation of the "$PdMeCl_2$" unit about the P···P axle in **53** (view along the P-Pd-P rod)

When the palladium(II) complex **51** was reacted with *excess* MeLi (3 equiv. or more), a cascade of transformations leading to the production of ethane occurred (Scheme 2 and Figure 4). In order to gain more information about this intriguing result, the methylation reaction was carried out at low temperature in d_8-thf in a NMR tube (Figure 5). Complex **51** was first treated with 1 equivalent of MeLi at –80ºC. Not surprisingly, complex **52** was by far the predominant species formed, complex **53** being still present. Adding 3 further equivalents of MeLi at –60ºC caused the appearance of *two new transient* species with concomitant disappearance of complex **52**.

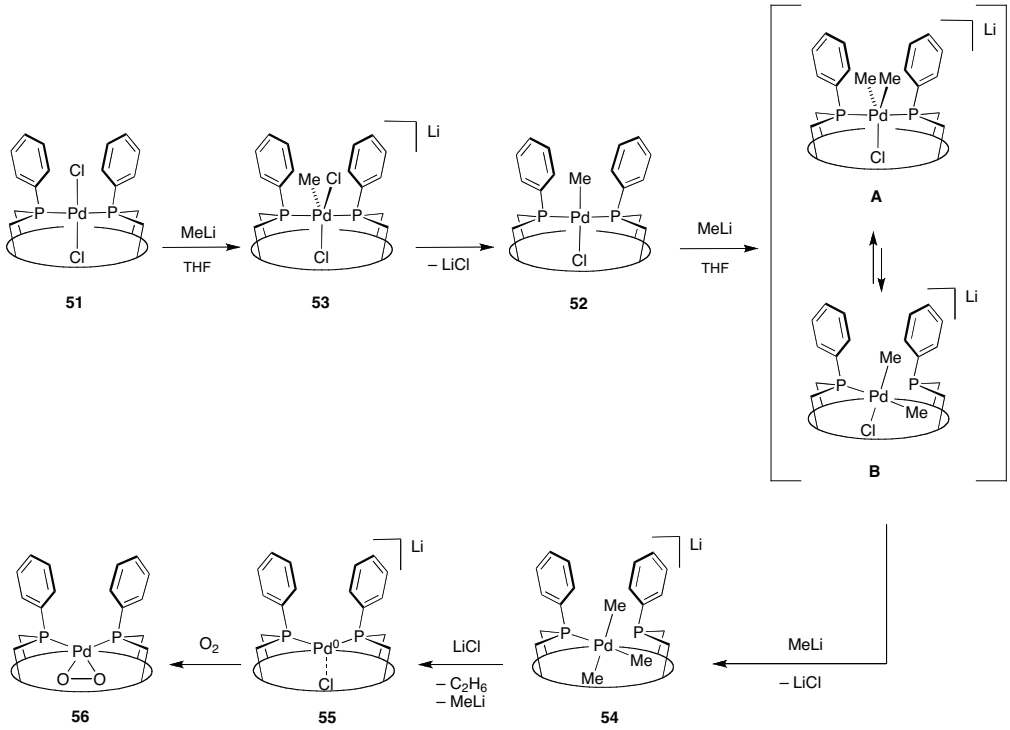

Scheme 2. Reaction pathway for the production of ethane from **51** and formation of dioxygen complex **56**.

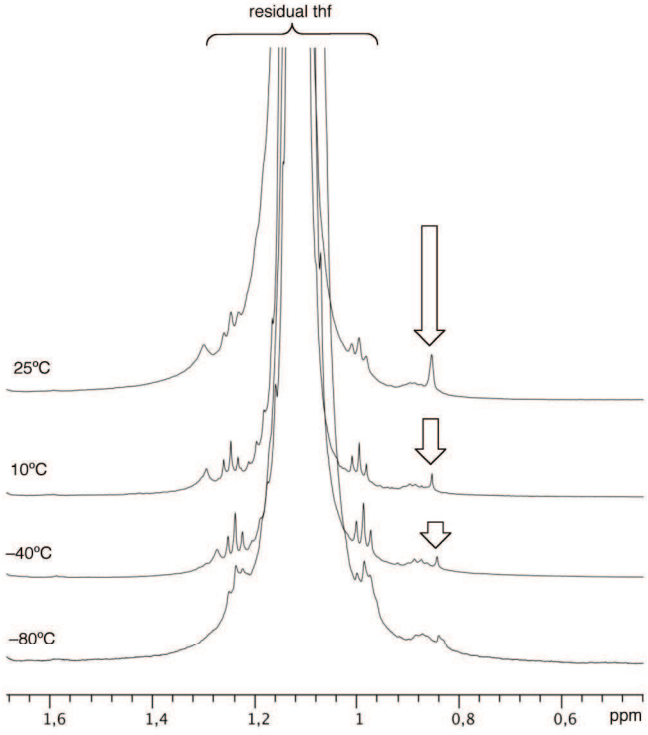

Figure 4. Variable temperature ^{1}H NMR study (zoom) of **51** in the presence of an excess of MeLi in d_8-thf at 500.1 MHz. Arrows indicate growing ethane concentration.

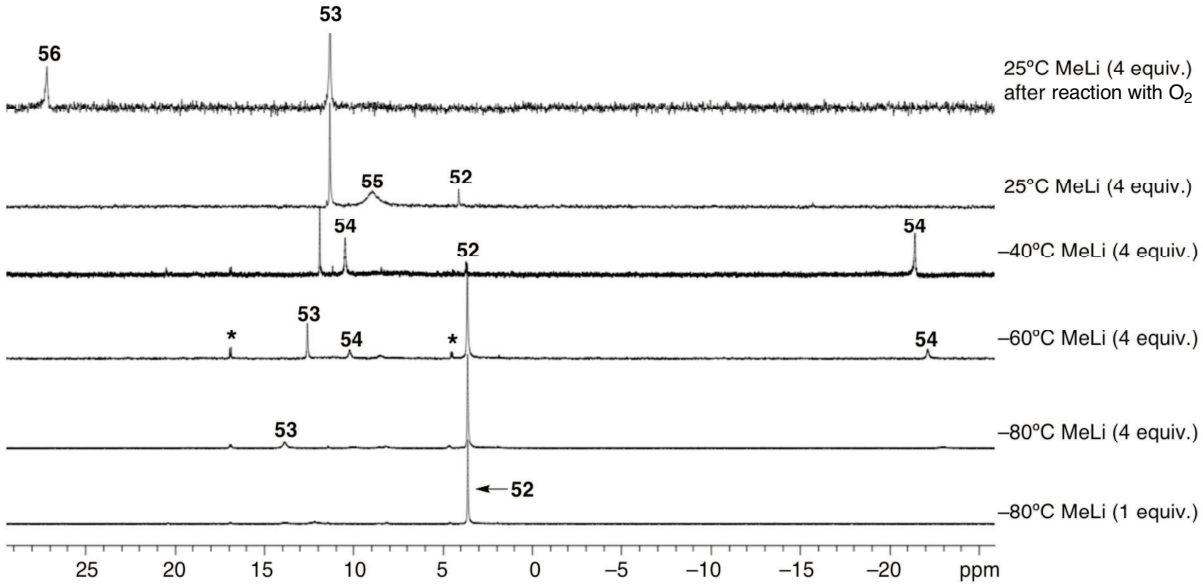

Figure 5. Variable temperature $^{31}P\{^{1}H\}$ NMR study of **51** in the presence of excess MeLi in d_8-thf recorded at 202.5 MHz. Asterisks denote traces of dinuclear species.

The major species detected at –40ºC is complex **54**. It comprises two non-equivalent phosphorus atoms, which resonate as two singlets having remarkably different chemical shifts, as deduced from its $^{31}P\{^{1}H\}$ NMR spectrum. One of them corresponds to a free phosphorus atom at δ = –21.4 ppm and the other to a coordinated one at δ = 11.2 ppm. The corresponding ^{1}H NMR spectrum (Figure 6) displays a doublet integrating for 6 equivalent methyl protons at δ = –0.68 ppm (^{3}J(PH) = 5.8 Hz) and a doublet at 0.01 ppm (^{3}J(PH) = 5.8 Hz) integrating for 3 methyl protons, corresponding to a "$PdMe_3$" fragment coordinated to a single phosphorus atom, as confirmed by a ^{1}H-$^{31}P\{^{1}H\}$ HMQC NMR experiment (Figure 7).

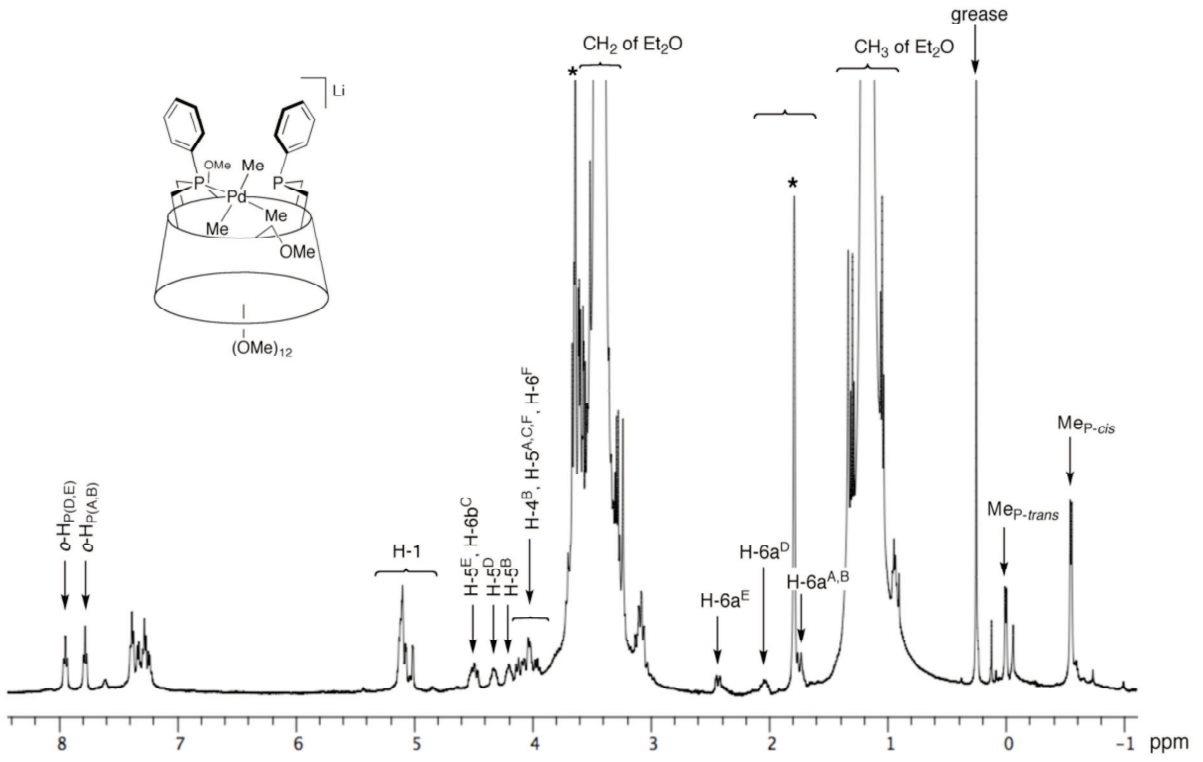

Figure 6. ^{1}H NMR spectrum of complex **54** recorded in d_8-thf at –40ºC at 500.1 MHz. Asterisks denote residual protic thf. Et_2O = diethyl ether.

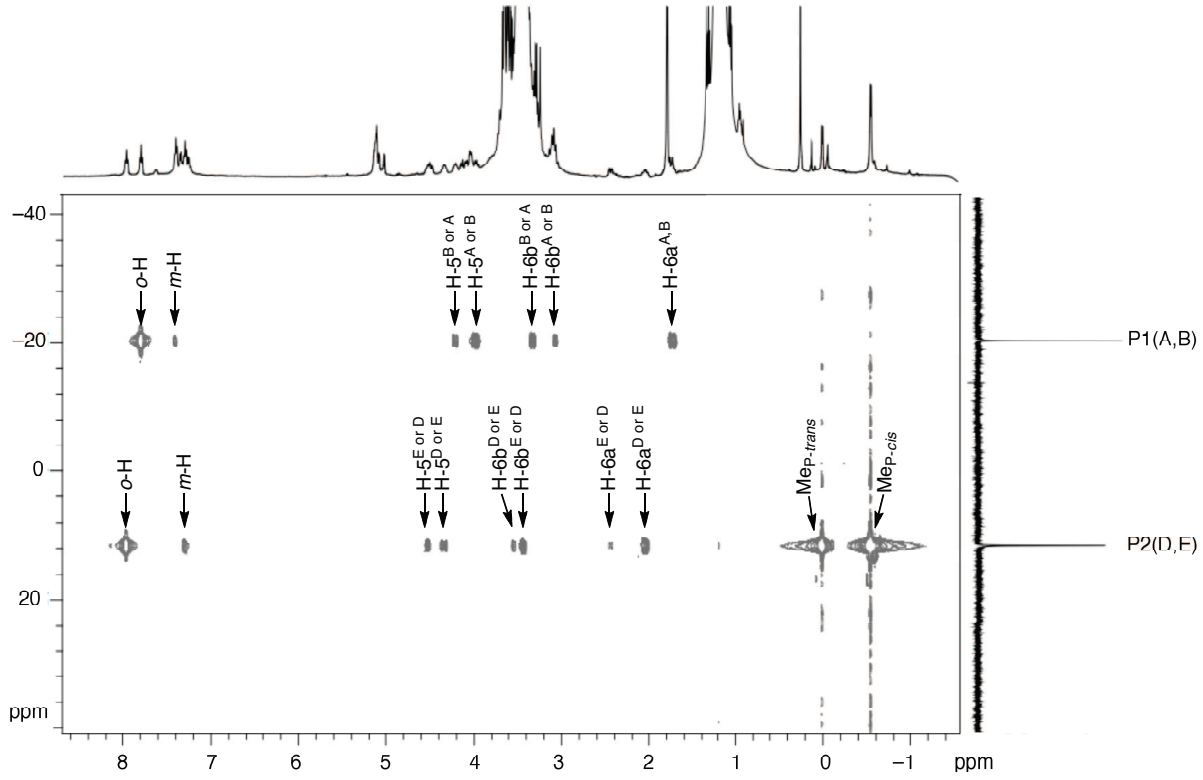

Figure 7. ^{1}H-^{31}P{^{1}H} HMQC NMR spectrum of complex **54** at –40ºC measured in d_8-thf at 500.1 MHz showing that the "$PdMe_3$" unit is bound to a single phosphorus atom.

Alternatively, complex **54** was quantitatively formed when treating a solution of pure **52** in d_8-thf with 4 equivalents of MeLi at –80ºC (Figure 8). To the best of our knowledge **54** is the first complex containing a "$PdMe_3$" fragment bound to a unique phosphorus atom of a potentially chelating diphosphine. Note that monophosphine complexes containing a "$PdMe_3$" fragment have already been reported. They were found stable at room temperature.[26]

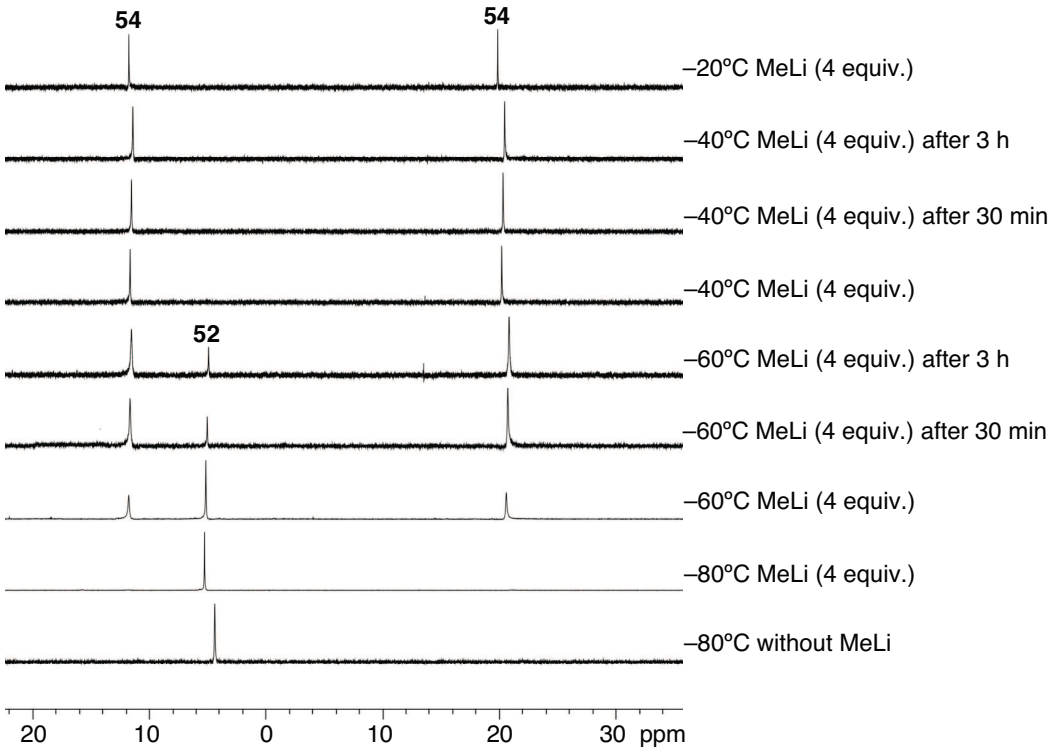

Figure 8. Variable temperature $^{31}P\{^1H\}$ NMR study of **52** in the presence of an excess of MeLi in d_8-thf recorded at 202.5 MHz showing quantitative formation of complex **54**.

The minor transient species (denoted with asterisks in Figure 5) observed in the range –80ºC/–40ºC gave rise to an AB system (δ = 4.4 and 16.9 ppm, ^2J(PP) = 16 Hz) in the $^{31}P\{^1H\}$ NMR spectrum, which is indicative of a C_1-symmetrical complex. As shown by a 2D ^1H-$^{31}P\{^1H\}$ HMQC NMR experiment, two methyl groups are present, each of them correlating with one of the phosphorus atoms. These findings are consistent with the formation of a dinuclear intermediate, the precise formulation of which could however not be devised.

Upon letting the reaction mixture reach 25ºC (Figure 5), complex **54** *rapidly disappeared* to give the Pd^0 complex **55** with concomitant evolution of ethane at $\delta = 0.78$ ppm (Figure 4).[27] Note that, in contrast to the observations made by other authors on methyl-Pd complexes,[17,28] ethane formation was here remarkably facile, as it started to occur already at –80ºC. The $^{31}P\{^1H\}$ NMR spectrum of **55** consists of a broad singlet at $\delta = 8.7$ ppm and the ^1H NMR spectrum confirms the presence of a C_2-symmetrical species. Note that there was no indication of the presence of a methyl group. The presence of a coordinated chlorido anion in **55** could *stricto sensu* spectroscopically could not be proven as the phosphorus peak is too broad to give rise to correlations with H-5 *intra*-cavity protons in the 2D ^1H-$^{31}P\{^1H\}$ HMQC NMR spectrum. However, this is very likely as the reaction of **52** with 4 equivalents of MeLi at –80ºC, led to complex **55** only when LiCl (2 equivalents or more) was added to the reaction mixture, in keeping with chlorine stabilization of the Pd^0 complex. When the amount of chloride anion was not sufficient, the Pd^0 complex **55** did not form and rapid decomposition of the ligand was observed. The existence of ionic $[Pd^0Cl(PR_3)_2]Li$ species has already been proposed by Negishi.[29]

Overall, the best way to rationalise the formation of the Pd^0 complex **55** (when starting from **51**) is to consider complexes **53** and **54** as key intermediates (Scheme 2). As shown by the above NMR experiments, the methylation reaction first leads to **52**, which forms after departure of a Cl^- anion from the pentacoordinated intermediate **53**. Nucleophilic attack of MeLi on complex **52** then affords **54**, this reaction possibly involving the equilibrating intermediates **A** and **B**. The next step is the reductive elimination of ethane which results in a palladium(0) complex, the stability of which probably depends of coordinating chlorine anions (formation of **55**), although stable 14 VE Pd^0 complexes containing a *trans*-spanning diphosphane as the sole ligand have recently been isolated.[31] Clearly, in the present case, additional stabilisation is provided by the CD cavity, which is a good receptor for metal-chloride fragments. Finally, it should be reminded here that reductive coupling of R–R moieties from square planar Pd-*monophosphine* complexes is well documented.[30]

Complex **55** is extremely sensitive to oxygen, as a couple of seconds are enough to oxidise it in the presence of air (Figure 5 and Scheme 2), producing the peroxo complex [Pd(η^2-O_2)(**TRANSDIP**)] (**56**). The latter turned out to be exceptionally stable in contrast with most reported palladium peroxo complexes.[32-37] This peroxo complex could be

subjected to column chromatography and stored at room temperature without noticeable decomposition. It transforms into the corresponding di(phosphine oxide) and black palladium when heated above 60ºC in the solid state. Although indefinitely stable in solution in most organic solvents, **56** underwent slow chlorination to afford **51** when dissolved in chloroform. The $^{31}P\{^{1}H\}$ NMR spectrum of **56**, recorded in C_6D_6, consists of a single peak at δ = 28.8 ppm, indicating that the complex has kept the C_2 symmetry of the ligand. As for complexes having CD-included chlorido ligands, two sets of H-5 protons belonging to bridging units are markedly downfield shifted (δ = 5.16 and 5.46 ppm), in keeping with an encapsulated peroxo unit (Figure 9).

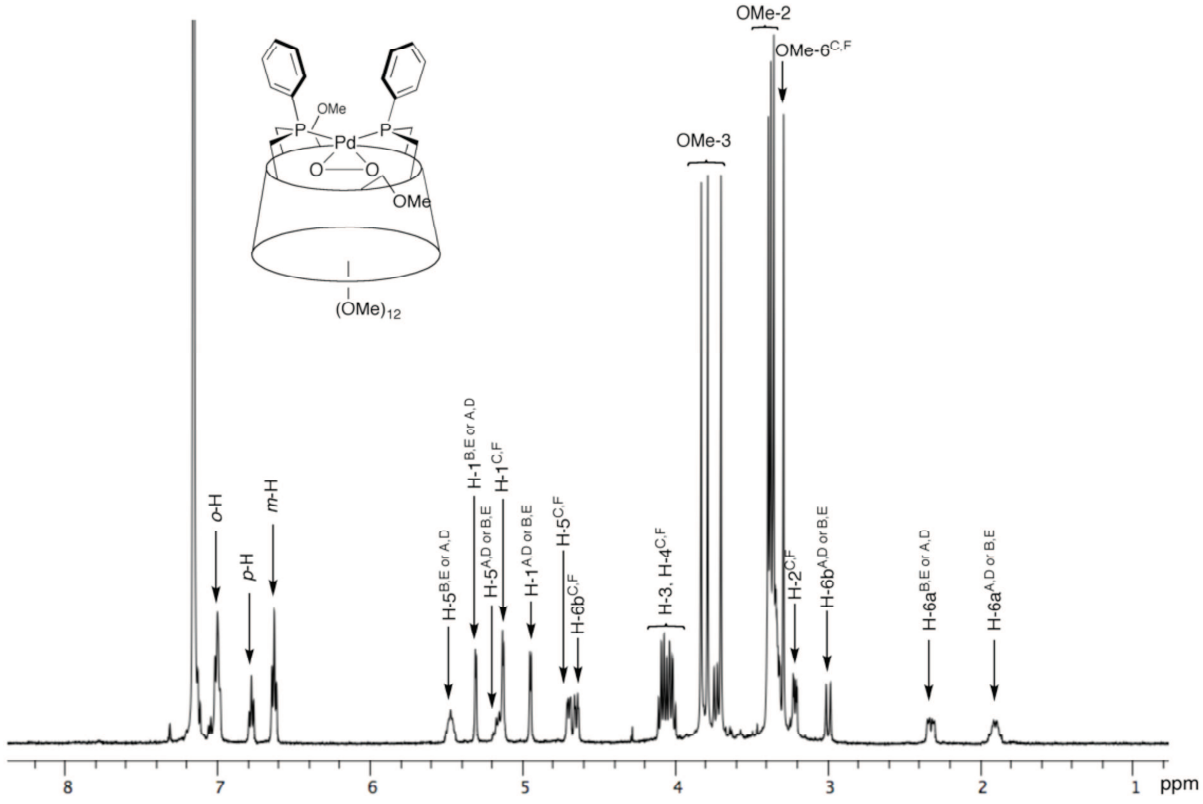

Figure 9. ^{1}H NMR spectrum of complex **56** in C_6D_6 measured at 300.1 MHz at 25ºC.

This feature was confirmed by an X-ray diffraction study (Figure 10 and Table 1). Two independent molecules are present in the unit cell. The oxygen atoms are tightly held between the aforementioned four CD H-5 protons, with distances of 2.59 (2.64) and 2.49 (2.48) Å, respectively for $CH^{A,D}\cdots O$ and $CH^{B,E}\cdots O$ separations. The O···O distance of 1.41 (1.45) Å is typical for such peroxo complexes.[36-39] The P-Pd-P angle, 112.4º (110.7º), the size of which is imposed by the triangular PdO_2 moiety, is so far the smallest observed in a **TRANSDIP**

complex, but is larger than in the only reported structure of a Pd peroxo chelate complex (P-Pd-P 104.5º).[40]

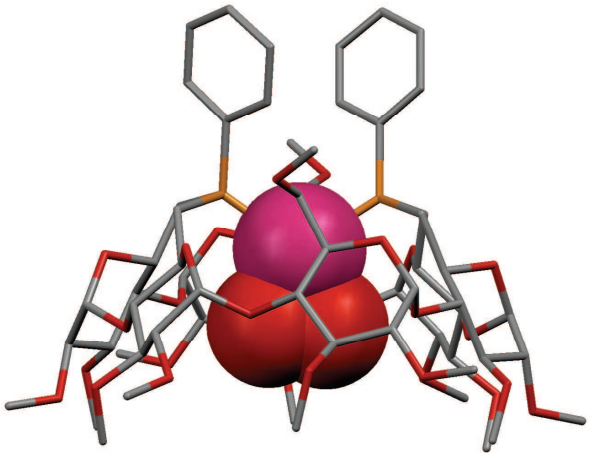

Figure 10. X-ray structure of the peroxo complex **56**. For clarity, only one molecule from the unit cell is shown and solvent molecules have been omitted.

Table 1. Selected bond lengths, distances and angles for 2(**56**)·3(CH_2Cl_2).

Molecule **56a**		Molecule **56b**	
Bond lengths and distances [Å]			
P–Pd	2.306(1)	P–Pd	2.295(1)
Pd–O	2.005(3)	Pd–O	1.993(3)
O–O	1.409(5)	O–O	1.454(6)
O···H-5^A	2.591	O···H-5^A	2.638
O···H-5^B	2.486	O···H-5^B	2.480
Angles[º]			
P-Pd-P	112.41	P-Pd-P	110.67
P-Pd-O	103.26	P-Pd-O	103.28
O-Pd-O	41.13	O-Pd-O	42.79

Treating **51** or **52** with excess MeLi is not the best method for obtaining **56**, as small amounts of the monomethylated complex **52** were always present. Two different methods were employed to achieve full conversion of **TRANSDIP** into **56**. The first one consists in

treating **51** with at least 2 equiv. of *n*BuLi and then leaving the resulting Pd^0 complex to react with air. Presumably, the reaction proceeds in this case via β-hydride elimination,[17] be a mono- or dialkylated species formed. Complex **56** can also be obtained quantitatively by reacting **TRANSDIP** with $[Pd(dba)_2]$ (dba = dibenzylideneacetone) in the presence of air. Remarkably, no reaction occurred when **TRANSDIP** was treated with $[Pd(dba)_2]$ without oxygen. It seems that **TRANSDIP** competes unfavourably with dba for coordination to palladium(0)[41] and only oxygen can drive the palladium complexation to completion, because of the unusual stability of the resulting peroxo complex **56**. It is noteworthy to mention that such reaction can only occur because **TRANSDIP** is not easily oxidised.

In summary, the rigid, chelating ligand **TRANSDIP** has proven an invaluable tool for monitoring the sequential formation of a carbon–carbon bond from a *trans*-chelated $PdCl_2$ complex. The most remarkable finding of this study concerns the dissociation of one of the two phosphorus atoms, which is required for allowing the carbon–carbon coupling step to occur. It should be emphasised that the proposed C–C bond forming step (**56** → **57**) contrasts with the one proposed by Amatore and Jutand for palladium-catalysed cross-coupling reactions, in which the coupling occurs directly within an anionic $[PdClAr(R)(PR_3)_2]^-$ intermediate.[25] We have further shown that the presence of the CD cavity is essential in stabilizing palladium(0) complexes via chlorine encapsulation as well as palladium peroxo species, which are known to decompose rapidly in many other systems. No doubt that methylated cyclodextrins represent a promising alternative to other cavities, *e. g.* calix[6]arenes,[42,43] for performing *intra*-cavity oxidations.

VI.2.2. A solvent dependent chlorine encapsulation in a molecular cavity

The above findings on an anionic chlorido palladium(0) intermediate encouraged us to look for other **TRANSDIP** chelate complexes containing a unique M-Cl moiety. We therefore embarked on the study of the stoichiometric reaction between **TRANSDIP** and complex [AuCl(tht)] (tht = tetrahydrothiophene), which constitutes a common source of the AuCl fragment. This reaction afforded quantitatively and exclusively complex **57** (Scheme 3). Chelate formation was inferred from the mass spectrum, which showed an intense peak at *m/z* = 1513.52 corresponding to the $[M - Cl]^+$ cation, and the $^{31}P\{^1H\}$ NMR ($CDCl_3$) spectrum which displayed a single peak at δ = 27.2 ppm. Interestingly, the ^{31}P NMR signal of

57 (δ = 27.2 ppm) appears at considerably lower field that that of the related chelate complex, [Au(**TRANSDIP**)]PF_6 (**58**) (δ = 38.4 ppm), which was crystallographically shown to have the $[PF_6]^-$ anion remote from the cavity.[10] Clearly, in these complexes, the gold atoms must experience different coordination environments.

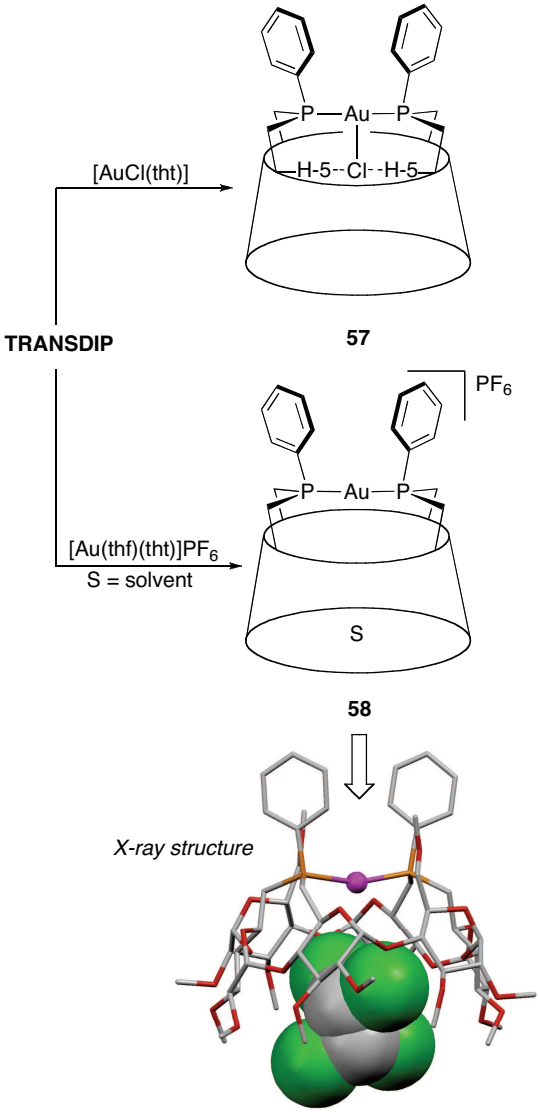

Scheme 3. Synthesis of anionic gold(I) complexes **57** and **58**. Dotted lines represent the interactions between the cavity and the chlorine anion. For clarity, the $[PF_6]^-$ anion in the solid state structure of **58** is not shown.

In fact, careful examination of the ^{1}H NMR spectra revealed significant differences in both complexes. The spectrum of complex **57** showed H-5 *intra*-cavity protons that are

strongly downfield shifted at δ = 4.87 and 5.22 ppm (Figure 11) with respect to those of **58** (δ = 4.24 and 4.36 ppm),[10] in keeping with encapsulation of the chloride anion in **57**. That the chloride anion interacts with the gold centre in **57** cannot be stated with certainty, but seems likely in view of the significant displacement of the phosphorus signal when compared to that of **58**. Note that, T-shaped $AuClP_2$ (P_2 = diphosphine) complexes have already been isolated,[44-46] although these are known to undergo straightforwardly structural rearrangements.[47-50]

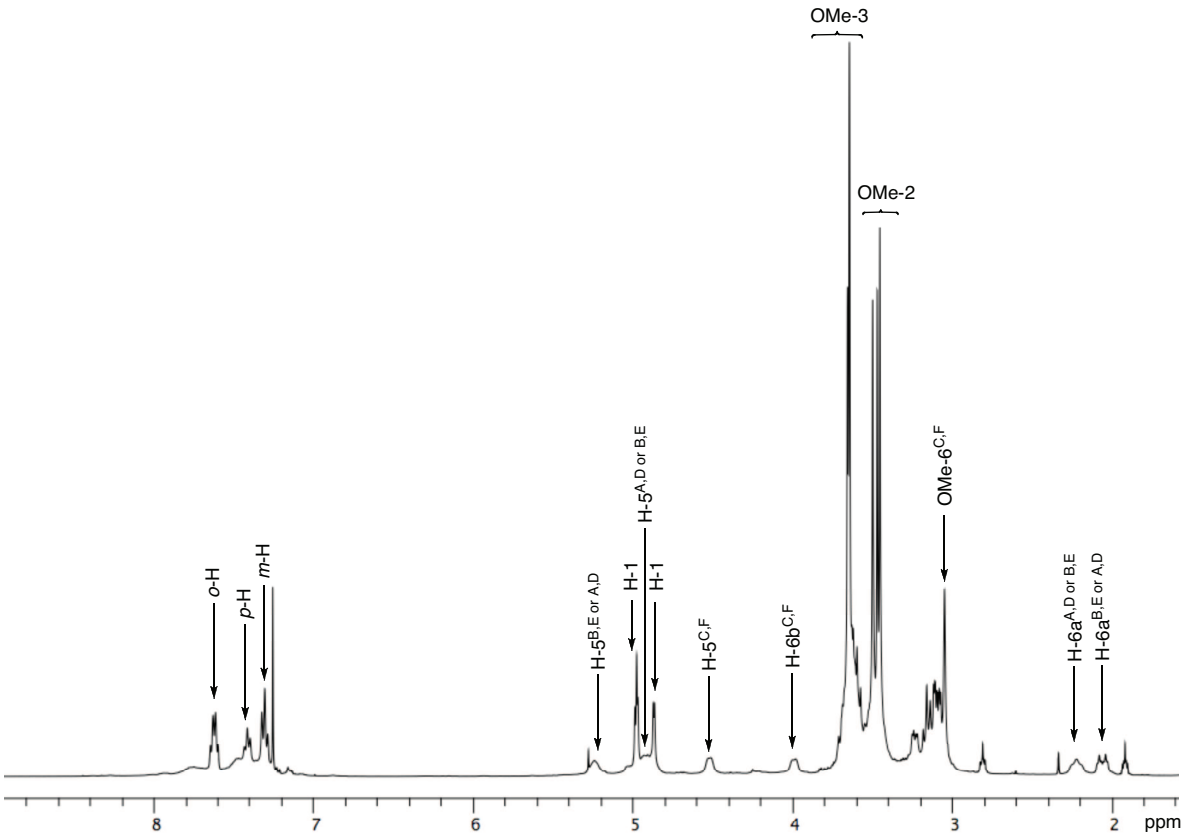

Figure 11. ^{1}H NMR spectrum of complex **57** in $CDCl_3$ measured at 300.1 MHz at 25ºC.

We observed that when carrying out the $^{31}P\{^{1}H\}$ NMR measurements of complex **57** in CD_2Cl_2 instead of $CDCl_3$, a second species at δ = 28.4 ppm, present in small amounts, appeared (Figure 12). Addition of NBu_4Cl (a chloride anion source) in excess to the solution caused full disappearance of the peak at δ = 28.4 ppm, **57** being then the only complex present. These observations are consistent with the existence of an equilibrium between the *endo*-complex **57** and a gold complex having a guest possibly coordinated to the metal, the structure of which could not be devised from spectroscopic analyses.

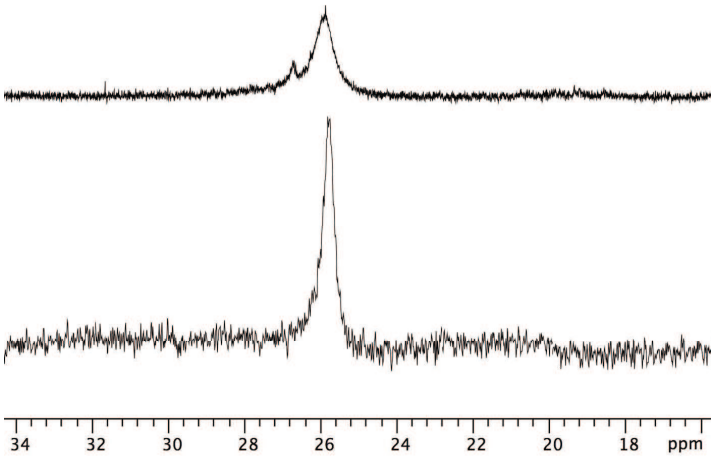

Figure 12. $^{31}P\{^{1}H\}$ NMR spectra of complex **57** (top) and after addition of excess NBu_4Cl (bottom) recorded in CD_2Cl_2 at 162.0 MHz at 25ºC.

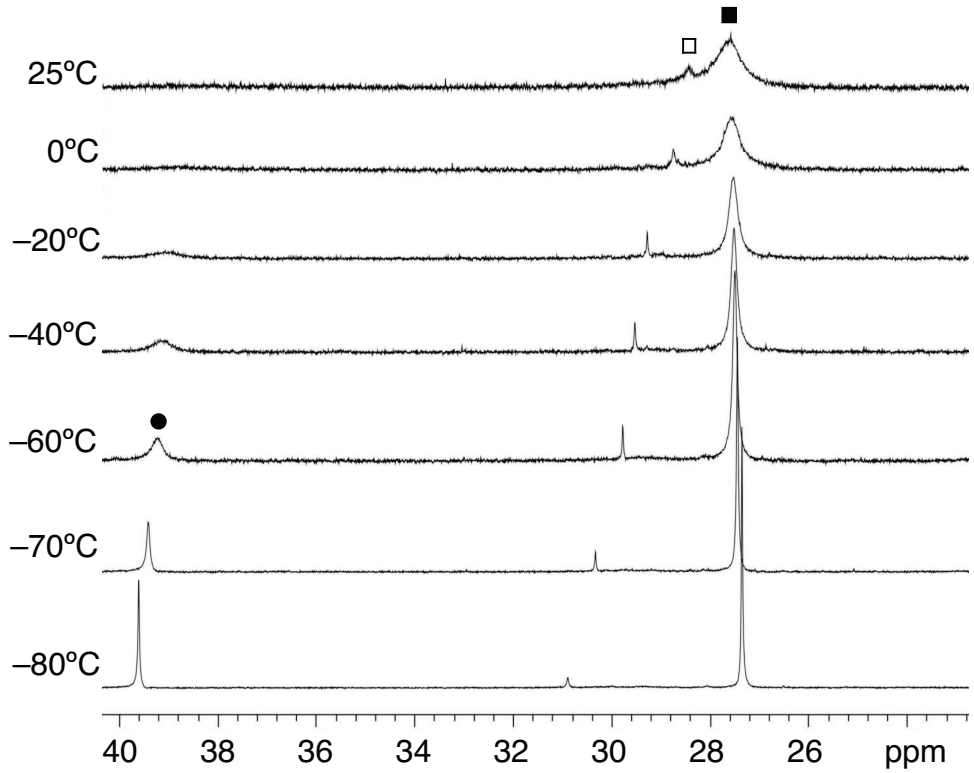

Figure 13. Variable temperature $^{31}P\{^{1}H\}$ NMR (CD_2Cl_2, 500.1 MHz) study, revealing the presence of three distinct species (filled square: T-shaped complex **57**; empty square: unknown species; filled circle: digonal complex **59**).

In order to get some further insight into the above equilibrium, a variable temperature (VT) $^{31}P\{^{1}H\}$ NMR study was carried out for **57** in CD_2Cl_2 (Figure 13). By decreasing the

temperature, a new species (**59**) appeared at δ = 39.6 ppm, the signal of which was broad at –20ºC and became gradually sharper upon lowering the temperature. Its chemical shift is nearly identical with that of the digonal, hexafluorophosphate complex **58** (δ = 38.6 ppm), so that it appears reasonable to assign to **59** a structure similar to the former complex.

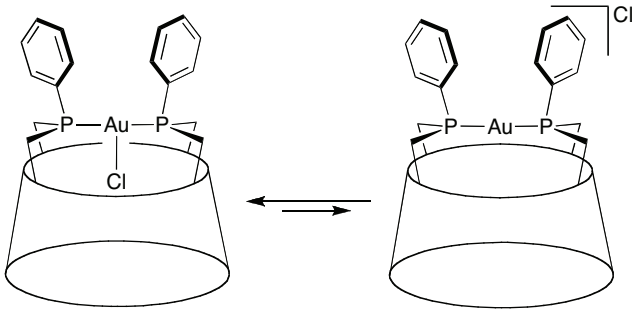

57 **59**

Scheme 4. *Intra*-cavity coordination processes occurring in [Au(**TRANSDIP**)]Cl in the presence of dichloromethane.

Although anion exchange inside the cavity of **TRANSDIP** had been observed previously, notably in [AgX(**TRANSDIP**)] (X = medium size anions) complexes,[11] an equilibrium which involves changes in the complex geometry (linear digonal *vs*. T-shaped trigonal) together with counterion coordination-decoordination is here seen for the first time in a **TRANSDIP** complex. It is noteworthy that T-shaped gold complexes of formula $[AuX(L)_2]$ (L = monophosphine) have been seen to crystallise in different polymorphs having various Au–X distances, although this was only observed in the case of X = Br, I, but not X = Cl.[51] Overall, these results show that **TRANSDIP** is perfectly suited for slowing down and therefore studying metal-centred processes taking place in CD cavities.

In conclusion, the above study is a new illustration of the fact that metallated CDs constitute powerful tools for visualising coordination processes occurring in a confined environment, the observed equilibrium being controlled by possible interactions between a guest and either the metal centre or the cavity walls, or both.

VI.3. Conclusion

In this chapter, we have shown that **TRANSDIP** constitutes a new molecular receptor-phosphine suited for probing the stepwise formation of a palladium promoted C–C bond. Unusual intermediates were identified, in particular the pentacoordinate complex **53**, the first [Pd(alkyl)X_2P_2] complex having *trans*-disposed phosphorus atoms, and the trialkyl-palladium complex **54** in which one phosphorus atom of (the hemilabile!) **TRANSDIP** is dissociated. On the other hand, the cavity was shown to play a major role for stabilizing Pd^0 complexes by allowing chlorine encapsulation and coordination. Similar properties were observed in gold(I) complexes. Finally, the isolation of a peroxo complex in which an O_2 ligand is fully embedded in a CD paves the way to the study of novel artificial metalloenzymes.

VI.4. Experimental section

VI.4.1. General procedures

All manipulations were performed in Schlenk-type flasks under dry nitrogen. Solvents were dried by conventional methods and distilled immediately prior to use. Deuterated solvents were passed down a 5 cm-thick alumina column and stored under nitrogen over molecular sieves (4 Å). Routine ^{1}H and $^{13}C\{^{1}H\}$ spectra were recorded on FT Bruker AVANCE 300, AVANCE 400 and AVANCE 500. ^{1}H NMR spectral data were referenced to residual protiated solvents (δ = 7.26 ppm for $CDCl_3$ and δ = 7.16 ppm for C_6D_6), $^{13}C\{^{1}H\}$ chemical shifts are reported relative to deuterated solvents (δ = 77.00 ppm for $CDCl_3$ and δ = 128.06 ppm for C_6D_6) and the $^{31}P\{^{1}H\}$ NMR data are given relative to external H_3PO_4. Mass spectra were recorded either on a ZAB HF VG analytical spectrometer using *m*-nitrobenzyl alcohol as matrix or on a Bruker MicroTOF spectrometer (ESI) using CH_2Cl_2, MeCN or MeOH as solvent. Elemental analyses were performed by the Service de Microanalyse, Institut de Chimie, Strasbourg. Melting points were determined with a Büchi 535 capillary melting-point apparatus. All commercial reagents were used as supplied. **TRANSDIP**,[10] complex **51**[10] and [AuCl(tht)][52] were prepared according to literature procedures. The numbering of the atoms within a glucose unit is as follows:

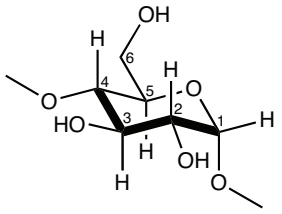

VI.4.2. Synthesis of compounds

***trans-P,P'*-Chlorido-methyl-{6^A,6^B,6^D,6^E}-tetradeoxy-6^A,6^B:6^D,6^E-bis[(*R*)-phenyl phosphinidene]-2^A,2^B,2^C,2^D,2^E,2^F,3^A,3^B,3^C,3^D,3^E,3^F,6^C,6^F-tetradeca-*O*-methyl-α-cyclodextrin}palladium(II) (52)**

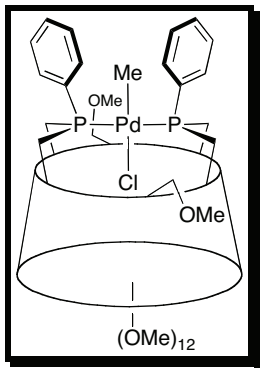

A solution of MeLi in diethyl ether (1.60 M, 0.050 mL, 0.080 mmol) was added dropwise to a solution of **51** (0.120 g, 0.080 mmol) in thf (5 mL) at –78ºC. The reaction mixture was then allowed to reach room temperature and stirred for a further 2 h before being evaporated to dryness. The residue was purified by column chromatography (SiO_2, CH_2Cl_2/MeOH, 95:5, *v*/*v*) affording complex **52** as a pale yellow solid (yield: 0.116 g, 99%). The spectroscopic data match those found in the literature.[10]

Lithium *trans-P,P'*-dichloro-methylo-{6^A,6^B,6^D,6^E}-tetradeoxy-6^A,6^B:6^D,6^E-bis[(*R*)-phenylphosphinidene]-2^A,2^B,2^C,2^D,2^E,2^F,3^A,3^B,3^C,3^D,3^E,3^F,6^C,6^F-tetradeca-*O*-methyl-α-cyclodextrin}palladate(II) (53)

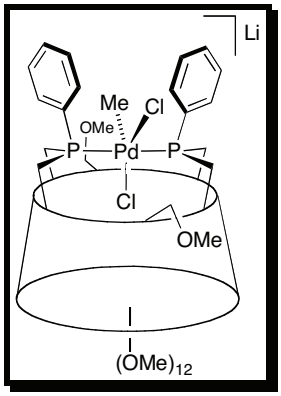

A solution of MeLi in diethyl ether (1.60 M, 0.050 mL, 0.080 mmol) was added dropwise to a solution of **51** (0.120 g, 0.080 mmol) in C_6D_6 (5 mL) at –78ºC resulting in the quantitative precipitation of **53**, which was recovered by filtration. This complex decomposes rapidly, which is the reason why we only provide selected characterization data. ^{1}H NMR (400.1 MHz, d_8-thf, 25ºC): δ (assignment by ^{1}H-^{31}P{^{1}H} HMQC) = –0.65 (t, 3 H, $^3J_{H,P}$ = 6.2 Hz, Me), 2.06 (m, 2 H, H-6a$^{A,D\text{ or }B,E}$), 2.35 (m, 2 H, H-6a$^{B,E\text{ or }A,D}$), 2.96 (m, 2 H, H-6b$^{A,D\text{ or }B,E}$), 3.35 (m, 2 H, H-6b$^{B,E\text{ or }A,D}$), 4.51 (m, 2 H, H-5$^{A,D\text{ or }B,E}$), 4.86 (m, 2 H, H-5$^{A,D\text{ or }B,E}$), 7.29 (m, 4 H, *m*-H), 7.51 (m, 4 H, *o*-H) ppm; ^{13}C{^{1}H} NMR (100.6 MHz, d_8-thf, 25ºC): δ = 3.30 (t, $^2J_{C,P}$ = 10.4 Hz, Me) ppm; ^{31}P{^{1}H} NMR (162.0 MHz, d_8-thf, 25ºC): δ = 11.1 (s) ppm; ^{31}P{^{1}H} NMR (162.0 MHz, C_6D_6, 25ºC): δ = 10.7 (s) ppm; MS (ESI-MS): *m/z* (%): 1525.50 (100) [*M* – Li + O]$^-$, 1509.48 (65) [*M* – Li]$^-$.

Lithium κ^1-*P,P'*-trimethylo-{6^A,6^B,6^D,6^E-tetradeoxy-6^A,6^B:6^D,6^E-bis[(*R*)-phenylphosphinidene]-2^A,2^B,2^C,2^D,2^E,2^F,3^A,3^B,3^C,3^D,3^E,3^F,6^C,6^F-tetradeca-*O*-methyl-α-cyclodextrin} palladate(II) (54)

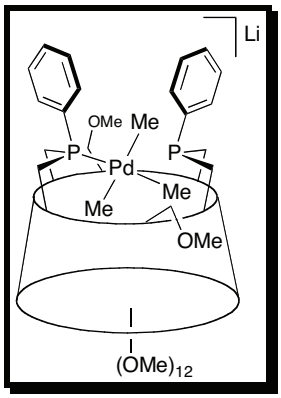

A solution of MeLi in diethyl ether (1.52 M, 0.16 mL, 0.243 mmol) was added dropwise to a solution of **52** (0.120 g, 0.081 mmol) in d_8-thf (0.6 mL) at –78ºC in a NMR tube. The reaction mixture was monitored by NMR spectroscopy until disappearance of **52** and complete formation of **54** at –40ºC. Assignment of each phosphorus atoms was made by arbitrarily designating glucose units *A* and *B* as the ones linked to the non-coordinated phosphorus atom. ^{1}H NMR (500.1 MHz, d_8-thf, –40ºC): δ (assignment by ^{1}H-^{1}H COSY, ^{1}H-^{31}P{^{1}H} HMQC and ^{1}H-^{13}C{^{1}H} HMQC) = –0.55 (d, 6 H, $^3J_{H,P}$ = 6.4 Hz, Me$_{P\text{-}cis}$), 0.00 (d, 3 H, $^3J_{H,P}$ = 6.1 Hz, Me$_{P\text{-}trans}$), 1.73 (1 H, H-6a$^{A\text{ or }B}$), 1.75 (1 H, H-6a$^{B\text{ or }A}$), 2.04 (1 H, H-6a$^{D\text{ or }E}$), 2.43 (1 H, H-6a$^{E\text{ or }D}$), 3.05-3.16 (4 H, H-2), 3.06 (1 H, H-6b$^{A\text{ or }B}$), 3.21-3.29 (2 H, H-2), 3.24 (s, 3 H, OMe-6), 3.32 (2, H-4$^{E\text{ or }D}$, H-6b$^{B\text{ or }A}$), 3.33-3.73 (6 H, H-3), 3.34 (1 H, H-4$^{D\text{ or }E}$), 3.35 (1 H, H-4$^{A\text{ or }B}$), 3.43 (1 H, H-6b$^{E\text{ or }D}$), 3.44 (s, 3 H, OMe-2), 3.46 (s, 3 H, OMe-6), 3.47 (s, 3 H, OMe-2), 3.48 (s, 3 H, OMe-2), 3.49 (s, 3 H, OMe-2), 3.52 (s, 6 H, OMe-2), 3.54 (1 H, H-6b$^{D\text{ or }E}$), 3.58 (s, 3 H, OMe-3), 3.59 (1 H, H-4$^{C\text{ or }F}$), 3.60 (s, 3 H, OMe-3), 3.62 (s, 6 H, OMe-3), 3.65 (s, 3 H, OMe-3), 3.67 (s, 3 H, OMe-3), 3.69 (1 H, H-4$^{F\text{ or }C}$), 3.71 (1 H, H-6a$^{C\text{ or }F}$), 3.80 (1 H, H-4$^{B\text{ or }A}$), 3.98 (1 H, H-5$^{A\text{ or }B}$), 4.03 (2 H, H-5$^{F\text{ or }C}$, H-6a$^{F\text{ or }C}$), 4.08 (1 H, H-5$^{C\text{ or }F}$), 4.13 (1 H, H-6b$^{F\text{ or }C}$), 4.20 (1 H, H-5$^{B\text{ or }A}$), 4.34 (1 H, H-5$^{D\text{ or }E}$), 4.48 (1 H, H-6b$^{C\text{ or }F}$), 4.52 (1 H, H-5$^{E\text{ or }D}$), 5.02 (d, 1 H, $^3J_{H\text{-}1,H\text{-}2}$ = 2.5 Hz, H-1), 5.07 (d, 1 H, $^3J_{H\text{-}1,H\text{-}2}$ = 4.1 Hz, H-1), 5.09-5.12 (3 H, H-1), 5.13 (d, 1 H, $^3J_{H\text{-}1,H\text{-}2}$ = 4.9 Hz, H-1), 7.25 (m, 1 H, *p*-H of P^{D,E}), 7.29 (t, 2 H, $^3J_{m\text{-}H,o\text{-}H}$ = $^3J_{m\text{-}H,p\text{-}H}$ = 7.0 Hz, *m*-H of P^{D,E}), 7.34 (m, 1 H, *p*-H of P^{A,B}), 7.39 (t, 2 H, $^3J_{m\text{-}H,o\text{-}H}$ = $^3J_{m\text{-}H,p\text{-}H}$ = 7.2 Hz, *m*-H of P^{A,B}), 7.79 (t, 2 H, $^3J_{o\text{-}H,m\text{-}H}$ = $^3J_{o\text{-}H,P}$ = 7.0 Hz, *o*-H of P^{A,B}), 7.95 (t, 2 H, $^3J_{o\text{-}H,m\text{-}H}$ = $^3J_{o\text{-}H,P}$ = 7.9 Hz, *o*-H of P^{D,E}) ppm; ^{13}C{^{1}H} NMR (125.8

MHz, d_8-thf, –40ºC): δ (assignment by ^{1}H-^{1}H COSY, ^{1}H,^{31}P{^{1}H} HMQC and ^{1}H-^{13}C{^{1}H} HMQC) = –2.27 [×2] (Me), 3.59 (Me), 26.80 (C-6$^{D\text{ or }E}$), 26.93 (C-6$^{A\text{ or }B}$), 34.13 (C-6$^{B\text{ or }A}$), 35.34 (C-6$^{E\text{ or }D}$), 56.63, 56.67 [×2], 56.79, 56.87 [×2] (OMe-2), 58.21, 59.38 (OMe-6), 61.13, 61.32 [×2], 61.58, 61.96, 62.14 (OMe-3), 65.99 (C-5$^{A\text{ or }B}$), 66.15(C-5$^{D\text{ or }E}$), 70.34 (C-5$^{E\text{ or }D}$), 70.57 (C-5$^{C\text{ or }F}$), 71.38 (C-6$^{F\text{ or }C}$), 71.60 (C-5$^{F\text{ or }C}$), 72.80 (C-6$^{C\text{ or }F}$), 72.85 (C-5$^{B\text{ or }A}$), 79.78–84.55 (C-2,C-3), 80.70 (C-4$^{B\text{ or }A}$), 82.13 (C-4$^{C\text{ or }F}$), 82.45 (C-4$^{F\text{ or }C}$), 87.28 (C-4$^{A\text{ or }B}$), 87.72 (C-4$^{D\text{ or }E}$), 89.28 (C-4$^{E\text{ or }D}$), 97.03, 97.68, 99.10, 99.65, 99.86, 100.07 (C-1), 127.36 (*m*-C of P^{D,E}), 127.73 (*p*-C of P^{D,E}), 128.70 (*m*-C of P^{A,B}), 128.83 (*p*-C of P^{A,B}), 133.04 (*o*-C of P^{A,B}), 133.18 (*o*-C of P^{D,E}) ppm, *ipso*-C could not be detected; ^{31}P{^{1}H} NMR (202.5 MHz, d_8-thf, –40ºC): δ = –21.4 (s, $P_{A,B}$), 10.5 (s, $P_{D,E}$) ppm. We do not provide microanalytical data or mass spectroscopy because of fast decomposition of the compound at room temperature.

Palladium complex 55

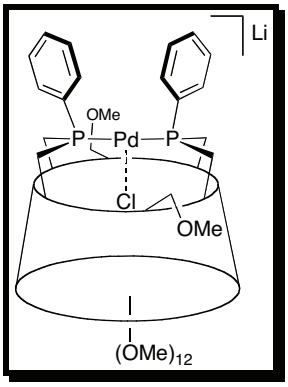

^{1}H NMR (500.1 MHz, d_8-thf, 25ºC): δ (assignment by ^{1}H-^{1}H COSY and ^{1}H-^{31}P{^{1}H} HMQC) = 1.96 (m, 2 H, H-6a$^{A,D\text{ or }B,E}$), 3.25 (m, 2 H, H-6a$^{B,E\text{ or }A,D}$) ppm; ^{31}P{^{1}H} NMR (202.5 MHz, d_8-thf, 25ºC): δ = 8.7 (s) ppm. Note that because of the broadness of the peaks, it was not possible to establish a full assignment based on ^{1}H and ^{13}C NMR spectroscopy. Attempts to retrieve microanalytical and mass spectroscopic data failed because of oxidation into complex **56**. Complex **55** is only stable when carrying the reaction in the presence of excess MeLi and LiCl.

***cis*-*P*,*P'*-Peroxo-{6^A,6^B,6^D,6^E}-tetradeoxy-6^A,6^B:6^D,6^E-bis[(*R*)-phenylphosphinidene]-2^A,2^B,2^C,2^D,2^E,2^F,3^A,3^B,3^C,3^D,3^E,3^F,6^C,6^F-tetradeca-*O*-methyl-α-cyclodextrin} palladium(II) (56)**

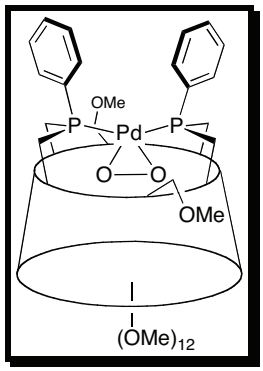

A solution of MeLi in diethyl ether (1.60 M, 0.21 mL, 0.335 mmol) was added dropwise to a solution of **51** (0.100 g, 0.067 mmol) in thf (10 mL) at –78ºC. The reaction mixture was allowed to reach room temperature over 12 h and was then evaporated to dryness. The residue was purified by column chromatography (SiO_2, CH_2Cl_2/MeOH, 95:5 to 92:8 *v*/*v*) affording traces of complex **52** (yield: 10 mg, 5%) and mainly complex **56** (yield: 0.093 g, 95%) as a pale brown solid. R_f (SiO_2, CH_2Cl_2/MeOH, 92:8, *v*/*v*) = 0.20; m.p. dec. >250ºC; ^{1}H NMR (500.1 MHz, C_6D_6, 25ºC): δ (assignment by COSY) = 1.85–1.93 (m, 2 H, H-6a$^{A,D\text{ or }B,E}$), 2.31 (dd, 2 H, $^2J_{H\text{-}6a,H\text{-}6b}$ = 16.2 Hz, $^3J_{H\text{-}6a,H\text{-}5}$ = 7.1 Hz, H-6a$^{B,E\text{ or }A,D}$), 2.99 (d, 2 H, $^2J_{H\text{-}6b,H\text{-}6a}$ = 14.3 Hz, H-6b$^{A,D\text{ or }B,E}$), 3.20 (dd, 2 H, $^3J_{H\text{-}2,H\text{-}3}$ = 9.6 Hz, $^3J_{H\text{-}2,H\text{-}1}$ = 3.4 Hz, H-2^{C,F}), 3.31–3.38 (m, 10 H, H-2^{A,B,D,E}, H-4^{A,B,D,E}, H-6b^{B,E}), 3.28 (s, 6 H, OMe), 3.34 (s, 6 H, OMe), 3.36 (s, 6 H, OMe), 3.36 (s, 6 H, OMe), 3.38 (s, 6 H, OMe), 3.69 (s, 6 H, OMe), 3.72 (d, 2 H, $^2J_{H\text{-}6a,H\text{-}6b}$ = 10.6 Hz, H-6a^{C,F}), 3.78 (s, 6 H, OMe), 3.82 (s, 6 H, OMe), 3.99–4.10 (m, 8 H, H-3, H-4^{C,F}), 4.64 (virtual dd, 2 H, $^2J_{H\text{-}6b,H\text{-}6a}$ = 10.2 Hz, $^3J_{H\text{-}6b,H\text{-}5}$ = 3.6 Hz, H-6b^{C,F}), 4.69 (virtual dd, 2 H, $^3J_{H\text{-}5,H\text{-}4}$ = 9.3 Hz, $^3J_{H\text{-}5,H\text{-}6b}$ = 2.3 Hz, H-5^{C,F}), 4.94 (d, 2 H, $^3J_{H\text{-}1,H\text{-}2}$ = 4.2 Hz, H-1$^{A,D\text{ or }B,E}$), 5.12 (d, 2 H, $^3J_{H\text{-}1,H\text{-}2}$ = 3.6 Hz, H-1^{C,F}), 5.14–5.18 (m, 2 H, H-5 $^{A,D\text{ or }B,E}$), 5.30 (d, 2 H, $^3J_{H\text{-}1,H\text{-}2}$ = 3.6 Hz, H-1$^{B,E\text{ or }A,D}$), 5.43–5.49 (m, 2 H, H-5 $^{B,E\text{ or }A,D}$), 6.62 (t, 4 H, ^3J = 7.5 Hz, *m*-H), 6.77 (t, 2 H, ^3J = 7.5 Hz, *p*-H), 6.99 (t, 4 H, ^3J = 7.5 Hz, *o*-H); ^{13}C{^{1}H} NMR (125.8 MHz, C_6D_6, 25ºC): δ (assignment by HMQC) = 31.92 (virtual t, $|^1J_{C,P} + {}^3J_{C,P'}|$ = 10.7 Hz, C-6$^{A,D\text{ or }B,E}$), 35.59 [×2] (virtual t, $|^1J_{C,P} + {}^3J_{C,P'}|$ = 7.6 Hz, C-6$^{B,E\text{ or }A,D}$), 57.40 [×2], 57.52 [×2], 58.57 [×2], 59.24 [×2], 61.74 [×2], 61.78 [×2], 62.02 [×2] (OMe), 64.40 [×2] (C-5$^{A,D\text{ or }B,E}$), 72.01 [×2] (C-5^{C,F}), 72.14 [×2] (br s with triplet shape, C-5$^{B,E\text{ or }A,D}$), 73.01 [×2] (C-6^{C,F}),

81.20 [×2], 81.69 [×2], 82.24 [×2], 82.41 [×2], 82.74 [×2], 84.09 [×2], 84.31 [×2] (C-2, C-3, C-$4^{C,F}$), 86.68 [×2] (virtual t, $|^3J_{C,P} + {}^5J_{C,P'}|$ = 10.1 Hz, C-$4^{A,D \text{ or } B,E}$), 89.62 [×2] (C-$4^{B,E \text{ or } A,D}$), 97.78 [×2] (C-$1^{B,E \text{ or } A,D}$), 98.46 [×2] (C-$1^{A,D \text{ or } B,E}$), 101.12 [×2] (C-$1^{C,F}$), 128.35 [×4] (*m*-C), 129.22 [×2] (*p*-C), 130.55 [×4] (virtual t, $|^2J_{C,P} + {}^4J_{C,P'}|$ = 10.2 Hz, *o*-C), 134.20 [×2] (m, *ipso*-C); ^{31}P {^{1}H} NMR (202.5 MHz, C_6D_6, 25ºC): δ = 28.8 (s) ppm; elemental analysis (%) calcd for $C_{62}H_{94}O_{28}P_2Pd$ (1455.76) C 51.15, H 6.51, found: C 51.30, H 6.72; MS (ESI-MS): *m/z* (%): 1455.47 (100) $[M + H]^+$.

Alternative method 1: **TRANSDIP** (0.150 g, 0.114 mmol) was added to a solution of $Pd(dba)_2$ (0.066 g, 0.114 mmol) in toluene (15 mL) in the presence of air at room temperature. After 2-3 hours, evaporation to dryness followed by column chromatography (SiO_2, CH_2Cl_2/MeOH, 92:8, *v*/*v*) afforded analytically pure complex **56** (yield: 0.165 g, 99%) as a pale brown solid.

Alternative method 2: A solution of *n*BuLi in hexanes (1.60 M, 0.21 mL, 0.335 mmol) was added dropwise to a solution of **51** (0.100 g, 0.067 mmol) in thf (10 mL) at –78ºC. The reaction mixture was allowed to reach room temperature over 12 h and was then evaporated to dryness. The residue was purified by column chromatography (SiO_2, CH_2Cl_2/MeOH, 92:8 *v*/*v*) affording analytically pure complex **56** (yield: 0.097 g, 99%) as a pale brown solid.

***P,P'*-Chlorido-{6^A,6^B,6^D,6^E-tetradeoxy-6^A,6^B:6^D,6^E-bis[(*R*)-phenylphosphinidene]-2^A,2^B,2^C,2^D,2^E,2^F,3^A,3^B,3^C,3^D,3^E,3^F,6^C,6^F-tetradeca-*O*-methyl-α-cyclodextrin}gold(I) (57)**

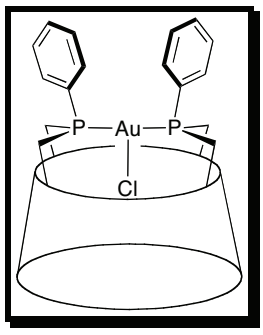

[AuCl(tht)] (0.048 g, 0.152 mmol) was added to a solution of **TRANSDIP** (0.200 g, 0.152 mmol) in CH_2Cl_2 (10 mL). After 30 minutes, the reaction mixture was evaporated to dryness affording pure **57** (0.234 g, 99%). Compound **57** decomposes when absorbed on

silica; m.p. dec. >250ºC; ^{1}H NMR (400.1 MHz, $CDCl_3$, 25ºC): δ (assignment by COSY) = 2.05 (dt, 2 H, $^{2}J_{H\text{-}6a,P} = {}^{2}J_{H\text{-}6a,H\text{-}6b}$ = 15.4 Hz, $^{3}J_{H\text{-}6a,H\text{-}5}$ = 5.1 Hz, H-6a$^{B,E\text{ or }A,D}$), 2.22 (d, 2 H, $^{2}J_{H\text{-}6a,P} = {}^{2}J_{H\text{-}6a,H\text{-}6b}$ = 10.6 Hz, H-6a$^{A,D\text{ or }B,E}$), 3.04 (s, 6 H, OMe), 3.05-3.26 (12 H, H-2, H-4^{A,B,D,E}, H-6b$^{A,D\text{ or }B,E}$), 3.44 (s, 6 H, OMe), 3.45-3.72 (10 H, H-3, H-4^{C,F}, H-6a^{C,F}) 3.46 (s, 6 H, OMe), 3.49 (s, 6 H, OMe), 3.63 (s, 12 H, OMe), 3.64 (s, 6 H, OMe), 3.98 (br s, 2 H, H-6b^{C,F}), 4.50 (br s, 2 H, H-5^{C,F}), 4.86 (d, 2 H, $^{3}J_{H\text{-}1,H\text{-}2}$ = 3.3 Hz, H-1), 4.87 (m, 2 H, H-5$^{A,D\text{ or }B,E}$), 4.96 (d, 2 H, $^{3}J_{H\text{-}1,H\text{-}2}$ = 3.6 Hz, H-1), 4.97 (d, 2 H, $^{3}J_{H\text{-}1,H\text{-}2}$ = 4.5 Hz, H-1), 5.22 (m, 2 H, H-5$^{B,E\text{ or }A,D}$), 7.30 (t, 4 H, $^{3}J_{m\text{-}H,o\text{-}H}$ = 7.5 Hz, $^{3}J_{m\text{-}H,p\text{-}H}$ = 7.5 Hz, *m*-H), 7.41 (t, 2 H, $^{3}J_{p\text{-}H,m\text{-}H}$ = 7.5 Hz, $^{4}J_{p\text{-}H,o\text{-}H}$ = 7.2 Hz, *p*-H), 7.61 (td, $^{3}J_{o\text{-}H,m\text{-}H} = {}^{3}J_{o\text{-}H,P}$ = 6.5 Hz, $^{4}J_{p\text{-}H,p\text{-}H}$ = 6.4 Hz, *o*-H) ppm; ^{13}C{^{1}H} NMR (100.6 MHz, $CDCl_3$, 25ºC): δ (assignment by HMQC) = 29.88-30.20 (C-6$^{A,D\text{ or }B,E}$), 37.16 (virtual t, $|{}^{2}J_{C,P} + {}^{3}J_{C,P'}|$ = 13.4 Hz, C-6$^{B,E\text{ or }A,D}$), 57.54, 57.66, 57.86 (OMe-2), 58.94 (OMe-6), 61.67, 61.94, 62.11 (OMe-3), 64.14 (C-5$^{A,D\text{ or }B,E}$), 68.73 (C-5$^{B,E\text{ or }A,D}$), 70.52 (C-5^{C,F}), 71.73 (C-6^{C,F}), 80.61, 80.74, 81.35, 81.51, 82.23, 82.76, 82.93 (C-2, C-3, C-4^{C,F}), 87.13 (C-4$^{A,D\text{ or }B,E}$), 89.24 (C-4$^{B,E\text{ or }A,D}$), 97.95, 98.39, 100.56 (C-1), 128.64 (virtual t, $|{}^{3}J_{C,P} + {}^{5}J_{C,P'}|$ = 4.7 Hz, *m*-C), 130.61 (*p*-C), 131.92 (virtual t, $|{}^{2}J_{C,P} + {}^{4}J_{C,P'}|$ = 7.4 Hz, *o*-C) ppm, *ipso*-C could not be detected; ^{31}P{^{1}H} NMR (162 MHz, $CDCl_3$, 25 ºC): δ = 27.2 (s) ppm; elemental analysis (%) calcd for $C_{62}H_{94}AuClO_{26}P_2 \cdot CHCl_3$ (1549.76 + 119.38): C 45.33, H 5.74, found: C 45.43, H 6.04; MS (ESI-TOF): *m/z* (%): 1513.52 (100) $[M - Cl]^{+}$.

V.4.3. X-ray crystallographic data for 56

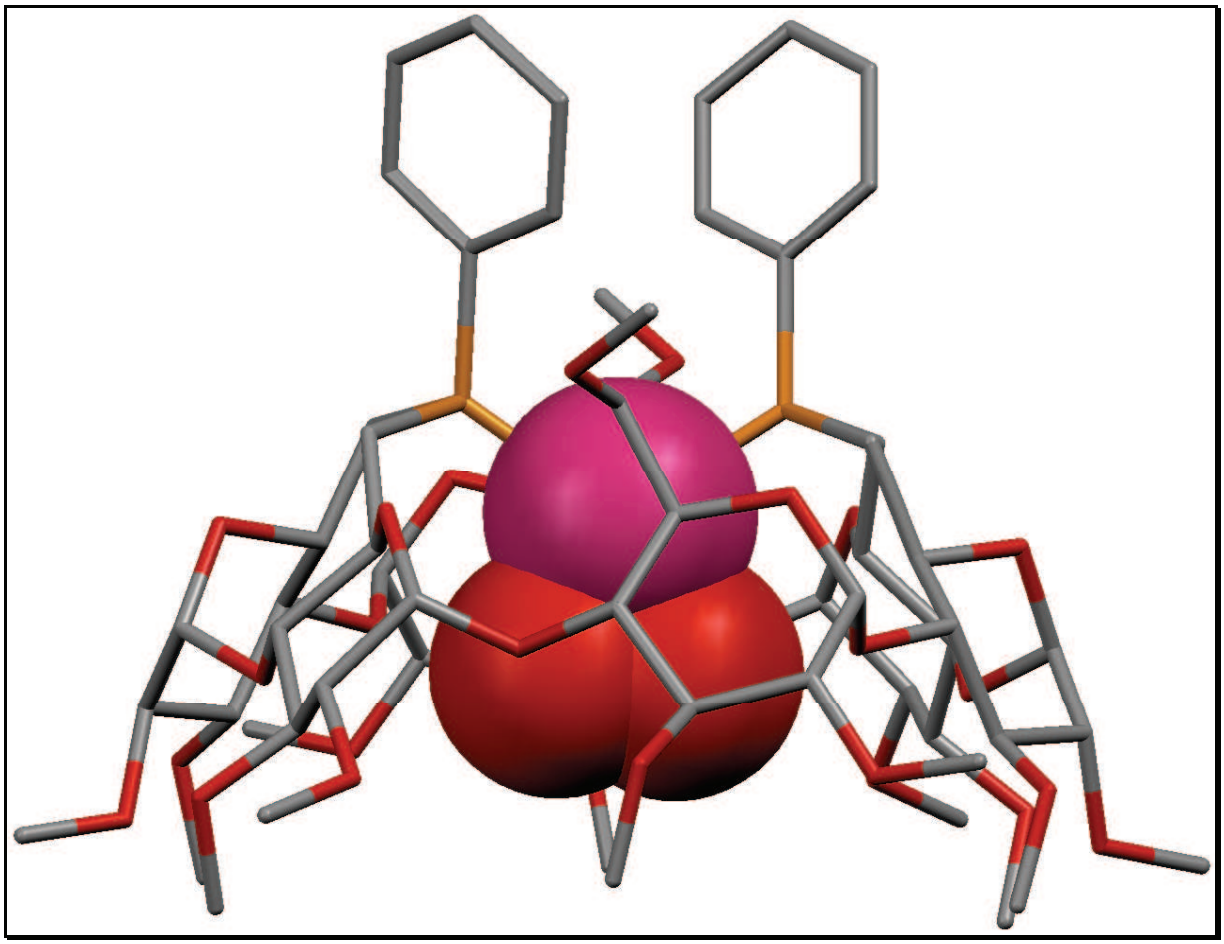

The X-ray structure determination was performed by Dr L. Toupet (University of Rennes, France). Single crystals were obtained by slow diffusion of pentane into a solution of **56** in dichloromethane. The sample was studied on a Oxford Diffraction Xcalibur Saphir 3 CCD with graphite monochromatised MoKα radiation (λ = 0.71073 Å). The structure was solved with SIR-97,[53] which revealed the non-hydrogen atoms of the molecule. After anisotropic refinement, many hydrogen atoms were found with a Fourier difference analysis. The whole structure was refined with SHELX-97[54] and full-matrix least-square techniques (use of F^2 magnitude; x, y, z, β_{ij} for Pd, Cl, C, O, P atoms, x, y, z, in riding mode for H atoms; 890 variables and 15915 observations with $I > 2.0\sigma(I)$; calcd $w = 1/[\sigma^2(F_o^2) + (0.0633\ P)^2]$ where $P = (F_o^2 + 2\ F_o^2)/3$ with the resulting R = 0.0379, R_w = 0.099 and S_w = 0.984; $\Delta\rho <$ 0.892 eÅ^{-3}. The absolute configuration (and thus the enantiomeric space group assignment) was determined by a *Flack* x parameter of 0.025 (15). A summary of the crystallographic data is given in Table 2. CCDC reference number 746930.

Table 2. Crystal data and structure refinement for 2(**56**)·3(CH_2Cl_2).

Crystal Data	
Crystal size	0.22 × 0.15 × 0.12 mm^3
Empirical formula	$C_{127}H_{194}Cl_6O_{56}P_4Pd_2$
M_r	3166.20
Crystal system	Monoclinic
Space group	*C*2
Temperature	120(2) K
Unit cell parameters	
a	15.8106(2) Å
b	24.3689(2) Å
c	18.9715(2) Å
α	90º
β	94.131(1)º
γ	90º
V	7290.48(13) $Å^3$
Z	2
D (calculated)	1.442 g/cm^3
F (000)	3316
□	0489 mm^{-1}
Data Processing and Reduction	
θ range for data collection	2.57 to 27.00º
Index ranges	-20 ≤ h ≤ 20, -31≤ k ≤ 31, -24≤ l ≤ 24
Reflections collected	72737
Independent reflections	15915 [R(int) = 0.0398]
Refinement method	Full-matrix least-squares on F^2
Data / restraints / parameters	19915 / 1 / 890
Goodness-of-fit on F^2	0.984
Final R indices [I > 2σ(I)]	R1 = 0.0379, *w*R2 = 0.0968
R indices (all data)	R1 = 0.0470, *w*R2 = 0.0990
Largest diff. peak and hole	0.892 and -0.915 $eÅ^{-3}$

VI.5. References

[1] C. A. Bessel, P. Aggarwal, A. C. Marschilok, K. J. Takeuchi, *Chem. Rev.* **2001**, *101*, 1031-1066.

[2] Z. Freixa, P. W. N. M. van Leeuwen, *Coord. Chem. Rev.* **2008**, *252*, 1755-1786.

[3] L. Poorters, M. Lejeune, D. Armspach, D. Matt, *Actual. Chim.* **2009**, *326*, 15-18.

[4] K. Issleib, G. Hohlfeld, *Z. Anorg. Allg. Chem.* **1961**, *312*, 169-179.

[5] N. J. DeStefano, D. K. Johnson, L. M. Venanzi, *Angew. Chem.* **1974**, *86*, 133.

[6] N. J. DeStefano, D. K. Johnson, L. M. Venanzi, *Helv. Chim. Acta* **1976**, *59*, 2683-2690.

[7] F. Bachechi, L. Zambonelli, L. M. Venanzi, *Helv. Chim. Acta* **1977**, *60*, 2815-2823.

[8] G. Bracher, D. M. Grove, L. M. Venanzi, F. Bachechi, P. Mura, L. Zambonelli, *Helv. Chim. Acta* **1980**, *63*, 2519-2530.

[9] E. Engeldinger, L. Poorters, D. Armspach, D. Matt, L. Toupet, *Chem. Commun.* **2004**, 634-635.

[10] L. Poorters, D. Armspach, D. Matt, L. Toupet, S. Choua, P. Turek, *Chem. Eur. J.* **2007**, *13*, 9448-9461.

[11] L. Poorters, D. Armspach, D. Matt, L. Toupet, P. G. Jones, *Angew. Chem. Int. Ed.* **2007**, *46*, 2663-2665.

[12] D. Armspach, D. Matt, *C. R. Chimie* **2011**, *14*, 135-148.

[13] J. Tsuji, *Palladium Reagents and Catalysts: Innovation in Organic Synthesis,* Wiley, Chichester, **1995**.

[14] J. Tsuji, *Palladium Reagents and Catalysts: New Perspectives for the 21st Century,* John Wiley & Sons, Ltd, Chichester, **2004**.

[15] A. Suzuki, *Angew. Chem. Int. Ed.* **2011**, *50*, 6722-6737.

[16] R. Jana, T. P. Pathak, M. S. Sigman, *Chem. Rev.* **2011**, *111*, 1417-1492.

[17] A. Gillie, J. K. Stille, *J. Am. Chem. Soc.* **1980**, *102*, 4933-4941.

[18] M.-N. Birkholz, Z. Freixa, P. W. N. M. van Leeuwen, *Chem. Soc. Rev.* **2009**, *38*, 1099-1118.

[19] R. C. Smith, C. R. Bodner, M. J. Earl, N. C. Sears, N. E. Hill, L. M. Bishop, N. Sizemore, D. T. Hehemann, J. J. Bohn, J. D. Protasiewicz, *J. Organomet. Chem.* **2005**, *690*, 477-481.

[20] L. Kaganovsky, K.-B. Cho, D. Gelman, *Organometalllics* **2008**, *27*, 5139-5145.

[21] L. Kaganovsky, D. Gelman, K. Rueck-Braun, *J. Organomet. Chem.* **2010**, *695*, 260-266.

[22] G. M. Gray, C. H. Duffey, *Organometalllics* **1994**, *13*, 1542-1544.

[23] C. Amatore, A. Jutand, A. Suarez, *J. Am. Chem. Soc.* **1993**, *115*, 9531-9541.

[24] C. Amatore, S. Aziz, A. Jutand, G. Meyer, P. Cocolios, *New. J. Chem.* **1995**, *19*, 1047-1059.

[25] C. Amatore, A. Jutand, *Acc. Chem. Res.* **2000**, *33*, 314-321.

[26] H. Nakazawa, F. Ozawa, A. Yamamoto, *Organometalllics* **1983**, *2*, 241-250.

[27] S. M. Reid, J. T. Mague, M. J. Fink, *J. Am. Chem. Soc.* **2001**, *123*, 4081-4082.

[28] E. Negishi, T. Takahashi, K. Akiyoshi, *J. Organomet. Chem.* **1987**, *334*, 181-194.

[29] E. Negishi, T. Takahashi, K. Akiyoshi, *J. Chem. Soc. Chem. Commun.* **1986**, 1338-1339.

[30] M. Pérez-Rodríguez, A. A. C. Braga, M. Garcia-Melchor, M. H. Pérez-Temprano, J. A. Casares, G. Ujaque, A. R. de Ler, R. Álvarez, F. Maseras, P. Espinet, *J. Am. Chem. Soc.* **2009**, *131*, 3650-3657.

[31] T. Schnetz, M. Röder, F. Rominger, P. Hofmann, *Dalton Trans.* **2008**, 2238-2240.

[32] G. Wilke, H. Schott, P. Heimbach, *Angew. Chem. Int. Ed.* **1967**, *6*, 92-93.

[33] C. J. Nyman, C. E. Wymore, G. Wilkinson, *J. Chem. Soc. A* **1968**, 561-563.

[34] M. Matsumoto, H. Yoshioka, K. Nakatsu, T. Yoshida, S. Otsuka, *J. Am. Chem. Soc.* **1974**, *96*, 3322-3324.

[35] T. Yoshida, S. Otsuka, *J. Am. Chem. Soc.* **1977**, *99*, 2134-2140.

[36] T. Yoshida, K. Tatsumi, M. Matsumoto, K. Nakatsu, A. Nakamura, T. Fueno, S. Otsuka, *New. J. Chem.* **1979**, *3*, 761-774.

[37] A. G. Sergeev, H. Neumann, A. Spannenberg, M. Beller, *Organometalllics* **2010**, *29*, 3368-3373.

[38] N. W. Aboelella, J. T. York, A. M. Reynolds, K. Fujita, C. R. Kinsinger, C. J. Cramer, C. G. Riordan, W. B. Tolman, *Chem. Commun.* **2004**, 1716-1717.

[39] G. Adjabeng, T. Brenstrum, C. S. Frampton, A. J. Robertson, J. Hillhouse, J. McNulty, A. Capretta, *J. Org. Chem.* **2004**, *69*, 5082-5086.

[40] W. Clegg, G. R. Eastham, M. R. J. Elsegood, B. T. Heaton, J. A. Iggo, R. P. Tooze, R. Whyman, S. Zacchini, *J. Chem. Soc. Dalton Trans.* **2002**, 3300-3308.

[41] C. Amatore, A. Jutand, *Coord. Chem. Rev.* **1998**, *178-180*, 511-528.

[42] G. Thiabaud, G. Guillemot, I. Schmitz-Alfonso, B. Colasson, O. Reinaud, *Angew. Chem. Int. Ed.* **2009**, *48*, 7383-7386.

[43] G. Izzet, J. Zeitouny, H. Akdas-Killig, Y. Frapart, S. Ménage, B. Douziech, I. Jabin, Y. Le Mest, O. Reinaud, *J. Am. Chem. Soc.* **2008**, *130*, 9514-9523.

[44] M. Barrow, H. B. Bürgi, D. K. Johnson, L. M. Venanzi, *J. Am. Chem. Soc.* **1976**, *98*, 2356-2357.

[45] M. Viotte, B. Gautheron, M. M. Kubicki, Y. Mugnier, R. V. Parish, *Inorg. Chem.* **1995**, *34*, 3465-3473.

[46] P. A. Cooke, S. D. Perera, B. L. Shaw, M. Thornton-Pett, J. D. Vessey, *J. Chem. Soc. Dalton Trans.* **1997**, *1997*, 435-438.

[47] S. J. Berners-Price, P. J. Sadler, *Inorg. Chem.* **1986**, *25*, 3822-3827.

[48] S. J. Berners-Price, R. J. Bowen, T. W. Hambley, P. C. Healy, *J. Chem. Soc. Dalton Trans.* **1999**, 1337-1346.

[49] A. Pintado-Alba, H. de la Riva, M. Nieuwhuyzen, D. Bautista, P. R. Raithby, H. A. Sparkes, S. J. Teat, J. M. López-de-Luzuriaga, M. C. Lagunas, *Dalton Trans.* **2004**.

[50] H. Ito, T. Saito, T. Miyahara, C. Zhong, M. Sawamura, *Organometalllics* **2009**, *28*, 4829-4840.

[51] G. A. Bowmaker, C. L. Brown, R. D. Hart, P. C. Healy, C. E. F. Rickard, A. H. White, *J. Chem. Soc. Dalton Trans.* **1999**, 881-889.

[52] R. Uson, A. Laguna, M. Laguna, *Inorganic Synthesis* **1989**, *26*, 85-91.

[53] A. Altomare, A. C. Burla, M. Camalli, G. Cascarano, C. Giacovazzo, A. Guagliardi, A. G. G. Moliterni, G. Polidori, R. Spagna, *J. Appl. Crystallogr.* **1998**, *31*, 74-77.

[54] G. M. Sheldrick, SHELXL-97, *Program for Crystal Structure Refinement,* University of Göttingen (Germany) **1997**.

Conclusion générale et perspectives

Cette thèse relève de la chimie des métallo-cavitands. Elle est consacrée à la synthèse et la chimie de coordination de podands phosphorés dérivés d'une β-cyclodextrine (β-CD) perméthylée. La caractéristique principale des ligands étudiés est d'avoir leur(s) centre(s) coordinateur(s) dirigé(s) vers l'intérieur du récepteur macrocyclique, ce qui en fait non seulement des coordinats de choix pour l'étude de réactions en espace confiné, mais également des outils potentiels pour la confection de catalyseurs supramoléculaires.

La **première partie** de ce mémoire donne une vision globale de la chimie des systèmes moléculaires associant de manière covalente un métal de transition à un récepteur cavital jouant le rôle de première et deuxième sphère de coordination.

Dans le **chapitre II**, nous avons développé plusieurs méthodes efficaces de synthèse d'α- et β-CD tetrafonctionnalisées reposant sur une stratégie de pontage régiosélectif d'unités glucose de la plateforme CD. L'une d'entre elles, qui fait appel à un réactif rigide et encombré de type $ClAr_2C–C_6H_4–CAr_2Cl$, a permis de préparer un ensemble de β-CD substituées au niveau des positions 6^A,6^B,6^D,6^E. La méthodologie mise en œuvre a, en particulier, conduit à une nouvelle diphosphine, **WIDEPHOS**, une β-CD équipée de deux entités phénylphosphinidène (PPh) pontant respectivement les paires d'unités glucose (A,B) et (D,E). La caractéristique principale de cette cavité est d'intégrer des atomes de phosphore *endo*-orientés. L'analogue disulfure a également été synthétisé. Un autre réactif de pontage employé est le chlorure de thionyle. Son utilisation a permis de préparer en deux étapes des α- et β-CD perméthylées dont les unités glucose A et B, ainsi que D et E, ont été reliées par une entité sulfate. L'accès à ces composés ouvre la voie à la préparation de nouvelles cyclodextrines polyfonctionnalisées, car les atomes de carbone pontés 6^A et 6^B (ainsi que 6^D et 6^E) n'ont pas la même réactivité par suite d'une différentiation stérique. Enfin, ce chapitre décrit deux nouvelles cyclodextrines ne comportant qu'un seul fragment PPh « introverti » analogue à ceux présents dans **WIDEPHOS**. Le pontage implique les atomes de carbone 6^A et 6^B pour la première et les atomes 6^A,6^C pour la seconde.

Le **chapitre III** est dédié à l'étude des propriétés chélatantes de **WIDEPHOS**. En dépit de la grande séparation entre ses deux atomes de phosphore, cette diphosphine forme facilement des complexes *chélate* avec les ions Au(I), Pd(II), Pt(II) et Rh(I). Les complexes obtenus sont exclusivement de stéréochimie *trans*. Cependant, en raison du non-alignement

des doublets libres des atomes de phosphore du ligand, rigidement ancrés sur la plateforme CD, les complexes chélate formés présentent une stéréochimie *trans* « imparfaite ». En effet, dans ces derniers, les angles de chélation P-M-P s'écartent d'environ 20º de la valeur idéale de 180º, et incidemment mettent le métal dans un état métastable. C'est précisément cette caractéristique qui déclenche le phénomène inédit d'*oschélation*, une sorte de mouvement de balancier du chélateur autour du centre métallique. Dans cette dynamique, les deux atomes de phosphore optimisent à tour de rôle leur liaison avec l'atome métallique. Les complexes formés à partir de **WIDEPHOS** ont constitué le point de départ pour le développement d'une chimie *intra*-cavité.

Le **chapitre IV** démontre l'aptitude de **WIDEPHOS** à former des complexes comportant deux centres métalliques confinés dans une cavité CD. Il s'agit des premiers exemples du genre. Les atomes métalliques y sont soit « indépendants », comme dans $[(AuX)_2$(**WIDEPHOS**)] (X = Cl, Br, I), soit reliés entre eux par un pont □-Cl, comme dans plusieurs espèces dipalladiées. Dans chaque type de structure, le confinement engendre des modifications sensibles de la stéréochimie de l'un des atomes métalliques par suite de contraintes stériques importantes dans l'espace cavital. Celles-ci se manifestent par un déplacement chimique anormal de l'un des signaux du spectre RMN ^{31}P, qui correspond à un recouvrement orbitalaire imparfait entre les orbitales mises en jeu dans la liaison M–P. Ce dernier est, dans certains cas, lui-même à l'origine d'un comportement oschélatant, mais qui contrairement au cas décrit plus haut mettant en jeu deux atomes de phosphore, implique alors une chélation de type *P,O*.

Dans le **chapitre V** sont décrites les propriétés complexantes de l'équivalent « monophosphine » (**L**) de **WIDEPHOS**. Ce coordinat monodentate « introverti » s'est avéré particulièrement adapté à la synthèse de complexes monophosphine de type $[PdCl_2(PR_3)(D)]$ (D = atome donneur de $2e^-$ autre que P). Des complexes de ce type sont actuellement très recherchés, car leurs performances en couplage croisé sont généralement supérieures à celles des versions bis-phosphine correspondantes. Un des composés obtenus est le complexe $[PdCl_2$**L**$(H_2O)]$, dont l'entité $\{PdCl_2(H_2O)\}$ est nichée au cœur de la cavité CD. La molécule d'eau coordinée y est stabilisée par des intéractions *intra*-cavité, d'une part avec la paroi interne de la CD, d'autre part avec une seconde molécule d'eau incluse. L'extrusion de la molécule d'eau par chauffage à reflux d'une solution du complexe dans le toluène provoque la coordination d'un groupement méthoxyle de la face primaire. Par ailleurs, le ligand **L**

catalyse efficacement la réaction de couplage croisé entre différents arylbromés et le styrène en présence de $Pd(OAc)_2$ (réaction d'Heck-Mizoroki). Les meilleurs résultats ont été obtenus avec une charge en catalyseur de 1 mol% et un ratio ligand/palladium de 1:1, ce rapport suggérant la formation d'une espèce active ne contenant qu'un seul ligand phosphine au cours du cycle catalytique. Enfin, quel que soit le substrat testé, l'activité du système **L**/Pd s'est avérée supérieure à celles du couple **WIDEPHOS**/Pd. Cette observation est probablement liée à un encombrement stérique autour du métal plus favorable pour **L** que pour la diphosphine.

Le **dernier chapitre** est consacré à l'étude de la formation d'éthane par réaction entre *trans*-[$PdCl_2$(**TRANSDIP**)] et un excès de MeLi. Pour rappel, **TRANSDIP** est un *trans*-chélateur authentique découvert en 2004 au laboratoire; sa structure est similaire à celle de **WIDEPHOS**, mais il est bâti sur une plateforme α-cyclodextrine. **TRANSDIP** ne se prêtant pas à la formation de complexes de stéréochimie *cis*, le complexe étudié ne constituait, à priori, pas un bon candidat pour la réalisation d'un couplage réducteur. Une étude détaillée *in situ* démontre la formation successive de plusieurs intermédiaires clés au cours de la réaction de formation d'éthane: a) une espèce pentacoordinée anionique, [$PdCl_2Me$(**TRANSDIP**)]Li, premier exemple de complexe de stéréochimie bipyramide trigonale $[PdCl_2Me(PR_3)_2]^-$ ayant deux atomes de phosphore *trans*-positionnés; b) le complexe [$PdMe_3$(**TRANSDIP**)]Li, dans lequel la diphosphine a subi la décoordination d'un des atomes de phosphore. C'est précisément ce complexe qui donne lieu à l'élimination d'éthane; c) le complexe [Pd^0Cl(**TRANSDIP**)]Li, analogue des complexes $[Pd^0Cl(PR_3)_2]^-$ observés par Jutand et Amatore dans des réactions de couplage carbone–carbone impliquant des monophosphines. Tous ces intermédiaires ont pu être visualisés spectroscopiquement grâce au confinement de la réaction qui provoque ainsi un ralentissement de la réaction et permet d'observer les diverses étapes. Le complexe [Pd^0Cl(**TRANSDIP**)]Li est facilement oxydé en présence d'air pour donner le complexe peroxo [$Pd(O_2)$(**TRANSDIP**)], exemple rare de cavité hébergeant une entité [MO_2]. L'extension de cette réaction à d'autres métaux permet d'envisager la synthèse de nouvelles métalloenzymes artificielles.

L'ensemble des résultats décrits dans ce mémoire pourra donner lieu à plusieurs nouveaux projets de recherche :

- L'utilisation de réactifs pontants pour la formation de dérivés tetrafonctionnalisés de la γ-CD, qui permettrait obtenir des analogues de **TRANSDIP** et **WIDEPHOS** bâtis sur une cavité encore plus grande et peut-être mieux adaptés à une chimie *intra*-cavitale.

- La synthèse et l'étude des propriétés complexantes et catalytiques des dérivés de CD comportant des fonctions non plus de type *phosphine* mais, par exemple, phosphite ou phosphoramidite.

- La synthèse de cyclodextrines hydrosolubles autorisant des réactions catalytiques en milieu aqueux.